G. M. Tarekul Islam
Shampa
Ahmed Ishtiaque Amin Chowdhury *Editors*

Water Management: A View from Multidisciplinary Perspectives

8th International Conference on Water and Flood Management

Springer

Water Management: A View from Multidisciplinary Perspectives

G. M. Tarekul Islam · Shampa ·
Ahmed Ishtiaque Amin Chowdhury
Editors

Water Management: A View from Multidisciplinary Perspectives

8th International Conference on Water and Flood Management

Springer

Editors
G. M. Tarekul Islam
Institute of Water and Flood Management (IWFM)
Bangladesh University of Engineering and Technology (BUET)
Dhaka, Bangladesh

Ahmed Ishtiaque Amin Chowdhury
Institute of Water and Flood Management (IWFM)
Bangladesh University of Engineering and Technology (BUET)
Dhaka, Bangladesh

Shampa
Institute of Water and Flood Management (IWFM)
Bangladesh University of Engineering and Technology (BUET)
Dhaka, Bangladesh

ISBN 978-3-030-95721-6 ISBN 978-3-030-95722-3 (eBook)
https://doi.org/10.1007/978-3-030-95722-3

© The Editor(s) (if applicable) and The Author(s), under exclusive license to Springer Nature Switzerland AG 2022
This work is subject to copyright. All rights are solely and exclusively licensed by the Publisher, whether the whole or part of the material is concerned, specifically the rights of translation, reprinting, reuse of illustrations, recitation, broadcasting, reproduction on microfilms or in any other physical way, and transmission or information storage and retrieval, electronic adaptation, computer software, or by similar or dissimilar methodology now known or hereafter developed.
The use of general descriptive names, registered names, trademarks, service marks, etc. in this publication does not imply, even in the absence of a specific statement, that such names are exempt from the relevant protective laws and regulations and therefore free for general use.
The publisher, the authors and the editors are safe to assume that the advice and information in this book are believed to be true and accurate at the date of publication. Neither the publisher nor the authors or the editors give a warranty, expressed or implied, with respect to the material contained herein or for any errors or omissions that may have been made. The publisher remains neutral with regard to jurisdictional claims in published maps and institutional affiliations.

This Springer imprint is published by the registered company Springer Nature Switzerland AG
The registered company address is: Gewerbestrasse 11, 6330 Cham, Switzerland

Preface

This book *Water Management: A View from Multidisciplinary Perspectives* presents the collection of selected papers from the 8th event of the International Conference on Water and Flood Management (ICWFM) held during March 29–31, 2021. This year, the conference added a new dimension not only because the program was held online due to the COVID-19 situation but because the pandemic taught us how to act when natural disasters and pandemic-like situations occur concurrently.

Said that, organizing the conference in virtual platform was less difficult compared to the challenges of selecting top articles from more than 200 scientific works presented in the conference. Thanks to the members of the Scientific Committee and Reviewers whose relentless effort has made this possible. It is gratifying to note that our initiative has brought together a multidisciplinary and global team of national and international academicians, researchers, experts, as well as practitioners contributing chapters to the book on the diverse physical, environmental, socio-economic, and institutional issues concerning Water Management. Our objective, and indeed, the driving force behind the book, has been to bring the current water management issues and knowledge throughout the world into the forefront of the scientific community and policymakers. We hope all this endeavor will prove valuable to academicians, policy planners, and development practitioners alike.

Finally, thanks to the Springer team for publishing this volume for two successive years. This particularly encourages early career researchers to contribute to the conference.

Dhaka, Bangladesh

Prof. G. M. Tarekul Islam
Shampa
Ahmed Ishtiaque Amin Chowdhury

Contents

Floods and Drainage

Causes and Management of Damaging Flood Incidences in Rapidly Urbanizing Areas of Kathmandu Valley: A Case Study of Flood Event in Bhaktapur District, Nepal

Purnima Acharya and Ashutosh Shukla

Abstract The ever-growing incidences of urban flooding that were previously anomalous have now started affecting many parts of Kathmandu Valley on a yearly basis. This study aims to understand the causes of urban floods and the adaptation/mitigation interventions being implemented through a case study of recurrent urban flooding in Bhaktapur District, Nepal. A Land Use Land Cover Change (LULCC) map to trace the local LULCC of the flood-affected area and precipitation data of Bhaktapur city was analysed to examine its contribution to the flood. Household surveys, FGD and key informant interviews were conducted to understand the mitigation and adaptation practices at household, community and national levels. The research revealed that the flooding impact has been increasingly severe in recent years, mostly due to poor mitigation efforts. Poor storm water management aggravated by disorganized human settlements in the right of way of the river contributes to scale up the infrequent overflows to overt flooding. Therefore, it is important to expand our understanding regarding causes and consequences of flooding events to inform urban planning. Considering current and potential adaptation strategies, this research makes suggestions for effective adaptive measures and adds to a global conversation about the future of sustainable cities.

Keywords Urban Flooding · LULCC · Climate Change · Storm water · Drainage

1 Introduction

The annual flood brought by heavy monsoon precipitation results in enormous damage to lives and properties, making regions of southern Asia vulnerable to floods (Mirza 2011). In addition, population growth and changes in land use have also increased human vulnerability to floods (Dewan 2015). The changes in land use not only bring changes in the geomorphology but also change the infiltration capacity of soils, which leads to increase in the amount of overland water flow causing floods

P. Acharya (✉) · A. Shukla
Nepal Engineering College, Bhaktapur, Nepal

© The Author(s), under exclusive license to Springer Nature Switzerland AG 2022

G. M. Tarekul Islam et al. (eds.), *Water Management: A View from Multidisciplinary Perspectives*,
https://doi.org/10.1007/978-3-030-95722-3_1

downstream. In addition, the changes in natural drainage and increased burden on existing drainage system, as a result of population growth, increase the likelihood of the system being overwhelmed (Salike and Pokharel 2017). With extreme rainfall events having more recurrent trends in the recent years (IPCC 2014), incidences of both pluvial and riverine flooding have been exacerbated.

Flooding has become a major problem in Kathmandu Valley, Nepal in recent years. Rapid urbanization and subsequent human led changes in the urban landscape has increased the imperviousness exacerbating the flood frequency. The flood incidences over the last one decade have increased in areas with no flooding events in the past, that also includes areas with relatively low precipitation in the catchment. In Hanumante River of Bhaktapur district, there have been two flood events within the four years producing widespread damages—the first one occurring on August 27, 2015 and the second on July 12, 2018 (Prajapati et al. 2018). This study mainly focuses on the flood incidence of July 12, 2018.

While incidences of urban flooding are on the rise all over Nepal, it remains one of the least explored areas in the field of disaster management (NWCF 2009). The challenges to flood hazard mitigation are essentially about instituting good governance (Rijal et al. 2018). The policy, as it exists, does not allow the government to impose necessary restrictions on private property, thus proving ineffective in preventing the unsustainable expansion of urban sprawl.

This research analyses the factors and processes accumulating in the urban areas responsible for the genesis of the flood event of July 12, 2018 in Hanumante River of Bhaktapur, Nepal. It also analyses the strings of adaptation and mitigation efforts implemented by the community and different levels of government. It also aims to draw key gaps in the policies, regulations and practices leaving the urban flooding unaddressed in the rapidly changing urbanscape and urban development plans.

2 Methodology

2.1 Study Area

The study area (Fig. 1) of this research lies in Madhyapur Thimi Municipality (MTM) in Bhaktapur District. Geographically, MTM lies at 27˚40′00″ to 27˚42′00″ N latitudes and 81˚22′30″ to 85˚25′00″ E longitudes, at an average elevation of 1320 m from the mean sea level. Much of the landscape of the municipality is plateau-like, located between Manohara and Hanumante Rivers, which includes conspicuous upland and lowland areas.

Hanumante River flows from north-east to south-west of Bhaktapur District with an average width ranging from minimum of 10 m in the dense urban sprawls to maximum of 20 m in peri-urban and rural areas. The catchment of the river is 143 km^2 stretching across 23.5 km (Sada 2012). The river includes numerous tributaries and among them Ghatte Khola, Kasan Khola, Kalighat Khola and Kaalcha khola are

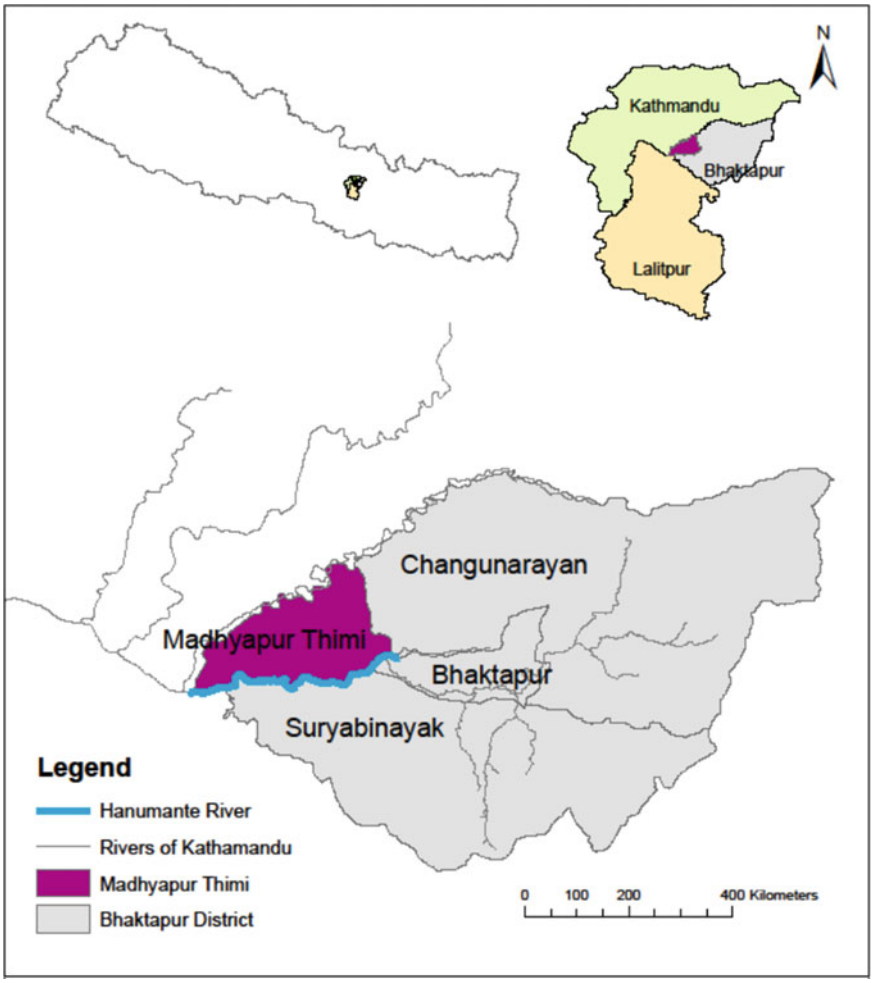

Fig. 1 Study area

important tributaries which join the river at different stretches. Specifically, the low land areas were in the focus of the study because these were the areas inundated in the flood event of July 12, 2018.

This research has used a case study approach and multi-perspective analysis: geographic, geomorphic, meteorological and socio-economic in unpacking the flood incidence of July 12, 2018 in Hanumante River that inundated Madhyapur Thimi Municipality. The following methodological tools were used.

2.2 Reconstruction and Mapping of the Studied Flood Event

The flood event of July 12, 2018 was reconstructed using secondary data collected from different published/unpublished sources and primary information was collected through the questionnaire survey with thirty-five people who faced the event. The primary information was also received from those associated to different social and humanitarian organizations and local governments who were involved in rolling rescue/relief operations following the event and mitigation efforts in the aftermath of the event. The information collected was validated with the recorded information of local government, civil society organizations, red-cross and district administration.

2.3 Reconstruction of Historical Events

Hanumante watershed is ungauged therefore longer-term hydrological data and records of flood history was not available. The Disaster Risk Reduction portal of the Ministry of Home Affairs which is responsible for maintaining records of the disaster event across the country did not have any record of flood events in Madhyapur Thimi and/or Hanumante. Similarly, Municipal Office, Department of Hydrology and Meteorology (DHM), Department of Irrigation and Water Resources (DIWR), Water and Energy Commission Secretariat (WECS), District Administration Office, Nepal Red Cross Society, Bhaktapur and District Police office had no archived information regarding historical flood events. In the absence of hydrological stations at any of its reach in the Hanumante River and unavailability of water flood records, hydrological analysis could not be done, so, the records of flood history were developed using information from the memory of the people.

2.4 Meteorological Data Analysis

The study used rainfall data maintained by the DHM to analyse the rainfall trend in the areas. For this purpose, daily rainfall data of the time period 1971–2018 of the nearest meteorological station (Nagarkot index no. 1043, Bhaktapur index no. 1052, and Changunarayan index no. 1059) were analysed using RCLIMDEX software (Zhanag and Yang 2004). These stations were selected by drawing Thiessen Polygon to establish possible contributions in Hanumante catchment. Out of three rainfall stations closer to Hanumante basin, the data of Bhaktapur station were only found to be homogeneous while conducting RH test and hence was only used for rainfall analysis.

RClimDex is a software package which is useful in calculating the climate extremes indices, required to monitor and detect climate change (Zhanag and Yang 2004). RClimDexuses R platform was used to perform and check the data quality

before computing the indices (Zhanag and Yang 2004). This study uses selected precipitation indices for the rainfall analysis and conducts quality control which checks the data input errors which also includes missing data as well. The RHtest software was applied for homogeneity testing of the rainfall data as it does not require any reference series and is available freely (Wang and Feng 2013).

2.5 Map Analysis

The study has analysed the changes in land use and land cover around Hanumante River in Madhyapur Thimi Municipality (MTM) where time series analysis was done from the late seventies to look into the decadal change. Due to limitation of the high-resolution images for detailed LULCC analysis in the small area along Hanumante River, this study uses aerial photographs of 1979 and 1992 which were available with the Department of Survey, Government of Nepal and the Google earth images of 2005 and 2018 which were downloaded and refined for the year 2005 and 2018. These images were used to develop the LULCC map for the lowlands of Madhyapur Thimi and Suryabinayak Municipality, that lies within 500 m width from the Hanumante River for the stretch of 7.13 km covering 7.34 km^2, to know the increase in built-up area along the Hanumante River, which is prone to flooding.

After georeferencing the aerial photographs in ArcGIS, digitization of the photograph was done using four classifications to look into the changes in the land use and land cover: (i) vegetation, (ii) water body, (iii) settlements and (iv) farmland and open space. Similarly, digitization of the Google earth image was done using the same classification and decadal land use and land cover changes were assessed.

2.6 Focus Group Discussion

Experiences and perceptions of the flood event, the changing rainfall pattern, causes and impacts of the flood events were collected from the urban poor, slum and squatter settlers, old inhabitants and recent migrants with their dwellings close to the river course through FGDs, with the following two groups having ten people in each of the groups. Series of questions were asked and documented.

i. Old habitants living in the upland of MTM but having farms in low land and
ii. Old and new migrants living in the lowland of MTM who at least experienced the flood incidence of July 12, 2018.

2.7 Key Informants' Interviews (KII)

Fourteen KIIs were conducted to collect information pertinent to plans, policies and strategies of the government; social, economic, infrastructural and environmental changes in the area and planned and autonomous adaptation practices rolled at different levels. The key informants included personnel working in KVDA, DHM, DOI (WRRDC), Smart Panni, HPCIDBC, MTM, Bhaktapur Municipality and Red Cross Society, including independent professionals and academicians and researchers.

2.8 Physical Observation of the Study Area

The land use pattern and the corridor development work in progress implemented by the High-Power Commission on Integrated Development of Bagmati Civilization (HPCIDBC) were observed as part of the study. At some sections the original width of the river was narrowed as a result of development of the road corridor, which was indicative of the encroachment in the river even by the government supported development programmes.

3 Results

3.1 Historical Flood Events in Hanumante River

The focus group discussion, household interviews and key informants' surveys showed that the lowland areas of MTM have had a past history of getting flooded intermittently at an interval of a few years but the magnitude of damage produced by the recent floods including on July 12, 2018 was unprecedented. In the past, there were no disturbances on the passage of flood and therefore the water level in the river receded within a few hours to few days' time. But the floodwater on July 12, 2018 stood in the area for more than 24 hours showing significant change in the recession of flood flow.

3.2 Analysis of Climatic Causes of the Flood

In order to analyse if the variability in rainfall has been responsible for the flood event, rainfall records of Bhaktapur meteorological stations were analysed using RCLIMDEX software. The catchment of the Hanumante River is 143 km^2 and almost all of the surface water of Bhaktapur is drained through this river. Therefore, when

it rains covering the entire catchment the volume of the water in the river rises, producing potential risk of flooding and inundation in the downstream areas.

3.2.1 Rainfall Frequency Analysis

Daily rainfall records of Bhaktapur Station for the period 1971–2018 were subjected to frequency analysis using Gumbel's Type I Extreme Distribution Function to estimate the return period of rainfall of different magnitude (Table 1).

The stations at Bhaktapur, Changunarayan and Nagarkot recorded 24-h rainfall of 129.6, 30, and 117 mm, respectively, on July 12, 2018. As the Bhaktapur station is considered representative to the study area and therefore contributor to the genesis of the flood event on the day, the return period of the event is calculated to be 8.4 years. This shows that the likelihood of recurrence of the flood event of the magnitude of July 12, 2018 is once in 8.4 years (Fig. 2).

Table 1 Estimated 24-hours rainfall for different return periods

S. No.	Return Period (years)	Rainfall (mm)
1	2	73.3
2	5	110.99
3	10	135.95
4	50	190.87
5	100	214.08

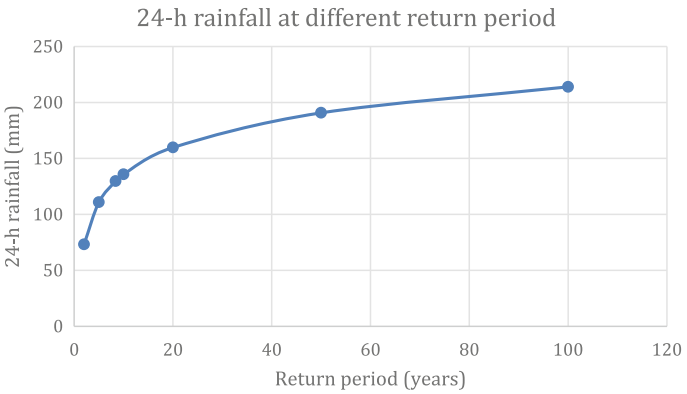

Fig. 2 Likely 24 hours rainfall at different return periods in Bhaktapur

3.2.2 Analysis of Rainfall Trend

This study maintained that one of the causes for the flooding event was extreme rainfall event. The five indices used in the study provide opportunity to look into antecedent rainfall conditions and persistence in the event, both proving bases to logically unpack the extremity of the event.

i. Trend of Annual Total Rainfall

The annual total rainfall analysis revealed a decreasing trend, but the trend was found non-significant as the *p*-value is 0.075 (i.e. non-significant at 5% level of significance). The decreasing trend in annual total rainfall would mean lower possibility flooding occurrences in the study area in future. However, relying on this observation to make any assessment of flooding trends in the study area would be grossly unrealistic for the fact that flood events are often results of extreme events and the runoff producing potential of the catchment and not necessarily the contribution of total annual rainfall in the catchment.

ii. Trend of Extreme Values

In order to analyse the likely contribution of extreme values responsible for the genesis of the flood event of the day, the highest daily rainfall amount (RX1day) and highest 5-days consecutive rainfall amount (RX5day) of Bhaktapur Station were subjected to trend analysis. The analysis revealed an increasing trend ($p = 0.521$) of highest daily rainfall while decreasing trend ($p = 0.719$) in 5-days consecutive rainfall total. However, this trend cannot be relied upon as both of the observed trends are very weak and non-significant.

iii. Trend of Consecutive Wet Days (CWD)

The observed trend in maximum consecutive wet days was noted to be decreasing significantly ($p = 0.041$) in the study area. This trend signals lowering of persistence in rainfall in future times, even in the monsoon. Lower CWD in the area even if there is not much change in the total amount of rainfall would mean lower runoff concentration to produce peak flow because runoff yield from catchment depends on antecedent moisture condition in the catchment besides the amount of the rainfall. Similar observations have been observed of the people living in the study area for a longer time, who revealed that monsoon rainfall in the area is no longer persistent. Number of days without rainfall in between two successive rainfall events has increased, unlike in the past.

iv. Simple daily intensity index (SDII)

In order to look into the trend of SDII in the study area, the SDII values of each year over the past 47 years (1971–2018) were plotted and it revealed a decreasing trend in the study area, which was non-significant ($p = 0.087$). This trend of SDII in the study area revealed decreasing rainfall amounts on the wet days to produce concentrated runoff causing flooding in the study area.

All the rainfall trend plots are shown in Fig. 3.

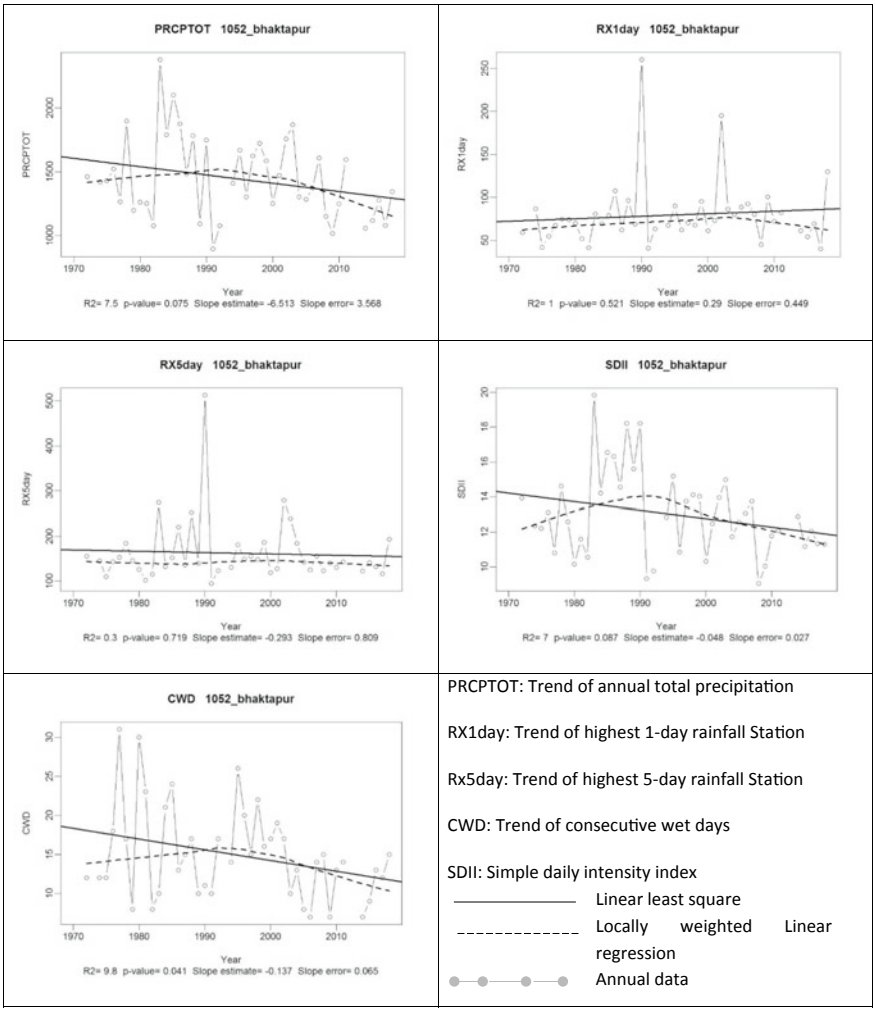

Fig. 3 Trend of rainfall analysis

3.2.3 People's Perception on Climatic Trend

People in the area recall significant shifts in the pattern of rainfall and seasonality indicating that the past moderate and persistent monsoon rainfall had mostly been of short duration with high intensity. Increased occurrence of high intensity rainfall event in the monsoon was attributed by most people to the cause of flooding in Hanumante River and inundation in the surrounding areas, however out of 35 local people who were interviewed, only a small number of people (less than 20%) pointed the rainfall to be the only cause of the flooding. They rather attributed changes in the land use, particularly changes brought in the natural drainage pattern as a result of rapid

infrastructure development to be the additional cause. This attribution signifies that they do distinguish rainfall amount and the surface water flow that the given amount of rainfall produces. This perception of rainfall excess clearly signifies people's knowledge of the changes occurring in the landscape and hydrological processes as a result of population growth and densification of human built infrastructures.

3.3 Analysis of LULCC

The study attempted to relate LULCC as a possible causal factor combining with rainfall for producing the flood event of July 12, 2018 in Hanumante River. The LULC maps of the area for different time periods covering a stretch of 500 m width on both sides of the river in Madhyapur Thimi Municipality were prepared. In addition, LULCC map of Kathmandu Valley was also prepared to relate the urbanization trend and related LULCC in the study area with the general trend in Kathmandu Valley.

3.3.1 LULCC of Kathmandu Valley

Land use map of Kathmandu Valley was prepared in Google Earth Engine (Gorelick et al. 2017) for the year 1988, 1998, 2009 and 2018 to assess the general trend of urbanization in the valley and to compare the resulting changes with the changes in the study area (Fig. 4). This was needed because LULCC in the study area cannot be looked at in isolation.

The LULCC analysis of the Kathmandu Valley shows that between 1988 and 2018, the size of the -developed area increased by 625% (Table 2). Much of this growth was found concentrated in three major urban centres: Kathmandu Metropolitan City, Lalitpur Metropolitan City and Bhaktapur Municipality. Human settlements were also found to be rapidly expanding in the peripheral areas, radiating to all directions, from the urban core mostly after the late nineties with 165.60% growth in the developed area from 1998 to 2009. This clearly reveals significant growth in the developed area in Kathmandu Valley over the last three decades.

3.3.2 LULCC of Study Area

In order to assess the land use change in the lowlands of Madhyapur Thimi that was engulfed into recurrent flooding and inundation on July 12, 2019, 7.34 km^2 of area that extended 500 m on either side of the Hanumante River for a stretch of 7.13 km, one side in Madhyapur Thimi and on the other side Suryabinayak Municipality, was analysed (Fig. 5). The periods selected for analysis included 1979, 1992, 2005 and 2018, to cover a time span of four decades (Fig. 6) and maps were prepared in ArcGIS. There has been significant expansion in the built-up area over the period 0f 2005–2018 (Table 3), it increased from 84.9 to 389.330 ha. On the other hand, there

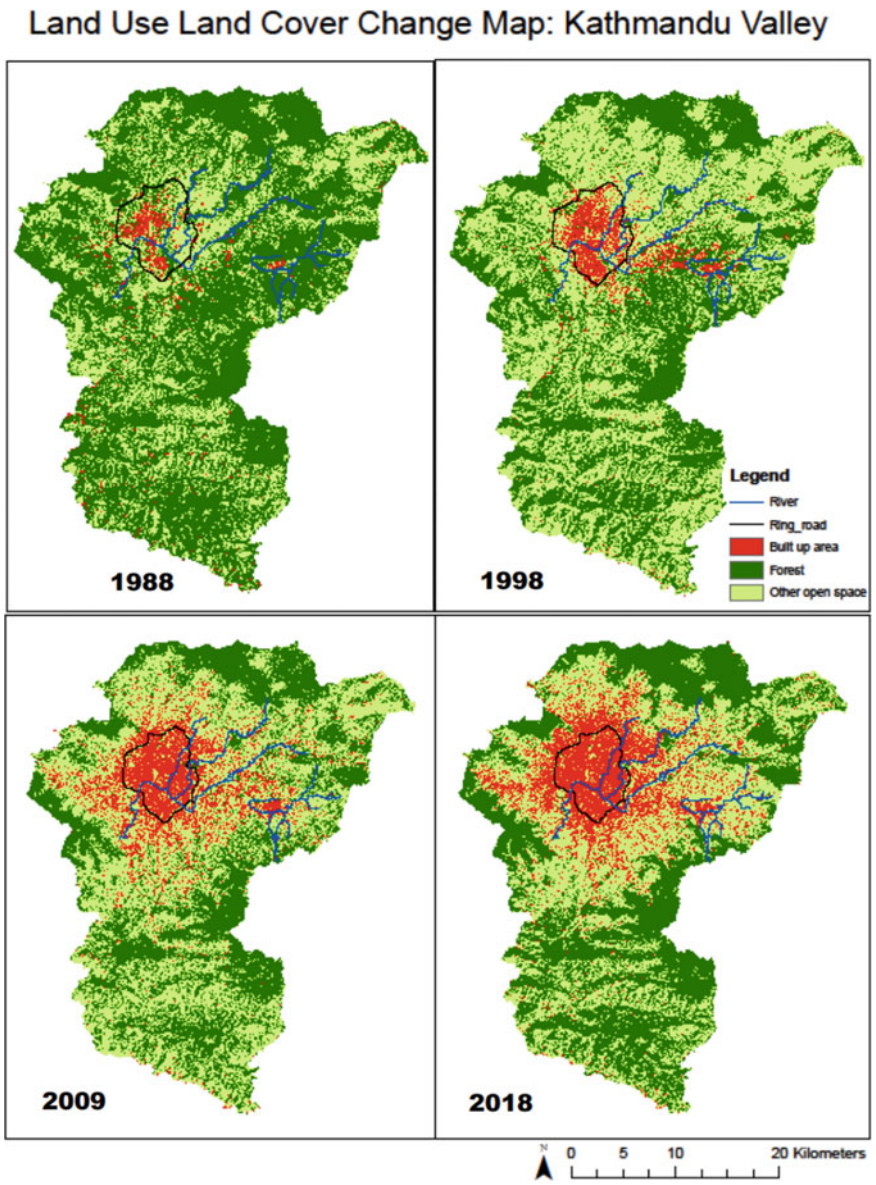

Fig. 4 Land Use Land Cover Change map of Kathmandu valley

Table 2 Land Use Changes in Kathmandu Valley (1988–2018)

	Area (ha)		
Year/Categories	Built-up area	Forest	Other (Agriculture, barren, open space)
1988	2023.74	61,379.73	29,336.76
1998	4212.81	43,420.77	45,106.65
2009	11,189.34	35,886.87	45,664.02
2018	14,678.71	39,475.98	38,586.84

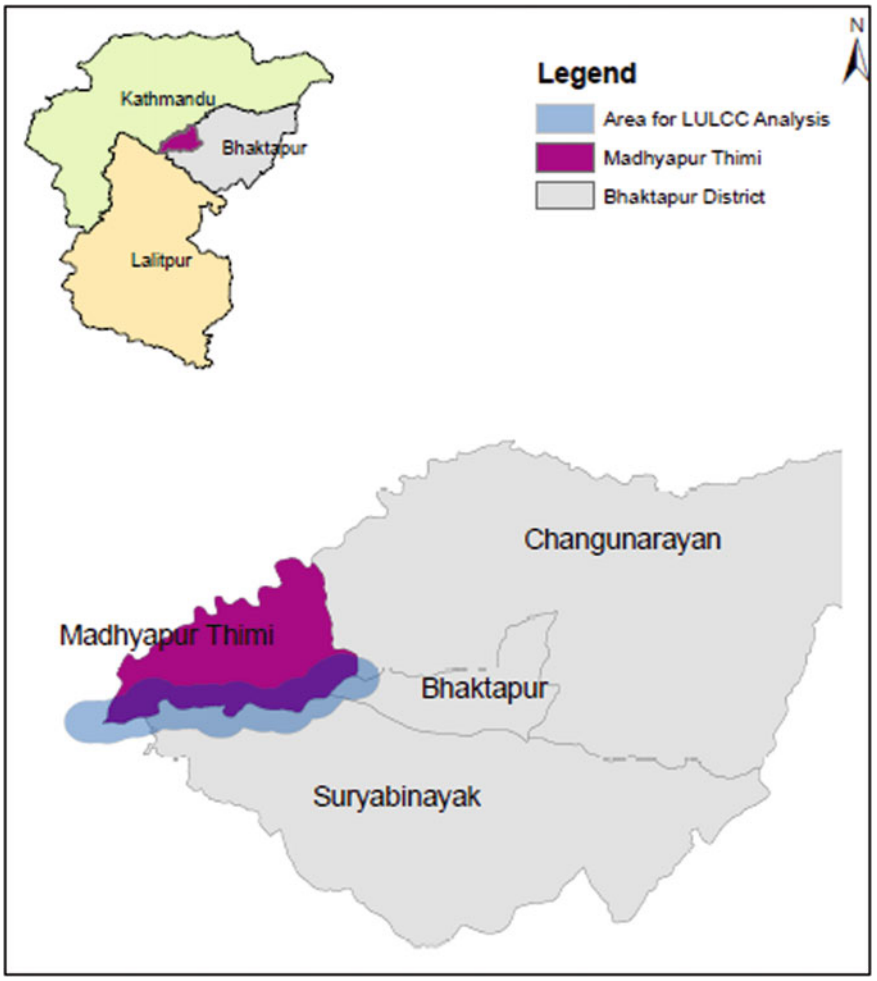

Fig. 5 The site location for LULCC in MTM

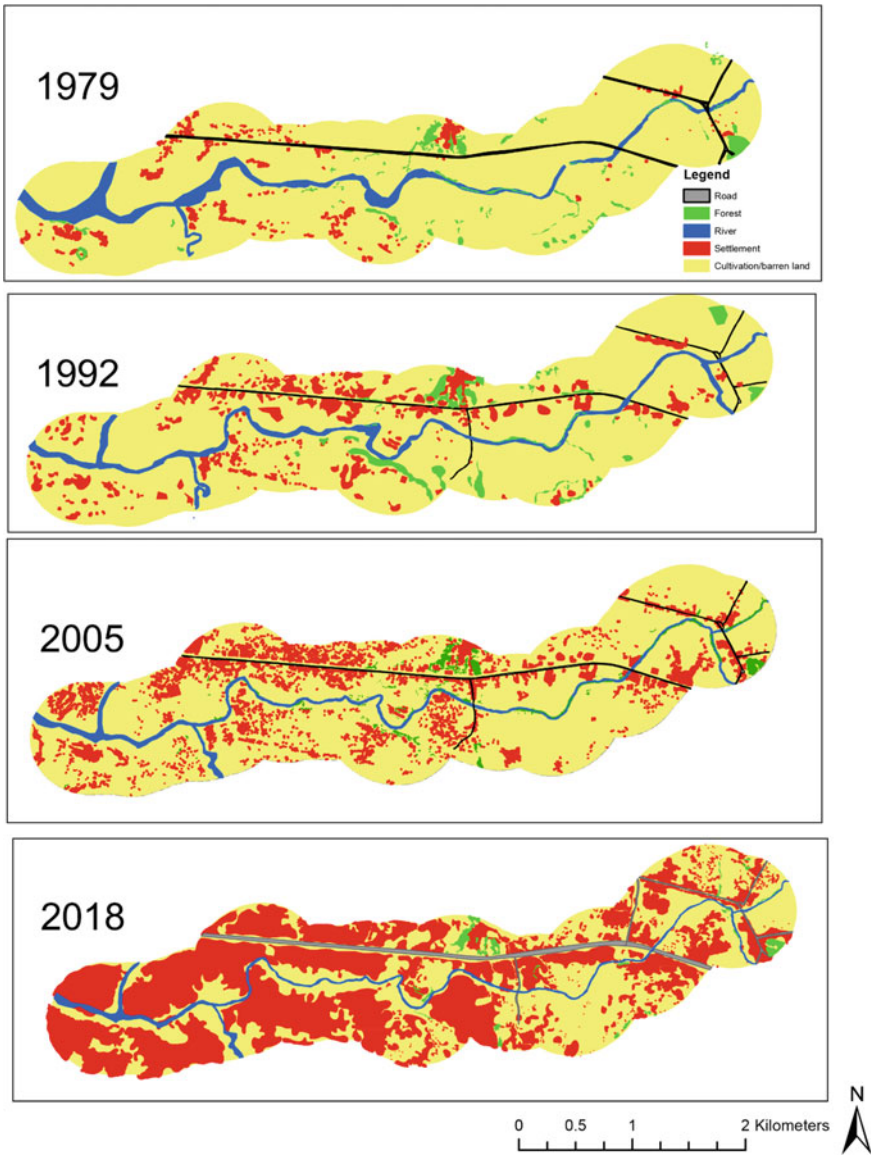

Fig. 6 LULCC map around Hanumante River

has been reduction in the area under agricultural use, water bodies and forest. This resonates with the information provided by the people that the extent of damages faced by the people in the flood event of July 12, 2018 was essentially due to growth in human settlement in close proximity of the river and not by the magnitude of the flood itself.

Table 3 Land use changes in the study area over 1979–2018

	Area (ha)				
Year/Categories	Settlement	Forest	River	Road	Cultivation/barren land
1979	19.00	23.73	41.33	6.24	643.34
1992	54.64	19.48	30.72	6.31	622.49
2005	84.96	14.69	15.32	6.31	612.36
2018	389.33	8.81	11.90	17.27	306.34

3.3.3 People's Observation on Urbanization vis-à-vis Trend of Flooding

This section presents the observation of the people living in the study area regarding the pattern of flooding and inundation in relation to urbanization and changes in the landscape along Hanumante River.

i. Growth in the Population and Human Settlements

The high rate of migration, development of roadways and conversion of agricultural land have developed physical barriers for surface water flowing back into the river during heavy rainfall. This has resulted in inundation for prolonged duration in the human settlements on both sides of the river. Nearly 67% of the respondents blamed the government for not having strict policies to regulate the land near the rivers.

ii. Encroachment into the Flood Plain

The key informants identified significant encroachment on the right of way of the river. The area adjoining the river was previously a farmland that had always been the flood plain of Hanumante River, but, at present, the entire area is covered by new settlements and commercial establishments. Unregulated conversion of the farmlands into settlements led it to emerge close to the river's waterway. Also, the natural barriers of endemic vegetation were gradually removed that resulted in floodplain and the riverbanks becoming weak, causing significant erosion due to bank cutting and sloughing. The sediments entered into the river and were deposited on the bed, causing the river bed to rise. The problem was aggravated when riverbank was used for dumping solid wastes by the municipal authorities of Bhaktapur and Madhyapur Thimi.

iii. Poor Storm water Management Practices

People attributed the problem of flooding and inundation to their inability to evacuate the excess water from the rainstorms quickly. With the reduction in the open spaces and porous land surface, the existing drainage system gets overwhelmed even with rainfall of moderate intensity. The overland flow from paved areas and human settlements, which generated suddenly following the rainfall event, when added to the river flow at lower reaches, aggravates flooding.

iv. Infrastructures Development without Drainage Considerations

Construction of new roads and other human built infrastructures brought changes in the natural drainage system and the routes for the flow of excess

water in the study area. There are several bridges along the Hanumante River and at these bridge crossings, the river section has been narrowed which blocks the natural flow of the river.

v. Erosion of Traditional Systems and Practices of Water Management

The respondents revealed that in the past, there were a number of ponds, natural drains, canals and open areas that buffered the flood water reducing damage. Drainage and excess water from the stone spouts went to the ponds downstream and during rainfall the ponds acted as a storage that was used in the pre-monsoon period for agriculture (Molden and McMahon 2019). In addition to this, surface runoff was also channelled into these ponds. These traditional systems and water management practices are now on the verge of extinction and the pace of development of new infrastructures hardly respects their existence and accrue importance.

vi. Landscape Level Changes Caused by Land Development

Local governments allow land developers to extract sand from hillocks on the river terraces in the valley, which is also common in Madhyapur Thimi. The damage caused to landscape and the environmental damage resulting from such practice of land development, which is rampant at present, is difficult to reverse. The sandy hillocks in the landscape have an important role in sustaining local hydrology for their ability to store water during and after rainfall. Highly permeable sand formation retains the water which would regulate runoff. The loss of the sandy hillocks in the landscape has been one of the reasons for urban flooding, particularly in the catchment of Hanumante River in Bhaktapur. With the loss of more porous sub-surface sandy formation rainwater moves out quickly to produce floods and inundation on the downstream.

3.4 Management of Flood

Management of flood involves minimizing the negative impacts, but they are difficult to eliminate altogether (Khanal 2018). Therefore, resilient adaptive strategy and mitigation efforts rolled at various levels is a cornerstone for minimizing loss and damage. In addition, it is imperative to explore sustainable solutions with regard to management techniques.

3.4.1 Adaptation and Mitigation Efforts Rolled at Household and Community Level

As stated in the preceding sections, the study area had been experiencing incidences of recurrent flooding in the past. Therefore, the case flood incidence was not new but the intensity and duration of flooding and inundation caused by it and the losses and damages suffered were alarming. The event has made people more cautious of repetition of events of similar or larger magnitude in the future.

People revealed that the magnitude of flooding and inundation, at least those that had occurred in the recent past including the event of July 12, 2018, has been so large and sudden, that this leaves very little scope at their end to cope with or adapt to them. People think this would require larger efforts and investment which would be beyond their reach and they foresee the importance of collective efforts and investment made by local governments. Nonetheless, some of the measures that they have started rolling at their end following the event to develop their adaptive capacity include:

- Shifting to other areas or at least shifting to live on the 1st and 2nd floor of the house.
- Raising the plinth level of new houses to ensure that the floodwater would not enter the house.
- Investing to develop raised masonry boundaries, to function as flood walls.

3.4.2 Adaptation and Mitigation Rolled at Local Government Level

Some of the initiatives that have started at the local level following the event have been: (i) removal of silt and cleaning of the river bed and banks annually with the aim of maintaining the river cross-section to allow the floodwater to pass the river channel quickly, and (ii) strengthening riverbanks by developing masonry and vegetated revetment at critical sections and strengthening the ghats and (iii) development of the road corridor, under the funding of the High-Power Commission on Integrated Development of Bagmati Civilization (HPCIDBC) which involves the development of a 20 m wide river followed by 20 m wide road on both sides, and construction of flood wall and retaining wall to strengthen the bank.

The hydrological report of this project reveals that the hydraulic calculation for flood is carried out for the 2- and 5-year return periods at the cross-section and bridge locations along the reaches of all rivers. Though the actual impact of the project is yet to be seen, the real risk is the infrastructure development under the project producing large and irreversible changes in the river environment. When inquired, 83% of the respondents opined that the corridor project development will address the problem while 17% of them maintained that the river width will be further narrowed, thus limiting the capacity of the river to dispose-off the runoff that often produces from extreme rainfall events. One obvious consequence that can be thought of is the disconnection between surface water and groundwater in the river environment as a result of creation of a physical barrier on the riverbank.

3.4.3 Adaptation and Mitigation Rolled at the Central Government Level

The past flood events and the one of July 12, 2018 does not seem to have produced enough concern at the level of central government agencies, those entrusted with the responsibility of decision making and issue policy directives, that urban flooding

and inundation is an impending hazard risk in the urban areas and the consequences could be grave if it remains unaddressed. Their focus continues to be on designing and rolling infrastructure solutions to the problem. One such example which is currently underway in the area is urban drainage development involving construction of trunk sewer lines on both sides of the river collecting sewage disposal of the household. The project is part of the urban water system improvement project of Kathmandu Upatyaka Khanepani Limited (KUKL), implemented through a Project Implementation Directorate (PID). The design of the project does not involve any focus on collection and management of storm water, which is the cause of flooding and inundation in the area.

4 Discussion

The flood event of July 12, 2018 was the result of several factors and processes, all combining to produce the flood event of the day. The rainfall trend analysis demonstrated an increase in the high intensity short duration rainfall events which also corroborated with the people's perception. With the increase in urbanization, the events of flooding are seen to be more deleterious and detrimental to the inhabitants in the floodplain. The analysis also shows that the likelihood of recurrence of the flood event of the magnitude of July 12, 2018 once in only 8.4 years. Given the fact that Bhaktapur station has historically witnessed the highest daily rainfall amount of 260 mm recorded in 1990, occurrence of rainfall events of this magnitude could produce even worse floods in the future if not addressed timely. This observation must draw the attention of local governments and the agencies responsible for the development and management of urban infrastructures and services. The Weather Forecast Division of Nepal (DHM) agrees that events of urban flooding, such as the one that occurred on July 12, 2018, are not solely the result of weather-related causes. Most of the time the genesis of urban flooding lies on poorly developed urban infrastructures and services.

The scope of mitigation and adaptation at the household level is much limited as the recurrent urban flood events require larger scale efforts, involving a multi-pronged approach of storm water management, improvement of drainage systems and regulation of infrastructure growth in the urban areas. Contrarily, the local government in the existing arrangement bears responsibility to roll preparedness but does not seem to have any organized and coordinated preparedness measures. Development of river corridors along Hanumante River undertaken by HPCIDBC was identified as the only major activity in the floodplain, although the primary objective of this was to develop road corridors and not for flood control.

The issues of disaster risk reduction and management (DRRM) remained outside the scope of urban development policies until the proclamation of Hyogo Framework (2005–2015) and Sendai Framework of Action (2015–2030). But, the attention has been only on the high intensity and episodic disasters, small yet recurrent disasters, such as urban flooding and inundation, continue to remain outside the radar of DRRM

especially in context of Nepal. One of the hard facts projected by the study is the lack of attention and priority for urban flooding and inundation in the existing regulatory codes and practices of Nepal. Nepal's Urban Development Policy (2007) and Urban Development Strategy (2017) considers 'resilience' as the guiding principle of urban development and emphasizes on sensible urban development, and these policy directives do set conceptual clarity for sustainable urban development. However, they do not provide for an operational mechanism to translate the policies into action on the ground. The land use zonation (LUZ) maps which are basic instruments to regulate the land use in the urban and rural areas have not been developed at the level of most municipalities. Even in Kathmandu Valley where these maps have been developed, it is yet to be implemented effectively. This is mainly due to the fair amount of ambiguity in the existing regulatory laws to impose restrictions on the development and uses of private land other than those for designated purposes.

4.1 Sustainable Solutions to Mitigate Urban Flooding

Kathmandu was once a city of culturally and religiously significant ponds that enabled urban development. These traditional systems are rapidly decreasing as the new development did not respect their existence, to add on, the new development did not care for the development of additional drainage facilities to compensate for this loss. This has certainly produced a regime of increased flooding and inundation in urban areas. The local knowledge that informed these ancient structures can be adapted to a modern context by improving drainage systems, groundwater recharge and rainwater storage. The use of traditional water storage systems in new development plans can have the potential of adapting local knowledge systems to solve this modern problem. Also, the dissipation of rainwater, especially its use to recharge groundwater, should be part of the mitigation plan for urban flooding problems.

There is no doubt that the change in local hydrology due to urbanization has contributed to an increase in the frequency of damaging flood incidences in Hanumante River and the damage suffered by the people. This change in the local hydrology is also exacerbated by other changes in land use such as the switch from rice to vegetable cultivation and the practice of increasingly leaving land fallow, as land without a cover crop does not hold water, it acts like a pavement during the deluges of the monsoon and disrupts the recharge cycle (Wrobley 2020). Therefore, planting rice could also be one of the solutions to hold the water.

For enabling resilient urban living, urban flooding and inundation should both be included in the urban development policy and programming. One of the major clauses to be included is the river waterway demarcation in order to avoid further encroachment along the river as well as maintenance of natural drainage in the urban areas. Planning and regulatory capacity of agencies, including local government, to regulate haphazard urbanization should be developed to restrict urban areas from turning into disaster hotspots.

5 Conclusion

The study intended to look into the factors and processes that were responsible for the onset of the flooding event of July 12, 2018. This involved a multi-perspective analysis involving analysis of rainfall data and LULCC in the catchment and flood plain of the river to establish their relationship with the incidence of flooding and inundation on the stated day. Alongside, the perception of the local people was collected to validate the finding.

While climatic factors control the inputs that set the processes for genesis of urban flooding, the physical changes in the urban landscape particularly those relating to land use and drainage system largely modulate the flow and flow rates to produce flooding damages resulting from the flood events caused to livelihoods of urban dwellers. The responsibility of mitigation and adaptation falls in the domain of local and central government. Infrastructure solutions that are developed to mitigate the impacts of the flood have negative consequences on the environment. As seen in most of the cases, in an attempt to develop permanent solutions, the river environment is changed. For example, solutions like building flood walls and developing road corridors along the river changes the flow regime by decreasing the river's right of way. The major problem of urban areas is the increasingly impervious surface, so the most important aspect of urban flood management is to look into rainwater management which is not sufficiently addressed and the worst part is that the storm water management does not even come in the purview of urban development in Nepal.

References

Dewan, Tanvir H. 2015. Societal Impacts and Vulnerability to Floods in Bangladesh and Nepal. *Weather and Climate Extremes* 7: 36–42.

Gorelick, Noel, Matt Hancher, Mike Dixon, Simon IIyushchenko, David Thau, and Rebecca Moore. 2017. Google Earth Engine: Planetary-Scale Geospatial Analysis for Everyone. *Remote Sensing of Environment* 202: 18–27.

IPCC. 2014. Climate Change 2014: Synthesis Report. Contribution of Working Groups I, II and III to the Fifth Assessment Report of the Intergovernmental Panel on Climate Change [Core Writing Team, eds. R.K. Pachauri and L.A. Meyer], 151, Geneva, IPCC.

Khanal, Bina. 2018. Recurrent Water Induced Disaster from Urban Flooding and the Resulting Livelihood Consequences: A Case Study of Dhobi Khola Catchment. M.Sc, Nepal Engineering College-Center for Postgraduate Studies (nec-CPS), Pokhara University.

Mirza, Monirul. 2011. Climate Change, Flooding in South Asia and Implications. *Regional Environmental Change* 11: 95–107.

Molden, Olivia, and Tyler McMahon. 2019. *Nepali Times.* 29, 11. Accessed November 30, 2019. https://www.nepalitimes.com/here-now/in-nepals-weather-erratic-is-the-new-normal/.

NWCF. 2009. *The Bagmati: Issues Challenges and Propspects.* Kathmandu: Nepal Water Conservation Foundation (NWCF).

Prajapati, Rajaram, Thapa Bhesh Raj, and Rocky Talch. 2018. *What Flooded Bhaktapur*. Kathmandu: My republica.

Rijal, Sushila, Bhagawat Rimal, and Sean Sloan. 2018. Flood Hazard Mapping of a Rapidly Urbanizing City in the Foothills (Birendranagar, Surkhet) of Nepal. *Land* 7 (2).

Sada, Rajesh. 2012. Hanumante River: Emerging Uses, Competition and Implication. *Journal of Science and Engineering* 1.

Salike, Inu Pradhan, and Jiba Raj Pokharel. 2017. Impact of Urbanization and Climate Change on Urban Flooding: A Case of the Kathmandu Valley. *Journal of Natural Resources and Development* 7: 56–66.

Wang, Xiaolan L., and Yang Feng . 2013. RHtestsV4 User Maual. *User Maual.* Toronto: Climate Research Division Atmospheric Science and Technology Directorate Science and Technology Branch, Environment Canada, July 20.

Wrobley, Madison. 2020. Groundwater Quality and Quantity Are Linked, and Neither Are Improving. *The Kathmandu Post Daily Newspaper* , January 21.

Zhanag, Xuebin, and Feng Yang. 2004. *RClimDex (1.0) User Manual.* User Manual, ON: Climate Research Branch, Environment Canada Downsview.

Urban Drainage Study for Gopalganj Pourashava Considering Future Climate Change Impacts

Faruque Abdullah, A. K. M. Saiful Islam, Afsara Tasnia, G. M. Tarekul Islam, Sujit Kumar Bala, and Nahruma Mehzabeen Pieu

Abstract This study focuses on an investigation, through hydraulic modelling, of the urban drainage systems in designing suitable drainage infrastructures for Gopalganj Pourashava by considering the possible impact of climate change on drainage. The daily rainfall data of Madaripur station from the Bangladesh Meteorological Department (BMD) for the base period of 1987–2016 has been analysed to prepare the IDF (Intensity–Duration–Frequency) curves for different return periods by fitting Extreme Value Type-1 (Gumbel) Distribution. Projected rainfall data has been obtained from 11 Regional Climate Models simulated considering high-end scenarios (RCP8.5) over the CORDEX South Asia domain for the near future (2017–2046). Design hyetographs were developed for 10 years 2-hour storm, which was later applied to generate runoff using the SWMM model. Water levels obtained from the frequency analysis at Atharobanki and the peak flow of Old Madhumati at Haridaspur for a 20-year return period are then used as boundary conditions for the model. Afterwards, natural canals which overtopped during the simulation have been identified. Finally, five alternative design conditions based on node flooding have been proposed to improve the urban drainage system. A comparison between the present and future drainage scenarios under different climate conditions has also been represented.

Keywords Climate change · Gopalganj · Hyetograph · SWMM · Urban drainage

1 Introduction

1.1 Background of the Study

The planet's hydrological cycle is likely to face severe impacts of climate change and global warming due to the enhanced effects of greenhouse gas (IPCC 2014).

F. Abdullah (✉) · A. K. M. S. Islam · A. Tasnia · G. M. T. Islam · S. K. Bala · N. M. Pieu
Institute of Water and Flood Management (IWFM), Bangladesh University of Engineering and Technology (BUET), Dhaka, Bangladesh

© The Author(s), under exclusive license to Springer Nature Switzerland AG 2022

G. M. Tarekul Islam et al. (eds.), *Water Management: A View from Multidisciplinary Perspectives*,
https://doi.org/10.1007/978-3-030-95722-3_2

The average annual runoff will increase in high latitudes, in equatorial Africa and Asia, and Southeast Asia, and will decrease in mid-latitudes and most subtropical regions (Arnell 1999). The Ganges–Brahmaputra-Meghna (GBM) basins are one of the world's most significant and complex river nexuses. The water resources of these river systems are highly vulnerable to global climate change (Solomon et al. 2007), which may have substantial insinuations on the livelihoods and well-being of the people in the region (Eriksson et al. 2009). Bangladesh is at the frontline of impending climate change impacts. It is one of the most densely populated countries in the world with a small geographic extent and is located in the deltaic setting of the GBM basins. This unique geographical location and proximity to the sea and monsoonal climate have made it more vulnerable to increasing natural disasters (Mondal et al. 2018). Varying levels of physical exposure, like storm surge, flooding, and changing weather patterns, exacerbated by sea-level rise, represent significant social and legal risks to its populations. Urban encroachment, rising sea levels, and increased high-frequency storm surges are expected to intensify urban drainage runoff impacting present infrastructures. An effective urban drainage design reduces the potential impact of new and existing developments concerning surface water drainage discharge. According to the 2011 population census of Bangladesh Bureau of Statistics, the urban population was about 27% of the total population in Bangladesh. Since independence, the average rate of urbanization is about 5% (Ahmed and Ahmed 2012), and the percentage share of the urban population has doubled, from 15% in 1974 to 28.4% in 2011 (BBS 2012). This extensive expansion of urban areas as well as its economy would need urban planning. The Pourashavas, which are district towns, would need to provide urban services to their citizens and provide a sustainable environment for sound living.

Rapid urbanization and substantial increase in built-up areas in Gopalganj Paurashava have taken place over the last few decades. These phenomena have facilitated a significant growth of impervious regions, hampered natural drainage patterns, and reduced detention basins, leading to a lower time of concentration and increased stormwater peak flow. Improper drainage systems very often lead to flooding, unsafe and unhygienic conditions for humans and animals, and damaging numerous establishments. Unfortunately, toxic substances, such as waste from markets, poly bags, household wastewater, fertilizer, and other chemicals, are regularly drained into stormwater drainage systems. These toxic chemicals lead to water pollution, proving unhealthy for fish, plants, and different water life, even killing them. Therefore, it is essential to plan for a coordinated stormwater drainage management system for the proficient regulation of stormwater quantity. The initial step for this management planning is to conduct a drainage analysis via computer modelling, which will be efficient in prescribing fitting solutions to manage drainage problems better.

In this study, EPA's Storm Water Management Model (SWMM), the most widely recognized model for urban drainage as well as sanitary sewer systems, is used for the assessment of present and future drainage capacity in Gopalganj Pourashava as part of the drainage and environmental management master plan under the Municipal Governance and Services Project (MGSP) of the Local Government Engineering Department (LGED). SWMM is unique because of its excellent ability to simulate

hydraulics and hydrology within the same interface compared to other commonly used models. The advantage of SWMM over other models is that it allows the users to prepare the inputs manually and run the model smoothly, thereby providing users access to all the functions and tools to create and edit data. EPASWMM 5.0 is a dynamic rainfall-runoff simulation model used for a single event or long-term assessment of runoff quantity and quality from urban areas (Rossman and Huber 2016). SWMM has been used in numerous sewer and stormwater studies throughout the world. It can design and size drainage system components for flood control, flood plain mapping of natural channel systems, develop control strategies for minimizing combined sewer overflows, and evaluate the impact of inflow and infiltration on sanitary sewer overflows, etc.

The Institute of Water and Flood Management (IWFM) of Bangladesh University of Engineering and Technology (BUET) has used SWMM for several studies relating to urban runoff and drainage (Khan and Chowdhury 1998; Khan et al. 2006; Chowdhury et al. 1998; Rahman et al. 1999; Asian Development Bank 2013). (Akter and Tanim 2016) used the SWMM model and spatial analysis in ArcGIS to identify urban-flood-prone areas in Chattogram that were validated using recent field studies. This study provided insights for flood management-related decision-making approaches to identify and emphasize the vulnerable flood-prone zones in the study area. Another study conducted by (Tarek et al. 2017) on the Chaktai Khal basin area in Chattogram used GeoSWMM to simulate and analyse the behaviour of flash floods in the watershed. Their analysis revealed that a maximum of 47% of the total study area is prone to flash floods during the rainy season, suggesting that SWMM can effectively analyse integrated flash floods in an ungauged urban system. According to (Cambez et al. 2008), SWMM can also produce a satisfactory outcome in the long-term modelling of a metropolitan area despite having any minor limitations in catchment hydrological description. Long-term simulations help compare different storage scenarios and sewage treatment plant capacities. (Hossain et al. 2019) indicated these limitations and concluded that event-based modelling of EPASWMM outperforms the continuous simulation approach in evaluating both direct runoff hydrograph and total runoff hydrograph. (Paul et al. 2013) led a study in three coastal towns—Amtali, Galachipa, and Pirojpur and used SWMM to evaluate the future drainage condition of these areas. Their research revealed that rapid urban development in coastal zones and climate change-induced sea-level rise would significantly increase inundation vulnerability compared to the baseline period. (Bai et al. 2018) used SWMM to assess the LID (Low Impact Development), a storm management technique at Sucheng district in China, under four different scenarios. The study indicates that runoff frequency reduces with increasing rainfall under all scenarios until it becomes stable with a certain rainfall amount. (Khadka and Basnet 2019) have found SWMM as an effective modelling tool for managing storm waters in major cities of Nepal, where the management of overflow from the existing drainage is a crucial issue. The study was conducted on the Barahi Chowk area of Lakeside, Pokhara, focusing on stormwater drainage design and also a comparison with the existing drainage system. Another application of SWMM is to estimate urban runoff peaks and volume. For example, a study done by (Rabori and Ghazavi 2018) assessed urban

flooding of a semi-arid area such as Zanjan city of Iran, concluding that this model can simulate urban peak flow with acceptable accuracy. (Jang et al. 2007) suggested SWMM for evaluating pre and post-development conditions of a metropolitan area to study hydrologic impact assessments. However, employing a synthetic hydrograph for pre-development and an urban hydrology model for post-development may introduce some unavoidable difficulties which can be resolved using a single SWMM model. The natural streams are converted to artificial drainage networks due to urbanization-induced land use change (Haase 2009). This phenomenon ultimately results in urban flooding in monsoon regarding high slopes and scarcity of a proper drainage management system. In this connection, the assessment of the rainfall-runoff process is essential, and (Babaei et al. 2018) used SWMM, which showed good accuracy for peak runoff simulation for Urmia city of Iran.

The prime goal of the study was to investigate the detailed hydrological and hydraulic analysis of the urban watersheds in determining suitable drainage systems for the study area incorporating the probable impact of climate change on drainage. Secondary objectives include hydraulic design and sizing of the primary and secondary canals for flood control, sizing detention facilities, and designing control strategies to minimize sewer overflows. SWMM was set up, tested, and simulated for present conditions and the near future (2017–2046). Impacts of climate change on the urban drainage system have also been considered to design climate-resilient urban infrastructures. Finally, a set of alternative solutions to the existing and future drainage issues have been recommended to improve the urban drainage capacity of Gopalganj Pourashava.

1.2 Study Area and Existing Drainage System

Gopalganj district, located at 23°000′47.67″ N 89°049′21.41″ E, stands on the bank of the Madhumati River. It is bounded by Faridpur district in the North, Pirojpur and Bagerhat in the South, Madaripur and Barisal in the East, and Narial in the West. Gopalganj Pourashava town is the district town of Gopalganj District that lies within the Sadar Upazila. After the liberation war, Gopalganj Sadar becomes Pourashava, consisting of 9 wards and 75 mahallas. The Local Government Engineering Department (LGED) has formulated a master plan for developing a practical and affordable solution to the stormwater drainage problem of Gopalganj Pourashava with an extension area that covers a total area of 35.32 sq. km (Fig. 1). The study area bears the characteristics of rapid urbanization, leading to a gradual encroachment of the natural canals and hindrance to the smooth flow of drainage water and thus has become a matter of suffering for the people of the Pourashava.

The natural canal system of the study area comprises four significant channels. The Old Madhumati River, now known as the Mora Modhumati, is the core natural drainage canal flowing through the centre of the town. The other three significant canals known as ‘Khals’ within the area have been originated from the Old Madhumati. But the gradual encroachment and unplanned infrastructures result in unstable

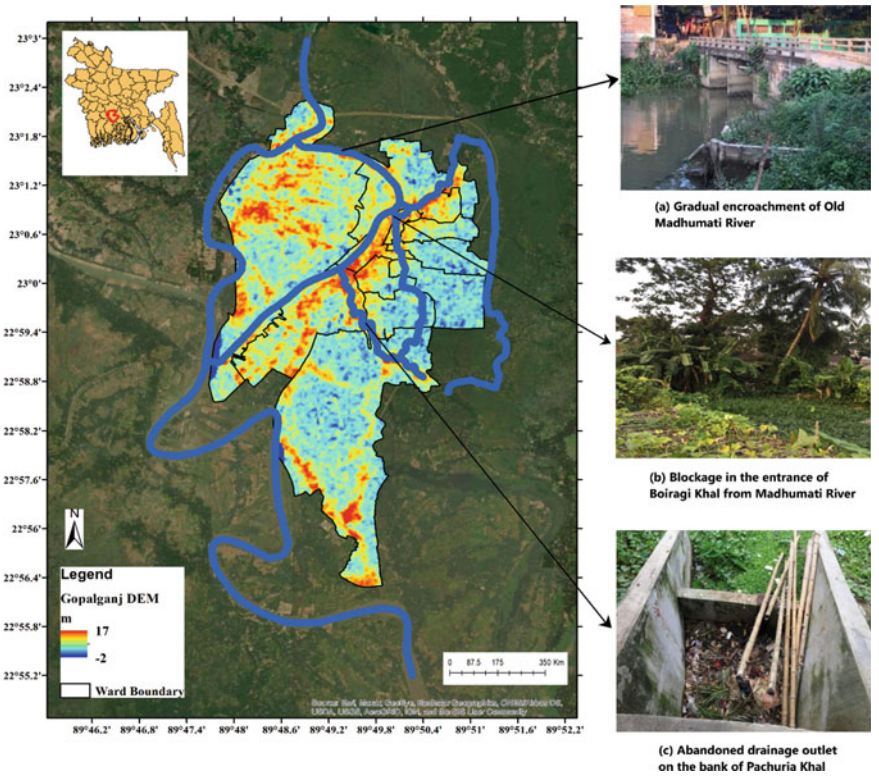

Fig. 1 Study area and existing drainage condition of the Pourashava

flow conditions, allowing the river to gain silt in some locations and hampering the natural flow from upstream to downstream. In this connection, discharge capacity has been decreased to a great extent which is the main factor behind the drainage congestion and waterlogging in the city area. Among the other three channels, Panshi Khal, which once actively carried flow from the Old Madhumati to the downstream, is now almost dry with a minimum flow circulation. Boiragi Khal is the most important of the three because it has the largest drainage outfalls from the market area. But the entrance from Madhumati is now totally blocked, and no water can enter Boiragi Khal from the river. So, to improve the present condition, the connectivity of the natural canals should be given first priority before talking about the artificial drainage conduits. Another disengaged channel, known as Pachuria Khal, meets Boiragi Khal and then carries the flow to the Bonnir Baor, which is considered one of the most significant outfalls for the entire catchment. The efficiency of the existing primary drainage network is also not satisfactory. The drainage channels got reduced both by horizontal and vertical dimensions in the city area. Once plied upon local launches and country boats, encroachment and siltation have turned these large canals into a non-distinguishable small drain. At present, the drain is clogged with market

garbage, water hyacinth, etc., creating blockages in several points. These locations are to be opened up again, in order to make the drain more effective and drain water towards the New Madhumati River.

2 Methodology

Several steps have been followed for the urban drainage modelling of the Gopalganj Pourashava. The analysis of rainfall data from available rain gauges involves separation of rainfall events, estimating the return periods of a certain durational rainfall, evaluating data inconsistency, etc. The stormwater model was developed using time series of daily and sub-daily rainfall events to determine runoff. Sub-catchments are hydrologic land units with dynamic terrain and drainage characteristics that route surface runoff to a single outlet point. These are delineated using spatial analysis of the existing digital elevation model or topological survey data. By utilizing the study area's land use map, sub-catchments are divided into permeable and impermeable subareas. Drainage systems have been mapped using a Digital Elevation Model (DEM) that was trained by existing drainage networks and then subjected to spatial analysis. The cross-sectional survey of the principal channels and drainage structures yielded information on the prevailing drainage characteristics of the area. Finally, a number of input parameters, such as soil characteristics, infiltration rate, manning's coefficient, etc., have been used based on field observation and literature review. The model has been simulated using the design storm scenarios. A hypothetical rainstorm event with a defined duration, temporal distribution, rainfall intensity, return period, and total depth of rainfall is referred to as a design storm. To analyse future climate change vulnerabilities, the SWMM model has been used to replicate design storm scenarios with and without climate change impacts. Statistical analysis has also been conducted to determine the design water level of the surrounding rivers used as boundary conditions of the model. Based on the design simulation results, the drainage network capacity has been assessed, and various alternative options have been suggested to improve the performance of the drainage networks. A similar exercise has been conducted for the future periods considering climate change where both the shift in land use pattern and evolution of rainfall and water levels of the surrounding rivers for future periods are considered for simulating the model.

2.1 Data Collection and Watershed Delineation

The combination of EPA's Storm Water Management Model (SWMM5) and GeoSWMM have been used in this study to conduct urban drainage modelling. For the stormwater drainage analysis, collecting and compiling all hydraulic and morphological data concerning the urban drainage systems and the surrounding rivers have

been ensured. For the watershed delineation, SRTM 1 Arc-Second Global DEM of 30 m resolution was collected from the USGS Global Data Explorer website. In addition, the historical daily rainfall data was collected from Bangladesh Meteorological Department (BMD), and the future projected rainfall information using regional climate models over the project area has been obtained from Mohammed et al. (2018). The required topographic data and bathymetry of the corresponding canals were collected through a field survey. Moreover, necessary information regarding existing drainage canals, cross drainage structures, bridges and culverts, and the projected land use change of the study area has been collected from the Local Government Engineering Department (LGED) and Gopalganj Pourashava office. The watershed delineation tool of GeoSWMM, the advanced version of EPA's SWMM5, has been used to delineate the sub-catchments of the study area. The process involves DEM clipping, stream burning, stream and outlet generation, watershed delineation, etc., as GeoSWMM facilitates users to conduct these operations using the ArcGIS interface directly. After delineating the sub-catchments and assigning the necessary properties for the corresponding streams, joints, and links, the whole project was then imported to the EPASWMM5 interface for the model development, simulation, and urban drainage modelling.

The drainage model has one upstream boundary and three downstream boundaries shown in Fig. 2(c). The upstream boundary is at the mouth of the Old Madhumati River, where it receives flow from the Madaripur Beel Route. The downstream boundary of the Old Madhumati River is at the confluence of the Madhumati River.

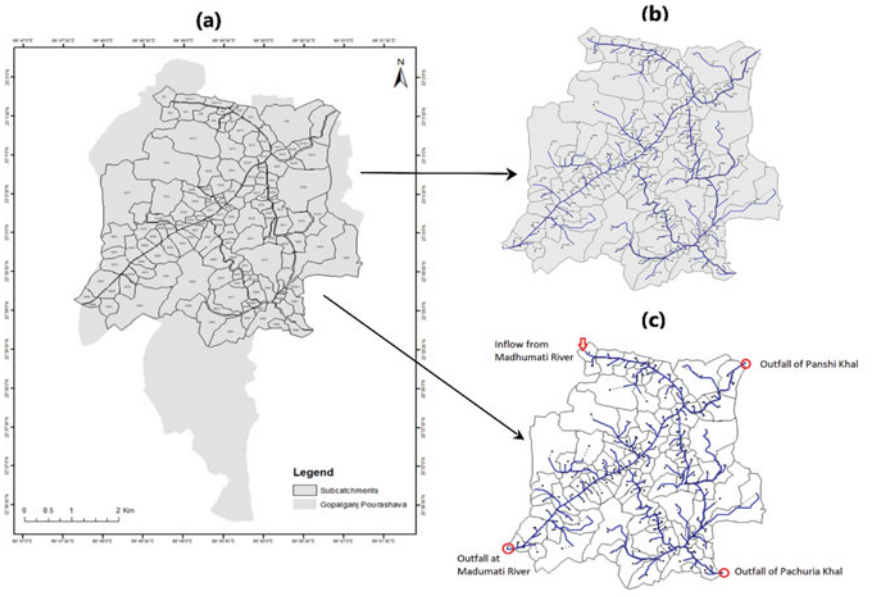

Fig. 2 **a** Delineated watersheds within the extension area. **b** streams, links, and joints within the watersheds. **c** locations of the inflow and stage boundaries for simulating SWMM

The downstream boundaries of Panshi Khal and Pachuria Khal have been considered as open water bodies.

2.2 Hydrologic Analysis

The hydrologic analysis mainly focuses on predicting the design water level and outflow through frequency analysis. The primary method in frequency analysis involves fitting various probability distribution functions to historical yearly peak water levels and discharge data at appropriate locations for the selected design return period (Paul et al. 2013). The design return period has been considered based on the size and importance of the proposed intervention. The gauge stations maintained by BWDB nearest to the Gopalganj Municipality are located at Haridaspur of Madaripur Beel Route and the off-take at Atharobanki of the Gorai-Madhumati-Haringhata-Baleswar River. Thus the water level data of Madaripur Beel Route at Haridaspur and Gorai-Madhumati-Haringhata-Baleswar River at Atharobanki have been used for frequency analysis. The discharge data of the Madaripur Beel Route at Haridaspur has been taken from (Hossain and Chowdhury 2018) where the highest recorded historical peak flow was 1550 m^3/s in 1998.

With regard to frequency analysis, five probability distribution functions (PDFs) were used. These were Pearson Type III (P3), Log Pearson Type III (LP3), Two-Parameter Log-Normal (LN2), Three-Parameter Log-Normal (LN3), and Gumbel (EV1) distribution. A probability plot correlation coefficient (PPCC) was used to test them later (Filliben 1975). The best-fitted PDFs are P3 for the annual maximum water level of Gorai-Madhumati-Haringhata-Baleswar River at Atharobanki (Table 1(b)) and Madaripur Beel Route at Haridaspur (Table 1(c)) and LN3 for the peak flow of the Madaripur Beel Route at Haridaspur (Table 1(a)).

For the yearly maximum water level and peak flow of the Madaripur Beel Route at Haridaspur and water level of Gorai-Madhumati-Haringhata-Baleswar River at Atharobanki, Fig. 3 illustrates probability diagrams with a 90% confidence interval. The observed values for the annual maximum water level of the Madaripur Beel Route at Haridaspur and the Gorai-Madhumati-Haringhata-Baleswar river at Atharobanki, as well as the yearly peak flow of the Madaripur Beel Route at Haridaspur, fit well within the 90% confidence interval of the adjusted P3 and LN3 distributions, respectively.

Following the importance and size of the proposed drainage master plan, a 20-year return period has been considered as the design return period as per the recommendations of Local Government Engineering Department. The design water levels of Madaripur Beel Route at Haridaspur and Gorai-Madhumati-Haringhata-Baleswar River at Atharobanki corresponding to a 20-year return period are 4.65 m and 4.07 m, respectively. The design peak flow of Madaripur Beel Route at Haridaspur corresponding to a 20-year return period is 1412 m^3/s.

Table 1 **a** Adjusted PDFs and associated PPCC values for annual maximum flow (m^3/s) of Madaripur Beel Route at Haridaspur. **b** Adjusted PDFs and associated PPCC values for annual maximum water level (m PWD) of the Gorai-Madhumati-Haringhata-Baleswar River at the off-take at Atharobanki. **c** Adjusted PDFs and associated PPCC values for annual maximum water level (m PWD) of Madaripur Beel Route at Haridaspur

PDFs	Return period				PPCC	Rank
	2.33	20	50	100		
(a) Annual peak flow (m3/s)						
LN2	782	1302	1503	1652	0.94394	5
LN3	731	1412	1792	2120	0.95838	1
P3	765	1398	1651	1840	0.95817	2
LP3	736	1414	1797	2138	0.95751	3
EV1	786	1374	1603	1774	0.94434	4
(b) Annual maximum water level (m PWD)						
LN2	3.07	4.79	5.43	5.89	0.90034	2
LN3	3.19	4.05	4.27	4.42	0.90027	3
P3	3.17	4.07	4.32	4.49	0.90211	1
LP3	3.34	3.77	3.78	3.78	0.82954	5
EV1	3.05	4.22	4.67	5.01	0.89983	4
(c) Annual maximum water level (m PWD)						
LN2	3.37	4.87	5.40	5.78	0.97838	4
LN3	3.50	4.62	4.94	5.15	0.98266	2
P3	3.48	4.65	4.99	5.22	0.98313	1
LP3	3.45	4.64	4.96	5.17	0.98110	3
EV1	3.37	4.78	5.33	5.74	0.97219	5

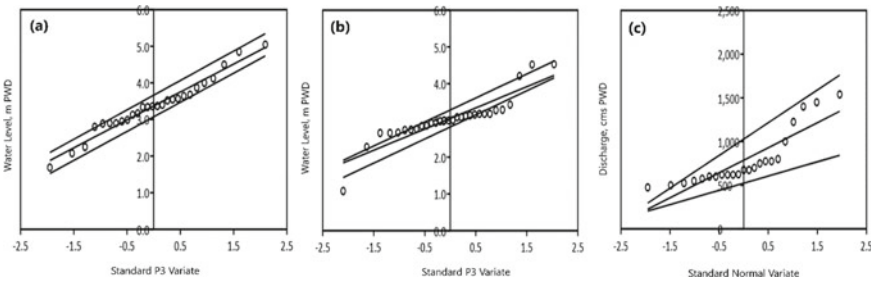

Fig. 3 Probability distribution diagram with 90% confidence interval of the **a** P3 distribution fitted to the annual maximum water level of Madaripur Beel Route at Haridaspur. **b** P3 distribution fitted to the annual maximum water level of the Gorai-Madhumati-Haringhata-Baleswar River at the off-take of Atharobanki. **c** LN3 distribution fitted to the annual peak flow of Madaripur Beel Route at Haridaspur

2.3 *Evaluation of Climate Change Impacts on Boundary Flows*

The Madaripur Beel Route has a connection with the Padma River, which receives flow both from the Ganges and Brahmaputra. Changes in future flow of the Ganges and the Brahmaputra due to climate change will influence the variations in the flows of the Madaripur Beel Route and other surrounding rivers. At IWFM, BUET, a semi-distributed hydrological model, SWAT has been applied to assess climate change's impact on the major river flow (Mohammed et al. 2017) under the HELIX research project. The Soil and Water Assessment Tool, SWAT (Arnold et al. 2012), was used to simulate future discharges with 11 different climate projections, as shown in Table 2.

Using the boundary discharge from the SWAT model, a one-dimensional hydrodynamic model HEC-RAS has been simulated to determine the changes of flow in the major rivers of Bangladesh (Mondal et al. 2018). The downstream boundary of the HEC-RAS was obtained from another three-dimensional modelling suite, Delft3D, which has incorporated the impact of sea-level rise from its open boundary conditions. In the fifth assessment report of IPCC (IPCC 2014), a global mean sea-level rise of 52–98 cm by the year 2100 under a very high emission scenario of RCP 8.5 and 36–71 cm under a moderate emission scenario of RCP 4.5 have been projected. For the Bay of Bengal, the IPCC projection is a little more comprehensive (25–73 cm under RCP 4.5). Based on IPCC's projections of global and local (Bay of Bengal) sea-level rise, a maximum sea-level rise of 1 m by 2100 and 0.31 m by 2050 has been anticipated for the Bay of Bengal. The downstream sea boundary of the Delft3D based coastal model has been modified according to these projections of sea-level rise. The HEC-RAS model has been rerun for flood discharges of 100 year return period to

Table 2 List of Regional Climate Models used in this study

Sl	Institute	GCM	RCM	Res	RCP
1	CSIRO	ACCESS1.0	CCAM-1391 M	0.5°	8.5
2	CSIRO	CCSM4.0	CCAM-1391 M	0.5°	8.5
3	SMHI	CNRM-CERFACS-CNRM-CM5	RCA4	0.5°	8.5
4	CSIRO	CNRM-CM5	CCAM-1391 M	0.5°	8.5
5	SMHI	ICHEC-EC-EARTH	RCA4	0.5°	8.5
6	CSIRO	MPI-ESM-LR	CCAM-1391 M	0.5°	8.5
7	MPI-CSC	MPI-M-MPI-ESM-LR	REMO2009	0.5°	8.5
8	SMHI	MPI-M-MPI-ESM-LR	RCA4	0.5°	8.5
9	SMHI	NOAA-GFDL-GFDL-ESM2M	RCA4	0.5°	8.5
10	SMHI	IPSL-CM5A-MR	RCA4	0.5°	8.5
11	SMHI	MIROC-MIROC5	RCA4	0.5°	8.5

generate stage hydrographs along the major rivers of the basin, and a significant increment in flood peaks has been observed due to climate change impacts.

Based on the SWAT simulation for baseline (1980–2009) and future (2070–2099) and the HEC-RAS model simulation from the studies mentioned in the previous paragraph, the anticipated changes in flow and water level due to climate change and sea-level rise impact have been incorporated with the urban drainage design analysis. As Madaripur Beel Route is a branch of the Arial Khan River, the evolution of discharge in Mawa has been taken as 6% by the end of the century, according to (Mondal et al. 2018). Similarly, variation in the Ganges' discharge at Gorai off-take is 29%, and the Brahmaputra at Dhaleswari is 14% by the end of this century resulting from climate change impacts. Considering this deviation, the possible increase in the peak discharge in Madaripur Beel Route at Haridaspur will be about 10% (one-third of the change in Ganges flow) by 2030 according to the study. Again, the peak water level difference due to sea-level rise in the Ganges at Gorai is about 62 cm, the Brahmaputra at Dhaleswari is 38 cm, and the Ganges at Mawa is about 54 cm by 2100. In this connection, the peak water level at Atharobanki has been considered to increase by about 21 cm (one-third of the change in the Ganges at Gorai for 2100) in the near future (2017–2046).

2.4 Rainfall Analysis

The rainfall analysis includes developing Intensity–Duration–Frequency (IDF) curves through the frequency analysis of rainfall data. This operation is followed by the generation of hyetographs used for rainfall-runoff analysis to estimate peak runoff rate. For Gopalganj Pourashava, daily rainfall data from 1977 to 2016 at the nearest station Madaripur regarding the present scenario has been collected from Bangladesh Meteorological Department (BMD). This data has been analysed and used for developing IDF curves for long and short duration rainfall and eventually hyetographs for the base period of 1987–2016. As climate change will influence the future precipitation trend, the rainfall data has also been projected for the Madaripur station for the near future (2017–2046). Here, eleven CMIP5 regional climate models have been used to produce a monthly delta. The maximum monthly value of 1-day rainfall (RX1) of each year of the baseline period (1987–2016) was calculated for each model. A similar analysis has been done for the near future (2017–2046). The percent differences between the averages of these two data sets indicate a delta for that particular month. A similar calculation was carried out for each month from April to October. These delta values were then used to project the future rainfall from the observed rainfall data set and develop consequent IDF curves and hyetographs. The Extreme Value Type I (Gumbel) Distribution has been used for creating the curves for different return periods. For generating the IDF curves regarding short-duration rainfall, the IDF curves for long-duration were plotted in log–log scale, which resulted in almost linear graphs. From the equations of those trend lines, rainfall intensities were found for different durations and return periods. The duration step was 10 min.

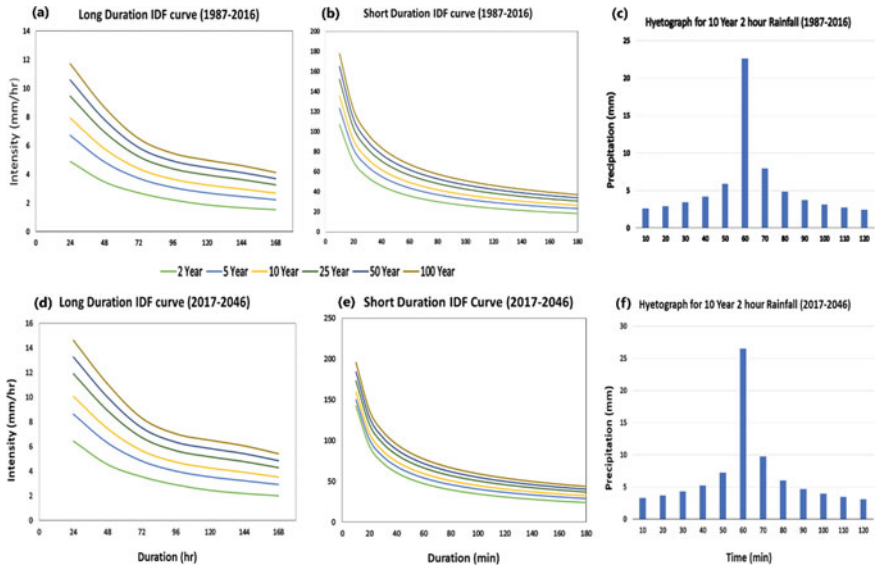

Fig. 4 **a** Long duration IDF curves. **b** short duration IDF curves for different return periods. **c** design hyetographs for 10-year 2-h rainfall for the baseline (1987–2016). **d** Long duration IDF curves. **e** short duration IDF curves for different return periods. **f** design hyetographs for 10-year 2-h rainfall for the near future (2017–2046)

Using these short-duration IDF curves, design hyetographs were then developed both for the present (1987–2016) and future climate change (2017–2046) scenarios using the alternating block method. A series of hyetographs were constructed for return periods of 2, 5, 10, 25, 50, and 100 years, with the 10-year 2-h hyetograph being chosen as the study's design hyetograph (Fig. 4).

3 Results and Discussions

3.1 Canal Capacity Assessment under Different Simulation Scenarios

SWMM model has been set up and simulated for the normal flood condition to assess the existing canal capacity. The model has also been run for the design condition, and finally considering the future climate change impacts to evaluate the necessity of designing a suitable and efficient urban drainage system for the study area. Due to the lack of observed water level and discharge data in the Old Madhumati River and other surrounding major canals, it was not possible to compare the model flow with the historical data. In the absence of the flow data in the channels, the model has been set up using insights from the drainage modelling of adjacent coastal cities used in

previous studies (Paul et al. 2013; Hossain and Chowdhury 2018). In addition, the primary calibration parameter, such as Manning's roughness coefficient, has been used in this study considering the soil type, land use pattern, and insights from a similar project in the nearby region conducted by IWFM (Asian Development Bank 2013). Table 3 summarizes the location and magnitude of all the inflow and stage boundaries of the SWMM model for the simulations under regular flooding, design flooding, and future climate change scenarios based on (Mondal et al. 2018; IWM 2011).

A model has been simulated for normal flood conditions (a flood with a 2.33 year return period), a 10-year 2-h design storm hyetograph considering climate change implications on precipitation, and also without considering climate change impacts. The maximum amount of discharge entering the Old Madhumati River from the Madhumati River is about 15%, based on the IWM study report. Therefore, the upstream inflow for the normal flood condition to the Old Madhumati River from the Madhumati River has been considered as 110 m^3/s which is 15% of the flow in Madhumati River (731 m^3/s) shown in Table 1(a). Similarly for the design storm condition with a 20-year return period, the design inflow to the Old Madhumati River has been set as 212 m^3/s (15% of 1412 m^3/s). For the design storm condition considering climate change impacts, an extra 10% increment to 212 m^3/s has been considered regarding the high-end climate scenario. A similar convention has been followed for the corresponding stage boundaries at Atharobanki and Haridaspur, as shown in Table 1(b) and (c), respectively. Considering the impact of sea-level rise in the downstream boundary, about 21 cm additional rise of water level has been included with 4.07 m water level at Atharobanki for a 20-year return period based on the outputs of (Mondal et al. 2018). For the stage boundaries at the outfall of Pachuria and Panshi Khal, normal depth has been considered. Manning's equation has been modified and the normal depth has been calculated for both the locations as 2.2 and 2.0 m, respectively.

Figure 5 indicates that the water surface has maintained a constant below 4 m threshold for the Old Madhumati River under normal flood conditions, representing similar findings compared to a study conducted by the Institute of Water Modelling back in 2009. It has also been found that water surface height maintains a 3.4–2.9 m range above the ground level in various canal sections in case of regular flooding. Under the design flooding condition, the range is 4.3–2.9 m, and for the climate change scenario, it is 4.4–2.9 m. The capacity of the drainage systems, including major canals, has been assessed for this high tide and high-intensity rainfall events for Gopalganj Pourashava at the normal flooding condition. Analysis of water surface profiles indicates that, except for a few locations, the capacity of the canal system is enough to drain the water during high tide. As ponding is allowed during the simulation, the overtopping margin would approximate the quantity of water overflowed. No significant overtopping has been observed along the canals under the present condition. Therefore, the existing drainage system is capable of carrying the flow of normal floods. Under design conditions, overtopping is noticed at six locations in the Old Madhumati River and one location in Boiragi Khal. The simulation considering climate change exhibits significant overtopping at eight locations in the Old

Table 3 Location and magnitude of the inflow and stage boundaries of the SWMM model regarding three simulation scenarios

Location	Node	Simulation Condition	Value	Boundary type	Remarks
Entrance of the Old Madhumati River	J1	Normal	110 m^3/s	Inflow	15% of the normal flood at Haridaspur in the Madhumati River
		Design	212 m^3/s		15% of the flow at Haridaspur in Madhumati River for 20-year return period flood
		Climate Change	233 m^3/s		15% of the design flood at Haridaspur in the Madhumati River for 20-year return period flood and additional 10% increment considering climate change
Outfall of the Old Madhumati River	O1	Normal	3.17 m	Stage	Normal flood stage at Atharobanki station in the Madhumati River
		Design	4.07 m		Stage at Atharobanki station on Madhumati River for 20-year return period flood
		Climate Change	4.28 m		Stage at Atharobanki station in the Madhumati River considering 20-year return period flood and additional 21 cm for climate change impact due to sea-level rise
Outfall of Pachuria Khal	O2	Normal	2.2 m	Stage	Normal depth
		Design	2.2 m		Normal depth
		Climate Change	2.2 m		Normal depth
Outfall of Panshi Khal	O3	Normal	2.0 m	Stage	Normal depth
		Design	2.0 m		Normal depth

(continued)

Table 3 (continued)

Location	Node	Simulation Condition	Value	Boundary type	Remarks
		Climate Change	2.0 m		Normal depth

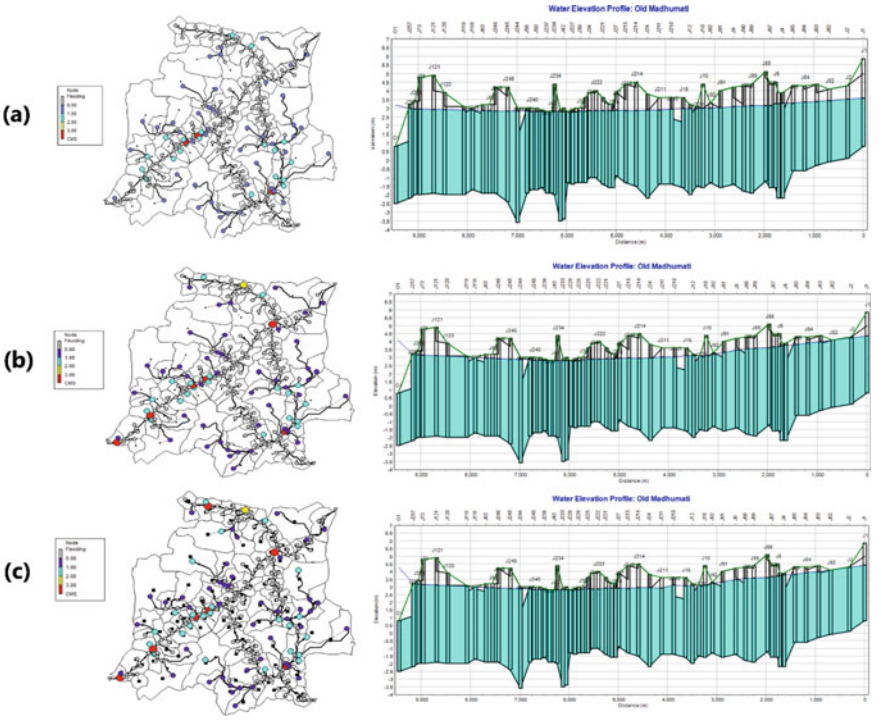

Fig. 5 Location of the nodes flooded and corresponding water surface profile of the Old Madhumati River under **a** normal flooding condition. **b** design flooding condition. **c** future climate change scenario

Madhumati River and Boiragi Khal. In general, the existing urban drainage system of the Pourashava is not capable of carrying the flow during the design condition and considering future climate change and sea-level rise impacts.

3.2 Alternative Design Options

SWMM simulation indicates that the drainage system of the study area will be suffering from urban flooding in the future. The drainage systems' present capacity, including the Old Madhumati River and other canals, is insufficient to drain the

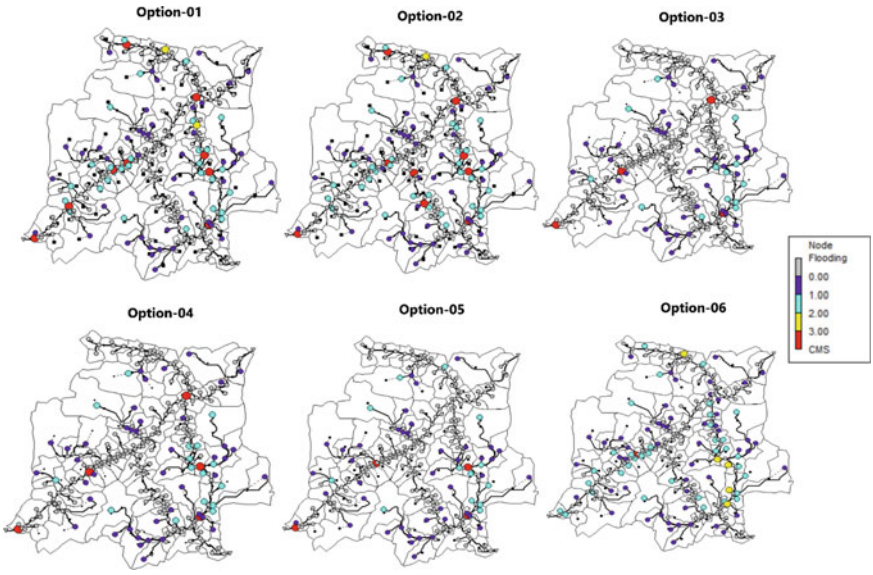

Fig. 6 Location of the nodes flooded under six alternative design options considering future climate change impacts

runoff generated from the design storm and climate change impacts on the rainfall, boundary inform, and sea-level rise. SWMM model has been simulated considering six alternative design scenarios, and Fig. 6 represents the location of the nodes flooded under these options, considering climate change scenarios. These alternative design options are

- Option 1: Establishing a connection between the Old Madhumati River and Boiragi Khal.
- Option 2: Establishing a connection between the Old Madhumati River and both Pachuria Khal and Boiragi Khal.
- Option 3: Dredging of the Old Madhumati River considering vertical bank protection using retention walls (rectangular channel).
- Option 4: Dredging of the Old Madhumati River considering vertical bank protection using retention walls (rectangular channel) and connecting Boiragi Khal with the Old Madhumati River.
- Option 5: Dredging of the Old Madhumati River and Boiragi Khal considering trapezoidal channel with bank protection and connecting Boiragi Khal with the Old Madhumati River.
- Option 6: Dredging of the Old Madhumati River, Boiragi Khal and Pachuria Khal considering trapezoidal channel section and connecting both Boiragi Khal and Pachuria Khal with the Old Madhumati River.

A summary of different options used to improve the urban drainage system and the comparison of node flooding for existing conditions and alternatives are presented in

Table 4. The least amount of node flooding is observed in the Old Madhumati River under Option 6. Considering the increase of the freshwater flow in Boiragi Khal, which will eventually reduce deposition of sediments and improve water quality, Option 6 has appeared to be more ecosystem friendly and less costly, in comparison with other options. However, dredging of Old Madhumati River, Boiragi Khal, and Pachuria Khal is essential in order to improve the overall carrying capacity.

It has been observed that urban runoff is wholly carried out by the improved trapezoidal section, and has established full connectivity of these surrounding Khals with the Old Madhumati River. Consequently, the overtopping is noticed only in a

Table 4 A comparison of simulations between existing conditions and alternative options for improving the performance of urban drainage system

Option		Old Madhumati	Boiragi	Pachuria
Existing	Connection with old Madhumati	—	NO	NO
	X-Section	Irregular	Irregular	Irregular
	Nodes flooded	7	1	0
1	Connection with old Madhumati	—	YES	NO
	X-Section	Irregular	Irregular	Irregular
	Nodes flooded	7	4	0
2	Connection with old Madhumati	—	YES	YES
	X-Section	Irregular	Irregular	Irregular
	Nodes flooded	5	3	2
3	Connection with old Madhumati	—	NO	NO
	X-Section	Rectangular	Irregular	Irregular
	Nodes flooded	3	1	0
4	Connection with old Madhumati	—	YES	NO
	X-Section	Rectangular	Irregular	Irregular
	Nodes flooded	3	2	0
5	Connection with old Madhumati	—	YES	NO
	X-Section	Trapezoidal	Trapezoidal	Irregular
	Nodes flooded	3	2	0
6	Connection with old Madhumati	—	YES	YES
	X-Section	Trapezoidal	Trapezoidal	Trapezoidal
	Nodes flooded	1	0	0

few locations through the whole canal system of the study area. Hence, Option 6 is recommended for the improvement of the drainage system of Gopalganj Pourashava.

3.3 Limitations of the Study

The following are some of the study's limitations:

- The proper catchment delineation of the study region necessitates the use of high-resolution DEM data. To build a high-resolution DEM for the study area, a comprehensive survey using ground stations or the purchase of high-resolution satellite images is required.
- The model could not be directly calibrated and tested due to a lack of site-specific observed data. However, it has been evaluated using secondary data from prior IWM and BWDB investigations. So it is really important to take necessary actions to solve the data scarcity problems of the study area for future research work. Water level from various significant canals and rainfall data in the research area should be collected continuously during the monsoon season for a number of storms. The major canals must be equipped with automatic water level and flow measurement devices, which should be kept operational throughout the season. Automated rain gauges can also be installed to record hourly rainfall data during storms.

4 Conclusion

In this study, the open source and community model SWMM developed by the EPA was used to analyse urban drainage system of Gopalganj Pourashava. Due to the lack of observed flow data in the canals, the model has been validated with similar study results in this region. Models seem reasonably adequate to capture the shape of the water surface profile of channels and stages of the surrounding rivers for normal flood conditions. The urban drainage system of the study area is already facing several challenges from natural hazards and human activities such as colossal sedimentation, illegal encroachments, instability of banks, poor connectivity of sanitary sewerage, solid waste disposal, etc. Again, various sections of the natural canals are overtopped for the design condition. Climate change impacts on the urban drainage systems of Gopalganj Pourashava would also cause overtopping and urban flooding in the Old Madhumati River, Boiragi Khal, and Pachuria Khal. It is essential to take necessary steps to combat urban flooding due to overflow depending on the importance of the location, cost, and land availability. In this study, some options to improve the urban drainage network have been considered. The best choice to resolve the drainage congestion is to dredge the Old Madhumati River, Boiragi Khal, and Pachuria Khal, considering a trapezoidal channel section with side slope 1:1.5 and connecting both Boiragi Khal & Pachuria Khal with the Old Madhumati River.

Based on the modelling study and field visits, a number of challenges were found, which will cause severe urban flooding in Gopalganj Pourashava. A summary of the recommendation to improve urban drainage systems has been presented as follows:

- The entrance of the Old Madhumati River is partially opened to avoid deposition of huge sediment load in the river, and dredging was found essential. This will bring more freshwater discharge into the Old Madhumati River from Madhumati River.
- The Old Madhumati River and other canals have been encroached upon illegally. Illegal possessions on both sides of canals should be re-occupied, and the canal's waterways should be marked.
- Because of the steep slope (1:1) and illegal pipe connections, the current bank protection of the canals is insecure in several areas. It should be designed in accordance with LGED standards for bank slopes (1:1.5), construction materials, compaction, and layouts.
- Household and commercial waste, along with sanitary sewage, are currently disposed of directly into the stormwater drainage system. To improve the water quality and reduce sedimentation in the canal, a separate sanitary sewage system is required. Before draining to canals and natural water bodies, wastewater from business and residential housing compounds should be treated at a sewage treatment plant (STP).
- Pipe drains have been found to work well; they are environmentally benign and carry less solid waste. When the discharge is high (>1.62 m^3/s), pipe drains with proper manhole spacing are highly recommended.
- Construction of two or more primary and secondary canals, rather than one tertiary-secondary canal, is advised when peak runoff exceeds the maximum capacity of the pipe drain connecting to the other side of the natural drainage system (e.g. Madhumati River).
- Solid wastes are currently disposed of in canals and river systems, reducing the canal's carrying capacity and degrading the ecosystem. In the Pourashava, solid waste management systems should be enhanced by scheduling collection, providing enough garbage bins, raising public awareness, and developing environmentally safe dumping locations. Again, the Department of Environment's Bangladesh Standards and Guidelines for Sludge Management (2015) should be followed while dealing with sludge from municipal and domestic sewage treatment plants (STP).
- Both Boiragi Khal and Panshi Khal are now cut off from the Old Madhumati River, causing increased sedimentation in the canal and environmental deterioration. These canals should be connected to the Old Madhumati by building appropriate water infrastructures such as bridges and culverts.
- Since they help to reduce peak urban floods ditches, ponds, and wetlands should all be identified, conserved, and excavated (if necessary).

Acknowledgements The authors would like to thank the Institute of Water and Flood Management (IWFM), BUET, who have provided the system components and support during the project

execution. The authors would also like to thank the Local Government Engineering Department (LGED) for the financial support under the Municipal Governance and Services Project (MGSP).

References

Ahmed, S.S., and Muntasir Ahmed. 2012. *Urbanization and Economic Development of Bangladesh: The Primacy of Dhaka and Competitiveness. 2009:* 1–21.

Akter, Aysha, and Ahad Hasan Tanim. 2016. Estimating Urban Flood Hazard Zones Using Swmm in Chittagong City. *Technical Journal River Research Institute* 13 (1): 87–101.

Arnell, Nigel W. 1999. Climate Change and Global Water Resources. *Journal of Global Environmental Change, Volume 9, Supplement 1*. https://doi.org/10.1016/S0959-3780(99)00017-5.

Arnold, J.G., D.N. Moriasi, P.W. Gassman, K.C. Abbaspour, M.J. White, R. Srinivasan, C. Santhi, et al. 2012. SWAT: Model Use, Calibration, and Validation. *Transactions of the ASABE* 55 (4): 1491–1508.

Asian Development Bank. 2013. People's Republic of Bangladesh: Strengthening the Resilience of the Urban Water Supply, Drainage, and Sanitation to Climate Change in Coastal Towns (Financed by the Japan Fund for Poverty Reduction), October: 596.

Babaei, Sahar, Reza Ghazavi, and Mahdi Erfanian. 2018. Urban Flood Simulation and Prioritization of Critical Urban Sub-Catchments Using SWMM Model and PROMETHEE II Approach. *Physics and Chemistry of the Earth* 105 (February): 3–11. https://doi.org/10.1016/j.pce.2018.02.002.

Bai, Yiran, Na Zhao, Ruoyu Zhang, and Xiaofan Zeng. 2018. Storm Water Management of Low Impact Development in Urban Areas Based on SWMM. *Water (Switzerland)* 11 (1). https://doi.org/10.3390/w11010033.

BBS. 2012. National Population and Housing Census 2011. *National Report.* Government of Bangladesh, National Planning Commission Secretariat, Bangladesh Bureau of Statistics.

Cambez, M.J., J. Pinho, and L.M. David. 2008. Using SWMM 5 in the Continuous Modelling of Stormwater Hydraulics and Quality, 1–10.

Chowdhury, J.U., Md. Rezaur Rahman, Sujit Kumar Bala, and A.K.M. Saiful Islam. 1998. Impact of 1998 Flood on Dhaka City and Performances of Flood Control Works. *Technical Report*. IWFM, BUET, Dhaka.

Eriksson, Mats, Xu Jianchu, Arun Bhakta Shrestha, Ramesh Ananda Vaidya, Santosh Nepal, and Klas Sandström. 2009. "The Changing Himalayas: Impact of climate change on water resources and livelihoods in the greater Himalayas." *Journal of Geophysical Research 114*.

Filliben, James J. 1975. The Probability Plot Correlation Coefficient Test for Normality. *Technometrics* 17 (1). https://doi.org/10.1080/00401706.1975.10489279.

Garrote, J., F.M. Alvarenga, and A. Díez-Herrero. 2016. Quantification of Flash Flood Economic Risk Using Ultra-Detailed Stage–Damage Functions and 2-D Hydraulic Models. *Journal of Hydrology* 541: 611–25. https://doi.org/10.1016/j.jhydrol.2016.02.006.

Haase, Dagmar. 2009. Effects of Urbanisation on the Water Balance—A Long-Term Trajectory. *Environmental Impact Assessment Review* 29 (4): 211–219. https://doi.org/10.1016/j.eiar.2009.01.002.

Hasan Tarek, Mehedi, Shah Md, Imran Kabir, and Adil Hassan. 2017. Application of Swmm for Analysis of Flash Floods in Urban Areas: A Case Study for Chaktai Khal Watershed in Chittagong.

Hossain, M.M., and Rumman Mowla Chowdhury. 2018. Hydro-Morphological Study for Rehabilitation of Old Madhumati River Using Mathematical Model. *Journal of Engineering Science* 03 (1).

Hossain, Sharif, Guna Alankarage Hewa, and Subhashini Wella-Hewage. 2019. A Comparison of Continuous and Event-Based Rainfall-Runoff (RR) Modelling Using EPA-SWMM. *Water (Switzerland)* 11 (3). https://doi.org/10.3390/w11030611.

Institute of Water Modeling (IWM). 2011. Hydrological and Morphological Study of Old Madhumati River under Rehabilitation of Old Madhumati River and Improvement of Surrounding Area of Gopalganj Pourashava. *Final Report* (April). Dhaka.

IPCC. 2014. 5th Assessment Report: Summary for Policymakers. *IPCC Fifth Asessement Report: Working Group III Mitigation of Climate Change.*

Jang, Suhyung, Minock Cho, Jaeyoung Yoon, Yongnam Yoon, Sangdan Kim, Geonha Kim, Leehyung Kim, and Hafzullah Aksoy. 2007. Using SWMM as a Tool for Hydrologic Impact Assessment. *Desalination* 212 (1–3): 344–356. https://doi.org/10.1016/j.desal.2007.05.005.

Khadka, Sanjay, and Keshav Basnet. 2019. Storm Water Management of Barahi Chowk Area, Lakeside, Pokhara, Nepal Using SWMM. *KEC Conference* 2 (1): 320–325.

Khan, M.S.A., and J.U. Chowdhury. 1998. Dhaka City Storm Water Quality Assessment. *Technical Report-1*. IWFM, BUET, Dhaka.

Khan, M.S., Md. Rezaur Rahman, Anisul Haque, Md. Munsur Rahman and G.M. Tarekul Islam. 2006. *Stormwater Flooding at BUET Campus: A Situation Report*. Institute of Water and Flood Management, BUET, Dhaka.

Mohammed, Khaled, A.K.M. Saiful Islam, G.M. Tarekul Islam, Md., Lorenzo Alfieri, Jamal Uddin Khan, Sujit Kumar Bala, and Mohan Kumar Das. 2018. Future Floods in Bangladesh under 1.5°C, 2°C, and 4°C Global Warming Scenarios. *Journal of Hydrologic Engineering* 23 (12): 04018050. https://doi.org/10.1061/(asce)he.1943-5584.0001705.

Mohammed, Khaled, A.K.M. Saiful Islam, G.M. Tarekul Islam, Lorenzo Alfieri, Sujit Kumar Bala, and Md. Jamal Uddin Khan. 2017. Impact of High-End Climate Change on Floods and Low Flows of the Brahmaputra River. *Journal of Hydrologic Engineering* 22 (10): 04017041. https://doi.org/10.1061/(asce)he.1943-5584.0001567.

Mondal, M. Shahjahan, A.K.M. Saiful Islam, Anisul Haque, Rashedul Islam, Subir Biswas, and Khaled Mohammed. 2018. Assessing High-End Climate Change Impacts on Floods in Major Rivers of Bangladesh Using Multi-Model Simulations. *Global Science and Technology Journal* 6 (2): 1–14.

Paul, S., A.K.M. Saiful Islam, G.M. Tarekul Islam, Ahsan Azhar Shopan, and Sujit Kumar Bala. 2013. Impact of Climate Change on Urban Drainage Systems in Three Selected Coastal Towns of Bangladesh. *International Conference on Climate Change Impacts and Adaptation* 397–406.

Rabori, Ali Moafi, and Reza Ghazavi. 2018. Urban Flood Estimation and Evaluation of the Performance of an Urban Drainage System in a Semi-Arid Urban Area Using SWMM. *Water Environment Research* 90 (12): 2075–2082. https://doi.org/10.2175/106143017x15131012188213.

Rahman, M.R., J.U. Chowdhury, and M. Salehin. 1999. Dhaka City Storm Water Quality Assessment. *Technical Report-2, R01/99.* IWFM, BUET, Dhaka.

Rossman, Lewis A., and Wayne C. Huber. 2016. Storm Water Management Model Reference Manual. *US EPA Office of Research and Development* III (January): 231. www2.epa.gov/water-research.

Solomon, S., D. Qin, M. Manning, Z. Chen, M. Marquis, K.B. Averyt, M. Tignor, and H.L. Miller. 2007. IPCC, 2007. Climate Change 2007: The Physical Science Basis. Contribution of Working Group I to the Fourth Assessment Report of the Intergovermental Panel on Climate Change.

Flood Propagation Processes in the Jamuna River Floodplain in Sirajganj

Ashik Iqbal, M. Shahjahan Mondal, M. Shah Alam Khan, Hans Hakvoort, and William Veerbeek

Abstract Monsoon flooding inundates a substantial part of Bangladesh, where 80% of the areas are floodplains. Sirajganj, located beside the Jamuna River in northwestern Bangladesh, is home to many communities living in the low-lying unprotected floodplains. The Ranigram village of Sirajganj has a hydraulic connection with the Jamuna River and is flooded almost every year. This study aims to explore how flood propagates in the floodplain, determine the water level variation in the floodplain with respect to the Jamuna River stage, and develop a hydrodynamic model of the flood propagation process in Ranigram. Water level gauges were installed at strategically selected locations in Ranigram, and flood data were collected during the 2018 and 2020 monsoons. In the R^2, NSE, MSE, and RMSE analyses, the observed floodwater level in Ranigram shows an excellent dynamic relation with the water level at Sirajganj on the Jamuna River. The statistical relation derived from the 2018 data is validated with the observed data of 2020. A two-dimensional hydrodynamic model is developed with HEC-RAS using a DEM generated with surveyed bathymetry and UAV-based data and is calibrated and validated with the observed water level data and flood images. The maps of flood arrival time, duration, and maximum extent and depth were extracted from the model. The outcomes of this study will be useful in flood risk and damage assessments and forecasting of floods in floodplain areas.

A. Iqbal (✉) · M. S. Mondal · M. S. A. Khan
Institute of Water and Flood Management, Bangladesh University of Engineering and Technology, Dhaka, Bangladesh

M. S. Mondal
e-mail: mshahjahanmondal@iwfm.buet.ac.bd

M. S. A. Khan
e-mail: msalamkhan@iwfm.buet.ac.bd

H. Hakvoort · W. Veerbeek
IHE Delft Institute for Water Education, Delft, The Netherlands
e-mail: h.hakvoort@un-ihe.org

W. Veerbeek
e-mail: w.veerbeek@un-ihe.org

© The Author(s), under exclusive license to Springer Nature Switzerland AG 2022

G. M. Tarekul Islam et al. (eds.), *Water Management: A View from Multidisciplinary Perspectives*,
https://doi.org/10.1007/978-3-030-95722-3_3

Keywords Flood propagation · Floodplain · Jamuna River · 2D hydrodynamic model · HEC-RAS

1 Introduction

Almost 80% of Bangladesh is consisted of floodplain land, which is considered flood-prone, and in average flood years, about 20% of the country's land area is flooded (Mirza 2002). Monsoon flooding from the river inundates a substantial part, especially the northern parts of Bangladesh, every year from early July to late September (Khan 2008). Many communities reside in the low topographical non-protected area of the riverside that is flooded by the river overtopping water. Such communities are entirely exposed and vulnerable even to flood events with low associated return periods. During floods, they are the first to be affected and cannot take enough precautions before the floodwater enters the locality (Mirza 2002). Residents of these areas often build their houses on elevated mounds as an indigenous technique to save their houses from flood exposure (Brammer 2010).

Due to climate change and riverbed siltation, flood events are becoming increasingly unpredictable and severe every year, and so the historical practice of living with water is being threatened by rising flood impacts (Biswas 2008; Mondal et al. 2018). In addition, the encroachment of wetlands and floodplains and the inadequate drainage capacity may increase the flood process's severity at the local level (Islam et al. 2010; Miller and Hutchins 2017; Avinash 2014). Bangladesh faces many challenges in flood management (Ali et al. 2018), where the implementation gap and poor planning and design of flood mitigation measures make the management system inadequate and ineffective (Vaz 2020; Brammer 2010). Nevertheless, a proper assessment of flooding is necessary for selecting and taking effective measures.

One of the most efficient non-structural flood impact mitigation measures is flood forecasting and early warning systems (Subramanya 2008). Proper assessment of the flooding process in inundated areas is a prerequisite for proper flood forecasting. The Flood Forecasting and Warning Center (FFWC) of the Bangladesh Water Development Board (BWDB) provides information of the river stage at critical locations along the major rivers in Bangladesh (FFWC 2018). The FFWC has developed danger levels for different locations to indicate the magnitudes of the expected flood conditions (FFWC 2018). These levels primarily indicate major events when evacuation and temporary relocation might be needed.

Sirajganj Sadar upazila (sub-district) has hydraulic interaction with the Jamuna River and is flooded every year due to the overtopping of the river (Islam et al. 2010). Many riverside areas and communities are not considered for protection from flooding with the embankment, and they suffer from the loss of houses and livelihoods (Ali et al. 2018). People of the locality do not get any proper location-specific flood information with indicative lead time. The flood information provided by FFWC is only based on the river stage, but there is no flood information for the locality. Nevertheless, better insight into the flood extent and depth distribution in the area is

essential for safety that impacts livelihoods since insight into local flood conditions is essential for appropriate responses (Hassan and Shah 2008). If the flood propagation process is appropriately understood, the consequent hazards for the flood in the locality can be forecasted; thus, the necessary measures can be taken.

Two-dimensional hydrodynamic modeling is an effective method for gaining insight into the propagation of floods (Meire et al. 2010). Such models typically rely on remote sensing data with subsequent coarse digital elevation models for river flooding (Rahman2015; Jain et al. 2018). Such practices are adequate for predicting the flood extent for relatively large areas (Jain et al. 2018; Yalcin 2020) but often lack the level-of-detail needed for sub-critical floods at the scale of local communities.

The main objective of this study is to explore the flood propagation process in the floodplain in the Ranigram area of Sirajganj. The specific objectives are (a) to find out the flood process in the Jamuna River floodplain through a statistical relationship with the river stage and (b) to develop a 2D hydrodynamic model in HEC-RAS with a UAV-enhanced high-resolution DTM, and to validate with field data at the local level.

2 Floods in Bangladesh

Floods are Bangladesh's most common natural disaster that affects people's lives and livelihoods. Bangladesh is located in the downstream of the three largest river systems in the world—the Ganges, the Brahmaputra, and the Meghna. The flat topography of the floodplain and the monsoonal climate make the country highly vulnerable to floods. The principal source of floods in Bangladesh is the river water from the overbank flows of these major river systems, which result from the runoff of prolonged high-intensity rainfalls during the monsoon over Nepal, India, and Bangladesh (Rahman and Salehin 2013). This massive discharge itself cannot be drained to the Bay of Bengal due to the high outfall water levels (Rahman and Salehin 2013). In addition, the construction of roads without sufficient cross drainage openings, alignment of roads transverse to the natural drainage paths, blockage of drainage channels by solid waste dumping, construction of cross-dams on some rivers, inadequate capacity of drainage sluices, and loss of connectivity between rivers and floodplains due to unplanned and unregulated anthropogenic activities are amplifying the frequency and magnitude of flood events (Rahman and Salehin 2013).

Overflowing rivers annually flood about one-fifth to one-third of the country from June to September. When the peak flows in the two major rivers, the Brahmaputra and the Ganges, synchronize, extreme floods occur with extensive coverage and duration (Rahman et al. 2006). An increasing variability is observed in the annually flooded area since the late 1980s (Fig. 1). As seen in the figure, some severe floods were experienced in 1988, 1998, 2007, and 2017, and some moderate floods in 1955, 1974, 1987, and 2004.

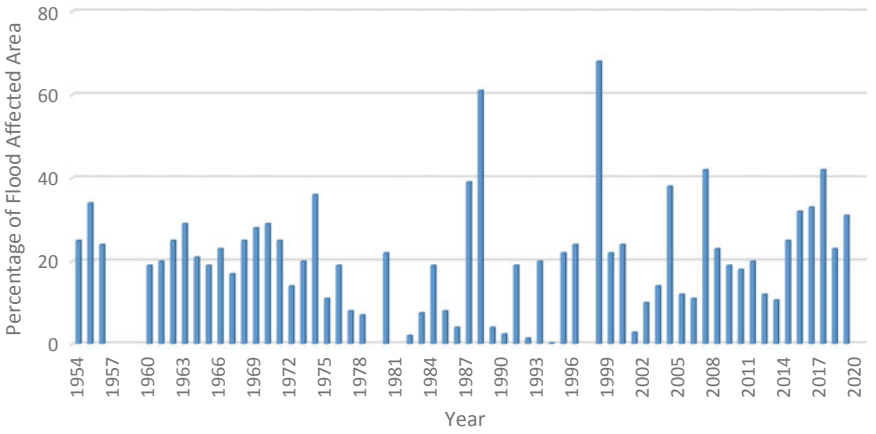

Fig. 1 Percentage of flood affected area in Bangladesh

3 Study Area

3.1 Description of the Area

Sirajganj is in the northwest of Bangladesh and is also one of the most flood-prone areas. It lies between 24°22′ and 24°37′N latitudes and between 89°36′ and 89°47′E longitudes. Out of 320 km^2 of total area of Sirajganj region, about 260 km^2 is designated as the land area and 60 km^2 as the riverine area (Islam and Miah 2012). Sirajganj is located along the Jamuna River and is flooded primarily by the riverine flood during the monsoon associated with high-intensity rainfall. Sirajganj experiences a sub-tropical monsoonal climate, typical of Bangladesh, with an average annual rainfall of 1610 mm (BBS 2016). The danger flood level at the Sirajganj station on the Jamuna River is set at 13.35 m PWD, which specifies that if this water level is crossed, the resulting flood will cause damage in the adjacent areas.

The Ranigram village in the Khokshabari union is a peri-urban area of the Sirajganj district and is adjacent to the Jamuna River (Fig. 2). The area of the village is 2.4 km^2 and is located outside the new 15.35 m PWD flood-control embankment of the Sirajganj town. It is surrounded on three sides by roads. Two crossbars exist in the north and south of the village.

3.2 Flood Occurring in the Ranigram Area

There exists a breach in the eastern shallow old embankment (Fig. 3) from which water enters the area. The Union Parishad water level gauge is just beside the water

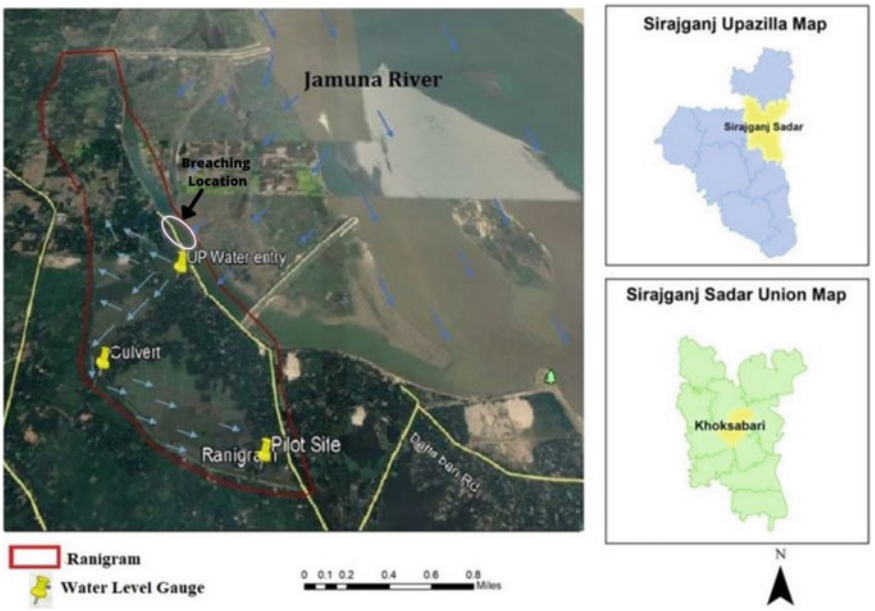

Fig. 2 Study area with gauge locations and flooding direction

Fig. 3 Breaching location beside Union Parishad from where water enters into the Ranigram area during **a** dry season and **b** monsoon

entry location. The breach profile is 10–30 m at the lowest portion of the breach and extends to 110–170 m at the high flood level.

At first, the bank spilled water from the Jamuna River flows from the north to the southeast side of the area between two crossbars. After that, water enters through the breach, and for high flood levels, the overtopping occurs in the shallow embankment. Then passing the breaching location, the water flows inside the village from south to north and east to west from the Union Parishad. Gradually, water reaches the whole northern part of the village and the culvert area in the middle-western part. From the

culvert area, water flows to the southern part of the village and reaches the Pilot Site area.

After entering the village, the water gets stacked because of the embankment roads on all three sides of the village. With the decrease of water level in the Jamuna River, the floodwater in the Ranigram village starts going out from the breaching point location. The whole flood water goes out in the same way as it entered, and little water remains in the ditches and lowlands that later dry up by evaporation.

4 Methodology

4.1 Methodological Framework

In Ranigram, three water level gauges are installed at strategically crucial locations to monitor the floodplain's water depth. From the flood depth, the water levels are calculated with proper benchmarking. The floodwater level data of the area is analyzed to understand the relation of the internal flood process with the external river stage of the Jamuna River by the coefficient of determination (R^2), Nash–Sutcliffe model efficiency coefficient (NSE), Mean Absolute Error (MAE), and Root Mean Square Error (RMSE) analysis (Mali et al. 2020). Secondary data on the water level of the Jamuna River is collected from BWDB.

A two-dimensional hydrodynamic model of the selected area is developed with HEC-RAS using a high-resolution DTM (Farooq et al. 2019; Jung et al. 2014). Water level and normal depth are used for boundary conditions for the model. Measured flood water level data of one water level gauge is used for the boundary condition and others for calibrating and validating the model (Yalcin 2020). The model is calibrated and validated using real flood scenarios. The flood maps of the flood extent and depth, arrival time, and duration are extracted from the simulation result. Figure 4 shows the methodological framework of the study.

4.2 Data Collection

The water level readings of the three installed gauges were closely monitored for the whole flood cycle of the years 2018 and 2020. The three water level gauges installed at the Union Parishad, Culvert, and Pilot Site are shown in Fig. 2. The distance from the Union Parishad gauge at the water entry location to the gauge at the Culvert is about 0.82 km. The distance from the gauge at the Culvert to the Pilot site gauge is about 1.35 km. The reduced level of each gauge location is measured with proper benchmarking. When the water started overtopping the river, the water depth at each gauge was collected regularly in the morning every day. Then, the water levels at the three locations were measured by adding the depths with the respective reduced

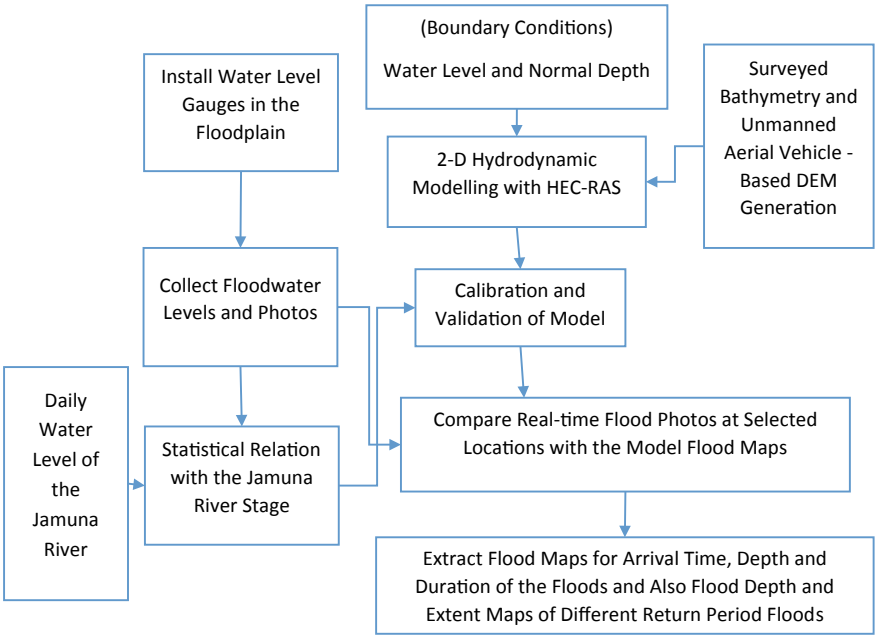

Fig. 4 Methodological framework of the study

levels. At the same time, the water level at Sirajganj station on the Jamuna River was recorded daily from the FFWC website of BWDB.

4.3 Statistical Relation

A relationship between the water level on the floodplain and that on the river was established using regression analysis. The simple linear regression method is used for establishing the relationship between the water level on the floodplain and that on the Jamuna River. The simple linear model is expressed using the following equation:

$$Y = aX + b + c \tag{1}$$

where Y is the dependent variable (the water level at the gauges in the floodplain), X is the independent variable (the water level on the Jamuna River at Sirajganj station), a is the slope of the regression line, b is the intercept, and c is the residual (error).

The R^2 is the quantification of the predictive extent of a regression model. It explains the strength of the relationship between the independent and dependent variables. If the R^2 of a model is 0.50, half of the observed variations are explained

by the model's inputs. The R^2 values range from 0 to 1 and are commonly stated as percentages from 0 to 100%. A higher R^2 value indicates a better fit of the model to the observed data (Freund et al. 2006).

4.4 Nash–Sutcliffe Model Efficiency Coefficient

The Nash–Sutcliffe model efficiency coefficient (NSE) is used to assess the predictive skill of a model. It represents the robustness of the model. NSE value close to 1 means the model quality is good, and if the value is negative, the model is unacceptable (Zeybek 2018). The NSE is calculated as one minus the ratio of the error variance of the modeled time-series divided by the variance of the observed time-series data. It is calculated using the following equation:

$$\mathrm{NSE} = 1 - \frac{\sum_{i=1}^{n} (Y_{\mathrm{obs}} - Y_{\mathrm{sim}})^2}{\sum_{i=1}^{n} (Y_{\mathrm{obs}} - Y_{\mathrm{mean}})^2} \tag{2}$$

where Y_{obs} is the observed data, Y_{sim} is the model data, and Y_{mean} is the mean of the observed data.

4.5 Mean Absolute Error

Mean Absolute Error (MAE) is an error function used for regression models. MAE is the sum of absolute differences between the measured and predicted values. So, MAE measures the average magnitude of errors in a set of predictions without considering their directions. The formula is:

$$\mathrm{MAE} = \frac{\sum_{i=1}^{n} |Y_{\mathrm{sim}} - Y_{\mathrm{obs}}|}{n} \tag{3}$$

where n is the number of data, Y_{sim} is the model data, Y_{obs} is the measured data, and $|Y_{\mathrm{sim}} - Y_{\mathrm{obs}}|$ is the absolute error.

4.6 Root Mean Square Error

Root Mean Square Error (RMSE) is the standard deviation of the residuals or simply called prediction errors. RMSE is a measure of how spread out these residuals are. Thus, RMSE represents how robust the data is around the line of best fit.

$$\text{RMSE} = \sqrt{\frac{\sum_{i=1}^{n} (Y_{\text{sim}} - Y_{\text{obs}})^2}{n}} \tag{4}$$

4.7 High-Resolution DEM

A high-resolution DEM was generated using a hybrid technique with Unmanned Aerial Vehicle (UAV) and measured bathymetry data of the Ranigram area. The Agisoft Metashape 1.5.2 software and ArcGIS 10.5 software were used for the DTM generation. The whole area was divided into two parts: (i) tree-canopy area and (ii) non-canopy area. The UAV data was used for the non-canopy areas of the village. The measured bathymetry data was used for the canopy areas which are covered by dense trees where UAV cannot penetrate to take land position data.

For the non-canopy area, the UAV-generated images were used along with a set of ground control points in the Agisoft Metashape 1.5.2 software to obtain a DTM for the Ranigram area. Many errors were found when compared with the actual field

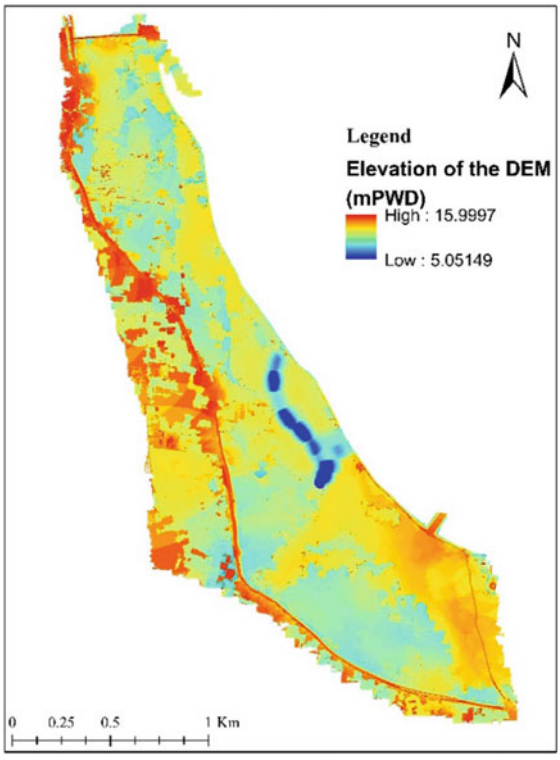

Fig. 5 High-resolution DEM of Ranigram

elevations. Some errors in the water-covered areas were corrected, and a manual correction was done in the location of a hydraulic structure (i.e., culvert). For the tree-canopy area, the measured bathymetry data was used. With this measured point elevation data for the tree-canopy area, a complementary DTM was generated using the Triangulated Irregular Network (TIN) methods from the point cloud. The two DTM models of the tree-canopy and the non-canopy area were merged into one to obtain the DTM of the Ranigram area (Fig. 5).

4.8 HEC-RAS 2D Model

The 2D hydrodynamic model was developed with HEC-RAS 5.0.7 software (Farooq et al. 2019; Jung et al. 2014). The high-resolution DEM of the Ranigram area was used in creating the terrain in the RAS Mapper. The projection was taken as WGS 1984—UTM zone 45 N. With satellite images, the horizontal position correctness of the terrain is checked. At first, the 2D flow perimeter of the study area was set. The shapefile of the Ranigram area was imported for the 2D flow area perimeter. The mesh was developed with computational points in 10 m $\times$ 10 m for the 2D area. Manning's roughness coefficients of 0.04 and 0.05 were used for agricultural land and housing land respectively in the 2D flow area.

Two external boundary condition lines were drawn. One boundary condition is at the breaching location beside the Union Parishad from where the water enters into the Ranigram area, and the other is in the south of the Ranigram village beside the pilot site. For the first boundary condition, the stage hydrograph was taken, and for the second boundary condition, the normal depth was taken. The daily flood water level at the water entry location beside the Union Parishad was used for stage hydrograph at boundary condition 1 with a 1-day interval. The average normal depth for the second boundary condition estimated from the measured water level data at the gauges and found to be 0.0001 was used for the floodplain of Sirajganj.

The model run was performed for the dates similar to the measured data. The model was run with a 1-min computation interval. The output of the model was taken for a 1-day interval. The water level at the Union Parishad was used as a boundary condition, and the water level reading at the Culvert and Pilot Site was used for calibrating and validating the model. The measured data of 2020 was used for the validation of the model.

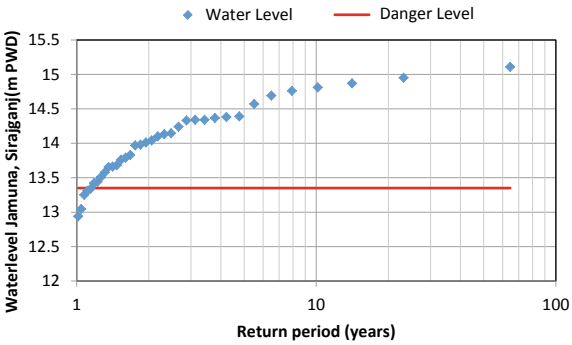

Fig. 6 Water level at Sirajganj station in the Jamuna River for different return periods

5 Results and Discussion

5.1 Frequency Analysis of the Jamuna River Water Level at Sirajganj

Water level data at Sirajganj station of the Jamuna from 1984 to 2020 (37 years) has been considered, and the Gumbel distribution is used for the frequency analysis. The water levels for different return period floods are shown in Fig. 6. The danger level is 13.35 m PWD. The Jamuna River crossed the danger level every year except for five years in the 37 years observed.

For a 1.18-year return period, the water level in the Jamuna River at Sirajganj crosses the danger level, and for a 2-year return period, the water level at the Jamuna River is 0.65 m above the danger level.

5.2 Statistical Analysis of the Jamuna River Water Level with the Flood Level in Floodplain

The flood depth data at each water level gauge in Ranigram village was collected during the flood season of 2018. The floodwater level for the corresponding depth was calculated for each day at each gauge. The water level at the Ranigram area is plotted with the water level of the Jamuna at Sirajganj station in Fig. 7. The co-relation with each gauge was found from the flood water level at the gauges in the Ranigram area. It is found that when there was a sudden rise or fall in the water level of the Jamuna River, the water level in the floodplain did not follow that trend.

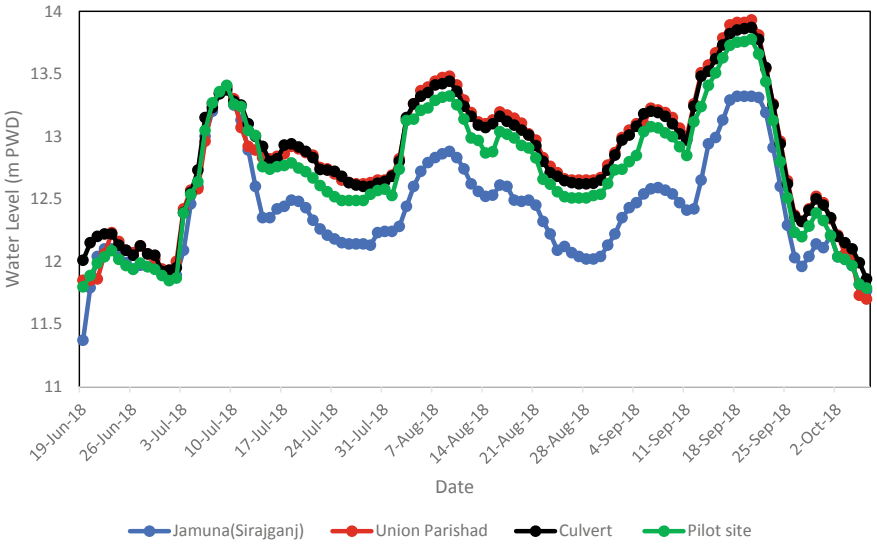

Fig. 7 Flood water level data in the Ranigram and Sirajganj station of Jamuna River in 2018

5.2.1 The Relation of Gauges with the Water Level of the Jamuna at Sirajganj

The water level data at the Ranigram area for each gauge was plotted with the water level of the Jamuna at Sirajganj station. From the plots in Fig. 8a–c, it is found that there is a linear relationship between the water level on the floodplain and the water level on the Jamuna River, and so with the data, a statistical relationship can be established using a simple regression method.

The statistical relation found between the Jamuna River water level and the water level at the Union Parishad according to (1) is given below:

$$Y_{\mathrm{UP}} = 1.1093X - 0.9437 \tag{5}$$

$$Y_{\mathrm{Culvert}} = 1.0635X - 0.3715 \tag{6}$$

$$Y_{\mathrm{PilotSite}} = 1.1072X - 1.0313 \tag{7}$$

where Y is the water level at Union Parishad, Culvert, and Pilot Site in Eqs. (5), (6), and (7), respectively, and X is the water level on the Jamuna at Sirajganj for the corresponding day. The relation and error in the model were analyzed using the Eqs. (2), (3), and (4).

The R^2 value is 0.79, 0.83, and 0.86, and the NSE is 0.795, 0.831, and 0.864 for Union Parishad, Culvert, and Pilot Site, respectively. In the error analysis, the MAE

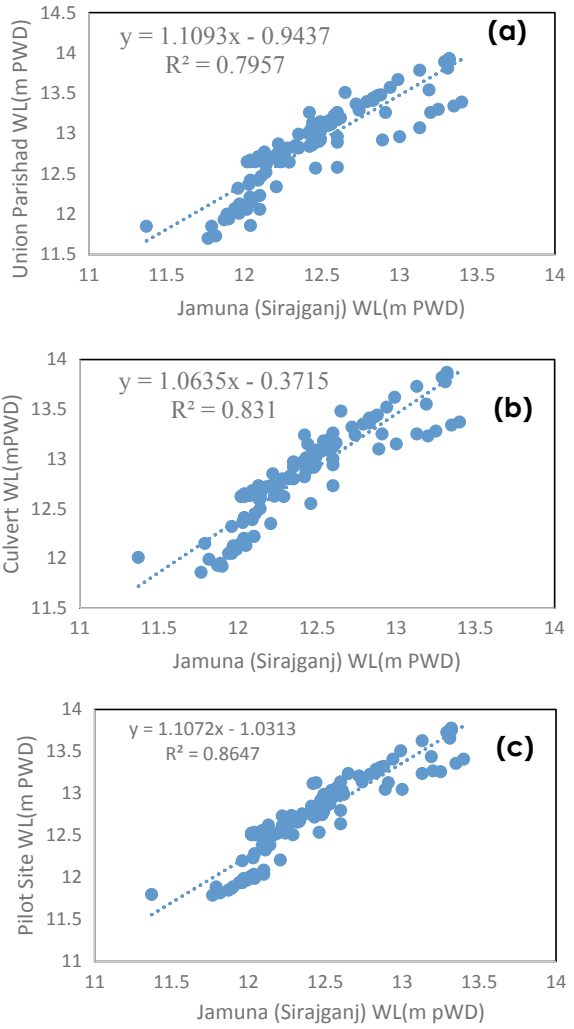

Fig. 8 Relation of the Jamuna River water level with the water level on the floodplain at **a** Union Parishad, **b** Culvert, and **c** Pilot Site for 2018

is found to be 0.017 m, 0.048 m, and 0.049 m, and the RMSE is 0.236 m, 0.201 m, and 0.184 m for Union Parishad, Culvert, and Pilot Site, respectively. The residual ranges from 0.267 m to −0.298 m, 0.276 m to −0.176 m, and 0.334 m to −0.240 m for Union Parishad, Culvert, and Pilot Site, respectively.

The simple linear equation derived from the measured daily data of 2018 indicates a good relation, and the model's error is not very high. This model can predict water levels at those locations from the water level of the Jamuna River. For low water levels, the relationship deviates more, and for high water levels, the relationship is better.

5.2.2 Validation of Statistical Relation with 2020 Data

Equations (5), (6), and (7) developed with the data of 2018 were validated using the measured data of 2020. First, the daily data of the Jamuna River of 2020 was inputted as the independent variable for each equation, and from the equations, the water level for each gauge was found. Figure 9a–c show the plot of the model and measured water levels at Union Parishad, Culvert, and Pilot Site, respectively.

The R^2 values are 0.975, 0.941, and 0.936, and the NSEs are 0.97, 0.92, and 0.87 for Union Parishad, Culvert, and Pilot Site, respectively.

Also, in the error analysis, the MAEs are found to be 0.137 m, 0.162 m, and 0.183 m, and the RMSEs are found to be 0.174 m, 0.267 m, and 0.301 m for Union Parishad, Culvert, and Pilot Site, respectively. The residuals range from 0.418 m to −0.392 m, 1.228 m to −0.370 m, and 1.355 m to −0.406 m for Union Parishad, Culvert, and Pilot Site, respectively.

From Fig. 9, it is found that the statistical equations perform very well for the 2020 data. The variation of model and measured water levels at all three gauges is very well captured, and the residuals are not very high.

5.3 HEC-RAS 2D Model Results

The two-dimensional HEC-RAS model incorporated with high-resolution DTM was developed, and the simulation results were calibrated and validated with the measured data of 2018 and 2020, respectively. The water level at the Union Parishad was used as a boundary condition, and the water levels at the Culvert and Pilot Site were used for calibrating and validating the model, respectively.

5.3.1 HEC-RAS Model Calibration

After the simulation, the computational cells at the Culvert and Pilot Site water level gauge locations were selected. The daily water surface elevation data of the cells was collected from the model output and is plotted with the measured water level of the gauges. For the set up, the model performs well for the floodplain in Sirajganj.

Figure 10a, b show the plot of HEC-RAS simulated and measured water levels at Culvert and Pilot Site, respectively. From the figure, it is seen that the simulated water level is matching with the pattern of the measured water level at both Culvert and Pilot Site. The R^2 values are 0.982 and 0.975, and the NSEs are 0.97 and 0.91 for the Culvert and Pilot Site, respectively. The MAEs are found to be 0.043 m and 0.131 m, and the RMSEs to be 0.068 m and 0.141 m for the Culvert and Pilot Site, respectively. The residuals range from 0.34 m to −0.07 m and 0.167 m to −0.271 m for the Culvert and Pilot Site, respectively.

So, from the calibration, it appears that the HEC-RAS model incorporated with high-resolution DTM performs very well when compared with the measured water

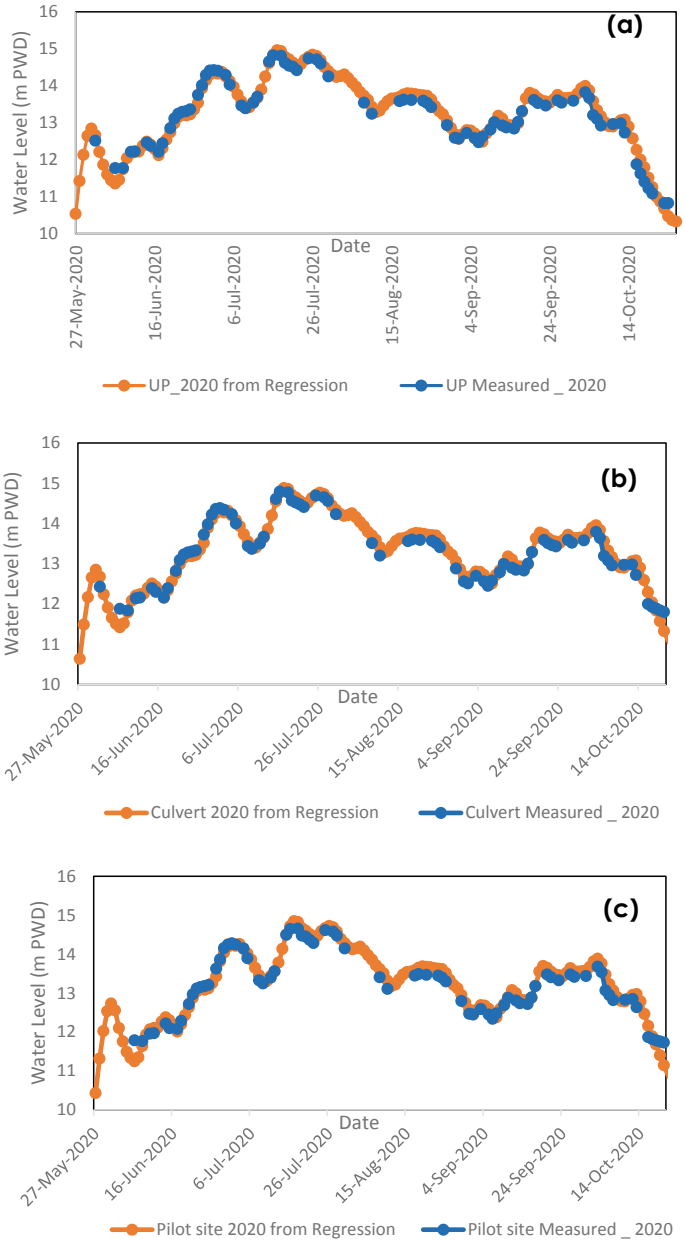

Fig. 9 Model water level with the measured water level in the floodplain at **a** Union Parishad, **b** Culvert, and **c** Pilot Site for 2020

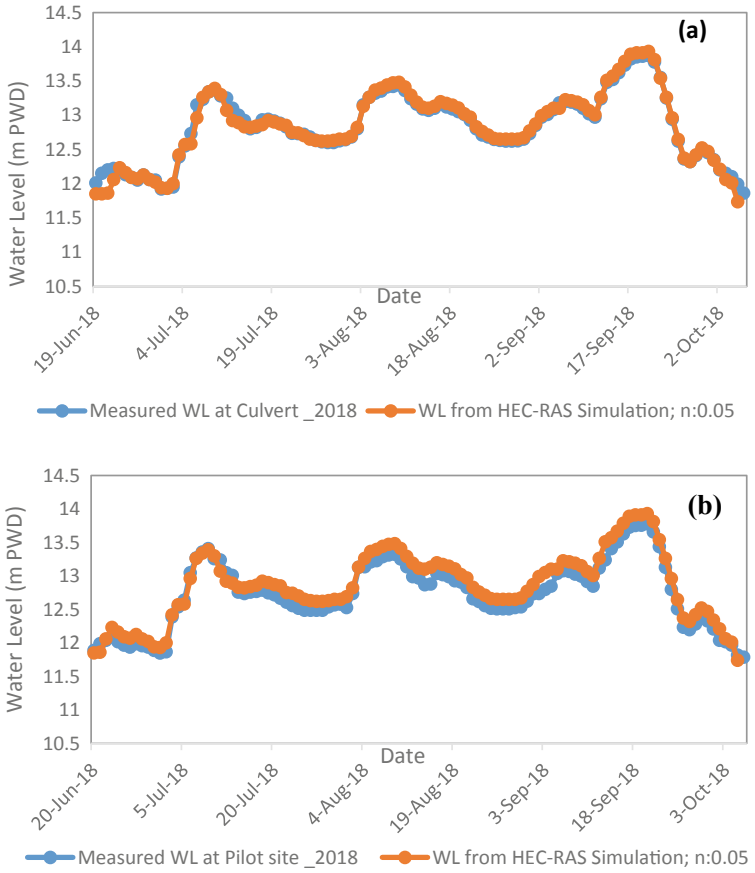

Fig. 10 HEC-RAS model calibration with simulated water level and measured water level in floodplain at **a** Culvert and **b** Pilot Site for 2018

level in the Ranigram area. Though there is some residual in the model, it is not very high.

5.3.2 HEC-RAS Model Validation

The water level data for 2020 at the Union Parishad derived from Eq. (5) was used in the HEC-RAS model. The 2D HEC-RAS model was run with the water level of 2020 as the boundary condition at the Union Parishad location. Figure 11a, b show the plots of HEC-RAS simulated and measured water levels in 2020 at the Culvert and Pilot Site, respectively.

The R^2 values are 0.963 and 0.948, and the NSEs are 0.82 and 0.87 for the Culvert and Pilot Site, respectively. The MAEs are 0.055 m and 0.189 m, and the RMSEs

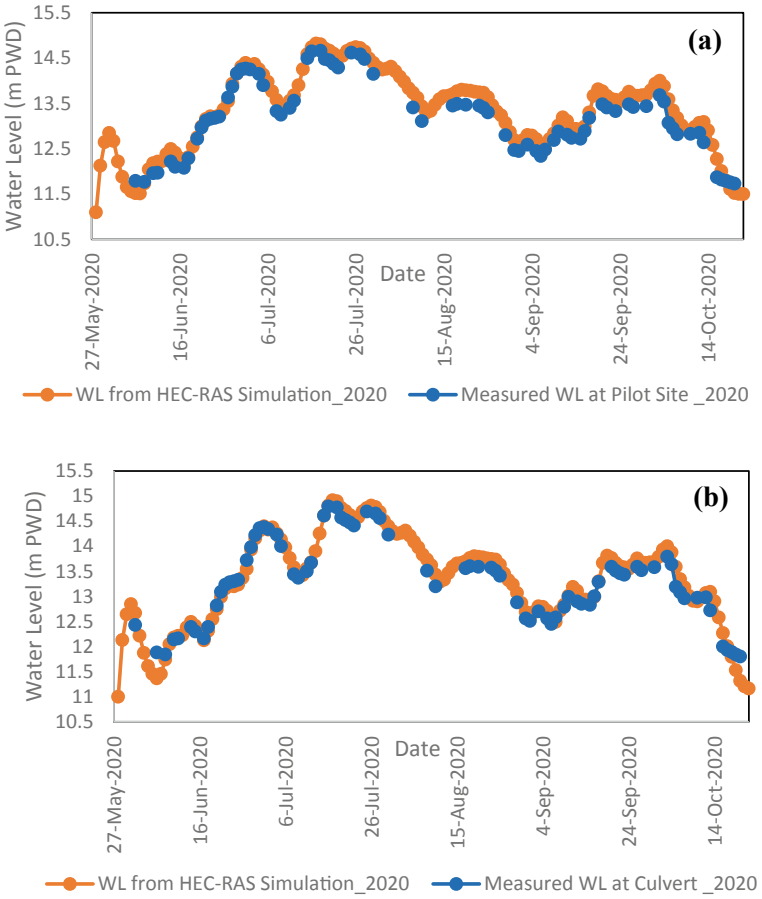

Fig. 11 HEC-RAS model validation with simulated water level and measured water level in floodplain at **a** Culvert and **b** Pilot Site for 2020

are 0.12 m and 0. 0.227 m for the Culvert and Pilot Site, respectively. The residuals range from 0.691 m to −0.08 m and 0.338 m to −0.667 m for the Culvert and Pilot Site, respectively.

From the analysis, it is found that the model performs very well when validated with the measured data of 2020. The residual is high at the beginning and end of the flood period, which means that in those days there is a sudden rise or fall in the water level in the Jamuna River.

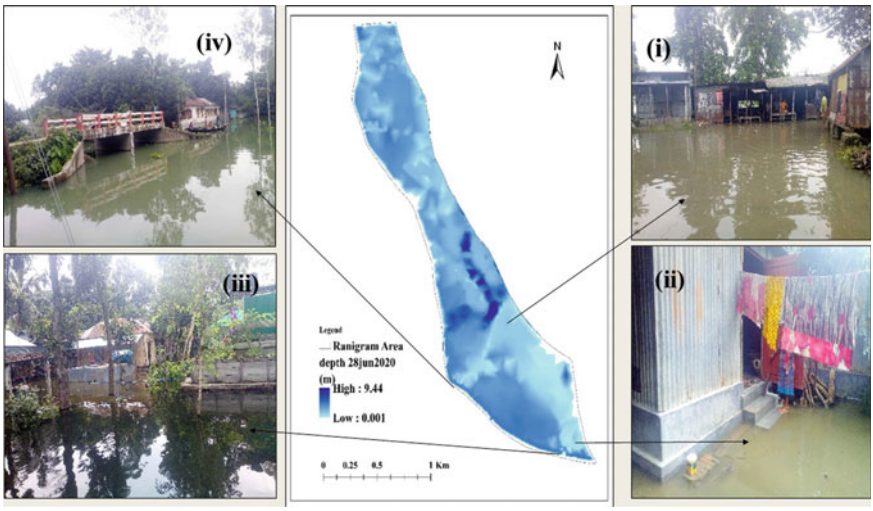

Fig. 12 Flood maps for 28 June 2020 with real-time photos in the floodplain of Ranigram

5.3.3 Model Comparison with Real-Time Photos of Some Specific Locations of Ranigram

The result of the model was also compared with an actual flood event in 2020. The photos were collected from crucial locations in Ranigram during the flood. On 28 June and 15 July 2020, photos were taken from the local market beside the Union Parishad, a retrofitted house, Pilot Site, and Culvert. The flood maps for the 28 June 2020 and 15 July 2020 were also exported from HEC-RAS, and the maps were compared at the locations of the photos. These are shown in Figs. 12 and 13, respectively.

The model-simulated flood maps show a similar flood scenario when compared with the photos of actual floods. Thus, the model with a high-resolution DEM can represent the real flood scenario at the locality of the floodplain.

5.4 Maps of Different Flood Parameters

The maps of flood arrival time, duration, and maximum depth and extent for the Ranigram area were extracted for both the 2018 and 2020 flood events (Fig. 14). At first, flooding started in the low-elevated croplands and reached the high-elevated housing within the following two to three weeks. The maximum duration of the flood was three months and twenty days, and four months and twenty days for 2018 and 2020, respectively. The flood information for any specific location in the village can be derived using these maps. The inundation depth in the wetlands is more than 9 m. The agricultural lowlands inundated for about 3.5 m, and the housing lands inundated

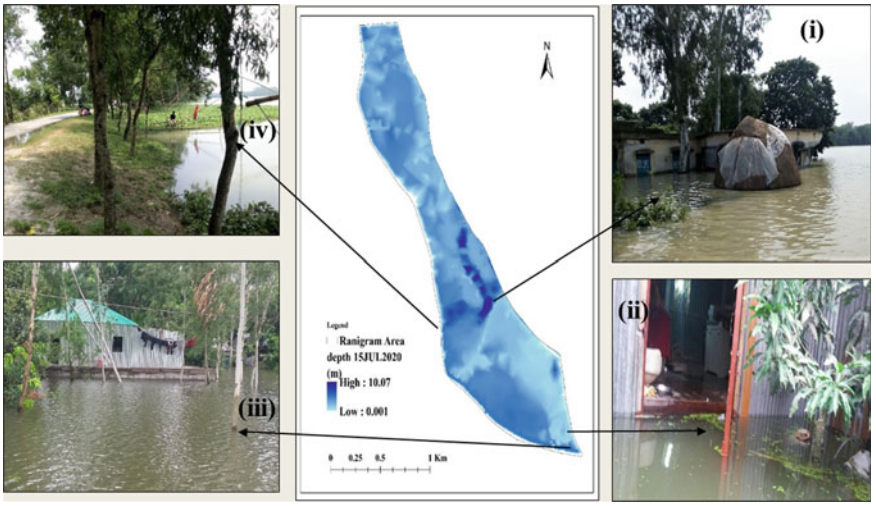

Fig. 13 Flood maps for 15 July 2020 with real-time photos in the floodplain of Ranigram

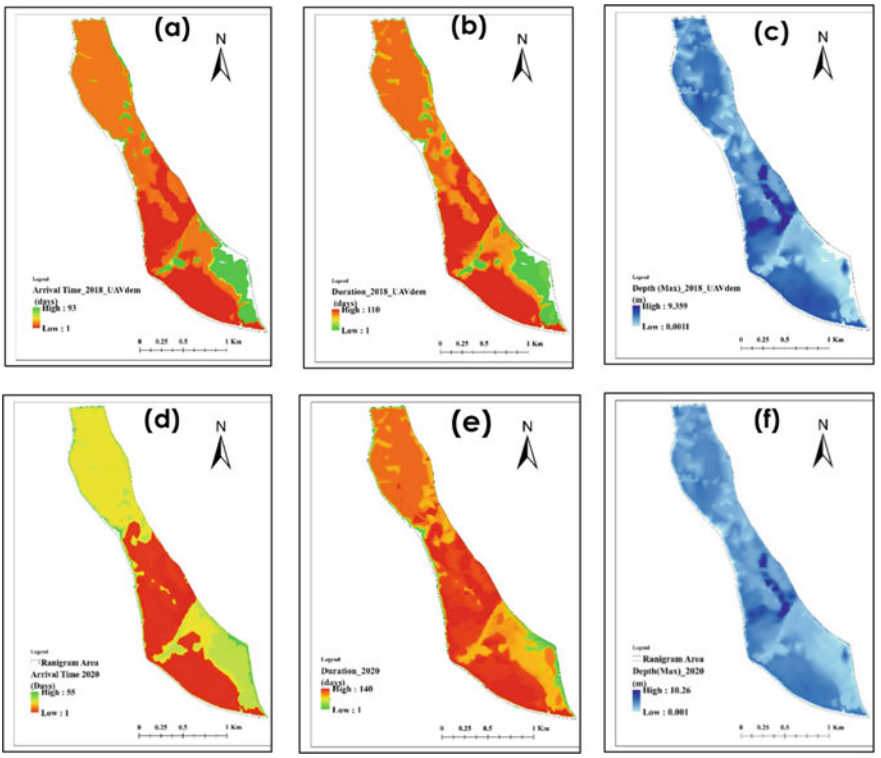

Fig. 14 Flood maps of **a** and **d** arrival time, **b** and **e** duration, and **c** and **f** maximum depth and extent for the flood events of 2018 and 2020, respectively

for more than 1 m. The flood events in the Ranigram area were severe in the years 2018 and 2020.

5.5 *Flood Maps of Ranigram for Different Return Periods*

The flood maps for different return periods are generated for Ranigram using the HEC-RAS model. Figure 15 shows the flood depth and extent maps of the Ranigram area for 1-, 2-, 10-, 20-, 50-, and 100-year return periods. From the maps, it is found that the agricultural lowlands get flooded every year. For a 2-year return period flood, the model shows complete flooding of the Ranigram area. During a 10-year flood event, the mounds with elevated houses are inundated for a depth of about 1.00–1.25 m, while during a 50-year flood the inundation depth is about 1.25–1.50 m. However, the inundation depth increases by 0.03 m only from a 50- to a 100-year return period flood.

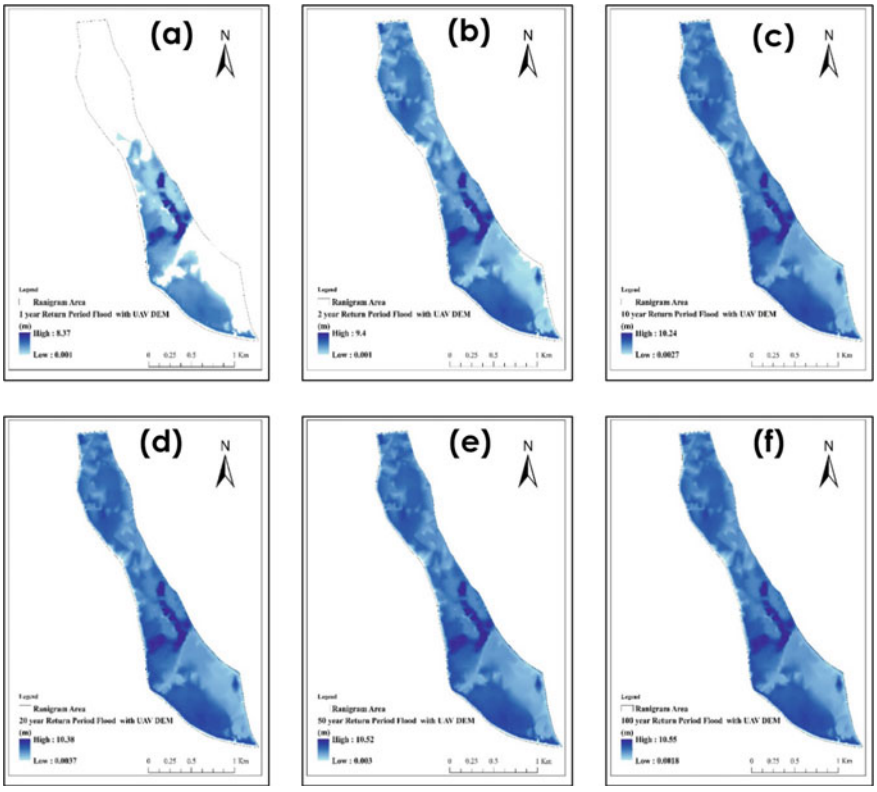

Fig. 15 Flood depth and extent maps for return periods of **a** 1 year, **b** 2 years, **c** 10 years, **d** 20 years, **e** 50 years and **f** 100 years in the Ranigram area

6 Conclusion

The flood in Ranigram area is found to be influenced almost entirely by the waters of the Jamuna River. Flooding in Ranigram increases with the corresponding increase in the Jamuna water levels and vice versa. The relation of floodwater level in the riverside area is linear and provides a good fit with the water level of the Jamuna River. The statistical equation can be useful in predicting the water levels at the gauge locations in the Ranigram area. A 2D hydrodynamic model with high-resolution DEM can represent a more accurate flood scenario at the local level. More field data frequency and UAV and survey bathymetry-based DEM can contribute to the accuracy level of the model. The flood maps representing arrival time, duration, and maximum depth and extent for the Ranigram area can be extracted from the hydrodynamic model. The flood information for any specific location of the floodplain can be obtained from the flood maps. This information can be helpful in flood risk and damage assessments and forecasting of floods in floodplain areas.

Acknowledgements Alhamdulillahi Rabbil Alamin. We praise and glorify the Lord, Allah Subhanahu wa taala, as He is ought to be praised and glorified. Authors would like to express gratitude to local NGO SHARP, Sirajganj for their cordial logistic support during field visit and data collection. This research is a part of the project "Community Resilience through rapid prototyping of flood proofing technologies in urban areas (CORE Bangladesh)" in the Urbanizing Deltas of the World-2 Program supported by The Netherlands Organization for Scientific Research (NWO) under project number W07.69.203.

References

Ali, Md.H., B. Bhattacharya, A.K.M.S. Islam, G.M.T. Islam, Md.S. Hossain, and A.S. Khan. 2018. Challenges for Flood Risk Management in Flood-Prone Sirajganj Region of Bangladesh. *Journal of Flood Risk Management* 12 (1): e12450. https://doi.org/10.1111/jfr3.12450.

Avinash, Shubha. 2014. Flood Related Disasters: Concerned to Urban Flooding in Bangalore, India. *International Journal of Research in Engineering and Technology* 03 (28): 76–83. https://doi.org/10.15623/ijret.2014.0328013.

BBS. 2016. Economic Census 2013—District Report: Sirajganj. Reproduction, Documentation & Publication (RDP) Section Bangladesh Bureau of Statistics, Bangladesh.

Biswas, Asit K. 2008. Management of Ganges-Brahmaputra-Meghna System: Way Forward. In *Management of Transboundary Rivers and Lakes*, 143–164. https://doi.org/10.1007/978-3-540-74928-8_6.

Brammer, Hugh. 2010. After the Bangladesh Flood Action Plan: Looking to the Future. *Environmental Hazards* 9 (1): 118–130. https://doi.org/10.3763/ehaz.2010.si01.

Farooq, Muhammad, Muhammad Shafique, and Muhammad Shahzad Khattak. 2019. Flood Hazard Assessment and Mapping of River Swat Using HEC-RAS 2D Model and High-Resolution 12-M Tandem-X DEM (Worlddem). *Natural Hazards* 97 (2): 477–492. https://doi.org/10.1007/s11069-019-03638-9.

FFWC. 2018. Annual Flood Report 2018. Processing and Flood Forecasting Circle, Bangladesh Water Development Board. Government of the People's Republic of Bangladesh.

Freund, Rudolf J., William J. Wilson, and Ping Sa. 2006. *Regression Analysis*, 2nd ed. Boston: Academic Press.

Hassan, Ahmadul, and Mohammad Aminur Rahman Shah. 2008. A Participatory Model for Flood Early Warning Dissemination. In *Third South Asia Water Research Conference On Innovative Modeling Approaches For IWRM*. Dhaka.

Islam, Sirajul, and Sajahan Miah. 2012. *Banglapedia: National Encyclopedia of Bangladesh*. Dhaka: Asiatic Society of Bangladesh.

Islam, Akm Saiful, Anisul Haque, and Sujit Kumar Bala. 2010. Hydrologic Characteristics of Floods in Ganges–Brahmaputra–Meghna (GBM) Delta. *Natural Hazards* 54 (3): 797–811. https://doi.org/10.1007/s11069-010-9504-y.

Jain, Sharad Kumar, Pankaj Mani, Sanjay K. Jain, Pavithra Prakash, Vijay P. Singh, Desiree Tullos, Sanjay Kumar, S.P. Agarwal, and A.P. Dimri. 2018. A Brief Review of Flood Forecasting Techniques and Their Applications. *International Journal of River Basin Management* 16 (3): 329–344. https://doi.org/10.1080/15715124.2017.1411920.

Jung, Younghun, Dongkyun Kim, Dongwook Kim, Munmo Kim, and Seung Lee. 2014. Simplified Flood Inundation Mapping Based on Flood Elevation-Discharge Rating Curves Using Satellite Images in Gauged Watersheds. *Water* 6 (5): 1280–1299. https://doi.org/10.3390/w6051280.

Khan, M. Shah Alam. 2008. Disaster Preparedness for Sustainable Development in Bangladesh. *Disaster Prevention and Management: An International Journal* 17 (5): 662–671. https://doi.org/10.1108/09653560810918667.

Mali, Vijay Kisan, B. Veeranna, Aditya Parik, and Soumendra Nath Kuiry. 2020. Experimental and Numerical Study of Flood Dynamics in a River-Network-Floodplain Set-Up. *Journal of Hydroinformatics* 22 (4): 793–814. https://doi.org/10.2166/hydro.2020.160.

Meire, Dieter, Liesbet De Doncker, Frederic Declercq, Kerst Buis, Peter Troch, and Ronny Verhoeven. 2010. Modelling River-Floodplain Interaction During Flood Propagation. *Natural Hazards* 55 (1): 111–121. https://doi.org/10.1007/s11069-010-9554-1.

Miller, James D., and Michael Hutchins. 2017. The Impacts of Urbanisation and Climate Change on Urban Flooding and Urban Water Quality: A Review of the Evidence Concerning the United Kingdom. *Journal of Hydrology: Regional Studies* 12: 345–362. https://doi.org/10.1016/j.ejrh.2017.06.006.

Mirza, M. Monirul Qader. 2002. Global Warming and Changes in the Probability of Occurrence of Floods in Bangladesh and Implications. *Global Environmental Change* 12 (2): 127–138. https://doi.org/10.1016/s0959-3780(02)00002-x.

Mondal, M. Shahjahan, A.K.M. Saiful Islam, Anisul Haque, Md. Rashedul Islam, Subir Biswas, and Khaled Mohammed. 2018. Assessing High-End Climate Change Impacts on Floods in Major Rivers of Bangladesh Using Multi-Model Simulations. *Global Science and Technology Journal* 6 (2): 1–14. https://zantworldpress.com/wp-content/uploads/2018/10/1.Mondal.pdf.

Rahman, Md. Mostafizur. 2015. Modeling Flood Inundation of the Jamuna River. M. Sc. thesis, Department of Water Resources Engineering, Bangladesh University of Engineering and Technology.

Rahman, Rezaur, and Mashfiqus Salehin. 2013. Flood Risks and Reduction Approaches in Bangladesh. In *Disaster Risk Reduction*, 65–90. https://doi.org/10.1007/978-4-431-54252-0_4.

Rahman, Rezaur, Anisul Haque, M. Shah Alam Khan, Mashfiqus Salehin, and Sujit Kumar Bala. 2006. Investigation of Hydrological Aspects of Flood-2004 with Special Emphasis on Dhaka City. Final Report, Institute of Water and Flood Management, Bangladesh University of Engineering and Technology, Dhaka.

Subramanya, K. 2008. *Engineering Hydrology*, 3rd ed. New Delhi: Tata McGraw-Hill.

Vaz, A. C. 2020. Coping with floods—the experience of Mozambique. 1st WARFSA/WaterNet Symposium: Sustainable Use of Water Resources, 1–2 November 2000, Maputo.

Yalcin, Emrah. 2020. Assessing the Impact of Topography and Land Cover Data Resolutions on Two-Dimensional HEC-RAS Hydrodynamic Model Simulations for Urban Flood Hazard Analysis. *Natural Hazards* 101 (3): 995–1017. https://doi.org/10.1007/s11069-020-03906-z.

Zeybek, Melis. 2018. Nash-Sutcliffe Efficiency Approach for Quality Improvement. *Journal of Applied Mathematics and Computation* 2 (11): 496–503. https://doi.org/10.26855/jamc.2018.11.001.

Co-creation of Flood Mitigation Technologies in Bangladesh to Strengthen Community Resilience

Nadia Nowshin, M. Shah Alam Khan, Hans Hakvoort, William Veerbeek, and Chris Zevenbergen

Abstract Most of the small- to medium-scale flood mitigation technologies in Bangladesh are planned, designed, and constructed in a top-down approach, ignoring the actual needs of the vulnerable communities and the appropriateness of the technology in the local context. This non-inclusive approach does not create ownership of the technology by the local communities and stakeholders, and undermines the sustainability of the technological solution. This paper presents the co-creation process and preliminary performance monitoring results of a few small-scale flood mitigation technologies implemented as pilots in the peri-urban area of Sirajganj, Bangladesh. Local communities, policy actors, and stakeholders were involved at various stages of planning, design, construction, management, and monitoring of these pilots. Sustainability scores of the technologies in their technical, economic, social, and environmental dimensions are assessed through a set of indicators. A comparative sustainability analysis of these technologies is performed based on the user experiences and expert opinions. It is concluded that successful technical performance and functional effectiveness, along with reasonable and fair costs, are the primary requirements for the sustainability of a flood mitigation technology to improve community resilience. This study also provides key policy recommendations for building community resilience in urban/peri-urban areas of Bangladesh to deal with flood risks.

Keywords Flood mitigation · Community resilience · Technology · Co-creation · Sustainable development

N. Nowshin (✉) · M. S. A. Khan
Institute of Water and Flood Management, Bangladesh University of Engineering and Technology, Dhaka, Bangladesh

H. Hakvoort · W. Veerbeek · C. Zevenbergen
IHE Delft Institute for Water Education, Delft, The Netherlands

© The Author(s), under exclusive license to Springer Nature Switzerland AG 2022

G. M. Tarekul Islam et al. (eds.), *Water Management: A View from Multidisciplinary Perspectives*,
https://doi.org/10.1007/978-3-030-95722-3_4

1 Introduction

Bangladesh is one of the largest floodplain and delta areas in the world and is highly vulnerable to floods due to its geographical location at the confluence of the Ganges, Brahmaputra and Meghna (GBM) rivers. The rapidly increasing population, the intensification of agriculture and the scale and dynamics of the river systems make floodplain management in Bangladesh a challenging task (Mirza 2003; Brammer 2004; Islam 2017). Although flooding is a natural process, human activities enhance the risks of flooding. Human activities that usually cause flooding include land use changes, clearance of vegetation, cultivation in steep slope areas, rapid and unplanned urbanization, poor design and maintenance of drainage system and settlement in floodplain areas (Sinthumule and Mudau 2019; Flower and Fortnam 2015; Kabir and Hossen 2019).

About 80% of Bangladesh is occupied by floodplain and is affected by river floods, rainwater floods and flash floods (Brammer 1990). Floodplains in Bangladesh are subject to riverine floods during the monsoon while the urban and peri-urban areas experience a combined effect of rainfall-induced floods and riverine floods. Flood damages become the most extensive when the three major rivers reach their peak stages at the same time. Rainfall-induced floods are caused by high-intensity local precipitation of long duration during the monsoon. It is projected that increased precipitation, higher transboundary water flows and sea level rise will increase the destructive power of monsoon floods in future, mainly in embanked areas (Dasgupta et al. 2011; Dewan et al. 2003). This will ultimately cause serious threats to the lives and livelihoods, particularly for the poor floodplain inhabitants and low income groups in urban and peri-urban areas (Sultana and Thompson 2019; Parvin et al. 2016).

Floods are the most widespread disaster risks to urban settlements of all sizes. According to the UN Office for Disaster Risk Reduction (UNDRR 2020), 4.03 billion people have been affected by floods over the last 20 years (2000–2019) due to the combined effect of population growth and climate change-induced sea level rise, storm surge, etc. The losses are expected to increase. To mitigate future losses, building flood resilience at the community level is an important component of an integrated flood risk management strategy that calls for measures that are customized to the local needs and often inspired by indigenous technologies (Keating et al. 2014).

Sustainable development as articulated in the ambitious UN agenda for global action on sustainable development calls for innovation. In developing countries, there is a growing recognition of the importance of experimentation and demonstration of local technological innovations at grassroots levels and marginalized communities, and to involve them in the innovation process (Smith et al. 2016; Goodman et al. 2017). Empowering local communities through their participation in flood management is an effective approach for successful flood governance practices over the long term. Additionally, sustainability needs to be considered during improvement

of flood resilience at local levels. Moreover, capitals should be utilized at community level through introduction of new, innovative and improvised technology, and enhancement of existing recovery practices of that community (Corsel 2015).

In Bangladesh, this particularly holds true for sustainable (or local) flood mitigation technologies where the communities also represent a significant market for small-scale entrepreneurs. Community stakeholders can help in finding an effective and sustainable intervention that matches each community's unique context and demand. Success crucially depends on the communities' involvement in the planning and decision-making processes, as well as on their engagement over the long term. Identifying the right interventions for boosting community resilience is only one part of the equation; other aspects include the local engagement in carrying them out (Deubelli 2019). Within this context, innovations in flood mitigation technologies often comprise of a process of incremental steps based on adjusting to existing, indigenous technologies, rather than on a radical new technology.

In general, the criteria for sustainable flood mitigation technology are: (i) technical and functional effectiveness, i.e., the capacity of measures to fulfill the primary function of risk management; (ii) economic sustainability, i.e., affordability; (iii) social sustainability, i.e., social acceptability; (iv) environmental sustainability, which assesses the impact of measures relative to all species, habitats and landscapes; and (v) institutional sustainability, which addresses the issue of governance (Edjossan-Sossou et al. 2014).

It follows from the above that the development of sustainable flood mitigation technologies should follow an inclusive co-creation process to effectively reduce flood vulnerability and to comply with long-term technical, economic and social goals (Montz and Grunfest 2002).

In this paper, we assess the sustainability of different flood mitigation technologies: Amphibious living unit, amphibious sanitation unit and retrofitted housing, etc. (for small- to medium-scale floods affecting local communities) by using a set of sustainability indicators (i.e., technical, social, economic and environmental) through a co-creation process in a demonstration site. The outcomes of the assessment have been used to develop policy recommendations for building community resilience in urban/peri-urban areas.

2 Study Area

Sirajganj district is one of the most vulnerable flood-prone areas of Bangladesh. Flood and water logging are some of the major disasters occurring in this area. The main cause of flooding in the area is the transboundary inflow from upstream catchment carried by the Jamuna River. Most of the *upazilas* are exposed to floods and subsequent river erosion. About 65% of the people of Sirajganj district are vulnerable to flooding (Rouf 2015).

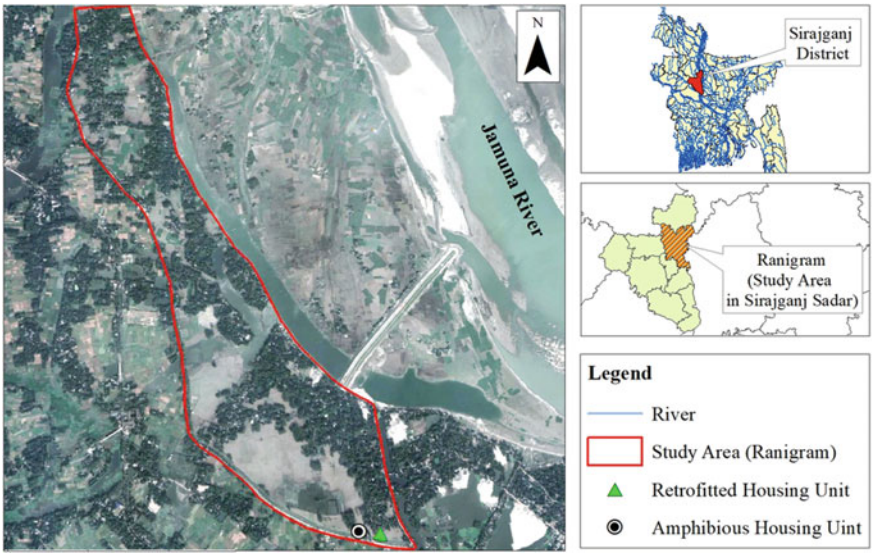

Fig. 1 Map showing the study area

The demonstration (pilot) site is located in Sirajganj (Fig. 1), one of the most flood-prone urban areas of Bangladesh. Yet this area is representative of the peri-urban regions in the floodplains of a large river, the Jamuna. Figure 2 shows the highest observed water level from 1984 to 2020 (37 years) in the Jamuna River at Sirajganj Station where the danger level is 13.35 m PWD. The figure shows that

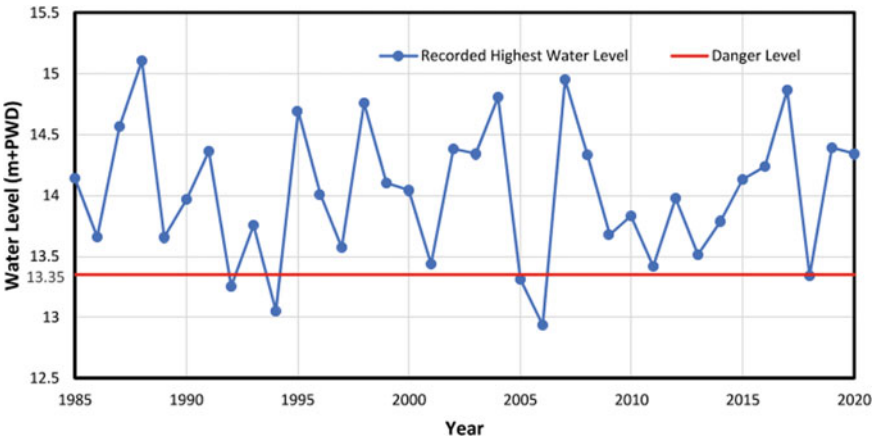

Fig. 2 Graph showing highest water lever in the Jamuna River at Sirajganj (*Source* Flood Forecasting and Warning Center, FFWC)

the water level crosses the danger level almost every year, except for the five years during this time period.

The study area is flooded for 140 days every year on an average which severely affects the local living condition and livelihoods (Fig. 3a). Since these areas face flood for almost five months per year, conducting normal year-round activities by the inhabitants of these floodplain areas is quite challenging. They face different types of socio-economic problems particularly during flood. Scarcity of pure drinking water has become acute in flood-affected areas as the tube-wells have been submerged.

Fig. 3 **a** Sirajganj Peri-urban area during flood, **b** amphibious living unit, **c** amphibious sanitation unit, **d** retrofitted house, **e** focus group discussion with user and manufacturer group, **f** local community participation during construction (*Source* CORE BD Team)

The inhabitants of the Sirajganj peri-urban area are involved in numerous low-paid income-generating activities such as day-laborers, carpenters, shop keepers, to name of a few. As they face flooding every year, they are trapped in a vicious cycle of poverty and hunger. During floods, the affected people have to put in all their efforts for managing food for survival. Due to the lack of savings, they can barely manage other basic needs and are forced to take personal loans that lead to more difficult conditions. Poor conditions during this period lead to various sicknesses, and they need to spend money for treatment purposes as well. They need pure and safe drinking water, ORS (oral rehydration solutions), sanitation facilities and non-food items (like *sari*, *lungi*, napkin/towel, mosquito net and lights at dark) along with emergency food support.

During the flood period, when water enters into the houses, the household belongings are completely damaged. Following the flood, they need to repair houses, sanitation units and other household commodities on a large scale. Due to the lack of savings, it is quite difficult for them to spend additional money for repairing their household items. Despite facing poverty, they have to repay this loan, which is a burden for them.

To study community resilience, specific households are selected from this area. Taking into account the vulnerabilities of the assigned households, this study offers three innovative small-scale flood mitigation technologies such as amphibious living unit (Fig. 3b), amphibious sanitation unit (Fig. 3c), and retrofitted house (Fig. 3d) in order to reduce the flood risks and enhance community flood resilience (CORE Bangladesh Project 2016).

3 Materials and Methods

Focus group discussions (FGDs) were conducted with users, manufacturers and flood-affected communities (Fig. 3e) to collect qualitative data and information. They shared their practical experiences during the construction period of these technologies and two flood periods (2019–2020) considering the social, economic and environmental governance and technical aspects. This qualitative information was converted to quantitative data by scores given on the basis of community feedback and the researcher's own perception and analysis. Finally, a comparative analysis was carried out to determine the performance and sustainability of the technologies. In addition, several meetings were carried out with different stakeholders, government officials and workshop owners. Workshops were conducted to exchange views between technology providers and the local community. Students from Sirajganj Polytechnic Institute participated in a design competition on the flood-proofed (amphibious) house. Moreover, the local community participated in the construction of the pilot flood-proofed houses (Fig. 3f).

Table 1 Stakeholder description and role

Stakeholder	Description	Role
Manufacturer	Dutch SMEs (flood mitigation technology providers), local mechanics and workshops, local construction material suppliers	Design and construction of the pilot technology, provide construction materials locally
Implementer	Netherlands Organization for Scientific Research, IHE-Delft, Bangladesh University of Engineering and Technology, Dutch SMEs	Financial, academic, research, technical and field support
User	Flood-affected community	Participated in planning, design and construction; provided land for pilot construction; provided local knowledge on flood processes and feasible options for mitigation
Policy maker	Local Government Engineering Department (LGED), Bangladesh Water Development Board (BWDB), Mayor (City Corporation), Union Parishad Chairman (UP Chairman), Local Leaders, Govt. Officials, Ward Commissioner, Socio-Economist and Technologist	Influence and implement flood mitigation policy at the local and national levels; adoption of the technology for up-scaling

3.1 Stakeholder Engagement

Stakeholders who had a role or interest in flood mitigation technology and community resilience were identified through extensive discussion, interviews and field visits. Some of these stakeholders were engaged with the research team from the inception; others were engaged at a later stage. The stakeholders were classified into four groups: Manufacturer, Implementer, User and Policy Maker on the basis of their activities and importance. Table 1 gives the descriptions and roles of these stakeholders.

3.2 Assessment of Resilience and Sustainability

Several flood mitigation technologies, i.e., amphibious living unit, amphibious sanitation unit, retrofitted house, etc., were introduced to test sustainability of flood mitigation solutions and to strengthen community resilience. The fundamental basis of this approach was to ensure co-creation of the technologies through a participatory process that would create ownership of the technologies and thus contribute to sustainability and resilience. Figure 4 shows the conceptual framework of this approach based on preliminary understanding of different factors that influence

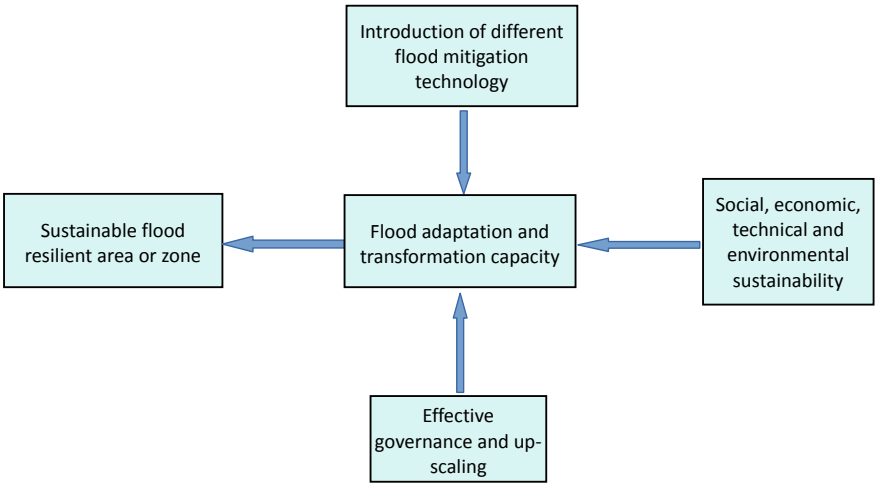

Fig. 4 Conceptual framework for resilience and sustainability of the co-creation process

sustainability and resilience. Subsequent verification and improvement of this framework and selection of indicators were carried out through a detailed discussion with stakeholders.

The framework shows that the adaptive and transformative capacities of the flood-affected communities are enhanced through the introduction of innovative and affordable technologies, effective governance and scaling up of these technologies. Scale up of these technologies will be ensured by proper governance and appropriate participation of policy actors in the decision-making process. The social, economic, technical and environmental sustainabilities of these technologies are important indicators that ultimately create the sustainable flood resilient area or zone.

3.3 Sustainability Dimensions and Indicators

Several indicators are selected to assess the sustainability of the flood mitigation technologies (Table 2). In this study, technical sustainability is considered as the most important dimension. The basic concept used here is that if a technology does not perform successfully, it will not sustain in the long run even if it is less expensive, socially acceptable and environment friendly. The order of importance of the other dimensions presented in Table 2 is determined with similar justifications.

Table 2 Sustainability indicators for different dimensions

Dimension	Indicator
Technical	Availability of local materials, availability of local labor, construction ability, technical performance, functional effectiveness
Economic	Return on investment, business agility, life-cycle costs, willingness to pay, employment, total capital cost, construction time
Social	Labor practices and decent work, society and customers, human health risk impact, acceptability to stakeholders, participation and responsibility of different stakeholders, wellbeing/happiness, quality of life, flexibility and adaptation
Environmental	Impact on environment, waste, material and resource (reusability and waste), pollution (land and water), impact of land use in ecosystem

3.4 Data Analysis

Flood mitigation technologies are evaluated in three steps. In the first step, a scoring scale is set for different sustainability indicators to evaluate the technologies. The scoring scale ranges from +2 to −2 (very good, good, neutral, bad and very bad), where positive and negative scores indicate favorable and adverse impacts of the technology, respectively.

In the second step, relative weights of the sustainability indicators are assigned on ad hoc basis (Canter 1996) based on public consultation and expert judgment. The weighted average score (I) (Eq. 1) for each alternative technology is determined for each domain (Technical, Economic, Social and Environmental) in this step.

$$I = \frac{\sum (W * \text{Score})}{\sum W} \tag{1}$$

where I = weighted average score, W = relative weight (Range: 1–3), and score = value assigned to each indicators on the basis of technical, economic, social and environmental performance of the technology based on information collected through field visits, focus group discussion (FGDs) and interviews.

Finally, the combined impact scores for the four dimensions are calculated to identify the best performing technology with respect to sustainability. In this step, relative weights of different dimensions are assigned based on unranked pair-wise comparison technique. Pair-wise comparison technique (unranked and ranked) for importance weighting basically involves a series of comparisons between decision factors or criteria. This technique allows the comparison of two criteria or factors at a time (Sims et al. 1991; Canter 1996; Elsheikh et al. 2015). In this study, this method compares two alternative choices which are expected to have independent impacts by ranking the parameters in pairs. Different combinations of the parameters are thus tested to find out the most influential parameter(s) and thus deciding on the relative weights (Canter 1996).

4 Results and Discussion

4.1 Evaluation of Alternative Technologies

Performance of these selected technologies are evaluated for the four dimensions, i.e., technical, economic, social and environmental.

The first technology is an amphibious living unit (Fig. 5a, b) which is built on an amphibious floating base where a special type of construction material (EPS—Expanded Polystyrene) is used. The house floats during flood and sits on a level ground after the flood water recedes.

The second technology is an amphibious sanitation unit (Fig. 5c, d). The floating base and technology in the sanitation unit are the same as in the amphibious living unit. This unit consists of two parts. The upper part is the toilet unit, while the lower part contains a constructed wetland (which filters the discharged wastewater by bioremediation) and a septic tank.

The third technology is a retrofitted house (Fig. 5e, f) in which a vertically-moving wooden floor is constructed as a floating base. PET (polyethylene terephthalate) bottles are used as the floating material in the wooden floor which moves up and down with the floodwater level.

Performance of these technologies are assessed through field visits, FGDs and interviews with the users and manufacturers. Scores and relative weights of the indicators are assigned in the four dimensions for each technology based on these interactions and expert judgment. Table 3 gives the weighted average scores of the technical indicators of sustainability for the amphibious living unit, amphibious sanitation unit and retrofitted house. For amphibious living unit, considering different advantages and disadvantages, the weighted average score is +0.6. Although the most important material, i.e., EPS is not locally available and is expensive, technically, however, the EPS base performed very well. The base floated immediately with the flood and perfectly set on the ground after the floodwater drained out. Since no anchor was in place initially, the EPS base needed some manual maneuvering to settle it down on the ground, although minor rolling was experiences. The local community and the manufacturers can build the superstructure easily. However, they need assistance to acquire the EPS and design the base. Moreover, EPS is found to degrade with prolonged submergence in water and rodent attack. Local manufacturers are able to repair the wooden frame, but are unable to replace the EPS blocks inside the frame. The superstructure remained stable and performed satisfactorily during the flood event. The users report a very high load-bearing capacity for this technology.

The weighted average score for the amphibious sanitation unit is −0.2. This score reflects the same difficulties with EPS as in the living unit, but also the additional difficulties with repair and maintenance. The superstructure and the appliances get damaged more rapidly, sometimes making it unusable. The local mechanics and plumbers are unable to fix these problems. The wooden superstructure is not suitable for the local weather and gets damaged rapidly.

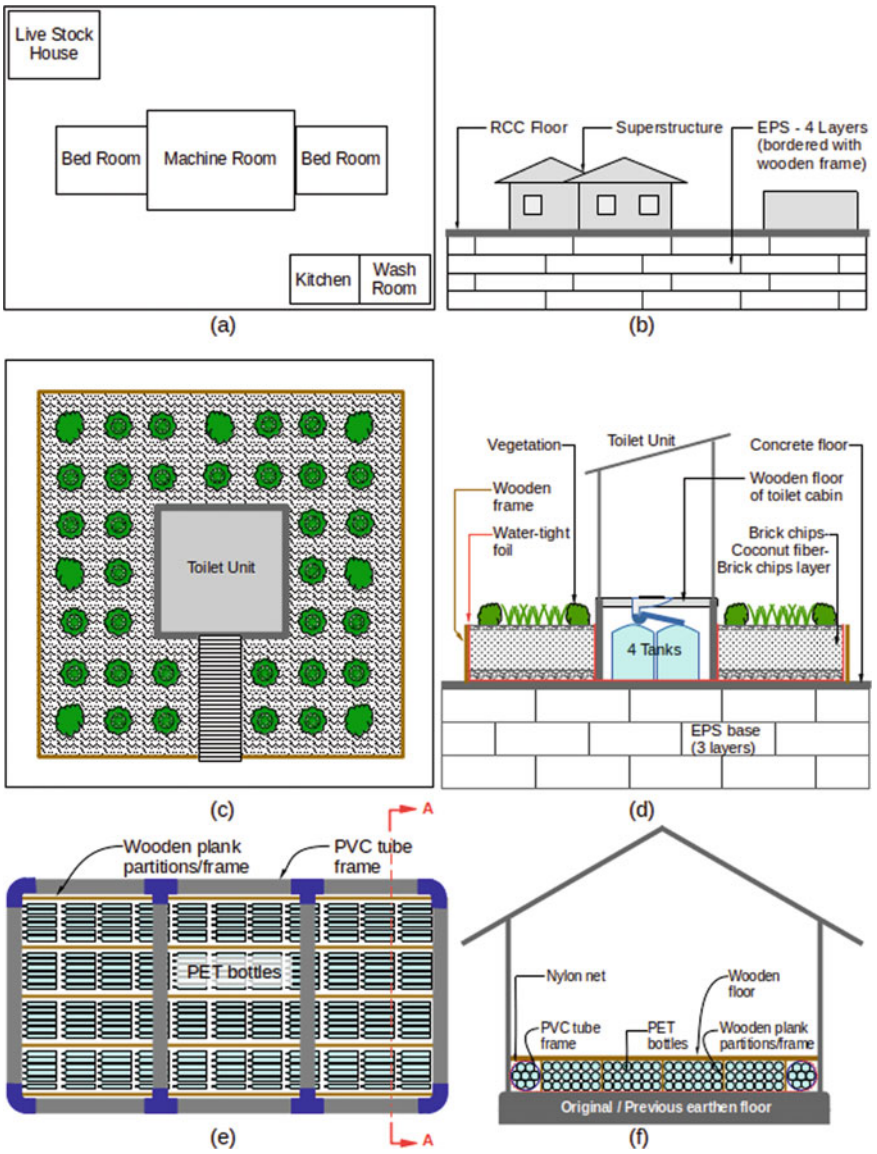

Fig. 5 **a** Schematic plan of amphibious living unit, **b** schematic elevation of amphibious living unit, **c** schematic plan of amphibious toilet unit with constructed wetland, **d** schematic section elevation of amphibious toilet unit with constructed wetland, **e** plan below the retrofitted wooden floor, **f** elevation of section A-A of retrofitted floor (*Note* All designs are not to scale)

Table 3 Weighted average scores for the **technical** indicators of sustainability

	Amphibious living unit			Amphibious sanitation unit			Retrofitted house		
Indicators	Relative weight (W)	Score	W * Score	Relative weight (W)	Score	W * Score	Relative weight (W)	Score	W * Score
Availability of local materials	1	−1.25	−1.25	1	−1.5	−1.5	1	2	2
Availability of local labor	1	1.25	1.25	1	−0.25	−0.25	1	2	2
Construction ability	1	−1.25	−1.25	1	−1.5	−1.5	1	1.25	1.25
Technical performance	2	1.65	3.3	2	1.65	3.3	2	1.8	3.6
Functional effectiveness	2	1.1	2.5	2	−0.75	−1.5	2	1	2
Σ(W) =	7			7			7		
Σ(W * Score) =	4.55			−1.45			10.85		
(Weighted average score) I_{Tech} =	0.6			−0.2			1.6		

Note On weighted average score: −2 to −1 = very bad; −1 to 0 = bad; 0 = neutral; 0 to +1 = good; +1 to +2 = very good

Local labor and local inexpensive material were used for the construction of the retrofitted house. The weighted average score for this technology is +1.6. The design and construction of this technology were much simpler compared to those of the amphibious units. The wooden floor floated perfectly with a reasonable load. Minimal obstructions were created during the vertical movement of the floor, which settled on the ground after floodwater drained out. No object was trapped under the floor. No major technical difficulties are reported for this technology. Minor technical problems occurred during the last two flood seasons, which were fixed by the users themselves. However, the users do not like the wooden floor, because it is visually unpleasant to them. They also reported infestation of insects inside the floor and a low load-bearing capacity of the floating base.

Table 4 gives the weighted average scores for the economic indicators of sustainability. The amphibious living unit has an economic score of +0.7 which is satisfactory/good. The users had to lose the land where they grew vegetables for extra income and household consumption. They used to sell their extra vegetables for around BDT 6,000 per year. Additionally, this technology is relatively expensive and not very suitable for the poor communities due to its high construction cost. On the other hand, this living unit saved the users from loss of household assets during the floods. The users moved all their valuables and perishable assets including cattle, looming machine, etc., to the amphibious house. The users are satisfied with the fact that they could operate their thread machine during floods, which is their primary source of livelihood.

Although the amphibious sanitation unit is constructed on the same land, the weighted average (economic) score for this technology is much lower (−0.6). The sanitation unit not only required a relatively high unit cost, but also high maintenance and repair costs, particularly during floods.

The economic weighted average score for the retrofitted house is +1.1. This score is in the range "very good" and results from the low construction cost as well as low maintenance and repair costs. The low cost is particularly appreciated by the poor flood effected community. However, the users were unable to keep their heavy looming machine on the wooden floor to continue their livelihood activities for about 1.5 months. The user used the floor as a storage space so no household items were damaged.

Although the amphibious living unit is quite expensive, this technology scores the highest (+1.305) in terms of social indicators of sustainability (Table 5). The reason behind the remarkable social acceptance is the high load-bearing capacity and technological flexibility; that is, it can be moved easily from one place to another during flood and can be set perfectly on the ground after flood. Moreover, this unit can be used in the charlands, flooded areas and water logged areas. The local community is very much interested in this technology. However, they would like to have this technology free of cost. Neighbors and relatives of the users stayed in this house and helped the users in the maintenance works. The only problem was the scarcity of drinking water. Since they were not affected by any waterborne diseases, they did not want to spend any money for water treatment. Various visitors, e.g., NGOs, LGED

Table 4 Weighted average scores for the **economic** indicators of sustainability

	Amphibious living unit			Amphibious sanitation unit			Retrofitted house		
Indicators	Relative weight (W)	Score	W * Score	Relative weight (W)	Score	W * Score	Relative weight (W)	Score	W * Score
Return on investment	1	−0.25	−0.25	1	−1.5	−1.5	1	0.75	0.75
Business agility	1	−2	−2	1	−2	−2	1	1.5	1.5
Life-cycle cost	1	−1	−1	1	0.25	0.25	1	2	2
Willingness to pay	2	2	4	2	0.875	1.75	2	0.5	1
Employment	1	1.25	1.25	1	0.75	0.75	1	1.5	1.5
Total capital cost	3	0.5	1.5	3	−2	−6	3	1	3
Construction time	2	2	4	2	0	0	2	1.375	2.75
Σ(W) =	11			11			11		
Σ(W * Score) =	7.5			−6.75			12.5		
(Weighted average score) I_{Eco} =	0.7			−0.6			1.1		

Note on weighted average score: −2 to −1 = very bad; −1 to 0 = bad; 0 = neutral; 0 to +1 = good; +1 to +2 = very good

Table 5 Weighted average scores for the **social** indicators of sustainability

	Amphibious living unit			Amphibious sanitation unit			Retrofitted house		
Indicators	Relative weight (W)	Score	W * Score	Relative weight (W)	Score	W * Score	Relative weight (W)	Score	W * Score
Labor practice and decent work	1	1.5	1.5	1	0.5	0.5	1	2	2
Society and customers	1	1.6	1.6	1	0.75	0.75	1	0.5	0.5
Human health risk impact	1	0	0	1	0.5	0.5	1	−1	−1
Acceptability to stakeholders	2	0.5	1	2	0	0	2	1	2
Participation and responsibility of different stakeholders	1	2	2	1	2	2	1	0.25	0.25
Wellbeing/happiness	1	1.25	1.25	1	0.5	0.5	1	2	2
Quality of life	2	1.5	3	2	0.5	1	2	1.25	2.5
Flexibility and adaptation	2	2	4	2	2	4	2	0.5	1
Σ(W) =	11			11			11		
Σ(W * Score) =	14.35			9.25			9.25		
(Weighted average score) I_{Soc} =	1.3			0.8			0.8		

Note On weighted average score: −2 to −1 = very bad; −1 to 0 = bad; 0 = neutral; 0 to +1 = good; +1 to +2 = very good

and people from faraway places, are increasingly coming to visit the living unit on a regular basis.

Although used by the same users, at the same location and having a similar technology, the amphibious sanitation unit scores +0.8 because of the difficulties and challenges in maintenance and repair due to the unavailability of expert electricians and plumbers locally. Visitors are curious also about this technology and appreciate this innovative technology and its usefulness. Public consultation indicates that the main social barriers for using this technology include congested toilet space, lack of privacy and malfunctioning of sewerage. In general, women are hesitant to use this unit, as it is placed at a higher ground and can be visible from a distance. Neighbors and the local community are very much interested in this technology, but they want this technology free of cost too. The users are happy to have this unit. However, they are not too comfortable using this unit as they are not completely satisfied with the use of the flushing mechanism and other unfamiliar systems. The toilet unit became electrified when rainwater entered the toilet unit. So they could not use the toilet unit when it was raining and was forced to use the regular toilets.

The retrofitted house scores +0.8 in terms of the social dimension. The users are happy to have this technology because at least they could save their household assets independently without bothering their neighbors. Their only demand is to strengthen this floor for more durability so they could keep more weight along with their looming/thread machine. However, the local community, neighbors, manufacturers or any government official/organization did not show any interest in this technology. Additionally, the user could not stay in this house during the last flood year (2020) because there is no attached toilet facility, and it is more difficult to access.

The amphibious living unit is located in an open environment that used to have many trees which attracted birds. Additionally, during the flood period, this location was the habitat for fish. Moreover, the users cultivated rice and vegetables during dry season. Construction of the amphibious unit changed this natural environment significantly. Although there is no direct wastewater discharge from the living unit, dumping of household wastes in the floodwater causes pollution. As a result of these considerations that followed a public consultation, the weighted average score of the environmental sustainability indicators is −0.3 (Table 6).

On the other hand, although the sanitation unit was constructed in the same location and caused the same environmental changes, the environmental sustainability score for this unit is +0.2. This higher score is due to the fact that the users and other respondents are satisfied with the way the wastewater discharge and environmental impacts are managed in this unit.

Construction of the retrofitted house did not cause any damage to trees or crops. The construction only modified the floor of an existing house. The main construction material is wood which is natural and environment friendly. The recycled plastic bottles used in the floor platform improved environmental pollution. However, there was some unpleasant odor emitting from the floor, specifically after the floodwater drains out. The users report infestation of the floor with insects and cockroaches.

Table 6 Weighted average scores for the **environmental** indicators of sustainability

	Amphibious living unit			Amphibious sanitation unit			Retrofitted house		
Indicators	Relative weight (W)	Score	W * Score	Relative weight (W)	Score	W * Score	Relative weight (W)	Score	W * Score
Impact on environment (positive/negative)	2	−2	−4	2	−2	−4	2	2	4
Waste (prevention of waste, recycling, disposal)	1	−2	−2	1	2	2	1	−1.5	−1.5
Material and resource (reusability and waste)	1	2	2	1	1.5	1.5	1	1.75	1.75
Pollution (land and water)	2	2	4	2	2	4	2	−1	−2
Impact of land use in ecosystem	1	−2	−2	1	−2	−2	1	1	1
Σ(W) =	7			7			7		
Σ(W * Score) =	−2			1.5			3.25		
(Weighted average score) I_{Env} =	−0.3			0.2			0.5		

Note On weighted average score: −2 to −1 = very bad; −1 to 0 = bad; 0 = neutral; 0 to +1 = good; +1 to +2 = very good

Considering these situations, the environmental sustainability score for the retrofitted house is +0.5.

4.2 Comparative Sustainability Analysis

Following the unranked pair-wise comparison method (Canter 1996), relative weights are assigned to each dimension of sustainability to calculate the combined sustainability score. The relative weights together define the overall sustainability score. In this study, for sustainability considerations, the technical performance was found to have preference over cost. For example, between two technology options, the option with a better technical performance could be selected to be more sustainable even if it is costlier. This results from the fact that the respondents placed higher importance (relative weight) on the technical indicators than the economic indicators.

Similarly, when two options or technologies have the same levels of technical and environmental performance, the option with higher economic advantage (cheaper) is selected even it has less social acceptability.

This concept is used in unranked pair-wise comparison method (Table 7) to fix the relative weights for different dimensions. This method compares the importance of a dimension/factor in relation to each of the other dimensions/factors. Total 10 pairs of comparison can be made among these 5 dimension/factors (4 dimensions + 1 dummy factor) because ${}^5C_2 = 10$. A weight of "1" indicates more important dimension/factor of a pair and "0" indicates a less important one. In this method, a factor-importance coefficient (FIC) of a factor or dimension is equal to the sum of all pair-wise assigned weights (S) divided by the sum of all weights (T1) for all dimensions/factors. A dummy factor is defined as that factor of each pair, deemed less important of the two, and acts as a "place keeper" to avoid skewness of the process (Canter 1996).

The technical dimension or the importance of sustainable flood resilience technology is considered the most important for sustainability and is assigned the highest weight, i.e., 40%. Long-term economic viability or the economic dimension is the next important dimension and is assigned a relative weight of 30%. This means that a technically feasible technology even with sound performance may not sustain if the long-term economic viability is very poor. With similar comparative considerations, 20% and 10% relative weights are assigned to the social and environmental dimensions of sustainability, respectively.

Finally, the combined sustainability scores for the three technologies are calculated by aggregating the sustainability scores (= relative weight * weighted average scores in Tables 3–6) determined for the four dimensions of sustainability (see Table 8). The retrofitted house is the most sustainable technology (score = +1.2), followed by the amphibious house (score = +0.7) and the sanitation unit (score = −0.1). The negative score for the sanitation unit indicates unsustainability of the technology.

Table 7 Unranked pair-wise comparison method for importance weight assignment

Factor/dimension	Assignment of weight										Row-wise sum (S)	Factor-importance coefficient FIC) = (S)/T1	Relative weight (RV) = (FIC*100) (%)
Social	0	0	1	1							2	0.20	20
Technical	1				1	1	1				4	0.40	40
Economic		1			0			1	1		3	0.30	30
Environmental			0			0		0		1	1	0.10	10
Dummy				0			0		0	0	0	0.00	0
Column total											T1 = 10	1	100

Note 1 = more important dimension/factor; 0 = less important dimension/factor

Table 8 Combined sustainability scores

		Weighted average score			Sustainability score		
Dimensions	Relative weight (RV) (%)	Amphibious living unit	Amphibious sanitation unit	Retrofitted house	Amphibious living unit	Amphibious sanitation unit	Retrofitted house
Technical	40	0.6	−0.2	1.6	0.243	−0.083	0.620
Economic	30	0.7	−0.6	1.1	0.205	−0.184	0.341
Social	20	1.3	0.8	0.8	0.261	0.168	0.168
Environmental	10	−0.3	0.2	0.5	−0.029	0.021	0.046
		Combined Sustainability Score			**0.7**	**−0.1**	**1.2**

4.3 Expert Opinion

Among different stakeholders, the technical and socio-economic experts provided very useful insights regarding the sustainability of these technologies. The experts agreed with the location selection and user group selection as well. As per the experts, these technologies are constructed in the safe zone. The real sustainability situation would be understood if these technologies faced extreme geographic or climatic conditions like near erosion-prone river banks, flash flood, cyclone, storm surge, strong wave, high tides, etc. The experts also expressed their concern over using costly and not easily obtainable foreign materials in the construction of amphibious units. They emphasized on inclusive design: local materials and feedback from local stakeholders. Technology transfer for local production can be initiated through government interventions (i.e., Dutch embassy, etc.). According to the experts, the toilet unit is the technology that is most in demand as it prevents pollution. But, it lacks easy access for elderly and other groups, and hence, some modifications regarding its capacity and access are suggested. As retrofitted house is constructed with local material, this technology is more feasible in terms of sustainability. For retrofitted house, reuse of plastic bottle is quite appreciable, as it reduces the problem of solid wastes. These plastic bottles are not exposed in direct sunlight. Therefore, no UV radiation occurred and no harmful elements were produced by the products. In addition to the introduction of these technologies, alternate employment opportunities need to be created simultaneously with existing livelihood through locally available capacity building programs. If the user group wants to avoid moving to shelter houses, they can build floating gardens, take on fish farming, etc., to keep them employed throughout the year. They can even construct a floating storage area to keep their agricultural production safe during floods.

4.4 Policy Recommendations

The following policy recommendations are made based on public consultation and the overall analysis and findings.

1. Any new intervention should be built based on the knowledge and technology that exists at the local level. This would ensure ownership and sustainability of the new technologies.
2. It is important to ensure participation of the local community of users, policy makers, skilled workers, and other stakeholders in the process of conceptualizing and constructing the pilot interventions. This would help develop ownership of the interventions and promote scale up of the technologies. Introducing ‘on the job’ technical education and training, investing in infrastructure that enables communities, and including access to information services, data, and the internet would help in this circumstance.

3. To ensure the sustainability of a technology, it is essential to understand the technical, economic, social and environmental complexities of improving and scaling up the technology in the backdrop of cultural and behavioral dynamics of the local context.
4. Needs' assessments would be conducted in consideration of social and political acceptability of changes, and incentives needed for behavioral changes.
5. BDP2100 should foster the inclusion of local level innovation in terms of ideas, regulations, governances and institutional reforms, stakeholder engagement, techniques and technologies; avoiding the trap of expecting conventional, large-scale engineering approaches to solely be able to cope with the future threats and ever changing demands.

5 Conclusion

This study conducted focus group discussions, workshops, meetings and interviewed the users, manufacturers and other local stakeholders in a peri-urban area of Sirajganj, Bangladesh, to assess the sustainability of some of the small-scale flood mitigation technologies that have been implemented. The combined sustainability of a technology is assessed by evaluating the indicators of the four dimensions of sustainability, i.e., technical, economic, social and environmental. Of the three technologies assessed, i.e., amphibious house, amphibious sanitation unit and retrofitted house, the retrofitted house is found to be the most sustainable technology. Based on public consultation, field observation and analysis of the collected data and information, it is concluded that successful technical performance and functional effectiveness are the primary requirement for sustainability of a flood mitigation technology to improve community resilience. In the technology adoption process, it is important to follow a co-creation approach where the stakeholders are engaged early on in the process so they have more ownership of the technology, are willing to pay for the technology, and are willing to co-invest to scale up and replicate the technology. Economic sustainability is the second requirement, which defines the communities' ability to afford the adoption of the technology. Social acceptability is another requirement which defines the quality of life, flexibility and adaptive capacity of the flood-affected community. The fourth, environmental sustainability, is important to assess the implementation of measures in relation to all species, habitats and landscapes.

It is essential to engage the local communities and relevant stakeholders including the local mechanics, small businesses and technical education institutions to ensure uptake, replication and scale up of the technology with appropriate modification in the local context.

In summary, this study suggests that efforts to boost community resilience and adaptive capacity would benefit from the sustainable development of flood mitigation technologies considering the technical, economic, social and environmental dimensions, and involvement of all relevant stakeholders in all stages of the process.

Acknowledgements Funding for the research leading to this article is provided by Netherlands Organization for Scientific Research, The Netherlands.

References

Brammer, Hugh. 1990. Floods in Bangladesh: Geographical Background to the 1987 and 1988 Floods. *The Geographical Journal* 156 (1): 12–22. https://doi.org/10.2307/635431.

Brammer, Hugh. 2004. *Can Bangladesh Be Protected from Floods?* Dhaka: The University Press Limited.

Canter, Larry W. 1996. *Environmental Impact Assessment*. Singapore: McGraw-Hill.

CORE Bangladesh Project. 2016. NWO. Accessed 19 May 2021. https://www.nwo.nl/en/projects/w-0769203.

Corsel, Denise. 2015. Addressing Worldwide Flood Concerns: Empowering Local Communities. MEI@75, June 15. https://www.mei.edu/publications/addressing-worldwide-flood-concerns-empowering-local-communities.

Dasgupta, Susmita, Mainul Huq, Zahirul Huq Khan, Md. Sohel Masud, Manjur Murshed Zahid Ahmed, Nandan Mujharjee, and Kiran Panday. 2011. Climate Proofing Infrastructure in Bangladesh: The Incremental Cost of Limiting Future Flood Damage. *The Journal of Environment & Development* 20 (2): 167–190. https://journals.sagepub.com/doi/10.1177/1070496511408401.

Deubelli, Teresa M. 2019. Flood Resilience Measurement for Communities: Boosting Community Resilience. Prevention Web, May 16. https://www.preventionweb.net/news/view/6549.

Dewan, A.M., Makoto Nishigaki, and Mitsuru Komatsu. 2003. Floods in Bangladesh: A Comparative Hydrological Investigation on Two Catastrophic Events. *Journal of the Faculty of Environmental Science and Technology, Okayama University* 8 (1): 53–62. http://ousar.lib.okayama-u.ac.jp/files/public/1/11503/20160527190938720714/008_053_062.pdf.

Edjossan-Sossou, A.M., O. Deck, M. Al Heib, and T. Verdel. 2014. A Decision-Support Methodology for Assessing the Sustainability of Natural Risk Management Strategies in Urban Areas. *Natural Hazards and Earth System Sciences* 14 (12): 3207–3230. https://doi.org/10.5194/nhess-14-3207-2014.

Elsheikh, Ranya Fadlalla Abdalla, Sarra Ouerghi, and Abdel Rahim Elhag. 2015. Flood Risk Map Based on GIS, and Multi Criteria Techniques (Case Study Terengganu Malaysia). *Journal of Geographic Information System* 7 (4): 348–357. https://doi.org/10.4236/jgis.2015.74027.

Flower, Ben, and Matt Fortnam. 2015. Urbanising Disaster Risk. Cambodia: People in Need Mission. https://www.preventionweb.net/files/submissions/47109_urbanisingdisasterriskreportinteractive.pdf.

Goodman, Jennifer, Angelina Korsunova, and Minna Halme. 2017. Our Collaborative Future: Activities and Roles of Stakeholders in Sustainability-Oriented Innovation. *Business Strategy and the Environment* 26 (6):731–753. https://doi.org/10.1002/bse.1941.

Islam, Mohammad N. 2017. *Living with Hazards*. Dhaka: University Grants Commission of Bangladesh.

Kabir, Md. Humayain, and Md. Nazmul Hossen. 2019. Impacts of Flood And Its Possible Solution in Bangladesh. *Disaster Advances* 12 (10): 48–57. https://www.researchgate.net/publication/336146425.

Keating, Adriana, Karen Campbell, Reinhard Mechler, Erwann Michel-Kerjan, Junko Mochizuki, Howard Kunreuther, JoAnne Bayer, Susanne Hanger, Ian McCallum, Linda See, Keith Williges, Ajita Atreya, Wouter Botzen, Ben Collier, Jeff Czajkowski, Stefan Hochrainer, and Callahan Egan. 2014. Operationalizing Resilience Against Natural Disaster Risk: Opportunities, Barriers, and a Way Forward. Zurich Flood Resilience Alliance. http://pure.iiasa.ac.at/id/eprint/11191/1/zurichfloodresiliencealliance_ResilienceWhitePaper_2014.pdf.

Mirza, M. Monirul Qader. 2003. Three Recent Extreme Floods in Bangladesh: A Hydro-Meteorological Analysis. *Natural Hazards* 28: 35–64. https://doi.org/10.1023/A:1021169731325.

Montz, Burrell E., and Eve Gruntfest. 2002. Flash Flood Mitigation: Recommendations for Research and Applications. *Global Environmental Change Part B: Environmental Hazards* 4 (1): 15–22. https://doi.org/10.3763/ehaz.2002.0402.

Parvin, Gulsan Ara, Annya Chanda Shimi, Rajib Shaw, and Chaitee Biswas. 2016. Flood in a Changing Climate: The Impact on Livelihood and How the Rural Poor Cope in Bangladesh. *Climate* 4 (4): 60. https://doi.org/10.3390/cli4040060.

Rouf, Tasnuva. 2015. Flood Inundation Map of Sirajganj District Using Mathematical Model. MSc. Thesis, WRE, BUET. Accessed 19 May 2021. http://lib.buet.ac.bd:8080/xmlui/handle/123456789/966.

Sims, Lynn O., Robert C. Knox, and Larry W. Canter. 1991. Protocol for Selecting an In-Tank Leak Detection Device. *International Journal of Environmental Studies* 39 (3): 163–176. https://doi.org/10.1080/00207239108710692.

Sinthumule, Ndidzulafhi I., and Ntavheleni V. Mudau. 2019. Participatory Approach to Flood Disaster Management in Thohoyandou. *Jàmbá: Journal of Disaster Risk Studies* 11 (3): a711. https://doi.org/10.4102/jamba.v11i3.711.

Smith, Adrian, Mariano Fressoli, Dinesh Abnol, Elisa Arond, and Adrian Ely. 2016. *Grassroots Innovation Movements.* London and New York: Routledge. https://www.taylorfrancis.com/books/mono/10.4324/9781315697888/grassroots-innovation-movements-adrian-smith-mariano-fressoli-dinesh-abrol-elisa-arond-adrian-ely.

Sultana, Parvin, and Paul Thompson. 2019. Livelihoods in Bangladesh Floodplains. In *Oxford Research Encyclopedia of Natural Hazard Science*. New York: Oxford University Press. Accessed 19 May 2021. https://doi.org/10.1093/acrefore/9780199389407.013.258.

UNDRR. 2020. Dramatic Rise in Climate over Last Twenty Years. UN Report. Accessed 21 June 2011. https://www.preventionweb.net/news/view/74121.

Urban Waterlogging Risk Profiling: The Case of Khatunganj Wholesale Commodity Market, Chattogram

Tasnim Alam Nishat, Dewan Salman Sunny, Rifat Talha Khan, Md.Reaz Akter Mullick, and Piyal Datta

Abstract Khatunganj, a busy trade region extending across an area along the Chaktai canal in Chattogram, has been severely affected by recurrent inundation for the last few years. The presented study used a reproducible methodology to develop a risk and vulnerability profile of Khatunganj connecting waterlogging with climate change scenario. For hydrologic-hydraulic modeling purpose, a model was set up on SWMM numerical modeling platform to simulate the discharge and water level at different points of the canal. Nine different scenarios of rainfall events were considered, where one actual rainfall event was taken, and the remaining scenarios were considered as design rainfall events. Using an inundation pattern combined with three other factors, namely, proximity to canal, structure type, and land use type of the area, the vulnerability of the area was assessed. Vulnerability of 224 households was calculated for low, average, and medium rainfall using the Household Sector Approach in ArcGIS. Analyses of the nine scenarios showed that even a 50% decrease in rainfall will generate a water level of 3.09 m to 3.84 m, whereas the elevation level of Khatunganj main road is between 2.9 m and 3.1 m. Results found that 27, 30, and 71 structures are very vulnerable at the time of low, medium, and high rainfall, respectively.

Keywords Khatunganj Commercial Area · Design rainfall · Flood inundation · Vulnerability · Risk profile

1 Introduction

Urban waterlogging refers to the phenomenon when a short duration intense rainfall event surpasses the urban drainage capacity and causes an adverse waterlogged situation (Xue et al. 2016). Rapid urbanization accelerates the change of urban land surfaces, typically by diminishing ecological land and expanding the impenetrable cover regions, which keeps water from penetrating into the soil (Deng et al. 2020).

T. A. Nishat · D. S. Sunny · R. T. Khan · M. A. Mullick (✉) · P. Datta
Department of Civil Engineering, Chittagong University of Engineering and Technology, Chittagong, Bangladesh
e-mail: reazmullick@cuet.ac.bd

© The Author(s), under exclusive license to Springer Nature Switzerland AG 2022

G. M. Tarekul Islam et al. (eds.), *Water Management: A View from Multidisciplinary Perspectives*,
https://doi.org/10.1007/978-3-030-95722-3_5

Another reason for urban waterlogging is heavy shower in urban areas, which is a result of intensified heat island effects occurring in recent years (Miller et al. 2014; Alexander et al. 2019). Most climate models and empirical evidence in the twenty-first century demonstrate that as the climate gets warmer, atmospheric water vapor increases, resulting in more intense and frequent precipitation events, which are likely to exacerbate the current drainage congestion scenario (Berndtsson et al. 2019). Following heavy rain showers, flash floods on urban streets and protracted flooding of low-lying areas have become a pervasive problem in various cities of Bangladesh, particularly in the port city and commercial capital of Chattogram. Chattogram makes significant contributions to the national economy, generating 40% of the country's industrial output, 80% of its international trade, and 60% of government revenue (E. Kabir 2016).

Khatunganj is the primary wholesale market for daily commodities in Chattogram and is vital not only for the economy of the city, but also for the entire national economy (Chowdhury 2011). Khatunganj was originally developed to serve as a business hub as it is situated at the bank of Chaktai canal, which was the gateway to inner land from the Chattogram Port. However, Khatunganj has been subject to severe waterlogging problem for about one and a half decades till date. Khatunganj traders reported suffering from excruciating costs due to waterlogging, as their storage of raw commodities is often destroyed. A very short duration rainfall results in waterlogging in all the alleys of this crowded market area (Quddusi 2017). Traders in Khatunganj suffered direct financial losses of around $60 million last year solely due to waterlogging (Barua 2021). The waterlogging problem at this wholesale market appears to have barely been resolved by the city managers and policy makers. Very little has been done to conduct a scientific study to assess the economic impacts of the current waterlogging scenario.

Researchers have introduced a range of different risk assessment methodologies for waterlogging. Peng-zhu et al. (2000) produced Hydrologic and Hydraulic (H&H) models for different precipitation frequencies and showed flood inundated conditions with geomorphologic classification mapping for the Lake Taihu region in China. The Hydrologic and Hydraulic model (H&H) in the watershed catchment is used to simulate flood, and to thereby evaluate the impacts of urban development and the effectiveness of watershed management (Nayeb Yazdi et al. 2019). The Storm Water Management Model (SWMM) is widely used in H&H in urban areas because it has shown the capability to simulate conveyance systems even in very small-scale (2 hectares) urban contexts (Nayeb Yazdi et al. 2019; Wanniarachchi and Wijesekera 2012). Jang et al. (2007) explored the suitability of SWMM as an urban hydrology modeling tool for post-development scenario development. Using hydrological modeling and GIS spatial analysis, Quan (2014) created a paradigm for waterlogging risk assessment under six hypothetical scenarios. The concept of multi-scenario analysis has piqued interest in waterlogging research in recent years. Its objective is to evaluate the different risks posed by a hazard, as well as the individual hazard intensity assigned to each aspect (Shi et al. 2010). For the Jing'an District of Shanghai, China, Yin et al. (2011) performed a scenario simulation to evaluate the risk of small-scale urban waterlogging disasters across various return

periods. Several other studies have applied the scenario analysis method to evaluate the risk of waterlogging (Dutta et al. 2003; Oliveri and Santoro 2000; Kleist et al. 2006). Several studies also argued that climate change has been a contributing factor to flood risk by raising the precipitation amount much higher than the average annual rainfall (Fleming et al. 2012; Hirabayashi et al. 2010). However, the severity of waterlogging hazard is only one of the factors that determine water risk and vulnerability. Other variables such as exposure play a part in risk profiling as well. When flooded land does not contain any components, there are no risks since zero exposure equals zero risk. Therefore, there is a need to evaluate exposure by modeling inundation degree for different scenarios (Shi et al. 2010). Han et al. (2006) carried out a research, where road exposure was evaluated using scenario simulation.

It is evident that the entire Chattogram city is faced with the problem of waterlogging every year. But a long-term solution for the overall city will only prolong the sufferings. Rather, an integrated solution based on a priority area can be effective and economically beneficial in the short term. Since the market at Khatunganj is of the wholesale kind, the stock is massive in general, and businessmen hardly get any time to transfer their products to a safe custody at the onset of waterlogging. The retail price of daily products in and around Chattogram city increases as an indirect effect. However, an intensive study on this prime location can prevent the loss of millions of dollars every year. Therefore, this study attempts to provide an answer to the research question: 'What is the extent of the inundation problem due to different rainfall scenarios and what would be the risk map of Khatunganj due to urban flooding considering climate change?'. Three objectives have been formulated to answer the research question-

1. To develop Hydrologic and Hydraulic model to simulate discharge and water level at Khatunganj from various rainfall and tidal scenarios.
2. Develop a methodology for waterlogging risk and vulnerability assessment with climate change scenarios and
3. To develop a risk and vulnerability profile of Khatunganj in relation to waterlogging with climate change scenario.

2 Study Area

Khatunganj is situated in the eastern part of the Chattogram city, alongside the famous Chaktai canal. This is the location where the Chaktai canal opens to the Karnafuli River. The geographic location of Khatunganj is at 22.330N and 91.840E. It is located at Ward No. 35 of Chattogram City Corporation. It is a relatively low-lying area within the city, situated only 3 m above the sea level. The temperature in the area has been found to vary from 14.5 to 39.3 ˚C during the monsoon season over the period of 1950–2002 (Nasher and Uddin 2015). Chattogram experienced a mean rainfall of 16 mm at dry season, 444 mm at pre-monsoon, 1857 mm at monsoon, and 267 mm at post-monsoon, for the period of 1949 to 2011 (Hasan et al. 2014). The city is located beside the Karnafuli River which is semi-diurnal in nature. Tidal ranges from chart

datum (ISLWL-Indian Spring Low Water Level which is 1.673 m below mean sea level) are 1.5 m–5.5 m (above ISLW) at Patenga, 1.5 m–4.8 m (above ISLWL) at Khal No. 10, and 1.2 m–4.2 m (above ISLW) at Sadarghat (S. M. I. Kabir and Ali 2017). Khatunganj is located at the downstream part of Murarpur-Bahaddarhat sub-catchment. The whole area becomes flooded following a period of extensive rainfall, as Chaktai canal cannot hold the water flowing from upstream (Fig. 1).

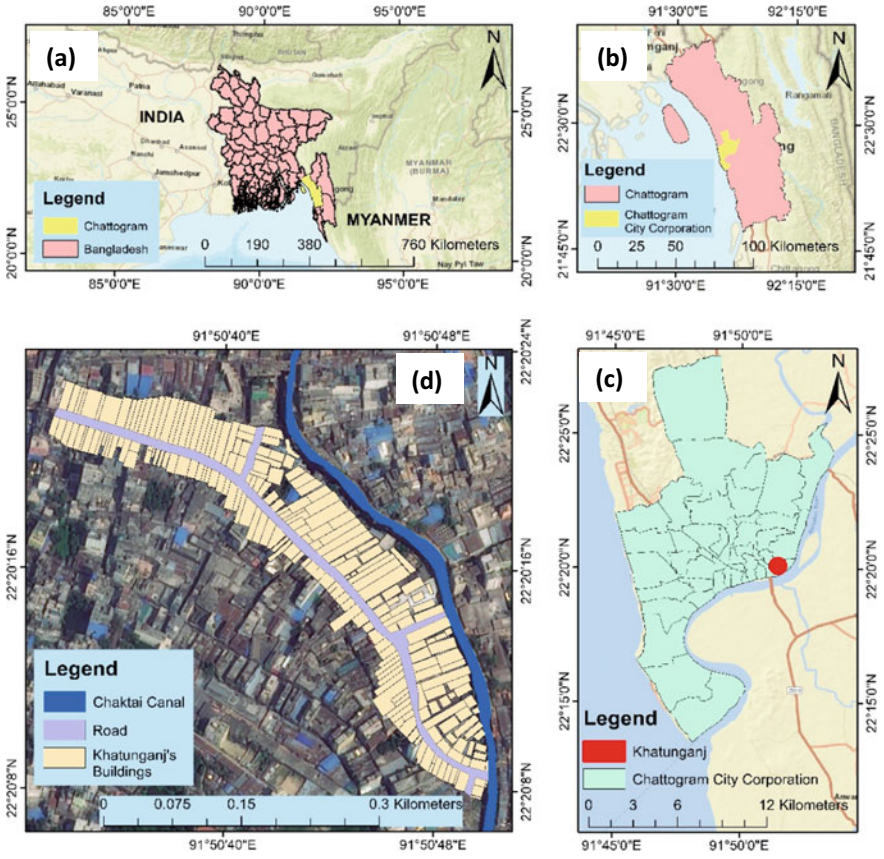

Fig. 1 **a** Bangladesh within world map; **b** Location of Chattogram within Bangladesh; **c** Chattogram City Corporation; **d** Location map of Khatunganj and Chaktai Canal in Chattogram

3 Methodology

3.1 Preparation of Digital Elevation Model (DEM)

Hydrologic processes and water resource issues are commonly investigated by using distributed watershed models. These watershed models require physiographic information such as configuration of the channel network, location of drainage divides, channel length and slope, and sub-catchment geometric properties. These parameters are usually gathered from secondary maps or field surveys. During the last two decades, this information is generally acquired directly from digital topographic representation, which is called 'Digital Elevation Model (DEM)' (Jenson and Domingue 1988).

Digital data generated by this approach also has the advantage that Geographic Information Systems (GIS) can easily import and analyze these data. The technical advancements made by GIS and the growing availability and quality of DEMs have greatly expanded the scope for application of DEMs to many hydrologic, hydraulic, water resources, and environmental research (Jenson and Domingue 1988).

Since the study site is not very large, a fine-scale Light Detection And Ranging (LiDAR)-generated DEM, preferably 0.5 m × 0.5 m, was required and was used for this study. ArcGIS 10.8 and ArcScene 10.8 were used to prepare and visualize the Digital Elevation Model (DEM), respectively.

3.2 Preparation of Digital Surface Model (DSM)

Digital Elevation Models (DEMs) have diverse and well-documented applications including visual impact assessment, hydrological modeling, flood prediction, and site suitability analysis. Automated elevation model creation from remotely sensed data may provide a representation of both the ground surface and the objects on that surface (Burrough et al. 1998). Digital Surface Models (DSMs) provide the option of extracting surface elevations to leave the surface DEM on the ground. This separation of over-surface feature information from ground information can provide a useful combination of data sets for many applications in the urban world. For example, comprehensive knowledge of ground surface elevation is necessary to predict flood inundation and the possible effects of sea-level rise, whereas a comprehensive model of man-made structures that will be impacted as a result is important for land owners, planning authorities, and insurance companies. Since the study site is not very large, a fine-scale LiDAR-generated DSM, preferably 0.5 m × 0.5 m, was used. ArcGIS 10.8 was used to produce Digital Surface Model (DSM), and ArcScene 10.8 was used to visualize it.

3.3 Watershed Analysis

Watershed or catchment delineation was carried out for the entire basin containing the Khatunganj sub-catchment. A watershed is the land area that drains water to the outlet (Chaktai canal) during a rainstorm. It is simply an area that drains surface water from high elevation to low elevation. For delineation of the catchment boundaries, at first, the drainage network was identified from field visits to the study site and its surrounding areas. The drainage network was then drawn in ArcGIS by manipulating the Aster 30 m resolution DEM using hydrological tools in ArcGIS. DEM filling function was performed to avoid irregular stream/drainage networks. For showing the direction of water flows out of each cell of a filled elevation raster, the flow direction tool was used. The flow accumulation tool was employed to tabulate the accumulated flow as the accumulated weight of all cells flowing into each downslope cell in the output raster. Stream networks were derived from a flow accumulation raster. Finally, raster data was converted to vector data and overlaid on satellite image for verification.

3.4 Hydrologic and Hydraulic Modeling

The Storm Water Management Model (SWMM), established by the US Environmental Protection Agency (EPA), is used to set up hydraulic models. The model simulates hydrologic response in dendritic watershed. A hydrological model can be described as a set of equations, which help to estimate runoff as a function of the various parameters used to describe the characteristics of the watershed. To estimate the extent and depth of inundation due to a specific storm, hydrologic and hydraulic modeling is required. Rainfall, basin characteristics, infiltration losses, calibration data, and different human effects are regarded as the data required for hydrological modeling. Cross section of the Chaktai canal at 89 points (Fig. 2), water level of Chaktai outfall for the year 2017, and discharge of Chaktai outfall for 3 months (June, July, and August) of 1983 were collected from Centre for Environment and Geographic Information Service (CEGIS). Rainfall data (1980–2017) for Chattogram was obtained from the Meteorological department (BMD).

To simulate the rainfall-runoff scenario, the Soil Conservation Service (SCS) curve number method was used for infiltration loss. Curve number of each basin was collected from Mishra and Singh (Mishra and Singh 2013) according to the relevant soil group (as presented in Fig. 3) and imperviousness (Fig. 4). The SCS unit hydrograph has been used to transform precipitation excess to direct run-off. In this regard, lag time (min) was required for the transform method and following equation was used to calculate the lag time (Hour),

$$\text{Lag time}(h) = \frac{2.587 \times L^{0.8} \times \left(\frac{1000}{\text{CN}} - 9\right)^{0.7}}{1900 \times H^{0.5}} \tag{1}$$

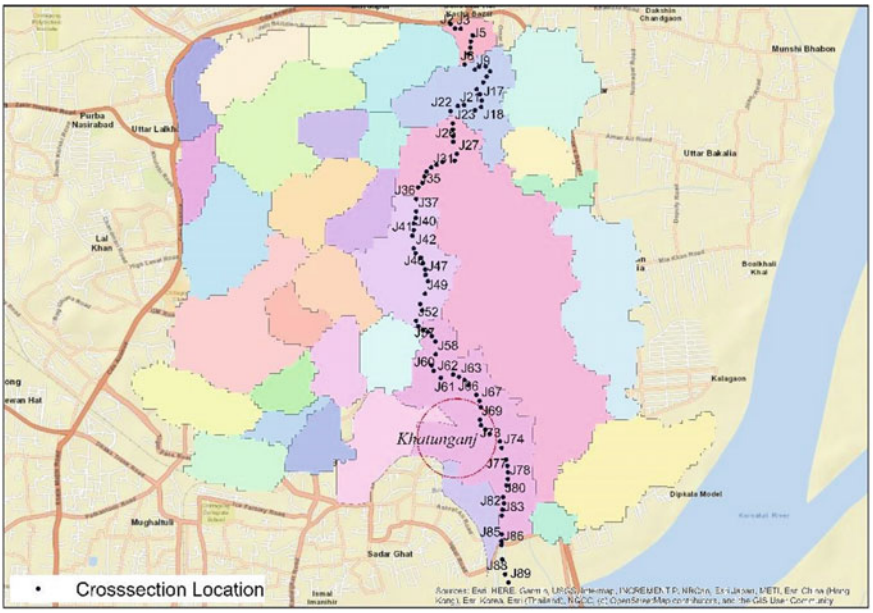

Fig. 2 Muradpur- Bahaddarhat basin with sub-catchments and cross-section points of Chaktai khal

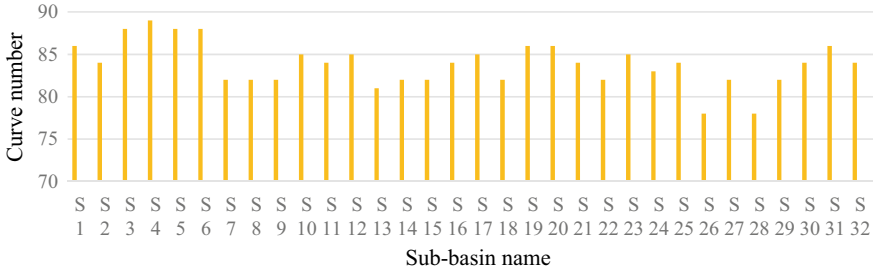

Fig. 3 Curve number of Muradpur-Chawkbazar basin

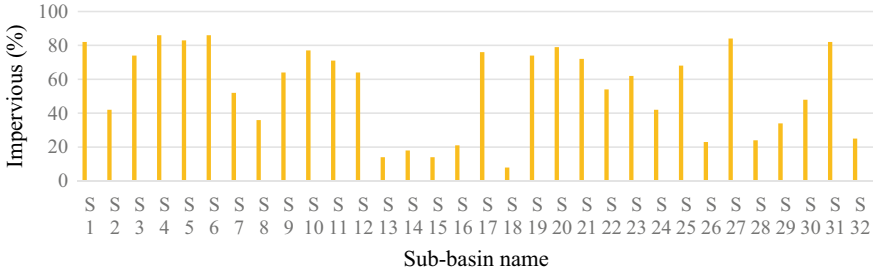

Fig. 4 % Imperviousness of Muradpur-Chawkbazar basin

Where, L = Hydraulic watershed length in meter = $110 \times A^{0.6}$;
A = Sub-catchment area in hectare;
CN = Curve number;
H = Average sub-catchment land slope in percentage.

Average sub-catchment land slope was calculated from DEM using ArcGIS interface. Due to lack of data availability, base flow was not used. Since most of the areas in the basins are urbanized and impervious, interception and surface method were also not used. Since the durations of the rainfall and resulting runoff events are relatively short, and the events mostly happen in the rainy season with highly humid conditions, evaporation losses are very low and are considered to be negligible (Schwab et al. 1993).

The model was run with an actual rainfall event i.e., the maximum rainfall event in 2017 on 05 July, and also simulated with a number of design rainfall events. The Rainfall Intensity-Duration-Frequency (IDF) curve has been used in this study to create the design of rainfall events. IDF curves graphically represent the amount of water that falls in a catchment within a given period of time. The following IDF relationship (Fig. 5) was used to extract the design rainfall events. IDF equation is based on the rainfall for the years 1980–2017 in Chattogram and follows the following equation.

$$\text{Rainfall intensity(mm/hr.)} = \frac{776.24 \times Tr^{0.217}}{Td^{0.563}} \tag{2}$$

where,
T_r = Return period in year;
T_d = Rainfall event duration in hour.

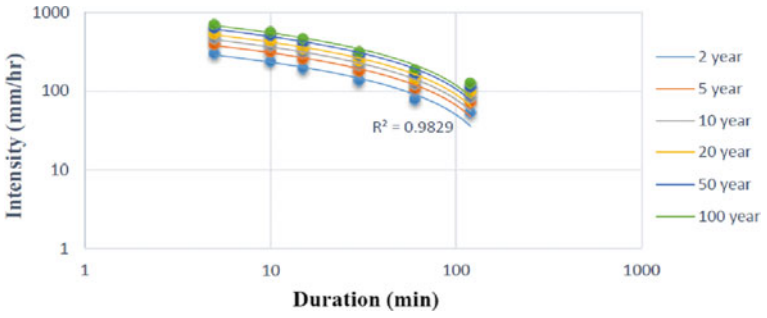

Fig. 5 IDF Curve of Chattogram City by Hershfield Method

Several scenarios with different critical design storms based on IDF analysis were generated using equations obtained from literature. The following scenarios have been considered:

1. **Scenario 1**: Max rainfall event in 2017 distributed over 24 h (Actual rainfall event scenario)
2. **Scenario 1 (A):** Max rainfall event in 2017 (2-h, High Tide)
3. **Scenario 2**: 2-h 20-year return period rainfall (High Tide)
4. **Scenario 3**: 2-h 50-year return period rainfall (High Tide)
5. **Scenario 4**: 2-h 50-year return period rainfall (Low Tide)
6. **Scenario 5**: 2-h 50-year return period rainfall (considering 50% rainfall decrease) (High Tide)
7. **Scenario 6**: 2-h 50-year return period rainfall (considering 50% rainfall decrease) (Low Tide)
8. **Scenario 7**: 6-h 50-year return period rainfall (High Tide)
9. **Scenario 8**: 2-h 50-year return period rainfall (considering Climate change 11% rainfall increment)

The resulting runoff from the hydrologic models of various sub-catchments was routed through the nodes, and conduits were added in the SWMM model. The cross-section properties of the conduits were selected as irregular shaped, and relevant data obtained from the bathymetric survey conducted by CEGIS was given as input. Dynamic wave routing and unsteady flow equations were used in simulating the model. The Manning's roughness coefficient, n-value was taken as 0.01. At the outlet, the boundary condition was set as 4.25 m water level (WL), based on the highest tide WL in the year 2017 due to water level data being available only for that year. To incorporate the scenario of climate change-induced sea-level rise, a 0.60 m rise was estimated (Ministry of Foreign Affairs of the Netherlands 2019), and 4.85 m WL was used to include the climate change scenario.

The entire catchment has been considered for hydrological modeling, and no boundary condition was imposed to the model. However, water level at the outfall of Chaktai canal has been used as the downstream boundary condition. The high and low tide condition water levels at the Chaktai outfall are considered as maximum and minimum boundary level. The WL is taken as 4.5 m and 1.5 m for high and low tide conditions, respectively, based on the tide chart published by the Chittagong Port Authority.

3.5 Inundation Maps

Inundation scenarios were illustrated using the simulation tool of ArcScene 10.8. DEM of a rectangular area covering Khatunganj was taken in ArcScene. 'Floating on a custom surface' was activated at 'Base Height' in 'Properties' of Arcscene. A blue color polygon was assigned to represent the inundation. At 'Animation Manager', a total of 13 keyframes were taken, out of which 11 keyframes represent the 11

inundation scenarios. The other two keyframes represent the starting and ending of the simulation. Again at 'Animation Manager', in the Translation:Z field of each keyframe, elevation values were set according to the water levels of the different rainfall scenarios. The simulation was run (simulation time was 48 h for Scenario-1 and 24 h for rest of the scenarios), and scenarios were exported in JPEG format.

3.6 Vulnerability and Risk Assessment

Under different hypothetical precipitation scenarios, the risk potential in Khatunganj is simulated using GIS. Vulnerability can be defined as the degree to which a system is susceptible to, or unable to cope with, unfavorable climate change impacts, such as climate variability and extremes. It is determined by the character, magnitude, and rate of climate change to which a system is subjected to, as well as the sensitivity and adaptive capacity of that system (IPCC 2001).

Four criteria were chosen to determine the vulnerability of Khatunganj to flooding caused by different rainfall scenarios. The four criteria are plinth level of the structure, proximity to Chaktai canal, structure type (kacha, pucca, or semi-pucca), and land use pattern.

Table 1 shows the respective weightages under each criterion of vulnerability.

Normalization of input data of each criterion is done using the following equation:

$$X_{\text{norm}} = \frac{X - \min(X)}{\max(X) - \min(X)} \tag{3}$$

Here, X is the criterion of vulnerability. The equation used to calculate vulnerability index for each structure was:

Table 1 Weightages for each criterion of vulnerability

Plinth	w	Proximity	w	Structure Type	w	Land Use	w
3 ft (1 m) below	6	1.05 m<	1	Paved (pucca)	1	Residential	1
2 ft (0.6 m) below	5	0.70 m–1.05 m	2	Semi-paved (semi-pucca)	2	Community Service	1
1 ft (0.3 m) below	5	0.35 m–0.70	3	Tin shed (kacha)	3	Mixed Use	2
Road level	4	0 m–0.35	4			Service Activity	2
1 ft (0.3 m) above	3					Manufacturing and Commercial activity	3
2 ft (0.6 m) above	2						
3 ft (1 m) above	1					Commercial activity	3

$$\text{Vulnerability} = \frac{\sum_{i=1}^{n} W_i X_i}{n} \tag{4}$$

Here, X is the criterion of vulnerability, W is the weight of individual criterion, and n is the number of criteria. The equation has been adopted and modified from the Household Sector Approach of Leon and Carlos for this research (Léon and Carlos 2006).

$$\text{Vulnerability} = (\text{Plinth} + \text{Proximity} + 0.8^{*}\ \text{Land Use} + 0.8^{*}\ \text{Structure Type})/4 \tag{5}$$

Weights of the criteria were given as per expert opinion.

A total of 224 structures were identified at the study site, and for each of the three flood scenarios of vulnerability analysis, these structures were classified into four classes of vulnerability: not vulnerable, less vulnerable, medium vulnerable, and very vulnerable.

For risk profiling, three categories have been documented—low rainfall which is lower than normal and it is 50 mm per day of hypothetical rain that creates up to 2.8 m water level; average rainfall that causes up to 3.5 m water level; and heavy rainfall that generates more than 3.5 m water level from the datum (the sea level).

Table 2 represents an overview of datasets used for the study and their collection sources, and Fig. 6 depicts a methodological flowchart.

Table 2 Data used with its source for the study

Parameter	Dataset	Data source
Watershed delineation	DEM	ASTER (USGS)
	Drainage network	Primary data (Field visit)
Bathymetry	Chaktai cannel cross-section (at 89 nodes)	CEGIS
Cannel Water level	Water level of Chaktai outfall of 2017	
Cannel Water discharge	Discharge of Chaktai outfall for 3 months (June, July and August) of 1983	
Precipitation	Rainfall data of Chattogram (1980–2017)	Meteorological department (BMD)
Landuse	Household GIS dataset	Chattogram Development Authority (CDA)

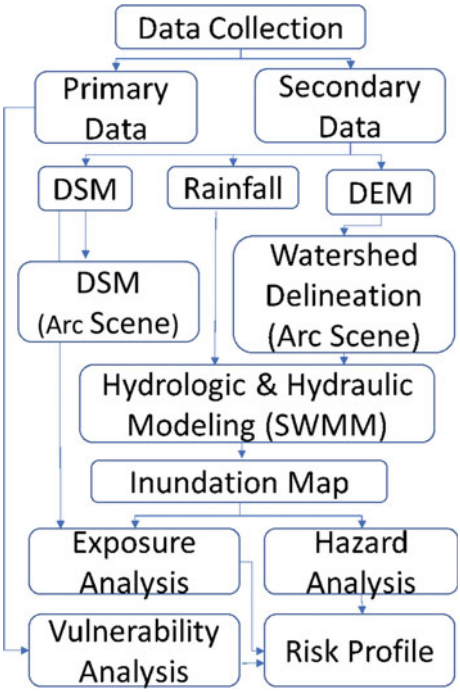

Fig. 6 Methodological flowchart

4 Results

4.1 Catchment Delineation

Figure 7 shows the catchment boundary of Muradpur-Chawkbazar basin with its divides, and Fig. 8 is focused on Khatunganj. 32 sub-basins have been identified in this Mudarpur-Chawkbzar basin. Since drainage water from these sub-basins contributes to the Chaktai canal, and also affects the waterlogging scenario at Khatunganj, all these sub-catchments were considered in the hydrological model.

4.2 Inundation Scenario with Actual and Design Rainfall

Design rainfall, which was generated from IDF curves, is used for every sub-catchment in the model. Table 3 presents the rainfall values that have been considered for the modeling in different scenarios and Figs. 9, 10, 11, and 12 depict the hyetographs of actual and design rainfall.

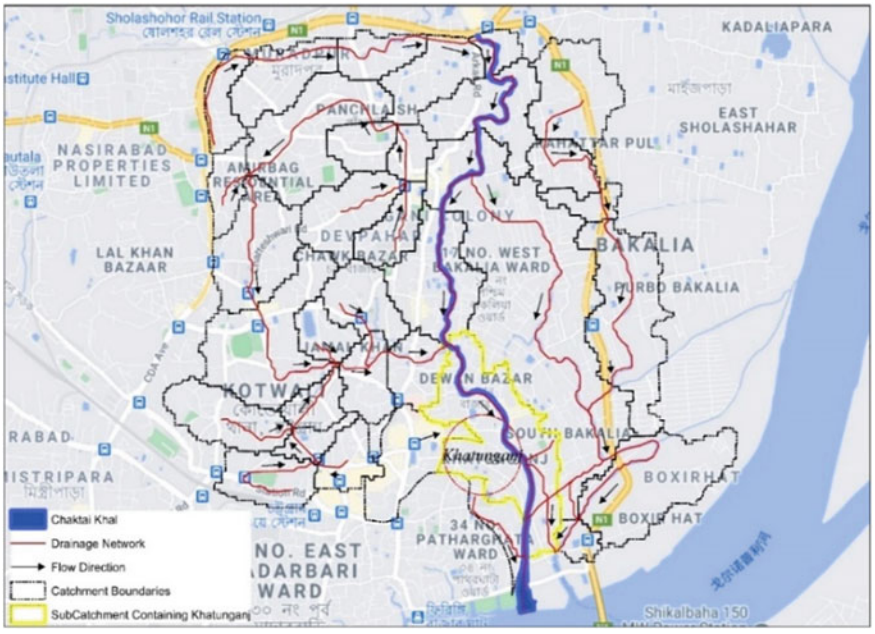

Fig. 7 Catchment area map adjacent to Chaktai

4.3 Discharge and Water Level

In different scenarios, the discharges (hydrograph) and water levels at the nodes (node 69 & 70) near Khatunganj have been considered for the study and presented in Fig. 13. For each scenario, the maximum discharge and WL have been reported.

4.4 Validation of SWMM Model

The model was run for the maximum rainfall as observed in the year 2017, since water level data is only available for that year. Corresponding inundation pattern was simulated using ArcGIS. Due to resource constraints and the unavailability of any other data for calibrating and validating the model, an indirect validation approach was used using satellite image. The simulated water inundation vicinity to Khatunganj area was compared with the actual flood inundation extent obtained from the satellite image of Sentinel-1. Sentinel-1 images have 10 m spatial resolution and perform well in case of inundation mapping in a cloudy environment (Tanim and Mullick 2017).

With the knowledge of an actual rainfall event on 05 July 2017, the model was run, and the extent of inundation was estimated. It was then compared with the

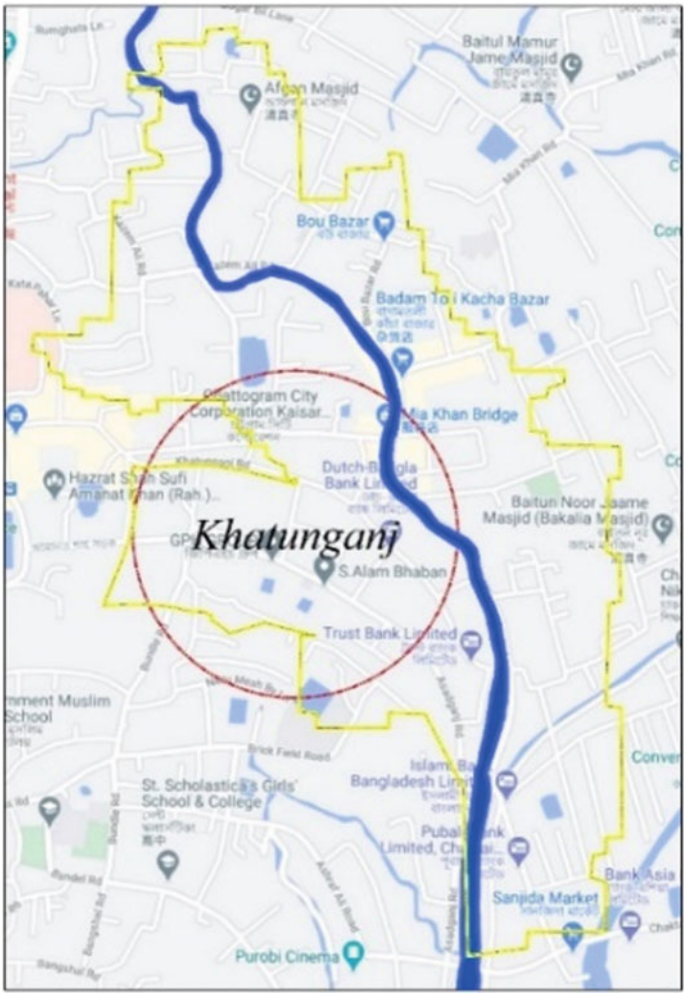

Fig. 8 Sub-catchment area containing Khatunganj

satellite image. Based on satellite image analysis, 32.35% of the study area was found as inundated on the day, whereas the simulation study found an inundation of around 39.11% of the area. The obtained results are quite compatible and the model can be considered as calibrated. Figure 14 presents the comparison between actual inundation as obtained from the satellite image and the simulated inundation from the actual rainfall on 05 July in 2017.

Table 3 Rainfall values considered for different scenarios

Scenario SL no	Scenario description	Rainfall value
S-1	Max rainfall event in 2017 distributed over 24 h (Actual Scenario)	222 mm
S-1 (A)	Max rainfall event in 2017 (2 h, High Tide)	222 mm
S-2	2-h 20 year return period rainfall (High Tide)	200.80 mm
S-3	2-h 50 year return period rainfall (High Tide)	244.98 mm
S-4	2-h 50 year return period rainfall (Low Tide)	244.98 mm
S-5	2-h 50 year return period rainfall (50% rainfall decrease and High Tide)	122.49 mm
S-6	2-h 50 year return period rainfall (50% rainfall decrease and Low Tide)	122.49 mm
S-7	6-h 50 year return period rainfall (High Tide)	395.94 mm
S-8	2-h 50 year return period rainfall (considering Climate change 11% rainfall increment)	271.92 mm

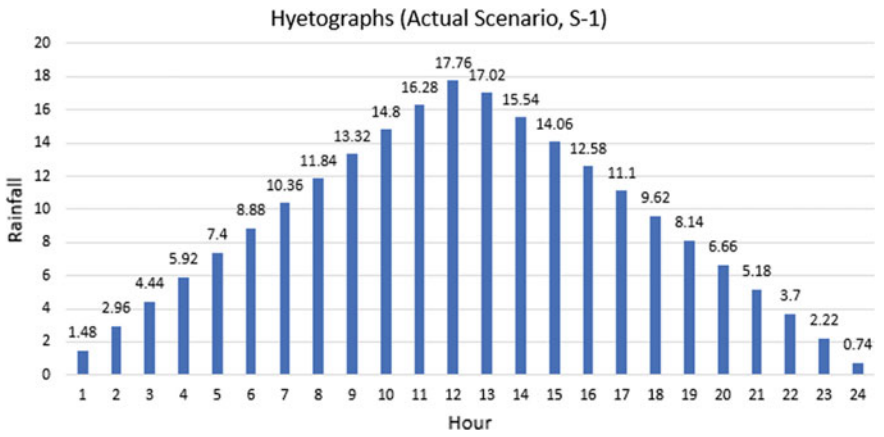

Fig. 9 Hyetographs of scenario 1

4.5 Inundation Maps

Percentages of inundated area are presented in Fig. 15. At hourly maximum rainfall, counted according to the actual scenario of 2017 (S-1), 39.1% area of Khatunganj got inundated. A 2-h, 50-year return period rainfall, considering 50% rainfall decrease and low tide (S-6), inundated 24.6% area of Khatunganj. At an extreme case, for 2-h 50-year return period rainfall, considering climate change and 11% rainfall increment (S-8), 49.08% of the total area of Khatunganj was found to be submerged. At the end, an inundation scenario (S-10) was assumed, which inundated 12.18% area of Khatunganj with a flood level of 2.56 m.

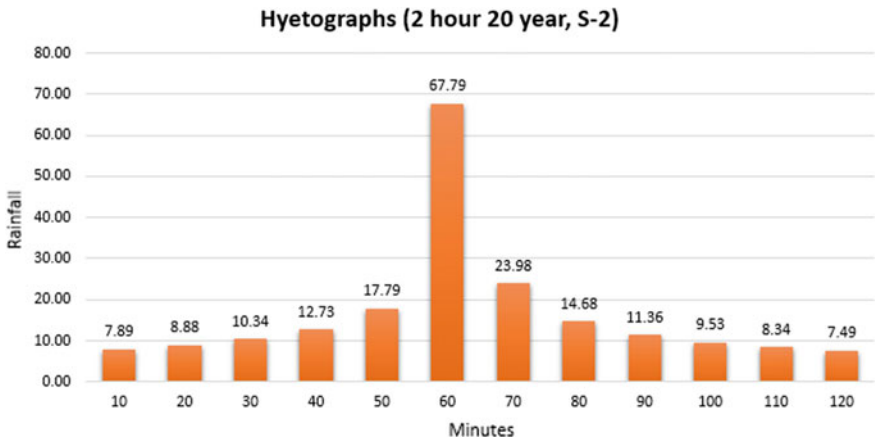

Fig. 10 Hyetographs of scenario 2

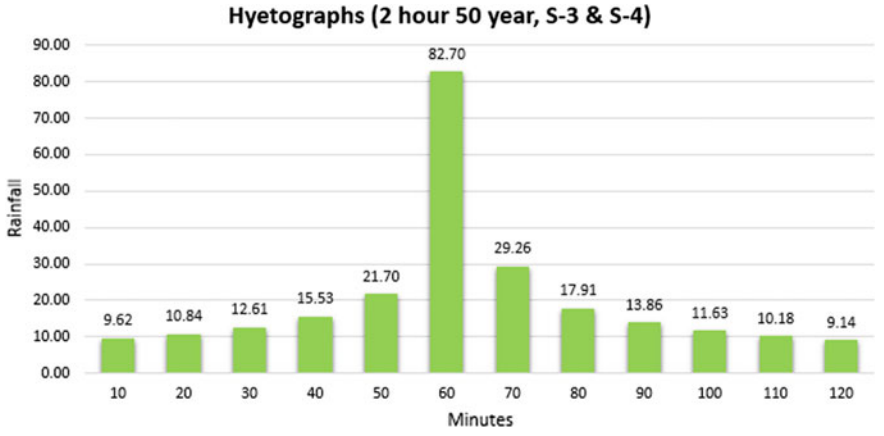

Fig. 11 Hyetographs of scenario 3 & 4

4.6 Vulnerability and Risk Analysis

Figures 16 represent the structural classification based on the four criteria i.e., plinth, proximity, structure type, and land use.

Figures 17, 18, and 19 demonstrate the vulnerability for different categories of rainfall. Table 4 documents the number of structures at risk due to different flood scenarios. In case of low rainfall, 122 structures were found as not vulnerable, and 27 structures to be very vulnerable. Besides, there were 33 less vulnerable and 42 medium vulnerable structures. In the event of average rainfall, 37 structures were found as not vulnerable, and 83 structures were less vulnerable. The number of medium and very vulnerable structures were 74 and 30, respectively. At the time

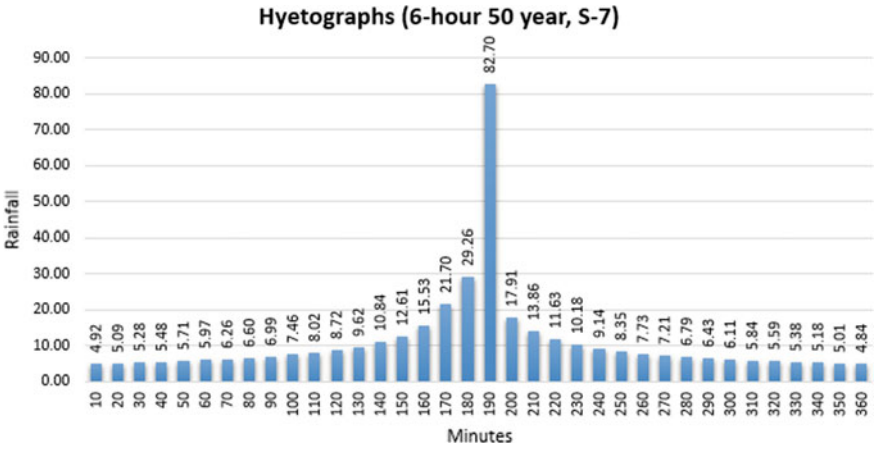

Fig. 12 Hyetographs of scenario 7

of heavy rainfall, every structure was vulnerable to some extent. There were 68 less vulnerable structures and 85 medium vulnerable structures. Additionally, 71 structures of Khatunganj were identified as very vulnerable at the time of heavy rainfall.

5 Discussion

Analysis shows that in all the different scenarios, the water level exceeds 3 m from the sea level (the datum), whereas the existing road level in Khatunganj varies between 2.9 m and 3.05 m from the datum. So, in the event of average to heavy rainfall, the Chaktai canal becomes overtopped, and the adjacent areas get flooded. The structures on both side of Khatunganj road have 3 types of plinth levels, namely, plinth elevation near to road level, below road level, and above road level. In fact, the site is very much historic, and majority of the structures in the area are very old. On the other hand, the road level is upgraded by the city authority from time to time. This results in a number of structures being lower than the road level. However, the plinth level of new structures is a bit high, even going up to 3 feet higher than the existing road level.

It was observed that tide events had a vital influence on the inundation for the same extent of rainfall. A 2-h 50-year return period rainfall creates a flood level 3.94 m at the time of high tide (S-3) and inundates 46.14% of Khatunganj area. On the contrary, the same amount of rainfall causes a 3.5 m flood at the period of low tide (S-4), submerging 36.23% of the total area. Similar influence was observed in case of scenarios S-5 and S-6. Considering 50% rainfall decrease, a 2-h 50-year return period rainfall generates 3.84 m flood at the time of high tide (S-5), but the same

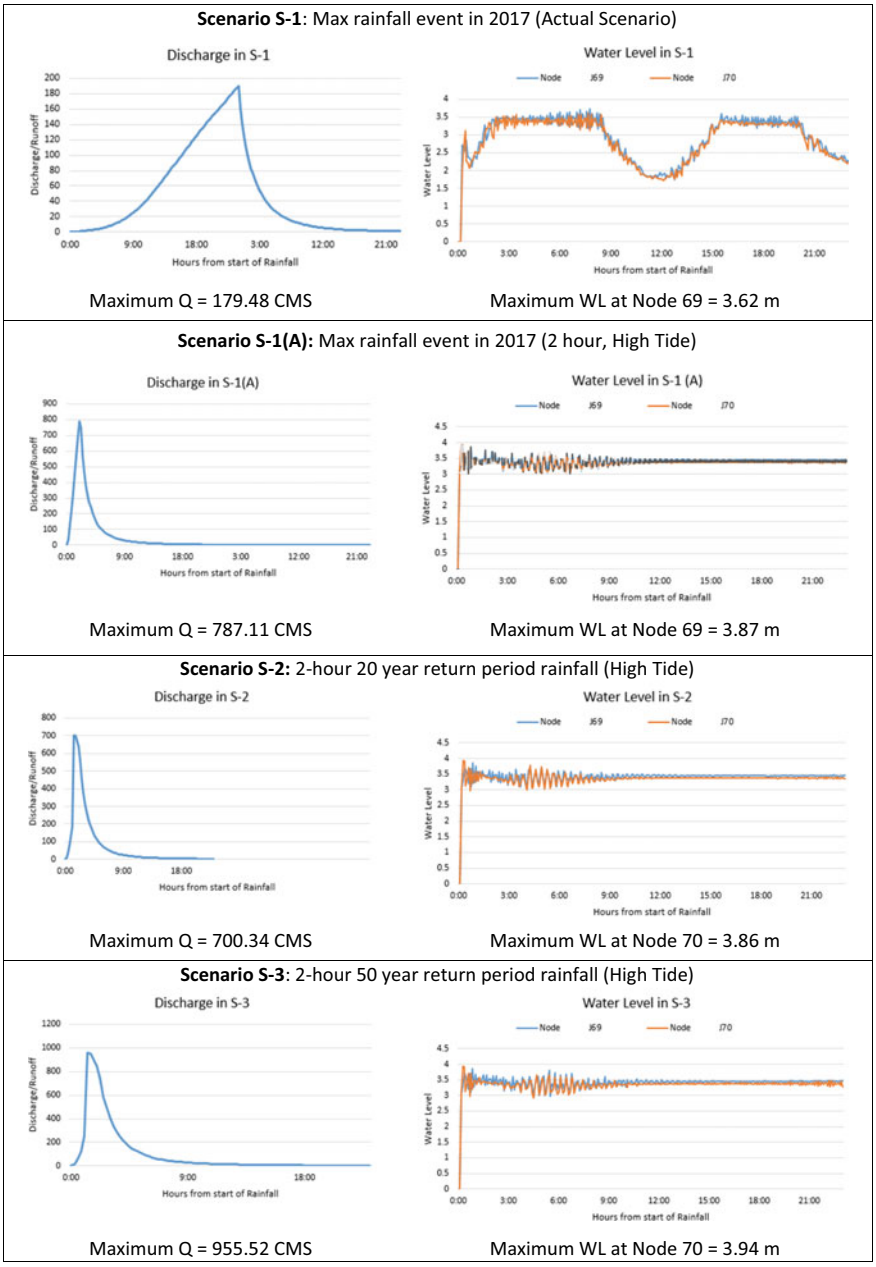

Fig. 13 Discharge and Water level for different scenario analyzed

Scenario S-4: 2-hour 50 year return period rainfall (Low Tide)

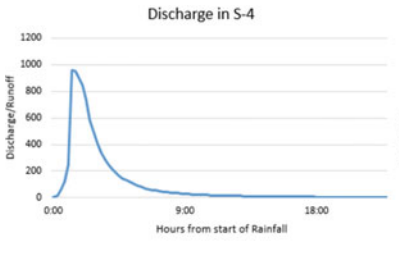

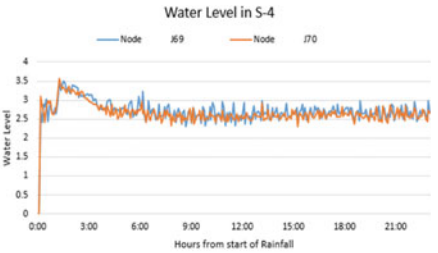

Maximum Q = 955.52 CMS

Maximum WL at Node 69: 3.5 m

Scenario S-5: 2-hour 50 year return period rainfall (considering 50% rainfall decrease) (High Tide)

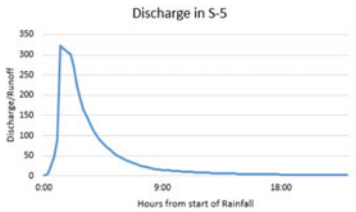

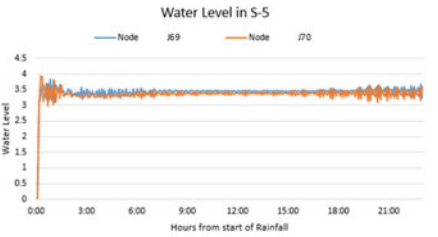

Maximum Q = 323.51 CMS

Maximum WL at Node 69: 3.84 m

Scenario S-6: 2-hour 50 year return period rainfall (considering 50% rainfall decrease) (Low Tide)

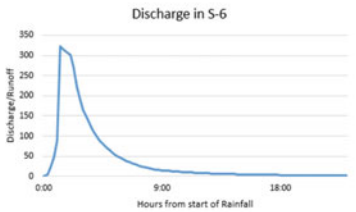

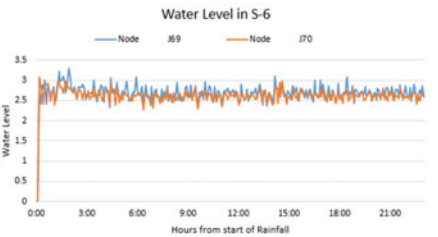

Maximum Q = 323.51 CMS

Maximum WL at Node 70: 3.09 m

Scenario S-7: 6-hour 50 year return period rainfall (High Tide)

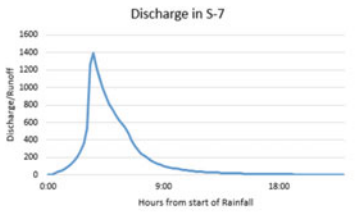

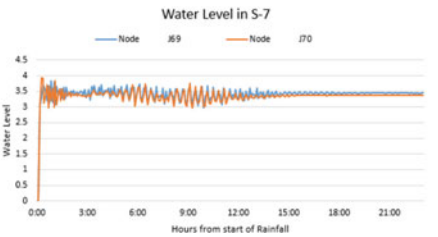

Maximum Q = **1394.27** CMS

Maximum WL at Node 69: 3.83 m

Fig. 13 (continued)

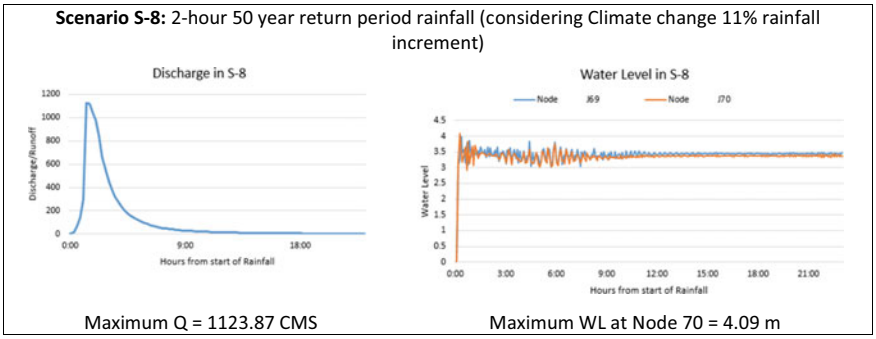

Fig. 13 (continued)

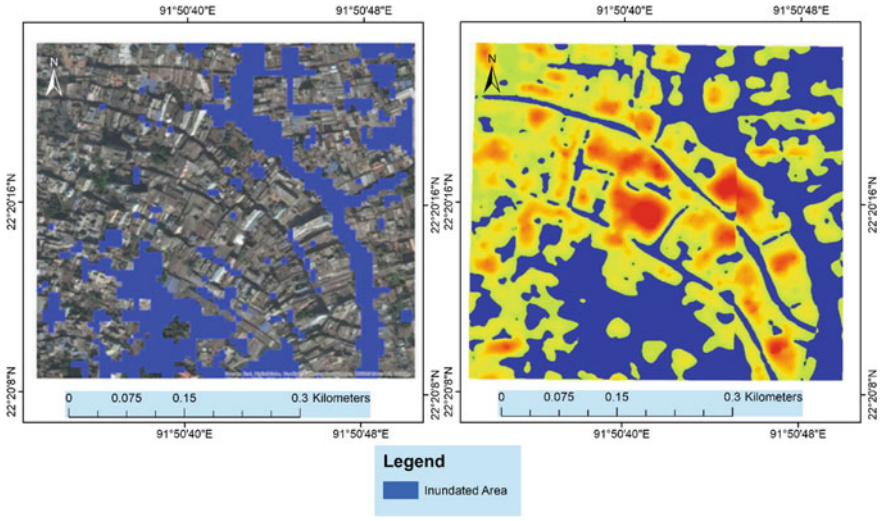

Fig. 14 Comparison between **a** Actual Flood Scenario obtained from Satellite and **b** Simulated Flood Scenario

rainfall generates a flood level of 3.09 m during low tide (S-6). Inundated area at the span of high tide (S-5) is 44.08%, and it drops down to 24.6% at the time of low tide.

Majority of the structures in Khatunganj area fall in the medium vulnerable class for all three rainfall cases. 122 structures out of 224 i.e., 54.4% of all structures in the area are not vulnerable at the time of low rainfall. However, event of high rainfall, all the structures have been found as vulnerable to various extent. Only 27 structures are very vulnerable in case of low rainfall. The number of very vulnerable structures rose up to 30 at the time of average rainfall, whereas 71 structures i.e., 31.7% of all structures in the area are very vulnerable at the time of heavy rainfall.

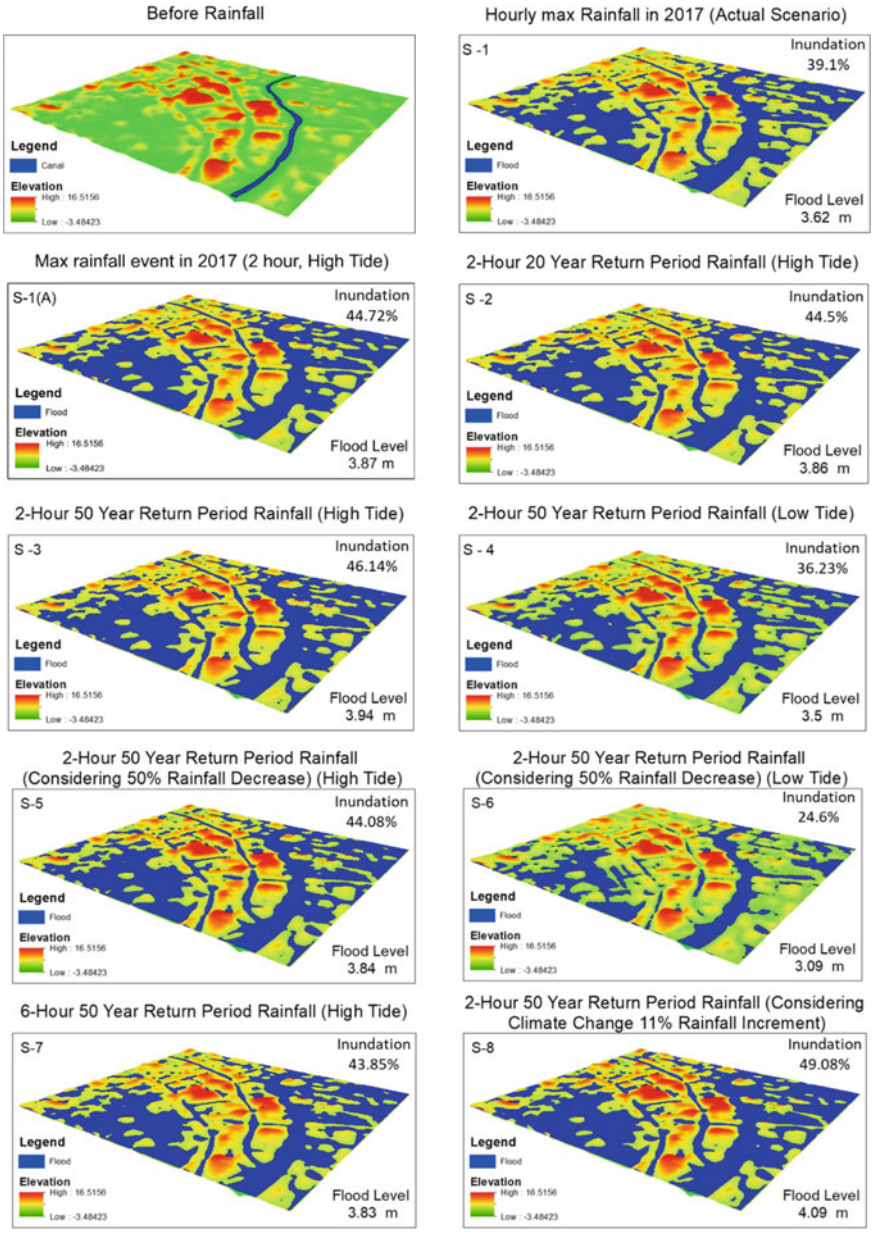

Fig. 15 Inundation pattern as obtained from model for different scenarios

Fig. 15 (continued)

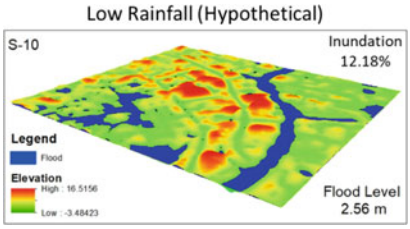

6 Conclusion

This study did an extensive analysis of the recurrent waterlogging problem in Khatunganj commercial area. A small rainfall results in an inundation in the area and the consequences are substantial economic loss in the commercial area. The study enumerated the vulnerability of the area due to waterlogging. To carry out such analysis, a hydrologic-hydraulic model was first developed to provide an inundation scenario and from the inundation scenario, vulnerability of each structure was assessed.

A model was formulated on the SWMM model platform, which provided discharge and water level at different canal points. Nine different scenarios on different rainfall events were simulated, where an actual rainfall event was taken from 05 July 2017, and remaining scenarios were set up as design rainfall events. Due to data scarcity, the model was calibrated using a satellite image of inundation extent from the actual rainfall.

In the event of any average to heavy rainfall, the Chaktai canal becomes overtopped, resulting in flooding of the surrounding areas. Average rainfall generates a WL of 3–3.5 m and the road level is about 2.9 to 3.1 m. Therefore, such a WL results in inundation of the Khatunganj main road with a water depth of 1 to 15 inch. Heavy rainfall with climate change scenario gives around 4.09 m WL, indicating around 1 m depth of water inundation of the road. All structures on both sides of the road will be submerged in such a scenario.

Majority of the structures in the area can be categorized as medium vulnerable for all three rainfall cases. In case of heavy rainfall, all structures are vulnerable to some extent. Water retention options, increased canal capacity, and regular maintenance of canal are extremely important for managing such a crisis.

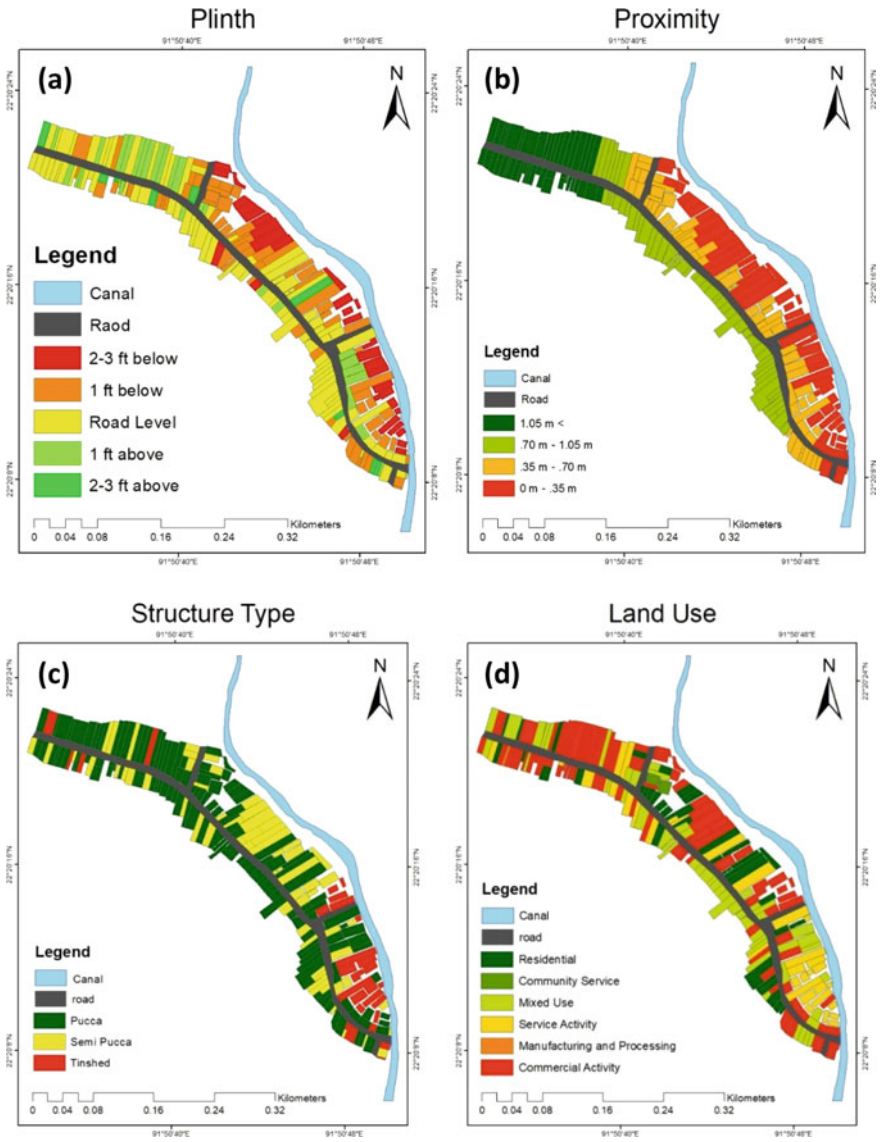

Fig. 16 Area Classification based on **a** plinth of the structure, **b** proximity to Chaktai canal, **c** structure type, **d** land use

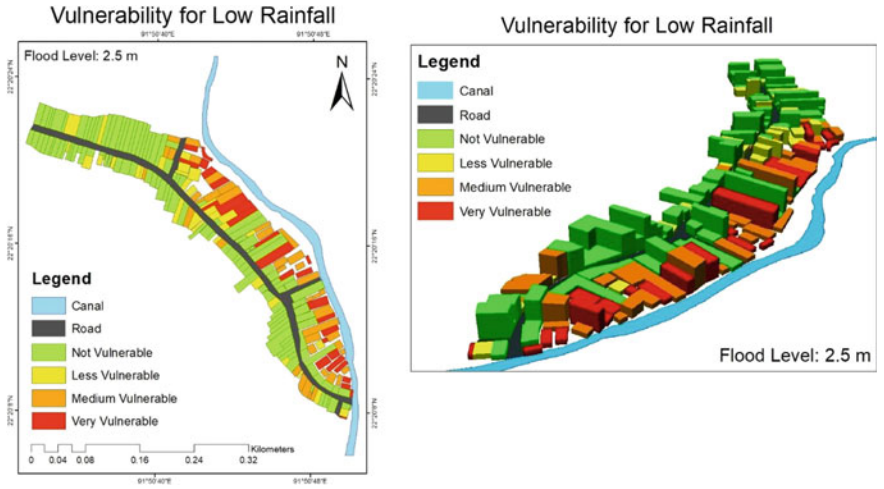

Fig. 17 Vulnerability for low rainfall

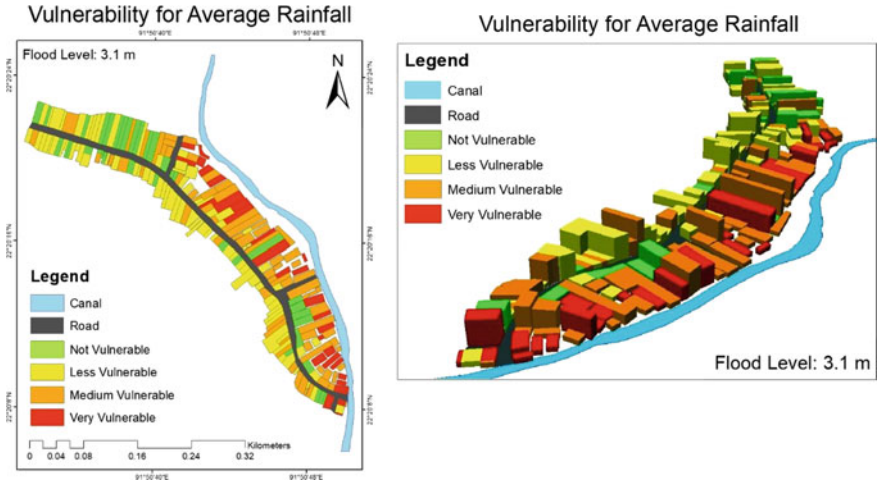

Fig. 18 Vulnerability for average rainfall

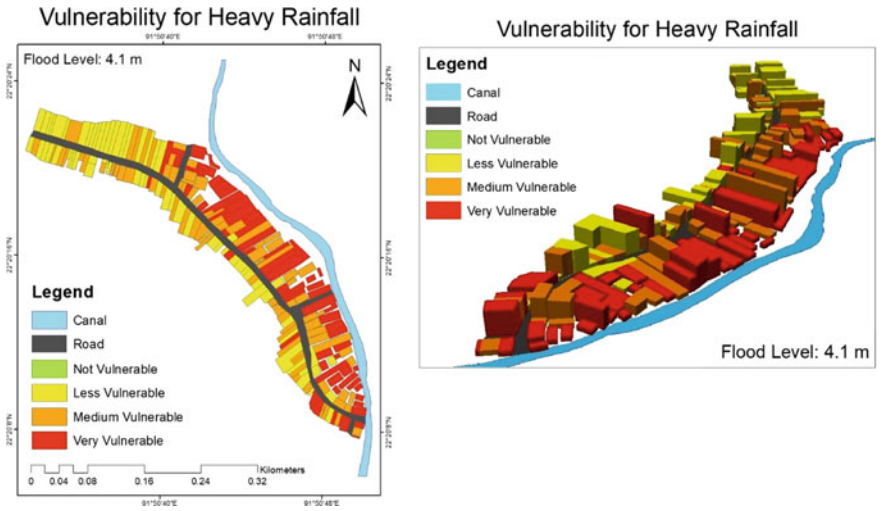

Fig. 19 Vulnerability for heavy rainfall

Table 4 Number of structures at risk due to different flood scenarios

	Low rainfall	Average rainfall	Heavy rainfall
Not vulnerable	122	37	0
Less vulnerable	33	83	68
Medium vulnerable	42	74	85
Very vulnerable	27	30	71
Total	224	224	224

References

Alexander, Kane, Suresh Hettiarachchi, Yixiao Ou, and Ashish Sharma. 2019. Can Integrated Green Spaces and Storage Facilities Absorb the Increased Risk of Flooding Due to Climate Change in Developed Urban Environments? *Journal of Hydrology* 579. Elsevier B.V.: 124201. https://doi.org/10.1016/j.jhydrol.2019.124201.

Barua, Dwaipayan. 2021. Khatunganj Lost over Tk 514cr to Waterlogging in 2020: Study. *The Daily Star*.

Berndtsson, R., P. Becker, A. Persson, H. Aspegren, S. Haghighatafshar, K. Jönsson, R. Larsson, et al. 2019. Drivers of Changing Urban Flood Risk: A Framework for Action. *Journal of Environmental Management* 240 (October 2018). Elsevier: 47–56. https://doi.org/10.1016/j.jenvman.2019.03.094.

Burrough, Peter A., Rachael A. McDonnell, and Christopher D. Lloyd. 1998. *Principles of Geographical Information Systems*. Oxford University Press. https://books.google.com.bd/

books?hl=en&lr=&id=kvoJCAAAQBAJ&oi=fnd&pg=PP1&dq=Burrough,+P.+A.,+%26+McDonnell,+R.+A.+(1998).+Principles+of+geographical+information+systems.+Oxford:+Oxford+University+Press&ots=aKI63ms3HG&sig=cxKiRofsF8-2ctO1IChRca9V6EM&redir.

Chowdhury, Mitoon. 2011. SPECIAL Century-Old Khatunganj Loses Its Glory. Bdnews24.Com.

Deng, Yu, Wei Qi, Bojie Fu, and Kevin Wang. 2020. Geographical Transformations of Urban Sprawl: Exploring the Spatial Heterogeneity Across Cities in China 1992–2015. *Cities* 105 (January). Elsevier: 102415. https://doi.org/10.1016/j.cities.2019.102415.

Dutta, Dushmanta, Srikantha Herath, and Katumi Musiake. 2003. A Mathematical Model for Flood Loss Estimation. *Journal of Hydrology* 277 (1–2): 24–49. https://doi.org/10.1016/S0022-1694(03)00084-2.

Fleming, K.M., P. Tregoning, M. Kuhn, A. Purcell, and H. McQueen. 2012. The Effect of Melting Land-Based Ice Masses on Sea-Level Around the Australian Coastline. *Australian Journal of Earth Sciences* 59 (4). Taylor & Francis: 457–467. https://doi.org/10.1080/08120099.2012.664828.

Han, Su Qin, Yi Yang Xie, Da Ming Li, Pei Yan Li, and Mei Ling Sun. 2006. Risk Analysis and Management of Urban Rainstorm Water Logging in Tianjin. *Journal of Hydrodynamics* 18 (5). China Ocean Press: 552–558. https://doi.org/10.1016/S1001-6058(06)60134-0.

Hasan, Zaheed, Sabiha Akhter, and Mamunul Islam. 2014. Climate Change and Trend of Rainfall in the South-East Part of Coastal Bangladesh. *European Scientific Journal* 10 (2): 25–39. https://www.researchgate.net/publication/260002503_CLIMATE_CHANGE_AND_TREND_OF_RAINFALL_IN_THE_SOUTH-EAST_PART_OF_COASTAL_BANGLADESH.

Hirabayashi, Yukiko, Shinjiro Kanae, Seita Emori, Taikan Oki, and Masahide Kimoto. 2010. Global Projections of Changing Risks of Floods and Droughts in a Changing Climate. *Hydrological Sciences Journal* 53 (4). Taylor & Francis Group: 754–772. https://doi.org/10.1623/HYSJ.53.4.754.

IPCC. 2001. Climate Change 2007: Impacts, Adaptation and Vulnerability.

Jang, Suhyung, Minock Cho, Jaeyoung Yoon, Yongnam Yoon, Sangdan Kim, Geonha Kim, Leehyung Kim, and Hafzullah Aksoy. 2007. Using SWMM as a Tool for Hydrologic Impact Assessment. *Desalination* 212 (1–3): 344–356. https://doi.org/10.1016/j.desal.2007.05.005.

Jenson, S.K., and J.O. Domingue. 1988. Extracting Topographic Structure from Digital Elevation Data for Geographic Information System Analysis, Vol. 54.

Kabir, Ekram. 2016. What's so Special About Chittagong. *Dhaka Tribune.*

Kabir, Shah Md Imran, and Mostafa Ali. 2017. Hydrodynamic and Morphological Simulation of Karnafuli River Using Cche2d Model. In *6th International Conference on Water & Flood Management (ICWFM-2017).* https://www.researchgate.net/publication/328007509_HYDRODYNAMIC_AND_MORPHOLOGICAL_SIMULATION_OF_KARNAFULI_RIVER_USING_CCHE2D_MODEL.

Kleist, L., A.H. Thieken, P. Köhler, M. Müller, I. Seifert, D. Borst, and U. Werner. 2006. Estimation of the Regional Stock of Residential Buildings as a Basis for a Comparative Risk Assessment in Germany. *Natural Hazards and Earth System Sciences* 6 (4): 541–552. https://doi.org/10.5194/nhess-6-541-2006.

Léon, Villagrán de, and Juan Carlos. 2006. *Vulnerability: A Conceptional and Methodological Review - UNU Collections.* Bonn: UNU- EHS. http://collections.unu.edu/view/unu:1871.

Miller, James D., Hyeonjun Kim, Thomas R. Kjeldsen, John Packman, Stephen Grebby, and Rachel Dearden. 2014. Assessing the Impact of Urbanization on Storm Runoff in a Peri-Urban Catchment Using Historical Change in Impervious Cover. *Journal of Hydrology* 515. Elsevier B.V.: 59–70. https://doi.org/10.1016/j.jhydrol.2014.04.011.

Ministry of Foreign Affairs of the Netherlands. 2019. *Climate Change Profile Bangladesh.* https://doi.org/10.1080/17565529.2014.977761.

Mishra, Surendra Kumar, and Vijay P. Singh. 2013. Soil Conservation Service Curve Number (SCS-CN) Methodology. *Water Science & Technology Library* 42.

Nasher, N.M. Refat, and M.N. Uddin. 2015. Maximum and Minimum Temperature Trends Variation over Northern and Southern Part of Bangladesh. *Journal of Environmental Science and Natural*

Resources 6 (2). Bangladesh Journals Online (JOL): 83–88. https://doi.org/10.3329/jesnr.v6i2.22101.

Nayeb Yazdi, Mohammad, Mehdi Ketabchy, David J. Sample, Durelle Scott, and Hehuan Liao. 2019. An Evaluation of HSPF and SWMM for Simulating Streamflow Regimes in an Urban Watershed. *Environmental Modelling and Software* 118 (January). Elsevier: 211–225. https://doi.org/10.1016/j.envsoft.2019.05.008.

Oliveri, Elisa, and Mario Santoro. 2000. Estimation of Urban Structural Flood Damages: The Case Study of Palermo. *Urban Water* 2 (3): 223–234. https://doi.org/10.1016/s1462-0758(00)00062-5.

Peng-zhu, X.U., Jiang Tong, and King Lorenz. 2000. Hydrologic/Hydraulic Modelling and Flood Risk Analysis for the West Tiaoxi. *Chinese Geographical Science* 10 (4): 309–318.

Quan, Rui Song. 2014. Rainstorm Waterlogging Risk Assessment in Central Urban Area of Shanghai Based on Multiple Scenario Simulation. *Natural Hazards* 73 (3): 1569–1585. https://doi.org/10.1007/s11069-014-1156-x.

Quddusi, Kazi S.M. Khasrul Alam. 2017. Water-Logging in Chittagong: Glimpses of Losses. *Daily Sun*.

Schwab, G.O., D.D. Fangmeier, W.J. Elliot, and R.K. Freveret. 1993. *Soil and Water Conservation Engineering*. New York: Wiley.

Shi, Yong, Chun Shi, Shi Yuan Xu, A. Li Sun, and Jun Wang. 2010. Exposure Assessment of Rainstorm Waterlogging on Old-Style Residences in Shanghai Based on Scenario Simulation. *Natural Hazards* 53 (2): 259–272. https://doi.org/10.1007/s11069-009-9428-6.

Tanim, Ahad Hasan, and Md. Reaz Akter Mullick. 2017. Application of Synthetic Aperture Radar Imagery for Inundation Mapping : A Case of Sylhet Flood Event 2017, no. September.

Wanniarachchi, S.S., and N.T.S. Wijesekera. 2012. Using SWMM as a Tool for Floodplain Management in Ungauged Urban Watershed. *Engineer: Journal of the Institution of Engineers, Sri Lanka* 45 (1): 1. https://doi.org/10.4038/engineer.v45i1.6944.

Xue, Fengchang, Minmin Huang, Wei Wang, and Lin Zou. 2016. Numerical Simulation of Urban Waterlogging Based on FloodArea Model. *Advances in Meteorology* 2016. https://doi.org/10.1155/2016/3940707.

Yin, Zhane, Jie Yin, Shiyuan Xu, and Jiahong Wen. 2011. Community-Based Scenario Modelling and Disaster Risk Assessment of Urban Rainstorm Waterlogging. *Journal of Geographical Sciences* 21 (2). Springer: 274–284. https://doi.org/10.1007/s11442-011-0844-7.

Hydrometeorological Hazards and Risk

A Remote Sensing-Based Approach for Analysis of Dry and Wet Periods of Bangladesh Based on Standardized Precipitation Index During 1981–2020

Saumik Mallik

Abstract Bangladesh, having a subtropical monsoon climate with wide seasonal fluctuations in rainfall, is susceptible to recurrent dry and wet periods. This study aims to measure the spatial and temporal variability of dry/wet periods at district level, based on timescale and intensity by analyzing satellite data from CHIRPS precipitation record for the past 40 years to calculate the standardized precipitation index (SPI). The frequencies of moderate, severe, and extreme dry and wet periods for both short and long timescales for individual districts are calculated by extracting and analyzing the individual SPI time series of the 64 districts in GIS and R through geospatial analysis and verified using past records of well-defined drought and flood. The results demonstrated that, within a period of 100 years, districts from Khulna and Rangpur division can anticipate about 18 droughts and 17 floods, respectively, of different intensities lasting 12 months on average, which is the highest in Bangladesh. As for droughts and floods lasting 3 months, districts from Barisal and Dhaka division lead, respectively, with about 66 droughts and 67 floods expected on average. The findings demonstrate that, based on timescale and intensity, the occurrences of dry/wet periods varied to a great extent across Bangladesh during the past 40 years.

Keywords Bangladesh · Remote sensing · Standardized precipitation index · Droughts and floods · Extreme events

1 Introduction

Global climate change, encompassing steady as well as abrupt shifts, has a considerable influence on land surface-atmosphere dynamics and local socio-economic development. Global warming, or progressive climate change, has a major impact on the hydrological cycle and atmospheric circulatory systems, altering the intensity and geographic distribution of precipitation (Parry et al. 2007; Arnell 1999), that in turn disrupts the local meteorological conditions and the regional agriculture sector.

S. Mallik (✉)
Department of Civil Engineering, Bangladesh University of Engineering and Technology, Dhaka 1000, Bangladesh

© The Author(s), under exclusive license to Springer Nature Switzerland AG 2022

G. M. Tarekul Islam et al. (eds.), *Water Management: A View from Multidisciplinary Perspectives*,
https://doi.org/10.1007/978-3-030-95722-3_6

Additionally, as a result of climate change, the frequency and intensity of extreme weather occurrences may alter (Rosenzweig et al. 2001), resulting in a variety of meteorological disasters such as floods, droughts, and rainstorms.

Despite considerable scientific and technological advancements and improvements in environmental management over the twentieth century, mankind continues to be affected by the repercussions of these meteorological disasters on a global scale (Krysanova, Vetter, and Hattermann 2008). Climate change is only one of several indicators of our previous inability to accomplish sustainable development (Green 2010), other indicators include the approach of peak oil (IEA 2009) and peak phosphorus (Cordell et al. 2009), as well as the challenge of satisfying global food needs (Molden 2013). It is essential to analyze the spatial and temporal variability of local extreme hydroclimatic events in order to garner a better understanding of recent climatic variations, their appearance in local areas, and to regularly keep track of drought and flood events. This insight will significantly assist in the advancement of integrated water resource management.

Conventional drought monitoring entails the study of rain-gage network measurements, which are more reliable when coupled with long-term satellite records (Khan et al. 2014; Bechle et al. 2013). Precipitation data from several meteorological stations in Bangladesh, provided by the Bangladesh Meteorological Department (BMD), is often utilized in a variety of research. However, this technique has numerous drawbacks, including spatial contiguity, data inaccessibility in remote regions, high maintenance costs, and near-real-time data unavailability to ordinary users (Pandey et al. 2020). Alternatively, spatially contiguous precipitation data enables a more accurate evaluation of drought and flood occurrences. Moreover, high-resolution satellite data has been frequently employed in recent years to characterize drought episodes spatiotemporally (Tao et al. 2016; Gao et al. 2018; Shrestha et al. 2017). The Climate Hazards Group's Infrared Precipitation with Station (CHIRPS) data is a newly developed high-resolution precipitation product derived from satellite data and integrated with weather stations observations. It has demonstrated significant potential in a variety of hydrological studies, including drought monitoring (Funk et al. 2014, 2015). Numerous regions in Asia, specifically in India, China, and Nepal, are demonstrating the use of CHIRPS records for real-time retrospective drought and flood study. Shrestha et al. (2017) used CHIRPS precipitation data to monitor drought in Nepal's Koshi River watershed and suggested the data's usefulness for such research. Additionally, the CHIRPS-based SPI is shown to have the capability of identifying drought events and their characteristics, suggesting it can be used as a novel source of information for drought monitoring across diverse regions of China (Gao et al. 2018; Zhong et al. 2019; W. Wu et al. 2019). Pandey et al. (2020) assessed the performance of high-resolution satellite precipitation datasets, including TRMM, PERSIANNCDR, and CHIRPS, in order to determine their effectiveness for drought monitoring. It was found that CHIRPS data had the highest accuracy when compared to the gridded gage dataset over their study area of central India.

Many drought-monitoring indicators have been developed (Ahmed et al. 2019; Alamgir et al. 2015). The standardized precipitation index (SPI) is the most straightforward, statistically robust, comprehensible, and independent of meteorological

variables among these (Keyantash and Dracup 2002). SPI is a probability-based statistic that indicates how much a given period's accumulative precipitation deviates from the average state. The index is spatially independent and performs excellently for expressing precipitation anomalies (McKee et al. 1993). In comparison to other physical processes-based indices and methodologies, such as the palmer drought severity index (PDSI), the SPI is straightforward to compute and implement. It only uses precipitation as input data, which eliminates the need for parameter calibration, making it especially well-suited for drought/flood monitoring in locations with a scarcity of hydrological data (Yuan and Zhou 2004). In a multitude of countries and regions, the SPI has been extensively utilized to classify dry and wet conditions, including Canada (Quiring and Papakryiakou 2003), China (Du et al. 2013), Iran (Moradi et al. 2011; Nafarzadegan et al. 2012), Italy (Piccarreta et al. 2004; Vergni and Todisco 2011), Korea (Min et al. 2003; Kim et al. 2009), and the United States (H. Wu et al. 2007).

Bangladesh's rainfall pattern is shifting as a result of global climate change (Shahid and Behrawan 2008; Rimi et al. 2019). This has resulted in an increase in the country's extreme weather events (Basher et al. 2018) and hydrological disasters (Mohsenipour et al. 2018). As a result of changes in rainfall patterns, Mohsenipour et al. (2018) noticed a drop in the return period of droughts from 1985 to 2014 at stations where it was high from 1961 to 1990, and vice versa in Bangladesh's most drought-prone areas. Bangladesh, which is located in tropical South Asia, has suffered many catastrophic droughts and floods as a result of precipitation shortages and excesses (Shahid and Behrawan 2008). These extreme occurrences resulted in protracted water scarcity or inundation, affecting agriculture, the environment, and public health (Keyantash and Dracup 2002). Population increases, agricultural expansion, land use changes, and industrial development all amplify the impact of these disasters ("Glossary of Terms" 2014). This necessitates a thorough knowledge of the geographical and temporal diversity associated with dry/wet cycles on various timescales.

Even though a substantial body of research has been conducted in Bangladesh on the spatial and temporal characteristics of droughts and floods (Mohsenipour et al. 2018; Rimi et al. 2019), no studies have been performed on a national scale in Bangladesh that quantify the spatial and temporal variability of dry/wet periods on a districts basis and focus on both timescale and intensity utilizing satellite data. The novelty of this work is that it uses a high-resolution precipitation product derived from satellite data in conjunction with rain-gage observations from 1981 to 2020 to explore the frequency of both dry and wet periods of varying intensities over both short- and long-term timescales using SPI. Remote sensing techniques have established themselves as an increasingly efficient strategy for researchers and policymakers (Kafy et al. 2021), and this study will contribute to the development and maintenance of the country's water resources, as well as limit the impact of extreme events to ensure sustainable management and planning.

2 Materials and Method

2.1 Study Area

The study area encompasses Bangladesh, situated in South Asia between latitudes 20°34′ and 26°38′ N and longitudes 88°01′ and 92°41′ E. Bangladesh is bounded by India on the west, north, and northeast and bordered on the south by Myanmar. The Bay of Bengal, with its extensive coastline, serves as the southern boundary. Excluding the higher elevations at the far southeast and the Sylhet division in the northeast, the majority of Bangladesh is less than 10 m above sea level. Agricultural land prevails in the country, since more than 50% of the entire geographical land was estimated to be cropped areas during 2019–2020 (Bangladesh Bureau of Statistics 2021). Bangladesh is particularly vulnerable to global climate change's escalating consequences. It is often struck by natural calamities, including flooding, drought, cyclones, and tidal bores (Bangladesh Bureau of Statistics 2015). Bangladesh has recently suffered drought on a frequent basis; on average, Bangladesh faces drought once every 2.5 years (Mondol et al. 2017).

2.2 Datasets

The preceding four decades (1981 to 2020) were chosen as study period for this work. This study makes use of gridded precipitation data from The Climate Hazards Group's Infrared Precipitation with Stations (CHIRPS) dataset. Estimates obtained from satellite data produce area-averaged values that typically underestimate the intensity of extreme precipitation events owing to complex geography. Precipitation grids generated from station data, on the other hand, suffer in more remote regions with fewer rain-gage stations. To construct gridded rainfall time series for seasonal drought monitoring and trend analysis, CHIRPS data contains in-house climatology—CHPclim, 0.05° resolution satellite images, and in situ station data from 1981 to the near-present. Its algorithm is based on a 0.05° climatology that (i) incorporates satellite data to represent sparsely gaged locations, (ii) incorporates daily, pentadal, and monthly 0.05° CCD-based precipitation estimates from 1981 to the present, (iii) blends station data to generate a preliminary information product with an average latency of about 2 days and a final product with an average latency of about 3 weeks, and (iv) uses an unique blending procedure to assign interpolation weight utilizing the spatial correlation structure of CCD-estimates (Funk et al. 2015).

2.3 The Standardized Precipitation Index (SPI)

Drought is quantified on the basis of the standardized precipitation index (McKee et al. 1993), which has also been recommended by the WMO for drought monitoring (WMO 2012). Additionally, wetter and drier climates can be portrayed in the same way since the SPI is standardized; hence, utilizing the SPI, wet periods can be analyzed and monitored just as well. The SPI transformation begins by applying a backward-looking moving average with a window length τ to the monthly precipitation data, resulting in accumulated precipitation time series. The SPI was computed for each month of this sequence of years at timeframes of $\tau = 3$ and $\tau = 12$ months in this study. The rest of this paper will refer to index values derived for window length using the notation SPI- τ. To determine SPI-3 and SPI-12, a new series was constructed for each month of the calendar year with components equal to the corresponding precipitation moving sums for each individual pixel within the study area. For example, the 3-month SPI for February 2000 was computed using the total precipitation from November 1999 to February 2000. Similarly, the 12-month SPI for February 2000 was calculated using the total precipitation from March 1999 to February 2000.

The cumulative precipitation series is then normalized individually for each calendar month. This is accomplished by assembling data from a single calendar month in a base period (e.g., all February values from 1981 to 2020) and fitting the data to a gamma distribution. The parameters of the gamma distribution are used to transform all the values of the associated months to those of the standard normal distribution, resulting in a mean SPI of zero for the pixel and desired period (Stagge et al. 2015; Edwards 1997). The area-averaged SPI time series for each of the 64 districts is then calculated in QGIS using the pixels contained inside the district borders.

The lowest bound for precipitation is zero, and their empirical distributions exhibit a positive skewness. As a result, the gamma distribution has been a popular choice for calculating the SPI. The gamma distribution was found to fit long-term precipitation data well, in accordance with earlier research (Stagge et al. 2015; Livada and Assimakopoulos 2007; Thom 1958). The gamma distribution is defined as follows in terms of a frequency or probability density function:

$$g(x) = \frac{1}{\beta^{\alpha}\Gamma(\alpha)} x^{\alpha-1} e^{-x/\beta}, \text{ for } x > 0 \tag{1}$$

where $\Gamma(\alpha)$ is the gamma function; x is the precipitation; and α and β are the shape and scale parameters, respectively.

For the 3- and 12-month timescales, the number of months N_i in each class of drought and flood intensity as defined in Table 1 was calculated. The number of droughts and floods every hundred years was then estimated as follows:

$$N_{i,100} = \frac{N_i}{i,n}.100 \tag{2}$$

Table 1 Meteorological drought and flood risks classification using SPI values (McKee et al. 1993)

SPI values	Class	Probability
2.0 and more	Extremely wet	0.023
1.5 to 1.99	Very wet	0.044
1.0 to 1.49	Moderately Wet	0.092
0.99 to 0.99	Near normal	0.682
−1.0 to −1.49	Moderately dry	0.092
−1.5 to −1.99	Severely dry	0.044
−2 and less	Extremely dry	0.023

where $N_{i,100}$ = the number of droughts/floods for a timescale i in 100 years.

N_i = the number of months with droughts/floods for a timescale i in the n-year set.

i = timescale (3, 12 months).

n = the number of years in the data set (=40).

Pre-processing of the CHIRPS satellite data included several intermediate steps such as cropping the study area, merging all netCDF format files into one netCDF file, editing variable names and units, and were done using BASH script. SPI values were calculated for each pixel within the study area using the open-source software package Climate Indices for Python (Adams 2017), which includes Python implementations of various climate index algorithms that provide a geographical and temporal portrait of the intensity of precipitation and temperature irregularities effective for climate monitoring and research. In QGIS, the pixels within a district border are used to calculate the area-averaged SPI value for each of the 64 districts. The resultant dataset is then imported into R, where the frequency of drought/flood occurrences of various intensities is analyzed. Timescale and intensity-based maps of long and short-term dry/wet periods are generated from the analysis.

McKee et al. (1993) defined drought intensities resulting from the SPI using the categorization system shown in the SPI value table below (Table 1). Additionally, they specified the parameters for a drought occurrence across all timescales. A drought episode occurs when the SPI remains persistently negative and maintains a magnitude of −1.0 or less. When the SPI turns positive, the event terminates. Similarly, a persistent positive SPI value of +1.0 or more is considered a flood episode.

In this study, a 3-month SPI is used to identify short-term or seasonal dry/wet events, while a 12-month SPI is used to detect long-term dry/wet events. Streamflow, reservoirs, and groundwater respond to longer-term precipitation anomalies of the order of 6 months to 24 months or more, whereas meteorological and soil moisture conditions (agricultural) respond relatively quickly to precipitation anomalies, typically within 1–6 months. SPIs with a shorter time horizon, such as 3-month SPIs, can give early warning of drought/flood and aid in determining the severity of the event.

3 Results

Three frequency-based maps for each of the intensities (moderate, severe, and extreme) are created for both long- and short-term dry and wet events, and a further four maps are generated based on the total number of events encountered by each district regardless of intensities using SPI analysis of 3- (short-term) and 12- (long-term) months, thus identifying districts with a greater prevalence of drought and flooding during a 40-year period (1981–2020). The SPI results are such classified into short- and long-term analysis, as well as three distinct intensities, in order to provide comparative analysis and to propose appropriate short- and long-term actions.

3.1 Spatial Distribution of the Frequency of Long-Term Dry/Wet Events in Bangladesh

The SPI-12 results are classed as long-term analysis, illustrating drought and flood rates for moderate, severe, and extreme intensities over all districts, with red color symbology emphasizing the most frequently affected areas (Fig. 1). The frequencies of long-term droughts and floods of individual districts, as well as the averaged frequencies for each of the seven divisions, are shown in Table 2.

Long-term SPI is a term that refers to the long-term effects of droughts on stream flow, reservoir storage, and groundwater level, and hence is connected to hydrological droughts. The incidence of moderate dry and wet periods is higher than the occurrence of severe or extreme dry/wet periods in the majority of the country's districts.

The north-eastern district of Sylhet is one of the least affected by long-term droughts. However, it is observed that its neighboring districts to the west have a higher frequency of extreme dry occurrences but are less likely to have moderate-to-severe events. Districts in the north-western Rajshahi and south-western Khulna regions are more likely to have long-term severe dry episodes, whereas districts throughout southern Bangladesh, including the Chittagong hill tracts region, have had regular moderate dry spells throughout the study period. Long-term study reveals a rise in frequency percentages, as seen in Table 2, which compares distinct drought and flood categories and their respective frequency percentages for 12 months SPI. It is found that in places prone to severe to extreme droughts, there is a significant likelihood of hydrological drought and depletion of ground water and stream flow, and thus necessitating the adoption of water conservation and management practices in those areas.

On the other hand, the central region of the country surrounding the capital Dhaka, extending up to the north-eastern Sylhet region, is more likely to encounter long-term extreme wet periods. As evidenced by the greater average frequency of these two divisions in Table 2, the south-west districts of Khulna and the northernmost districts of Rangpur division are more prone to long-term moderate-to-severe wet events than other regions.

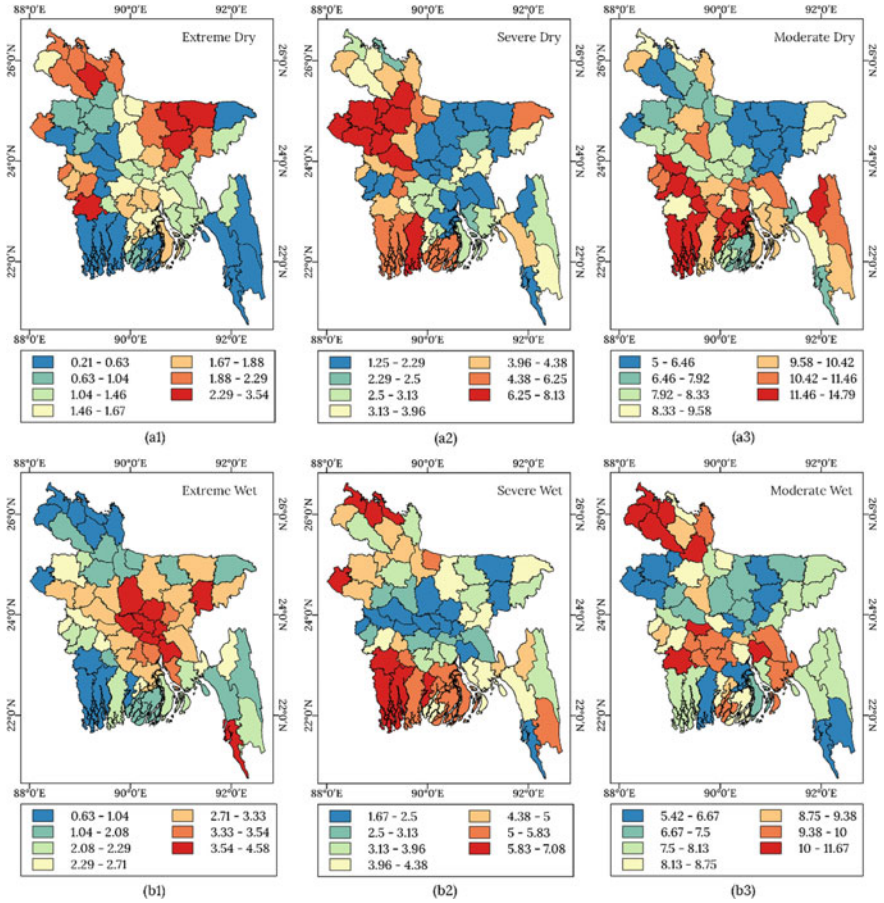

Fig. 1 Spatial distribution of the frequency (in %) of long-term dry periods (**a**) and frequency of long-term wet periods (**b**) of different intensities (extreme, severe, and moderate)

3.2 Spatial Distribution of the Frequency of Short-Term Dry/Wet Events in Bangladesh

The results of the 3-month SPI are classified as short-term analysis (Fig. 2) since they primarily give estimates of the effects of dry/wet periods on a short timescale. Short-term drought and flood frequencies for each individual districts and divisions were calculated for moderate, severe, and extreme intensities, as shown in Table 3, and districts having a greater drought/flood frequency were highlighted in red on the maps. The 3-month SPI is useful for estimating short- and medium-term moisture conditions in agriculture, since it offers an estimate of seasonal precipitation, which indicates a deviation from total precipitation. For instance, at the end of February, the 3-month SPI compares the December–January–February precipitation total for

Table 2 The frequency of occurrences of long-term dry and wet periods of various intensities in different districts in Bangladesh between the years 1981 and 2020

Division	District	Extreme dry (%)	Severe dry (%)	Moderate dry (%)	Extreme wet (%)	Severe wet (%)	Moderate wet (%)
Barisal	Barguna	0.83	6.25	8.13	1.88	4.17	10
	Barisal	1.67	2.29	12.29	3.33	5.21	6.04
	Bhola	1.88	2.71	10.42	2.29	5.63	7.08
	Jhalokati	1.88	3.13	10.63	2.5	5.63	9.38
	Patuakhali	0.63	5.83	7.71	2.08	5.83	8.75
	Pirojpur	1.67	3.33	12.08	1.04	6.88	8.33
	Average	**1.43**	**3.92**	**10.21**	**2.19**	**5.56**	**8.26**
Chittagong	Bandarban	0.21	3.33	10.42	2.29	5.83	6.67
	Brahamanbaria	1.46	3.75	6.25	3.13	4.17	7.92
	Chandpur	1.67	1.25	9.38	3.96	2.29	11.25
	Chittagong	0.21	4.17	9.58	2.08	4.38	8.13
	Cumilla	1.25	1.88	11.46	3.33	3.13	9.58
	Coxs Bazar	0.21	2.29	7.29	3.75	2.29	5.42
	Feni	1.46	3.54	7.71	2.5	4.58	9.58
	Khagrachhari	1.25	1.67	11.88	2.71	4.58	8.13
	Lakshmipur	1.46	2.5	9.79	3.54	4.38	7.92
	Noakhali	1.46	2.71	10.42	2.29	4.17	10
	Rangamati	0.42	2.92	11.25	2.08	3.96	8.13
	Average	**1.01**	**2.73**	**9.58**	**2.88**	**3.98**	**8.43**
Dhaka	Dhaka	1.46	2.29	8.13	4.58	2.29	6.04
	Faridpur	1.67	2.71	9.79	2.92	3.13	9.58
	Gazipur	1.88	2.29	8.33	4.38	1.67	7.5
	Gopalganj	1.88	2.71	11.46	3.13	3.54	9.79
	Jamalpur	1.67	5.63	7.29	1.25	5	7.92
	Kishoreganj	2.5	2.5	5.83	3.33	3.33	6.25
	Madaripur	1.88	3.13	8.54	3.54	3.75	9.58
	Manikganj	1.46	1.67	8.13	4.38	2.08	8.54
	Munshiganj	1.67	2.71	11.25	3.75	2.71	9.17
	Mymensingh	2.29	2.29	5	2.92	4.38	6.88
	Narayanganj	1.67	3.75	7.08	4.58	2.5	7.5
	Narsingdi	2.08	3.75	5.42	3.54	4.38	6.25
	Netrakona	3.54	2.08	5.63	1.88	3.75	6.46
	Rajbari	0.63	5	8.13	3.33	1.88	10.63
	Shariatpur	1.88	1.67	10.63	3.54	3.75	8.75
	Sherpur	1.67	4.38	8.33	1.25	5.83	8.33

(continued)

Table 2 (continued)

Division	District	Extreme dry (%)	Severe dry (%)	Moderate dry (%)	Extreme wet (%)	Severe wet (%)	Moderate wet (%)
	Tangail	1.67	2.29	8.13	4.17	2.5	7.5
	Average	**1.85**	**2.99**	**8.06**	**3.32**	**3.32**	**8.04**
Khulna	Bagerhat	0.63	6.88	9.79	2.29	5.83	6.67
	Chuadanga	1.88	2.29	11.46	2.29	2.92	8.96
	Jessore	2.5	4.17	9.17	0.83	6.04	10.42
	Jhenaidah	2.29	2.08	12.08	2.29	4.17	8.75
	Khulna	0.63	5.63	12.71	1.04	6.46	7.92
	Kushtia	1.88	4.17	12.29	2.71	2.5	7.71
	Magura	0.42	5	13.33	2.5	5	10
	Meherpur	2.08	4.38	10.83	2.5	2.08	8.33
	Narail	1.46	3.75	13.75	1.67	5.21	10
	Satkhira	0.63	4.58	14.79	0.63	6.67	8.13
	Average	**1.44**	**4.29**	**12.02**	**1.88**	**4.69**	**8.69**
Rajshahi	Bogra	0.83	7.5	10	1.46	3.96	8.75
	Joypurhat	0.83	7.29	7.92	2.29	5	6.67
	Naogaon	1.04	7.29	7.08	2.71	4.58	5.63
	Natore	1.04	6.88	8.33	3.13	3.13	7.08
	Nawabganj	2.08	7.92	5.63	1.04	6.67	6.04
	Pabna	0.21	6.46	8.33	3.33	2.5	7.08
	Rajshahi	0.42	8.13	8.33	2.92	4.58	6.25
	Sirajganj	0.42	4.17	11.04	3.13	2.92	9.38
	Average	**0.86**	**6.96**	**8.33**	**2.5**	**4.17**	**7.11**
Rangpur	Dinajpur	2.29	3.96	6.46	2.08	3.54	10.83
	Gaibandha	0.83	7.5	7.92	1.25	4.79	11.04
	Kurigram	2.29	4.38	10.21	0.83	3.33	9.79
	Lalmonirhat	2.29	2.5	9.17	0.63	6.88	8.75
	Nilphamari	2.29	3.33	5.83	1.04	6.04	10.63
	Panchagarh	2.29	3.13	8.96	0.63	7.08	10.42
	Rangpur	2.71	4.17	7.71	1.04	5	9.38
	Thakurgaon	1.67	4.38	10.21	1.04	5	11.67
	Average	**2.08**	**4.17**	**8.31**	**1.07**	**5.21**	**10.31**
Sylhet	Habiganj	2.08	2.29	5.63	3.96	2.29	8.13
	Maulvibazar	1.25	3.96	9.17	3.33	3.54	7.71
	Sunamganj	3.33	2.08	5.42	3.13	1.88	7.5
	Sylhet	0.63	4.79	9.58	2.08	4.38	7.71

(continued)

Table 2 (continued)

Division	District	Extreme dry (%)	Severe dry (%)	Moderate dry (%)	Extreme wet (%)	Severe wet (%)	Moderate wet (%)
	Average	**1.82**	**3.28**	**7.45**	**3.13**	**3.02**	**7.76**

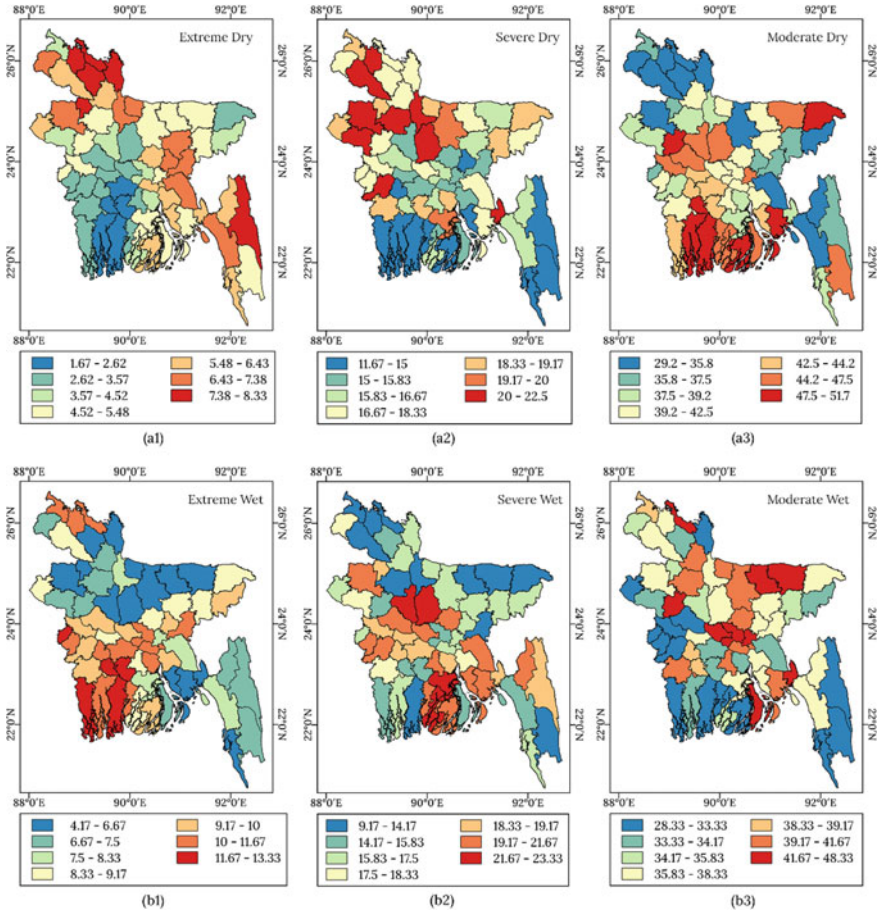

Fig. 2 Spatial distribution of the frequency (in %) of short-term dry periods (**a**) and frequency of short-term wet periods (**b**) of different intensities (extreme, severe and moderate)

that year against the December–January–February precipitation totals for all years. Short-term analysis indicates a greater likelihood of extreme droughts in the bulk of districts in the country's northernmost area of Rangpur and east to south-eastern Chittagong region, according to the 3-month SPI. Severe droughts are prevalent in northern Bangladesh, while moderate droughts affect the middle to south-western parts of the country. Short-term severe to extreme wet episodes are more prevalent

Table 3 The frequency of occurrences of short-term dry and wet periods of various intensities in different districts of Bangladesh between the years 1981 and 2020

Division	District	Extreme dry (%)	Severe dry (%)	Moderate dry (%)	Extreme wet (%)	Severe wet (%)	Moderate wet (%)
Barisal	Barguna	4.17	16.67	45	9.17	22.5	35
	Barisal	5	20	38.33	8.33	23.33	38.33
	Bhola	5	15.83	47.5	7.5	15.83	45
	Jhalokati	5	15.83	46.67	9.17	22.5	33.33
	Patuakhali	5.83	13.33	49.17	10	20.83	32.5
	Pirojpur	3.33	14.17	47.5	11.67	21.67	30.83
	Average	**4.72**	**15.97**	**45.7**	**9.31**	**21.11**	**35.83**
Chittagong	Bandarban	5	11.67	47.5	7.5	13.33	33.33
	Brahamanbaria	6.67	15.83	36.67	11.67	14.17	36.67
	Chandpur	5.83	15.83	42.5	10	18.33	36.67
	Chittagong	6.67	16.67	35.83	8.33	15.83	37.5
	Cumilla	6.67	17.5	29.17	8.33	21.67	34.17
	Coxs Bazar	5.83	12.5	39.17	6.67	16.67	28.33
	Feni	5.83	20.83	39.17	5.83	19.17	48.33
	Khagrachhari	5.83	16.67	33.33	7.5	21.67	38.33
	Lakshmipur	5.83	14.17	44.17	6.67	20	36.67
	Noakhali	5	17.5	48.33	5	20	41.67
	Rangamati	7.5	12.5	37.5	7.5	19.17	33.33
	Average	**6.06**	**15.61**	**39.39**	**7.73**	**18.18**	**36.82**
Dhaka	Dhaka	4.17	16.67	41.67	11.67	15	44.17
	Faridpur	2.5	15.83	43.33	11.67	19.17	34.17
	Gazipur	5.83	15.83	40	9.17	20.83	40.83
	Gopalganj	2.5	19.17	44.17	13.33	15.83	34.17
	Jamalpur	6.67	21.67	38.33	8.33	14.17	38.33
	Kishoreganj	6.67	16.67	40	9.17	16.67	38.33
	Madaripur	3.33	16.67	42.5	9.17	20.83	40
	Manikganj	3.33	18.33	42.5	10	20.83	45
	Munshiganj	5.83	15.83	42.5	11.67	16.67	40.83
	Mymensingh	5	20	34.17	4.17	16.67	41.67
	Narayanganj	5	15.83	45.83	8.33	17.5	44.17
	Narsingdi	6.67	15	37.5	10	17.5	36.67
	Netrakona	5	18.33	41.67	6.67	11.67	45.83
	Rajbari	3.33	15.83	43.33	9.17	19.17	36.67
	Shariatpur	4.17	19.17	39.17	10.83	19.17	34.17
	Sherpur	6.67	19.17	40.83	6.67	16.67	40.83

(continued)

Table 3 (continued)

Division	District	Extreme dry (%)	Severe dry (%)	Moderate dry (%)	Extreme wet (%)	Severe wet (%)	Moderate wet (%)
	Tangail	3.33	20.83	45	5.83	22.5	38.33
	Average	**4.71**	**17.7**	**41.32**	**9.17**	**17.7**	**39.66**
Khulna	Bagerhat	1.67	15	51.67	13.33	14.17	33.33
	Chuadanga	3.33	17.5	40.83	10.83	20.83	33.33
	Jessore	3.33	19.17	40.83	10	18.33	40.83
	Jhenaidah	3.33	20.83	38.33	10	21.67	31.67
	Khulna	1.67	13.33	48.33	10.83	17.5	34.17
	Kushtia	5	17.5	45	10	19.17	32.5
	Magura	3.33	13.33	44.17	10.83	19.17	39.17
	Meherpur	5	18.33	36.67	12.5	17.5	30
	Narail	1.67	16.67	50.83	12.5	15	39.17
	Satkhira	3.33	11.67	44.17	12.5	15.83	33.33
	Average	**3.17**	**16.33**	**44.08**	**11.33**	**17.92**	**34.75**
Rajshahi	Bogra	5	22.5	38.33	7.5	13.33	41.67
	Joypurhat	7.5	19.17	37.5	6.67	19.17	35.83
	Naogaon	6.67	22.5	31.67	6.67	20	38.33
	Natore	5	18.33	48.33	7.5	15	43.33
	Nawabganj	5.83	19.17	39.17	9.17	17.5	31.67
	Pabna	3.33	16.67	46.67	10	21.67	32.5
	Rajshahi	4.17	21.67	39.17	7.5	18.33	34.17
	Sirajganj	4.17	15.83	45	5.83	22.5	35.83
	Average	**5.21**	**19.48**	**40.73**	**7.61**	**18.44**	**36.67**
Rangpur	Dinajpur	5.83	22.5	35	9.17	10.83	38.33
	Gaibandha	5.83	17.5	40.83	7.5	16.67	41.67
	Kurigram	7.5	18.33	35.83	6.67	17.5	28.33
	Lalmonirhat	8.33	18.33	33.33	10.83	9.17	45.83
	Nilphamari	7.5	20.83	31.67	10.83	14.17	37.5
	Panchagarh	4.17	19.17	36.67	10.83	11.67	39.17
	Rangpur	8.33	18.33	35.83	6.67	15.83	34.17
	Thakurgaon	6.67	17.5	33.33	7.5	18.33	35.83
	Average	**5.02**	**17.31**	**41.08**	**9.02**	**17.87**	**37.22**
Sylhet	Habiganj	5	19.17	37.5	9.17	17.5	35.83
	Maulvibazar	4.17	18.33	35	10	16.67	34.17
	Sunamganj	5	16.67	45.83	6.67	12.5	46.67
	Sylhet	3.33	19.17	48.33	9.17	14.17	37.5

(continued)

Table 3 (continued)

Division	District	Extreme dry (%)	Severe dry (%)	Moderate dry (%)	Extreme wet (%)	Severe wet (%)	Moderate wet (%)
	Average	**4.38**	**18.34**	**41.67**	**8.75**	**15.21**	**38.54**

in Bangladesh's central and south-western areas, compared to moderate wet periods which are prevalent in the central and north-eastern regions.

Additionally, there is a notable change in the frequency percentages—they increase for both dry and wet periods of all intensities as the timescale decreases. Tables 2 and 3 illustrate this by comparing the frequency percentages for various events in the 3- and 12-month SPI. By identifying critical districts i.e., the districts highlighted in red in the generated maps, short-term solutions to meet agricultural objectives, such as achieving optimal soil moisture and minimizing agricultural drought risks, may be proposed for those regions. It is prudent to take appropriate steps early in response to moderate dry/wet episodes that have the potential to deteriorate into severe occurrences over longer time frames.

3.3 Spatial Distribution of the Total Number of Dry/Wet Events in Bangladesh Since 1981

The districts with the largest number of dry/wet events, regardless of intensity, are depicted in Fig. 3. It is apparent that nearly the whole western Bangladesh is prone to long-term dry episodes, but short-term dry episodes are more frequent in the southern districts of the Barisal division and portions of the north and north-eastern districts of Sylhet and Rajshahi division. Similarly, whereas the northern and southern sections of the nation are more susceptible to long-term wet periods, the central region of

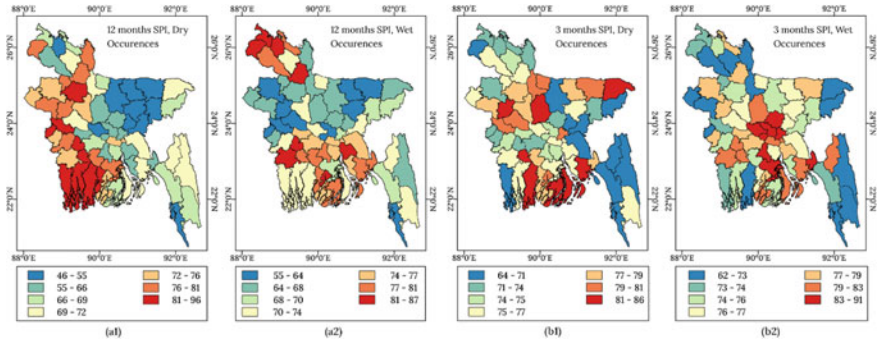

Fig. 3 Spatial distribution of the total number of long-term (**a**) and short-term (**b**) dry months and wet months in Bangladesh between 1981 and 2020

Bangladesh is more prone to short-term wet periods. It is worth noting that while certain districts (e.g., Dhaka) are prone to frequent short-term wet periods, they are one of the least affected areas in terms of long-term wet periods. This confirms the spatial variability of dry/wet periods in terms of timescales.

3.4 Evaluation of SPI-3 and SPI-12 in 40 years

SPI time series was constructed at different time intervals of three and twelve months to assess their potential utility for identifying dry/wet periods and monitoring the risk of extreme events. Figure 5 shows the SPI time series for the eastern Sylhet and northern Rangpur regions from 1981 to 2020 on 3- and 12-month time periods, as well as the occurrence of past major flood and drought events in the region.

Dry/wet seasons vary according to timescale. When timescale is small, the SPI oscillates frequently above and below zero. On longer periods, the SPI varies slowly as precipitation changes. When a 12-month period is used, the drought episodes are more concentrated and persist longer than the more dispersed 3-month drought events—they occur more frequently and last less time. This is a feature that has been seen in a variety of other locations: McKee et al. (1993) in Colorado, USA, Lloyd-Hughes and Saunders (2002) in Yorkshire, UK, and Szalai and Szinell (2000) in Szarvas, Hungary.

Figure 4 depicts the variability of the SPI in the Sylhet and Rangpur districts over 3- and 12-month intervals from 1981 to 2020. The findings confirm the assertions made previously. SPI demonstrates a high frequency of shift between dry and rainy periods over short time frames. Dry and wet phases shift less frequently and last longer as timescales increase.

Longer timescales (SPI of 12 months or more) are better for detecting historically major drought and flood incidents. Drought episodes lasting 12 months or longer (SPI-12 < -1.5) were recorded in Sylhet in 1994, 2007, and 2019 and in Rangpur in 1994, 2007, and 2014. In Sylhet, severe to extreme flood episodes occurred in 1988, 2004, 2010, and 2017; while in Rangpur, severe to extreme flood events occurred in 1984, 1988, 1998, and 2020. Rangpur had a succession of extremely dry years from 2007 to 2015, with the detrimental impacts of droughts reaching an apex in 2014. During the study period, Sylhet, on the other hand, had interchanging years of dry/wet periods.

On shorter timescales, the frequent seasonal and inter-annual precipitation fluctuations are more apparent, resulting in a large number of events and, thus, a greater frequency. On a short timescale, the class of moderate events has the highest monthly frequency, at 40–45% for moderate dry episodes and 35–40% for moderate wet episodes. On the contrary, 8–12% for moderate dry and 6–10% for moderate wet episode frequency are observed in terms of longer timescale, both of which are highest among the classes. The shorter timescale SPI values are more scattered and fluctuate rapidly, whereas the longer timescale SPI values are localized in a series of

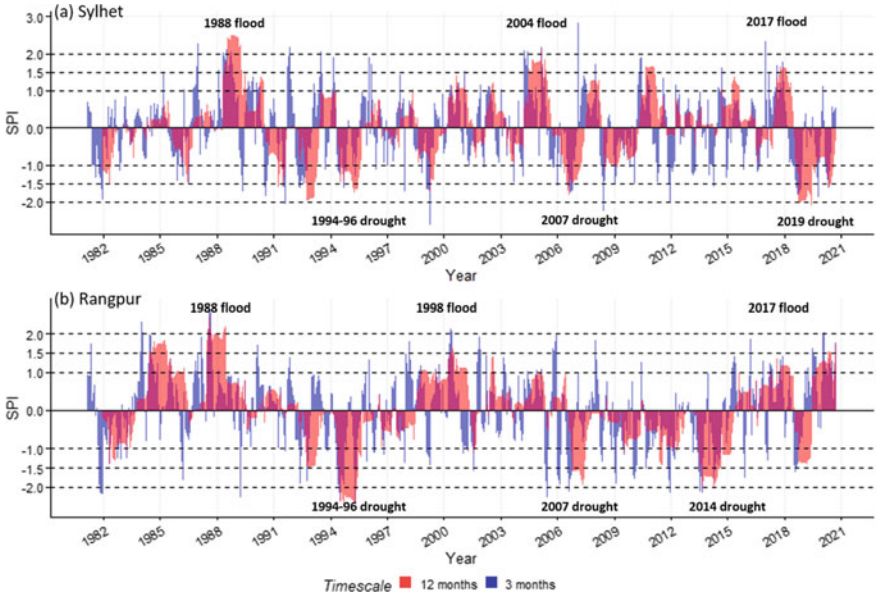

Fig. 4 The temporal evaluation of SPI-3 and SPI-12 averaged over districts of (**a**) Sylhet and (**b**) Rangpur

consecutive months within a year or the next few years (e.g., the Rangpur district's dry years of 2007–2015).

By translating the observed number of dry/wet events to the number of occurrences in 100 years using Eq. (2), one can anticipate for the district of Sylhet approximately 15 droughts and 14 flood events of varying intensities lasting 12 months (Table 2), as well as approximately 71 droughts and 61 flood episodes of varying intensities lasting 3 months (Table 3). Using a similar method, comparable estimations can be generated for other districts as well. The aforementioned data, derived from the SPI study, provides extremely useful information about the local climates found across Bangladesh. For many years, it has been asserted that this is a region prone to droughts and floods, but only the SPI for various timescales and intensities allows for the visualization of the spatial link between the number of months with droughts/floods for various timescales, frequency, and length.

4 Conclusions

Since point-based observations limit spatiotemporal analysis of precipitation, effective drought monitoring is hindered. High-resolution satellite precipitation data products, when combined with in situ observations, have been shown to be an excellent alternative data source for spatiotemporal drought analysis. The open-source

CHIRPS data products are accessible at multiple temporal scales and have a great potential for drought and flood detection and evaluation in near real-time. This study evaluated the district-wide dry/wet event characteristics for Bangladesh from 1981 to 2020 using the CHIRPS data generated SPI. The findings of this study show that the standardized precipitation index SPI is extremely useful in identifying and characterizing local dry and wet periods. Since it just requires precipitation data, the SPI is straightforward to use. It is feasible to determine the frequency of droughts and floods that are the result of rainfall anomalies in previous periods using different timescales for which it is computed. The study looked at the number of months in which drought/flood events were recognized at the 3- and 12-month timescales and found that, depending on the timing and intensity of the event, there is a significant geographical diversity of dry/wet period recurrence frequency across Bangladesh. Based on the three classes of intensities, the highest frequencies of long-term dry periods were observed in divisions of Rangpur (Extreme-2.08%), Rajshahi (Severe-6.96%), and Khulna (Moderate-12.02%), whereas long-term wet periods were prevalent in divisions of Dhaka (Extreme-3.32%) and Rangpur (Severe-5.21% and Moderate-10.31%). Moreover, short-term analysis depicted a different scenario, with the Chittagong division (Extreme-6.06%), the Rajshahi division (Severe-19.48%), and the Barisal division (Moderate-45.7%) observed as the most frequently affected by short-term dry periods; and the Khulna division (Extreme-11.33%), the Barisal division (Severe-21.11%), and the Dhaka division (Moderate-39.66%) observed as the most short-term flood-prone divisions. Using previous rainfall data, the current study aids in comprehending severe dry/wet occurrences in different locations of the country. Furthermore, the findings may aid in the planning of essential steps to control regional drought and flood, reducing the negative effects of extreme weather occurrences across Bangladesh.

References

Adams, James. 2017. Climate_indices, an Open Source Python Library Providing Reference Implementations of Commonly Used Climate Indices. https://github.com/monocongo/climate_indices.

Ahmed, Kamal, Shamsuddin Shahid, Eun-Sung. Chung, Xiao-jun Wang, and Sobri Bin Harun. 2019. Climate Change Uncertainties in Seasonal Drought Severity-Area-Frequency Curves: Case of Arid Region of Pakistan. *Journal of Hydrology* 570: 473–485.

Alamgir, Mahiuddin, Shamsuddin Shahid, Manzul Kumar Hazarika, Syams Nashrrullah, Sobri Bin Harun, and Supiah Shamsudin. 2015. Analysis of Meteorological Drought Pattern During Different Climatic and Cropping Seasons in Bangladesh. *JAWRA Journal of the American Water Resources Association* 51 (3): 794–806.

Arnell, Nigel W. 1999. Climate Change and Global Water Resources. *Global Environmental Change* 9: S31-49.

Bangladesh Bureau of Statistics (BBS). 2015. Disaster-Related Statistics 2015 Climate Change and Natural Disaster Perspectives. Ministry of Planning, Government of the People's Republic of Bangladesh: Dhaka, Bangladesh.

Bangladesh Bureau of Statistics (BBS). 2021. Yearbook of Agricultural Statistics-2020. Ministry of Planning, Government of the People's Republic of Bangladesh: Dhaka, Bangladesh.

Basher, Md Abul, Mathew Alexander Stiller-Reeve, A.K.M. Saiful Islam, and Scott Bremer. 2018. Assessing Climatic Trends of Extreme Rainfall Indices over Northeast Bangladesh. *Theoretical and Applied Climatology* 134 (1): 441–452.

Bechle, Matthew J., Dylan B. Millet, and Julian D. Marshall. 2013. Remote Sensing of Exposure to NO2: Satellite Versus Ground-Based Measurement in a Large Urban Area. *Atmospheric Environment* 69: 345–353.

Cordell, Dana, Jan-Olof. Drangert, and Stuart White. 2009. The Story of Phosphorus: Global Food Security and Food for Thought. *Global Environmental Change* 19 (2): 292–305.

Du, Juan, Jian Fang, Wei Xu, and Peijun Shi. 2013. Analysis of Dry/Wet Conditions Using the Standardized Precipitation Index and Its Potential Usefulness for Drought/Flood Monitoring in Hunan Province, China. *Stochastic Environmental Research and Risk Assessment* 27 (2): 377–387.

Edwards, Daniel C. 1997. Characteristics of 20th Century Drought in the United States at Multiple Time Scales. Air Force Inst of Tech Wright-Patterson AFB OH.

Funk, Chris, Pete Peterson, Martin Landsfeld, Diego Pedreros, James Verdin, James D. Rowland, Bo E. Romero, Gregory Husak, Joel Michaelsen, and Andrew Verdin. 2014. A Quasi-Global Precipitation Time Series for Drought Monitoring. *US Geological Survey Data Series* 832 (4): 1–12.

Funk, Chris, Pete Peterson, Martin Landsfeld, Diego Pedreros, James Verdin, Shraddhanand Shukla, Gregory Husak, James Rowland, Laura Harrison, and Andrew Hoell. 2015. The Climate Hazards Infrared Precipitation with Stations—A New Environmental Record for Monitoring Extremes. *Scientific Data* 2 (1): 1–21.

Gao, Feng, Yuhu Zhang, Xiulin Ren, Yunjun Yao, Zengchao Hao, and Wanyuan Cai. 2018. Evaluation of CHIRPS and Its Application for Drought Monitoring over the Haihe River Basin, China. *Natural Hazards* 92 (1): 155–172.

"Glossary of Terms." 2014. *Scandinavian Journal of Public Health* 42 (14_suppl): 178–190. https://doi.org/10.1177/1403494813515131.

Green, Colin. 2010. Towards Sustainable Flood Risk Management. *International Journal of Disaster Risk Science* 1 (1): 33–43.

IEA. 2009. World Energy Outlook 2009 – Analysis - IEA. https://www.iea.org/reports/world-energy-outlook-2009.

Kafy, Abdulla - Al, Abdullah Al Rakib, Kaniz Shaleha Akter, Zullyadini A. Rahaman, Abdullah-Al Faisal, Saumik Mallik, N.M. Refat Nasher, Md. Iquebal Hossain, and Md. Yeamin Ali. 2021. Monitoring the Effects of Vegetation Cover Losses on Land Surface Temperature Dynamics Using Geospatial Approach in Rajshahi City, Bangladesh. *Environmental Challenges*: 100187. https://doi.org/10.1016/j.envc.2021.100187.

Keyantash, John, and John A. Dracup. 2002. The Quantification of Drought: An Evaluation of Drought Indices. *Bulletin of the American Meteorological Society* 83 (8): 1167–1180.

Khan, Sadiq I., Yang Hong, Jonathan J. Gourley, Muhammad U. Khattak, and Tom De Groeve. 2014. Multi-Sensor Imaging and Space-Ground Cross-Validation for 2010 Flood along Indus River, Pakistan. *Remote Sensing*. https://doi.org/10.3390/rs6032393.

Kim, Do-Woo, Hi-Ryong Byun, and Ki-Seon Choi. 2009. Evaluation, Modification, and Application of the Effective Drought Index to 200-Year Drought Climatology of Seoul, Korea. *Journal of Hydrology* 378 (1–2): 1–12.

Krysanova, Valentina, Tobias Vetter, and Fred Hattermann. 2008. Detection of Change in Drought Frequency in the Elbe Basin: Comparison of Three Methods. *Hydrological Sciences Journal* 53 (3): 519–537.

Livada, I., and V.D. Assimakopoulos. 2007. Spatial and Temporal Analysis of Drought in Greece Using the Standardized Precipitation Index (SPI). *Theoretical and Applied Climatology* 89 (3): 143–153.

McKee, Thomas B., Nolan J. Doesken, and John Kleist. 1993. The Relationship of Drought Frequency and Duration to Time Scales. In *Proceedings of the 8th Conference on Applied Climatology* 17: 179–183. Boston.

Min, Seung-Ki, Won-Tae Kwon, E-Hyung Park, and Youngeun Choi. 2003. Spatial and Temporal Comparisons of Droughts over Korea with East Asia. *International Journal of Climatology: A Journal of the Royal Meteorological Society* 23 (2): 223–233.

Mohsenipour, Morteza, Shamsuddin Shahid, Eun-sung Chung, and Xiao-jun Wang. 2018. Changing Pattern of Droughts during Cropping Seasons of Bangladesh. *Water Resources Management* 32 (5): 1555–1568.

Molden, David. 2013. *Water for Food Water for Life: A Comprehensive Assessment of Water Management in Agriculture*. Routledge.

Mondol, Md, Anarul Haque, Iffat Ara, and Subash Chandra Das. 2017. Meteorological Drought Index Mapping in Bangladesh Using Standardized Precipitation Index during 1981–2010. *Advances in Meteorology* 2017.

Moradi, H.R., M. Rajabi, and M. Faragzadeh. 2011. Investigation of Meteorological Drought Characteristics in Fars Province, Iran. *CATENA* 84 (1–2): 35–46.

Nafarzadegan, A.R., M. Rezaeian Zadeh, M. Kherad, H. Ahani, A. Gharehkhani, M.A. Karampoor, and M.R. Kousari. 2012. Drought Area Monitoring During the Past Three Decades in Fars Province, Iran. *Quaternary International* 250: 27–36.

Pandey, Varsha, Prashant K. Srivastava, R.K. Mall, Francisco Munoz-Arriola, and Dawei Han. 2020. Multi-Satellite Precipitation Products for Meteorological Drought Assessment and Forecasting in Central India. *Geocarto International*, 1–20.

Parry, Martin, Osvaldo Canziani, Jean Palutikof, Paul van der Linden, and C.E. Hanson. 2007. *Intergovernmental Panel on Climate Change Contribution of Working Group I to the Fourth Assessment Report of the Intergovernmental Panel on Climate Change.* Cambridge and New York: Cambridge University Press.

Piccarreta, Marco, Domenico Capolongo, and Federico Boenzi. 2004. Trend Analysis of Precipitation and Drought in Basilicata from 1923 to 2000 within a Southern Italy Context. *International Journal of Climatology: A Journal of the Royal Meteorological Society* 24 (7): 907–922.

Quiring, Steven M., and Timothy N. Papakryiakou. 2003. An Evaluation of Agricultural Drought Indices for the Canadian Prairies. *Agricultural and Forest Meteorology* 118 (1–2): 49–62.

Rimi, Ruksana H., Karsten Haustein, Myles R. Allen, and Emily J. Barbour. 2019. Risks of Pre-Monsoon Extreme Rainfall Events of Bangladesh: Is Anthropogenic Climate Change Playing a Role. *Bulletin of the American Meteorological Society* 100: S61–65.

Rosenzweig, Cynthia, Ana Iglesius, Xiao-Bing Yang, Paul R. Epstein, and Eric Chivian. 2001. Climate Change and Extreme Weather Events-Implications for Food Production, Plant Diseases, and Pests.

Shahid, Shamsuddin, and Houshang Behrawan. 2008. Drought Risk Assessment in the Western Part of Bangladesh. *Natural Hazards* 46 (3): 391–413. https://doi.org/10.1007/s11069-007-9191-5.

Shrestha, Narayan K., Faisal M. Qamer, Diego Pedreros, M.S.R. Murthy, Shahriar Md Wahid, and Mandira Shrestha. 2017. Evaluating the Accuracy of Climate Hazard Group (CHG) Satellite Rainfall Estimates for Precipitation Based Drought Monitoring in Koshi Basin, Nepal. *Journal of Hydrology: Regional Studies* 13: 138–151.

Stagge, James H., Lena M. Tallaksen, Lukas Gudmundsson, Anne F. Van Loon, and Kerstin Stahl. 2015. Candidate Distributions for Climatological Drought Indices (SPI and SPEI). *International Journal of Climatology* 35 (13): 4027–4040.

Tao, Hui, Thomas Fischer, Yan Zeng, and Klaus Fraedrich. 2016. Evaluation of TRMM 3B43 Precipitation Data for Drought Monitoring in Jiangsu Province, China. *Water* 8 (6): 221.

Thom, Herbert C S. 1958. A Note on the Gamma Distribution. *Monthly Weather Review* 86 (4): 117–122.

Vergni, L., and F. Todisco. 2011. Spatio-Temporal Variability of Precipitation, Temperature and Agricultural Drought Indices in Central Italy. *Agricultural and Forest Meteorology* 151 (3): 301–313.

WMO. 2012. Standardized Precipitation Index User Guide. https://library.wmo.int/doc_num.php?explnum_id=7768.

Wu, Hong, Mark D. Svoboda, Michael J. Hayes, Donald A. Wilhite, and Fujiang Wen. 2007. Appropriate Application of the Standardized Precipitation Index in Arid Locations and Dry Seasons. *International Journal of Climatology: A Journal of the Royal Meteorological Society* 27 (1): 65–79.

Wu, Wenqi, Yungang Li, Xian Luo, Yueyuan Zhang, Xuan Ji, and Xue Li. 2019. Performance Evaluation of the CHIRPS Precipitation Dataset and Its Utility in Drought Monitoring over Yunnan Province, China. *Geomatics, Natural Hazards and Risk* 10 (1): 2145–2162.

Yuan, Wen-Ping., and Guang-Sheng. Zhou. 2004. Comparison Between Standardized Precipitation Index and Z-Index in China. *Chinese Journal of Plant Ecology* 28 (4): 523.

Zhong, Ruida, Xiaohong Chen, Chengguang Lai, Zhaoli Wang, Yanqing Lian, Haijun Yu, and Xiaoqing Wu. 2019. Drought Monitoring Utility of Satellite-Based Precipitation Products Across Mainland China. *Journal of Hydrology* 568: 343–359.

Indigenous Knowledge and Practices of the Small Ethnic Communities of Asia–Pacific Island Countries in Facing Hydro-Meteorological Hazards

Mahfuzul Haque

Abstract Tsunami of 2004 brought with it unprecedented damages to the lives and livelihoods of people in 12 Indian Ocean nations. This was by far, the worst disaster in the recent past, resulting in a high death toll and a huge devastation. Studies conducted during the post-tsunami period among the coastal communities of the island nations in South Asia and the Pacific found survival strategies of the local community in the face of disasters. This paper examined resilience of the coastal and small island communities in Indonesia, the Philippines, Timor-Leste and Solomon Islands in the Asia–Pacific; Andaman and Nicobar Islands in the Indian Ocean; and Bangladesh coast in the Bay of Bengal in the face of earthquake, tsunami and hazards like cyclones, floods and tidal surges. Based on animal behavior, activities of celestial bodies, environment; material culture; traditional, religious and faith-based beliefs and practices, the local community was able to develop a coping mechanism for themselves with these hydro-meteorological disasters. The paper argues that as the indigenous communities practice their traditional knowledge, they could save themselves from the earthquake and tsunami-related disasters. The paper further argues that they have been living with natural disasters over generations based on their indigenous knowledge and practices.

Keywords Andaman and Nicobar Island · Bangladesh coast · Ethnic communities · Indigenous knowledge and practices · Tsunami

1 Introduction

According to UNESCO's program on Local and Indigenous Knowledge Systems (LINKS), local and indigenous knowledge refers to the understandings, skills and philosophies developed by societies with long histories of interaction with their natural surroundings (Hiwasaki et al. 2014). This definition states that local and indigenous knowledge is one that is dynamic. The term local and indigenous

M. Haque (✉)
Adjunct Faculty, Department of Sociology, Bangladesh University of Professionals, Dhaka, Bangladesh

© The Author(s), under exclusive license to Springer Nature Switzerland AG 2022

G. M. Tarekul Islam et al. (eds.), *Water Management: A View from Multidisciplinary Perspectives*,
https://doi.org/10.1007/978-3-030-95722-3_7

knowledge is comparable to local and traditional knowledge, indigenous technical knowledge and endogenous knowledge.

Functional knowledge of local people is generally known as Indigenous Knowledge (IK) living in a particular ethno-cultural and agro-ecological condition. Indigenous knowledge is developed through experience sharing and normally passes from one generation to another orally, and it remains in operation in all aspects of community life and continues to be there in unwritten forms (Amin 2000; Haque 2013). It is often mentioned that unwritten knowledge is vulnerable to being lost; local wisdom has a tendency to remain present in the villages, old towns, markets and other places. IK generally sticks around in a holistic way in their knowledge, beliefs and perceptions, mainly among the people living in rural environments (Warner 1991; Sillitoe et al. 1998). According to Walker et al. (1991), this is a knowledge held collectively by a specific community.

Generally, indigenous knowledge is not codified or written in formal language. IK mostly remains in verbal form and passes on from one generation to another. It is increasingly felt that IK is a resource that should be promoted and preserved in order to complement scientific knowledge while developing appropriate plans and policies for people in the rural areas. IK refers to knowledge, values, concepts, perceptions and beliefs of a specific community. It is essentially a diverse and multi-faceted knowledge system with a distinct language. Sillitoe (2000) stated that contrary to "top down" interventions, IK has followed a "bottom-up" or "grassroots" process. Generally found in rural areas in unwritten form and in informal discussions, IK could be distinguished by scientific knowledge available in written and codified language and literature.

The term "indigenous" is synonymous with "traditional" and "local", distinguishing this knowledge from that of scientific knowledge developed by formal research studies undertaken by education institutions (Mustafa 2000; Haque 2019). IK continues to be used by rural people in natural resource management, conservation of fisheries, livestock and healthcare practices. Sillitoe et al. (1998) stated that indigenous knowledge relates to any knowledge held collectively by a population mostly inhabiting in rural areas. IK may incorporate knowledge of any kind including that of socio-cultural practices and natural resource management.

Importance of local knowledge and practices cannot be avoided. It is to be noted that knowledge and practices of the local community cannot be called as primitive or unscientific. The local community, however, is exposed to modern knowledge. They have not disowned their indigenous knowledge and practices assimilated over generations. It is true that local knowledge is eroding fast and much has been lost with the modernization and rapid spread of foreign technology introduced from outside. The development practitioners are of the opinion that indigenous knowledge needs to be promoted and documented before it goes into oblivion.

McAdoo et al. (2008) stated that there are a number of international agreements that recognize the value of indigenous knowledge for sustainable development. This includes the Rio Declaration 1992; Agenda 21, 1992; Convention on Biological Diversity, 1992; World Summit on Sustainable Development, Johannesburg,

2002; and the work of International Decade (1995–2004) for the World's Indigenous Peoples.

In line with the Hyogo Framework for Action 2005–2015 and Sendai Framework for Disaster Risk Reduction 2015–2030, national disaster risk reduction strategies are to incorporate the local knowledge of the indigenous communities practiced over generations. One of the five main drivers of the Hyogo Framework was strong community engagement for effective disaster risk reduction. Among the priority actions, the Framework observed that people are to be made aware of indigenous knowledge and traditional practices for risk reduction and mitigation. On the other hand, the Sendai Framework, 2015–2030 emphasized on "indigenous knowledge and practices and coping strategy of the local community in facing challenges of natural disaster". Emphasizing on the role of the stakeholders, it said that the indigenous peoples, through their experience and traditional knowledge, provide an important contribution to the plans and policies concerning disaster risk reduction.

The hydro-meteorological hazard discussed in this article is atmospheric, hydrological or oceanographic in nature, that may cause loss of life, injury, property damage, loss of livelihoods and services, social and economic disruption and environmental damage. The hazards discussed in this article are caused by hydro-meteorological events like floods, cyclones, tidal surges and tsunami.

With a brief description on indigenous knowledge and practices, the paper deliberates on survival strategies of these coastal and small ethnic communities. The paper examined how their age-old beliefs were found handy in time of disasters, like earthquake and tsunami. The paper suggests that indigenous knowledge and practices need to be integrated with science before it can be used in policies, education and actions related to hydro-meteorological hazards. This article is divided into five sections. The introduction deliberates on the definitional issues of indigenous knowledge and practices and the emphasis given by the Hyogo and Sendai Frameworks on incorporating indigenous knowledge and practices in disaster management policies and plans. The introduction is followed by a series of case studies concerning the experiences of the coastal and small ethnic communities of the Asia–Pacific Islands; Andaman and Nicobar Islands and the Bangladesh Coasts. The last section concludes that indigenous knowledge and practices need to be integrated with science before it can be used in policies, education and actions related to disaster risk reduction and climate change.

2 Methodology

The paper is based on secondary sources of literature, books and journals available in print and electronic media. Interviews were also held with some authors on indigenous knowledge and practices, both at home and abroad, in order to understand the link between disaster and its understanding by the coastal and small ethnic communities, based on their age-old beliefs. Efforts were taken to obtain confirmation regarding this delicate linkage through communication with some relevant

authors. Views and comments received from the audience present in the conference were further checked and incorporated prior to finalizing the paper.

3 Asia–Pacific Islands

Primary hydro-meteorological hazards faced by the communities in Asia–Pacific island nations are typhoons, storms, tidal surges, heavy rainfall, floods and landslides. Coastal communities have also observed climatic changes, such as warmer days and nights, changes in rainfall patterns and more frequent and stronger cyclonic storms. These are mainly seen in the Philippines. In Indonesia, more frequent monsoons, tropical cyclones, coastal erosion and land subsistence are noticeable. The primary problems in Timor-Leste are tropical cyclones with heavy rainfall, and prolonged dry and extended rainy seasons resulting in floods, landslides and droughts (Hiwasaki et al. 2014). In addition to earthquakes and tsunamis, there have been incidences of volcanic eruptions from some of the active volcanoes that are present here.

Coastal and small island communities, over the generations, have been observing changes in the environment and have gathered a wealth of knowledge and practices closely related to hydro-meteorological hazards. The local people are able to closely observe and monitor changes in their environment by looking at the seas, clouds, animals, plants and insects. The changes of position in celestial bodies, like the moon, sun, and stars also help them understand the advent of hydro-meteorological hazards. These small island communities also suffer from food crises as they get isolated from the mainland, and communication is disrupted during hazardous situations.

Hiwasaki et al. (2014) stated that the communities predict heavy rainfall or strong winds by observing clouds, waves, winds, sun and the stars. Their local and indigenous knowledge is based on the (a) observations of animal behavior; (b) observations of celestial bodies; (c) observations of the environment; (d) material culture; and (e) traditional and faith-based beliefs and practices. They look for changes in the texture of clouds (thin or thick), color (white, dark, yellow or red), location (over the mountains or the sea) and movement (to and from the coast), including speed (fast) and direction (vertical or horizontal). They observe how the sky changes color, as well as the direction and height of the waves. The direction of winds and temperature; the position and size of the sun; and visibility and constellations of stars are signs that communities commonly look out for. The islanders shared that they can smell a foul odor from the sea signaling that a storm or typhoon is coming.

In some Pacific coastal islands, people watch movements of animals, insects and plants for predicting hazards. In the islands of Timor-Leste, leaches and caterpillars are seen before typhoons. When banana tree leaves fall to the ground without strong winds, people in the Philippines prepare for storms or typhoons (Hiwasaki et al. 2014). In Timor-Leste and Indonesian islands, birds, usually migratory, are important signs of changing seasons and duration. In the islands of Philippines, various animals are used to forecast hazards as the rays jump consecutively in the sea in summer, the fast movement of sea snakes and hermit crabs going inland or climbing up trees.

These observations are also considered as signs of other hazards like flooding and landslides. Similar to predictions and warnings, islanders have also developed ways to prevent or mitigate such hazards, using local materials. They plant local trees to safeguard their houses from the storm. They have developed various ways to ensure food security during storms and droughts. They use salt to preserve fish and often smoke-dry them. People used to consume locally available fruits, tuber and roots in the aftermath of a disaster when external relief took time to come. In order to protect their houses from storms and strong winds, they use local structures, materials and plants.

In Solomon Islands in 2007, an earthquake of magnitude 8.1 hit the islands' western province. The earthquake caused severe damages to structures in the region. Coral reefs were damaged, and the earthquake triggered landslides, caused uplift and subsidence and generated a sizable tsunami resulting in the death of 52 people (McAdoo et al. 2008). There was less than a three-minute separation time between the earthquake and the tsunami in the Solomon Islands, and the indigenous peoples based on their traditional knowledge and practices were still able to survive. The number of casualties would have been higher had the local community not applied their indigenous knowledge.

What happened was that the water of the coral lagoon was drained out when the shaking stopped exposing the seafloor. The tsunami advanced within ten minutes later. The following two or three waves hit the area like high tides. Expecting the advance of the incoming tsunami, the indigenous people of the island moved toward the steep hills, and the village elders and heads of household ensured safety of the children and made proper evacuation anticipating the approach of another big wave. The people, at least 50, who died during the Solomon Islands tsunami, were mostly immigrants from the mainland with no such memory. Such localized knowledge related to natural disasters could also be used effectively during early warning and response.

4 Andaman and Nicobar Islands

The Andaman and Nicobar Islands in the midst of the Indian Ocean, some 1,200 km off the eastern coast of India, were severely devastated by an earthquake of 9.0 magnitude followed by tsunami waves during the early hours of 26 December 2004. Out of 572 islands, only 38 were able to live (Sekhsaria 2017). These islands are inhabited by some primitive tribal groups, who came from Africa some 20,000 years ago. With various "development" activities like urbanization, tourism, modernization, these primitive tribes gradually lost their culture and identity. Now there are only 92 *Ongees*, 43 Great *Andamanese*, 350 *Jarawa*, 100 *Sentinelese* and over 250 *Shompens* (Reddy 2018), who constitute the "Particularly Vulnerable Tribal Groups" of Andaman and Nicobar Islands.

During the 26 December 2004 tsunami, the southern islands of the archipelago, the Nicobar Islands were worst hit (Reddy 2013; Sekhsaria 2014). Geologically,

the Andaman and Nicobar Islands represent the highest peaks of an under-water mountain range. Of the 3,513 people reported dead and missing, only 64 were from the Andaman group of islands, the remaining 3,449 were from various southern islands in Nicobar (Reddy 2018). It is to be noted that these islands were about 180 km from the epicenter of the earthquake in Aceh province in Sumatra (Singh et al. 2018; Sekhsaria 2017). The Sumatra–Andaman earthquake, which caused the 2004 Indian Ocean tsunami, is estimated to have released energy equivalent to 23,000 Hiroshima-type atomic bombs. In Banda Aceh, the landmass closest to the quake's epicenter, tsunami waves topped 100 feet. The earthquake-induced tsunami affected the areas in Malaysia, Myanmar and Thailand. The giant wave later reached the coasts of Bangladesh, India, Maldives and Sri Lanka. Hours later, it reached the shores of the Seychelles, Kenya, Somalia and Tanzania in East Africa. Although the final figure varies as per different sources, the total casualty may vary between 250,000 and 300,000 (Shaw 2006).

The deep-ocean earthquake shook the islands for several minutes followed by eight consecutive tsunami waves. As the islands were mostly flat, the people were made easy victims of the incoming waves. The tsunami swept across some islands causing land subsidence with little signs of human habitation. Uprooted trees were found floating around in the sea, and the coast was clogged with damaged corals. Various parts of the islands were deformed, and the island was overall reduced in size. Although, Nicobar Islands sustained a heavy loss of lives and property, the other primitive tribe, the *Ongees* in Little Andaman Islands, could however escape to safety. The island experienced 6–10 m high waves followed by the earthquake. Soon after the earthquake, about 83 *Ongees* packed up and ran through the forest to a safer place in the high hills (Pandya 2005). Their primitive tribal wisdom helped them to sense the imminent danger of tsunami waves.

They consider earth tremors as frequent events and have been living in such situations for years. According to them, with the advent of *giyangejebey* (tsunami), the water dries up and goes away from the land very quickly, and similar to the motion of breathing-in and -out of the body, the sea water had to come back very rapidly with more force. *Giyangejebey* in *Ongee* language is a verb meaning "solid earth becoming fluid like the sea water" (Pandya 2005). It is not only solids melting in to liquids, but also liquids becoming solids again. They saw the water and knew that more land would soon be covered with sea and angry spirits would descend down to hunt them away. They believed that the *Ibedangey* (ancestral spirits) would come down to help them if they remained united (Chandi and Andrews 2010).

According to *Ongees*, the *Lololokobey* (earthquakes) are frequent and natural. They associate earthquakes with the creation of dead ancestors crossing over to another-world and becoming spirits (Pandya 2005). The image of rising water levels, as in the case of tsunami, has often been referred to as floods, a disaster associated since mythical times with the destruction of fire by rising water levels. There is a cultural practice among the primitive tribes in Andaman and Nicobar Islands to save fire from being extinguished by water, meaning fire should remain burning for their safety.

Based on their age-old cultural wisdom, the *Ongees* got concerned on the morning of the giant tsunami when they saw the rapidly receding water line, something that signaled to them that the "ancestral spirits" were angry and were shaking the pillar-like tree trunk on which the sea rests. According to the *Ongees* tradition, when the spirits get angry, the wind directions change, and spirits move from sea to forest during September–October and move from the forest to sea during July to August (Pandya 2005). In the state of anger, the spirits often hurl down huge boulders taken from stars at the sea. Earthquakes are experienced by the impact of the boulders touching the sea surface.

On the morning of tsunami, when the water line receded, the *Ongees* immediately gathered on the shores with their baskets, bows and arrows and hurled stones at the sea, for they wanted the spirits to believe that the community was still left behind submerged under the rising water level, so that the spirits remained at the spot looking for those who had hurled stones at them while other spirits continued to shake the earth. Unlike the settlers, the *Ongees* did not wait to see aftermaths of the earthquake, which to them was a regular event. Many lives of the settler communities were lost because they were looking at the receding sea, oblivious to the fact that the killer waves were coming from behind.

The *Ongees*' idea of living in the future is based on their cultural notion of when to move and where to move. In fact, the *Ongees*, as stated by Pandya (2005), usually move to the interior forest or coastal area and set up traditional residential structures known as *korale* (single family shelters) or *beraley* (communal huts). This practice of translocation has always made the *Ongees* adept at packing up essentials and moving on in response to seasonal changes.

The *Sentinelese* and *Jarawas* are the communities, who also continue to use their knowledge networks for livelihood security. Like others, they are the hunter-gatherer tribes. The *Jarawas* know the forests they live in. They are familiar with the medicinal plants and the use of special herbs for driving away bees from bee-hive (Chandi 2010; Sekhsaria 2014). It is also learnt that sensing imminent danger of tsunami, the most isolated and fierce primitive tribe in the North Sentinel island, the *Sentinelese* were able to leave their homestead and escape to the highland forests for safety, although it is not known if they lost property and lives during the incident. Indian helicopters with relief materials had to abort their mission as they faced a hail of arrows from these tribes.

5 Bangladesh Coastal Islands and the *Haors*

The coastal islands of Bangladesh on the Bay of Bengal are periodically vulnerable to hydro-meteorological disasters like floods, cyclones, tidal surges and salinity intrusion. Threat of sea level rise due to climate change is also looming. The 710 km coastal line covering many small and newly emerged *charlands* (shoals) are subjected to tropical cyclones and storm surges that regularly devastate vast areas with salinity intrusion and prolonged inundation, incurring loss of lives and damages to crops. The

coastal area comprises of 47,201 sq.km (32% of the country) of Bangladesh within 19 districts in 147 Upazilas (Rasheed 2008). The area is populated by 35 million people (2005) representing 29% of the total population.

Because of the very proximity with the Bay of Bengal, the coastal population, especially the *charland* people have developed through a process of adaptation, many coping strategies and techniques in line with the local environment. These coping strategies are based on their local knowledge and practices gathered over the generations. Unfortunately, much of the knowledge is lost as they remain undocumented. Nevertheless, people in disaster-prone areas still nurture such knowledge in their myths, beliefs and traditions (Haque 2019).

The coastal landmass of Bangladesh is periodically subjected to hydro-meteorological disasters, like cyclones and tidal surges causing loss of lives and properties. In the last 150 years, 35 devastating cyclones have hit the Bangladesh Coast (Haque 2019). Generally, April–May and November are the months of cyclones and associated tidal surges in Bangladesh. Around 330,000 people in the coastal islands of Bangladesh died as a result of the cyclone and tidal surges of 12 November 1970, and another 138,882 people died on 29 April 1991 (Haque 2019). Bangladesh recently faced a number of devastating cyclonic storms and associated tidal surges, including Sidr in 2007, Aila in 2009, Mohasen in 2013, Bulbul in 2019 and Amphan in 2020, causing loss of lives and damages to standing crops and property. It is to be noted that loss of lives has decreased substantially in recent cyclonic storms. This was possible due to a paradigm shift in disaster management, from relief and rehabilitation to disaster risk reduction. Improved cyclone warning system, fast evacuation to cyclone shelters and coping strategies of the local communities, which helped in bringing down loss of lives to a great extent.

According to Hassan 2000, the people of the coast could identify, anticipate and predict cyclones through the following observations: (a) wind direction; (b) temperature and salinity of sea water; (c) color and shape of the clouds; (d) appearance of a rainbow; and (e) behavior of certain bird species. Regarding the direction of wind, the people in the coast believed that a wind blowing from the south-east is more likely to create a storm, while the wind direction from the north-east has the potential to generate a cyclone but not a severe one. The wind direction is also associated with other attributes i.e., a rise in sea water temperature, red-colored cloud and the appearance of a rainbow if it is day time, suggesting formation of deep depression in the sea. In most cases, such depressions are formed near the Andaman Islands. Abnormal behavior of the birds residing in trees is regarded as a signal of a rapid storm approaching.

People have also developed some survival strategies during and after a cyclonic event. They are simple tactics like holding onto and binding themselves to trees; looking for more dependable places like embankments and polders; using floating items such as timber, thatched roof, straw piles and bunches of coconuts are some of the survival strategies; these represent spontaneous survival strategies. Generally, external help and relief goods appear a couple of days after the disaster. During this intermediary period while they are waiting for relief, people eat stems and roots of edible plants. For drinking purposes, they often resort to drinking rain water, as

cyclones are always followed by rain for several hours. In the absence of rainwater, they drink green coconut water. Due to unavailability of medicines, generally, the victims depend on herbal medicines for treating minor injuries and diarrheal diseases.

As they construct their houses, they use roofing materials and design it in such a way that the roofs have a sloping toward the wind direction. They plant local varieties of plants surrounding their homesteads. Haque (2000) states that in Sandwip Island in the south of Bangladesh, people plant *Hurma* (*Persimmon*) trees, which are strong and can withstand tidal waves. The lives of many people were saved during the April 1991 cyclone, as they held on mangrove trees, like *Keora* (*Sonneratia apetala*) and *Sundari* (*Heritiera fomes*). Another interesting phenomenon was that during tidal surges, people tied rafts to coconut trees so that they rose and fell with the changing water levels (Haque 2000).

In the north-eastern *haor* (low depression of wetland) of Bangladesh, a study was conducted to understand local knowledge and practices regarding early warnings of a disaster like heavy rainfall, hailstorm or flash floods. Local proverbs such as "abundance of mango will bring floods and abundance of jackfruit will increase rice production", or "abundance of mango and paddy will bring flood" are commonly used for forecasting early warnings of floods (Islam and Bremer 2016). These "local scientists", mostly elderly people interpret early warnings of floods or rainfall by observing the behavior of animals, birds, insects or amphibians. According to them, snakes will come to their house before a major flood. Frogs croaking in the month of March (Bengali month of *Chaitra*) is a warning for rainfall. If grass hoppers are flying too high in the middle of April, rainfall will occur. If cattle return to their home or birds return to their nests, it is sign that a big storm is coming, and if herons are flying erratically, then this is a particular sign of a northwesterly storm. Likewise, a persistent southerly wind may be a precursor to heavy rainfall. If water levels rise coinciding with a cold breeze, a flash flood may be coming. Often senior citizens are able to provide early warnings based on their experiences and wisdom. The *Haor* communities continue to interpret natural signs to predict the weather, because many say that meteorological weather forecasting systems are incorrect, not location-specific or inaccessible (Islam and Bremer 2016).

6 Conclusions

The critical role that indigenous knowledge and practices can play in addressing hazards and improving disaster preparedness is now recognized by disaster risk reduction specialists. They are yet to be generally used and practiced by communities, scientists, policymakers and the policy executives. It is believed that local and indigenous knowledge needs to be integrated with science before it can be used in policies, education and actions related to disaster risk reduction and climate change. It is important that such knowledge is promoted to increase the resilience of local communities against impacts of hazards and climate change. Local and indigenous

knowledge is key to increasing resilience of coastal and small island communities to hydro-meteorological hazards, like tsunami, earthquake and the impacts of climate change. It is true that indigenous knowledge and practices of the small ethnic communities have limitations. They mostly remain in oral forms and are not well documented. There is a move by the academics to validate the knowledge with scientific understanding. Hiwasaki et al. (2014) are of the opinion that a process could be initiated to identify, document, validate local and indigenous knowledge and integrate this knowledge with science. They termed it as "Local and Indigenous Knowledge and Practices, Inventory, Validation and Establishing Scientific Knowledge (LIVE)". Through this method, Hiwasaki et al. (2014) gave scientific explanations to indigenous knowledge like (a) observations of animal behavior; (b) observations of celestial bodies; (c) observations of environment; (d) material culture; and (e) traditional and faith-based beliefs and practices. Hiwasaki et al. observed that the key to successful implementation of "LIVE Scientific Knowledge" tool is the commitment of all stakeholders to develop an action plan through a participatory process.

There is no denying that resilience of coastal and small ethnic communities to meteorological hazards depends on documentation and promotion of their indigenous knowledge and practices. Proper validation and scientific explanation of this knowledge would help the scientists, policymakers and practitioners in developing an effective country-specific disaster management plan. Following recommendations of the Hyogo and Sendai Framework for Disaster Risk Reduction, it is suggested that efforts are to be taken to document and validate the local knowledge and practices of the island and small ethnic communities of Asia–Pacific, Andaman and Nicobar and Bangladesh coast to hydro-meteorological hazards, and incorporate them in all policies, plans and strategies of countries with similar socio-environmental situations. The 2004 Indian Ocean earthquake and tsunami was a great reawakening, which called for concerted actions for disaster risk reduction to be undertaken by the countries and nations bordering the seas.

References

Amin, M.N. 2000. Potential Use of Indigenous Knowledge in Sustainable Conservation of Plant Diversity in Bangladesh. In *Of Popular Wisdom: Indigenous Knowledge and Practices in Bangladesh*, ed. N. A. Khan and S. Sen. Dhaka: Bangladesh Resource Centre for Indigenous Knowledge.

Chandi, M. 2010. Colonization and Conflict Resolution in the Andaman Islands: Learning from Reconstruction of Conflict Between Indigenous and Non-indigenous Islanders. In *The Jarawa Tribal Reserve Dossier, Cultural & Biological Diversities in the Andaman Islands*, ed. P. Sekhsaria and V. Pandya. Paris: UNESCO.

Chandi, M., and H. Andrews. 2010. The Jarawa Tribal Reserve: The Last Andaman Forest. In *The Jarawa Tribal Reserve Dossier, Cultural & Biological Diversities in the Andaman Islands*, ed. P. Sekhsaria and V. Pandya. Paris: UNESCO.

Haque, M. 2000. Indigenous Knowledge and Practices in Disaster Management in Bangladesh. In *Of Popular Wisdom: Indigenous Knowledge and Practices in Bangladesh*, ed. N.A. Khan and S. Sen. Dhaka: Bangladesh Resource Centre for Indigenous Knowledge.

Haque, M. 2013. Indigenous Knowledge and Practices in Disaster Management. In *Environmental Governance: Emerging Challenges for Bangladesh*. Dhaka: AH Development Publishing House.
Haque, M. 2019. Indigenous Knowledge and Practices in Disaster Management: Experiences of the Coastal People of Bangladesh. In *Disaster Risk Reduction: Community Resilience and Responses*, ed. B. Zutshi, A. Ahmed, and A.B. Srungarapati. Palgrave Macmillan, Springer Nature Singapore.
Hassan, S. 2000. Indigenous Perceptions, Predictions and Survival Strategies Concerning Cyclones in Bangladesh. In *Of Popular Wisdom: Indigenous Knowledge and Practices in Bangladesh*, ed. N.A. Khan and S. Sen. Dhaka: Bangladesh Resource Centre for Indigenous Knowledge.
Hiwasaki, L., E. Luna, Syamsidik, and R. Shaw. 2014. Process for Integrating Local and Indigenous Knowledge with Science for Hydro-Meteorological Disaster Risk Reduction and Climate Change Adaptation in Coastal and Small Island Communities. *International Journal of Disaster Risk Reduction* 10 (2014): 15–27.
Islam, AKM. S., and S. Bremer. 2016. Signs of the Weather. *Dhaka Tribune*, 4 June.
McAdoo, B.G., A. Moore, and J. Baumwoll. 2008. Indigenous Knowledge and the Near Field Population Response During the 2007 Solomon Islands Tsunami. *Nat Hazards*, 22 January. https://doi.org/10.1007/s11069-008-9249-z.
Mustafa, M. 2000. Towards an Understanding of Indigenous Knowledge. In *Indigenous Knowledge Development in Bangladesh: Present and Future*, ed. P. Sillitoe. Dhaka: The University Press Ltd.
Pandya, V. 2005. When Land Became Water, Tsunami and the *Ongees* of Little Andaman Island. *Anthropology News*, March.
Rasheed, K.B.S. 2008. *Bangladesh, Resources and Environmental Profile*. Dhaka: AH Development Publishing House.
Reddy, S. 2013. *Clash of Waves: Post Tsunami Relief and Rehabilitation in Andaman and Nicobar Islands*. New Delhi: Indos Books.
Reddy, S. 2018. New Andamans: The Aftermath of Tsunami in the Andaman and Nicobar Islands. In *The Asian Tsunami and Post Disaster Aid*, ed. S. Reddy. Singapore: Springer Nature.
Sekhsaria, P. 2014. *The Last Wave, An Island Novel*. India: HarperCollins.
Sekhsaria, P. 2017. *Islands in Flux, The Andaman and Nicobar Story*. India: Harper Litmus.
Shaw, R. 2006. Indian Ocean Tsunami and Aftermath: Need for Environment-Disaster Synergy in the Reconstruction Process. *Disaster Prevention and Management* 15 (January, 1).
Sillitoe, P., ed. 2000. *Indigenous Knowledge Development in Bangladesh: Present and Future*. Dhaka: The University Press Limited.
Sillitoe, P., P. Dixon, and J. Barr. 1998. IK Research on Floodplains of Bangladesh: The Search for a Methodology. *Grassroots Voice* 1 (1): 5–15.
Singh, S.J., M. Fischer-Kowalski, and W. Hass. 2018. The Sustainability of Humanitarian Aid: The Nicobar Islands as a Case of 'Complex Disaster'. In *The Asian Tsunami and Post Disaster Aid*, ed. S. Reddy. Singapore: Springer Nature.
Walker, D.H., F.L. Sinclair, and R. Muetzelfeldt. 1991. *Formal Representation and Use of Indigenous Ecological Knowledge about Agroforestry Practices: A Pilot Phase Report*. School of Agricultural and Forests Sciences, UK: University of Wales, Bangor.
Warner, K. 1991. *Shifting Cultivators: Local Technical Knowledge and Natural Resource Management in the Humid Topics*. Food and Agriculture Organization of the United Nations.

Driving Factors of Destination Choices Due to Riverbank Erosion Along the Brahmaputra River

Sahika Ahmed and Sonia Binte Murshed

Abstract Riverbank erosion is one of the most common natural disasters in Bangladesh. The after-effect of the flood is one of the major reasons behind this calamity. Recently, the Brahmaputra riverbank has eroded severely due to frequent flooding events. As a consequence, the inhabitants of these areas are forced to migrate. This study was conducted at Dewanganj in Jamalpur district, located at Brahmaputra River's left bank. We carried out qualitative research incorporating semi-structured and unstructured interviews, direct observations, and participatory rural appraisal (PRA) tools to understand the internal displacement dynamics and the victims' problems. Moreover, we divided the study area into five zones, i.e., island char, government land, attached char, Gucchogram, upazilla, and town, to understand the spatial aspects of the displacement pattern. The surveys were done from September 2019 to January 2020 to capture the devastating flood-induced bank erosion impact of the year 2019. It was noticed that a significant number of people have displaced during this time frame. This study area's displacement dynamics are controlled by a total number of 14 push and pull factors. These push and pull factors show significant temporal and spatial variations. Among them, the most important are the amount of resources, land price, land elevation, help from government and NGOs, distance from ancestors place, etc. The displacement pattern largely depends on these factors. This study describes an approach to assist planners and policymakers in framing the current displacement processes and their causes. It will also help plan a better settlement policy for the affected people, which unfortunately is a considerable part of the current population.

Keywords Internal displacement · Riverbank erosion · Push factors · Pull factors · Flood · Brahmaputra River

S. Ahmed (✉) · S. B. Murshed
Institute of Water and Flood Management, Bangladesh University of Engineering and Technology, Dhaka, Bangladesh

© The Author(s), under exclusive license to Springer Nature Switzerland AG 2022

G. M. Tarekul Islam et al. (eds.), *Water Management: A View from Multidisciplinary Perspectives*,
https://doi.org/10.1007/978-3-030-95722-3_8

1 Introduction

Bangladesh, a riverine country, faces riverbank erosion every year. This forces millions of its population to displace from their place of origin (Alam et al. 2020; M.F. Islam and Rashid 1970). Being located at the downstream of the Ganges, Brahmaputra, and Meghna Rivers, the combined flow (both water and sediment) has a significant impact in shaping its hydro-morphology. An extreme amount of sediments from the Himalayan Mountains is transported by a large monsoon flow to the sea through the delta of Bangladesh. Consequently, the large rivers behave rather unpredictably with the permanent risk of riverbank erosion (M. Rahman 2013). Nearly 2.4 billion m. tons of sediment flows through the rivers of Bangladesh per year (M. Rahman 2013). This huge amount of washed-out fine soils from the upstream channels are easily transported downstream and deposited as islands or attached chars. This phenomenon results in river velocity's unpredicted flow path at different places and cause erosion (M. Rahman 2013).

Also, climate change indicates an alteration in temperature and rainfall patterns, affecting flood magnitude and frequency. Erosion is the after-effect of floods, and the incidence of abnormal floods is increasing day by day. Environmental impacts, increased rainfall intensity, infrastructural development activities, and poor drainage facilities are responsible for increased incidence of abnormal flood in recent years (Emdad Haque and Zaman 1993). Moreover, as mentioned before, another cause behind this unpredictable erosion-accretion behavior is the massive amount of sediments arising from all the river channels of Bangladesh.

Riverbank erosion has catastrophic impacts on the riverine households, which causes long-term or permanent loss of land (Penning-Rowsell et al. 2013; Haque and Zaman 1989). People affected by riverbank erosion move for safety and shelter almost immediately, and then later on move permanently for survival from associated practical hazards. It harms the social, economic, psychological, and cultural life of the survivors. Millions of people in Bangladesh are bound to displace or migrate permanently every year in search of household, earning sources, and cultivable land. The reasons behind their displacement root in many factors, including education, health, and better livelihood options. When erosion leads to displacement, people choose places to move to according to these factors. The erosion victims mainly displace to other places in the months between July and October. Most of them face this kind of displacement about 5–7 times in their lives (Afreen 2009). As the Brahmaputra is predominantly braided and extremely dynamic, erosion and accretion actions are very common (Mondal et al. 2015; Saikia et al. 2019). One hundred and twenty-seven miles of Brahmaputra, in the lower reach, has eroded almost 30 villages from 2007 to 2017 (Shetu et al. 2017). Even today, erosion is continuing at the rate of nearly 2000 hectares per year (Alam et al. 2020). Dewanganj is an Upazila of Jamalpur district which is severely affected by riverine floods and riverbank erosion every year (Haque et al. 2021). This area is situated at the left bank of the Brahmaputra River. The unprotected rural area in the Jamalpur district (left bank of the Brahmaputra River) has a total surface of about 174 km^2 and a population

of approximately 146,000 people (BBS 2014). As there is no riverbank protection measures in this rural area, erosion occurs more frequently than on the right bank. Local victims suffer devastating floods just before the erosion takes place (Mondal et al. 2015). This area loses a huge amount of land every year due to riverbank erosion. Inhabitants face loss of households, cultivated lands, and other properties. A significant number of riverine households face internal displacement multiple times. To improve this situation, a planned policy on the resettlement of erosion victims will be helpful if it includes measures for sustainably enhancing the living conditions.

Most research studies on erosion-prone areas (viz. Ashworth et al. 2000; Azam et al. 2019; Baki and Gan 2012, etc.) dealt with the impact and factors of erosions, migration, and the geomorphological scenario of the area. Migration policy or how people manage to settle in a new place is not focused on in most previous studies. A few studies (viz. Zetter 2012; M.S. Rahman and Gain 2020; M.F. Islam and Rashid 1970) have done some research work on the rehabilitation process. As such, this study mainly focuses on the factors behind choosing the destination after erosion has occured.

This study mainly focuses on the sufferings of the erosion victims while choosing places for habitation after erosion has occured. Specifically, this paper discusses (a) dominant driving factors behind the selection of displacement destinations and (b) the spatial variation of push–pull factors.

2 Study Area

The site was selected after observing the severity of flood and erosion in existing literature and secondary data. The study area is located near the downstream course of the Brahmaputra, which shifted to this location after the catastrophic flood and earthquake in 1787. The average channel width is 11 km (Sarker et al. 2003). The water and sediment discharge of the Brahmaputra River is dominated by the annual monsoon rainfall (Ashworth et al. 2000), as more than 80% of the river basin's yearly precipitation occurs during this season. Bank materials of the Brahmaputra River consist of loosely packed silt and fine sand with less than 1% clay, so they are highly susceptible to erosion. The bank erosion rate is as high as 1 km per year (Klaassen et al. 1993). The mean monthly temperature varies from 12º Celsius in January to 35.8º Celsius in July. The humidity of this area is high and is the highest in monsoon between June and October.

The location map of the study area is shown in Fig. 1.

Brahmaputra River is eroding its left bank at Dewanganj Upazila of Jamalpur, and this area is also prone to riverine monsoon floods. The erosion-accretion process of the Brahmaputra River develops several small and large sand bars, knows as "Chars." Chars that are connected with the mainland are known as "attached chars," whereas the chars without any connection to their surrounding area are known as "island chars." Our study area includes these two types of chars in addition to three different locations of the mainland. These are: (i) island char named Halkar Char

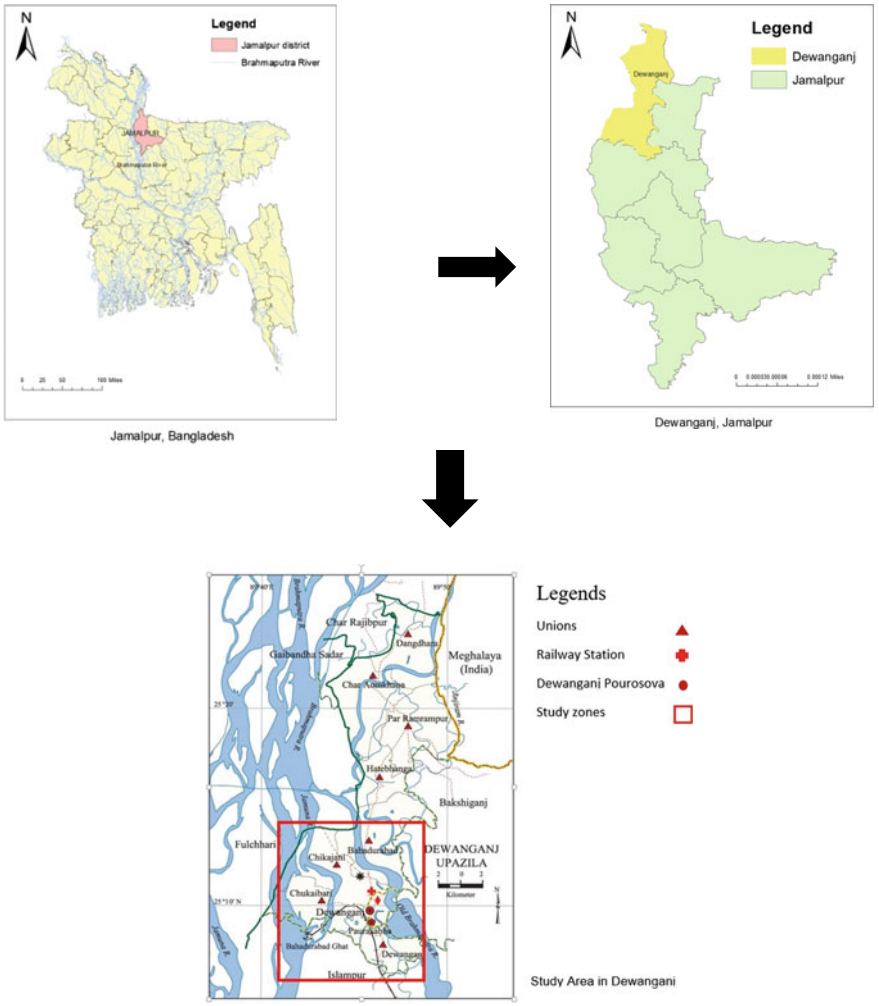

Fig. 1 Map of the study area

(Tiner Char), (ii) two attached chars named Kholabari and Chikajani, (iii) two clustered villages named Gujimari Guccho Gram and Adorsho Gram, (iv) two illegally occupied government land named Badeshshariyabari rail line slum and Chakuriya rail line slum, and finally, (v) the Dewanganj town. These are low-lying areas at the floodplain of the Brahmaputra River and located at latitude 25.3 North and longitude 89.76 East.

Charlands in the study area are agriculturally very productive due to their soil fertility. Also, living there is comparatively cheaper than in other areas. However, these islands are prone to devastating riverbank erosion and flooding. The condition of Dewanganj town is quite different as it is only affected by floods. Most of the

people in the islands are farmers. Men typically work in the field when women are engaging in homestead gardening and animal husbandry. Both men and women work in the field during harvesting. After a devastating erosion or flooding event, these people lose their earning source as well as their house. Almost every year, they have to rebuild their houses somewhere else and find a new income source. Displacements due to erosion are very common in the study area.

3 Methodology

This research is mainly based on primary qualitative data, where a set of data collection methods were used. At first, a reconnaissance survey was done to identify the inhabitants' current situation and the severity of different natural disasters in recent years. Though they face consecutive floods and erosions every year, the resettlement or displacement after being affected by erosion was the primary source of suffering. Satellite images from Google Earth Pro were also analyzed to understand the extent of erosion. From the field-level surveys, the factors which influence them in choosing the destinations were identified.

The reconnaissance survey was done with the help of local government officials and political persons. However, the following field surveys were done without involving official and political persons to understand the local perceptions without getting any biased information. After identifying displacement as their primary suffering due to erosion, a total of 15 household surveys were done. In each survey, there were 25–30 persons. These surveys helped to identify the factors that influenced people when they choose a place for living. Moreover, we followed the open questionnaire format for our survey, which helped local people express their thoughts and conceptions without limitations. In these household surveys, both men and women participated separately. After these surveys, three Focused Group Discussions (FGDs) were done with official persons to confirm some of the factors behind choosing migration destinations. These FGDs were done with local primary teachers, local political persons (members, chairman), and local government authorities (UNO or subdistrict executive officer & TNO thana executive officer). These FGDs and household surveys were the main primary sources of collected data.

During the second field visit, the study area was divided into five categories based on the five different land types. These are: island char, attached char, illegally occupied government land, cluster village (Gucchogram), and Dewanganj town. After that, ten FGDs were conducted with the local groups of those selected five places. From our first visit, we have identified a total of 14 factors that helped in choosing migration destinations. So, prioritizing these factors was the main focus of the FGDs of the second visit. These FGDs were done with structured questionnaires where the factors were classified into two groups (push factors and pull factors), and then, the evaluation of these factors was done. The dominant driving factors were then ranked by structured questionnaire surveys. The questionnaire surveys were based on the

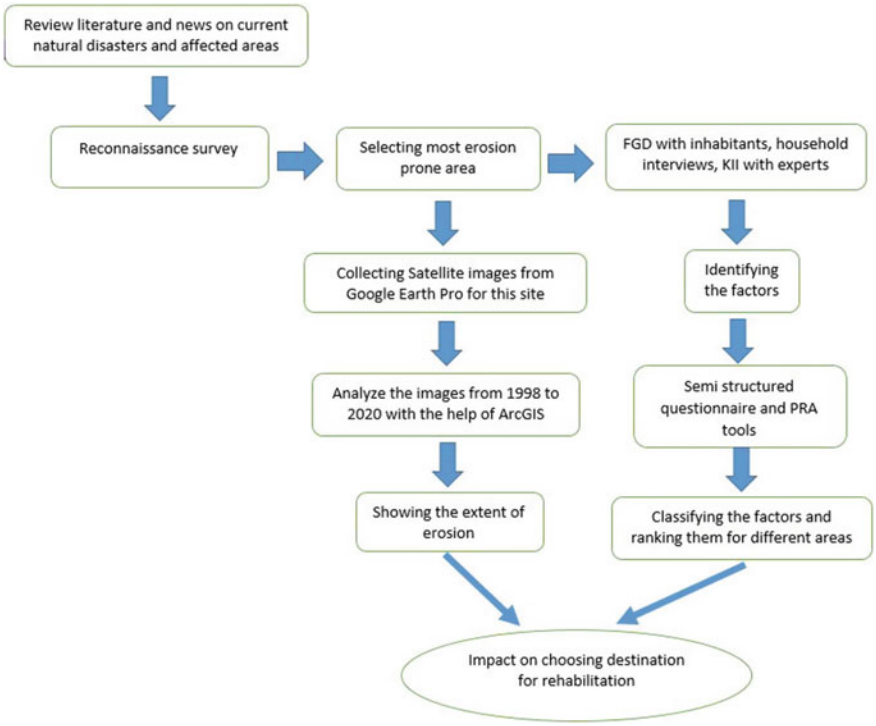

Fig. 2 Methodology of this study

preference ranking tool of PRA. The final ranking was achieved after analyzing all the outputs from FGDs and questionnaire surveys (Fig. 2).

4 Results and Discussions

The erosion that occurred in 2019 had nearly destroyed a whole union named Kholabari with government buildings, pakka (or concreted) houses, schools, mosques, and concrete roads. Many government infrastructures eroded in Dewanganj. Many of the inhabitants shared the incident of the Harindhara embankment, which eroded ten years ago. From then onward, this area does not have any concrete embankment. As such, people are suffering from more severe erosion now, and the recent devastating flood of 2019 broke the past records of severity.

Due to erosion, the inhabitants are forced to settle in different places every year. Choosing a destination for migration is not easy as there are lots of uncertainties involved in this process. The extent of erosion is also unpredictable. From Fig. 3, the Landsat satellite image of 2020 shows that the distance of the left riverbank from the railway station was 3.74 km, whereas this distance was 5.63 km in 1998. So, this

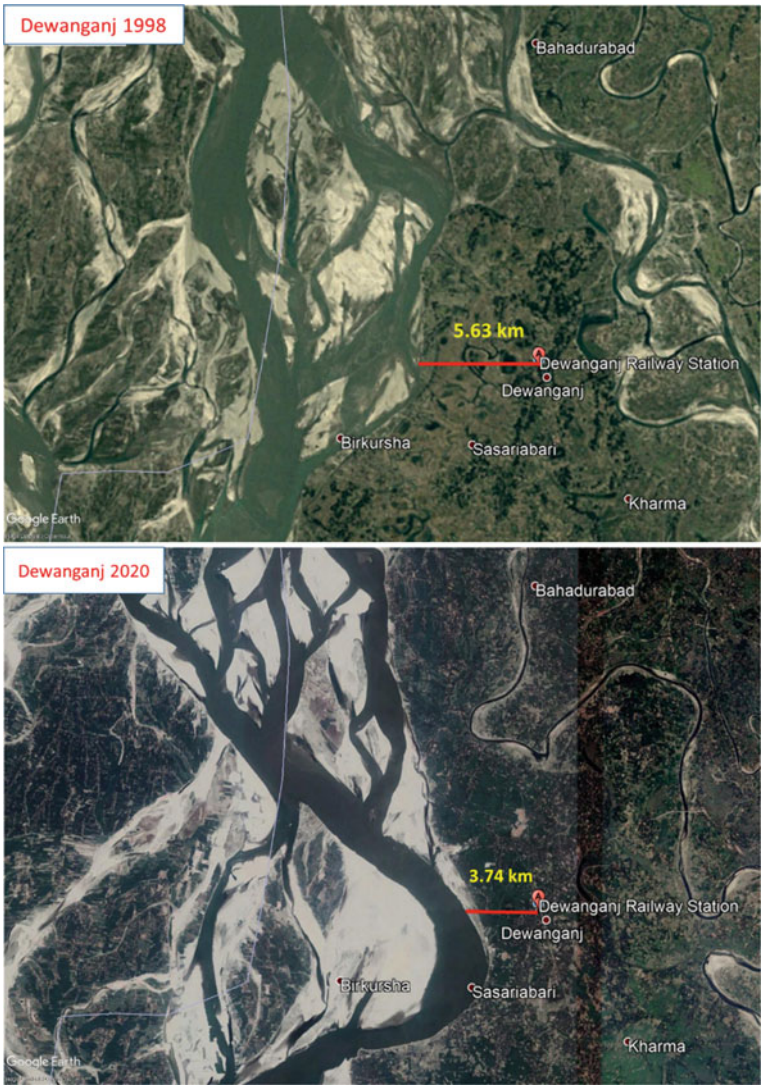

Fig. 3 A comparison of satellite images of the Brahmaputra riverbank at Dewanganj between **a** 1998 and **b** 2020

extreme riverbank erosion destroyed many people's land and belongings, along with government infrastructures.

A total of 15 factors were identified (Table 1) as push and pull factors from the FGDs, household interviews, and Key Informant Interviews (KIIs). Push factors force people to move away from their inhabitation, whereas pull factors motivate people to move into a new location for different socioeconomic reasons. These 15 factors act differently for people of different zones. The factors are given in Table 1.

Table 1 Factors identified from FCDs

Study zone	Push factors	Pull factors
Island char	Erosion Lower income facilities Lower land elevation Marital status Distance from origin Poor education facilities Inferior living condition Manpower	Surplus of resources Daily expenses Pastureland Relative's Land Land cost Link with political persons Government help or NGO's help
Attached char	Lower income facilities Erosion Daily expenses Lower land elevation Distance from origin Scarcity of resources Manpower Link with political persons Marital status	Government help or NGO's help Relative's Land Better education facilities Land Cost Pastureland Better living condition Link with political persons
Government land	Lower income facilities Manpower Distance from origin Erosion Relative's land Marital status Scarcity of resources Inferior living condition Barren land Daily expenses	Government help or NGO's help Link with political persons Land cost Higher land elevation Better education facilities
Gucchogram	Lower land elevation Marital status Erosion Relative's land Barren land Lower income facilities Manpower Poor education facilities Distance from origin Daily expenses	Land cost Government help or NGO's help Link with political persons Better living condition Surplus of resources

(continued)

Table 1 (continued)

Study zone	Push factors	Pull factors
Dewanganj town	Erosion Lower income facilities Poor education facilities Land cost Daily expenses Barren land Scarcity of resources	Better living condition Distance from origin Higher land elevation

Another key focus of our study is to understand the spatial variation among the push and pull factors. The preference ranking tool helped to prioritize the 15 key factors that have been identified. Tables 2 and 3 show the preference ranking of push and pull factors, respectively.

The above results show the local inhabitants' varying acceptance levels when it comes to different push and pull factors. Our findings also depict that the major push factors are almost common in these areas.

Due to riverbank erosions, the inhabitants of these areas become vulnerable from different perspectives; for example, they do not have any long-term plans or security of education, income facilities, and health. After being homeless, they face various inconveniences every day. In addition to riverbank erosion, the unstable and unplanned condition of their lives creates other reasons for their displacement. This study shows that the other factors excluding erosion can sometimes become the main reason for displacement of people in a particular area. The different zones have different types of benefits. Local people usually take benefits from the surrounding environment and have become accustomed to it. That is a major reason for people's non-migratory behavior. They prefer to displace to places nearer to their origins.

Push factors were identified as factors which make them compelled or interested in going for new habitation. Displaced households were interviewed to understand the local push factors. The ranking tables (Tables 2 and 3) show that erosion, one of the topmost push factors, is common across the five different zones. These devastating phenomena compelled them to find new accommodations. Though it is supposed to be ranked top among all the factors, it is noticeable that the need for income facilities remains unbeatable. With the development of education and living style, more and more people are searching for earning sources beyond their living places. Besides, the opportunity for different types of jobs is rare in these locations. Most of the people earn their livelihood by cultivation, fishing, and temporary work on government projects. There are some facilities for academic work in Dewanganj town, but that is not enough for all the educated and skilled persons of these areas. Also, women do not have many facilities over there. For survival, many women are forced to move into city areas to work in the garments sectors, domestic sectors, etc. So, lack of income facilities is found to be one of the primary reasons for permanent migration.

Table 2 Ranking of push factors across five zones of Dewanganj Upazila

Ranking of push factors of different places	Island char	Attached char	GOVT land	Gucchogram	Dewanganj town
1	Erosion	Lower income facilities	Lower income facilities	Lower land Elevation	Erosion
2	Lower income facilities	Erosion	Manpower	Marital Status	Lower income facilities
3	Lower land elevation	Daily expenses	Distance from Origin	Erosion	Poor education facilities
4	Marital Status	Lower land elevation	Erosion	Relative's Land	Land cost
5	Distance from origin	Distance from Origin	Relative's Land	Barren land	Daily expenses
6	Poor education facilities	Scarcity of resources	Marital Status	Lower income facilities	Barren land
7	Inferior living condition	Manpower	Scarcity of resources	Manpower	Scarcity of resources
8	Manpower	Link with political persons	Inferior living condition	Poor education facilities	N/A
9	N/A	Marital Status	Barren land	Distance from Origin	N/A
10	N/A	N/A	Daily expenses	Daily expenses	N/A

Due to the occurrence of devastating floods every year, land elevation is also an essential factor here. Naturally, island chars are not permanent. These locations face erosion and deposition more frequently than any other zones. Subduction of soil is also very common. So, these people who live in less elevated land suffer the most during flooding events. Hence, elevated land is very desirable and often gets prioritized as migration destinations. Also, local inhabitants in gucchograms and attached chars do not lose any chance to migrate or displace to higher elevated locations.

In addition, the erosion victims want to migrate to safer locations immediately after losing their homesteads. In those cases, the distance of migrated destinations is not an issue. Nevertheless, they always plan to return to their origin, near their lost household, after being settled. However, sometimes, the opposite case happens. If the number of adults and earning members is high in a family, they usually migrate to cities and do not plan to return.

Table 3 Ranking of pull factors across five zones of Dewanganj Upazila

Ranking of pull factors of different places	Island char	Attached char	GOVT land	Gucchogram	Dewanganj town
1	Surplus of resources	Government help or NGO's help	Government help or NGO's help	Land Cost	Living Condition
2	Daily expenses	Relative's Land	Link with political persons	Government help or NGO's help	Distance from Origin
3	Pastureland	Better education facilities	Land Cost	Link with political persons	Higher land Elevation
4	Relative's Land	Land Cost	Higher land Elevation	Better living condition	N/A
5	Land Cost	Pastureland	Education	Surplus of resources	N/A
6	Link with political persons	Better living condition	N/A	N/A	N/A
7	Government help or NGO's help	Link with political persons	N/A	N/A	N/A

Usually, families want to settle their daughters (after marriage) at distant places from the origin to keep them free from the suffering of erosion. Also, in recent days, male and female inhabitants, who are not unmarried, move to towns by themselves and stay there permanently by marrying someone and settling there.

The facility of education and health service is very inferior in island chars. In island char areas, very few families consider poor education opportunities as the push factors for choosing their migration destinations. The exception is Dewanganj town, where the migration rate due to education facilities is relatively higher.

In the island chars, the daily expense is very low as the amount of natural resources is very high. They do not have to pay much for their food and fuels as the charland areas are productive enough to supply these demands at a meager cost or no cost at all. Besides, the living standard of the local inhabitants of island char is very low. Therefore, many families with lower income facilities prefer island char when displacing after erosion. Getting help from relatives is another critical factor in choosing new

destinations. A significant number of people chose to shift close to relatives immediately after displacement. Moreover, if anyone has any professional or family link with any political persons, it is easier to get land in island char. The amount of cultivable land and pasture is abundant in island chars, which is a pull factor for the people with lower income from the other three zones, excluding Dewanganj town.

The vast amount of natural resources is the main pull factor of island chars which influences them not to choose other locations except another island char. Also, the land cost is relatively very low here. However, the reliefs from government or NGOs seldom reach the island chars. The people in attached chars, goverment lands, and gucchograms are more likely to benefit from relief services. Hence, access to relief services works as a pull factor for these places.

The displaced people who are illegally residing in goverment lands seek help from political persons, as they are afraid of eviction. That is why a link with a political persons is a pull factor for the area. Elevated land is also a pull factor here as it saves them from the severity of floods. The education system and the developed medical facilities are the pull factors for all the areas, excluding island char. In gucchograms, the land is given by the government of Bangladesh and is free of cost. That is why people living here do not want to displace easily.

Though these ranking positions seem different in different seasons according to their existing situation (such as during the season of riverbank erosion it is the main and top-ranking push factor, but in the dry season they may focus on income facilities or other factors), this study has focused on the overall sufferings and preferences of the inhabitants. This study is done in both wet and dry seasons and the final output is the merged conclusion of their overall condition.

These two tables (Tables 1 and 2) introduce the ranking of the factors. Nevertheless, if we can understand the reason behind these rankings, it will be easy to identify the needs and sufferings of these people. It will help to design and plan for better habitation for them. To develop the condition of these people, a better adaptation strategy to natural disasters is essential. Moreover, a further study on the driving factors will also be helpful in this matter.

5 Conclusion

Natural disasters cannot be avoided or stopped as these are beyond the control of humankind. Poor people who are continuing to lose their properties due to these disasters remain poor. Land losses make their condition even more vulnerable; it hampers the lifestyle of an entire community. Although we cannot control these situations, the implication of some planned projects to help victims return to their usual lifestyle will make a huge difference in the ultimate development of a society.

In Bangladesh, people who are living by the river are facing issues of riverbank erosion every year. So displacement of habitation is common after these incidents. People living in different zones have different choices and demands, which should be kept in mind when planning any policy for rehabilitating these people.

The government of Bangladesh has already taken projects, including Gucchogram (cluster village), under the Adarsha Gram Project. Although the project was planned for people affected by cyclones, many cluster villages are also made in the erosion-prone areas in recent years. Ranking the push and pull factors behind their choice of rehabilitation place would be helpful to achieve sustainability of such projects.

The output of this case study has shown the difference of choices in different zones by ranking these factors. Also, with the help of the push factors' ranking, the importance of common factors like governmental help or NGO's help, land cost, and link with political persons is easily noticeable. The factors known as pull factors (such as high land elevation, better income facilities, surplus of natural resources, better education facilities, protective measures against flood and erosion) should be introduced and ensured in the zones where necessary. In contrast, the factors known as push factors (such as poor income facilities, inferior living conditions, scarcity of resources) should be eliminated or adapted in feasible and secure ways.

Acknowledgements This study was funded by the South Asia Consortium for Interdisciplinary Water Resources Studies (SaciWATERs) as part of their South Asian Water (SAWA) Leadership program grant. The authors are also grateful to the local people of Dewanganj Upazila. Special thanks to Sumaiya Binte Islam, Khadizatul kubra, and Md. Shadhin Hossain for helping to gather field information during the Covid era.

Appendix

See Figs. 4 and 5.

	1	2	3	4	5	6	7	8	
1	×	1	1	1	1	1	1	1	Erosion
2		×	3	4	5	2	7	8	2	Inferior living condition
3			×	3	3	×	3	3	3	Lower income facilities
4				×	5	4	7	8	4	Poor education facilities
5					×	5	5	5	5	Lower land Elevation
6						×	7	8	6	Manpower
7							×	7	7	Marital Status
8								×	8	Distance from origin

(a) 1>3>5>7>8>4>2>6

	1	2	3	4	5	6	7	8	9	
1	×	1	3	1	1	1	1	1	1	Erosion
2		×	3	2	5	2	2	8	9	2	Scarcity of resources
3			×	3	3	3	3	3	3	3	Lower income facilities
4				×	5	6	4	8	9	4	Link with political person
5					×	5	5	5	9	5	Lower land Elevation
6						×	6	8	9	6	Manpower
7							×	8	9	7	Marital Status
8								×	9	8	Distance from Origin
9									×	9	Daily expenses

(b) 3>1>9>5>8>2>6>4>7

	1	2	3	4	5	6	7	8	9	10	
1	×	1	3	1	1	6	7	1	1	1	Erosion
2		×	3	4	2	6	7	8	9	2	2	Inferior living condition
3			×	3	3	6	7	8	9	3	3	Relative's Land
4				×	4	6	7	8	9	4	4	Scarcity of resources
5					×	6	7	8	9	5	5	Barren land
6						×	6	6	6	6	6	Lower income facilities
7							×	7	9	7	7	Manpower
8								×	9	8	8	Marital Status
9									×	9	9	Distance from Origin
10										×	10	Daily expenses

(c) 6>7>9>1>3>8>4>2>5>10

	1	2	3	4	5	6	7	8	9	10	
1	×	1	1	4	1	6	1	8	1	1	1	Erosion
2		×	2	2	2	6	2	8	2	2	2	Relative's Land
3			×	3	3	6	3	8	3	3	3	Barren land
4				×	4	6	4	8	4	4	4	Lower income facilities
5					×	6	7	8	5	6	5	Poor education facilities
6						×	6	6	6	6	6	Lower land Elevation
7							×	8	7	8	7	Manpower
8								×	8	8	8	Marital Status
9									×	9	9	Distance from Origin
10										×	10	Daily expenses

(d) 6>8>1>2>3>4>7>5>9>10

	1	2	3	4	5	6	7		
1	×	1	1	1	1	1	1	1	Erosion
2		×	2	2	5	6	2	2	Land Cost
3			×	4	5	6	7	3	Scarcity of resources
4				×	5	6	7	4	Barren land
5					×	5	5	5	Lower income facilities
6						×	6	6	Poor education facilities
7							×	7	Daily expenses

(e) 1>5>6>2>7>4>3

Fig. 4 Ranking of push factors for different zones **a** Island char, **b** Attached char, **c** Government land, **d** Gucchogram, and **e** Dewanganj Town

	1	2	3	4	5	6	7		
1	×	1	3	4	1	1	7	1	Relative's Land
2		×	3	4	2	2	7	2	Land Cost
3			×	3	3	3	3	3	Surplus of resources
4				×	4	4	7	4	Pastureland
5					×	6	7	5	Government help or NGO's help
6						×	7	6	Link with political person
7							×	7	Daily expenses

(a) 3>7>4>1>2>6>5

	1	2	3	4	5	6	7		
1	×	2	3	4	5	6	1	1	Better living condition
2		×	2	2	2	6	2	2	Relative's Land
3			×	3	5	6	3	3	Land Cost
4				×	5	6	4	4	Pastureland
5					×	6	5	5	Better education facilities
6						×	6	6	Government help or NGO's help
7							×	7	Link with political person

(a) 6>2>5>3>4>1>7

	1	2	3	4	5		
1	×	1	3	4	1	1	Land Cost
2		×	3	4	5	2	Better education facilities
3			×	3	3	3	Government help or NGO's help
4				×	4	4	Link with political person
5					×	5	Higher land Elevation

(c) 3>4>1>5>2

	1	2	3	4	5		
1	×	2	1	4	5	1	Better living condition
2		×	2	2	2	2	Land Cost
3			×	4	5	3	Surplus of resources
4				×	4	4	Government help or NGO's help
5					×	5	Link with political person

(d) 2>4>5>1>3

	1	2	3		
1	×	1	1	1	Better living condition
2		×	3	2	Higher land Elevation
3			×	3	Distance from Origin

(d) 1>3>2

Fig. 5 Ranking of pull factors for different zones **a** Island char, **b** Attached char, **c** Government land, **d** Gucchogram, and **e** Dewanganj Town

References

Afreen, Farzana. 2009. Study on Bank Erosion and Its Impact on the Livelihood of the Local People: A Case Study along the Nabaganga River. M.Sc in WRD, Institute of Water and Flood Management, Bangladesh University of Engineering and Technology.

Alam, G.M. Monirul, Khorshed Alam, Shahbaz Mushtaq, Md Nazirul Islam Sarker, and Moazzem Hossain. 2020. Hazards, Food Insecurity and Human Displacement in Rural Riverine Bangladesh: Implications for Policy. *International Journal of Disaster Risk Reduction* 43. https://doi.org/10.1016/j.ijdrr.2019.101364.

Ashworth, Philip J., James L. Best, Julie E. Roden, Charles S. Bristow, and Gerrit J. Klaassen. 2000. Morphological Evolution and Dynamics of a Large, Sand Braid-Bar, Jamuna River, Bangladesh. *Sedimentology*. https://doi.org/10.1046/j.1365-3091.2000.00305.x.

Azam, Gausul et al. 2019. *Climate Change and Natural Hazards Vulnerability of Char Land (Bar Land) Communities of Bangladesh: Application of the Livelihood Vulnerability Index (LVI).* Global Social Welfare, Springer.

Baki, Abul Basar M., and Thian Yew Gan. 2012. Riverbank Migration and Island Dynamics of the Braided Jamuna River of the Ganges-Brahmaputra Basin Using Multi-Temporal Landsat Images. *Quaternary International* 263: 148–61.

BBS. 2014. Population & Housing Census-2011. *Bangladesh Bureau of Statistics.*

Emdad Haque, C., and M.Q. Zaman. 1993. Human Responses to Riverine Hazards in Bangladesh: A Proposal for Sustainable Floodplain Development. *World Development* 21 (1): 93–107. https://doi.org/10.1016/0305-750X(93)90139-Z.

Haque, C.E., and M.Q. Zaman. 1989. Coping with Riverbank Erosion Hazard and Displacement in Bangladesh: Survival Strategies and Adjustments. *Disasters* 13 (4): 300–314. https://doi.org/10.1111/j.1467-7717.1989.tb00724.x.

Haque, M.M., Islam, S., Sikder, M.B., and Islam, M.S. 2021. Assessment of Flood Vulnerability in Jamuna Floodplain: A Case Study at Jamalpur District, Bangladesh. *Research Square*, 1–18.

Islam, M.D. Fakrul, and A.N.M. Baslur Rashid. 1970. Riverbank Erosion Displacees in Bangladesh: Need for Institutional Response and Policy Intervention. *Bangladesh Journal of Bioethics*. https://doi.org/10.3329/bioethics.v2i2.9540.

Klaassen, G.J., E. Mosselman, and H. Brühl. 1993. On the Prediction of Planform Changes in Braided Sand-Bed Rivers. *Advances in Hydro-Science and -Engineering.*

Mondal, M. Shahjahan, M. Aminur Rahman, Nandan Mukherjee, Hamidul Huq, and Rezaur Rahman. 2015. Hydro-Climatic Hazards for Crops and Cropping System in the Chars of the Jamuna River and Potential Adaptation Options. *Natural Hazards* 76 (3): 1431–1455. https://doi.org/10.1007/s11069-014-1424-9.

Penning-Rowsell, Edmund C., Parvin Sultana, and Paul M. Thompson. 2013. The 'Last Resort'? Population Movement in Response to Climate-Related Hazards in Bangladesh. *Environmental Science and Policy* 27: S44-59. https://doi.org/10.1016/j.envsci.2012.03.009.

Rahman, Md Sadequr, and Animesh Gain. 2020. Adaptation to River Bank Erosion Induced Displacement in Koyra Upazila of Bangladesh. *Progress in Disaster Science* 5. https://doi.org/10.1016/j.pdisas.2019.100055.

Rahman, M.R. 2013. Impact of Riverbank Erosion Hazard in the Jamuna Floodplain Areas in Bangladesh. *Journal of Science Foundation* 8 (1–2): 55–65. https://doi.org/10.3329/jsf.v8i1-2.14627.

Saikia, Lalit, Chandan Mahanta, Abhijit Mukherjee, and Suranjana Bhaswati Borah. 2019. Erosion–Deposition and Land Use/land Cover of the Brahmaputra River in Assam, India. *Journal of Earth System Science* 128 (8). https://doi.org/10.1007/s12040-019-1233-3.

Sarker, Maminul Haque, Rob Koudstaal, and Mustafa Alam. 2003. Rivers, Chars and Char Dwellers of Bangladesh. *International Journal of River Basin Management*. https://doi.org/10.1080/15715124.2003.9635193.

Shetu, M.S.R., M.A. Islam, K.M.M. Rahman, and M. Anisuzzaman. 2017. Population Displacement due to River Erosion in Sirajganj District: Impact on Food Security and Socio-Economic Status. *Journal of the Bangladesh Agricultural University* 14 (2): 191–99.

Zetter, R. 2012. Shelter and Settlement for Forcibly Displaced People. In *International Encyclopedia of Housing and Home*, 330–335. https://doi.org/10.1016/B978-0-08-047163-1.00024-2.

Bivariate Drought Risk Estimation Using a Multivariate Standardized Drought Index in Marathwada Region, India

Rajarshi Datta and Manne Janga Reddy

Abstract Drought is a natural disaster that can cause water scarcity and damage to crop yields. Rather than conventionally used univariate drought monitoring indices, this study applied the parametric Multivariate Standardized Drought Index (MSDI) for drought monitoring in the Marathwada region. The index is constructed using historical time series of precipitation and soil moisture by engaging copula functions. The drought conditions characterized by MSDI are then compared with two univariate drought indices. Two significant drought characteristics, duration, and severity are identified using the MSDI and fitted probability models. The best-fit marginal distributions were selected by performing goodness-of-fit tests and standard performance measures. Three Archimedean copulas and two meta-elliptical copulas were applied for bivariate modelling of drought characteristics, and their suitability was evaluated using goodness-of-fit tests. Subsequently, the drought risks for the study region have been assessed using the constructed copula-based joint distribution models. The results highlight the importance of multivariate drought risk assessment in the study region.

Keywords Drought · Copula · Risk · Precipitation · Soil moisture · Joint distribution

1 Introduction

Droughts are natural disasters that have detrimental effects on various sectors. The concept of drought and different types of droughts have been widely reviewed (Mishra

R. Datta (✉) · M. J. Reddy
Department of Civil Engineering, Indian Institute of Technology Bombay, Mumbai, India

M. J. Reddy
e-mail: mjreddy@iitb.ac.in

M. J. Reddy
Interdisciplinary Programme in Climate Studies, Indian Institute of Technology Bombay, Mumbai, India

© The Author(s), under exclusive license to Springer Nature Switzerland AG 2022

G. M. Tarekul Islam et al. (eds.), *Water Management: A View from Multidisciplinary Perspectives*,
https://doi.org/10.1007/978-3-030-95722-3_9

and Singh 2010). Drought events and their impacts are often region-specific because of regional differences in hydro-meteorological variables and socioeconomic factors. In general, meteorological drought can be defined as a prolonged deficiency in rainfall in a particular area, compared to the statistical multi-year mean. Drought is triggered by anthropogenic activities such as deforestation and groundwater extraction, as well as climatic variability (i.e. temperature and precipitation anomaly). These activities can impact the local water balance and alter the propagation of droughts (Liu et al. 2016). Moreover, global warming caused by human activities can make drought events worse by intensifying their severity and duration (Ahmadalipour et al. 2017).

The meteorological, hydrological, agricultural, and socioeconomic drought types are the four main drought classifications. Meteorological drought is defined as precipitation deficiency over a region for an extended period. When meteorological drought is prolonged, the surface and sub-surface water levels deplete, and it leads to hydrological drought. If the soil moisture and rainfall are inadequate to sustain the crop growth, then eventually, the crop starts wilting, resulting in agricultural drought. Socioeconomic drought begins when existing resources become further incapable of meeting the growing water demands (Liu et al. 2020).

Drought indices are numerical expressions based on climatic and hydrological variables, which are used for assessing drought's impact and defining drought characteristics. In the past decades, various drought indices have been introduced, and among them, the Palmer Drought Severity Index (PDSI) and the Standardized Precipitation Index (SPI) are commonly applied for drought monitoring (Mishra and Singh 2010). The PDSI is based on a physical water balance model (Palmer 1965). McKee et al. (1993) derived the SPI, which utilizes long-term rainfall records.

The Standardized Soil Moisture Index (SSI) (Hao and AghaKouchak 2013) is similar to the SPI, which uses soil moisture as its input parameter. Hao and AghaKouchak (2013) presented the Multivariate Standardized Drought Index (MSDI) by combining the rainfall and soil moisture data, which can be applied for agro-meteorological drought monitoring.

The copula functions developed by Sklar (1959) are handy functions that can be useful for capturing joint dependency between the random variables, irrespective of their marginal distribution. Hence, several studies (Janga Reddy and Ganguli 2012; Ganguli and Reddy 2012; Mirabbasi et al. 2012) applied a copula-based framework for drought frequency analysis.

Recent reviews (Hao and Singh 2015) emphasize the monitoring of drought from a multivariate perspective. Motivated by the above facts, the study takes up two main objectives (1) to compare the historical drought events based on MSDI, SPI, and SSI; and (2) to apply copula-based modelling to assess the agro-meteorological drought risks based on 3-month MSDI in the study region.

The rest of the paper is arranged as follows: The study area, dataset, and methodology are described in Sect. 2. The application, results, and discussion are presented in Sect. 3. Section 4 presents the conclusions of the study.

2 Materials and Methodology

2.1 Study Area and Dataset

The meteorological subdivision of Marathwada is situated in the central and south-eastern parts of Maharashtra state. The geographical extent of latitudes of the region is 17°35'N–20°40'N, and the expansion of longitudes is 74°40'E–78°15'E as shown in (Fig. 1). The entire region is divided into eight districts, covering an area of 64,590 km^2. The annual rainfall over Marathwada is 826 mm, more than 80% of which is dependent on the southwest monsoon. A tropical semi-arid climate prevails in the region, and the farmers in the area experience severe distress. The highest temperature (45 °C) is observed during May, and the coldest temperature (11 °C) occurs in December.

This study used the rainfall data of 91 grid points over the Marathwada region prepared by the India Meteorological Department (IMD), Pune (Pai et al. 2014). This data has a spatial resolution of 0.25° × 0.25°, and we extracted the data for all the grid points from 1980–2019. The Thiessen polygon approach has been adopted to compute the average areal precipitation over the Marathwada Region. The Thiessen polygons depicted the representation area of each grid, which has been used in the computation of mean precipitation. The monthly root zone soil moisture (RZSM) was downloaded from the Modern-Era Retrospective analysis for Research

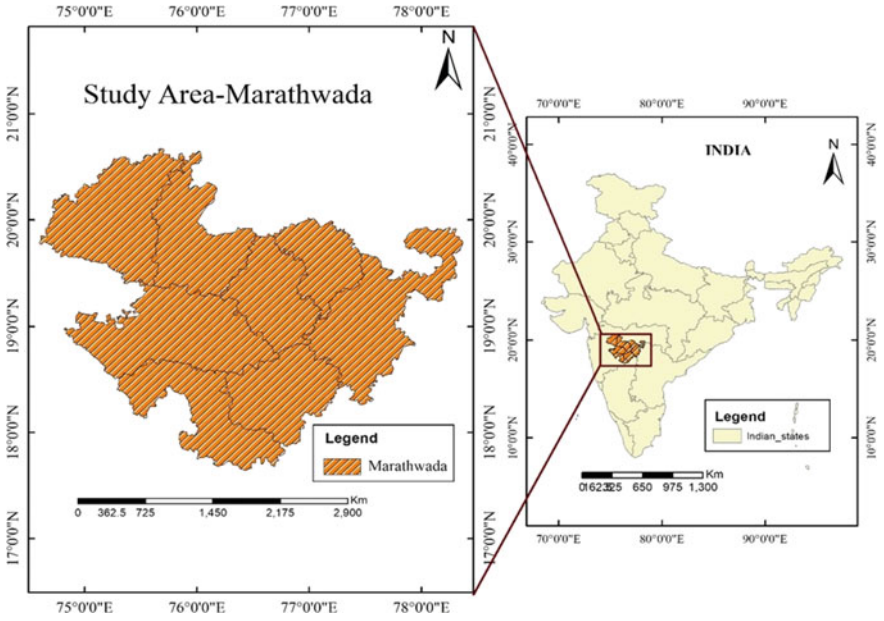

Fig. 1 Location map of the study region

and Applications 2 (MERRA-2) (Gelaro et al. 2017; Reichle et al. 2017) for the duration 1980–2019 from (https://gmao.gsfc.nasa.gov/reanalysis/MERRA-2/data_access/). The spatial resolution of the dataset is 0.5° latitude × 0.625° longitude, which is resampled to 0.25° latitude × 0.25° longitude by bilinear interpolation. The mean moisture content over 0–100 cm depth of soil is considered as the root zone soil moisture (m^3/m^3). Sathyanadh et al. (2016) assessed different soil moisture (SM) datasets against India Meteorological Department's in-situ measurements spread over India. The MERRA SM product exhibited a good correlation with the in-situ measurements. Several drought-related studies worldwide have used the MERRA soil moisture product (Farahmand and AghaKouchak 2015; Agutu et al. 2020; Chen et al. 2020).

2.2 Methodology

2.2.1 Formation of Standardized Indices

McKee et al. (1993) recommended two-parameter gamma distribution for obtaining the cumulative distribution function (CDF) from the observed rainfall data. The gamma probability density function (PDF) is expressed as:

$$g(\chi) = \frac{1}{\beta^{\alpha}\Gamma(\alpha)}\chi^{\alpha-1}e^{-\frac{\chi}{\beta}} \tag{1}$$

where $\Gamma(\alpha)$ represents the gamma function, α and β stand for the shape and rate parameters respectively, and χ is a random variable that accepts non-negative and nonzero values. By taking $t = \frac{\chi}{\beta}$, the cumulative probability $G(\chi)$ can be expressed as:

$$G(\chi) = \frac{1}{\Gamma(\hat{\alpha})}\int_0^{\chi} t^{\hat{\alpha}-1}e^{-t}dt \tag{2}$$

Equation 2 is not applicable for zero rainfall values. The modified CDF can be written as:

$$H(\chi) = q + (1-q)G(\chi) \tag{3}$$

In the above equation, q is the probability of zero precipitation. The CDF of the mixed distribution can then be transformed to the CDF of the standard normal distribution to obtain the standardized precipitation index.

Unlike SPI, there is no specific recommendation regarding best-fit distribution for soil moisture. Farahmand and AghaKouchak (2015) used a non-parametric approach by fitting soil moisture data to an empirical distribution. The SSI values in their study

were in the range of −2 to + 2, whereas it is observed that, in general, the values of the standardized indices lie between −3 and + 3. According to (Soľáková et al. 2014), the fact that parametric distribution captures extreme values better than their non-parametric counterparts can partly explain this result. Zhang et al. (2017) applied the gamma distribution to characterize SPI and SSI over the four Northern Indian states of the Indo-Gangetic plain. Following this work, we have used the gamma distribution to compute SSI over the Marathwada region.

2.2.2 Copula

Sklar (1959) first introduced the copula functions. One-dimensional marginal distribution functions can be joined or 'coupled' to construct multivariate distribution functions using copulas (Nelsen 2007). The copula functions can exhibit the dependence pattern among multiple random variables, and they are considered an efficient tool for joint distribution modelling (Joe 1997; Nelsen 2007).

Sklar's theorem gives the explicit definition of the copula, which is restated below. If $x_1, x_2, \ldots\ldots x_n$ are n random variables, and their corresponding marginal distribution functions are given as $G_1(x_1), G_2(x_2) \ldots\ldots .., G_n(x_n)$, then the copula function C can merge those univariate distributions to produce their joint cumulative distribution:

$$\begin{aligned} G(x_1, x_2, \ldots., x_n) &= C\{G_1(x_1), G_2(x_2) \ldots\ldots .., G_n(x_n)\} \\ &= C(u_1, .., u_n), \forall x_1, x_2, \ldots x_n \in R \end{aligned} \tag{4}$$

The study used three Archimedean and two elliptical copulas for the multivariate modelling. The functional form of the different copulas and their parameter ranges are presented in Table 1. (Zhang and Singh 2019) can be referred for more details regarding the copula functions.

2.2.3 Estimation of the Copula Parameters

The maximum pseudo-likelihood (MPL) technique has been adopted for deriving the parameters. In this method, instead of parametric distributions, the copula parameters are estimated using rank-based empirical marginal distributions. The maximization of the pseudo-log-likelihood function gives the required parameters. Given a random vector $X \in \{X_{i,1}, ..., X_{i,d}\}$, the pseudo-likelihood can be computed as follows:

$$L_\theta = \sum_{i=1}^{n} \ln\left[c_\theta\{U_{i,1}, ..., U_{i,d}\}\right] \tag{5}$$

where $U_{i,d} = \frac{R_{i,d}}{n+1}, d = 2$ and $R_{i,d}$ is the ranked data of $X_{i,d}$.

Table 1 List of the copula families

Copula class	Type	Copula CDF $C_\theta(u, v)$	Parameters Θ
Archimedean	Clayton	$max\left(\left[u^{-\theta} + v^{-\theta} - 1\right]^{\frac{-1}{\theta}}, 0\right)$	$\theta \in [-1, \infty)\backslash\{0\}$
	Gumbel-Hougaard	$\exp\{-[(-lnu)^\theta + (-lnv)^\theta]^{\frac{1}{\theta}}\}$	$\theta \in [1, \infty)$
	Frank	$-\frac{1}{\theta}\ln\left\{1 + \frac{(e^{-\theta u}-1)(e^{-\theta v}-1)}{(e^{-\theta}-1)}\right\}$	$\theta \in (-\infty, \infty)\backslash\{0\}$
Elliptical	Gaussian	$\Phi_R\left(\Phi^{-1}(u), \Phi^{-1}(v), \rho\right)$	$-1 \leq \rho \leq 1$
	Student's t	$\int_{-\infty}^{t_v^{-1}(u)} \int_{-\infty}^{t_v^{-1}(v)} \frac{1}{2\Pi\sqrt{1-r^2}}\left\{1 + \frac{x^2 - 2rxy + y^2}{v(1-r^2)}\right\}^{-\frac{v+2}{2}} dxdy$ $t_v(x) = \int_{-\infty}^{x} \frac{\Gamma\left(\frac{v+1}{2}\right)}{\sqrt{\Pi v}\Gamma\left(\frac{v}{2}\right)}\left(1 + \frac{y^2}{v}\right)^{-\frac{v+1}{2}} dy$	$v > 2, r \in (0, 1]$

Then we can estimate the required parameter as:

$$\hat{\theta} = \arg\max\{L_\theta\} \tag{6}$$

2.2.4 Selection of Best Copula

In general, the copula function with the highest likelihood can be considered as the best-fit copula. However, goodness-of-fit tests are required to ensure the suitability of the copula model. These tests are formulated by considering the distance between the empirical and theoretical copulas. The Cramer-von Mises (CvM), Anderson–Darling (AD), and Integrated Anderson–Darling (IAD) test statistics have been computed to decide the best performing copula model.

The empirical copula function is expressed as (Genest and Favre 2007):

$$\begin{aligned} C_n &= \frac{1}{n}\sum_{i=1}^{n} I\left(\frac{R_{i,1}}{n+1} \le u_1, \frac{R_{i,2}}{n+1} \le u_2\right) \\ u &= (u_1, u_2) \in [0,1]^2 \end{aligned} \tag{7}$$

where u_1 and u_2 are random variables and the indicator function of set A is denoted by I.

The CvM test statistic can be expressed as:

$$S_n = \sum_{i=1}^{n} \left\{C_n\left(U_{i,1}, U_{i,2}\right) - C_\theta\left(U_{i,1}, U_{i,2}\right)\right\}^2 \tag{8}$$

where C_n and C_θ are empirical and theoretical copula, respectively.

The Anderson–Darling and Integrated Anderson–Darling statistics can be expressed as (Ane and Kharoubi 2003):

$$AD = \max_{1\le i\le n, 1\le j\le n} \frac{|C_n(i/n, j/n) - C_\theta(i/n, j/n)|}{\sqrt{C_\theta(i/n, j/n)[1 - C_\theta(i/n, j/n)]}} \tag{9}$$

$$IAD = \sum_{i=1}^{n}\sum_{j=1}^{n} \frac{[C_n(i/n, j/n) - C_\theta(i/n, j/n)]^2}{C_\theta(i/n, j/n)[1 - C_\theta(i/n, j/n)]} \tag{10}$$

In the above equations, the order statistics of random variables are represented by i and j.

2.2.5 The Formulation of the Multivariate Standardized Drought Index (MSDI)

The parametric MSDI (Hao and AghaKouchak 2013) is adopted for drought characterization in the study. The MSDI integrates the SPI and SSI and can be expressed as:

$$MSDI = \Phi^{-1}(p) \tag{11}$$

where p is the joint cumulative probability of the joint distribution of precipitation and soil moisture.

$$p = P(U < u, V < v) = C[F_U(u), F_V(v)] \tag{12}$$

where C is the copula function, and $F_U(u)$, $F_V(v)$ are the CDFs of the random variable U and V, respectively. The joint CDF of precipitation and soil moisture is inversely transformed by the standard normal distribution, resulting in the construction of MSDI, as given in Eq. 11.

2.2.6 Drought Identification and Characterization

The concept of run theory (Yevjevich 1967) is applied for computing two drought characteristics—duration and severity. Based on the theory, a threshold is defined. We considered a threshold value of −0.8 (Hao and AghaKouchak 2013). If the index falls below the threshold, a drought event is identified, and the event terminates if the index value is greater than the threshold value. The consecutive time interval (in months) between the onset and termination of a drought event is known as the duration (D), and severity (S) is the summation of the index value over the time interval. The maximum absolute value of the index over the duration is known as drought peak (P). The drought inter-arrival time (L) is the consecutive number of months counting from the starting point of a drought episode to the onset of the next episode (Song and Singh 2010) (Fig. 2).

2.2.7 Return Period Analysis of Droughts

The computation of the return period is necessary for analysing drought risk. In this study, we computed two different cases of bivariate return periods and inter-compared them with univariate drought frequency. The univariate return periods for duration and severity can be separately expressed using the following equations (Willems 2000; Kim and Valdés 2003):

$$T_d = \frac{E(I_d)}{1 - F_D(d)} \tag{13}$$

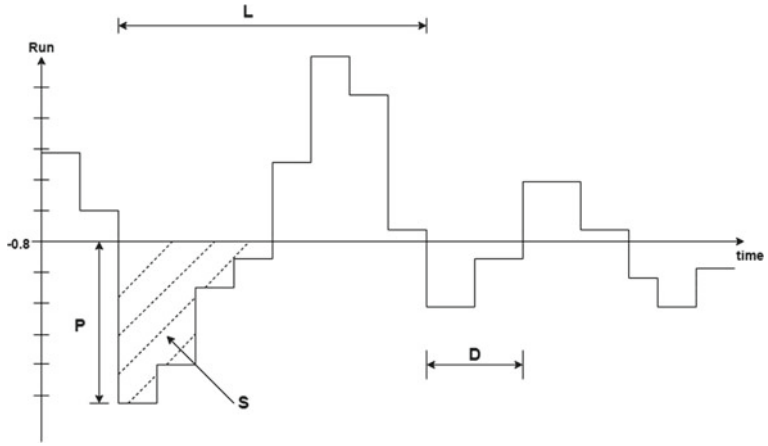

Fig. 2 Illustration of the drought events. ***Note*** *D* is *Duration, P* is *Peak, S* is *Severity, L* is *Inter arrival time*

$$T_s = \frac{E(I_d)}{1 - F_S(s)} \tag{14}$$

In the above equations, T_d = Return period considering duration is greater than or equal to a particular value, and T_s = Return period considering severity is greater than or equal to a specific value. $E(I_d)$ is the expected inter-arrival time, $F_D(d)$ and $F_S(s)$ are the CDF of duration and severity, respectively.

However, when the underlying random variables are mutually correlated, the multivariate return period plays a more significant role in the design criteria. The drought events are considered bivariate, and hence the return period should be computed while considering the joint behaviour of the drought characteristics. The joint return period can be evaluated for two separate cases (Shiau 2003): the 'OR' case in which duration *or* severity is exceeding or equal to a specific magnitude, and the 'AND' case where the duration *and* severity is exceeding or equal to a particular magnitude, which is designated by T_{DS}^{OR} and T_{DS}^{AND} respectively as:

$$T_{DS}^{AND} = \frac{E(I_d)}{1 - F_D(d) - F_S(s) + C(F_D(d), F_S(s))} \tag{15}$$

$$T_{DS}^{OR} = \frac{E(I_d)}{1 - C(F_D(d), F_S(s))} \tag{16}$$

where C is the selected copula function.

Table 2 Copula parameters and corresponding test statistics for modelling of MSDI

Copula Functions	Parameter Value	Log-likelihood	AIC	S_n	AD	IAD
Clayton	1.0145	85.477	−168.9542	0.8818	0.2098	4.5726
Frank	5.9684	**161.4117**	**−320.8235**	**0.1328**	**0.1903**	**1.0652**
Gumbel-Hougaard	1.8244	135.4227	−268.8454	0.2807	0.1912	1.7045
Gaussian	0.6729	144.6373	−287.2746	0.2580	0.1893	1.6540

3 Results and Discussion

3.1 Selection of Best Copula for MSDI Construction

The present study investigated agro-meteorological droughts considering the inputs of rainfall and soil moisture and performed drought analysis using SPI, SSI, and MSDI. Four copulas were evaluated to measure the mutual dependence between precipitation and soil moisture. The estimated copula parameters using the MPL approach and the associated goodness-of-fit test statistics are given in Table 2. The Frank copula is further selected to construct MSDI at a 3-month time scale (MSDI-3) for the study region.

3.2 Performance Assessment of MSDI

The MSDI has been compared with SPI and SSI at a 3-month time scale (SPI-3 and SSI-3), and the plot is depicted in Fig. 3. The MSDI may not give the same duration and severity as other univariate indices, because the joint distribution at any given quantile of the univariate distribution may not be the same. As seen from the previous analysis, Frank copula has been selected for constructing the joint index. The initial hypothesis is that the copula-based MSDI would perform better than SPI and SSI.

During the entire study period of 1981–2019, SPI and SSI, in many cases, manifested substantial differences within severity and duration. If we consider a period, for instance, 2008–2013, it is observed that the onset of drought is exhibited by the SPI before the SSI.

The inter-comparison indicates that MSDI could capture the severity of drought similar to SSI, and drought onset identical to the SPI. It was also observed that when both the univariate indices indicate drought, MSDI also showed drought. The MSDI index was further applied for bivariate drought risk estimation in the Marathwada region.

A total of 48 drought events were recognized from the estimated MSDI-3 series. Summary statistics of drought characteristics for the study period of 1981–2019 are presented in Table 3.

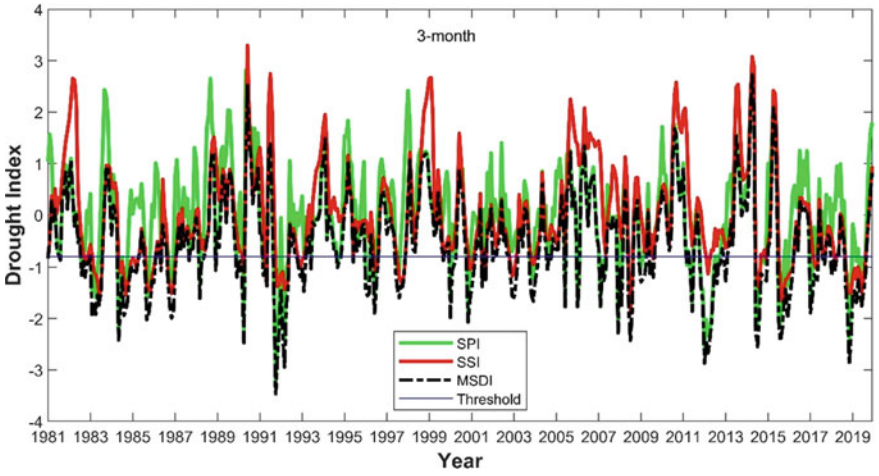

Fig. 3 Parametric drought indices at 3-month time scale for the Marathwada region

Table 3 Summary statistics of droughts based on MSDI, SSI, and SPI in the Marathwada region

Climate variables	Statistics	Drought Index		
		MSDI	SSI	SPI
Drought	Number of droughts	48	29	41
	Average inter-arrival time (months)	9.75	16	11.32
Duration (months)	Mean	3.85	3.55	2.29
	Maximum	12	12	8
	Standard deviation	3.05	3.07	1.62
	Skewness	1.22	1.54	1.42
	Kurtosis	3.99	4.78	5.15
Drought severity	Mean	5.54	3.99	3.18
	Maximum	20.97	14.71	15.09
	Standard deviation	5.42	3.75	2.84
	Skewness	1.55	1.42	2.17
	Kurtosis	4.67	4.24	8.85

Pearson's correlation coefficient, along with Kendall's tau and Spearman's rho, have been computed to check the dependence between two drought variables. Table 4 illustrates the correlation coefficient and associated *p*-values. The results indicated a significant correlation between drought characteristics.

Table 4 Dependence pattern between drought characteristics in terms of correlation

Drought Index	Dependence Measure	Duration-Severity	*P*-value for correlation
MSDI	Pearson's Correlation (r)	0.97	$1.18e^{-30}$
	Kendall's τ	0.89	$5.597e^{-17}$
	Spearman's rank correlation (ρ)	0.97	$9.28e^{-30}$

3.3 Marginal Distribution Selection for Drought Characteristics

The selection of appropriate marginal distribution is required for drought risk estimation. The study tested several parametric distributions to select the optimum distributions for fitting both duration and severity. The study applied the maximum likelihood (ML) approach for parameter estimation of the distributions. The performance of each distribution was evaluated using the Kolmogorov–Smirnov (KS) test and associated *p*-value at 5% significance level, along with Akaike information criteria (AIC), and the results are illustrated in Table 5. From Table 5, it can be seen that for the duration only for the Weibull distribution, the *p*-value is greater than the significance level (0.05). In the case of severity, all the selected distributions have a *p*-value greater than the significance level. The plot of CDF and PDF for distributions fitted to both the drought characteristics are presented in Fig. 4. From the results, the Weibull distribution was selected for modelling both duration and severity.

Table 5 Performance comparison between fitted probability models

Drought Index	Drought variables	Distributions	Shape	Scale	KS	p-value ($\alpha = 0.05$)	AIC
MSDI	Duration	Gamma	1.74	2.21	0.19	0.047	222.24
		Weibull	1.35	4.22	**0.18**	**0.083**	223.55
		Lognormal	1.04	0.82	0.21	0.027	**220.40**
		Exponential	3.85	-	0.23	0.011	227.52
	Severity	Gamma	1.23	4.50	0.12	0.501	263.33
		Weibull	1.09	5.74	**0.12**	0.511	263.94
		Lognormal	1.25	1.00	0.13	0.346	**259.93**
		Exponential	5.54	-	0.14	0.276	262.27

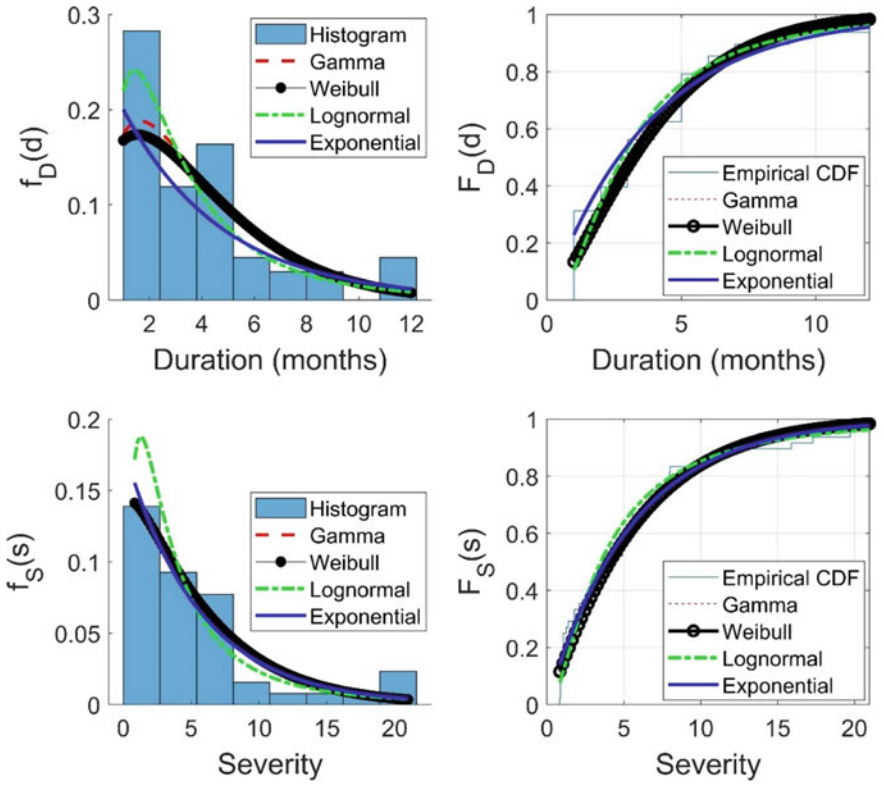

Fig. 4 PDF and CDF plots for the fitted probability distribution of duration and severity

3.4 Analysis of the Joint Distribution of Drought Variables by Applying Copulas

The joint distribution of the two drought characteristics is formulated using a suitable copula function. Five copula functions were evaluated to select the best copula for bivariate modelling. The maximum pseudo-log-likelihood approach has been adopted in this study for the estimation of copula parameters. The fitted parameters and related log-likelihood estimates are listed in Table 6. The Frank copula has the highest log-likelihood value, followed by the Gumbel-Hougaard copula. The AIC value of the Frank copula is the least among all the copulas considered in the study. Further, the results of distance-based statistics AD and IAD are also listed in Table 6.

It is observed that the AD and IAD values are least for Frank copula as well, and hence the Frank copula is chosen for estimating bivariate drought risk.

Table 6 The estimated parameters of copula and comparison of their performance

Copula Family	Copula Parameter	LL	AIC	S_n	AD	IAD
Clayton	$\theta = 4.115$	33.921	−65.843	0.236	0.397	1.307
Frank	$\theta = 24.469$	**61.760**	**−121.520**	**0.101**	**0.391**	**0.676**
Gumbel-Hougaard	$\theta = 5.873$	60.387	−118.774	0.114	0.401	0.746
Gaussian	$\rho = 0.950$	54.464	−106.929	0.128	0.397	0.804
t-copula	$\vartheta = 5.025$, $r = 0.962$	56.266	−108.532	0.115	0.395	0.726

3.5 Bivariate Frequency Analysis of Droughts

3.5.1 Comparison of the Univariate and Bivariate Drought Return Period

The joint distributions derived using the selected copula function are further applied for computing two primary return periods, the 'OR' case and the 'AND' case. The average inter-arrival time of drought is 9.75 months for the period of 1981 to 2019. Table 7 presents drought severity and duration for 5, 10, 20, 50, and 100 years of univariate return periods. For instance, in the case of a univariate return period of 20 years, the severity is greater than 16.68, and the duration is greater than 10.04 months, respectively. The comparison of univariate with bivariate return periods computed using the Frank copula is also presented in Table 7.

On the contrary, if we consider joint behaviour of the drought characteristics, it is observed from Table 7 that the return period for the 'AND' case where $D \geq 10.04$ and $S \geq 16.68$ is 39.33 years; whereas the return period for 'OR' case where $D \geq 10.04$ or $S \geq 16.68$ is equal to 13.41 years, as presented in Table 7. In a nutshell, in the case of a 3-month time scale of MSDI, compared to a single variant return period of 20 years, the bivariate return period for the 'AND' case is increased by 96.65%, and if we consider the 'OR' case, then the return period decreased by 32.95%. Moreover, it is noticed that compared to univariate return periods, the bivariate return period for the 'AND' condition is higher, 'and' the 'OR' condition is lower. It can be inferred from the analysis that the 'OR' condition overestimates the drought risks, and the

Table 7 Univariate and bivariate return periods and their associated return periods in the Marathwada region

Return Period (T) (years)	Duration (months)	Severity	T_{DS}^{AND}	T_{DS}^{OR}
5	6.59	9.92	6.04	4.27
10	8.37	13.34	14.56	7.62
20	10.04	16.68	39.33	13.41
50	12.10	21.01	174.57	29.18
100	13.58	24.22	601.6	54.53

'AND' condition underestimates the drought risks. Hence, both these estimates are useful to understand and manage drought risks in the region.

4 Conclusions

To manage water resources under drought conditions, it is necessary to characterize droughts using appropriate drought indices and analyze the associated drought risks. Rather than considering only one aspect, the effect of several drought-causing variables on the phenomena will give us a broad idea about the spatiotemporal assessment of drought. Therefore, this study used precipitation and soil moisture-based index for adequate drought characterization and risk estimation. The drought was modelled using MSDI at a 3-month time scale for the Marathwada region. The Archimedean and meta-elliptical families were evaluated for modelling joint distribution of duration and severity. Univariate and bivariate joint return periods for 'OR' and 'AND' cases were computed to understand the drought risks in the region. The main findings from the study are:

i. The Frank copula was ranked best-fit function for constructing parametric joint distribution for computing MSDI.
ii. MSDI showed good efficacy in monitoring droughts in the region in terms of identifying the drought events and evaluating their characteristics for the period of analysis; their values are in concordance with SPI and SSI.
iii. The results of bivariate dependency analysis indicated Frank copula as the most suitable copula for constructing joint distribution between duration and severity.
iv. The univariate return period for the study region was higher than the 'OR' case joint return period but lower than the 'AND' case return period. The study deduced that the 'OR' case joint return period would overestimate the drought risk while the risk will be underestimated when the 'AND' case is considered.

Acknowledgements The authors would like to thank the various organizations that provided support for the study. Department of Science and Technology (SPLICE–Climate Change Programme), Government of India, Project #DST/488/CCP/CoE/140/2018 for funding support; the India Meteorological Department (IMD), the Modern-Era Retrospective analysis for Research and Applications, Version 2 (MERRA-2) of NASA for providing the datasets used in this study.

References

Agutu, N. O., J. L. Awange, C. Ndehedehe, and M. Mwaniki. 2020. "Consistency of Agricultural Drought Characterization over Upper Greater Horn of Africa (1982–2013): Topographical, Gauge Density, and Model Forcing Influence." *Science of the Total Environment* 709: 135149. https://doi.org/10.1016/j.scitotenv.2019.135149.

Ahmadalipour, Ali, Hamid Moradkhani, and Mehmet C. Demirel. 2017. A Comparative Assessment of Projected Meteorological and Hydrological Droughts: Elucidating the Role of Temperature. *Journal of Hydrology* 553: 785–797. https://doi.org/10.1016/j.jhydrol.2017.08.047.

Ane, Thierry, and Cécile. Kharoubi. 2003. Dependence Structure and Risk Measure. *The Journal of Business* 76 (3): 411–438. https://doi.org/10.1086/375253.

Chen, Nengcheng, Ronghui Li, Xiang Zhang, Chao Yang, Xiaoping Wang, Linglin Zeng, Shengjun Tang, Wei Wang, Deren Li, and Dev Niyogi. 2020. "Drought Propagation in Northern China Plain: A Comparative Analysis of GLDAS and MERRA-2 Datasets." *Journal of Hydrology* 588: 125026. https://doi.org/10.1016/j.jhydrol.2020.125026.

Farahmand, Alireza, and Amir AghaKouchak. 2015. A Generalized Framework for Deriving Nonparametric Standardized Drought Indicators. *Advances in Water Resources* 76: 140–145. https://doi.org/10.1016/j.advwatres.2014.11.012.

Ganguli, Poulomi, and M. Janga Reddy. 2012. "Risk Assessment of Droughts in Gujarat Using Bivariate Copulas." *Water Resources Management* 26 (11): 3301–3327. https://doi.org/10.1007%2Fs11269-012-0073-6.

Gelaro, Ronald, Will McCarty, Max J. Suárez, Ricardo Todling, Andrea Molod, Lawrence Takacs, Cynthia A. Randles, Anton Darmenov, Michael G. Bosilovich, and Rolf Reichle. 2017. The Modern-Era Retrospective Analysis for Research and Applications, Version 2 (MERRA-2). *Journal of Climate* 30 (14): 5419–5454. https://doi.org/10.1175/jcli-d-16-0758.1.

Genest, Christian, and Anne-Catherine. Favre. 2007. Everything You Always Wanted to Know about Copula Modeling but Were Afraid to Ask. *Journal of Hydrologic Engineering* 12 (4): 347–368. https://doi.org/10.5040/9781472547675.ch-002.

Hao, Zengchao, and Amir AghaKouchak. 2013. Multivariate Standardized Drought Index: A Parametric Multi-Index Model. *Advances in Water Resources* 57: 12–18. https://doi.org/10.1016/j.advwatres.2013.03.009.

Hao, Zengchao, and Vijay P. Singh. 2015. Drought Characterization from a Multivariate Perspective: A Review. *Journal of Hydrology* 527: 668–678. https://doi.org/10.1016/j.jhydrol.2015.05.031.

Janga Reddy, M., and Poulomi Ganguli. 2012. "Application of Copulas for Derivation of Drought Severity–Duration–Frequency Curves." *Hydrological Processes* 26 (11): 1672–1685. https://doi.org/10.1002%2Fhyp.8287.

Joe, Harry. 1997. *Multivariate Models and Multivariate Dependence Concepts*. CRC Press. https://doi.org/10.1201/9780367803896.

Kim, Tae-Woong, and Juan B Valdés. 2003. "Nonlinear Model for Drought Forecasting Based on a Conjunction of Wavelet Transforms and Neural Networks." *Journal of Hydrologic Engineering* 8 (6): 319–328. https://doi.org/10.1061//ASCE/1084-0699/2003/8:6/319.

Liu, Suning, Haiyun Shi, and Bellie Sivakumar. 2020. "Socioeconomic Drought under Growing Population and Changing Climate: A New Index Considering the Resilience of a Regional Water Resources System." *Journal of Geophysical Research: Atmospheres* 125 (15): e2020JD033005. https://doi.org/10.1029%2F2020jd033005.

Liu, Xianfeng, Xiufang Zhu, Yaozhong Pan, Shuangshuang Li, Yanxu Liu, and Yuqi Ma. 2016. Agricultural Drought Monitoring: Progress, Challenges, and Prospects. *Journal of Geographical Sciences* 26 (6): 750–767. https://doi.org/10.1007/s11442-016-1297-9.

McKee, Thomas B., Nolan J. Doesken, and John Kleist. 1993. "The Relationship of Drought Frequency and Duration to Time Scales." 17: 179–183. In Proceedings of the 8th Conference on Applied Climatology.

Mirabbasi, Rasoul, Ahmad Fakheri-Fard, and Yagob Dinpashoh. 2012. "Bivariate Drought Frequency Analysis Using the Copula Method." *Theoretical and Applied Climatology* 108 (1): 191–206. https://doi.org/10.1007%2Fs00704-011-0524-7.

Mishra, Ashok K., and Vijay P. Singh. 2010. A Review of Drought Concepts. *Journal of Hydrology* 391 (1–2): 202–216. https://doi.org/10.1016/j.jhydrol.2010.07.012.

Nelsen, Roger B. 2007. *An Introduction to Copulas*. New York: Springer-Verlag. https://doi.org/10.1007/0-387-28678-0.

Pai, DS, Latha Sridhar, M Rajeevan, OP Sreejith, NS Satbhai, and B Mukhopadhyay. 2014. "Development of a New High Spatial Resolution (0.25× 0.25) Long Period (1901–2010) Daily Gridded Rainfall Data Set over India and Its Comparison with Existing Data Sets over the Region." *Mausam* 65 (1): 1–18. https://doi.org/10.1007/s00382-014-2307-1.

Palmer, Wayne C. 1965. *Meteorological Drought*. Vol. 30. US Department of Commerce, Weather Bureau.

Reichle, Rolf H, Clara S Draper, Qing Liu, Manuela Girotto, Sarith PP Mahanama, Randal D Koster, and Gabrielle JM De Lannoy. 2017. "Assessment of MERRA-2 Land Surface Hydrology Estimates." *Journal of Climate* 30 (8): 2937–60. https://doi.org/10.1175/jcli-d-17-0121.1.

Sathyanadh, Anusha, Anandakumar Karipot, Manish Ranalkar, and Thara Prabhakaran. 2016. Evaluation of Soil Moisture Data Products over Indian Region and Analysis of Spatio-Temporal Characteristics with Respect to Monsoon Rainfall. *Journal of Hydrology* 542: 47–62. https://doi.org/10.1016/j.jhydrol.2016.08.040.

Shiau, J.T. 2003. Return Period of Bivariate Distributed Extreme Hydrological Events. *Stochastic Environmental Research and Risk Assessment* 17 (1): 42–57. https://doi.org/10.1007/s00477-003-0125-9.

Sklar, M. 1959. Fonctions de Repartition an Dimensions et Leurs Marges. *Publications Institute Statistics University Paris* 8: 229–231.

Soľáková, Tatiana, Carlo De Michele, and Renata Vezzoli. 2014. Comparison between Parametric and Nonparametric Approaches for the Calculation of Two Drought Indices: SPI and SSI. *Journal of Hydrologic Engineering* 19 (9): 04014010. https://doi.org/10.1061/(asce)he.1943-5584.0000942.

Song, Songbai, and Vijay P. Singh. 2010. Frequency Analysis of Droughts Using the Plackett Copula and Parameter Estimation by Genetic Algorithm. *Stochastic Environmental Research and Risk Assessment* 24 (5): 783–805. https://doi.org/10.1007/s00477-010-0364-5.

Willems, Patrick. 2000. Compound Intensity/Duration/Frequency-Relationships of Extreme Precipitation for Two Seasons and Two Storm Types. *Journal of Hydrology* 233 (1–4): 189–205. https://doi.org/10.1016/s0022-1694(00)00233-x.

Yevjevich, Vujica M. 1967. "Objective Approach to Definitions and Investigations of Continental Hydrologic Droughts." Colorado State University. Libraries. https://doi.org/10.1016/0022-1694(69)90110-3.

Zhang, Lan, and V. P. Singh. 2019. *Copulas and Their Applications in Water Resources Engineering*. Cambridge University Press, Cambridge. https://doi.org/10.1017/9781108565103.

Zhang, Xiang, Renee Obringer, Chehan Wei, Nengcheng Chen, and Dev Niyogi. 2017. "Droughts in India from 1981 to 2013 and Implications to Wheat Production." *Scientific Reports* 7 (1): 1–12. https://doi.org/10.1038/srep44552.

High-Quality Historical Flood Data Reconstruction in Bangladesh Using Hidden Markov Models

Max Mauerman, Elizabeth Tellman, Upmanu Lall, Marco Tedesco, Paolo Colosio, Mitchell Thomas, Daniel Osgood, and Arifuzzaman Bhuyan

Abstract Historical data on flood hazard is critical for the design of climate risk management policies. Parametric weather insurance typically requires at least 20–30 years of historical data for accurate risk pricing. However, the current sources of satellite data on flood inundation in Bangladesh are limited. Although passive microwave (PMW) measurements reach back to 1992, they are imprecise and at coarse spatial resolution (25–3.125km^2). Sentinel-1 measurements are more precise (at 10m^2 resolution) but are only consistently available from 2017 onwards. We present a method for reconstructing the high-quality signal of Sentinel-1 data for pre-2017 years using its statistical relationship to PMW—a "data fusion" process. Our data fusion is based on a Bayesian Hidden Markov Model (HMM), in which both Sentinel-1 and PMW are modelled as realizations of an unobserved, time-dependent discrete variable representing flood state. Evaluated against the actual Sentinel-1 in

M. Mauerman (✉) · D. Osgood
International Research Institute for Climate and Society, Columbia University, New York, NY, USA
e-mail: mmauerman@iri.columbia.edu

E. Tellman
School of Geography, Development and Environment, University of Arizona, Tucson, Arizona, USA
e-mail: btellman@arizona.edu

U. Lall
Department of Earth and Environmental Engineering, Columbia University, New York, NY, USA

M. Tedesco
Lamont-Doherty Earth Observatory, Columbia University, New York, NY, USA

P. Colosio
Department of Civil, Environmental, Architectural Engineering and Mathematics, University of Brescia, Brescia, Italy

M. Thomas
Department of Mathematics, Columbia University, New York, NY, USA

A. Bhuyan
Bangladesh Flood Forecasting and Warning Centre, Dhaka, Bangladesh

© The Author(s), under exclusive license to Springer Nature Switzerland AG 2022

G. M. Tarekul Islam et al. (eds.), *Water Management: A View from Multidisciplinary Perspectives*,
https://doi.org/10.1007/978-3-030-95722-3_10

Sylhet division, the "fused" data series has a Spearman correlation of 65%. The fused series also has a 71% Spearman correlation with stream gauge measurements of water levels. On both metrics of correlation, the simulated series achieves an improvement over using PMW alone. We discuss how this simulated data could be used to improve parametric flood insurance.

Keywords Flooding · Insurance · Bangladesh · Data fusion · Remote sensing

1 Introduction

1.1 Overview

Floods have a greater human cost than any other disaster, having affected 2.3 billion people globally from 1995 to 2015 (UNISDR 2015). This cost falls disproportionately on marginalized populations (Winsemius et al. 2018; Tellman et al. 2020)—in the world's 77 lowest-income countries, 92% of disaster costs are not covered by international assistance (RMS 2017). There is a need for financial risk management strategies to cover these hazards—only 3% of this financing gap is covered by any kind of insurance (RMS 2017). Bangladesh in particular is among the world's most flood-prone countries—flood extent covers 25% of the country's area in a normal year and can reach over 60% in an extreme year (Mirza 2002).

Disaster insurance has been recognized as a way to mitigate catastrophic setbacks like floods and help the economically vulnerable escape poverty traps (Barnett et al. 2008)**.** In particular, agricultural index insurance—in which payouts are based on sensor measurements of areas' weather hazards rather than individual claims assessments—has been promoted by many international organizations and foreign assistance agencies (Osgood and Shirley 2012; Benami et al. 2021) as a sustainable way to provide affordable financial protection in developing nations.

However, the potential advantages of index insurance depend on the availability of timely climate data that accurately reflects populations' exposure to weather hazards (Benami et al. 2021). For example, in Bangladesh, flood risk estimation has been typically based on stream gauge water levels, but the stream gauge network is limited in its coverage and cannot convey the full picture of floods' inundated area. A workshop with government, NGO, and private sector stakeholders in Bangladesh identified inadequate risk exposure and monitoring data as the main obstacle to scaling up weather index insurance, particularly flood insurance. (ICCAD 2013).

Advances in radar-based satellite flood mapping technology could help meet this need, but the historical record of these new high-resolution products is short, limiting their utility for insurance. There is a need for statistical methods to reconstruct high-quality historical flood risk information in countries like Bangladesh. Here, we present a data fusion approach based on Bayesian Hidden Markov Models, which combines a high-resolution satellite with a short record (2017–present) and a lower

spatial resolution satellite with a longer record (1992–present) to design flood risk insurance products.

The first part of our paper describes the flood data sources used, along with their practical advantages and disadvantages. The second part introduces the principle of Hidden Markov Models and demonstrates how a well-identified HMM can be fitted to our Bangladesh flood data, using Bayesian methods. Finally, the third part of our paper demonstrates how our reconstructed flood data series has a high degree of correlation with other, independently measured proxies of flood risk, and describes how it could be used to improve index insurance—ultimately leading to risk management products that are both more accurate and more sustainably priced.

1.2 Disaster Index Insurance

Parametric disaster insurance, also known as index insurance, is a type of insurance product designed to pay out based on a proxy for weather hazards, rather than on individual claims assessments as in conventional indemnity-based insurance. The most common such proxy is satellite data on weather conditions, which has the advantages of being timely, low- or no-cost, and global in their coverage (Osgood and Shirley 2012; Benami et al. 2021).

A typical satellite-based index insurance contract is designed to cover an entire geographically contiguous area, such as a county-level administrative unit. These areas are known as the "unit areas of insurance" (UAIs). Satellite weather data is typically spatially averaged over the UAI to arrive at a single value for each insured area. This value is compared against the contract "trigger", an agreed-upon threshold beyond which the insurance product will pay out. Trigger values are often defined in reference to some historical return period; for instance, many index insurance products are tuned such that they are expected to pay out one out of every 5 or one out of every 10 years (Benami et al. 2021; Barnett et al. 2008). If the insurance contract triggers in a given UAI, all claimants in that area receive a payout.

A common issue with index insurance is "basis risk"; that is, the mismatch between insurance payouts and claimants' actual losses. Basis risk is a particular issue for satellite-based insurance, where sensor biases and imprecisions in measurement mean products may fail to pay out during critical loss years (Osgood et al. 2018). There is a growing body of literature on how to quantify basis risk in index insurance and adjust contracts to minimize it (Osgood and Shirley 2012; Benami et al. 2021; Carter et al. 2017).

Satellite-based index insurance has most commonly been applied to drought or excess of rainfall. There is increasing interest in applying similar methods to flood insurance—Bangladesh is the first country to pilot an index insurance product for floods (United News of Bangladesh 2020) that is based on direct estimates of inundated area rather than on rainfall (as in CCRIF 2015). However, satellite data on flood frequency and inundation extent of suitable quality for insurance remains limited.

1.3 Satellite Flood Estimation

Satellites can detect the inundated area of large flood events in rural areas by classifying areas that are distinguishable as water from space (Pekel et al. 2016; Cooley et al. 2017; Ji et al. 2018; Feng et al. 2019; Jones 2019). Radar satellite observations are particularly useful for flood mapping because clouds do not obscure their observations.

However, among the current radar-based remote sensing flood products, there is a tradeoff between accuracy, precision, and length of record, as detailed in Sect. 2. Products based on passive microwave estimates of soil moisture have a record of several decades, but have a very coarse resolution. In contrast, products based on synthetic aperture radar offer a much higher resolution—however, regular measurements only exist from early 2017 onward. Additionally, passive microwave sensors may be more prone than synthetic aperture sensors to false positives from non-flood sources of soil moisture, such as agricultural irrigation. Because rice irrigation requires standing water, rice fields irrigated during the dry season can often appear to be inundated both from the ground and consequently from satellites (Thomas et al. in pub).

1.4 Data Fusion

The tradeoff between temporal length and spatial resolution described above presents a quandary for index insurance projects, as an ideal index not only has low basis risk (i.e. its measurements accurately reflect the hazard that claimants face on the ground) but also has enough historical data to usefully inform risk pricing. Since a typical index insurance contract is designed to pay out once out of every 5–10 years on average, having a precise estimate of the magnitude of rare events is critical. Uncertainty in this regard could lead to unsustainably priced financial instruments and / or be passed on to the buyer in the form of higher risk premia (Osgood and Shirley 2012; Bell et al. 2013).

A potential way to combine the advantages of short, high-quality satellite sources, and longer, noisier satellite sources is to use statistical methods to reconstruct what the high-quality source *would have measured* in years before its record, using the longer but noisier source as a proxy. This class of solutions is known as "data fusion", and has many applications throughout climate science (Bellone et al. 2000; Hughes et al. 1999; Robertson et al. 2003; Xie et al. 2018). Zeng et al. (2020) present a data fusion method to combine synthetic aperture radar and passive microwave satellites, but this method is based on fitting a quadratic function to a very small (fewer than 50) number of data points—and thus is likely prone to overfitting. A promising alternative approach is to treat the parametric relationship between the two series as a time-varying process, the dynamics of which are guided by a simple rule—so-called Hidden Markov Models (HMMs). HMMs have been used by climate scientists

to reconstruct phenomena like wind speed and rainfall (e.g. Robertson et al. 2003); here, we apply them to the problem of reconstructing division-level fractional flooded area.

2 Data

We consider two sources of satellite data on fractional flooded area for this paper: Sentinel-1 ("S1") and passive microwave SSM/I ("PMW"). For the reasons detailed below, we believe that S1 is less likely to suffer from biases in extreme event estimation than PMW—however, its record is significantly shorter. This is what motivates the application of data fusion techniques.

2.1 Sentinel-1

The Sentinel-1 satellite product is a two-satellite constellation of Synthetic-Aperture Radar (SAR) sensors launched by the European Space Agency in April 2014 and April 2016, respectively. Typical of SAR sensors, Sentinel-1 features the ability to capture images through clouds, haze, and at night-time (Rahman and Thakur 2018). Sentinel-1 data usable for insurance is available over Bangladesh from 2017 to present at a current average revisit time of ~ 4.2 days, although this comes as a result of a primarily 2- and 10-day overpass schedule. Spatial resolution is 10 m. Data in this study is used in two transmit/receive radar polarizations—Vertical–Vertical (VV) and Vertical-Horizontal (VH)—and two overpass directions—Ascending and Descending.

We use a flood detection algorithm developed by adapting the Sentinel-1 statistical deviation flood algorithm proposed in DeVries et al. (2020). An adapted algorithm is proposed which adds a baseline selection method, an additional threshold on the VH band, and spatial smoothing. A dry-baseline period is derived from the minimum 45-days of a soil moisture time series over the studied area. We then compute a mean and standard deviation image for both polarizations and both overpass directions from Sentinel-1 images within this baseline period. From these images, a z-score image is computed at every time step where Sentinel-1 data is available 2017–Present. A binary (water or not water) water map is created from the z-score image by marking any pixel as water if the vv or vh z-score value is < -2.5. Finally, spatial smoothing is applied, at both 2- and 4-pixel radii. A pixel is classified as flooded if either the 2-pixel radius mean is > 0.6 *or* the 4-pixel radius mean is > 0.4.

Fractional flooded area over an administrative area is computed by dividing the total sum of water in the region by region area. A time series of fractional flooded area can accordingly be calculated at any administrative level in Bangladesh by iterating over every Sentinel-1 overpass. For this study, we use estimates by division for three divisions in the north: Rajshahi, Sylhet, and Rangpur.

2.2 Passive Microwave SSM/I

Passive microwave (PMW) sensors measure the electromagnetic radiation naturally emitted by the Earth surface, expressed as brightness temperature (ULABY 1982). Because of their sensitivity to wet and dry surfaces, different approaches have been proposed in the past aimed at monitoring large flood events continuously (CHOUDHURY 1989; Galantowicz 2002; Groeve 2010; Tangdamrongsub et al. 2021). In fact, the peculiarities of PMW spaceborne records are their long and continuous temporal coverage (at least every other day since 1979) and the large spatial coverage (global). On the other hand, the relatively coarse spatial resolution of 25 km^2 has always been a major limitation of this dataset. Recently, in the framework of the NASA MeASUREs project, a new gridding algorithm called rSIR technique (Brodzik and Long 2016) has been applied to PMW records to produce a new dataset at the enhanced resolution of 3.125 km^2.

Here, we apply a variation of the algorithm proposed by Groeve (2010) to the enhanced resolution PMW data from the Special Sensor Microwave / Imager (SSM/I) and the Special Sensor Microwave Imager / Sounder (SSMI/S) at Ka- band (37 GHz, horizontal polarization) collected during the ascending pass of the satellite between 1992 and 2019. The algorithm is based on the assumption that spatially close pixels have similar land surface properties and on the choice of a dynamically computed calibration brightness temperature to detrend the time series from temperature seasonality.

The measured (M) brightness temperature value of each pixel is considered as linear combination of water and land brightness temperature contributions, proportionally to the fractional area, and can be expressed as:

$$\begin{aligned} T_{b,measurement} &= (1-w)T_{b,land} + wT_{b,water} \\ &= T_{measurement}\left[(1-w)\varepsilon_{land,measurement} + w\varepsilon_{water}\right] \end{aligned} \tag{1}$$

where w is the water fractional area, ε_{water} the water emissivity, ε_{land} the land emissivity and $T_{measurement}$ the physical temperature at the measured pixel.

The measured brightness temperature (M, "wet" or "dry") is normalized with respect to a calibration brightness temperature value (C), chosen to represent the driest condition of a certain area (i.e. $w = 0$) as

$$T_{b,calibration} = T_{b,land} = T_{calibration}\varepsilon_{land,calibration} \tag{2}$$

where $T_{calibration}$ is the physical temperature of the calibration pixel. For nearby pixels, we consider valid the fundamental assumption of equal emissivities $\left(\varepsilon_{land,measurement} \approx \varepsilon_{land,calibration} \approx \varepsilon_{land}\right)$ and equal temperatures $(T_{calibration} = T_{measurement})$.

Finally, we compute the calibrated signal s (or M/C) as the ratio between the measurement and the calibration brightness temperatures. This quantity is dependent on the water fraction only, increasing when w decreases.

$$s = M/C = T_{b,measurement}/T_{b,calibration} \approx 1 - w(1 - \varepsilon_{water}/\varepsilon_{land}) = f(w) \quad (3)$$

In order to automatically select the calibration pixel, Groeve (2010) suggested the 95th percentile in a 7 by 7 pixels moving window (30,625 km^2). Here we use the 95th percentile in a 14 by 14 pixels moving window, according to preliminary analysis of the time series of calibration values.

Groeve (2010) defined as flood magnitude the number of standard deviations from the mean of the signal s. According to this definition, regular (large) flood events are identified with flood magnitude equal to 2. Here we consider a flood magnitude of 2 as threshold to identify flood events.

As with Sentinel-1, these pixel-level binary indicators of flood presence are spatially averaged to arrive at an estimate of fractional flooded area for a region (here, three divisions in the north: Rajshahi, Sylhet, and Rangpur).

2.3 Tradeoffs Between Sentinel-1 and Passive Microwave

Passive microwave sensors have at least three potential sources of noise for flood detection—soil moisture, rainfall, and coarse spatial resolution—that are less of a problem in active radar sensors like Sentinel-1.

As described above, passive microwave sensors detect water by changes in brightness temperature. Passive microwave sensors are typically used to assess soil moisture, in part because they are so sensitive to wet soils (Fang et al. 2018; Sabaghy et al. 2018). Wet soil (that is not flooded or has standing water present) can cause a similar drop in brightness temperature to inundated area. Thus, it can be difficult to distinguish the signal from an irrigated and actively cultivated field to one that is simply waterlogged, from one with standing water.

Similarly, heavy rainfall can interfere with the signature of surface conditions in PMW. Microwave algorithms over land depend on scattering signals, and the signals of atmospheric precipitation and surface type can be difficult to distinguish (Scheel et al. 2011).

Regarding spatial resolution, Fig. 1 illustrates the size of the smallest resolvable flood event each sensor is capable of detecting. Passive microwave resolution is 3.125km^2; in contrast, Sentinel-1 resolution is 10m^2. The significantly higher resolution of Sentinel-1 means it is much more able to discriminate the signal of flood events from non-flood events. Similarly, floods in areas adjacent to permanent bodies of water may be undetectable by passive microwave, as the signature of flooding is indistinguishable from that of permanent water for co-located pixels.

To illustrate the advantages of higher spatial resolution in practical terms, Fig. 2 illustrates 6 different satellite measurements of the same flood event in northern Bangladesh**.** We can see how in Sentinel-1, riverine overflow is clearly resolvable, while in passive microwave, the entire study area comprises less than a single pixel.

The biases described above are apparent in a comparison of each sensor's estimated fractional flooded area in Sylhet division (Fig. 3). All data are aggregated to

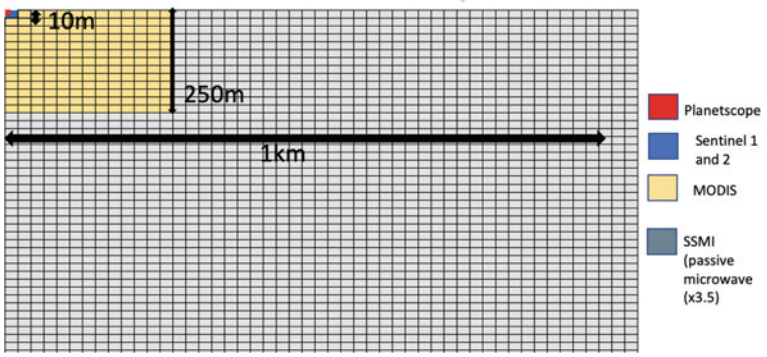

Fig. 1 Comparison of satellite flood products' resolution and measurement frequency. Figure reproduced from Tellman et al. (2021)

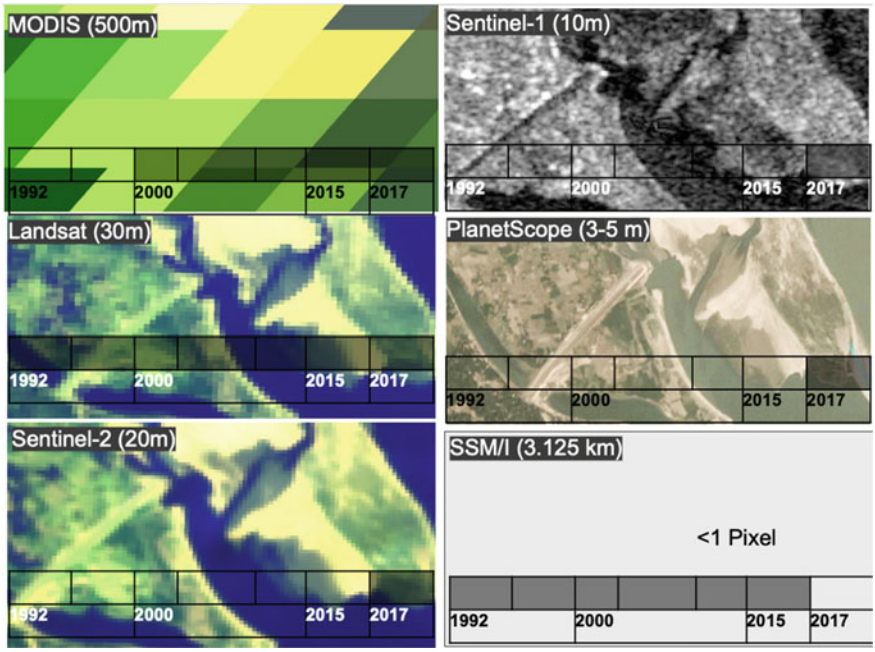

Fig. 2 Comparison of satellites' view of a flood event in northern Bangladesh

the dekadal (10-day) time scale by taking the maximum value over each dekad—a convention followed for the rest of this paper.

In the planting season, PMW exhibits erroneous spikes from seasonal irrigation around December to January, whereas Sentinel-1 does not. Likewise, the tendency of the PMW signal to saturate leads to a much more "jagged" time series than Sentinel-1 during the rainy season, with transient peaks and valleys in fractional flooded area.

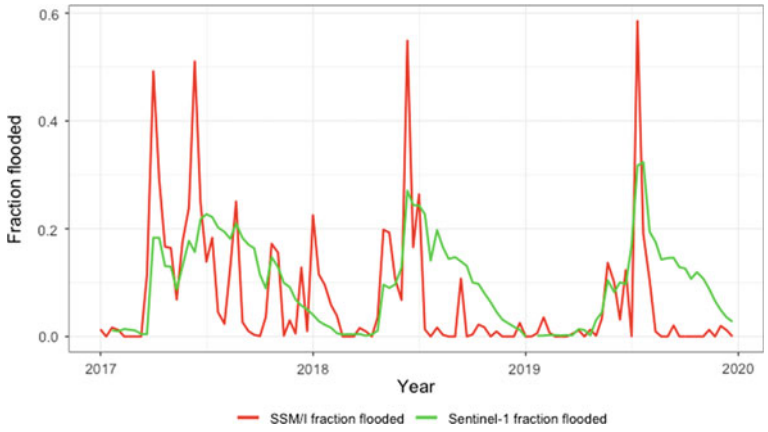

Fig. 3 Comparison of S1 and PMW SSM/I flooded area in Sylhet

Since index insurance is based on the accurate measurement of the magnitude of extreme events, these biases present a major practical problem.

However, visualizing the joint distribution of the two series over each quarter of the year (Fig. 4) suggests a way forward. We can see that within each quarter, the linear relationship between the two series is fairly strong, even as the magnitude of the relationship varies over seasons. This suggests that data fusion models which allow the relationship between the predictor and predicted series to vary as a function of time could be promising. The following section explores such a model in detail.

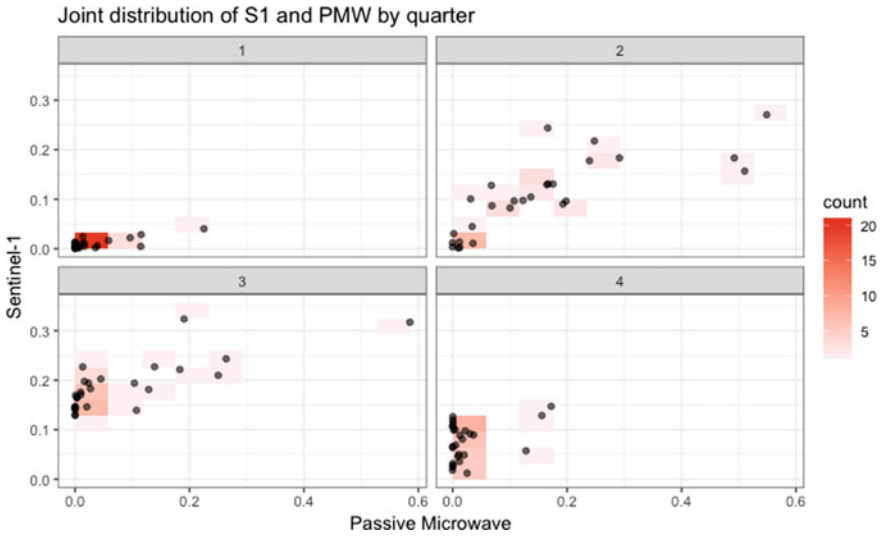

Fig. 4 Joint distribution of S1 and PMW flooded area by quarter of the year

2.4 Validation Data

To establish a benchmark for the reliability of our data fusion model (and its improvement over existing satellite products), we need an external source of data on the timing and severity of flood events to compare it to. While no data source is "perfect", events that are independently reflected in multiple sources are more likely to reflect actual weather risk phenomena and not idiosyncratic noise or bias.

For this paper, our validation data comes from a dataset of stream gauge water levels obtained from the Bangladesh Flood Forecasting and Warning Centre (FFWC). This data is available from 2008 to 2019 and is measured on a biweekly frequency (with some irregularity) over the rainy season (May–October) only. Of the 53 gauges available, we select 1 in each division for comparison on the basis of the highest maximum value over the observation period, under the intuition that this gauge is likely the most representative of flood events in the district. As with the satellite data, the stream gauge data is temporally aggregated up to the dekadal (10-day) level, taking the maximum value over each dekad.

3 Methodology

3.1 Model Overview

A Markov process is a simple rule for describing a phenomenon which depends on its past values. In its simplest form, a first-order Markov process can take a finite number of discrete states, and its state in period t depends only on its state in t-1. A "transition probability matrix" describes the likelihood of going from state i in period t-1 to state j in period t, as in Fig. 5.

Weather and climate dynamics have considered Markov processes for rainfall (wet/dry states), temperature (continuous variables with autoregressions), and other variables, with transition probabilities (or autoregressions) that may be seasonally variable (Robertson et al. 2003; Bellone et al. 2000; Xie et al. 2018; Hughes et al. 1999). In the machine learning literature, Hidden Markov Models (HMMs) were introduced where we do not observe the Markov state directly; rather, the dynamics of the state variable (continuous or discrete) are believed to be influenced by a hidden or latent variable. The underlying dynamics, including the transition probabilities of the discrete hidden states need to be inferred directly from the observed state variable alone. For our application, we consider that the hidden state may refer to a flood signature over the domain that is seen by both the Sentinel-1 and the PMW. This hidden state or signature influences the relationship or correspondence between these two variables.

In our study's observation model, the distribution of Sentinel-1 in each state is described by a Gaussian distribution. In a univariate model, the distribution of S1 over each state would have fixed mean and variance. However, this is a data *fusion* model,

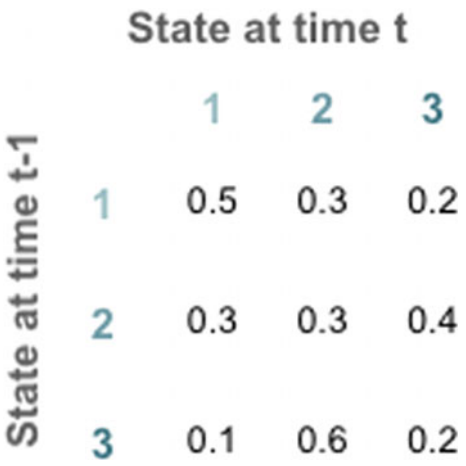

Fig. 5 Example of transition probability matrix

with two variables—S1 (the observations) and PMW (the predictor). Therefore, the mean of the S1 distribution in each state is not fixed, but is instead a scalar function of PMW at each time step. This is functionally equivalent to running a linear regression of S1 on PMW where the slope coefficient is allowed to vary by Markov state. Formally, the observation model is:

$$S1_t = N(\beta_s PMW_t, \sigma_s) \tag{4}$$

Where $S1_t$ is the estimated Sentinel-1 fractional flooded area at time t, PWT_t is the passive microwave fractional flooded area at time t, and β_s and σ_s are unique constants for each hidden state s.

We chose a Gaussian observation model because it is straightforward to model one series as a linear function of another in this framework. In practice, however, the joint distribution of S1 and PMW is often non-normal (as with many climate phenomena, there is a long tail of rare extreme events), so it would be valuable to explore other link functions in future work. (Running the model in logarithms was not found to improve its fit.)

We consider a model with three hidden states for this paper. A 3×3 transition matrix describes the probability of transitioning from state i in period t-1 to state j in period t (as detailed above). The model also requires an estimate of the initial state probability at $t = 0$.

We fit the model using a Hamiltonian Monte Carlo Bayesian sampling method in the Stan statistical package (Gelman et al. 2015); full details of the Bayesian model priors are available in the appendix. This method gives us a full estimated distribution for the values of each parameter in the model: the transition probabilities, the initial state probability, and the mean and variance of the observation model at each hidden state. We keep the priors as weak as possible; the only restriction given is that the observation distribution must be bounded by [0,1] so that the predicted fractional flooded area has a sensical interpretation.

3.2 Data Fusion Method

Once we have fit the model, we can use it for retrospective prediction. The first step of prediction is to fit the likeliest hidden state path to the PMW data we have. To do this, we use the Viterbi algorithm (Forney 1973), which computes the most likely sequence of hidden states **Z*** iteratively, from the initial probability at t = 0 to the final period T:

$$Z^* = \left(\arg\max_{z1} p(S1_{1:T}) \ldots, \arg\max_{zT} p(Z_T | S1_{1:T}) \right) \tag{5}$$

We have to make one additional assumption, which is that the Viterbi path learned from PMW alone (since that is all we observe pre-2017) is a reasonable proxy for the Viterbi path in the joint model. As long as we think both sensors are picking up the same underlying weather dynamics, this is a reasonable assumption.

The second step of prediction is to simulate what the Sentinel measurement would have been at each time step, given the likeliest hidden state and the PMW observation. Since there is uncertainty in both of these steps—both in the posterior distribution of estimated parameters as well as the underlying observation distribution—it is informative to run an ensemble of predictions. Figure 6 summarizes the entire data fusion process.

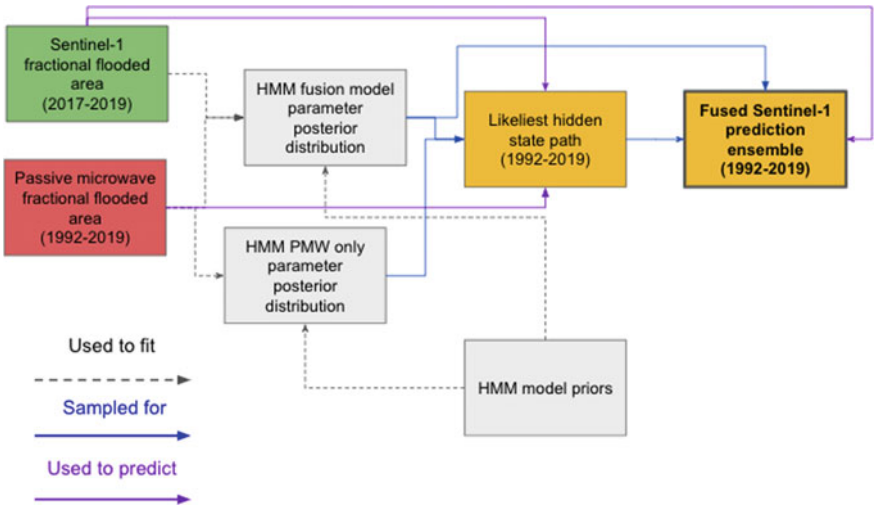

Fig. 6 Data fusion method schematic

4 Results

We fit our model separately to three administrative divisions in the north of Bangladesh—Rajshahi, Sylhet, and Rangpur. For each, we fit the model on S1 and PMW data from 2017 to 2019, then use the model to estimate fractional flooded area back to 2008, the beginning of the FFWC stream gauge record. The results shown in this section focus on Sylhet; the conclusion discusses the model's applicability to other areas.

4.1 Model Identification

The first question we can ask is whether the model parameters appear to be well-identified. In a Monte Carlo-based programme like Stan, identification is typically estimated through convergence statistics like R-hat (Gelman et al. 2015). Stan solves for the posterior distribution of model parameters by running a number of parallel simulations ("chains") starting from different points in the solution space. We would expect the chains to converge eventually if the model is well-identified. We do in fact see that in our model (Fig. 7).

Figure 8 shows the median Viterbi path (likeliest path of hidden states) as calculated from the model's posterior distribution.

Figure 8 depicts what the final simulated S1 series looks like, 2008–2019. The median of the prediction ensemble is shown in dark grey, and the 25th–75th quantile spread is shown in light grey. The actual S1 observation record is shown in green (Fig. 9).

For simplicity's sake, we will collapse the prediction distribution at each time step to its median for the subsequent evaluation steps. We consider two metrics for

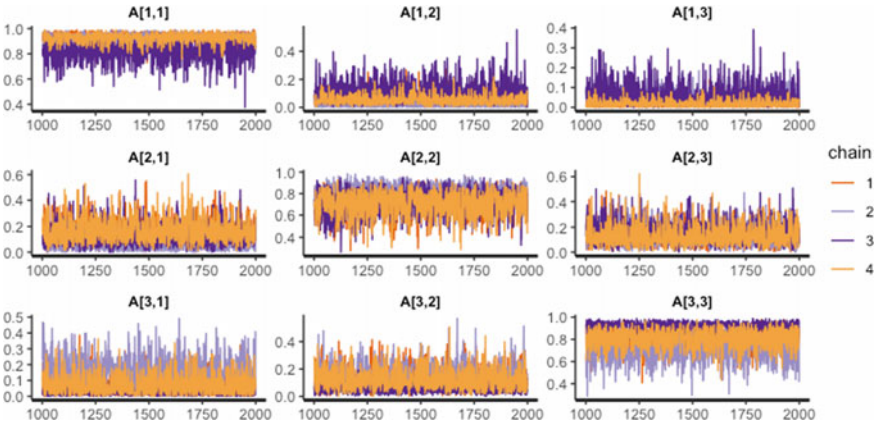

Fig. 7 Convergence graphs for HMM transition matrix parameters

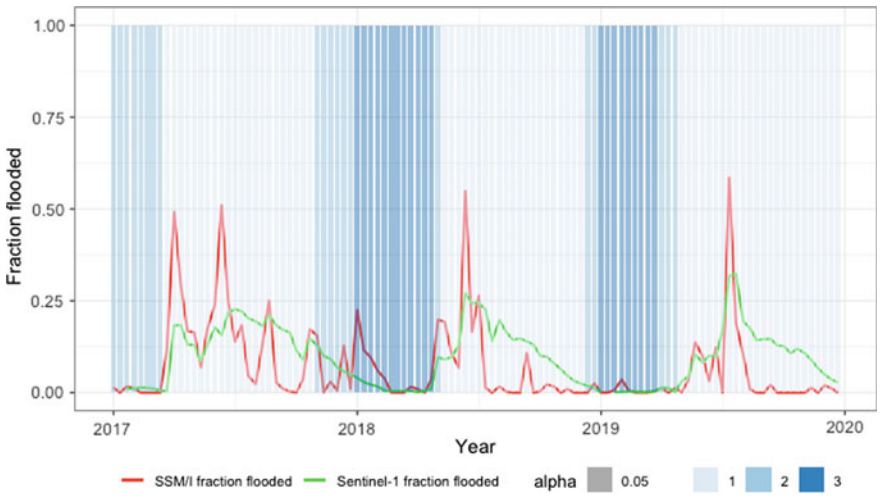

Fig. 8 Viterbi path for Sylhet superimposed on flood data

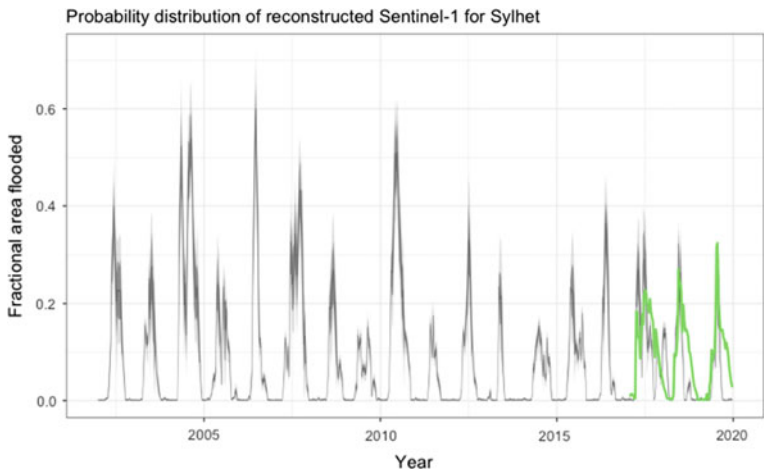

Fig. 9 Estimated Sentinel-1 probability distribution from data fusion model, Sylhet

model evaluation: Its quality of fit to the Sentinel-1 data (predictive accuracy) and its correlation with independently measured data on flood risk from stream gauges (external validity). On each of these metrics, we can compare our data fusion series against PMW, to establish that it improves on existing instruments.

Table 1 Correlation between data fusion results and observed Sentinel-1

n = 108	Data fusion model (Standard error)	SSM/I alone (Standard error)
Pearson correlation with S1	0.72 (0.10)	0.55 (0.15)
Spearman correlation with S1	0.64 (0.10)	0.45 (0.15)

4.2 Predictive Accuracy

The first evaluation step is to establish is how well-simulated S1 correlates with actual S1, shown in Table 1.

4.3 External Validity

The second evaluation step is to establish external validity; in other words, how well our simulated series correlates with independently measured sources of data on flood risk. Our external risk data comes from the FFWC dataset on directly measured water level from stream gauges, 2008–2019, described in Sect. 2. Table 2 describes these results.

Overall, we can see that our data fusion model is both an accurate (Spearman correlation of 64%) predictor of S1 and corresponds strongly (Spearman correlation of 71%) with stream gauge data in Sylhet—and that on both counts, it represents an improvement over using passive microwave alone, although this improvement is not statistically significant.

Our data fusion model did not perform as well in the other two divisions studied, Rajshahi, and Rangpur. The model is not as well-identified and the resulting predictions do not perform as well on either of our two evaluation metrics. This may be due to the time scale of the variation in the linear relationship between S1 and PMW in these areas. In Sylhet, erroneous spikes in the PMW series occur on an irregular basis and are relatively transient, lasting only 2 or 3 dekads. An HMM model with a dekadal time scale is well suited to identifying and correcting for these anomalies. In contrast, the other two divisions exhibit a relationship between S1 and PMW that is relatively constant over the season. In these cases, the HMM model struggles to

Table 2 Correlation between data fusion results and stream gauge water level

n = 288	Data fusion model (Standard error)	SSM/I alone (Standard error)
Pearson Corr. with Stream Gauge	0.51 (0.15)	0.47 (0.15)
Spearman Corr with Stream Gauge	0.71 (0.08)	0.63 (0.10)

fit the data, classifying most observations in a single state. Models that allow the relationship between the two series to vary on a quarterly or seasonal relationship may be more suited to the conditions in these areas.

5 Policy Application

The ultimate goal of this data fusion effort is to generate better data for index insurance design. One aspect of a quality index insurance data source is low basis risk—that is, that it accurately reflects the actual harvest risk from weather that claimants experience. We have already demonstrated that both the actual and simulated Sentinel-1 fractional flooded area have a stronger correlation with stream gauge data than passive microwave data alone does—and that this better correlation likely relates to the physical properties of the sensor, as described in Sect. 2 (for further discussion of this point, see Thomas et al. (in pub)).

However, another important aspect of a quality index insurance data source—and the primary motivation for this paper—is its length. Most index insurance contracts are calibrated to pay out during extreme events—for instance, 1-out-of-5-year or 1-out-of-10-year floods. Some projects estimate the magnitude of such events directly, using empirical quantiles of the data record; others use parametric methods like the extreme value distribution (Chowdhury et al. 1991). Either way, Sentinel-1's four years of data are insufficient for this purpose. Data fusion unlocks a much longer record, going back to 1992.

The following graph illustrates the information that data fusion adds in Rajshahi division—we can see that some of the biggest flood events in the modern record, such as 2007**,** lie outside Sentinel-1's record. Without such years in the record, any potential index insurance product would likely be miscalibrated against the true level of risk. Figure 10 illustrates the maximum flood extent in Sylhet in the observed Sentinel-1 data (green series) and in the fused data (grey series).

Ultimately, we expect the information from our data fusion method should make flood index insurance products both more accurately and more affordably priced.

6 Conclusion

In sum, we have demonstrated that a Hidden Markov Model applied to fractional flooded area data from the Sentinel-1 and SSM/I sensors is a promising approach for reconstructing high-quality historical flood risk information in parts of the world where there are major data gaps, like Bangladesh. The model is well-identified, yields demonstrable improvements over existing products, and has clear utility for policy applications like insurance.

Other data fusion models may be able to improve over HMM in this setting, and approaches that model variation in the functional relationship over a seasonal

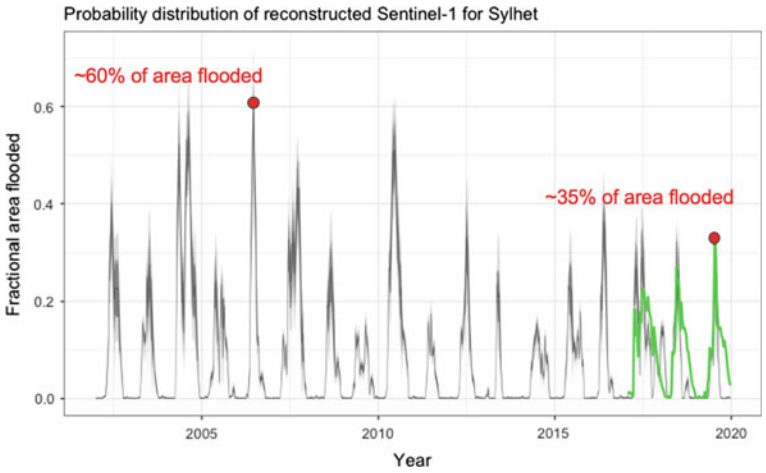

Fig. 10 Comparison of highest fractional flooded area in the Sentinel-1 observation record vs. the data fusion results

timescale—rather than 10-day periods—may be a particularly valuable direction for future work. Additionally, this paper takes the administrative division as the unit of analysis for simplicity's sake, but spatial aggregation may be better related to areas of similar climatology and hydrology—another direction for future work. Finally, as mentioned in the previous section, more work could be done to quantify the financial benefits of the reduction in uncertainty and basis risk that this model provides in an insurance setting.

As climate change portends an increase in the likelihood and severity of major floods in vulnerable countries like Bangladesh, a better understanding of the historical record is key for policymakers. Our work in this paper not only illustrates the past, but also provides the material to design better financial instruments against risk in future.

Acknowledgements Stream gauge data is provided courtesy of the Bangladesh Flood Forecasting and Warning Centre (FFWC).

This work is undertaken as part of the Columbia World Project, ACToday, Columbia University in the City of New York. ACToday funding was used to support IRI staff time and conference fees.

Model fitting was done with the Stan statistical package (https://mc-stan.org/) and Stan code adapted from Luis Damiano, Michael Weylandt and Brian Peterson's Hidden Markov Model routines (https://luisdamiano.github.io/BayesHMM).

Appendix

Bayesian Model Priors

Observation model priors:

$$\beta_s = Uniform(0, 1)$$

$$\sigma_s = Uniform(0, 1)$$

Transition model priors:

$$P_{i,j} = Dirichlet(\alpha_1 = 1, \alpha_2 = 1, \alpha_3 = 1)$$

Initial distribution priors:

$$P_0 = Dirichlet(\alpha_1 = 1, \alpha_2 = 1, \alpha_3 = 1)$$

References

Barnett, Barry, Christopher Barrett, and Jerry R. Skees. 2008. Poverty Traps and Index-Based Risk Transfer Products. *World Development* 36 (10): 1766–1785.

Bell, Andrew R., Daniel E. Osgood, Benjamin I. Cook, Kevin J. Anchukaitis, Geoffrey R. McCarney, Arthur M. Greene, Brendan M. Buckley, and Edward R. Cook. 2013. Paleoclimate Histories Improve Access and Sustainability in Index Insurance Programs. *Global Environmental Change* 23 (4): 774–781. https://doi.org/10.1016/j.gloenvcha.2013.03.003.

Bellone, Enrica, James P. Hughes, and Peter Guttorp. 2000. A Hidden Markov Model for Downscaling Synoptic Atmospheric Patterns to Precipitation Amounts. *Climate Research* 15 (1): 1–12. https://doi.org/10.3354/cr015001.

Benami, Elinor, Zhenong Jin, Michael R. Carter, Aniruddha Ghosh, Robert J. Hijmans, Andrew Hobbs, Benson Kenduiywo, and David B. Lobell. 2021. Uniting Remote Sensing, Crop Modelling and Economics for Agricultural Risk Management. *Nature Reviews Earth & Environment* 2 (2): 140–159. https://doi.org/10.1038/s43017-020-00122-y.

Brodzik, M. J., and D. G. Long. 2016. "MEaSUREs Calibrated Enhanced-Resolution Passive Microwave Daily EASE-Grid 2.0 Brightness Temperature ESDR, Version 1." NASA National Snow and Ice Data Center DAAC. https://doi.org/10.5067/MEASURES/CRYOSPHERE/NSIDC-0630.001.

Carter, Michael, Alain de Janvry, Elisabeth Sadoulet, and Alexandros Sarris. 2017. Index Insurance for Developing Country Agriculture: A Reassessment. *Annual Review of Resource Economics* 9 (1): 421–438. https://doi.org/10.1146/annurev-resource-100516-053352.

CCRIF. 2015. "The CCRIF Excess Rainfall (XSR) Model." https://www.ccrif.org/sites/default/files/publications/technical-materials/CCRIF_Excess_Rainfall_Model_2016_web.pdf.

Choudhury, Bhaskar J. 1989. "Monitoring Global Land Surface Using Nimbus-7 37 GHz Data Theory and Examples." *International Journal of Remote Sensing* 10 (10): 1579–1605. https://doi.org/10.1080/01431168908903993.

Chowdhury, Jahir, Jery Stedinger, and Li-Hsiung Lu. 1991. "Goodness-of-Fit Tests for Regional Generalized Extreme Value Flood Distributions." *Water Resources Research—WATER RESOUR RES* 27 (July): 1765–76. https://doi.org/10.1029/91WR00077.

Cooley, Sarah W., Laurence C. Smith, Leon Stepan, and Joseph Mascaro. 2017. Tracking Dynamic Northern Surface Water Changes with High-Frequency Planet CubeSat Imagery. *Remote Sensing* 9 (12): 1306. https://doi.org/10.3390/rs9121306.

DeVries, Ben, Chengquan Huang, John Armston, Wenli Huang, John W. Jones, and Megan W. Lang. 2020. "Rapid and Robust Monitoring of Flood Events Using Sentinel-1 and Landsat Data on the Google Earth Engine." *Remote Sensing of Environment* 240 (April): 111664. https://doi.org/10.1016/j.rse.2020.111664.

Fang, Bin, Venkataraman Lakshmi, Rajat Bindlish, and Thomas J. Jackson. 2018. "Downscaling of SMAP Soil Moisture Using Land Surface Temperature and Vegetation Data." *Vadose Zone Journal* 17 (1): 170198. https://doi.org/10.2136/vzj2017.11.0198.

Feng, Dongmei, Colin J. Gleason, Xiao Yang, and Tamlin M. Pavelsky. 2019. Comparing Discharge Estimates Made via the BAM Algorithm in High-Order Arctic Rivers Derived Solely From Optical CubeSat, Landsat, and Sentinel-2 Data. *Water Resources Research* 55 (9): 7753–7771. https://doi.org/10.1029/2019WR025599.

Forney, G.D. 1973. The Viterbi Algorithm. *Proceedings of the IEEE* 61 (3): 268–278. https://doi.org/10.1109/PROC.1973.9030.

Galantowicz, J. 2002. High-Resolution Flood Mapping from Low-Resolution Passive Microwave Data. *IEEE International Geoscience and Remote Sensing Symposium.* https://doi.org/10.1109/IGARSS.2002.1026161.

Gelman, Andrew, Daniel Lee, and Jiqiang Guo. 2015. Stan: A Probabilistic Programming Language for Bayesian Inference and Optimization. *Journal of Educational and Behavioral Statistics* 40 (5): 530–543. https://doi.org/10.3102/1076998615606113.

De Groeve, Tom. 2010. Flood Monitoring and Mapping Using Passive Microwave Remote Sensing in Namibia. *Geomatics, Natural Hazards and Risk* 1 (1): 19–35. https://doi.org/10.1080/19475701003648085.

Hughes, J.P., P. Guttorp, and S.P. Charles. 1999. A Non-Homogeneous Hidden Markov Model for Precipitation Occurrence. *Journal of the Royal Statistical Society: Series C (applied Statistics)* 48 (1): 15–30. https://doi.org/10.1111/1467-9876.00136.

ICCAD. 2013. "Weather Index Insurance: Lessons Learned and Best Practices for Bangladesh." http://icccad.net/wp-content/uploads/2015/12/Weather-Index-Insurance-lessons-and-best-practices.pdf.

Ji, Luyan, Peng Gong, Jie Wang, Jiancheng Shi, and Zhiliang Zhu. 2018. Construction of the 500-m Resolution Daily Global Surface Water Change Database (2001–2016). *Water Resources Research* 54 (12): 10270–10292. https://doi.org/10.1029/2018WR023060.

Jones, John W. 2019. Improved Automated Detection of Subpixel-Scale Inundation—Revised Dynamic Surface Water Extent (DSWE) Partial Surface Water Tests. *Remote Sensing* 11 (4): 374. https://doi.org/10.3390/rs11040374.

Mirza, Monirul. 2002. Global Warming and Changes in the Probability of Occurrence of Floods in Bangladesh and Implications. *Global Environmental Change* 12 (July): 127–138. https://doi.org/10.1016/S0959-3780(02)00002-X.

Osgood, Daniel, Bristol Powell, Rahel Diro, Carlos Farah, Markus Enenkel, Molly E. Brown, S. Greg Husak, Lucille Blakeley, Laura Hoffman, and Jessica L. McCarty. 2018. Farmer Perception, Recollection, and Remote Sensing in Weather Index Insurance: An Ethiopia Case Study. *Remote Sensing* 10 (12): 1887. https://doi.org/10.3390/rs10121887.

Osgood, Daniel, and Kenneth E. Shirley. 2012. "The Value of Information in Index Insurance for Farmers in Africa." In *The Value of Information: Methodological Frontiers and New Applications*

in Environment and Health, edited by Ramanan Laxminarayan and Molly K. Macauley, 1–18. Dordrecht: Springer Netherlands. https://doi.org/10.1007/978-94-007-4839-2_1.

Pekel, Jean-François., Andrew Cottam, Noel Gorelick, and Alan S. Belward. 2016. High-Resolution Mapping of Global Surface Water and Its Long-Term Changes. *Nature* 540 (7633): 418–422. https://doi.org/10.1038/nature20584.

RMS. 2017. "RMS—Executive Summary." RMS. https://forms2.rms.com/DFID-Executive-Summary.html.

Robertson, Andrew, Sergey Kirshner, and Padhraic Smyth. 2003. "Hidden Markov Models for Modeling Daily Rainfall Occurrence over Brazil," December.

Sabaghy, Sabah, Jeffrey P. Walker, Luigi J. Renzullo, and Thomas J. Jackson. 2018. Spatially Enhanced Passive Microwave Derived Soil Moisture: Capabilities and Opportunities. *Remote Sensing of Environment* 209 (May): 551–580. https://doi.org/10.1016/j.rse.2018.02.065.

Scheel, M. L. M., M. Rohrer, Ch. Huggel, D. Santos Villar, E. Silvestre, and G. J. Huffman. 2011. "Evaluation of TRMM Multi-Satellite Precipitation Analysis (TMPA) Performance in the Central Andes Region and Its Dependency on Spatial and Temporal Resolution." *Hydrology and Earth System Sciences* 15 (8): 2649–2663. https://doi.org/10.5194/hess-15-2649-2011.

Tangdamrongsub, Natthachet, Chalita Forgotson, Chandana Gangodagamage, and Joshua Forgotson. 2021. The Analysis of Using Satellite Soil Moisture Observations for Flood Detection, Evaluating over the Thailand's Great Flood of 2011. *Natural Hazards.* https://doi.org/10.1007/s11069-021-04804-8.

Tellman, Beth, Upmanu Lall, Pierre Gentine, and Venkat Lakshmi. 2021. "Mapping Flood Impacts Using Multi-Sensor Satellite Data Fusion in Urban Areas." NASA Terrestrial Hydrology.

Tellman, Beth, Cody Schank, Bessie Schwarz, Peter D. Howe, and Alex de Sherbinin. 2020. Using Disaster Outcomes to Validate Components of Social Vulnerability to Floods: Flood Deaths and Property Damage across the USA. *Sustainability* 12 (15): 6006. https://doi.org/10.3390/su12156006.

Thomas, Mitchell, Elizabeth Tellman, Ben DeVries, Akm Saiful Islam, Michael Steckler, Max Goodman, and Maruf Billah. in pub. "A Sentinel-1 Inundation Time Series Algorithm for Flood Index Insurance Applications in Bangladesh."

ULABY, F. T. 1982. "Microwave Remote Sensing Active and Passive." *Rader Remote Sensing and Surface Scattering and Emission Theory* II: 848–902.

UNISDR. 2015. "The Human Cost of Weather-Related Disasters 1995–2015." https://www.undrr.org/publication/human-cost-weather-related-disasters-1995-2015.

United News of Bangladesh. 2020. "WFP, Oxfam, Green Delta Insurance Join Hands to Protect Labourers," 2020. https://www.unb.com.bd/category/Bangladesh/wfp-oxfam-green-delta-insurance-join-hands-to-protect-labourers/55503.

Winsemius, Hessel C., Brenden Jongman, Ted I. E. Veldkamp, Stephane Hallegatte, Mook Bangalore, and Philip J. Ward. 2018. Disaster Risk, Climate Change, and Poverty: Assessing the Global Exposure of Poor People to Floods and Droughts. *Environment and Development Economics* 23 (3): 328–348. https://doi.org/10.1017/S1355770X17000444.

Xie, Miao, Zhe Jiang, and Arpan Man Sainju. 2018. "Geographical Hidden Markov Tree for Flood Extent Mapping." In *Proceedings of the 24th ACM SIGKDD International Conference on Knowledge Discovery & Data Mining*, 2545–54. KDD '18. New York, NY, USA: Association for Computing Machinery. https://doi.org/10.1145/3219819.3220053.

Zeng, Ziyue, Yanjun Gan, Albert J. Kettner, Qing Yang, Chao Zeng, G. Robert Brakenridge, and Yang Hong. 2020. "Towards High Resolution Flood Monitoring: An Integrated Methodology Using Passive Microwave Brightness Temperatures and Sentinel Synthetic Aperture Radar Imagery." *Journal of Hydrology* 582 (March): 124377. https://doi.org/10.1016/j.jhydrol.2019.124377.

Rivers, Coasts and Estuaries

Impact of Coriolis Force on the Flow Field and Sedimentation in Ideally Shaped Tidal Basins

Nazeat Ameen Iqra, Mohammad Asad Hussain, and M. Shah Alam Khan

Abstract Tidal basins under the Tidal River Management projects in Bangladesh exhibit complex morphological patterns consisting of substantial spatial and temporal variability of sedimentation. Sedimentation in the tidal basin is controlled by various physical and hydraulic factors. Therefore, it is indispensable to understand the dominant factors behind these morphological patterns. Flow field and sedimentation pattern in Pakhimara Beel (tidal basin), located in southwestern Bangladesh, are being investigated under the present study. Large-length scales of the beel, shallow water depth, and low depth-averaged velocity created by the hydraulic gradient of sediment-laden flows lead to Rossby number (defined as $\mathrm{Ro} = U/fL$) < 1, making the system susceptible to the effect of Coriolis force. This condition alters the flow field and, thereby, the sedimentation pattern. Four ideally shaped computation domains with varying depth, inlet channel location, and orientation have been investigated through the Delft3D model. The results indicate that, for all domains, the flow velocity is deflected towards the right in the northern hemisphere due to Coriolis effect. It is found that at large peripheral areas of the beel with substantially low flow velocity, the circulations are influenced by Coriolis force, and higher sediment deposition occurs for higher latitudes. The results imply that the deposition patterns in large tidal basins are significantly influenced by Coriolis effect.

Keywords Five Coriolis effect · Rossby number · Tidal River Management (TRM) · Tidal basins · Delft3D

1 Introduction

The Ganges–Brahmaputra-Meghna (GBM) river system carries more than a billion tons of sediments every year (Gain et al. 2017). Along with the Bay of Bengal, the coastal zone of Bangladesh is geomorphologically and hydrologically dominated by the GBM system (Ahmad 2019). Although the land subsidence rate of this region

N. A. Iqra (✉) · M. A. Hussain · M. S. A. Khan
Institute of Water and Flood Management, Bangladesh University of Engineering and Technology, Dhaka, Bangladesh

© The Author(s), under exclusive license to Springer Nature Switzerland AG 2022

G. M. Tarekul Islam et al. (eds.), *Water Management: A View from Multidisciplinary Perspectives*,
https://doi.org/10.1007/978-3-030-95722-3_11

is 2–3 mm/year, it is compensated by the large sediment supply (Nicholls et al. 2016). Excluding the Sundarbans mangrove ecosystem, larger part of the southwest coastal zone of Bangladesh is highly diverse and dynamic (Brammer 2014; Gain et al. 2017), characterized by an agro-ecological system with extensive tidal rivers, streams, and tidal basins (Mutahara et al. 2017), and has a potential impact of a rising sea level due to global warming (Brammer 2014). Since the 1960s, coastal polders (earthen embankments) have been constructed in the southwest region of the country, to provide protection from floods and to increase agricultural production (Gain et al. 2017). However, because of the interruption of natural tidal flow to the tidal floodplains, siltation has taken place in the adjacent tidal rivers, causing prolonged waterlogging and drainage congestion in the coastal polders (Rashid et al. 2013). As a result, further sediment accretion process is interrupted, and these polders have lost 1–1.5 m of elevation with respect to mean water level (Auerbach et al. 2015). To address these complex problems, a temporary restoration of controlled tidal flooding in polders was introduced conceptually as Tidal River Management (TRM) (van Staveren et al. 2014). TRM has been considered as an effective approach for sustainably managing the southwest coastal area (Nowreen et al. 2014). The temporary floodplains inundation process involves: (i) restoring tidal flooding (twice-daily) by means of temporary and partial removal of embankments (or polders); (ii) scouring the adjacent river bed; and (iii) depositing sediments within the tidal basins (the lowest parts of the polders) (van Staveren et al. 2017). Generally, it has been seen that at the beginning of the operation, the sedimentation was relatively low. Sediment deposition occurred during the monsoon season compared to the dry season. Sediment deposition was higher close to the opening of the tidal basin and decreased gradually to the furthest end of the tidal basins. This uneven sedimentation inside tidal basins hinders the main purpose of TRM and ultimately created drainage congestion. To tackle the problem, appropriate measures such as compartmentalization or rotation of openings were required (Gain et al. 2017).

The concept of restoring controlled tidal flooding in basins is inspired by the projects of the Dutch delta (Islam et al. 2020), involving the lowering or complete removal of embankment sections, subsequently restoring tidal flood dynamics. But the significant difference in the dynamic sediment deposition patterns needs to be adequately understood (van Staveren et al. 2017). Understanding the behaviour of the tides that cause fluctuating water levels and the in and outflow of water; water facilitating the movement of suspended sediment is highly recommended by van Staveren et al. (2017). In order to achieve the goals of TRM and the effective sediment accumulation process, many studies have been conducted from Bangladesh's perspective. Amir et al. (2013) modelled a concept of compartmentalization of the tidal basin with embankments and observed that the sedimentation spreads uniformly after gradual removal of embankments along the connecting river. Islam et al. (2020) and Talchabhadel et al. (2018) used multiple inlets and flow regulation in their numerical model to achieve uniform sediment spreading. Also, the relation of inlet cross-sectional area and tidal volume, which directly indicates the amount of sediment load, was observed by Shampa and Pramanik (2012) numerically and Talchabhadel et al. (2017) experimentally.

The small depth-average velocity in most parts of the beel, created by the hydraulic gradient of sediment-laden flows from inlet channels, and large-length scales of the beels make the influence of Earth's rotational effect, e.g. the Coriolis effect important on the flow field and sedimentation pattern (Wells 2007, 2009) in these artificially compounded water bodies. Wells (2009) used analogue laboratory experiments to study the influence of Coriolis forces upon the depositional patterns of turbidity currents. His results showed that when the density of the sediment-laden flow was kept constant with increasing rotation rates (e.g. latitudes) the length scale decreases, which means a systematic reduction in the radius within which most of the particles are deposited. In other words, the Rossby radius of deformation determines the deposition patterns. Ahn et al. (2016) investigated the influence of Coriolis force on upstream water flows and showed that the 'Rossby number' decreases with the increase of latitude, keeping inflow velocity and approach length constant (except at the equator where Rossby becomes infinity). The scale at which Coriolis forces become important is best expressed by the Rossby number, defined as $\mathrm{Ro} = U/fL$, where U is a depth-averaged velocity, L the length scale and the Coriolis frequency, f, is characterized by $f = 2\mathrm{w}\sin\theta$, where w is the earth's rotation speed (can be assumed to be a constant of 7.292×10^{-5} rad/s) and θ is the latitude. Coriolis forces will become significant when $\mathrm{Ro} < 1$ (Wells 2009; Cossu et al. 2010). When $\mathrm{Ro} < 1$ Coriolis forces will result in a significant deflection of the turbidity current to the right in the Northern hemisphere (Wells 2009). Cossu et al. (2010) observed that in the northern hemisphere, the right-hand channel levee being noticeably higher than the left-hand levee, which indicates the effect of Coriolis forces upon turbidity currents. The influence of Coriolis in sediment deposition patterns is recognized by many authors such as Unger and Nemeth (2013). The authors used remote sensing techniques to estimate the effect of Coriolis force for the Tisza River and found the right bank is higher than the left bank, and the westward shifting of the river is due to the impact of Coriolis force. Huijts et al. (2006, 2009) also showed the rightward deflection of sedimentation influenced by Coriolis force. So, the impacts of Coriolis force on sedimentation focusing on controlled flooding as in the case of TRM projects may be an important factor to study the sedimentation patterns inside the beels.

The present study intends to focus on the extent of Coriolis force influencing the sedimentation process through numerical experiments in idealized model domains. Idealized models can be a handy tool for studying the influence of various dynamic factors, keeping the geometry of the channel and other parts of the domain simple (Maskell et al. 2014). From previous studies, idealized models have been used to simulate lateral estuarine circulation and the implications for sediment transport and estuary morphology (Chen and Sanford 2009a), the vertical estuarine structure and salt transport (Chen and Sanford 2009b), the flood and ebb dominance of sediment transport (Robins 2008), the dependency of tides and storm surge on cannel depth (Familkhalili and Talke 2016). Among very few idealized model-based researches for the assessment of TRM in Bangladesh, a numerical model for solving drainage congestion (Shampa and Pramanik 2012) and the influence of inlet cross-section on sedimentation (Talchabhadel et al. 2017) can be found. In the present study, the effect of the Coriolis force on sediment accumulation is investigated under the

different latitudes conditions, and also the sediment deposition characteristics have been discussed for selected geometric features of these idealized domains.

2 Study Area

Since 1997, the polders in the southwest region of Bangladesh have been subject to TRM. After that, many tidal basins went through the TRM operation. Till now, the timeline of the TRM operation for the different tidal basins (beel) is shown in Table 1 (Talchabhadel et al. 2016).

The study area is Pakhimara Beel (tidal basin), located in the Khulna division of the southwest (SW) region (Fig. 1). It lies between 22°41′45″N, 89°13′33″E and 22°39′34″N, 89°15′17″E and covers 7 km^2 (Gain et al. 2017) having an average slope of 0.2%. For the TRM project operation, the adjacent Kobadak River is connected to the beel through a man-made link canal of 1.5 km length and 40 m maximum bottom width at −1.1 m PWD (the datum for the Public Works Department of Bangladesh with the zero datum at 0.46 m below MSL is called PWD). The flow and transport processes of the beel are dominated by tidal dynamics as there is no regulated gate to control the flow from the river through the canal. The average tidal ranges during pre-monsoon, monsoon, and dry seasons are 2.4 m, 1.5 m, and 2 m, respectively. On average, the measured Suspended Solid Concentration (SSC) at Balia on Kobadak River is 0.84 kg/m^3, 0.58 kg/m^3, 0.37 kg/m^3, respectively, during pre-monsoon, monsoon, and dry season (Islam et al. 2020). Cohesive particles dominate the suspended sediments as the median grain size is 64 μm. Maximum sediment concentration was found during April.

Before TRM, the beel had a mean elevation of 0.57 m PWD. After 1.5 years, a survey was conducted to assess the sediment deposition progress inside the beel. The mean elevation was found to be 1.17 m PWD. Though the land level increased due to sediment deposition, a significantly uneven distribution of sediments was found. Sediments mostly deposited close to the inlet mouth, and the elevation at the peripheral portions of the beel remained unchanged (Islam et al. 2020).

Table 1 The timeline of the TRM in Bangladesh

	1997	1998	1999	2000	2001	2002	2003	2004	2005	2006	2007	2008	2009	2010	2011	2012	2013	2014	2015	2016	2017	2018	2019	2020	2021
Beel Bhaina																									
Beel Kedaria																									
Beel Khuksia																									
Beel Kapalia																									
Beel Pakhimara*																									

*The study area

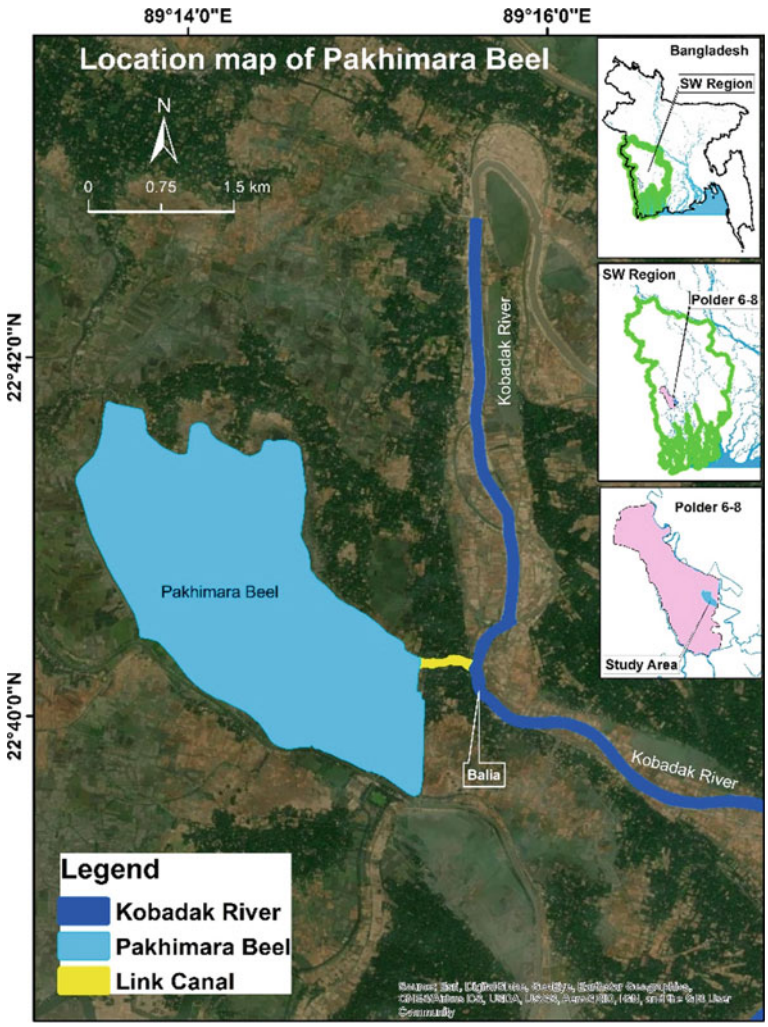

Fig. 1 Map of the study area

3 Methodology

A depth-averaged two-dimensional Delft3D numerical model has been configured with idealized geometry and boundary conditions which are derived from the field conditions. Delft3D-Flow (Delft3D-FLOW 2011) model is a multidimensional (2D or 3D) open-source hydrodynamic and sediment transport model solving the unsteady shallow water equations. It is a computational tool for coastal, river, and estuarine areas which can simulate flow, sediment transport, wave, and morphological developments. A rectangular grid (Cartesian frame of reference) is considered as a simplified

form of a curvilinear grid. The total number of grid cells in the computation domain is 61468. The size of grid cells is smaller in the river and connecting channel, and the size of grid cells increases inside the beel. The surface area of the grid cells varies from 24 m^2 to 660 m^2. From the measured water level data in the study area, it is found that the tidal range in the Kobadak River is 2.6 m. A sinusoidal tidal water level variation (ignoring tidal asymmetry) is used as downstream boundary keeping tidal range 2.6 m resembling the study area. Keeping similarity with observed data, relatively low river discharge (varying from 25 ~ 70 m^3/s) is used as an upstream boundary as the model is simulated for 30 days of the dry period. The applied water level and discharge data for 24 h at the model boundary are shown in Fig. 2.

For the model domain, an idealized bathymetry is used, keeping the maximum depth of 3.5 m for the beel. The maximum depth of the canal and the river is 3.5 m and the width are 30 m and 50 m, respectively. The sediment size of the coastal rivers was studied by Mahiuddin (2017) and they found that silt content in the suspended sediment is more than 50% and sand content ranged from 16 to 24%, while clay content ranged from 18 to 23%. For the present study, sand is considered to be 24% as non-cohesive soil, and silt and clay to be 76% as cohesive soil. Suspended sediment concentration (=0.84 kg/m^3) (Islam et al. 2020) is divided into this same percentage for the present research. The applied median sediment diameter, d_{50} is equal to 64 μm. The critical bed shear stress of the model for sedimentation and erosion is 1000 N/m^2 and 0.01 N/m^2, respectively. The manning roughness coefficient 0.03 $s/m^{1/3}$ was used for this model study.

In the present research, several ideally shaped domains are constructed resembling the study area to investigate the impact of beel geometry on flow field and sedimentation (Fig. 3). To understand the impact on the flow field and sedimentation, the model domains were run for two latitudes: 22.7° N and 0° N. Four ideally shaped computation domains with varying orientation and depth have been subjected to the investigation (Fig. 3). Scenario (i) is a rectangular-shaped domain with a constant

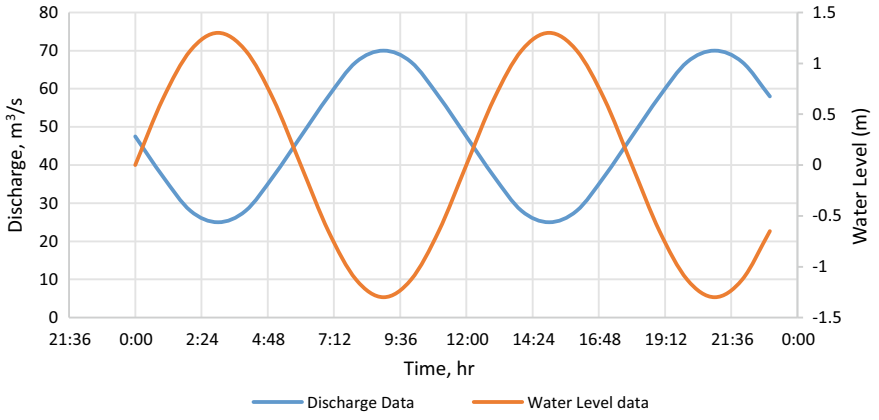

Fig. 2 The model upstream boundary discharge and downstream boundary tidal water level data

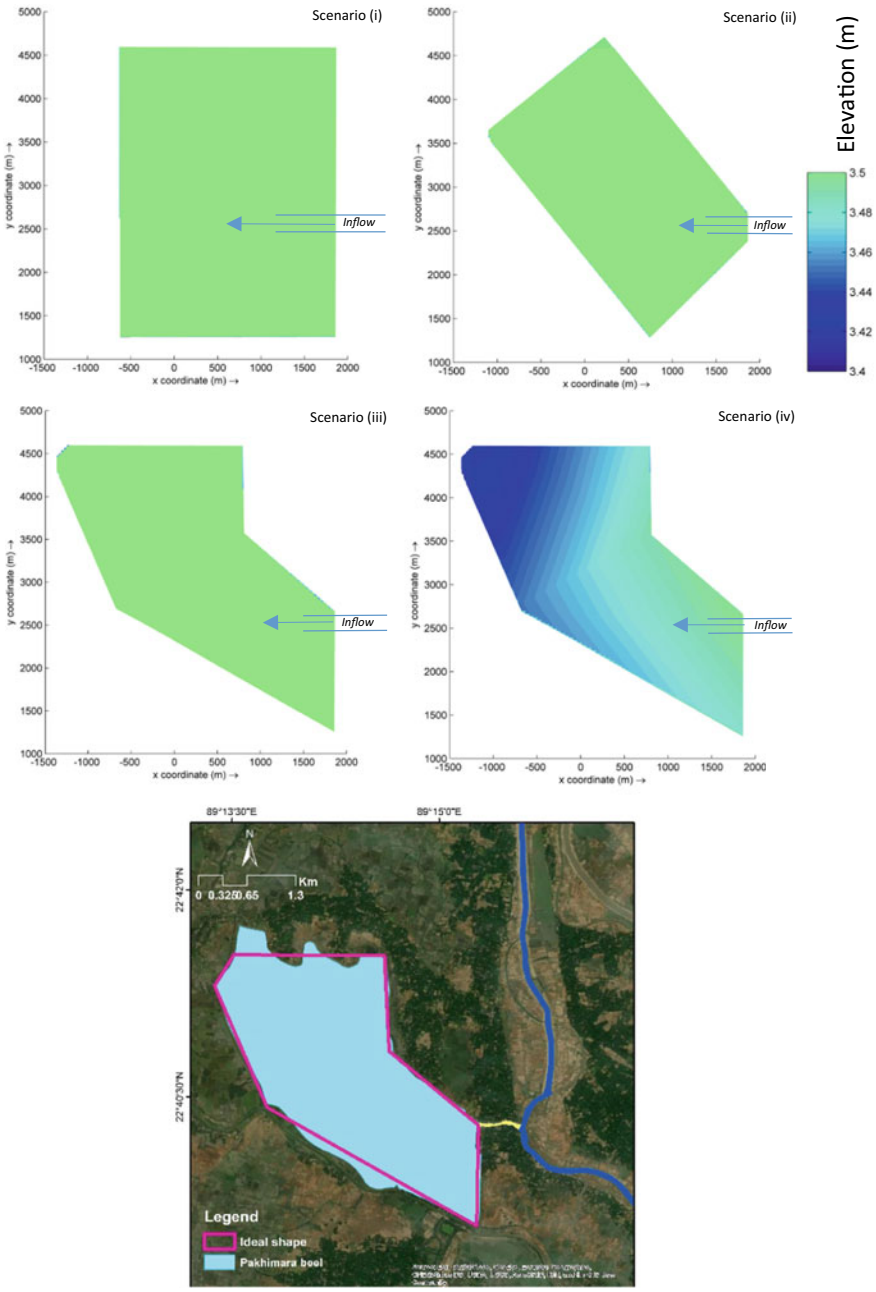

Fig. 3 Four scenarios of the idealized shaped domains

depth of 3.5 m; Scenario (ii) is the same domain tilted towards the left forming the similar orientation of the study area keeping the previous depth; Scenarios (iii) and (iv) the model domains are further extended towards north connected with the titled domain of Scenario (ii). The domain for Scenario (iii) has a constant depth while that for Scenario (iv) partially consists of a sloped bottom. Due to the unavailability of the detailed bathymetry of the study area, the concept of an ideal-shaped domain is used. Also, the main objective of the study is to identify the influence of the physical factors such as Coriolis force on the sediment deposition in the beel. Therefore, the ideal-shaped domain has been experimented numerically. Although the Scenarios (iii) and (iv) ideally represent the actual beel, before analysing them, the simpler shape in Scenarios (i) and (ii) was considered. The concept of sequential change of domains is found to be helpful to identify the sedimentation in terms of shape, orientation, and bathymetry. Also, for all the scenarios and in both latitudes, the model parameters including boundary conditions and physical parameters are kept the same only to focus on the impact of Coriolis force.

4 Results and discussion

4.1 Testing the Coriolis Effect in the Study Area

At first, to examine whether the flow field of the beel in the study area (at 22.7° N latitude) is influenced by the Coriolis effect, the Rossby number (Ro) is calculated for a range of depth-average velocities and beel sizes (representing length scales). Table 2 shows the calculated Rossby numbers at 22.7° N latitude for depth-average velocities 1 ~ 20 cm/s and length scales of 0.5 ~ 5 km. Values with Ro < 1 are shaded in the table. Calculated values show that for a length scale of 2 km, Rossby numbers Ro remain less than unity for depth-average velocity of up to 10 cm/sec.

As already mentioned, whether the Coriolis force should be taken into account or not depends on the Rossby number to be equal or less than 1. Rossby number (Ro $= U/fL$) is dependent on the flow velocity, Coriolis frequency, and length. In Table 2, it is shown that the Rossby number varies with velocity and beel size at a fixed latitude. We assume our domain is under Coriolis influence. So, the max value of

Table 2 Changes of Rossby number with depth-average velocity and length scale at a given latitude

Depth average velocity (cm/s)	Beel size (km)									
	0.5	1	1.5	2	2.5	3	3.5	4	4.5	5
1	0.36	0.18	0.12	0.09	0.07	0.06	0.05	0.04	0.04	0.04
2	0.71	0.36	0.24	0.18	0.14	0.12	0.10	0.09	0.08	0.07
5	1.78	0.89	0.59	0.44	0.36	0.30	0.25	0.22	0.20	0.18
10	3.55	1.78	1.18	0.89	0.71	0.59	0.51	0.44	0.39	0.36
15	5.33	2.66	1.78	1.33	1.07	0.89	0.76	0.67	0.59	0.53
20	7.10	3.55	2.37	1.78	1.42	1.18	1.01	0.89	0.79	0.71

Rossby number, Ro has to be equal to one. At a certain latitude when Ro = 1, from Rossby formula, we get that the length of influence is proportional to the velocity ($L \sim U$). Based on this concept, the length scale (L) is measured for each scenario. The velocity will decrease as the flow spreads across the domain. At the mouth of the basin, the flow velocity will be high but the velocity will drop tremendously after crossing a certain distance from the mouth of the canal.

Figure 4 shows the length scale of influence calculated for each domain keeping latitude at 22.7 degrees. Figure 4 shows that for Scenario (i), after 1300 m, the Coriolis force should be taken into account. For Scenario (ii), the value is 1200 m, and for Scenario (iii) and Scenario (iv), the value is 1000 m which means that if the domain is bigger, the Coriolis influence zone is larger. So, at the mouth of the link canal, the inertia force dominates the flow and Coriolis force can be neglected. And after a certain distance, the Coriolis force also contributes to the flow field and thereby sediment distribution.

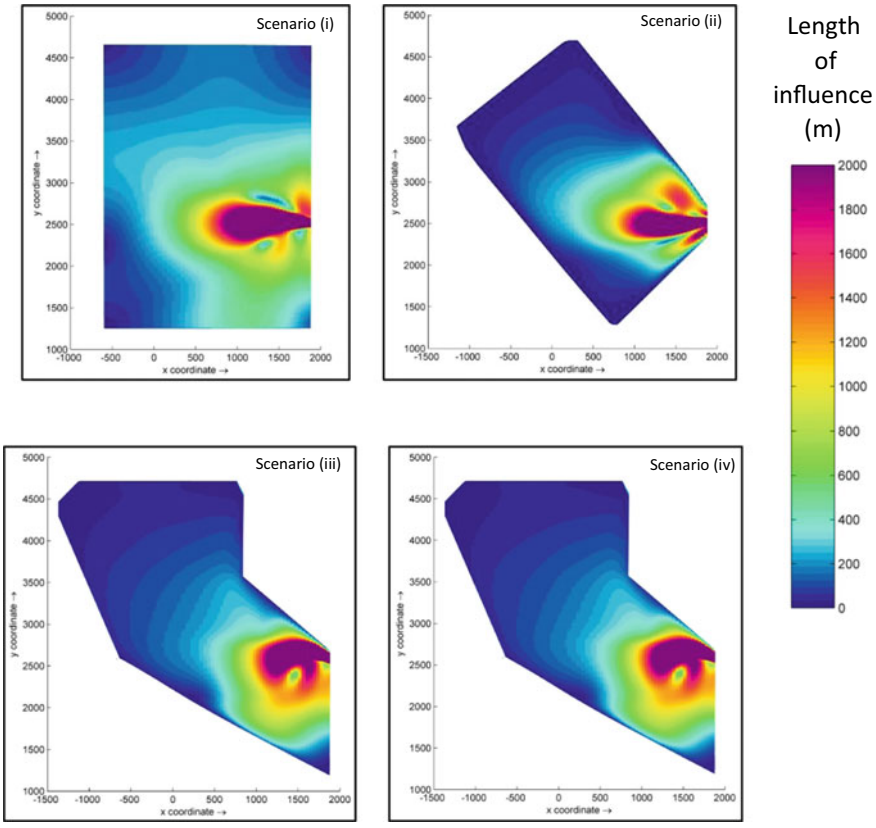

Fig. 4 The length scale variation for the four scenarios

5 Results from Numerical Experiments

For all the numerical experiments performed during the present study, the forcing factors like downstream tidal water level, upstream river discharge, and friction factors were kept constant. This ensures that when the latitude is altered i.e. the Coriolis coefficient is changed, the modified flow field and thereby the change in sedimentation are only caused by the Coriolis force. We anticipate that the change in the flow field and sedimentation caused by the change in Coriolis force will be very small but in field conditions, it may play an important role in combination with all other forcing factors.

At first, spatial distribution of depth-average velocities during peak flood for the four computation domains are presented in Fig. 5, where the left panel shows the depth-average velocities at 0° latitude and the right panel shows the same for 22.7° latitude.

From Fig. 5, it is evident that at the mouth of the link canal, jet-flow with flow separation phenomenon appears due to high inertia force for all the domains at both latitudes. But at locations \away from the mouth of the link canal depth, average flow velocities are less than 10 cm/s even during peak flood periods. So, it can be expected that the flow field in the areas away from the mouth of the link canal is influenced by the Coriolis force. From the same figure, with the change of beels' orientation and depth, the change in spatial extent of the zone where the influence of Coriolis force is expected to be significant can be clearly identified. For Scenarios (i) and (ii), the shape of the jet-flow area appears to be elliptical shape, whereas for Scenarios (iii) and (iv), they are circular. This is same for both the latitudes. But the spatial distribution for depth-average velocities at the peripheral areas show some difference between 0° latitude (left panel) and 22.7° latitude (right panel). This difference must be due to the impact of the Coriolis effect as the other forcing forces have been kept constant. To observe the difference in depth-average velocities in the peripheral areas, cross-sections across the peripheral areas are plotted. Figure 6 shows the cross-sectional view of the depth-average velocities for four scenarios comparing the two latitudes.

The difference in depth-average velocities in the peripheral areas are clearly visible from the cross-sectional profiles (for the northern part, 1500 m away, and for the southern part, 1200 m away from the mouth of the canal) of Fig. 6. Especially for Scenarios (iii) and (iv), it is clear that at higher latitude, depth-average velocity is higher and the difference is prominent in the northern part. This phenomenon might be due to the fact that the flow entering into the beel through the link canal is being deflected towards the right by the Coriolis force. As a result, at higher latitude where the Coriolis effect is larger, the depth-average velocity becomes significantly higher in the northern part.

Next, the spatial variation of accumulated sedimentation after 30 days of model runs for Scenarios (i), (ii), (iii), and (iv) at 0° latitude (left panel) and 22.7° latitude (right panel). Similar to the flow field, it is evident that at the mouth of the link canal, significant accumulation of sediment occurs for all the domains at both latitudes.

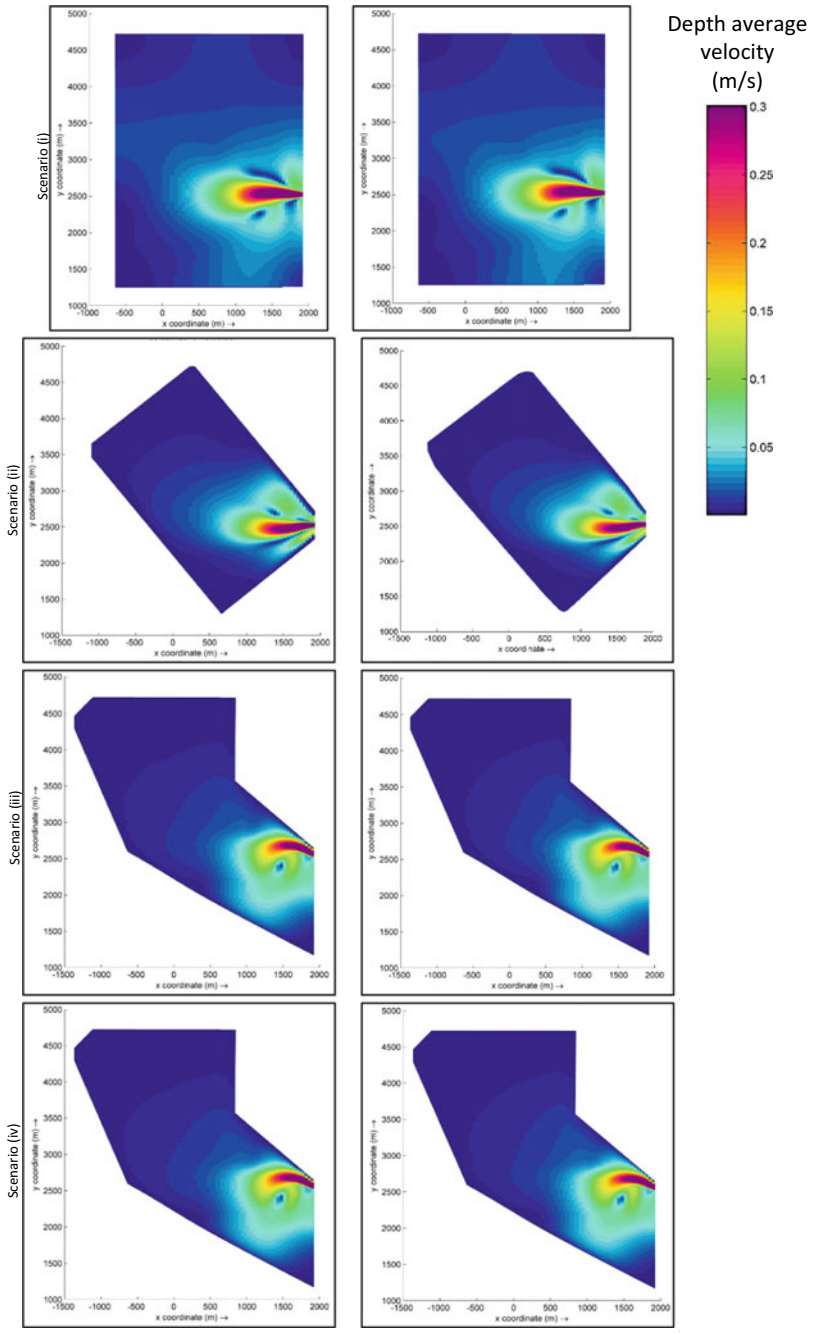

Fig. 5 Spatial distribution of depth-average velocities during peak flood for Scenarios (i), (ii), (iii), and (iv) at 0° latitude (*left panel*) and 22.7° latitude (*right panel*)

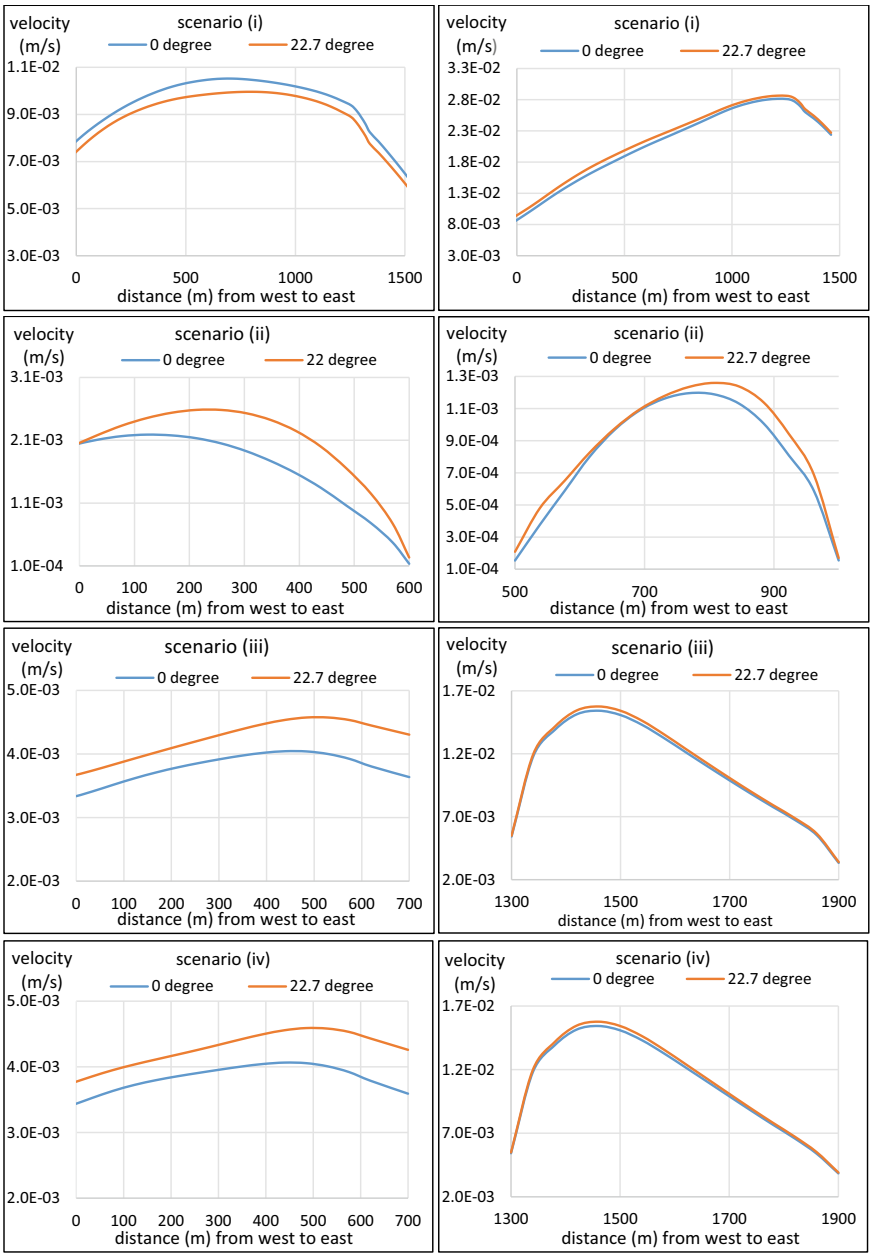

Fig. 6 Cross-sectional profiles of depth-average velocities for two latitudes at the northern part (*left panel*) and southern part (*right panel*)

But at locations away from the mouth of the link canal, amount of sedimentation is very small even after the same time durations. The flow field in these areas which is away from the mouth of the link canal is influenced by the Coriolis force. The spatial distribution for sedimentation at the peripheral areas shows some difference between 0° latitude (left panel) and 22.7° latitude (right panel).

Next, the spatial distribution of sedimentation of the four domains and cross-sectional profiles for sedimentation at the northern and southern peripheral areas of the domains are plotted to observe the difference in sedimentation due to the change in latitude. Figure 7 shows the spatial distribution and Figure 8 shows the cross-sectional view of the sedimentation for four scenarios comparing the two latitudes. The significant difference of sediment deposition at two latitudes cannot be identified from the spatial map in Fig. 7. However, uneven sediment distribution in the domains is noticeable. Also, along the domain peripheral, it is evident that the sediment accumulation varies with the depth variation. Such as for Scenario (iv), along the southwest peripheral, the deposition is lower than for Scenario (iii).

The difference in sedimentation in the northern peripheral areas is clearly visible from the cross-sectional profiles of Fig. 8 (northern part). It is clear that at higher latitude, sedimentation is higher at the northern parts of the beels. Like depth-average velocity distributions, this phenomenon again might be due to the fact that the flow entering into the beel through the link canal is being deflected towards the right by the Coriolis force, and as a result, higher sediment is being deposited in the northern peripheral areas of the beels. So, at higher latitude where the Coriolis effect is larger, sedimentation becomes significantly higher in the northern part.

According to (Wells 2009), for higher latitude, one will expect a smaller radius of sedimentation and a higher deflection of sedimentation towards the right. Thus, with the increase of latitude, the deposition decreases at a certain radius and increases towards the right. From Fig. 8 (southern part), it can be seen that for 0°, the deposition is higher than 22.7°. This indicates that the radius of sedimentation decreases with increasing latitude. This is because at a lower latitude, due to smaller particle size, the settling velocity increases. This makes the turbidity current weaker and sediment spreads in more area. The d_{50} of the sediment particle is 64 μm with a settling velocity of 0.0025 m/s, which is small enough to keep the sediment in suspension, making the flow velocity slower to spread more under the influence of earth rotation. Also, in Fig. 8 (southern part) for Scenario (i), the deposition increases from west to east, whereas for Scenarios (ii), (iii), and (iv), the deposition decreases. This is due to the orientation of the domains of Scenarios (ii), (iii), (iv) such that the flow deflecting towards the right carrying most of the sediment. As a result, the deposition in the southeast part of the domains of Scenarios (ii), (iii), and (iv) is lower than in the southwest.

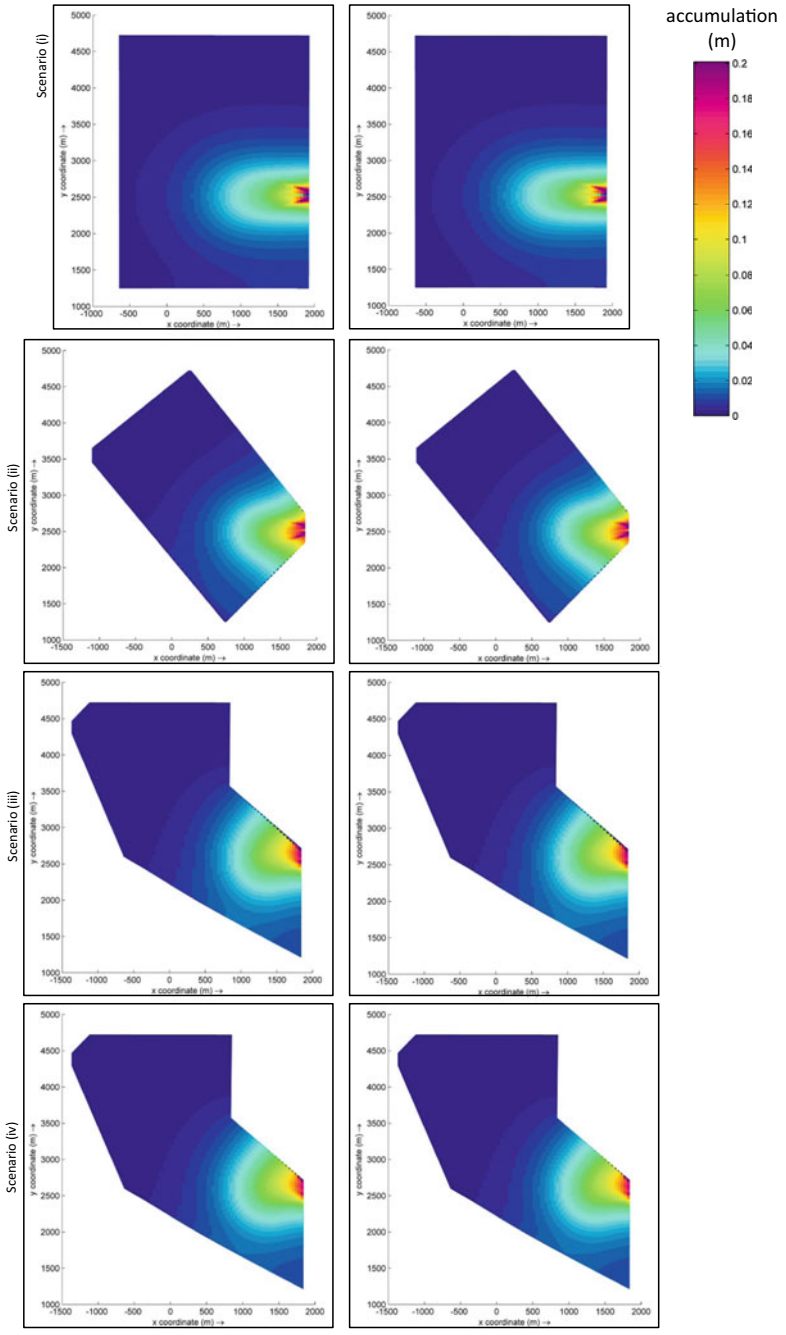

Fig. 7 Spatial distribution of accumulated sediment deposition after 30 days of model runs for Scenarios (i), (ii), (iii), and (iv) at 0° latitude (*left panel*) and 22.7° latitude (*right panel*)

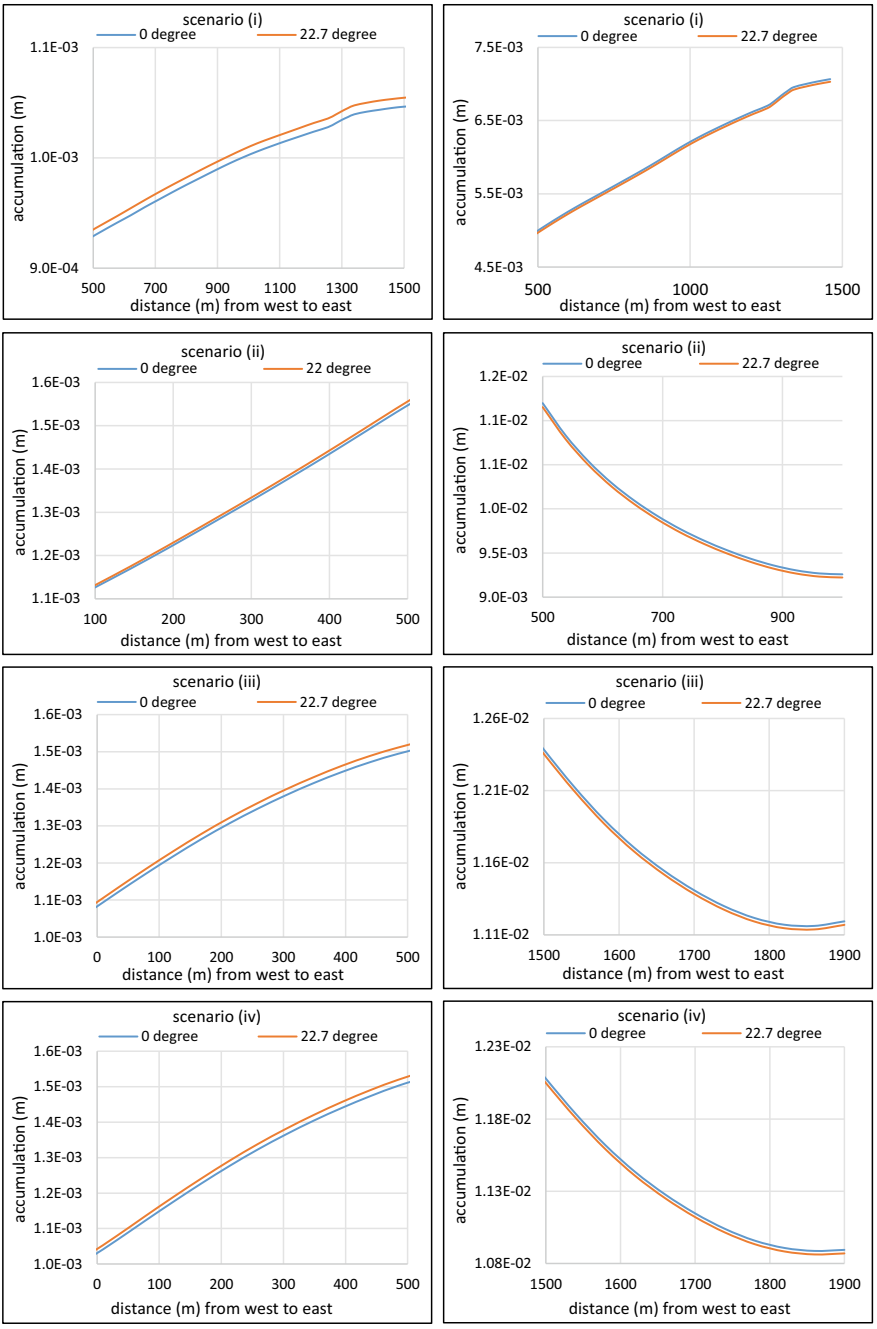

Fig. 8 Cross-sectional profiles of sedimentation for two latitudes at the northern part (*left panel*) and southern part (*right panel*)

6 Conclusions

Even and adequate sedimentation in the beel is the most necessitated objective to be achieved for an effective and successful TRM operation. So, determining the extent of influence of physical and hydraulic factors controlling the sedimentation process is indispensable. The impact of Coriolis force on sedimentation is minor yet hard to neglect. This study shows how Coriolis force impacts the spatial distribution of sedimentation at a different latitude. The Rossby number is a very helpful parameter to determine the influence of Coriolis force in the study area. The 'radius of deformation' which is expressed as length scale in this study can be determined based on Rossby number equal to one. In this study, the spatial sediment distribution in an idealized domain at the two different latitudes shows that the depth of sedimentation is more in higher latitude and it is deflected towards the right side of the inlet while the opposite happens at the left side of the domain. The Coriolis force is negligible at the mouth of the link canal where the velocity is mostly dominated by the inertia force. After a certain length (=1000 m on average), the Coriolis force dominates. The authors believe that this study will add another perspective to focus on the causes of uneven sedimentation in the tidal basin in terms of TRM and how Coriolis force incorporates with other physical and hydraulic factors.

Acknowledgements The research was funded by the 'Living Polders' project of the Institute of Water and Flood Management (IWFM), Bangladesh University of Engineering and Technology (BUET), Bangladesh.

References

Ahmad, Hafez. 2019. Bangladesh Coastal Zone Management Status and Future Trends. *Journal of Coastal Zone Management* 22 (1): 1–7. https://doi.org/10.4172/2473-3350.1000466.

Ahn, S.H., Y.X. Xiao, X.Z. Zhou, J. Zhang, C.J. Zeng, Y.Y. Luo, W. Xu, and Z.W. Wang. 2016. Numerical Analysis of Coriolis Effect on Low-Head Hydraulic Turbines. *IOP Conference Series: Earth and Environmental Science* 49 (2): 022012. https://doi.org/10.1088/1755-1315/49/2/022012.

Amir, Md. Sharif Imam Ibne, M. Shah Alam Khan, Mohammad Masud Kamal Khan, Mohammad Golam Rasul, and Fatema Akram. 2013. Tidal River Sediment Management—A Case Study in Southwestern Bangladesh. *International Journal of Geological and Environmental Engineering* 7 (3): 175–185.

Auerbach, L.W., S.L. Goodbred Jr., D.R. Mondal, C.A. Wilson, K.R. Ahmed, K. Roy, M.S. Steckler, C. Small, J.M. Gilligan, and B.A. Ackerly. 2015. Flood Risk of Natural and Embanked Landscapes on the Ganges-Brahmaputra Tidal Delta Plain. *Nature Climate Change* 5 (2): 153–157. https://doi.org/10.1038/nclimate2472.

Brammer, Hugh. 2014. Bangladesh's Dynamic Coastal Regions and Sea-Level Rise. *Climate Risk Management* 1: 51–62. https://doi.org/10.1016/j.crm.2013.10.001.

Chen, Shih-Nan, and Lawrence P. Sanford. 2009a. Lateral Circulation Driven by Boundary Mixing and the Associated Transport of Sediments in Idealized Partially Mixed Estuaries. *Continental Shelf Research* 29 (1): 101–118. https://doi.org/10.1016/j.csr.2008.01.001.

Chen, Shih-Nan, and Lawrence P. Sanford. 2009b. Axial Wind Effects on Stratification and Longitudinal Salt Transport in an Idealized, Partially Mixed Estuary. *Journal of Physical Oceanography* 39 (8): 1905–1920. https://doi.org/10.1175/2009jpo4016.1.

Cossu, R., M.G. Wells, and A.K. Wåhlin. 2010. Influence of the Coriolis Force on the Velocity Structure of Gravity Currents in Straight Submarine Channel Systems. *Journal of Geophysical Research* 115 (C11). https://doi.org/10.1029/2010jc006208.

Delft3D-FLOW, U.M. 2011. WL| Delft Hydraulics, the Netherlands.

Familkhalili, R., and S.A. Talke. 2016. The Effect of Channel Deepening on Tides and Storm Surge: A Case Study of Wilmington, NC. *Geophysical Research Letters* 43 (17): 9138–9147. https://doi.org/10.1002/2016gl069494.

Gain, Animesh K., David Benson, Rezaur Rahman, Dilip Kumar Datta, and Josselin J. Rouillard. 2017. Tidal River Management in the South West Ganges-Brahmaputra Delta in Bangladesh: Moving Towards a Transdisciplinary Approach? *Environmental Science & Policy* 75: 111–120. https://doi.org/10.1016/j.envsci.2017.05.020.

Huijts, K. M. H., H. M. Schuttelaars, H. E. de Swart, and A. Valle-Levinson. 2006. Lateral entrapment of sediment in tidal estuaries: An idealized model study. *Journal of Geophysical Research* 111 (C12). https://doi.org/10.1029/2006jc003615.

Huijts, K. M. H., H. M. Schuttelaars, H. E. de Swart, and C.T. Friedrichs. 2009. Analytical study of the transverse distribution of along-channel and transverse residual flows in tidal estuaries. *Continental Shelf Research* 29 (1): 89–100. https://doi.org/10.1016/j.csr.2007.09.007.

Islam, Md. Feroz, Hans Middelkoop, Paul P. Schot, Stefan C. Dekker, and Jasper Griffioen. 2020. Enhancing Effectiveness of Tidal River Management in Southwest Bangladesh Polders by Improving Sedimentation and Shortening Inundation Time. *Journal of Hydrology* 590: 125–228. https://doi.org/10.1016/j.jhydrol.2020.125228.

Mahiuddin, Md. 2017. Siltation Pattern and Pedogenesis in the Coastal Zone of Bangladesh. PhD Dissertation, University of Dhaka.

Maskell, J., K. Horsburgh, M. Lewis, and P. Bates. 2014. Investigating river–surge interaction in idealised estuaries. *Journal of Coastal Research* 294: 248–259. https://doi.org/10.2112/jcoastres-d-12-00221.1.

Mutahara, Mahmuda, Jeroen F. Warner, Arjen E. J. Wals, M. Shah Alam Khan, and Philippus Wester. 2017. Social Learning for Adaptive Delta Management: Tidal River Management in the Bangladesh Delta. *International Journal of Water Resources Development* 34 (6): 923–943. https://doi.org/10.1080/07900627.2017.1326880.

Nicholls, R.J., C.W. Hutton, A.N. Lázár, A. Allan, W.N. Adger, H. Adams, J. Wolf, M. Rahman, and M. Salehin. 2016. Integrated Assessment of Social and Environmental Sustainability Dynamics in the Ganges-Brahmaputra-Meghna Delta, Bangladesh. *Estuarine, Coastal and Shelf Science* 183: 370–381. https://doi.org/10.1016/j.ecss.2016.08.017.

Nowreen, Sara, Mohammad Rashed Jalal, and M. Shah Alam Khan. 2014. Historical Analysis of Rationalizing South West Coastal Polders of Bangladesh. *Water Policy* 16 (2): 264–279. https://doi.org/10.2166/wp.2013.172.

Rashid, Md. Bazlar, Arif Mahmud, Md. Kamrul Ahsan, Md. Hossain Khasru, and Md. Ashraful Islam. 2013. Drainage Congestion and Its Impact on Environment in the South-Western Coastal Part of Bangladesh. *Bangladesh Journal of Geology* 26: 359–371.

Robins, Peter. 2008. Present and Future Flooding Scenarios in the Dyfi Estuary, Wales, U.K. Countryside Council for Wale.

Shampa, and Md. Ibne Mayaz Pramanik. 2012. Tidal River Management (TRM) for Selected Coastal Area of Bangladesh to Mitigate Drainage Congestion. *International Journal of Scientific & Technology Research* 1 (5): 1–6.

Staveren, Martijn F. van, Jeroen F. Warner, and M. Shah Alam Khan. 2017. Bringing in the Tides. From Closing Down to Opening Up Delta Polders Via Tidal River Management in the Southwest Delta of Bangladesh. *Water Policy* 19 (1): 147–164. https://doi.org/10.2166/wp.2016.029.

Staveren, Martijn F. van, Jeroen F. Warner, Jan P.M. van Tatenhove, and Philippus Wester. 2014. Let's Bring in the Floods: De-Poldering in the Netherlands as a Strategy for Long-Term Delta Survival? *Water International* 39 (5): 686–700. https://doi.org/10.1080/02508060.2014.957510.

Talchabhadel, Rocky, Hajime Nakagawa, and Kenji Kawaike. 2018. Sediment Management in Tidal River: A Case Study of East Beel Khuksia, Bangladesh. In ed. A. Paquier and N. Rivière. E3S Web of Conferences 40: 02050. https://doi.org/10.1051/e3sconf/20184002050.

Talchabhadel, Rocky, Hajime Nakagawa, Kenji Kawaike, Masakazu Hashimoto, and Nassim Sahboun. 2017. Experimental Investigation on Opening Size of Tidal Basin Management: A Case Study in Southwestern Bangladesh. *Journal of Japan Society of Civil Engineers, Ser. B1 (Hydraulic Engineering)* 73 (4): I_781–1_786. https://doi.org/10.2208/jscejhe.73.i_781.

Talchabhadel, Rocky, Hajime Nakagawa, and Kenji Kawaike. 2016. Experimental Study on Suspended Sediment Transport to Represent Tidal Basin Management. *Journal of Japan Society of Civil Engineers, Ser. B1 (Hydraulic Engineering)* 72 (4): I_847–1_852. https://doi.org/10.2208/jscejhe.72.i_847.

Unger, Zoltan, and Nemeth Istvan. 2013. Estimation of the Coriolis-Force Size for Tisza River. *Carpathian Journal of Earth and Environmental Sciences* 8 (2): 201–208.

Wells, M.G. 2007. Influence of Coriolis Forces on Turbidity Currents and Sediment Deposition. *Particle-Laden Flow, ERCOFTAC Series* 11: 331–343. https://doi.org/10.1007/978-1-4020-6218-6_26.

Wells, M.G. 2009. How Coriolis Forces Can Limit the Spatial Extent of Sediment Deposition of a Large-Scale Turbidity Current. *Sedimentary Geology* 218 (1–4): 1–5. https://doi.org/10.1016/j.sedgeo.2009.04.011.

The Impact of Small Tributaries Flood in the Braided Plain of Large River

Md. Manjurul Hussain, Shampa, Juwel Islam, Md. Shibbir Ahmed, Md. Ashiqur Rahman, and Md. Munsur Rahman

Abstract Flooding of the braided Brahmaputra-Jamuna River causes significant economic losses in the northern region of Bangladesh every year. Presently, the intensity and timing of floods are mainly captured by the water level at a few selected stations of the river. Flood Forecasting and Warning Centre (FFWC) of the Bangladesh Water Development Board (BWDB) is officially mandated to regularly disseminate the water level for several rivers during the flood season. The water levels along the Brahmaputra-Jamuna at some strategic stations (such as Chilmari, Bahadurabad, Sirajganj etc.) are playing an important role for the above flood warning system in the North-Central part of Bangladesh. The right bank tributaries to the Brahmaputra-Jamuna River—the Teesta and the Dharla—are contributing rapid (flashy in nature) flow to the system, the effects of which are still unidentified. This study investigates the effects of the variations of flood flow of these tributaries on the flooding of the Brahmaputra-Jamuna basin at the local level by using the 2D hydrodynamic model. A 225 km long hydrodynamic model domain was set along the Brahmaputra-Jamuna, including the most vulnerable floodplain of Dharla and Teesta at Kurigram and Jamalpur districts, respectively. The results show that the variation of flow of the tributaries is trivial to the flood level at the stations where BWDB is capturing water-level data. However, the tributaries' flow has considerable effects on Charland flooding. In addition, the results demonstrate that the flood depth of some places in the char lands varies more than one metre for the variation of the contribution it receives from the tributaries. These observations indicate that the above fact for flood forecasting and warning systems will be important, especially for the Charland area in the Brahmaputra-Jamuna system.

Keywords Brahmaputra-Jamuna · Dharla · Teesta · Tributaries · Charland · Flooding

Md. M. Hussain (✉) · Shampa · J. Islam · Md. S. Ahmed · Md. A. Rahman · Md. M. Rahman
Institute of Water and Flood Management (IWFM), Bangladesh University of Engineering and Technology, Dhaka, Bangladesh

© The Author(s), under exclusive license to Springer Nature Switzerland AG 2022

G. M. Tarekul Islam et al. (eds.), *Water Management: A View from Multidisciplinary Perspectives*,
https://doi.org/10.1007/978-3-030-95722-3_12

1 Introduction

Bangladesh is one of the world's most natural disaster-prone country where floods, storm surges, cyclones, riverbank erosions and droughts are frequent occurrences (Nasreen 2004). Among these natural disasters, flood represents one of the most dominant ones. Flood is a regular feature in Bangladesh due to its geographical setting influenced by the overflow of major rivers and their tributaries and distributaries (Karim and Mimura 2008; Mamun et al. 2019; Younus et al. 2007). Catastrophic flooding events, for example, floods from the years 1988, 1998 and 2020, are a highly critical issue for the country which causes untold suffering to millions of people. The effect of catastrophic floods can be devastating and result in appreciable damage to crops and houses, severe riverbank erosion with consequent loss of homesteads, schools and land, as well as loss of human lives, livestock and fisheries (Pramanik 1991). If we consider basin-wise flooding, the mighty Brahmaputra-Jamuna has been the main contributor to most of the catastrophic flood cases in Bangladesh (NAWG 2020).

The Brahmaputra-Jamuna River, draining from the northern and eastern slopes of the Himalayas, is 2900 km long, wherein the reach length is 240 km in Bangladesh (Bhuiyan 2014). Geologically, it is one of the youngest rivers in the world (Archana et al. 2012). Because of abnormal flood and tectonic activity, the Brahmaputra River began to flow through a new course known as Jamuna from 1787 (Uddin et al. 2011). The right bank of the Jamuna was once a part of the Teesta floodplain, and now through the Dudhkumar and Dharala distributary of the Jamuna, is part of the bigger floodplain. Several distributaries of the Brahmaputra-Jamuna flow through the left bank floodplain which is later sub-classed as the Brahmaputra-Jamuna floodplain. The southern part of this sub-region was once a part of the Ganges floodplain (Paul 2011). The Brahmaputra-Jamuna River contributes ~51% of the water discharge and 38% of the sediment yield to the Ganges–Brahmaputra-Meghna (GBM) system (Schumm and Winkley 1994). The river is braided in nature with a width of up to 15 km and average depths of 6 m to 7 m (Klaassen and Vermeer 1988; Shampa 2019a). It has three main tributaries in the left bank i.e. Dudhkumer, Dharla and Teesta, and three main distributaries in the right bank which are Old Brahmaputra, Jenai and Dhaleswari (see Fig. 1).

The transboundary Teesta River is one of the major contributors or tributaries of Brahmaputra-Jamuna. The river flows through five northern districts of Bangladesh, which are Gaibandha, Kurigram, Lalmonirhat, Nilphamari and Rangpur (Rangpur Division), comprising an area of 9667 sq.km, 35 thanas and 5427 villages with an estimated population of 9.15 million as of 2011. The river plays a key role in flushing silt and sediment deposited during the dry season is a lifeline for irrigation, agriculture, farming, fishing and navigation in the region. This transboundary river is encroached by many dams and barrages both in India and Bangladesh. In the rainy season, excessive flow is dispensed by these dams and barrages, causing floods in the downstream areas (Rahman and Ali 2016). The river Teesta experiences several peaks during the monsoon season causing local floods. For example, in the year 2017, the

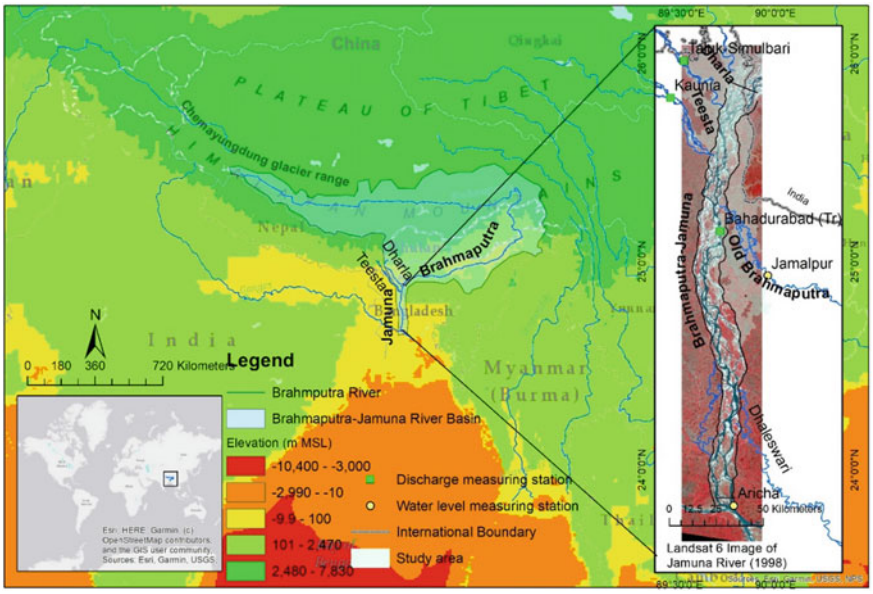

Fig. 1 The Brahmaputra-Jamuna River and its major tributaries and distributaries

water level crossed the danger level at Dhalia Point of Teesta for more than 6 days, a resulting in low-lying areas being submerged for several days (FFWC 2018). Among the other tributaries, Dharla is one of the major contributors to Brahmaputra-Jamuna. It originates in the Himalayas and enters Bangladesh through the Lalmonirhat district and flows as the Dharla River until it meets the Brahmaputra-Jamuna River near the Kurigram District (Fig. 1). Dharla River, along with the Brahmaputra River, has substantial influence on floods and riverbank erosion in different districts of Bangladesh (Pal et al. 2017). For example, the water level of the Dharla river at Kurigram point remained above the danger level for more than 30 days due to the 1998 floods, as a result of which the area was inundated for a long time (FFWC 2018). While the overall flooding situations of past events (i.e. 1987, 1988, 1998, 2007) are quite well documented, the contribution of these two major tributaries in the flooding of the Brahmaputra-Jamuna is yet to be known (Best et al. 2007; Dewan et al. 2003; Islam and Chowdhury 2002; Mosselman 2006).

Nevertheless, human activities such as land use and construction of infrastructure, such as dams, barrages, bridges, artificial levees, are continuously altering the river regime. Given the large-scale approach, it is important to understand the sub-regions scale details of the flooding characteristics. In recent decades, flood damage has been increasing all over the world, due to high population growth, economic activities in floodplain areas, and intensified precipitation due to climate change (Albano et al. 2017; Kvočka et al. 2016; Munich Re 2015). Bangladesh is no exception (Dewan 2015). Although the country has been able to significantly reduce the loss of lives due to floods, the economic loss and damage have increased over the decades (Ferdous

et al. 2019; Mechler and Bouwer 2015). The recent monsoon floods of 2020 affected about 30 districts in Bangladesh, of which 15 districts were severely hit. The damage was comparatively higher in the Brahmaputra-Jamuna floodplain areas of the Kurigram and Jamalpur districts. More than 50% of the area in 59 unions of 7 Upazilas of Jamalpur district , and 59 unions of 9 Upazilas of Kurigram district, were flooded (NAWG 2020).

Against this backdrop, this study attempts to deduce the impact of flood flow of Teesta and Dharla tributaries on the river basin of Brahmaputra-Jamuna including its char areas. Specifically, the study attempts to identify the impacts of tributary flow on flood hazard parameters, such as flood depth, duration and velocity, of the major Brahmaputra-Jamuna River using 2D hydrodynamic simulations. The flooding condition of the year 1998 has been considered as the base, and three hypothetical conditions have been generated based on the flow of Dharla and Teesta. As a study area, the major flood-prone unions of Kurigram and Jamalpur districts were considered as shown in Fig. 1. The next section of the paper describes the methodology of this study. The impact of the tributary flood is illustrated in the last parts.

2 Methodology

For this research, we used a well-calibrated and validated 2D hydrodynamic model by Shampa (2019b) and Shampa et al. (2017). Delft3D (flow version 4.00.01.000000), an open-source software, was used to develop the numerical model (Lesser et al. 2004). In the hydrodynamic part, Navier–Stokes-based two-dimensional depth-averaged shallSow water (for incompressible free surface flow) equations with consideration of Boussinesq approximations were used to solve the model. A short description of the model is given below.

The continuity equation was used to calculate conservation of mass (1)

$$\frac{\partial h}{\partial t} + \frac{\partial (hu)}{\partial x} + \frac{\partial (hv)}{\partial y} = 0 \tag{1}$$

Conservation of momentum in the x-direction is shown by Eq. (2)

$$\frac{\partial u}{\partial t} + u\frac{\partial u}{\partial x} + v\frac{\partial u}{\partial y} + g\frac{\partial \zeta}{\partial x} + \frac{gn^2}{\sqrt[3]{h}}\left(\frac{u\left(u^2+v^2\right)}{h}\right) - v_h\left(\frac{\partial^2 u}{\partial x^2} + \frac{\partial^2 u}{\partial y^2}\right) = 0 \tag{2}$$

Conservation of momentum in the y-direction is shown by Eq. (3)

$$\frac{\partial v}{\partial t} + u\frac{\partial v}{\partial x} + v\frac{\partial v}{\partial x} + g\frac{\partial \zeta}{\partial x} + \frac{gn^2}{\sqrt[3]{h}}\left(\frac{v\left(u^2+v^2\right)}{h}\right) - v_h\left(\frac{\partial^2 v}{\partial x^2} + \frac{\partial^2 v}{\partial y^2}\right) = 0 \tag{3}$$

where ζ is water level elevation with respect to a datum (here in m); h represents water depth (m) u, v is depth average velocity in the x and y directions (m/s); g is the gravitational acceleration (m/s^2); v_h denotes kinetic eddy viscosity (m^2/s); n represents the Manning's coefficient (sm-1/3). The terms $v_h\left(\frac{\partial^2 u}{\partial x^2}+\frac{\partial^2 u}{\partial y^2}\right)$ and $v_h\left(\frac{\partial^2 v}{\partial x^2}+\frac{\partial^2 v}{\partial y^2}\right)$ in Eqs. (2) and (3) represent the horizontal Reynold's stress under the eddy viscosity concept neglecting the shear stress along the closed boundaries. The model area consists of the whole Brahmaputra-Jamuna River and parts of Dudhkumar, Dharla, Teesra and Old Brahmaputra rivers encompassing a length of 246 km and an average width of 33 km. The total area has been divided into 127 × 893 cells curvilinear grids to perform the 2D hydrodynamic simulation. For the bathymetry data, the interpolated data from the measured bathymetry of BWDB for the year 1998 was considered. For the topographic data, Shuttle Radar Topography Mission data of the year 2014 was used. Figure 2 shows the model grid and bathymetry. The boundary data of discharge and the water level have been collected from BWDB. The observed/generated discharge data of Brahmaputra-Jamuna, Teesta, Dharla and Dudhkumar River are considered as the upstream boundary condition. At the same time, observed/generated water levels of Brahmaputra-Jamuna

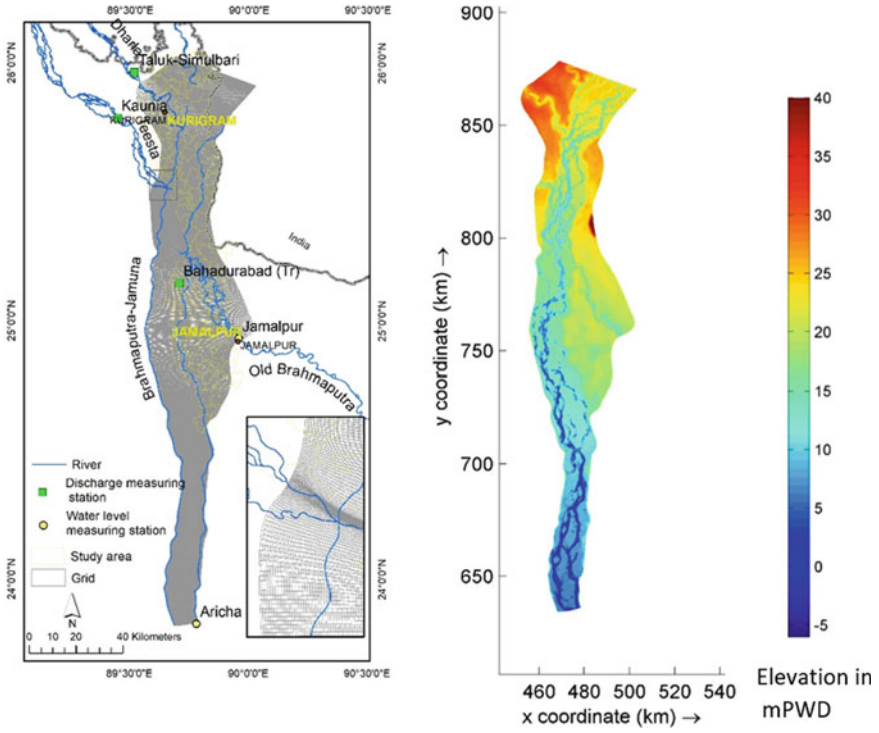

Fig. 2 Model grid and bathymetry

(Aricha), Old Brahmaputra (Jamalpur), are considered as the downstream boundary condition.

For this research, two types of conditions have been considered which are base and hypothetical conditions as shown in Table 1. Three types of scenarios were set up for the hypothetical conditions—(i) the discharge value of the Teesta-Dharla River is Zero (Both Zero); (ii) the discharge value of Dharla is Zero (Dharla Zero) and (iii) the discharge value of Teesta is Zero (Teesta Zero). All models run at the 100-year return periods condition reflecting the flood of 1998. The boundary condition of the base condition, $BJ_a D_a T_a$ is shown in Fig. 3.

From the simulation results, flood information such as the area of inundation, depth of inundation, duration of inundation and flow velocity has been extracted for three temporal conditions (pre-flood, post-flood and peak flood). Depth of inundation and

Table 1 Scenario considered in this study

Scenarios	Criteria
Base condition, $BJ_a D_a T_a$	Flood of 1998
Hypothetical condition	
Both Zero $BJ_a D_0 T_0$	Discharge of Dharla and Teesta is zero But Brahmaputra-Jamuna has the same discharge of the flood 1998
Dharla Zero, $BJ_a D_0 T_a$	Discharge of Dharla is zero But Brahmaputra-Jamuna and Teesta have the same discharge of the flood 1998
Teesta zero $BJ_a D_a T_0$	Discharge of Teesta is zero But Brahmaputra-Jamuna and Dharla have the same discharge of the flood 1998

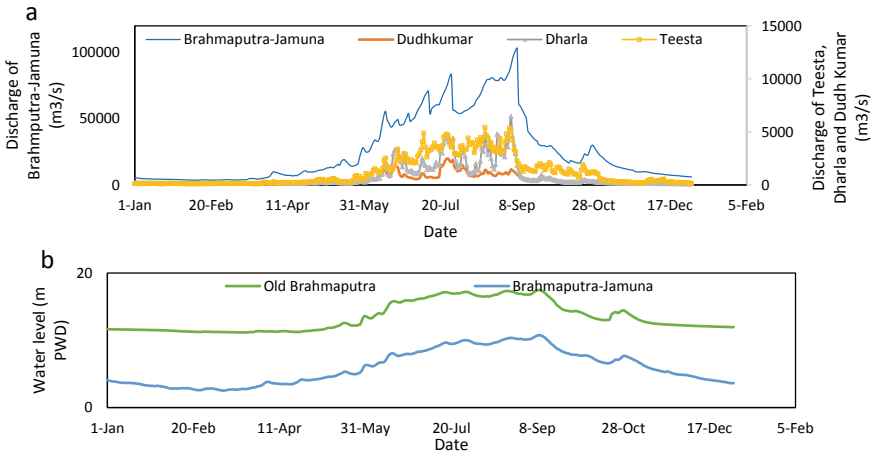

Fig. 3 Boundary conditions of the model for Base condition, $BJ_a D_a T_a$. **a** Upstream discharge boundary. **b** Downstream water-level boundary

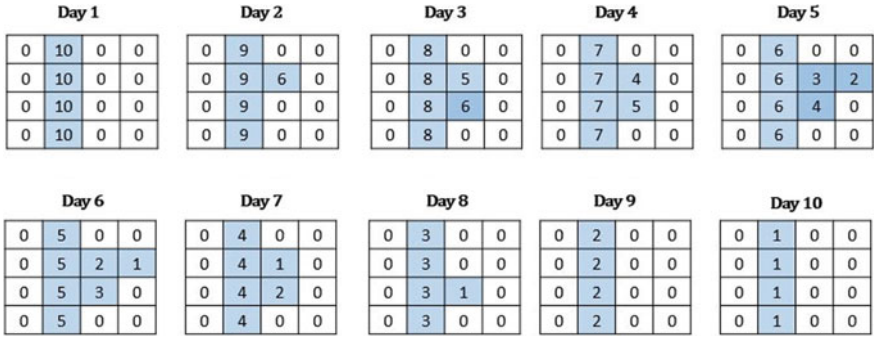

Fig. 4 Flood duration calculation process, where blue indicates water in that cell

flow velocity were directly extracted from model results, and duration was calculated from the depth of inundation. Calculations were done separately for every individual cell. If one cell contains water continuously for several days, then it was counted backwards to find the duration for every day in that cell (Fig. 4). After extracting all the results, a comparison was made between actual and hypothetical conditions to determine the influence of tributary rivers.

3 Results

3.1 The Flood Characteristics

Before discussing the hypothetical condition results, it is important to examine the character of the actual flooding (base) condition. Figure 5 shows the flood-hydrograph characteristics of the considered rivers at the base or actual condition $BJ_a D_a T_a$. It is evident from this figure that the Brahmaputra-Jamuna carried more than 90% (annual average) of flow during the considered year (Fig. 5a). However, during the peak monsoon, the sharing of Dharla (6.25%) and Teesta (5.26%) increased slightly (around 1% to 2%). But this slight increase had an impact on local water levels. Figure 5b shows the 7-day moving average of the rate of rising of water-level hydrograph of the Bahadurabad at Brahmaputra-Jamuna, Teesta at Kaunia and Dharla at Taluk-Simulbari. It is evident from this figure that the rise of Dharla and Teesta caused an increase of the hydrograph of the Brahmaputra-Jamuna each time. This phenomenon contributes to the local flooding.

Figure 6 shows the flooding depth and extent for different conditions at peak monsoon. It confirms that when the river discharge is nil either in Dharla ($BJ_a D_0 T_a$), or Teesta ($BJ_a D_a T_0$) or both ($BJ_a D_0 T_0$, c), the flooding depth is 0 m to 0.30 m lower than the base condition. Though the areal extent was almost similar in all conditions (Kurigram 55% and Jamalpur 43%).

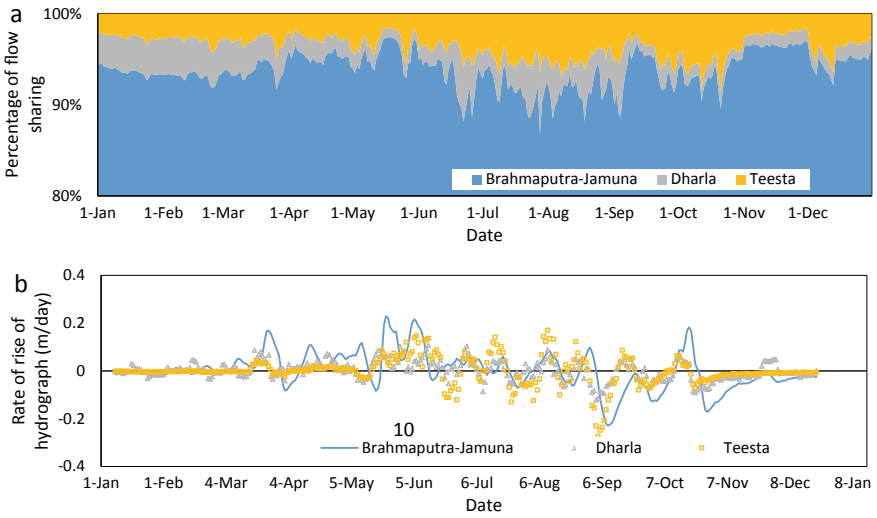

Fig. 5 The flood-hydrograph characteristics of the considered rivers at the base condition $BJ_a D_a T_a$. **a**. The percentage of flow sharing in actual condition, **b**. 7-days moving average of rate of rising of water-level hydrograph of the considered rivers

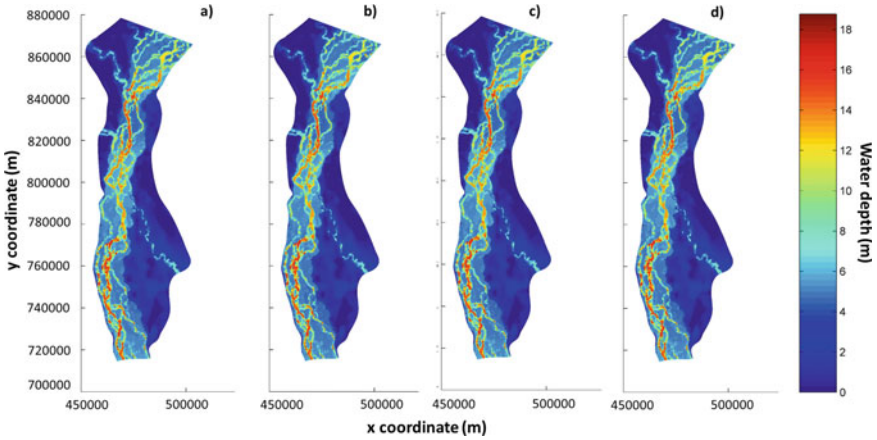

Fig. 6 Water depth (in m) of **a** base $BJ_a D_a T_a$, **b** both zero $BJ_a D_0 T_0$, **c** Dharla zero $BJ_a D_0 T_a$, **d** Teesta zero $BJ_a D_a T_0$ condition at peak-flooding time

3.2 Flood Depth

The simulation results showed that at base condition, $BJ_a D_a T_a$, the average flooding depth varies between 2.06 m and 3.37 m in the study domain as shown in Table 2. However, at Both Zero condition, the depth was lowered by 3.8% and 3.6% in

Table 2 Flooding depth of the considered cases the study domain

Scenarios	Average flooding depth (in m)		
	Pre-monsoon	Monsoon	Post-monsoon
Base condition, $BJ_a D_a T_a$	2.06	3.37	2.15
Hypothetical condition			
Both zero $BJ_a D_0 T_0$	1.98	3.25	2.11
Dharla zero, $BJ_a D_0 T_a$	2.03	3.30	2.14
Teesta zero $BJ_a D_a T_0$	2.02	3.32	2.12

pre-monsoon and monsoon periods correspondingly. In the post-monsoon season, the depth was similar to that of the base condition (1.86%). The impact of flooding depth in $BJ_a D_0 T_a$ and $BJ_a D_a T_0$ conditions was prominent in monsoon time. In Dharla Zero condition $BJ_a D_0 T_a$, the depth was decreased by 2.07% whereas in Teesta Zero condition $BJ_a D_a T_0$, it was found to be 1.48% less than that of the base condition. The special comparison of flood depth among the base, $BJ_a D_a T_a$ and hypothetical scenarios (Both Zero $BJ_a D_0 T_0$, Dharla Zero $BJ_a D_0 T_a$, Teesta zero $BJ_a D_a T_0$) is shown in Fig. 7. It indicates that the floodwater depth increases 0 m to 0.3 m due to both Dharla and Teesta River discharge. Whereas, the contribution to Jamuna flood depth for only Dharla or Teesta is 0 to 0.15 m (Fig. 7). The maximum variation found in peak flood conditions and the variation in post-flood conditions are negligible.

Here, the area-specific analysis was done by differentiating the flooding of inland and char areas in the two districts. At base condition, the average depth of flooding during the monsoon season was 5.44 m and 0.30 m in Kurigram district's char land and inland area, respectively. In pre-monsoon and post-monsoon seasons, the flooding depth was 67% and 59% lower in char areas, whereas the depth was 0.07 m in both pre and post-monsoon seasons for inland areas. In Jamalpur, the flooding depth was higher in inland areas (0.34 m) but lower in char areas (5.22 m) in comparison to the Kurigram district during monsoon season. In the char areas of Jamalpur, the depth was 70% and 57% lower than the monsoon season in pre and post-monsoon seasons, respectively. In inland areas of Jamalpur, the depth was 0.10 m in both pre and post-monsoon periods. Figure 8 shows the flood depth difference between the base condition and all hypothetical conditions. It is evident from this figure that the alteration of tributary discharge affects the flooding depth of char areas in both districts mostly. The maximum difference (0.22 m) was found in the chars of Jamalpur district in Both Zero $BJ_a D_0 T_0$ conditions during monsoon time. In the case of the chars of Kurigram, it was 0.12 m. The influence of Teesta was greater (0.07 m in char and 0.1 m in inland) in flooding depth than Dharla compared to the base condition.

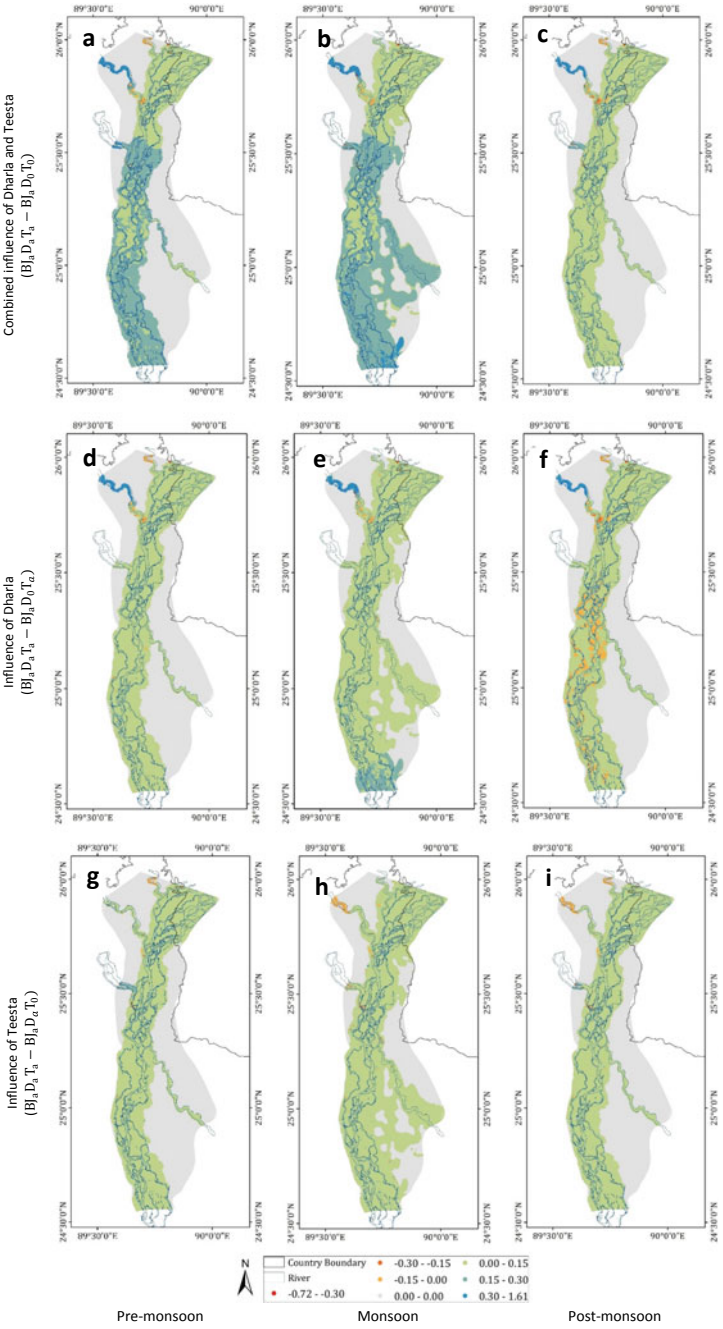

Fig. 7 Difference of flood depth between base and hypothetical condition

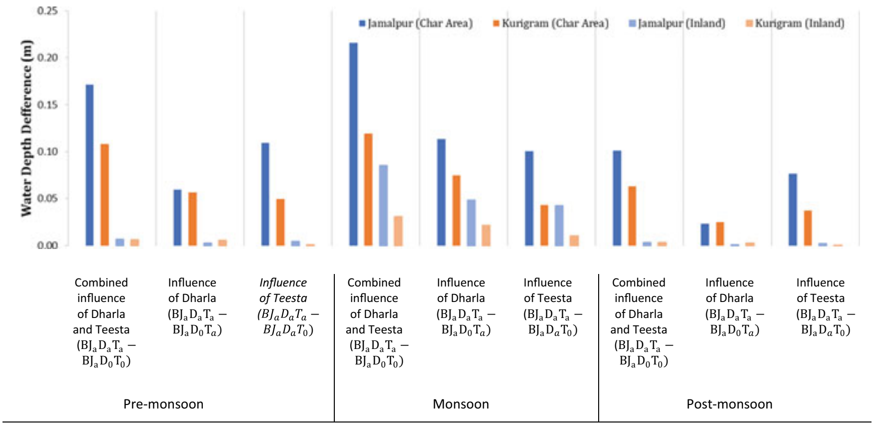

Fig. 8 Flood depth difference between base and hypothetical condition

3.3 *Flood Duration*

Duration is one of the major hazard parameters for floods. The study area consists of inland and char areas. The flood duration was found to be relatively low for inland areas, whereas the chars experienced very high duration flood. The results show that in the base condition, the flood duration varies from 0 to 115 days. But in Both Zero condition $BJ_aD_0T_0$, the duration was only 1% less. The influence of Dharla (0 days) was greater than Teesta (1 day) on flood duration. Figure 9 shows the difference map of flood duration among the considered scenarios in pre-monsoon, monsoon and post-monsoon periods. It is evident from this figure that the influence of the tributary discharge was similar during these three timelines. When considering the discharge of both tributaries to be nil ($BJ_aD_aT_a - BJ_aD_0T_0$), the flooding duration reduced to two days compared to the base condition (Fig. 9a–c). The effect of the Dharla on flood duration was insignificant (nearly 1 day) due to its flashy nature of the hydrograph. But it resulted in local flood in the Kurigram district (Fig. 9d–f). Due to the influence of Teesta, the flood duration may increase by nearly three days (Fig. 9g–i). Figure 10 shows the difference in flood duration in char and inland areas in both districts. This figure depicts that due to the influence of tributary discharge, the highest flood duration altered around 4 days in char areas and 1 day in inland areas. The chars of Jamalpur areas are more susceptible to long-duration flooding compared to Kurigram district's flood. The influence of tributary discharge inland flood duration is insignificant (about one day).

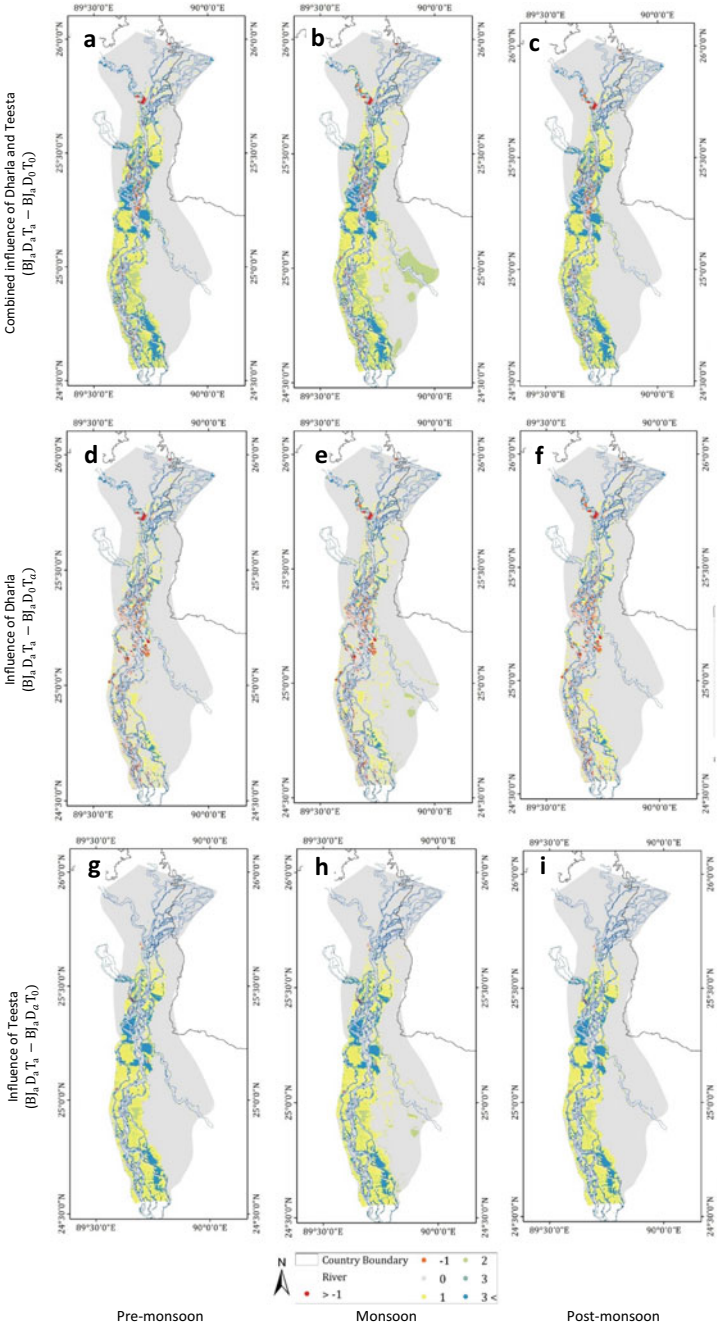

Fig. 9 Difference map of flood duration among the considered scenarios

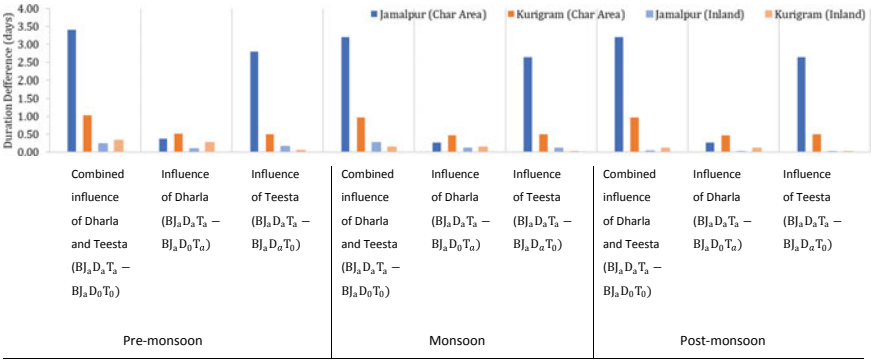

Fig. 10 Flood duration difference between base and hypothetical condition

3.4 Flood Velocity

Figure 11 shows the histogram plot of velocity magnitude in different scenarios. The *x*-axis showed the velocity magnitude class while the *y*-axis shows the number of grid cells containing that velocity in the model domain. As the study domain contains the land of various elevations, the range of velocity distribution is quite large. For example, the near channel area of chars has very low elevation compared to the floodplain or mid-char areas. Therefore, we consider the histogram plot for comparing the velocity of different cases. All the subfigures of Fig. 11 show two peaks due to the variation of velocity in low-lying and higher elevated areas. It depicts that unlike the flood duration, the flooding velocity shows seasonal variation. In base condition ($BJ_aD_aT_a$), during the pre-monsoon period, the velocity magnitude varies from 0 m/s to 2.26 m/s. In the inland areas, the velocity varies between 0 and 0.22 m/s, and when near the channel, it ranges between 0.44 m/s and 0.89 m/s, maintaining an average velocity of 0.40 m/s. During the monsoon period, the maximum velocity was found to be 2.51 m/s, wherein the average velocity increases by 1.5 times. In the post-monsoon season, the velocity distribution was quite similar to the pre-monsoon season (Fig. 11a–c). The distribution pattern of the hypothetical cases was similar to that of the base condition (Fig. 11d–l). In the pre-monsoon period, the velocity magnitude ranges from 0 m/s to 2.3 m/s with the average value of 0.38 m/s in all hypothetical conditions. In the monsoon season, the maximum velocity was found to be 2.53 m/s ($BJ_aD_0T_0$) with an average value of 0.60 m/s. In the post-monsoon season, a maximum velocity of 2.3 m/s ($BJ_aD_aT_0$) was noted, wherein the average velocity was 0.40 m/s. Figure 12 shows the spatial distribution of the difference of flood velocity magnitude among the considered scenarios. It illustrates that the contribution in velocity magnitude of Dharla and Teesta varies between − 0.015 m/s and 0.030 m/s. The main variation was observed at the lower left bank of Brahmaputra-Jamuna in peak-flooding conditions as this section has better floodplain connectivity (the right bank of the study domain was partially embanked).

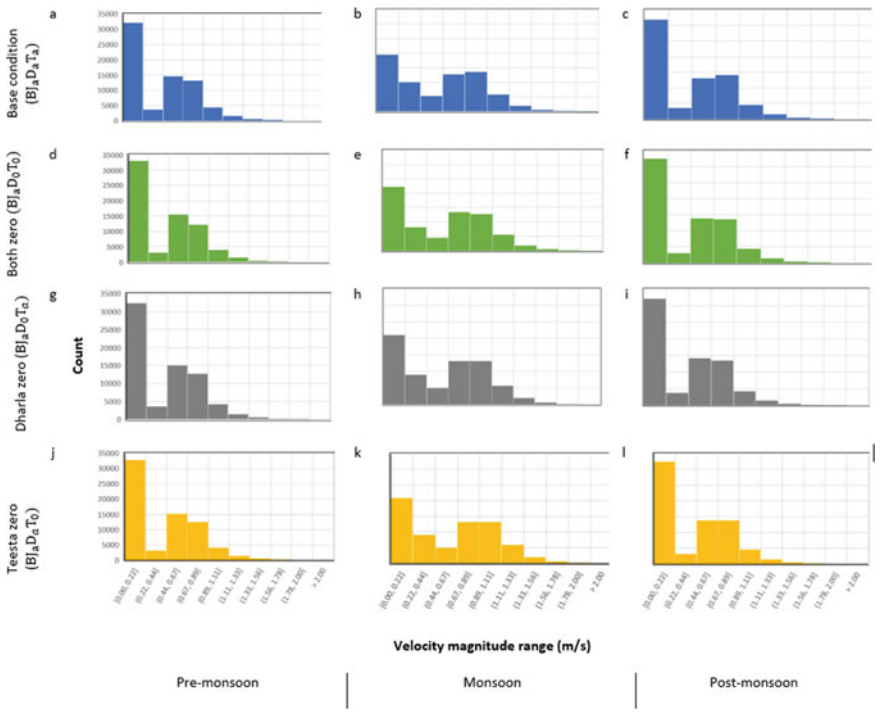

Fig. 11 Distribution of velocity magnitude of the considered cases

At base condition, the average velocity was 0.97 m/s in Kurigram district's char areas, whereas in Jamalpur it was 0.93 m/s as the valley slope is higher in Kurigram. But for the inland areas, the flooding velocity was 0.15 m/s in Kurigram and 0.25 m/s in Jamalpur. As the inland area of Kurigam contains partial embankment, it hampered the drainage path of the floodwater. The contribution of the tributary in velocity increment or decrement in char and inland areas was very small (0.01 m/s).

4 Discussion

Brahmaputra-Jamuna River is one of the major rivers in Bangladesh, and a lot of studies have been conducted on the Brahmaputra-Jamuna River floods (Best et al. 2007; Dewan et al. 2003; Islam and Chowdhury 2002; Mosselman 2006). But no previous study has been done to investigate the contribution of its tributaries. In this study, we tried to find the impact of tributaries by comparing different flood parameters (inundation depth, flood duration, flow velocity) in different conditions (base, $\mathrm{BJ}_a D_a T_a$, Both Zero $\mathrm{BJ}_a D_0 T_0$, Dharla Zero $\mathrm{BJ}_a D_0 T_a$, Teesta Zero $\mathrm{BJ}_a D_a T_0$). The results show that the inundation depth varies up to 3.8% due to contribution of Teesta

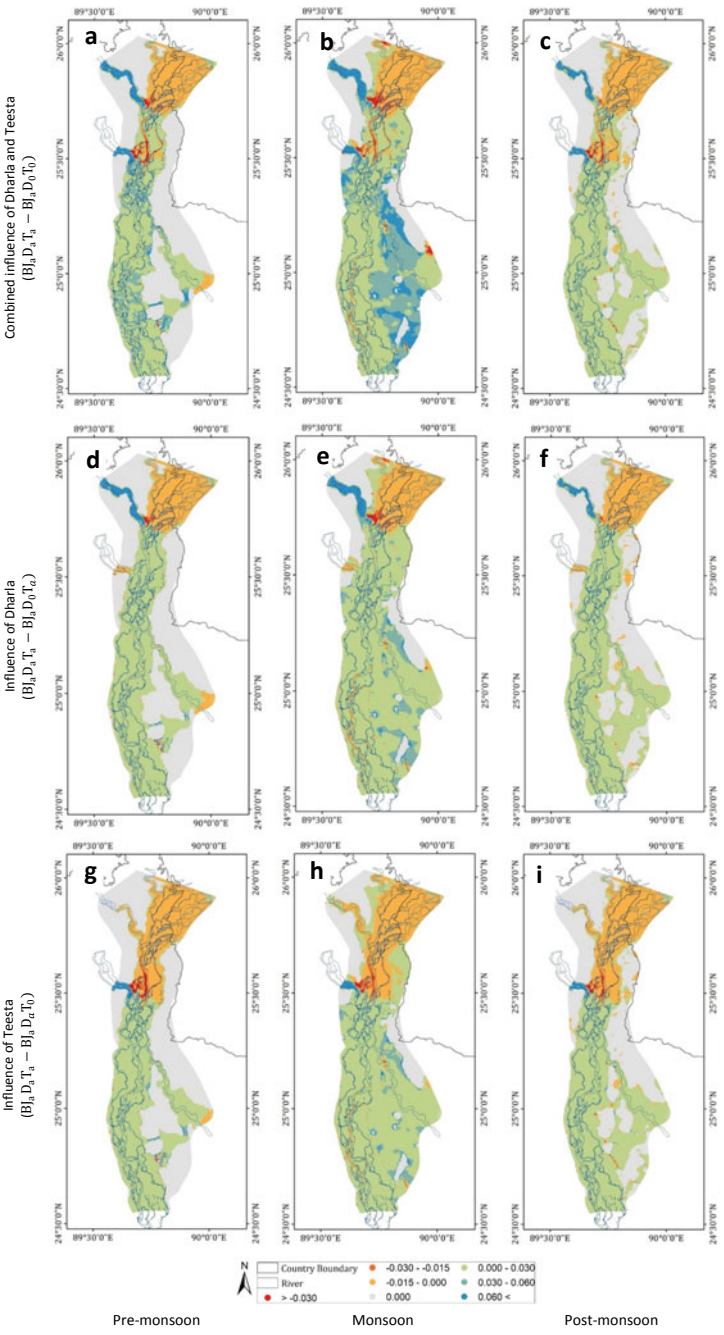

Fig. 12 Spatial distribution of flood velocity magnitude change among the considered scenarios

and Dharla river water. Islam and Chowdhury (2002) claims that, continuous inflow of high discharge for more than two and half months occurred in the Brahmaputra-Jamuna in 1998, which is consistent with the base condition $BJ_a D_a T_a$ results. The contribution in velocity magnitude of Dharla and Teesta varies between -0.015 m/s and 0.030 m/s. The study also found that Teesta and Dharla only contribute to 10% of discharge water in Brahmaputra-Jamuna River. The large difference between the river discharge of Brahmaputra-Jamuna and Teesta and Dharla is the probable reason for this small impact in Brahmaputra-Jamuna floods.

Although the aerial extent of flooding is largely dependent on the flooding pattern of the Brahmaputra-Jamuna, tributary flooding affects local flood conditions especially in the char areas. The flooding depth increase by up to 0.20 m due to the flooding conditions of the tributaries. The flooding duration can increase by up to three days due to the influence of the Teesta and Dharla. The flooding velocity was influenced by the presence of the local infrastructure (e.g. embankments). The downstream district Jamalpur was found to be more susceptible to flooding. The recent flood of the year 2020 has also shown a similar damage trend in Jamalpur (NAWG 2020).

This study aimed to gather new insights into the impact of tributaries on the Brahmaputra-Jamuna floods, by undertaking analyses that have not been conducted before. However, this study only accounted for Brahmaputra-Jamuna high flood (100-year return periods) condition. For a comprehensive understanding of the nature of Brahmaputra-Jamuna's tributaries, other types of scenarios (such as the high flood in Dharla-Teesta, normal flood in Jamuna etc.) can be investigated.

5 Conclusion

In this study, we investigate the influence of the flow of Teesta and Dharla river tributaries on flooding of the Brahmaputra-Jamuna. The study found that the rise of water level in the Dharla and Teesta rivers cause an increase in the water level of the Brahmaputra-Jamuna each time, which results in local floods, especially in char areas. The impact of Teesta is higher in terms of flood depth, duration and velocity compared to Dharla River. The downstream reach (i.e. Jamalpur district in this case) is more susceptible to tributary flooding. The char and inland flooding characteristics are significantly different. The flooding depth increases almost 25 times in char lands relative to inland flooding. The flood duration increases nearly 18 times in char lands and velocity may increase ninefold in char areas compared to inland areas. Therefore, similar flood adaptation techniques in inland and char areas may be inappropriate. It is expected that the results of this study will contribute to Brahmaputra-Jamuna's long-term flood risk management planning.

Acknowledgements This work was carried out under the Institute of Water and Flood Management (IWFM), BUET project titled "Developing Institutional Framework for Flood Preparedness Program (FPP)" funded by the National Resilience Programme (NRP) of the Government of

Bangladesh with the technical assistance of United Nations Development Programme (UNDP), UN Women and United Nations.

References

Albano, R., L. Mancusi, A. Sole, and J. Adamowski. 2017. FloodRisk: A Collaborative, Free and Open-Source Software for Flood Risk Analysis. *Geomatics, Natural Hazards and Risk* 8: 1812–1832. https://doi.org/10.1080/19475705.2017.1388854.

Archana, S., G. RD, and S. Nayan. 2012. RS-GIS Based Assessment of River Dynamics of Brahmaputra River in India. *Journal of Water Resource and Protection.* https://doi.org/10.4236/jwarp.2012.42008.

Best, J.L., P.J. Ashworth, M.H. Sarker, and J.E. Roden. 2007. The Brahmaputra-Jamuna River, Bangladesh. *Large Rivers: Geomorphology and Management*: 395–430.

Bhuiyan, S.R. 2014. Flood Hazard and Vulnerability Assessment in a Riverine Flood Prone Area: A Case Study.

Dewan, A., M. Nishigaki, and M. Komatsu. 2003. Floods in Bangladesh: A Comparative Hydrological Investigation on Two Catastrophic Events. *Journal of the Faculty of Environmental Science and Technology, Okayama University* 8: 53–62.

Dewan, T.H. 2015. Societal Impacts and Vulnerability to Floods in Bangladesh and Nepal. *Weather and Climate Extremes* 7: 36–42. https://doi.org/10.1016/j.wace.2014.11.001.

Ferdous, M.R., A. Wesselink, L. Brandimarte, G. Di Baldassarre, and M.M. Rahman. 2019. The Levee Effect Along the Jamuna River in Bangladesh. *Water International* 44: 496–519. https://doi.org/10.1080/02508060.2019.1619048.

FFWC. 2018. Annual Flood Report. *Bangladesh Water Development Board (BWDB).*

Islam, A., and J.U. Chowdhury. 2002. Hydrological Characteristics of the 1998 Flood in Major Rivers.

Karim, M.F., and N. Mimura. 2008. Impacts of Climate Change and Sea-Level Rise on Cyclonic Storm Surge Floods in Bangladesh. *Global Environmental Change, Globalisation and Environmental Governance: Is Another World Possible?* 18: 490–500. https://doi.org/10.1016/j.gloenvcha.2008.05.002.

Klaassen, G., and K. Vermeer. 1988. Confluence Scour in Large Braided Rivers with Fine Bed Material. In *Proceedings of the International Conference on Fluvial Hydraulics*, pp. 395–408. Budapest, Hung: Int. Assoc. Hydraul. Res.

Kvočka, D., R.A. Falconer, and M. Bray. 2016. Flood Hazard Assessment for Extreme Flood Events. *Natural Hazards* 84: 1569–1599. https://doi.org/10.1007/s11069-016-2501-z.

Lesser, G.R., J.A. Roelvink, J.A.T.M. van Kester, and G.S. Stelling. 2004. Development and Validation of a Three-Dimensional Morphological Model. *Coastal Engineering* 51: 883–915. https://doi.org/10.1016/j.coastaleng.2004.07.014.

Mamun, M.A., N. Huq, Z.F. Papia, S. Tasfina, and D. Gozal. 2019. Prevalence of Depression Among Bangladeshi Village Women Subsequent to a Natural Disaster: A Pilot Study. *Psychiatry Research* 276: 124–128.

Mechler, R., and L.M. Bouwer. 2015. Understanding Trends and Projections of Disaster Losses and Climate Change: Is Vulnerability the Missing Link? *Climatic Change* 133: 23–35. https://doi.org/10.1007/s10584-014-1141-0.

Mosselman, E. 2006. Bank Protection and River Training Along the Braided Brahmaputra-Jamuna River, Bangladesh. *Braided Rivers: Process, Deposits, Ecology and Management* 36: 279–287.

Munich Re. 2015. Weather Catastrophes and Climate Change. *Münchener Rückversicherungs-Gesellschaft*.

Nasreen, M. 2004. Disaster Research: Exploring Sociological Approach to Disaster in Bangladesh. *Bangladesh e-Journal of Sociology* 1: 1–8.

NAWG. 2020. Monsoon Floods 2020, Coordinated Preliminary Impact and Needs Assessment. Needs Assessment Working Group (NAWG), Bangladesh.

Pal, P.K., A. Rahman, and A. Yunus. 2017. Analysis on River Bank Erosion-Accretion and Bar Dynamics Using Multi-Temporal Satellite Images. *American Journal of Water Resources* 5: 132–141.

Paul, B.K. 2011. *Environmental Hazards and Disasters: Contexts, Perspectives and Management*. John Wiley & Sons.

Pramanik, M. 1991. Environmental Vulnerability in Bangladesh-Paper Presented in the UNDP. In *ESCAP Workshop on Regional Development Issues and Environment*, 18–21. Dhaka: Bangladesh, November.

Rahman, M.M., and M.M. Ali. 2016. Flood Inundation Mapping of Floodplain of the Jamuna River Using HEC-RAS and HEC-GeoRAS. *Journal of PU* 3: 24–32.

Schumm, S.A., and B.R. Winkley. 1994. *The Variability of Large Alluvial Rivers.* ASCE.

Shampa, 2019a. Hydro-Morphological Study of Braided River with Permeable Bank Protection Structure. Doctoral Thesis, Kyoto University 102.

Shampa, 2019b. Hydro-Morphological Study of Braided River with Permeable Bank Protection Structure. Thesis, Kyoto University, Japan 153.

Shampa, Y. Hasegawa, H. Nakagawa, H. Takebayashi, and K. Kawaike. 2017. Dynamics of Sand Bars in Braided River: A Case Study of Brahmaputra-Jamuna River. *Journal of Japan Society of Natural Disaster Science* 36: 121–135.

Uddin, K., B. Shrestha, and M.S. Alam. 2011. Assessment of Morphological Changes and Vulnerability of River Bank Erosion Alongside the River Jamuna Using Remote Sensing. *Journal of Earth Science and Engineering* 1.

Younus, M.A., R. Bedford, and M. Morad. 2007. Food Security Implications of Failure of Autonomous Crop Adaptation to Extreme Flood Events: A Case Study in Bangladesh.

Water Infrastructure and Development

Hybrid Coast Protection Approach in Bangladesh: A Case Study on Effectiveness of Small-Scale Forest in Reducing Surge Induced Inundation and Supporting Local Livelihoods

Mita Kazi Samsunnahar

Abstract Polders are subject to significant threats and often fail to protect the hinterland during cyclone induced storm surges. This study investigated the impact of mangrove afforestation in attenuating storm surge impacts on the embankment, as well as the social benefits of adapting this measure. Hydrodynamic model Delft-3D and ArcGIS 10.3 have been used to simulate, calculate and visualize coastal flood inundation condition. Primary and secondary source information were used to validate the model and assess social benefits of afforestation. For polder 47/4, the presence of 1.61 km^2 afforestation on the foreshore, protected additional 3 km^2 land from inundation during cyclone Sidr. While increasing polder height to 7 m slightly influenced inundation extent by reducing it 0.3 km^2, additional afforestation of the same roughness as exists now, helped to further reduce inundation depth in the hinterland. Social benefits provided by the existing forest were also considerable as local people collect fuelwood and Nipa palm regularly. While fuelwood was used for non-commercial uses, Nipa palm, on the other hand, was used by poor village women for preparing mats to sell at the local market. From the collected data, net benefit of this forest was calculated to be Tk. 5990.68 ($70.20)/hectare/year.

Keywords Storm surge · Coastal protection · Nature-based infrastructure · Afforestation · Social benefits

1 Introduction

As a vast majority of the world population lives near the coast (Nichols and Small 2002), protecting coastal zones from adverse climatic phenomena is a major concern. Over the last few decades, climate change risks, extreme weather conditions, coastal flooding etc. have been increasing and they are expected to further worsen in the future. Traditionally, coastal areas of the world have been protected by engineering structures which exhibit high effectiveness initially. But gradually, interference with

M. K. Samsunnahar (✉)
Davidson Laboratory, Stevens Institute of Technology, Hoboken, USA
e-mail: kmita@stevens.edu

© The Author(s), under exclusive license to Springer Nature Switzerland AG 2022

G. M. Tarekul Islam et al. (eds.), *Water Management: A View from Multidisciplinary Perspectives*,
https://doi.org/10.1007/978-3-030-95722-3_13

surrounding nature (De Vriend et al. 2015) and incapability to keep up with rapidly changing coastal conditions (Sutton-Grier et al. 2015), often undermines their original purpose (Jones et al. 2012). This has made researchers look for more sustainable and effective ecosystem-based solutions to the issue. Ecosystem-based Adaptation entails a wide range of ecosystem management activities targeted at increasing resilience and reducing vulnerability of people and the environment. Many new nature-based concepts with different names (De Vriend et al. 2015; Beck and Shepard 2012; Cheong et al. 2013; NYS 2013; Ferrario et al. 2014; Arkema et al. 2013) have been introduced, as recent global catastrophes, such as the Indian super cyclone, and hurricanes Katrina, Irene and Sandy, have raised awareness regarding the challenges and potential mitigation plans to protect people and property (Das and Vincent 2009; Reddy et al. 2016). Pure nature-based approaches are often not feasible because they take substantial amount of time and space to implement (Sutton-Grier et al. 2015). Using a combination of both built and natural infrastructures, it provides a scope to capitalize on the strengths of both, minimizing the weaknesses of each. This type of hybrid approach incorporates the intentioned use of natural and engineered features to produce engineering functions in combination with ecosystem services and social benefits (Bridges et al. 2013; Simm et al. 2016; Fink 2016), where "bio-based" solutions alone are likely to be ineffective. Examples from the USA (Heerden and Ll 2007) and the UK (van Slobbe et al. 2013) have shown tremendous performance of hybrid infrastructures during cyclones and regular wave action. Since the concept of hybrid infrastructure is new, no research has yet been conducted in the context of Bangladesh on this topic.

Bangladesh is widely recognized as one of the most disaster-prone countries of the world with its repetitive cycle of floods, cyclones and storm surges. The coastal zone is particularly vulnerable to climate-related impacts, especially cyclones, with a severe cyclone striking the Bangladesh coast every three years (GoB 2008). Loss of human lives and destruction of assets during these cyclones are primarily attributed to surge waves (Chowdhury et al. 1993). Major cyclonic storms of 1970 and 1991 together caused death of nearly half a million people and economic losses exceeded US$200 billion (Quadir 2008). Polders have always been under significant threat during cyclone, and failure of polders has caused severe damages to the housing and agricultural sector. During cyclone Sidr in 2007, total damages to over 2000 km of embankments and other critical water control structures amounted to about BDT 4.9 billion (US$71 million) (GoB 2008). The total length of embankment of 49 sea facing polders is 957 km, of which only 60 km has forest belts; and in many areas, the existing forest belt is degraded (Dasgupta et al. 2010). So, it is essential to take measures for enhancing the degree of protection of polders by providing afforestation.

Under the Coastal Embankment Rehabilitation Project (CERP- II), it was seen that afforestation in the foreshore area can play a very important role in the protection of embankments against wave action. Placed between "hard measures" like embankments, and the open sea greenbelts can help in reducing the impact of storm surge on the embankments, thereby increasing their lifespan and reducing the cost of maintenance and augmentation (CEGIS 2016). Moreover, it also has the potential of

providing significant amount of revenue through harvesting of forest resources. So, in the Coastal Embankment Improvement Project (CEIP-I), along with increasing polder height, Bangladesh Water Development Board (BWDB) has planned limited afforestation on the foreshore to protect the embankment and reduce maintenance cost.

Coastal greenbelts have long been seen as an important strategy for reducing the vulnerability of coastal populations to climate-related hazards in Bangladesh, and the country has over five decades of experience in coastal afforestation and reforestation. Over 140,000 ha of mangroves have been planted as social forestry along the coast since the 1960s (UNDP 2015). Also, to combat the adverse effects of climate change induced coastal hazards, the Bangladesh Forest Department (BFD) has initiated the afforestation project titled Climate Resilient Participatory Afforestation and Reforestation Project (CRPARP). While BWDB and BFD are separately taking measures to protect the coastal region, their efforts to integrate coastal embankment and coastal greenbelt planning and management have been limited till date (UNDP 2015). This study aims to demonstrate the possible outcomes of such an integration.

Also in delineating afforestation, previous studies have only considered width of afforestation, orientation of greenbelt and suitability of trees (CEGIS 2016) as design criteria for coastal belt. But if resistance provided by designed afforestation was considered, it would provide a smore comprehensive view about attaining desired protection during cyclonic storm surges. This study aims to take into consideration this important parameter along with afforestation width, to assess the effectiveness of hybrid intervention (integration of coastal embankment and foreshore afforestation) in providing protection.

Although several studies have been conducted to quantify the benefits of Sundarbans mangrove forest (Abdullah et al. 2016; Islam et al. 2019; Slam et al. 2020), very few studies have focused on community-based afforestation in the coastal belt of Bangladesh (Chow 2015). Understanding people's attitudes towards this type of small-scale afforestation project may help design them as part of social forestry programmes. Inclusion of benefits assessment of local people will increase the acceptability of hybrid intervention as a long-term adaptive measure to protect coastal communities from cyclonic hazards in Bangladesh.

2 Study area

This study was conducted in polder 47/4, situated at Kalapara upazila in Patuakhali district, which is a highly disaster-prone area of Bangladesh. Kalapara upazila (located at 21.9861°N and 90.2422°E) has a total area of 492.102 km^2, bounded by Amtoli upazila on the north and west, Rabnabad channel on the east and the Bay of Bengal to its south. The polders in Kalapara upazila are presented in Fig. 1. The Polder 47/4 is bounded by polder 46 on the north, polder 47/1, 47/2 and 47/3 on the west, polder 47/5 and Rabnabad channel on the east and Kuakata and the Bay of Bengal on the south (Fig. 1).

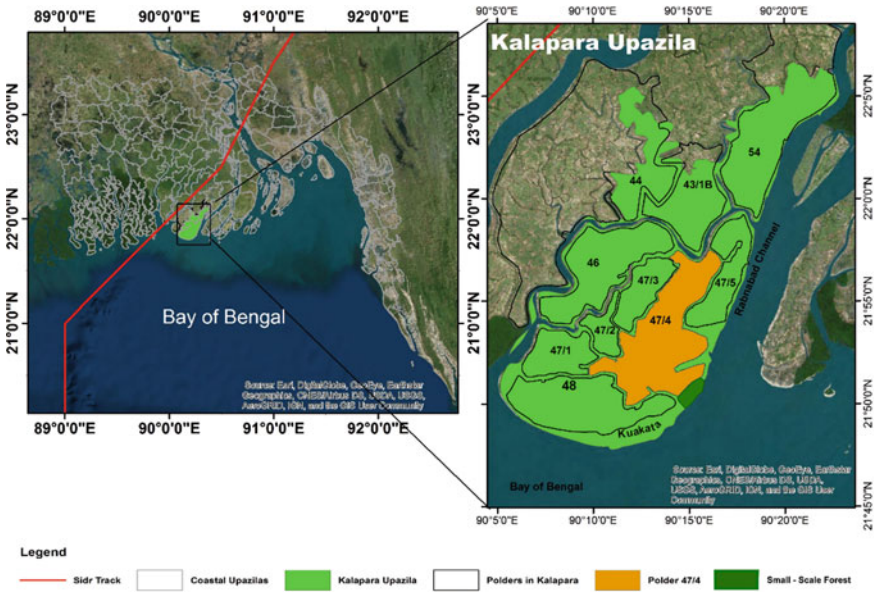

Fig. 1 Map of study area

Polder 47/4 was selected for this study due to its exposure to cyclones and cyclone induced storm surges. Because of its proximity to the sea and poor embankment condition, local people are severely affected by cyclones, storm surges and salinity intrusion, making this area as one of most climate vulnerable areas of Patuakhali (GoB 2013). In a reconnaissance survey, local people confirmed breaching of polder 47/4 at different points during Cyclone Sidr. Cyclones of moderate intensity like Aila and Mohasen have also damaged resources of this area. Since 1966, this polder has been performing as a defence mechanism against tidal flooding and storm surges. But in all these years, apart from occasional minor maintenance work, no noticeable rehabilitation work has been done. Thus, this polder has become vulnerable to extreme forces like storm surges. For this study, polder 47/4 represents a highly vulnerable exposed polder from the coastal region of Bangladesh. This polder has a small-scale mangrove forest, locally known as Dhulaswar Forest, consisting of mature trees along the foreshore of the embankment, which provides an ideal condition for conducting this research. The outcomes of this research will help to understand the general role of mangrove as an additional protective measure during extreme cyclonic events. Inclusion of benefits assessment of forest goods, along with assessing the role of mangrove plantation in reducing storm surge induced flood inundation for polder 47/4, will depict the suitability of hybrid intervention as a long-term adaptive measure at the community level.

3 Methodology

This study employs a technical perspective to investigate the effectiveness of mangrove plantation in the foreshore of the earthen embankment in protecting coastal communities from storm surge impacts. It also focuses on the social benefits of a small afforestation project in polder 47/4 by quantifying the services this small man-made forest provides to the local community. In this section, the methodology of data collection, description of models and tools and techniques related to the study are described.

3.1 Model Description

In this study, a calibrated and validated model of Bangladesh coast is set up using the Delft-3D hydrodynamic model, and then used to study the impact of mangrove afforestation in attenuating the devastating impact of storm surges. Delft3D hydrodynamic model is a computational tool which can simulate flow, sediment transports, waves, water quality, morphological developments and ecology for coastal, river and estuarine areas. Delft3D-FLOW solves the unsteady shallow water equation in two dimensions (depth-averaged) or in three dimensions (Delft Hydraulics 2006). Delft3D flow model coupled with the cyclone generated from the Delft-Dashboard is utilized to simulate coastal flooding for different cyclones. The data extracted from simulation has been processed using ArcGIS to produce maps.

3.2 Basic Model Setup

Delft-3D model domain extends from 21°03 ‘00 “N to 24° 00 ‘00 “N and 86°00 ‘00 “E to 94°00 “00 ‘E. The open sea is bounded parallel to latitude 20°00 ‘00 “N, and the land domain considers all the 19 coastal districts of Bangladesh. A detailed description of model domain, upstream and downstream boundary conditions, land topography, river bathymetry, land use and land cover data can be found in the study conducted by Al Azad et al. (2018). The model has been validated for Cyclone Mora (Al Azad et al. 2018), and cyclone Sidr (Mita 2019).

3.3 Modification of the model

Since the study area is a segment of the entire model, to modify this portion according to field data, several parameters such as polder height, width, actual polder height, mangrove afforestation properties (length, width, composition and density) etc. are

collected from the field for incorporating in the coastal model. In addition to field measurements, several Focus Group Discussions (FGDs) and Key Informant Interviews (KII) have been conducted. As Delft-3D considers impact of land cover as resistance, Manning's roughness coefficient is calculated from collected properties of trees. Detailed description of these methods will be discussed in this section.

3.3.1 Polder Height Modification

To better represent the existing height of polder in the model, primary data related to polder characteristics (width, slope etc.) is collected from several locations of polder 47/4. From collected data, height of polder is modified in the coastal model which initially had design height as input.

3.3.2 Quantification of Mangrove Plantation Properties

As for afforestation, general ideas regarding the area of the plantation, vegetation composition, vegetation characteristics etc. were acquired from Key Informant Interviews (KII) with foresters. Vegetation characteristics and vegetation composition were then observed during the transect walk. Later, using Google map/Satellite image, area of afforestation is determined again along with its length and width. The density of the plantation is represented as Manning's roughness coefficient in DELFT-3D model. In this study, Manning's roughness coefficient of existing forest is determined by using a direct technique (Chow 1959). In a densely wooded floodplain, size of tree trunks is a major contributing factor in determining roughness coefficient. In this type of locations, vegetation density can be calculated by counting the number of trees and measuring the trunk size of the trees in a representative sample area. The n value can be computed by using Eq. 1.

$$\mathrm{n} = n_0 \sqrt{1 + \left(\frac{c_* \sum A_i}{2gAL}\right)\left(\frac{1}{n_0}\right)^2} R^{4/3} \tag{1}$$

Where,

n_0= Manning's boundary-roughness coefficient excluding the effect of the vegetation (a base n),

C_*= The effective-drag coefficient for the vegetation in the direction of the flow,

ΣA_i=The total frontal area of vegetation blocking the flow in the reach,

G = The gravitational constant,

A = The cross-sectional area of the flow,

L = Length of the channel reach being considered, and.

R = The hydraulic radius.

Cowan (Chow 1959) developed a procedure for estimating the effects of these factors to determine the value of n for a channel. By altering Cowan's procedure, the

following equation is developed to compute the value of *n* for floodplain (Arcement & Schneider 1989),

$$n_0 = (n_b + n_1 + n_2 + n_3 + n_4)m \tag{2}$$

where,

n_b = a base value of *n* for floodplain's natural materials, n_1 = a correction factor for the effect of surface irregularities on the floodplain, n_2 = a value for variations in shape and size of the floodplain cross section, (value = 0 for floodplain), n_3 = a value for obstructions on the floodplain, n_4 = a value for vegetation and flow conditions on the floodplain and m = a correction factor for meandering of the channel (Value = 1 for floodplain).

Vegetation density calculation

Another required parameter for calculating Manning's n, vegetation density ($\frac{\sum A_i}{AL}$ term in Eq. 1), is determined for each subsection. To determine the roughness coefficient more accurately, data is collected from two subsections of the forest. Subsections are chosen based on spatial variance in tree density. A representative sample area of 30 m by 15 m is chosen to represent the roughness of the subsections accurately. The floodplain is divided into subsections based on spatial geometric and (or) roughness differences in different parts of the forest. In this study, two sample areas of 15 m by 15 m along the cross section and in the flow direction are taken to calculate roughness. The representative sections are selected based on the recommendation of local foresters for obtaining close to accurate representative vegetation density. A section of 15 m length perpendicular to the flow direction is marked in the sample area. Every tree within 7.5 m along either side of this marked line is counted. The total area occupied by the trees ($\sum A_i$) in the sampling area can be computed from the number of trees, their diameter and the depth of flow in the floodplain. Once the vegetation area, $\sum A_i$, is determined, the vegetation density can be computed by using following equation,

$$Veg_g = \frac{\sum A_i}{AL} = \frac{h \sum n_i d_i}{hwl} \tag{3}$$

where,

$\sum n_i d_i$ = the summation of number of trees multiplied by tree diameters, h = height of water in floodplain, w = width of sample area and l = length of sample area.

3.4 Assessing Benefits of Livelihood Groups

To ensure sustainability of the plantation, it is very important to involve the local community in the process of operation and maintenance. That will only be possible if the plantation can be considered as community resources. Quantification of

extractable benefits from small-scale plantation can help policy makers, relevant implementing agencies and the local people to better understand its impact the on local economy, and accordingly design the plantation in a manner whereby locals can get benefited without the main purpose of the plantation being harmed.

To assess the benefits of different local people from mangrove plantation, Participatory Rural Appraisal (PRA) tools, such as, Focus Group Discussions (FGD), Key Informant Interviews (KII) have been used. Field visits were made to the study area to collect data about the dependency of people on forest resources. In three different Focus Group Discussions with local people living in proximity to forest areas, data regarding the quantity of different goods extracted from forest, purpose of collection and the market value of each good were collected. Total collection quantities, costs, gross values and net values of fuelwood and other goods are calculated from estimated harvests. Seasonal variation in the extraction of materials from the forest has also been given emphasis while collecting data. Also, during FGDs, variation in dependency is also sorted into three different categories. During several Key Informant Interviews with residents as well as local foresters, data collected during FGD are cross-checked. Later using all collected data, the formulation of total net value density, or periodic net benefits (PNB) per hectare, for a forest patch a is calculated using the conceptual model developed by Chow (2015). The fundamental equation is:

$$\mathrm{PNB_a/ha} = \left(\sum_i \sum_g \left[(P_a - C_G(D_a)) X_g - F_g \right]_{a,i} - M_a \right) \Big/ H_a \tag{4}$$

Where for every good g and collector i,

P_g = the market price, C_G = the variable production cost (e.g. transportation cost), X_g = the extracted quantity, F_g = the fixed production cost, M_a = the forest management cost (in this case paid by government), H_a = the patch size and D_a = the distance of forest patch from the village.

4 Results and discussions

The results of this study are presented in two parts: the first part will focus on the numerical simulations of several scenarios to demonstrate how the presence of plantation can influence storm surge induced flooding during Cyclone Sidr (IMD 2021), which is one of the most devastating cyclones in the history of Bangladesh (JSCE 2008a) and the most destructive one for polder 47/4. In the second part, the benefits of residents from this small-scale plantation will be presented to address several important yet understated factors, that are important for designing this hybrid approach in a sustainable manner.

4.1 Effectiveness of Plantation on Reducing Surge Induced Flooding

The roughness value for the floodplain is determined by selecting a base value (n_b) for the natural bare soil surface of the floodplain, and then adding adjustment factors due to vegetation density, irregularity in surface and obstructions in flow path by using Eq. 2. The adjustments are made based on observation, judgement, experience and guidance from previous studies (Chow 1959). For this study, the base roughness (n_b) is assumed to be 0.025 which is consistent with assumptions made by Jisan et al. (2018) and Zhang et al. (2012). Using Eq. 2, Manning's boundary-roughness coefficient excluding the vegetation in two subsections are calculated to be 0.31 and 0.53, respectively, after making reasonable assumptions. The values of vegetation density from field measurements are 0.35 and 0.5, respectively. Then using Eq. 1, the Manning's roughness coefficient values for two subsections are 0.11 and 0.13. For simplicity, the average of two values 0.12 has been used in the model to represent the forest. The polder height has been measured in several locations and the average measured value of 4.51 m has been incorporated in the model. As mentioned earlier, Cyclone Sidr making landfall to the west of the study area is simulated to assess the effectiveness of plantation in reducing storm surge impacts. Generally, the portion of coastline which experiences onshore winds, usually experience high surge levels and vice versa (Needham and Keim 2011). So, ideally, if the forest is present in the onshore wind direction, it will provide additional resistance to the storm surge. Cyclone Sidr brought onshore winds and a high storm surge on the existing Dhulaswar forest, and thus it is considered as an ideal scenario for studying the effectiveness of afforestation in reducing storm surge impacts. In case of cyclones making landfall in the central and eastern region of the Bangladesh coast, the wind will blow in the offshore direction during cyclone landfall near Dhulaswar forest. This is due to anticlockwise rotation of the cyclone system. So theoretically, the area will experience negative to no surge. But due to weather anomalies, the water level may get higher than usual in few post-landfall tide cycles, and in this case, the forest will provide additional resistance. The forest also protects the embankment from regular tidal water-level fluctuations and wave actions. Assessing the effectiveness of afforestation during tidal conditions and various wave actions is beyond the scope of this study.

4.2 Scenario One: Role of Existing Afforestation

Inundation map from the model generated data is presented below (Fig. 2) for this scenario. From this map, it is observed that heavy inundation has occurred in the north-eastern side of the afforestation. Maximum inundation depth is more than 3 m. Slight inundation (depth 0.01–0.5 m) is observed in the land behind the afforestation. Distribution of inundated land under determined categories is given in Fig. 7. Here,

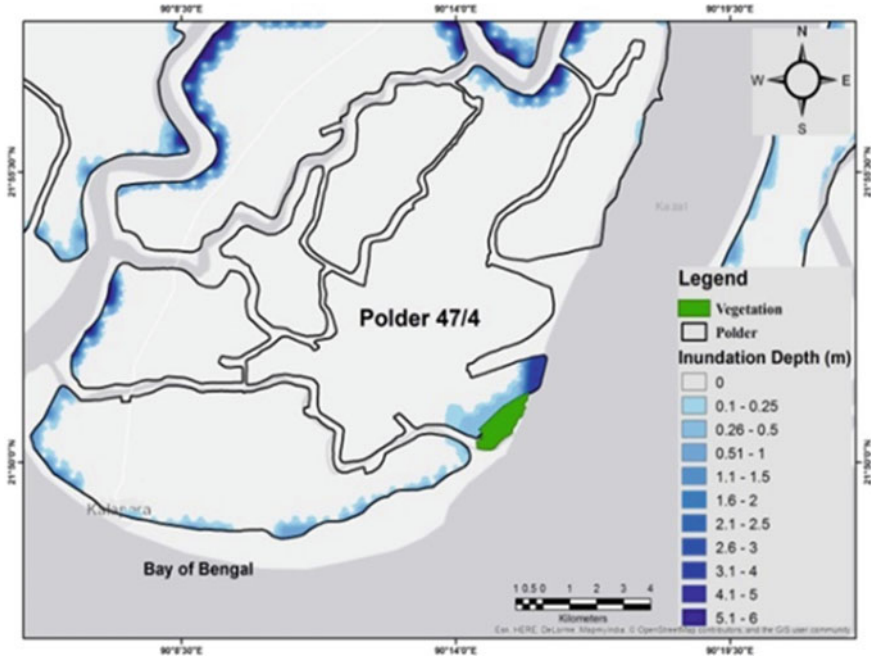

Fig. 2 Inundation map of polder 47/4 considering existing afforestation

inundation free land inside the polder is about 63.69 km^2. About 6.63% of the land inside this polder is inundated during cyclone Sidr.

During the field visits, local people verified that the flooding occurred from the exact location where the model simulated result shows significant inundation during cyclone Sidr (Fig. 3). As a result, the polder was breached, and later they repaired the polder. After a year of Sidr, while doing maintenance work, BWDB also took additional measures to protect the slope. When asked about water depth during Sidr, responses from locals varied widely. Some claimed that the highest water depth reached about 10–12 ft (3.05–3.66 m), while others suggested the highest level to be 15–18 ft (4.57–5.49 m). However, the polder started breaching when the water level reached about 4.5 ft. (1.37 m), according to people residing near the polder.

4.3 Scenario Two: Without Afforestation on the Foreshore

In this hypothetical scenario, the role of Dhulaswar mangrove forest is tested by assuming absence of plantation on the foreshore of the polder. It can be observed from Fig. 4 that the inundated area has increased from the previous scenario. Especially behind the imaginary barren land, the inundation has increased, which implies that presence of afforestation had previously reduced inundation in this portion. Overall,

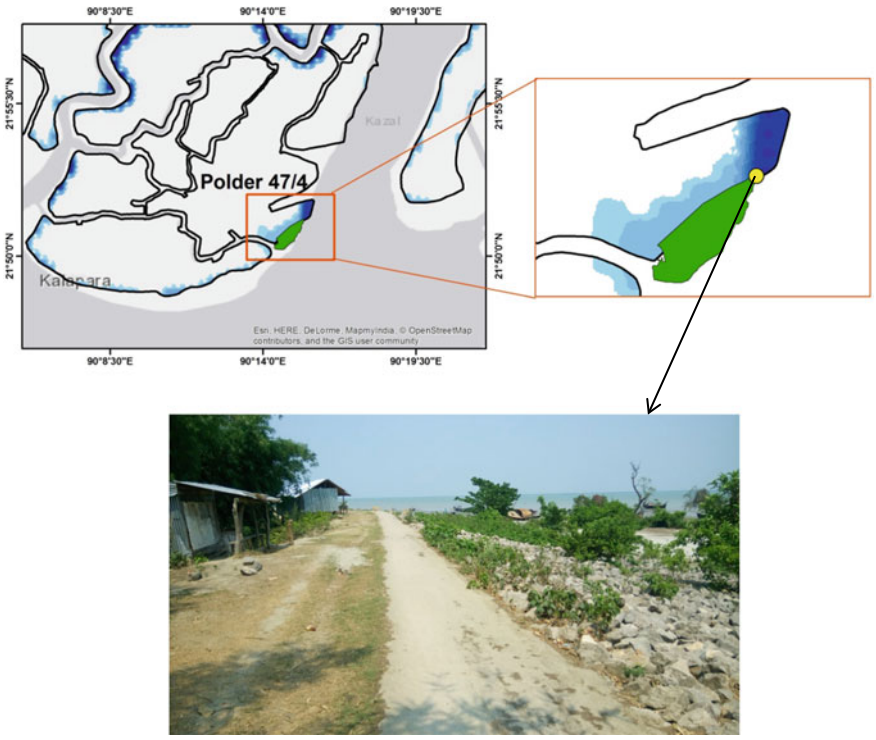

Fig. 3 Inundated area from model and image taken from field visit of same location

10.60% of the area under polder 47/4 is inundated in the absence of afforestation on the foreshore. The total inundation free area has reduced to about 60 km^2 (Fig. 7).

Comparing Figs. 3 and 4, it can be said that the presence of small-scale mangrove forest on the foreshore has played a significant role in reducing inundation in polder 47/4. Presence of this small-scale forest saved additional 3 km2 land from surge induced inundation.

4.4 Scenario Three: Conventional Coast Protection Approach (Actual Afforestation with Polder Height 7 m)

Traditionally, the Bangladesh coast has been protected by polders from storm surges and tidal flooding. Under the CEIP project of BWDB, the adjacent polder (polder 48) is to be raised as high as 7 m to protect the area inside the polder from coastal flooding, as the current height has proved to be inadequate in past few events. Since neither the present polder height nor the afforestation is deemed adequate to provide protection from storm surges during cyclone Sidr, this scenario assesses the effect

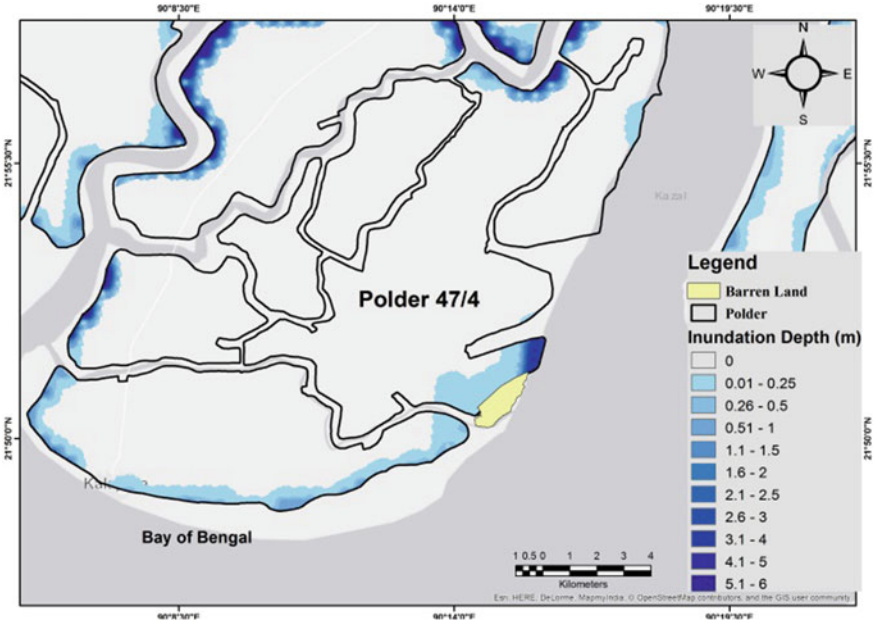

Fig. 4 Inundation map of polder 47/4 without afforestation on the foreshore

an increase in polder height can have on flooding conditions. So, the polder is taken as 7 m high for this scenario and pictorial representation of the results are given in Fig. 5.

Here, as it is seen in Figs. 2 and 5, the rise of polder from 4.73 m to 7 m does not exhibit a substantial change in inundation free area. When polder height is increased, the inundation free area has increased to slightly higher than the existing polder with the afforestation on the foreshore (63.39 to 63.71 km^2), reducing area of low inundation water depth (Fig. 7). Area under high water depth remains unaffected although the polder height is increased by almost 2.5 m.

4.5 Scenario Four: Hybrid Intervention (Increased Afforestation Area with Existing Polder Height)

As the polder height of 7 m is not adequate to prevent flooding inside the polder, in this case, the most affected portion on polder is covered by about 1.2 km width of hypothetical plantation on the foreshore, keeping the polder height 4.5 m. The width is determined considering width of existing forest and available land on the foreshore. Here, the map shows that the afforestation is very effective in decreasing inundation depth in the vulnerable portion of the polder (Fig. 6). The maximum water depth plummeted to below 1 m from previous depth of about 3 m inside the

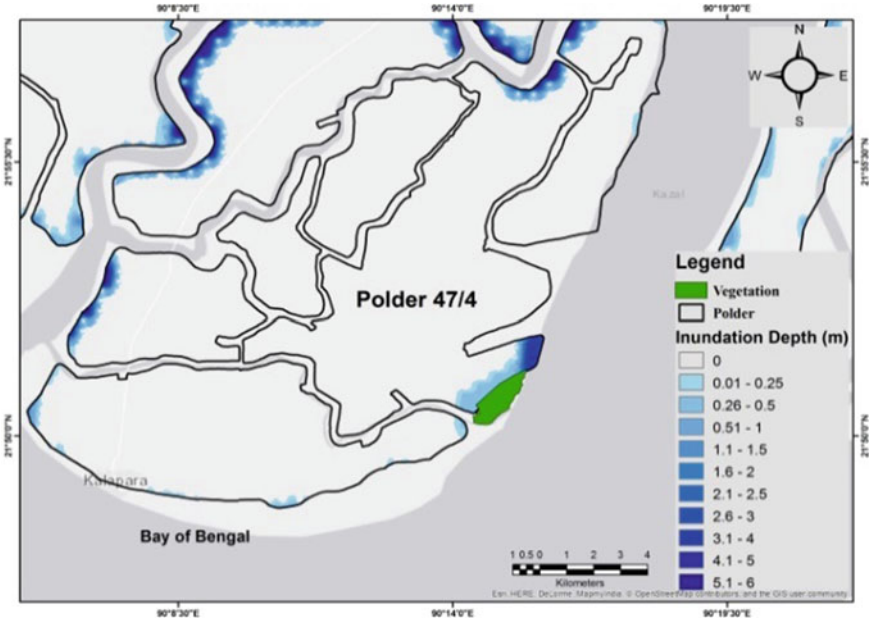

Fig. 5 Inundation map of polder 47/4 increasing polder height to 7 m along with existing afforestation on the foreshore

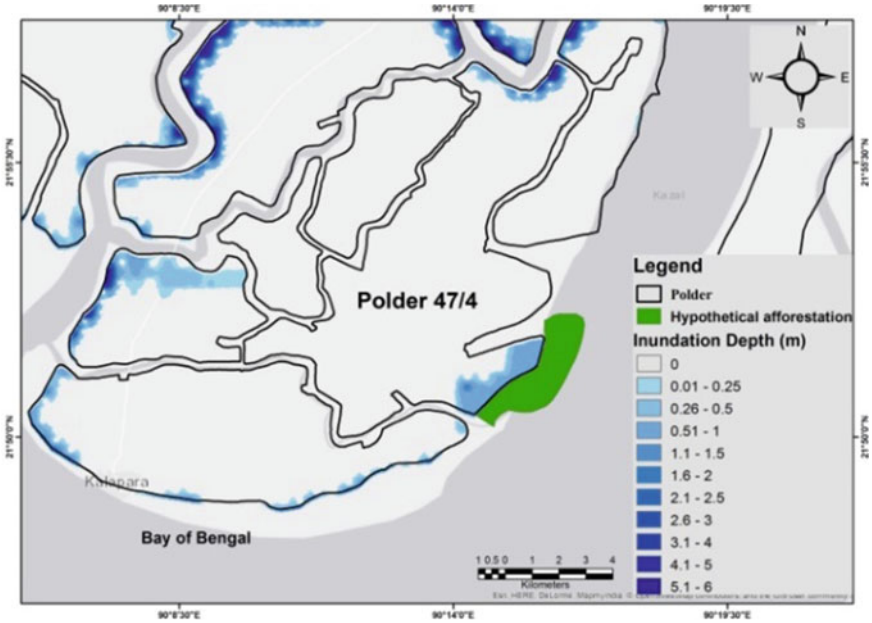

Fig. 6 Inundation map of polder 47/4 increasing afforestation area on the foreshore along with existing polder having height of 4.73 m

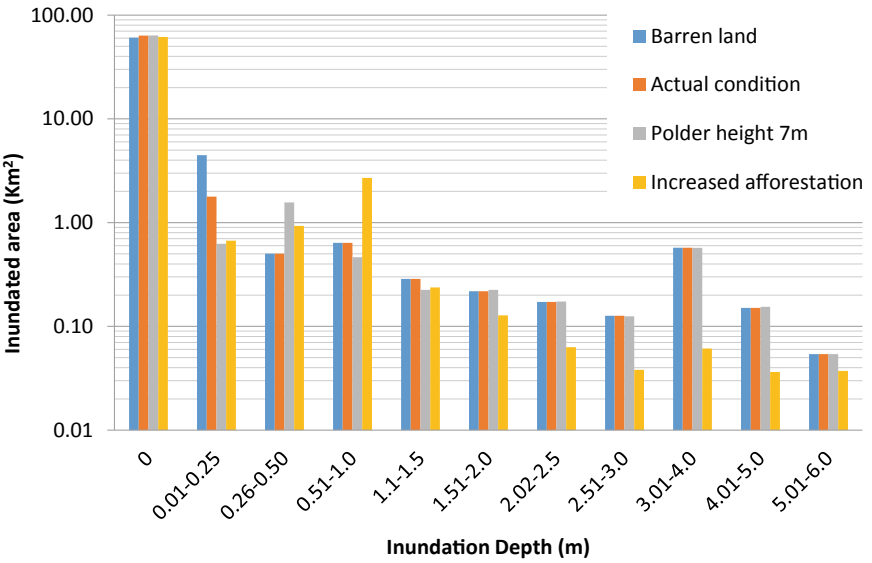

Fig. 7 Classification of inundated area for different inundation water categories

polder. From Fig. 6, it is found that, increased afforestation has significant impact in reducing higher surge depth inside the polder.

4.6 Comparison of Scenarios

For polder 47/4, it is true that existing afforestation exhibits a positive impact on attenuating storm surge inundation inside the polder during cyclone Sidr, as inundation free area increased from 60.70 to 63.40 km^2 with the presence of existing afforestation. In other words, if Dhulaswar reserved forest was not present in the foreshore, the inundated area would be about 3 km^2 area more. Conventional approach of increasing polder height, however, does not play a significant role in reducing inundation extent for this polder for cyclone Sidr. A polder height of 7 m can free 63.7 km^2 areas from inundation, which is 0.3 km^2 more than the inundation free land for existing condition. So, only increasing polder height may not be the most viable solution to keep the polder area protected. While there is a change in overall inundation area, as the modelled forest is same as found in the field, efficacy of presence of plantation is not properly visible, as the most vulnerable portion of the polder is beyond forest coverage. Because of that, in the following Fig. 6, for first three scenarios, variations in inundated area for higher water depths (1.5 m–6.0 m) have not changed. When the vulnerable portion of polder is covered by forest, area under higher water depth (1.5 m–6.0 m) reduced (Fig. 7) significantly, although a

noticeable reduction in inundation free area is not observed. Local complex hydrodynamics and intricate network of water bodies often play a pivotal role in determining the efficacy of afforestation measures. Even if the spatial extent (horizontal extent) of flooding remains unaffected, water depth over land (vertical extent) can be significantly reduced by afforestation. In this case, proposed increased afforestation scenario is very effective.

4.7 Social Benefits of Mangrove Afforestation

Afforestation does not only function as a shield during storm surges, it also provides local people with fuelwood, leaf litter, leaves for thatch, poles for construction, honey, cattle fodder etc. all year round. Data for assessing the benefits of mangrove afforestation has been collected from the residents of Dhulaswar village. Two FGDs were conducted directly by the author. Because of local norms, females were reluctant to speak publicly and hence the author interviewed a few of them individually. Apart from this, several KIIs were conducted with local foresters, the Executive Engineer of the Bangladesh Water Development Board (BWDB) and local community members.

During the focus group discussions and interviews it appeared that local people are very aware regarding the benefits of local afforestation. All of them agreed that Dhulaswar forest is an important resource for their village, and they concede with the fact that this forest needs to be protected. Among the ecosystem services the forest offers, local people mentioned that they are directly benefitted from the forest as they collect fuelwood and leaves, use the forest as gazing ground and collect raw materials to make mats. They also acknowledge that during adverse weather, the forest works as a protective shield. In general, when the sea is rough, afforestation in the foreshore reduces the impact of stormy winds in the hinterland. Local people could also recall the service provided by the afforestation during cyclone Sidr. During FGDs, they claimed that, during cyclone Sidr, the afforestation protected the embankment behind it from surge waves. As a result, the embankment only breached where it is exposed to the sea. They believe, if the afforestation did not exist, the damages would have been much greater than it actually were.

4.7.1 Collected Goods and Uses

Among numerous extractable and non-extractable benefits provided by the small-scale forests, in this study, dominant extractable benefits have been quantified. The Forest Department prohibits the felling of whole trees but allows the collection of non-main stem material such as branches, leaves and pneumatophores. Residents of Dhulaswar village mainly collect firewood (mainly wood branches and dried leaves) and Nipa palm (Locally known as Kewa pata). Nipa palm (Nypa fruticans) is easily found in this forest and the adjacent area. During high tides and rainy season, the forage area in the forest is considerably limited to local people. During low tides,

people can collect fuelwood from anywhere in the forest. As the forest is adjacent to the embankment (used as village road), local people can easily access the forest on foot. Moreover, as locals can extract regenerable mangrove species, they only need permission from local foresters to enter the forest. According to the beneficiaries, collected wood from this forest is not used for commercial purposes. All the families use the collected fuelwood for cooking. Contrary to fuelwood, Nipa Palm is collected to make mats, which are later sold at the village market.

4.7.2 Variation in Collection Patterns for Fuelwood

During data collection, local people were also requested to point out governing parameters affecting their forage for goods throughout the year. Among several issues, such as the distance of forest from home, safety, available work force, transportation facilities and seasonal variation, it is found from the discussion that the amount of goods collected from forest and the frequency, largely varies with the distance of household from the forest, and also with the season. Detailed analyses of these parameters are discussed below:

(i) Variation in collection pattern with distance.

Figure 8 represents the change in dependency on mangrove plantation for fuelwood as a function of distance. The figure is prepared from information collected during FGDs with active participation of local people.

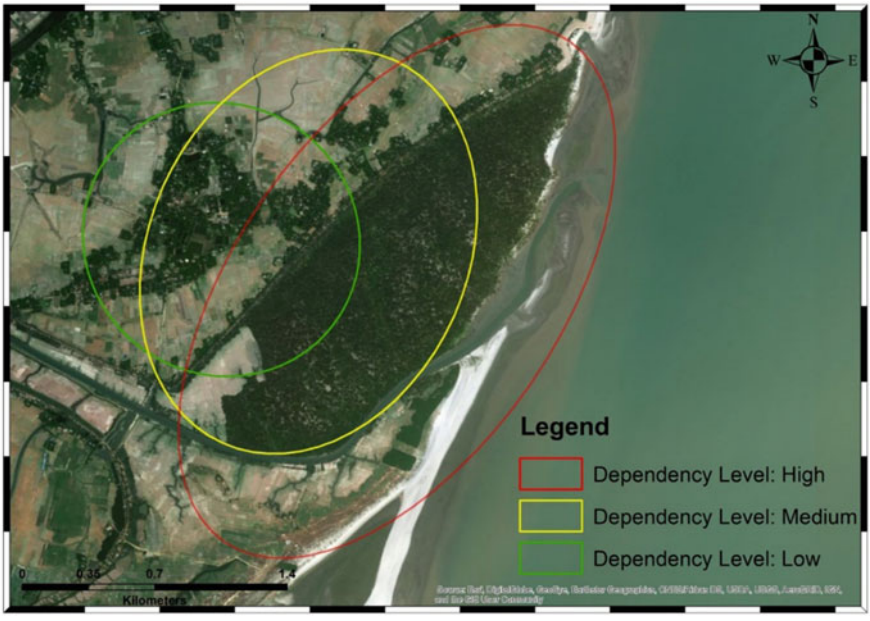

Fig. 8 Variation of dependency on forest for fuelwood with distance

In Fig. 8, the ellipsoids depict the level of dependency of local people on the forest for combustible fuelwood. People living adjacent to the forest depend highly on the forest and they forage almost the entire afforested area to collect wood (marked by the red ellipsoid in the Fig. 8). There are about 60 families living in the red zone, and the forest provides about 65% of total fuelwood consumed in a year. From the edge of the forest, people living in about a strip of roughly 350 m–450 m are benefitted the most from this afforestation of about 1.7 km^2 (represented as red ellipsoid in the Fig. 8). By the yellow ellipsoid, families of medium dependency are categorized along with their forage distance. As estimated number of 80 families living in about 400 m distance from the end of red zone fall in this category. Nearly 42% of annual needs of residents in this zone are fulfilled with firewood from this mangrove forest. The forage area of residents of this category is marked by yellow ellipsoid. Lastly, about 25 families living in a strip of 200 m–320 m (marked as green ellipsoid) is slightly dependent on the forest for fuelwood. About 25% of required fuelwood is collected from this forest. The remaining demand for firewood is fulfilled by non-mangrove trees, which local businessmen sell at village markets. From the collected data, it can be seen that as the distance between residence and forest increases, the dependency level for fuelwood collection decreases significantly. During FGDs, local people pointed out a number of reasons for this. First, there is no convenient local transport to move collected fuelwood. People usually walk on foot towards their destination after collecting wood, which hinders significant amount of fuelwood collection at a time. As a result of this inconvenience, people living 1 to 1.5 km away from the afforestation, prefer to buy their wood from the weekly village market. People living outside the ellipsoids rarely collect goods from the forest, and hence they are excluded from further data analysis.

(ii) Seasonal variation in the collection of fuelwood.

In addition to the distance, dependency of local people on the mangrove plantation generally varies with the change in seasons. During FGDs, local people split an entire year into two distinct categories considering the frequency of foraging and the extracted quantity of firewood. These are summer and dry season. According to them, summer season lasts from April to September, and dry season is from October to March. During the FGDs, people estimated their average dependence on the mangrove plantation for firewood by estimating the percentage of required fuelwood collected in a month, frequency of foraging and the monthly extracted quantity of firewood. The seasonal variation of three categories of users and related data are represented in the Table 1.

As presented in Table 1, according to local people, people of high, medium and low dependency extract more of their required fuelwood during dry season than summer. During summer, dependence of people on the forest decreases significantly. For people with medium and low dependency for fuelwood, an even sharper decrease is observed. This is because during majority of the summer season, the weather is very hot and humid, and sometimes, because of torrential rain, all the dried leaves and dead branches are dampened, making them difficult to use. As a result, people in general find it inconvenient to collect wet fuelwood. Especially, people living at a significant distance from the forest, find it very difficult to forage. As mentioned

Table 1 Seasonal variation in the collection of fuelwood

Property	Season	Dependency Level		
		High	Medium	Low
Percentage of fuelwood collected (monthly need)	Summer	40%	15%	5–7%
	Dry	90%	70%	40%
Frequency of forage (Monthly)	Summer	8–10 times	3–4 times	1–2 times
	Dry	At least 16 times	8–10 times	4–8 times
Monthly Extracted Quantity (in Kgs)	Summer	40–60	30–35	20
	Dry	90–120	60–85	Less than 40

*All the values presented in the table are approximated by local stakeholders

earlier, the road network of the village is also not good enough, so they are unable to use any vehicles to move the fuelwood. So, people are not willing to go through the trouble of collecting wet fuel, carrying them on foot and then drying them before using in the summer season. So, they mostly prefer to buy fuel from the local market. As a result, the frequency of forage drops largely during the summer. However, in the winter or dry season, residents of the village, both men and women, are more willing to collect fuelwood from the forest. As the weather is more convenient during the winter, it is less tiresome for people to collect wood and carry it back to their home. Since the weather is mostly sunny during the winter, people often collect slightly wet wood and later dry it at home before using.

Figure 9 illustrates the seasonal benefit provided by the forest for three types of users. As stated earlier, overall people get more benefits in the winter than in the summer season. Though people with high dependency levels gets more benefit as individual households, in this Figure, households under medium dependency show a seasonal benefit of about Tk. 745.34 ($8.73) which is greater than for the high dependency zone (Tk. 670.81/ $7.86). This is because the number of households in this category is 20 greater than that of the high dependency ones. For summer season, however, seasonal benefit remains inversely proportional to the distance, despite the population in the medium dependency zone being considerably larger. Beneficiaries with low dependency levels, show very little use of fuelwood (in monetary terms) both in winter (Tk. 93.17/ $1.09) and summer (Tk. 46.58/$0.55).

4.7.3 Benefits Provided by Nipa Palm

Nipa Palm is mainly collected and used by village women to make mats which are later sold in the weekly village market. It is mostly women from unprivileged families who are engaged in making mats. From interviews with local women, it is found that mats prepared from Nipa Palm make significant contributions to the monthly income of about 20–25 families. On average, each family can make 10 mats a week. Later these mats are sold at the village market by male members of the families. Presence of afforestation has thereby created a source of income for underprivileged women.

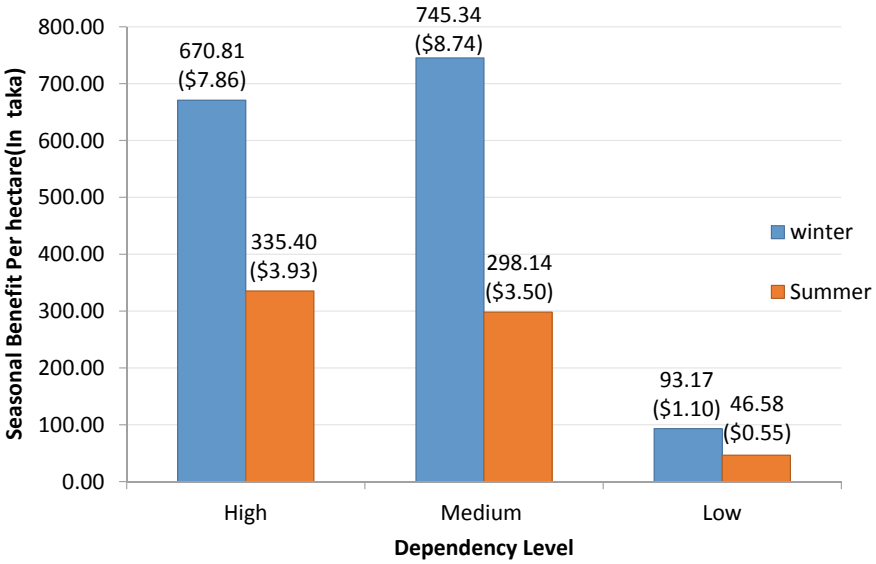

Fig. 9 Comparative change in seasonal benefit per hectare for fuelwood in three categories of user. (1 USD = 85.34Taka, August 2021)

4.7.4 Net Benefit Per Hectare

Net benefit of Dhulaswar forest has been calculated using conceptual model (Eq. 4). For this forest, locals claimed that there are no transportation costs (fixed or variable) involved. Also, collectors never use fuelwood for commercial purposes. So, the benefits provided by the forest for fuelwood is only the market value of the good, which is Tk. 2.6 (US$0.03) per kilogram in this study. Each mat prepared from Nipa palm is sold at about Tk. 120 (US$1.41) in the local market. The transportation cost of carrying these mats to the market is slightly more than Tk. 100 (US$1.17) per month. So, the benefit provided by Nipa Palm is calculated from subtracting the transportation cost from the market price of the mats. Also, from FGDs with the local forester, management cost of the forest (in this case provided by the Forest Department) is found to be Tk. 9000 (US$105.46) per month. Lastly, the summation of net benefits of each product is then divided by the area of afforestation which is 161 hectares. All these data are used in the conceptual model to get Table 2.

5 Conclusions

This study was conducted to examine the effectiveness of mangrove plantation in reducing storm surge induced inundation, and in the provision of services to local people at polder 47/4 in Kalapara Upazila of Patuakhali district in Bangladesh. A

Table 2 Calculation of net benefit per hectare

Products	Benefit Per year (in taka)	Variable cost per year in taka	Management cost per year (in taka)	Net benefit/hectare/year (in Taka)
Fuel wood	3,52,500 ($4130.53)	0	1,08,000 ($1265.52)	5990.68 ($70.20)
Nipa Palm	69,600 ($815.56)	2,400 ($28.12)		

validated coastal model of Bangladesh was used to simulate and analyze how the presence of small-scale plantation can have a positive impact in reducing flood inundation during cyclone Sidr. For Dhulaswar reserved forest in polder 47/4, existence of this forest has been found to have saved an additional 3 km^2 from coastal flooding during cyclone Sidr. Comparing conventional coast protection approaches with hybrid intervention, it is found that providing plantation to offer predetermined resistance can be integrated as a feasible alternative, with existing polder height in lieu of increasing polder height in places where land is available or because of local hydrodynamics during cyclone, a certain portion of polder poses more threat to breach.

Plantation also offers economic benefits to local people. In case of polder 47/4, services provided by the mangrove ecosystem vary with the distance of the forest from households, and there is also a seasonal variation in terms of foraging. These can be important factors in determining the composition of vegetation species for the coastal green belt, especially if the plantation project is designed as participatory forestry. In this study, direct extractable benefits from Dhulaswar forest are quantified to be Tk. 5990.68 (US$70.20) per hectare per year.

Appendix

Model Domain

Validation of Model for Cyclone Sidr

From storm surge validation, trial runs are executed in Delft-Dashboard. The simulations also include tidal constituents from open boundary for both events. For the Sidr 2007 cyclone, Indian Meteorological Department (IMD) estimated maximum wind speeds of about 60 m/s during landfall and the lowest central pressure of the cyclone to be 944 hPa with a pressure drop of 66 hPa during landfall. The couple model run was performed for the entire cyclone period of 5 days from its generation at 0000 UTC, 11 November 2007, to its dissipation on 0000 UTC, 16 November 2007.

The model results were observed to perform well while calculating the inundation extent for S 2007 (Fig. 11). High water-level values were also extracted for the same

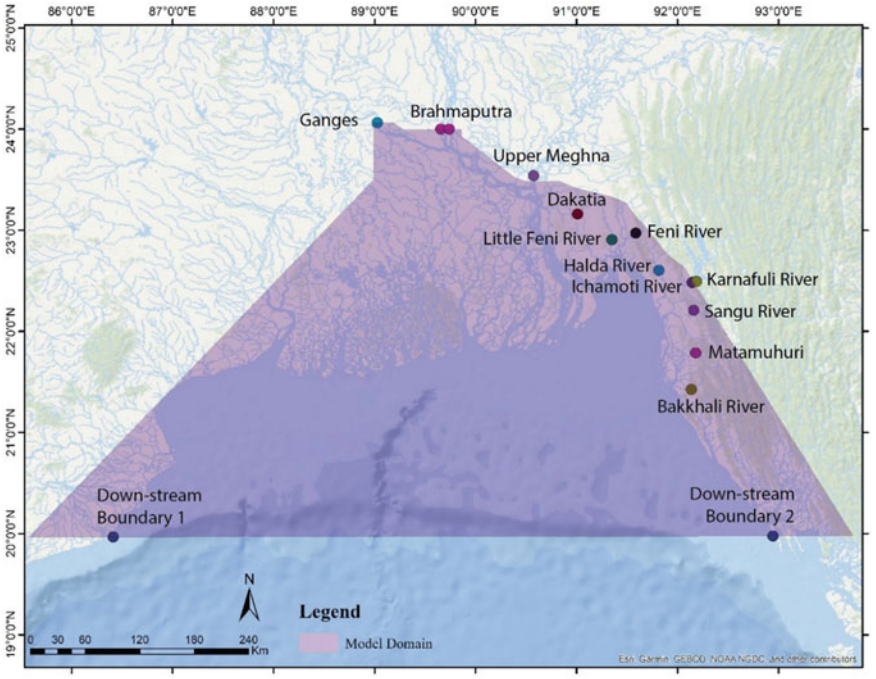

Fig. 10 Model domain along with upstream and downstream boundary of the model. (Al Azad et al. 2018)

locations (Table 3) from previous studies conducted by JSCE, 2008b, Lewis et al. 2013 and Deb and Ferreira, 2017 (Table 3). The computed storm surge was found to vary between 2.0 and 6.0 m along the coastal districts and estuaries where Sidr 2007 made landfall, and previous studies also demonstrated similar results on the same locations (Table 3).

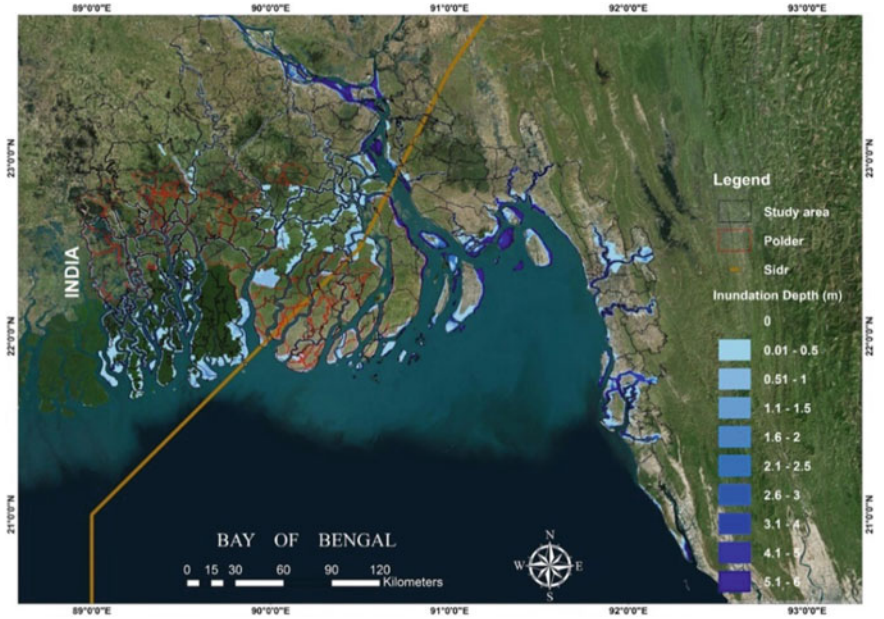

Fig. 11 Inundation map of cyclone Sidr. (Haque et al., 2018)

Table 3 Comparison of model outcomes with high water levels (HWLs) extracted from existing studies on storm surge modelling in Bangladesh coast for cyclone Sidr

Location	Hiron Point	Khepupara	Chittagong	Cox's Bazar
Coordinates	21.81	21.88	22.19	21.46
	89.49	90.10	91.92	91.92
Model data	2.31	5.86	3.12	2.1
JSCE,2008	2.2	5.9	3.0	2.0
% of error (between Model data and JSCE 2008)	−5%	0.68%	−4%	−5%
Lewis et al. (2013)	2.5	5.5	3.2	2.0
% of error (between model data and Lewis et al., 2013)	7.6%	−6.55%	2.5%	−5%
Deb and Ferreira (2017)	2.5	6.0	3.0	1.7
% of error (between model data and Deb and Fererra 2016)	7.6%	2.33%	−4%	−23.53%

Sample Area for Manning's Roughness Calculation

Fig. 12 Manning's roughness calculation sample area (a) Section-1: less dense area (represented by orange box) and another one is (b) Section-2: comparatively denser area (represented by the blue box)

Polder Height Measurement

Table 4 Measured dimensions of polder at selected locations

Location	GPS coordinate (in decimal degree))	Height (m)	Width(m)	Landward slope (degree)	Seaward slope (degree)
Point 1	21.8479, 90.2453	4.8	4.8	55	42
point 2	21.8413, 90.2385	5.43	4.01	60	44
Point 3	21.8443, 90.2192	3	4.42	69	50

Fig. 13 Photos of locals collecting and using firewood and nipa plam from the forest (*Source* Author)

Fig. 13 (continued)

Fig. 13 (continued)

Fig. 13 (continued)

References

Abdullah, Abu Nasar, Natasha Stacey Mohammad, Stephen T. Garnett, and Bronwyn Myers. 2016. Economic Dependence on Mangrove Forest Resources for Livelihoods in the Sundarbans, Bangladesh. *Forest Policy and Economics* 64: 15–24. https://doi.org/10.1016/j.forpol.2015.12.00.

Al Azad, A. S. M. Alauddin, Kazi Samsunnahar Mita, Md Zaman, Marin Akter, Tansir Zaman Asik, Anisul Haque, Mohammad Asad Hussain, and Md Rahman. 2018. Impact of tidal phase on inundation and thrust force due to Storm Surge. *Journal of Marine Science and Engineering* 6 (4): 110. https://doi.org/10.3390/jmse6040110.

Arcement Jr, G. J., & Verne R. Schneider. 1989. *Guide for Selecting Manning's Roughness Coefficients for Natural Channels and Flood Plains.* United States Geological Survey Water-supply Paper 2339. https://doi.org/10.3133/wsp2339.

Arkema, Katie K., Greg Guannel, Gregory Verutes, Spencer A. Wood, Anne Guerry, Mary Ruckelshaus, Peter Kareiva, Martin Lacayo, and Jessica M. Silver. 2013. Coastal Habitats Shield People and Property from Sea-Level Rise and Storms. *Nature Climate Change* 3 (10): 913–918. https://doi.org/10.1038/nclimate1944.

Beck, Michael W., and C. Shepard. 2012. *Coastal Habitats and Risk Reduction.* World Risk Report. Berlin: Bundnis Entwicklung Hilft.

Bridges, Todd, R. Henn, S. Komlos, D. Scerno, T. Wamsley, and K. White. 2013. *Coastal Risk Reduction and Resilience: Using the Full Array of Measures.* Washington, DC. http://sagecoast.org/docs/sci_eng/USACE_Coastal_Risk_Reduction_final_CWTS_2013-3.pdf. Accessed June 27, 2021.

CEGIS (Center for Environmental and Geographic Information Services). 2016. Final Report of Technical Study for Mapping of Potential Greenbelt Zone in the Coastal Regions of Bangladesh. Dhaka: CEGIS.

Cheong, So-Min, Brian Silliman, Poh Poh Wong, Bregje Van Wesenbeeck, Choong-Ki Kim, and Greg Guannel. 2013. Coastal Adaptation with Ecological Engineering. Nature Climate Change 3 (9): 787–791. https://doi.org/10.1038/nclimate1854.

Chow, Jeffrey. 2015. Spatially Explicit Evaluation of Local Extractive Benefits from Mangrove Plantations in Bangladesh. *Journal of Sustainable Forestry* 34 (6–7): 651–681. https://doi.org/10.1080/10549811.2015.1036454.

Chow, Ven T. 1959. Open-Channel Hydraulics. McGraw-Hill Civil Engineering Series.

Chowdhury, A., R. Mushtaque, Abbas U. Bhuyia, A. Yusuf Choudhury, and Rita Sen. 1993. The Bangladesh Cyclone of 1991: Why So Many People Died. *Disasters* 17 (4): 291–304. https://doi.org/10.1111/j.1467-7717.1993.tb00503.x.

Das, Saudamini, and Jeffrey R. Vincent. 2009. Mangroves Protected Villages and Reduced Death Toll During Indian Super Cyclone. *Proceedings of the National Academy of Sciences* 106 (18): 7357–7360. https://doi.org/10.1073/pnas.0810440106.

Dasgupta, Susmita; Huq, Mainul; Khan, Zahirul Huq; Ahmed, Manjur Murshed Zahid; Mukherjee, Nandan; Khan, Malik Fida; Pandey, Kiran. 2010. Vulnerability of Bangladesh to Cyclones in a Changing Climate: Potential Damages and Adaptation Cost. Policy Research Working Paper no. WPS 5280. World Bank. Last accessed on June 26, 2021. Available online at https://openknowledge.worldbank.org/handle/10986/3767.

De Vriend, Huib J., Mark van Koningsveld, Stefan GJ Aarninkhof, Mindert B. de Vries, and Martin J. Baptist. 2015. Sustainable Hydraulic Engineering Through Building with Nature. *Journal of Hydro-environment research* 9 (2): 159–171. https://doi.org/10.1016/j.jher.2014.06.004.

Deb, M., and C.M. Ferreira. 2017. Potential Impacts of the Sunderban Mangrove Degradation on Future Coastal Flooding in Bangladesh. *Journal of Hydro-Environment Research* 17: 30–46.

Ferrario, Filippo, Michael W. Beck, Curt D. Storlazzi, Fiorenza Micheli, Christine C. Shepard, and Laura Airoldi. 2014. The Effectiveness of Coral Reefs for Coastal Hazard Risk Reduction and Adaptation. *Nature Communications* 5 (1): 1–9. https://doi.org/10.1038/ncomms4794.

GoB 2008. *Cyclone Sidr in Bangladesh Damage, Loss, and Needs Assessment for Disaster Recovery and Reconstruction.* Dhaka: Government of Bangladesh assisted by International Development Community with Financial Support from the European Commission.

GoB. 2013. *Disaster Report*. Department of Disaster Management, Ministry of Disaster Management and Relief: Government of the People's Republic of Bangladesh.

Hydraulics, WL Delft. 2006. *Delft3D-FLOW: Simulation of Multidimensional Hydrodynamic Flows and Transport Phenomena, Including Sediments, User Manual*. Delft, Holland: Deltares.

India Meteorological Department (IMD). 2021. Ministry of Earth Sciences, Government of India. Available online: http://imd.gov.in. Accessed June 27, 2021.

Islam, Md Nazrul, Nabila Hasan Dana, Khandkar-Siddikur Rahman, Md Tanvir Hossain, Moin Uddin Ahmed, and Abdulla Sadig. 2019. Nypa Fruticans Wurmb Leaf Collection as a Livelihoods Strategy: A Case Study in the Sundarbans Impact Zone of Bangladesh. *Environment, Development and Sustainability*, 1–18. https://doi.org/10.1007/s10668-019-00438-w.

Jisan, Mansur Ali, Shaowu Bao, and Leonard J. Pietrafesa. 2018. Ensemble Projection of the Sea Level Rise Impact on Storm Surge and Inundation at the Coast of Bangladesh. *Natural Hazards and Earth System Sciences* 18 (1): 351–364. https://doi.org/10.5194/nhess-18-351-201.

Jones, Holly P., David G. Hole, and Erika S. Zavaleta. 2012. Harnessing Nature to Help People Adapt to Climate Change. *Nature Climate Change* 2 (7): 504–509. https://doi.org/10.1038/nclimate1463.

JSCE. 2008a. *Investigation Report on the Storm Surge Disaster by Cyclone Sidr 2007*. Investigation Team of Japan Society of Civil Engineering, Bangladesh. Available at: http://www.jsce.or.jp/report/46/files/Bangladesh_Investigation.pdf. Accessed 27 June, 2021.

JSCE. 2008b. *Investigation Report on the Storm Surge Disaster by Cyclone Sidr 2007*. Investigation Team of Japan Society of Civil Engineering, Bangladesh. Available at: http://www.jsce.or.jp/report/46/files/Bangladesh_Investigation.pdf. Retrieved at November 2018.

Lewis, M., P. Bates, K.J. Horsburgh, J. Neal, and G. Schumann. 2013. A Storm Surge Inundation Model of the Northern Bay of Bengal Using Publicly Available Data. *Quarterly Journal of the Royal Meteorological Society* 139: 358–369.

Mita, Kazi Samsunnahar. 2019. Role of Mangrove Plantation in Improving Embankment Safety and Supporting Local Livelihoods. M.Sc. Thesis. Bangladesh University of Engineering and Technology.

Needham, Hal, and Barry D. Keim. 2011. Storm Surge: Physical Processes and an Impact Scale. Recent Hurricane Research-Climate, Dynamics, and Societal Impacts. Anthony Lupo, IntechOpen. Available online: https://www.intechopen.com/download/pdf/15338. Accessed August 28, 2021. https://doi.org/10.5772/15925.

NYS 2100 Commission. 2013. Recommendations to improve the strength and resilience of the Empire State's Infrastructure. New York State Official Report, Andrew Cuomo, Governor. last accessed on June 26, 2021. http://www.governor.ny.gov/assets/documents/NYS2100.pdf.

Quadir, Dewan Abdul. 2008. *Tropical Cyclones: Impact on Coastal Livelihoods: Investigation of the Coastal Inhabitants of Bangladesh.* Dhaka: IUCN Bangladesh Country Office.

Reddy, Sheila MW., Gregory Guannel, Robert Griffin, Joe Faries, Timothy Boucher, Michael Thompson, Jorge Brenner, et al. 2016. Evaluating the Role of Coastal Habitats and Sea-Level Rise in Hurricane Risk Mitigation: An Ecological Economic Assessment Method and Application to a Business Decision. *Integrated Environmental Assessment and Management* 12 (2): 328–344. https://doi.org/10.1002/ieam.1678.

Santiago Fink, Helen. 2016. Human-Nature for Climate Action: Nature-Based Solutions for Urban Sustainability. *Sustainability* 8 (3): 254. https://doi.org/10.3390/su8030254.

Simm, Jonathan, Amy Guise, David Robbins, and Jason Engle. 2016. US North Atlantic Coast Comprehensive Study: Resilient Adaptation to Increasing Risk. In *Coastal Management: Changing Coast, Changing Climate, Changing Minds*, 639–649. ICE Publishing. https://doi.org/10.1680/cm.61149.639.

slam, M.N., Dana, N.H., Rahman, KS. et al. 2020. Nypa Fruticans Wurmb Leaf Collection as a Livelihoods Strategy: A Case Study in the Sundarbans Impact Zone of Bangladesh. Environ Dev Sustain 22, 5553–5570. https://doi.org/10.1007/s10668-019-00438-w.

Small, Christopher, and Robert J. Nicholls. 2003. A Global Analysis of Human Settlement in Coastal Zones. *Journal of Coastal Research*, 584–599. Accessed on June 27, 2021. http://www.jstor.org/stable/4299200.

Sutton-Grier, Ariana E., Kateryna Wowk, and Holly Bamford. 2015. Future of Our Coasts: The Potential for Natural and Hybrid Infrastructure to Enhance the Resilience of Our Coastal Communities, Economies and Ecosystems. *Environmental Science & Policy* 51: 137–148. https://doi.org/10.1016/j.envsci.2015.04.006.

UNDP. 2015. Integrating Community-Based Adaptation into Afforestation and Reforestation Programmes in Bangladesh. Government of Bangladesh, Bangladesh Forest Department, Dhaka.

Heerden, Van, and Ivor Ll. 2007. The Failure of the New Orleans Levee System Following Hurricane Katrina and the Pathway Forward. *Public Administration Review* 67: 24–35. https://doi.org/10.1111/j.1540-6210.2007.00810.x.

Van Slobbe, E., J. de Huib, S. Vriend, K. Lulofs. Aarninkhof, Marjan de Vries, and P. Dircke. 2013. Building with Nature: In Search of Resilient Storm Surge Protection Strategies. *Natural Hazards* 66 (3): 1461–1480. https://doi.org/10.1007/s11069-012-0342-y.

Zhang, Keqi, Huiqing Liu, Yuepeng Li, Hongzhou Xu, Jian Shen, Jamie Rhome, and Thomas J. Smith III. 2012. The Role of Mangroves in Attenuating Storm Surges. *Estuarine, Coastal and Shelf Science* 102: 11–23. https://doi.org/10.1016/j.ecss.2012.02.021.

Assessing the Consequences of Large-Scale Stabilization of the Padma River on Its Flow Hydraulics Using a Combined 1D-2D Hydrodynamic Model

Subir Biswas and M. Shahjahan Mondal

Abstract Bangladesh is in a unique geographic location dominated by floodplains and consists of three large and extremely dynamic rivers—the Ganges, the Brahmaputra, and the Meghna. The Government of Bangladesh has policies and plans regarding water resource management, disaster risk reduction, and land reclamation from the riverbed. Such policies and plans include narrowing down, channelizing and stabilizing the Padma River, and constructing structures on its floodplains. The rehabilitation and construction of embankments along the river have been suggested under the stabilization programs. However, such stabilization may result in a change of hydraulic characteristics of the Padma River. Very little studies have been done to assess the effects of such large-scale stabilization on the hydraulic behavior of the river. This study has set up a coupled 1D-2D hydrodynamic model using HEC-RAS for the Padma River system and simulated the potential impacts of such stabilization. The Padma River, its distributaries, and adjoining areas are included in the model setup. The model is calibrated for the 1998 flood and validated for the 2004 flood using the observed water level. Further calibration and validation at the floodplain have been done using the primary highest flood level data, and through a qualitative comparison of flood inundation with satellite images, respectively. It has been found that the model can simulate the observed variation of these floods quite satisfactorily. The simulation results reveal that the peak discharge of the 1998 flood can increase by 20% in the Padma River under a stabilized condition. The peak flood level in the river can increase by 51 cm, and the maximum average velocity by 25% due to the stabilization. The outcomes of this study will be useful in training the river and designing other interventions for river management.

Keywords River stabilization · Padma River · Embankment · River hydraulics · 1D-2D-coupled HEC-RAS model

S. Biswas (✉) · M. S. Mondal
Institute of Water and Flood Management (IWFM), Bangladesh University of Engineering and Technology (BUET), Dhaka, Bangladesh

© The Author(s), under exclusive license to Springer Nature Switzerland AG 2022

G. M. Tarekul Islam et al. (eds.), *Water Management: A View from Multidisciplinary Perspectives*,
https://doi.org/10.1007/978-3-030-95722-3_14

1 Introduction

Bangladesh is located at the most downstream of the world's largest delta. It consists of floodplains of the Ganges, Brahmaputra, and Meghna rivers, and their numerous tributary and distributary rivers. About 80% area of the country consists of the combined delta of these three international rivers (Islam 2011). This unique geographic location makes Bangladesh highly vulnerable to flooding. In general, four types of floods occur in this country: flash floods, riverine floods, tidal floods, and floods due to storm surge. Riverine floods are the most common and such floods occur in many parts of the country almost every year. Heavy monsoon rainfall and synchronization of flood-peaks of the major rivers are generally considered to be the main causes of this flood. Normally, during the monsoon season, 25–30% of the area is inundated, but during extreme flood events, 50–70% area of the country can be subject to inundation (Hossain 2003). The floods of the years 1988 and 1998 inundated about 61% and 68% area of the country, respectively (FFWC 2018). Floods cause significant damage to crops, lives, and property every year. The 1998 flood damaged an estimated 15,000 km of roads, 14,000 schools, over 500,000 homes, thousands of bridges and culverts, and 2.04 million metric tons of rice crop production (Ninno et al. 2001).

The Government of Bangladesh (GoB) has undertaken many policies, plans, and projects for better water resource management and disaster risk reduction. Such policies, plans, and projects (e.g., Flood Control, Drainage and Irrigation Projects, Flood and Riverbank Erosion Risk Management Investment Programs) include channelization and stabilization of the major rivers and reclamation of lands from the river beds to increase economic activities on the floodplains (NHC 2013, BWDB 2014, GED 2017). It has become a common practice to construct earthen embankments (also known as levees or dykes in some countries) along the rivers to confine the river flows within the river cross-sectional areas, and to thereby prevent flooding of the floodplains. During the 1960s, many earthen embankments were constructed along the major rivers for flood protection. The GoB has constructed a total of 16,261 km of embankments including 5757 km of coastal embankments (BWDB 2019). Similarly, the ongoing and future initiatives of GoB for water resource management and disaster risk reduction indicate that the Padma River will be narrowed down to a single channel and stabilized through engineering works. The average width of the Padma River will be reduced to 5.3 km from 10.6 km by the year 2030 through channelization and riverbank stabilization (NHC 2013). There will be embankments on both sides of the river to protect life and property from flooding. However, such flood-control embankments and engineering works may result in a change of hydraulic characteristics of the river, which may have both positive and negative impacts (Baird et al. 2015). Also, to design stabilization structures like flood-control embankments along the river, necessary analysis must be conducted to understand the future behavior of the river (e.g., changed discharge, water level, and velocity) under the proposed stabilized condition. This stabilization impact can be determined through hydrodynamic model simulations. However, very little studies have been done to assess the effects

of large-scale stabilization on the hydraulic behavior of the rivers. In this study, the impact of large-scale stabilization of the Padma River on its discharge, water level, and velocity magnitude is assessed through a combined one- and two-dimensional (1D-2D) HEC-RAS model simulation for the Padma River system. Among the available models for hydraulic simulation, the HEC-RAS, developed by the U.S. Army Corps of Engineers, provides automated floodplain mapping and analysis with effective, proficient, and standard results. The combined 1D-2D HEC-RAS model is more suitable for a large river network having a floodplain, where a more detailed flow field is necessary (Brunner 2014).

2 Study Area and Methodology

Considering the strategies of the Bangladesh Delta Plan 2100 about river stabilization, this study investigates similar stabilization impacts on the Padma River, which is one of the three major rivers in Bangladesh. The River Ganges confluences with the Brahmaputra-Jamuna River at Goalundo and holds the name as the Padma River. This part of the river mainly has meandering characteristics, but in some reaches, it shows similarity to the braided and straight patterns both spatially and temporally (McLean et al. 2012). At Chandpur, the Padma River joins the Upper Meghna River and holds the name as the Lower Meghna River and flows to the Bay of Bengal (BWDB 2011). Due to its connectivity with the sea via the Lower Meghna, the Padma River experiences tidal influence. The Padma River and its floodplains have been considered as the study area in this study (Fig. 1).

The Padma River has a total length of about 120 km. The length of the river considered in this study is about 94 km, and the total area of the floodplain is about 2843 km^2. Required data for this study have been collected from primary and secondary sources. Secondary data include water level, discharge, and river bathymetry, digital elevation model (DEM), satellite images, and others. Some of these data were already available with the Institute of Water and Flood Management (IWFM), and others were collected from the Water Resources Planning Organization (WARPO) and Bangladesh Water Development Board (BWDB). Primary data were collected during the field visits. A 1D-2D-coupled HEC-RAS model for the Padma River System was set up. The model was calibrated with the measured data for the 1998 flood and validated independently with the measured data of the 2004 flood. After calibration and validation of the model, embankments on both banks of the Padma River were added using lateral structure along the river. Afterward, the model was rerun, and the results were analyzed through a comparison with the measured data. For the impact analysis, the 1998 flood was chosen as it is historically the highest flood in the Padma River floodplain.

Fig. 1 Study Area shown on the Google Earth map

2.1 Development of 1D-2D-Coupled HEC-RAS Model

As the study area consists of a deltaic floodplain, its topography is moderately flat. The Padma River also has tidal influences. The water from the river can easily enter the floodplain during high tide and depart the floodplain during low tide, especially in the monsoon season (Mondal et al. 2018). These floodplains act as storage reservoirs and play an important role in river hydraulics. So, a combined 1D-2D model was developed to simulate the flooding pattern where the rivers are modeled as the 1D elements and the floodplains are modeled as the 2D elements.

First, the 1D river network of the study area has been developed in the Geometric Data of the HEC-RAS model. The Padma River and its distributaries have been delineated using the River Reach tool following the centerline and deepest channel as a guide. After delineation of the river network, the bathymetries of the rivers were entered into the HEC-RAS Geometry. In the network, the Padma River, as well as its distributaries (the Arial Khan, the Kirtinasa, and the Joynagar-Ganganagar), is included. The current model setup covers a total length of about 262 km of river network including the Padma River and its distributaries as 1D element. Of these, the Padma River itself covers a length of about 94 km. For an accurate determination of the energy gradient, the measured cross-sections have been interpolated using

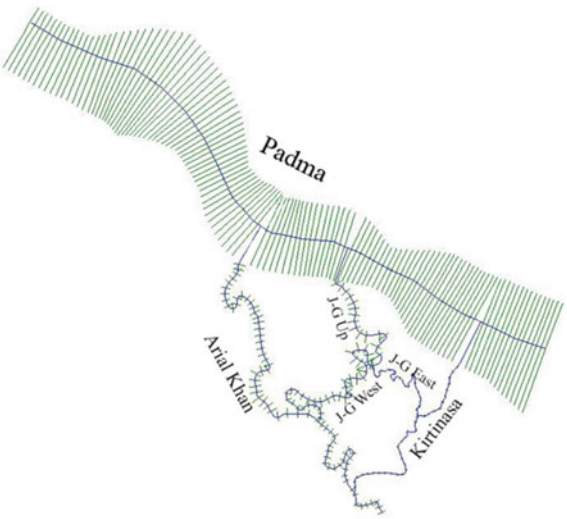

Fig. 2 A schematic showing the river network used in the coupled 1D-2D HEC-RAS model

additional master cords. A schematic showing the river network used in the model is given in Fig. 2.

After developing the 1D river network, the 2D flow area is added by drawing a 2D flow area polygon and developing the 2D computational mesh. For the development of the 2D floodplain, a terrain model is created in the HEC-RAS and is then added in the RAS Mapper. The resolution of the terrain model is a limiting factor for determining the quality of the hydraulic model. A high-resolution terrain model is essential to create a detailed and accurate hydraulic model. A DEM with a 500 m resolution from WARPO has been used to create the terrain model. The DEM resolution was further improved by using the topographical survey data collected in some selected areas by IWFM (2018). The raster DEM was saved in a float file format as required in the HEC-RAS. The raster file of the study area has been added to the RAS Mapper by using the new terrain layer tool. The raster file has been converted into the GeoTIFF (*.tif) file format by RAS Mapper (Brunner 2016). The terrain model has been further improved by using the cross-section data in the RAS Mapper. The terrain model of the study area thus created is shown in Fig. 3.

The terrain file is then opened in the Geometric Data Window of the HEC-RAS for creating a 2D flow area. A 2D flow area is added by drawing a 2D flow area polygon boundary in the Geometric Data Window. Due to the flat topography, the river water can easily exchange between the river and the floodplain with changes in the stages. Nowadays, the floodplains in many places are obstructed by highways, roads, and flood-control embankments. So, only the unobstructed parts of the floodplain act as storage areas. Such barriers and terrain contour lines were used as a guide to select the 2D area extent, as suggested in the HEC-RAS User Manual (Brunner 2016). It is found through several unsteady flow simulations, that a little change in the extent of 2D floodplain areas has no impact on the model outputs such as maximum water

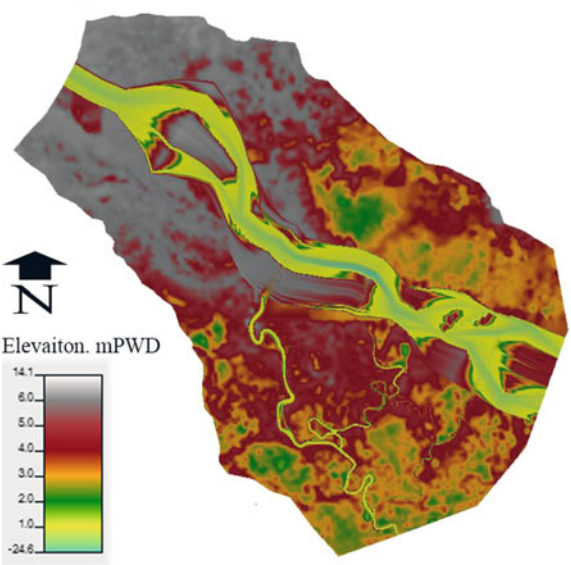

Fig. 3 Terrain model developed for the study area

level and velocity (Biswas et al. 2020). The number of 2D areas in the model is six, and the total area is about 2843 km^2. After drawing the 2D flow area polygon boundary, the 2D computational mesh and hydraulic property tables for the 2D cells and cell faces have been created. A 100 m $\times$ 100 m grid resolution has been used for the computational mesh.

After developing the 2D computational mesh, it has been connected with the 1D river using lateral structures from the Geometry Data Window. Here, a series of weir structures on each riverbank has been created to establish the connectivity between the 1D river and the 2D flow area.

2.2 Boundary Conditions

The model setup used in this study is for an unsteady flow simulation and thus requires the boundary and initial conditions. There is one upstream discharge boundary, two downstream water level boundaries, and five 2D area peripheral boundaries which act as the outflow boundary conditions. The locations of the boundaries are shown in Fig. 4. Here, the green arrow shows the upstream boundary, the two yellow arrows show the two downstream water level boundaries, and the red lines show the five peripheral boundaries.

The upstream boundary of this model is at Baruria Transit (SW91.9L) on the Padma River where the mean daily discharge (MDD) has been used. The two downstream boundaries are on the Padma River and on the Arial Khan River. The water levels at these boundaries for the year 1998 are obtained from a 1D hydrodynamic

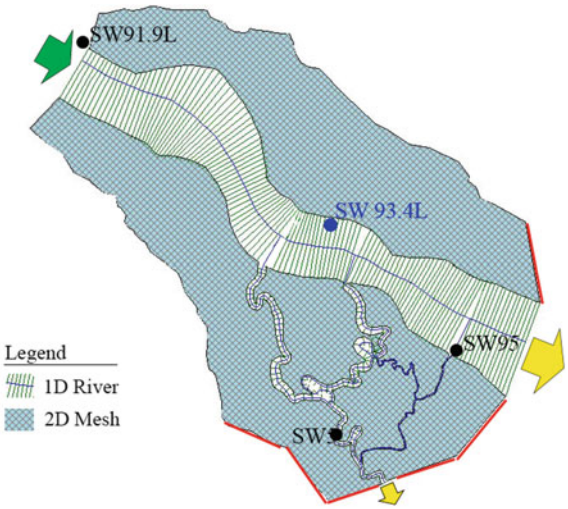

Fig. 4 Locations of the boundaries in the HEC-RAS model

HEC-RAS model developed by IWFM (2018) and Mondal et al. (2018) which was well-calibrated for the 2014 flood and validated for the 1998 and 1988 floods. Since the two downstream boundaries experience tidal influence, three hourly water level has been used as the boundary conditions at the downstream. For the year 2004, for both the downstream boundary conditions, such as Madaripur (SW5) on the Arial Khan and Sureswar (SW95) on the Padma River, the water levels were used after slope analysis as they are located further downstream. Observed discharge at Baruria Transit and water level on the Padma and Arial Khan were used as an initial condition. The peripheral outflow boundaries are modeled with normal depth. The normal depth boundary conditions can be used at locations where the flow leaves a 2D flow area or at an open-ended reach. Here, the peripheral boundaries are located on the floodplain where measured data (e.g., water level) are not available. So, the normal depth is used as recommended by Brunner (2016). Roy (2019) also used a similar approach. It requires entering a friction slope of that area to use the normal depth as a boundary condition. The friction slope should be based on the land slope at the vicinity of the 2D flow area boundary condition line. This friction slope is used in Manning's equation to compute a normal depth for each given flow, based on the cross-section underneath the 2D boundary condition line. In this model, there are five outflow boundaries where the average bed slope at the vicinity of the boundary has been used as an estimate of the friction slope. Two of them are located near the Padma River where a friction slope of 0.0002 has been used, and for others located near the Arial Khan River and open floodplain, a friction slope of 0.0001 has been used.

2.3 Model Simulations

After completing the model setup, the unsteady flow simulations were performed from 4 June to 22 September for the years of 1998 and 2004, to estimate the flood-peaks with a computational time interval of one minute. HEC-RAS solves either the full 2D Saint Venant equations or the 2D Diffusion Wave equations during the unsteady flow simulation. The governing equations for surface flow can be written as below:

$$\frac{\partial \zeta}{\partial t} + \frac{\partial p}{\partial x} + \frac{\partial q}{\partial y} = 0 \tag{1}$$

$$\frac{\partial p}{\partial t} + \frac{\partial}{\partial x}\left(\frac{p^2}{h}\right) + \frac{\partial}{\partial y}\left(\frac{pq}{h}\right) = -\frac{n^2 p g\sqrt{p^2+q^2}}{h^2} - gh\frac{\partial \zeta}{\partial x} + pf + \frac{\partial}{\rho \partial x}(h\tau_{xx}) + \frac{\partial}{\rho \partial y}(h\tau_{xy}) \tag{2}$$

$$\frac{\partial q}{\partial t} + \frac{\partial}{\partial y}\left(\frac{q^2}{h}\right) + \frac{\partial}{\partial x}\left(\frac{pq}{h}\right) = -\frac{n^2 q g\sqrt{p^2+q^2}}{h^2} - gh\frac{\partial \zeta}{\partial y} + qf + \frac{\partial}{\rho \partial y}(h\tau_{yy}) + \frac{\partial}{\rho \partial x}(h\tau_{xy}) \tag{3}$$

where, ζ = surface elevation, p = specific flow in the x direction, q = specific flow in the y direction, h = water depth, g = gravitational acceleration, n = Manning's resistance coefficient, f = Coriolis, ρ = water density, τ = components of the effective shear stress.

Equation 1 is the continuity equation and Eqs. 2 and 3 are the momentum equations. The acceleration terms in the Saint Venant equations can be neglected in most practical applications and then these become simple parabolic equations, known as the diffusive wave equations (Ponce 1990).

The full 2D Saint Venant equations are sometimes referred to as the full 2D shallow water equations. The user can select either of the equations. In general, the 2D Diffusion Wave equations allow the model to run faster and have greater stability properties. Quiroga et al. (2016) considered both options, the full Saint Venant equations and the 2D diffusion wave equations. They found that both methods provide the same results, but simulation solving the 2D diffusion wave equations was about 20 times faster. In this study, Diffusion Wave equations have been used as this model simulates only the monsoon flood.

As most of the DEMs used in the HEC-RAS model are from the year 2001, the year 1998 was chosen for the model calibration, and the year 2004 for the model validation. Also, the highest flood in the study area was observed in 1998, and there was a moderate flood in 2004. Using the boundary and initial conditions for each year, the model was run and the computed stage hydrographs were compared with the observed stage hydrographs to judge the performance of the model. As the model calculates

water level at all points within the model domain, the simulated water level has been compared with the Bhagyakul gage (SW 93.4L) station's observed water level to calibrate and validate the model. Bhagyakul is an intermediate gage station on the Padma River and is located near the center of the model domain. Manning's roughness coefficients for the main channel and floodplain were the principal calibration and validation parameters. The final calibrated and validated roughness parameters are found to be higher for the overbank areas ($n = 0.030$) and lower for the main channels ($n = 0.025$) and the highest in the floodplain ($n = 0.05$–0.06). Calibration at the 2D floodplain for 1998 has been done by comparing the survey data on the highest flood level and model-simulated highest water level for the same location. Validation at the 2D floodplain for 2004 has been done by a qualitative comparison between the MODIS image and the model-simulated flood inundation map. A similar approach for comparison of the 2D model flood inundation with the available satellite images has been used by many apprentices (Nishat 2017; Roy 2019; Tazin 2018).

There are many ways to evaluate a model's performance. Moriasi et al. (2007) have proposed guidelines for evaluation of model performance and recommended model evaluation techniques. They recommended quantitative statistics with graphical techniques. They divided quantitative statistical techniques for model performance evaluation into three major categories: standard regression, dimensionless, and error-index. In this study, three extensively used quantitative statistical performance indicators, namely Coefficient of Determination (R^2) as standard regression, Coefficient of Nash–Sutcliffe Efficiency (NSE) as dimensionless, and Root Mean Square Error (RMSE) as error-index, have been used for comparison of the simulated daily average water level with the observed daily average water level.

The embankments have been modeled using lateral structures along the river. There is an embankment on the left bank of the Padma River (Dhaka Southwest Project Embankment). The embankments were initially built with set-back distances from the active channel of around 1.5 km (NHC 2013). This distance has been followed as a setback to locate the embankment (lateral structure) in this model, with a few changes in some critical areas. The height of the embankment has been set in such a way that water cannot enter the floodplain. So, all the water remains within the river cross-sectional area for simulation under such a stabilized condition. Afterward, the results have been analyzed.

3 Results

In this 1D-2D-coupled model simulation, a spatially variable Manning's roughness coefficients were the principal calibration parameters. The calibration and validation results for the 1D river and 2D floodplains are discussed below.

3.1 Calibration and Validation Results

The model-simulated water level for Bhagyakul (SW 93.4L) on the Padma River is shown in Fig. 5 along with the observed water level at the same station. The figure shows that the water level has been simulated very well, except at the beginning. The inconsistency at the beginning could be due to the warm-up time required for an unsteady flow model to become stable. Elsewhere, the model captures the variation in the stage hydrograph at Bhagyakul reasonably well.

The highest measured water level at Bhagyakul was found to be 7.50 mPWD on 10 September and the highest simulated water level was 7.57 mPWD on the same day. Thus, the model-simulated water level was only about 7 cm higher than the measured water level at the peak. Also, it is seen from the figure that, the model could capture the variation in major part of the monsoon hydrograph very well. Since this study is mainly concerned with the peak flood period, the simulation results can be considered quite satisfactory. Since we are simulating the water level of 1998 using recent river bathymetries, and the river network used is very large, this small discrepancy could be expected and the model result can be considered to be acceptable. During calibration, the values of R^2 and NSE were found to be 0.98 and 0.95, respectively. These values indicate that the simulated water level is very close to the observed water level and also within the satisfactory range. The RMSE was found to be 0.20 m.

The validation of the model has been done for the year 2004. The comparison of the observed and simulated discharge hydrographs at Bhagyakul (SW 93.4L) is shown in Fig. 6.

It is seen from the figure that, the model captures the variation in major part of the monsoon hydrograph very well, with some discrepancy at the beginning of the hydrograph like the calibration year 1998. However, the peak does not match precisely in this case. This may be due to the unexpected drops in the observed discharges before the peak (on 15 and 22 July 2004) at Baruria Transit which was used as the upstream boundary. Otherwise, the simulation result can be considered quite satisfactory. In the validation, the values of R^2 and NSE have been found to be 0.98 and 0.90, respectively, which indicate that the simulated water level is very

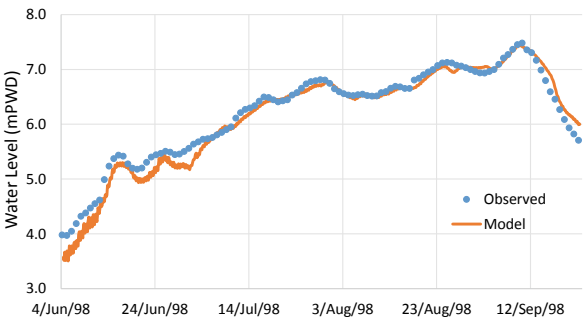

Fig. 5 Comparison of simulated and observed water levels at Bhagyakul on the Padma River for 1998

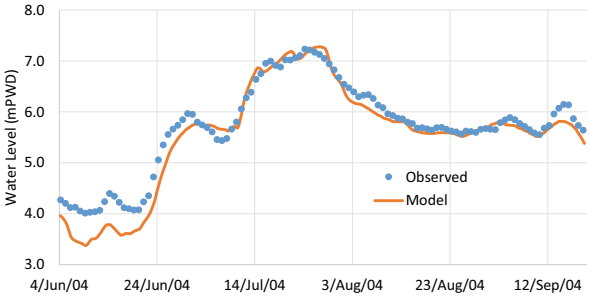

Fig. 6 Comparison of simulated and observed water levels at Bhagyakul on the Padma River for 2004

close to the observed water level and also within the satisfactory range. The RMSE was found to be 0.27 m.

3.2 Comparison of Flooding at 2D Floodplain

A comparison of flooding at 2D floodplain has been done through the comparison of the highest flood levels from the field survey, and the model simulation for the 1998 flood. The survey was conducted by IWFM during April–June of 2017, on the maximum flood level of the 1998 flood in Shariatpur and Madaripur districts covering an area of about 80 km^2. Those surveyed points are within this model domain. A relation between the surveyed maximum flood level and the modeled maximum flood level is shown in Fig. 7.

It is found that the model-simulated maximum flood level is 19 cm higher on average than the survey data, and the highest difference is 55 cm. The values of R^2 and NSE have been found to be 0.85 and 0.61, respectively, which fall within a satisfactory range. The RMSE was found to be 0.25 m.

A comparison of flooding at 2D floodplain has been done by comparison with the available satellite images for the 2004 flood. The qualitative comparison has been done for two situations—before flood conditions and during flood conditions. Figures 8 and 9 show the comparisons between flood inundation maps from MODIS, and that from the model for both before the flood and during the flood conditions.

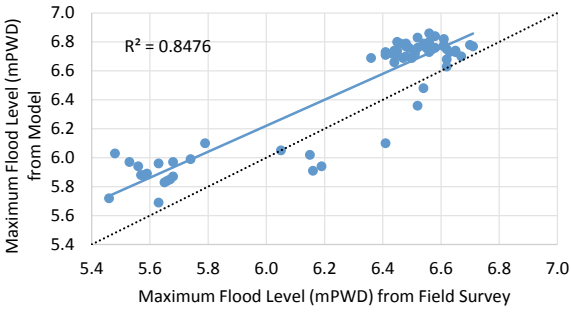

Fig. 7 Comparison of maximum flood levels between field survey and model simulation for 1998 flood

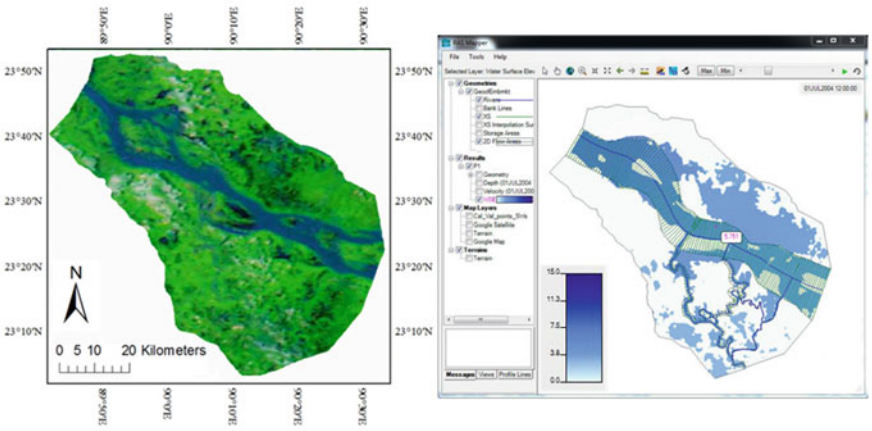

Fig. 8 Before-flood Inundation maps from MODIS (left) and model (right) on the 01 July 2004

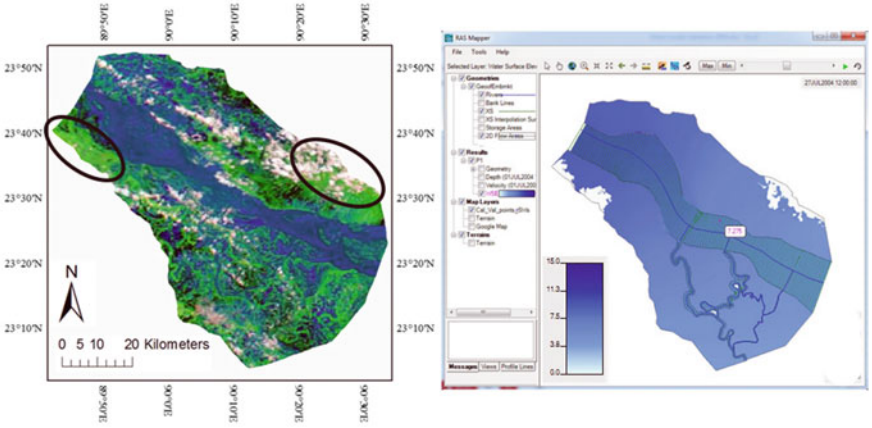

Fig. 9 During-flood inundation maps from MODIS (left) and model (right) on the 27th July 2004

Figure 8 shows the before-flood situations. On the left, there was no flood in the MODIS inundation map on 01 July 2004. Here, the green color shows the non-water zone, whereas the blue area and the green area with blue shade show the flood water zone. On the right, there is almost no flood in the model-generated inundation map on the same day. Here, the blue part shows the flood water zone, and the white part shows the non-water zone (Fig. 8).

The observed average water level on 01 July 2004 was 5.95 mPWD and the model-generated water level was 5.75 mPWD at 12 pm at Bhagyakul (SW 93.4L) gage station.

Figure 9 shows the during-flood situations. On the left is the MODIS inundation map on 27 July 2004 and on the right is the model-generated inundation map on the same day.

Here also, the blue area indicates the floodwater zone in the figures. On the left side of Fig. 9, the MODIS image shows that the green areas with any blue shade on the floodplain were actually inundated. Areas not inundated are marked by circles for easy visualization. So, almost all areas were flooded except the areas near the 2D boundary at the upstream right side and downstream left side of the Padma River. The observed average water level on 27 July 2004 was 7.13 mPWD and the model-generated water level was 7.28 mPWD at 12 pm at the Bhagyakul gage station on the same day.

Some higher areas have been flooded in the model which shows some discrepancy with the satellite image. This may be due to the initial condition of the model or the DEM quality. In this study, the DEM has been used with 500 m resolution, so some areas might have become lower at the time of DEM processing or terrain creation. Otherwise, the comparison between observed flooding from satellite imagery and simulated flooding from model results is found to be satisfactory.

3.3 Stabilization Impact Analysis

Under the stabilized condition, the river channel will not change its course and there will be flood-control embankments on both sides of the river. As both the river banks will be stabilized and flood-control embankments will be constructed, water will not enter into the floodplains even in a high flood situation. So, the hydraulic behavior of the Padma River will change under the recommended stabilized condition. Figures 10 to 12 represent the changes in such behaviors of the Padma River. The water will remain within the river that was previously used to enter into the floodplains. So, the river will carry more water under the stabilized condition. As a result, the discharge, water level, and velocity will increase under the stabilized condition. Figure 10 shows the change in the discharge of the Padma River at Mawa gage station (SW93.5L) under the stabilized condition.

In Fig. 10, the blue line represents the model-simulated discharge without stabilization at Mawa (present condition). The orange line represents the discharge at Mawa under the stabilized condition. A considerable rise in discharge is found after

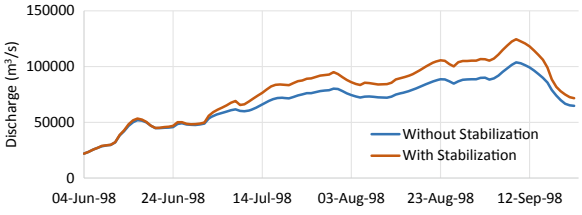

Fig. 10 Change in discharge at Mawa due to the stabilization of the Padma River

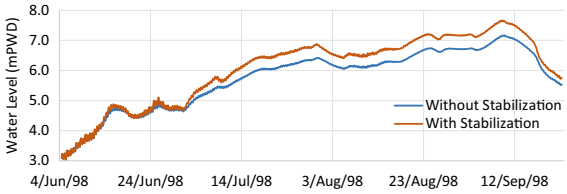

Fig. 11 Change in water level at Mawa due to the stabilization of the Padma River

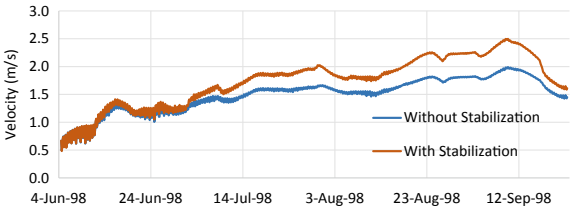

Fig. 12 Change in maximum average velocity magnitude near Mawa due to the stabilization of the Padma River

the 1st July. On average, 16.28% increase in discharge is found from 1 July to 22 September and 20.04% increase in discharge is found at the peak. The daily average peak discharge without stabilization is found to be 103,766 m^3/s and with stabilization 124,559 m^3/s on 9 September 1998 from the model simulation.

Figure 11 shows the change in the water level of the Padma River at Mawa under the stabilized condition. Here, the blue line represents the model-simulated water level without stabilization at Mawa (present condition), and the orange line represents the water level at Mawa under the stabilized condition (Fig. 11).

A considerable rise in water level is found after 1 July 1998. On average 6.22% (0.39 m) increase in water level is found from 1 July to 22 September, and 7.14% (0.51 m) increase in water level is found at the peak. The without-stabilization water level is 7.15 mPWD, and with-stabilization water level is 7.67 mPWD on 9 September 1998 at Mawa.

Figure 12 shows the change in the maximum average velocity magnitude of the Padma River near Mawa under the stabilized condition. Here, the blue line represents the model-simulated maximum average velocity magnitude without stabilization near Mawa (present condition), and the orange line represents the maximum average velocity magnitude under the stabilized condition (Fig. 12).

A rise in maximum average velocity magnitude is found after 1 July 1998. On average, 18.67% increase in maximum average velocity magnitude is found from 1 July to 22 September, and 26.74% increase in maximum average velocity magnitude is found on 8 September. The peak of the maximum average velocity magnitude is 1.99 m/s for without stabilization, and 2.50 m/s for the stabilization condition on 9 September 1998 near Mawa. A 25.43% increase in maximum average velocity magnitude is found during the peak, while the maximum change occurs on the previous day.

4 Discussion

This study has developed an important tool for assessing the future hydraulic behavior of the Padma River (e.g., changed discharge, water level, velocity) under the proposed stabilized condition. The study reveals that the stabilization will make the floodplain of the river flood-free. But the discharge, water level, and velocity magnitude will increase as demonstrated by the findings of this study. This information can be valuable for designing the hydraulic structures, such as fixing the heights of the flood-control embankment, bridges, roads, and others within the area.

Along with resource constraints, this study has some further limitations. Though the Padma River carries a huge amount of sediment load, the impact of sedimentation, local scour, and erosion have not been considered by the study. The local rainfall effect and possible climate change impacts in the future have not been considered. The resolution of the DEM is 500 m, which is also a limiting factor. These limitations could have resulted in some deviations of the model results from the measured data. Calibration and validation results show some overestimation of the water level on the floodplain and hence the inundated area, which is more likely due to the DEM resolution and quality. The qualitative comparison of the flood inundation map is also a limiting factor of this study. Quantitative comparison was not possible as the processed MODIS images were collected from Roy (2019) which is a secondary source. But the calibration and validation of water level at Bhagyakul on the Padma River indicate the high reliability of this model. From the values of the coefficient of model performance evaluation, it can be said that this 1D-2D-coupled HEC-RAS model setup can simulate the hydraulic behavior of the Padma River and its floodplains undoubtedly well. This mathematical model is able to calculate the hydraulic parameters at all locations within the model domain for both 1D and 2D areas very well. So, simulations of different possible conditions in the future using this model setup can be highly acceptable.

Stabilization intended will have beneficial impacts by preventing flood damage to agriculture and infrastructure within the area. Under the stabilized condition with flood embankment, the values of the hydraulic parameters will increase. The peak discharge of 100 years of return period, like the 1998 flood, will be increased by 20% at the Padma River. The water will not enter into the floodplain under the stabilized condition. It was also found during the field survey that the floodplains are getting little to no water due to the newly built embankment, especially in Shibchar area of Madaripur district and Jajira area of Shariatpur district. The river training embankment for the Padma Multipurpose Bridge is blocking the channels that are used to connect those floodplains with the Padma River. It has been found from the interviews and group discussions with the local people, that they are not getting water from those channels. As a result, they are facing water deficiency for growing crops. The areas are becoming arid day by day, and the local environment is changing rapidly. Local people anticipate that these channels will be lost in the future. The

people living in the floodplains of the Padma River are largely dependent on agriculture and fishery-based livelihoods. They are already experiencing the negative impacts of the embankment.

So, before the construction of the flood control and river stabilization embankment, the environmental impact on the entire region should be assessed, as several negative impacts may occur in the future. Floodplain aquatic habitats can be degraded due to reduced flooded areas and loss of hydrologic connectivity. This will adversely affect the floodplain-dependent open-water fish migration as well as wetland biodiversity. These impacts can in turn adversely affect the nutrition, health, and economic status of poor people in the area. Drainage congestion problems might occur as water may be entrapped in the area due to the construction of a new embankment. There is a need to develop a comprehensive river stabilization plan to identify potential stabilization solutions with minimal impacts on the river and floodplain environment. The off-takes of the distributaries can be stabilized in such a way that it allows stable dry season flows to pass and normal beneficial flooding to occur during the monsoon season, while restricting high damaging floods through regulations.

5 Conclusion

The Government of Bangladesh has already undertaken many initiatives for better water resource management and disaster risk reduction in the country. Some of these initiatives include the policy regarding stabilization and channelization of the Padma River. The stabilization plans include rehabilitation and construction of flood-control embankments, which can change the hydraulic behavior of the river. The stabilization impacts can be simulated and analyzed through a hydrodynamic model like HEC-RAS. In a country like Bangladesh, where data are very limited and resources are scarce, such modeling approaches can give reasonable predictions of required scenarios.

In this study, an HEC-RAS-coupled 1D-2D model of the Padma River system has been developed for evaluating the stabilization impacts on the hydraulic behavior of the river. The rivers have been modeled as a 1D flow area, and the floodplains have been modeled as a 2D flow area. Model calibration has been performed for the years 1998, and validation for the year 2004, where Manning's roughness coefficient 'n' was the main calibration and validation parameter. Further calibration and validation at the floodplain have been done using the observed highest flood water level, and the flood inundation area with the MODIS images, respectively. The results have shown a good performance of the model.

After calibration and validation, the model has been run according to the stabilization plan. The floodwater cannot enter into the floodplain and remains within the cross-sectional area under the stabilized condition. This results in an increase in discharge, water level, and velocity in the river. It is found that the peak discharge of the 1998 flood can increase by 20% with an average increase of 16% at Mawa on the Padma River. On average, 0.39 m increase in water level has been found with 0.51

m increase in the peak water level at Mawa. The average increase in the maximum average velocity has been found to be 19%, with the increase of 25% in the peak water level for the Padma.

The findings from this study will provide valuable information regarding the future stabilization impacts on river hydraulics in the Padma River and its floodplain. It is expected that the outcomes of this study will be useful for the authorities responsible for flood management and disaster risk reduction in the study area.

Acknowledgements The authors would like to thank all the survey respondents and participants of the group discussions, for providing valuable information. Special thanks go to Mr. Santosh Karmaker, a former student of the Department of Civil Engineering, BUET, Mr. Shahriar Shafayet Hossain, a former student of IWFM, BUET, and the IWFM survey team for accompanying the authors during the field survey. The authors are also grateful to the faculties and laboratory technician of IWFM, BUET for their assistance. Finally, the valuable comments and suggestions provided by the anonymous reviewer are gratefully acknowledged.

References

Baird, Drew C., Lisa Fotherby, Cassie C. Klumpp, and S. Michael Sculock. 2015. *Bank Stabilization Design Guidelines.* Denver: U.S. Department of the Interior, Bureau of Reclamation Technical Service Center.

Biswas, Subir, M. Shahjahan Mondal, and Md. Rashedul Islam. 2020. Simulating Flood Risk Due to Climate Change in the Padma River System Using the 2D HEC-RAS Model. 5th International Conference on Civil Engineering for Sustainable Development (ICCESD), 7–9 February 2020, Khulna.

Brunner, Gary W. 2014. *Combined 1D and 2D Modeling with HEC-RAS*. Davis, CA: US Army Corps of Engineers, Hydrologic Engineering Center.

Brunner, Gary W. 2016. *HEC-RAS River Analysis System, 2D Modeling User's Manual*. Davis, CA: US Army Corps of Engineers, Hydrologic Engineering Center.

BWDB (Bangladesh Water Development Board). 2011. *Rivers of Bangladesh.* Dhaka, Bangladesh.

BWDB. 2014. *Bangladesh: Flood and Riverbank Erosion Risk Management Investment Program.* Dhaka, Bangladesh.

BWDB. 2019. *Sixty Years of Water Resource Management & Development in Bangladesh.* Dhaka, Bangladesh.

FFWC (Flood Forecasting and Warning Centre). 2018. *Annual Flood Report 2018*. Flood Forecasting & Warning Centre, Processing & Flood Forecasting Circle. Dhaka: Bangladesh Water Development Board.

GED (General Economics Division). 2017. *Bangladesh Delta Plan 2100*. Bangladesh Planning Commission, Government of the People's Republic of Bangladesh. Dhaka, Bangladesh.

Hossain, A. N. H. Akhtar. 2003. *Integrated Flood Management Case Study Bangladesh: Flood management.* Technical report. The Associated Programme on Flood Management, World Meteorological Organization.

Islam, M. N. Nabiul. 2011. *Impacts of Urban Floods from Micro-Macro Level Perspectives: A Case Study of Bangladesh.* Chisinau: Lambert Academic Publishing.

IWFM. 2018. *Hydrology and Morphology Study Work Under Detail Feasibility Study for Bangabandhu Sheikh Mujib International Airport Project*. Bureau of Research: Testing and Consultation, Bangladesh University of Engineering and Technology, Dhaka, Bangladesh.

McLean, D.G., Jose A. Vasquez, Knut Oberhagemann, and Maminul H. Sarker. 2012. Padma River Morphodynamics Near Padma Bridge. River Flow 2012—Proceedings of the International Conference on Fluvial Hydraulics 1: 741–747.

Mondal, M. Shahjahan, A.K.M. Saiful Islam, Anisul Haque, Md. Rashedul Islam, Subir Biswas, and Khaled Mohammed. 2018. Assessing High-End Climate Change Impacts on Floods in Major Rivers of Bangladesh Using Multi-Model Simulations. *Global Science and Technology Journal* 6 (2): 1–14.

Moriasi, Daniel N., Jeffrey G. Arnold, Mi-chael W. Van Liew, Ronald L. Bingner, R. Daren Harmel, and Tamie L. Veith. 2007. Model Evaluation Guidelines for Systematic Quantification of Accuracy in Watershed Simulations. *Transactions of the ASABE* 50 (3): 885–900. https://doi.org/10.13031/2013.23153.

NHC (Northwest Hydraulic Consultants). 2013. *Bangladesh: Main River Flood and Bank Erosion Risk Management Program: Final Report, Main Report*. Dhaka.

Ninno, Carlo del, Paul A. Dorosh, Lisa C. Smith, and Dilip K. Roy. 2001. *The 1998 Floods in Bangladesh: Disaster Impacts, Household Coping Strategies, and Response.* Research report No.: 122. Washington D.C.: International Food Policy Research Institute.

Nishat, Ummay. 2017. *Flood Inundation Mapping of Jamuna River Floodplain Using HEC-RAS 2D Model* (B.Sc. Thesis). Dhaka: Department of Water Resources Engineering, Bangladesh University of Engineering and Technology.

Ponce, V.M. 1990. Generalized Diffusion Wave Equation with Inertial Effects. *Water Resources Research* 26 (5): 1099–1101.

Quiroga, V., S. Moya, K. Udo. Kure, and A. Mano. 2016. Application of 2D Numerical Simulation for the Analysis of the February 2014 Bolivian Amazonia Flood: Application of the New HEC-RAS Version 5. *RIBAGUA-Revista Iberoamericana Del Agua* 3 (1): 25–33. https://doi.org/10.1016/j.riba.2015.12.001.

Roy, Binata. 2019. *A Study on Fluvial Flood Hazard and Risk Assessment of Arial Khan River Floodplain Under Future Climate Change Scenarios* (M.Sc. Thesis). Dhaka: Department of Water Resources Engineering, Bangladesh University of Engineering and Technology.

Tazin, Tasmia. 2018. *Flood Hazard Mapping of Dharala Floodplain using HEC-RAS 1D/2D Coupled Model* (M.Sc. Thesis). Dhaka: Department of Water Resources Engineering, Bangladesh University of Engineering and Technology.

Water and Livelihood Security

A Sustainability Index for Assessing Village Tank Cascade Systems (VTCs) in Sri Lanka

E. M. G. P. Hemachandra, N. D. K. Dayawansa, and Ranjith Premalal De Silva

Abstract Traditional Village Tank Cascade systems (VTCs) are a connected series of tanks where the excess water in upstream tanks is collected and reused by the downstream tanks. These are highly sustainable irrigation systems in the Dry zone landscape of Sri Lanka from ancient times. At present, these systems are under threat of deterioration due to continuous human interventions. Even though a number of studies have identified different parameters to assess VTCs, none of them have addressed the social, environmental and economic sustainability within a single assessment. Since the sustainability of VTCs should achieve the equilibrium of its ecological, hydrological, agricultural and social subsystems and cultural norms, it is important to incorporate all these factors in the sustainability assessment. Considering this background, the objective of this study was to develop an index to assess the sustainability of VTCs in an integrated manner. The index was developed with 8 physical-environmental parameters and 13 socioeconomic parameters. The relative importance of each parameter was identified through a Multi-Criteria Analysis. The developed index can be used in assessing the sustainability of any of the VTCs as well as the individual tanks in a 0 to 100 scale, which can be used for comparing and prioritizing the cascades for rehabilitation and development activities.

Keywords Village Tank Cascade Systems (VTCs) · Sustainability · Index Development · Parameters

1 Introduction

The undulating landform in the dry zone of Sri Lanka has allowed ancient kings to construct village tanks/tank cascade systems (VTCs) by obstructing the natural

E. M. G. P. Hemachandra (✉)
Postgraduate Institute of Agriculture, University of Peradeniya, Peradeniya, Sri Lanka
e-mail: gimhani@agri.pdn.ac.lk

N. D. K. Dayawansa · R. P. De Silva
Department of Agricultural Engineering, Faculty of Agriculture, University of Peradeniya, Peradeniya, Sri Lanka

© The Author(s), under exclusive license to Springer Nature Switzerland AG 2022

G. M. Tarekul Islam et al. (eds.), *Water Management: A View from Multidisciplinary Perspectives*,
https://doi.org/10.1007/978-3-030-95722-3_15

drainage system for the purpose of irrigation and other rural water requirements. According to the definition of Madduma Bandara (1985) "Cascade System is a connected series of tanks organized within a meso-catchment of the dry zone landscape, for storing, conveying, and utilizing water from an ephemeral rivulet."

The upstream tanks in the cascade system collect water from rainfall and runoff while the downstream tanks receive water due to the drainage, seepage, surface runoff and direct rainfall to the tank. Therefore, the excess water of an upstream tank used by its command area is drained to the downstream tank and used for irrigating its command area (Panabokke et al., 2001). A representative diagram of a village tank cascade system is presented in Fig. 1.

The communities living in these areas have very close interactions with the VTCs since most of their livelihood activities are closely associated with village tanks and their ecosystems. Considering the ecological components and the sustainable land use system associated with the VTCs, they were once considered as highly sustainable agro-ecosystems. As a result, communities reaped multiple benefits from them including efficient rainwater storage to be utilized during dry season, flood control, provision of water for agriculture, domestic needs, livestock, maintenance of a high groundwater level, facilitation of growth of reeds, etc. Thus, the VTCs are considered as multi-purpose systems (Panabokke et al., 2001). Hence, based on specific functions and components of VTCs, Dharmasena (2020) has defined the cascade system as an ecosystem in the dry zone landscape of Sri Lanka which sustainably fulfills basic needs to humans, plants and animals using water, soil, air and vegetation.

Even though these systems were sustainable in the past, they are gradually deteriorating due to intense anthropogenic activities (Dharmasena, 2010). The level of deterioration is varying from cascade to cascade hence prioritization is important in restoration/rehabilitation activities. Since the sustainability of the cascade system

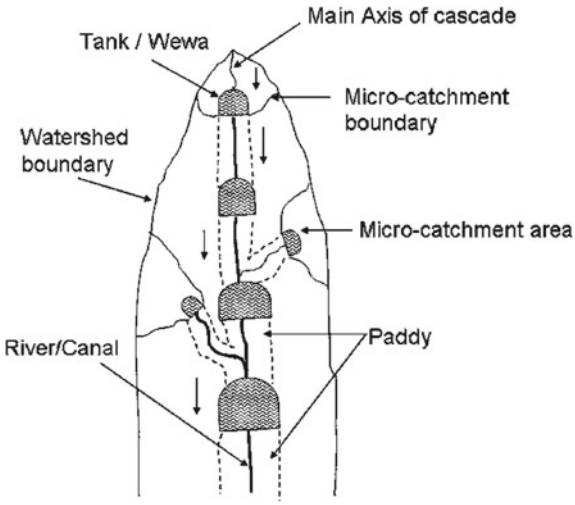

Fig. 1 Representative diagram of a village tank cascade system (*Source* Bandara et al., 2008)

includes the equilibrium of its subsystems such as ecological, hydrological, agricultural, social systems and cultural norms (Marambe et al., 2012), incorporation of all these factors is needed to assess the sustainability.

A number of parameters have been identified in the past studies to assess the sustainability of VTCs (Sakthivadivel et al., 1994; Dharmasena and Goodwill, 1999; Dharmasena, 2009; Perera, 2016). In general, social, environmental and economic factors collectively influence the sustainability of tanks/VTCs, and hence, it is difficult to consider only one group of factors in sustainability assessment. Integration of these different parameters into a single assessment strategy has not been addressed in the past studies. An index which can incorporate all possible parameters which are influential on the sustainability of VTC/individual village tanks will be helpful to identify and compare the status of these systems. These assessments will facilitate the managers to focus on most susceptible systems to introduce remedial measures. In addition, this type of sustainability assessment method will support continuous monitoring of these systems to obtain optimum services from them. Accordingly, planning and management of the VTCs should be done with a broad understanding of principles and mechanisms of the cascade system functions (Geekiyanage and Pushpakumara, 2013).

2 Methodology—Development of a Sustainability Index to Assess VTCs

The VTCs consist of a variety of subsystems, which include the ecological system of forests, aquatic habitats and common areas, the water management system of structures and the system of water distribution, the agricultural system, the social system with well-established formal and informal institutional setup and the cultural and spiritual norms which are helpful for simple and conflict free life (Marambe et al., 2012). Therefore, the sustainability of VTCs is a measure of how these subsystems utilize the resources to provide services while maintaining a sustainable ecosystem balance.

2.1 Identification of Variables/Parameters of Sustainability of VTCs

Twenty-one parameters of sustainability of VTCs were considered by using existing parameters, improving the parameters and developing new parameters. Four of them were taken as it is from the existing literature and seven parameters were newly developed by improving the existing parameters. Additionally, ten new parameters that have not been considered in past studies were developed to include the essential factors which influence the sustainability of the VTCs. All the parameters used in this

Table 1 Parameters of sustainability index of VTCs

No	Existing parameters	New parameters developed by improving existing parameters	Newly developed parameters
1	Ratio of Catchment area: Water surface area of tank (Sakthivadivel et al., 1994)	Live storage of the tank/Total irrigation command area (Dharmasena, 2009)	Presence of aquatic plants in village tanks (% coverage)
2	Frequency of spilling the tanks within a specific period of time (per year) (Sakthivadivel et al., 1994)	Existence of ecological components (Sangrama, 2018)	Existence and Performances of farmer organizations
3	Agro-well density (Dharmasena and Goodwill, 1999)	Percentage of forest cover in the catchment (Perera, 2016)	Healthy agricultural practices—Organic fertilizer usage
4	Cropping intensity (paddy) (Sakthivadivel et al., 1994; Dharmasena, 2009)	Presence of risky land uses in the catchment (Samarasinghe and Dayawansa, 2011)	Percentage of farmers who practice in water conservation strategies
5		Population density in the cascade system (Jayarathne et al., 2010)	Percentage of young farmers involved in agriculture
6		Severity of human-elephant conflict (Perera, 2016)	People's awareness of cascade system functions
7		Percentage of *Samurdhi* beneficiaries (Jayarathne et al., 2010)	Women's participation in cascade activities
8			Multiple water uses/users
9			Average paddy yield in *Maha* (Major cultivation) season
10			Number of cascade related projects implemented during last 10 years

study are presented in Table 1. A detailed description of the parameters is presented under "Development of sustainability Index."

2.2 Development of the Sustainability Index

A conceptual framework of the sustainability index was developed incorporating all the contributing parameters (Fig. 2). The parameters were then categorized into two major groups of physical-environmental parameters and socioeconomic parameters, based on the applicability of remedial and rehabilitation measures of VTCs after the sustainability assessment. It would be difficult to address physical and environmental

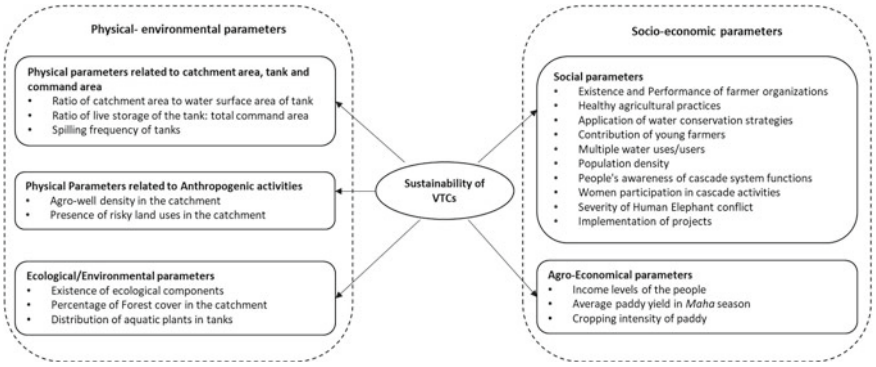

Fig. 2 Conceptual framework of developing the sustainability Index

parameters as they are high costly and will require political interventions and the approvals of many institutions and authorities. However, with the help of individuals or community-based organizations in a given cascade system, there is more flexibility when it comes to addressing social and economic parameters.

2.2.1 Calculation of Parameters and Normalization Scales

Different parameters are measured in different units and are in different scales. When developing an index, it is important to bring them to a common scale to identify their contribution to VTC sustainability. Therefore, the actual parameter values were converted into a 0–100 linear scale as stated below.

- **Physical and Environmental Parameters**

I. **Ratio of Catchment area: Water surface area of tank**

This parameter is looking for the hydrologic potential of the individual tanks or the tank cascade system. According to Sakthivadivel et al., (1994) a ratio of 7.5 is required to have an adequate hydrological potential. It implies that the area of the catchment should be 7.5 times as large as the water surface area of the tank which is a measure of the capacity of a small tank. Accordingly, a ratio larger than 7.5 would have high hydrologic potential and less than that value would have low hydrologic potential (Sakthivadivel et al., 1994). Assuming that with the reduction of the ratio, the sustainability of the cascade is reducing, the normalized score (linear) was developed according to Table 2.

II. **Ratio of live storage of the tank: Total command area**

Based on the major uses of a reservoir, its capacity is divided into three components: live storage/active storage, dead storage and flood storage. The live storage is used to supply water to the downstream, hydropower generation and recreational purposes.

Table 2 Score of "Ratio of Catchment area: Water surface area of tank" and "Ratio of Live storage of tank (ha.m): Command area (ha)"

Category	Ratio of Catchment area: Water surface area of tank	Ratio of Live storage of tank (ha.m): Command area (ha)	Score
i	< 1	< = 0.25	0
ii	1– < 2.5	0.25–0.5	25
iii	2.5– < 5	0.5–0.75	50
iv	5– < 7.5	0.75–1	75
v	> = 7.5	> = 1	100

The dead storage is used for sediment deposition, while the flood storage is used for controlling floods and its adverse impacts to the downstream (Loucks and Van Beek, 2017). Therefore, only the live storage is available for irrigation water supply in village tanks. When the command area increases compared to the live storage of the tank, then there is high pressure on irrigation water requirement. This can often result in water scarcity. On-farm water requirement of 3-month paddy variety in *Maha* season under Reddish Brown Earth (RBE) moderately drained soil is 1057 mm, and it is 948 mm under Low Humic Gley soil (*LHG)* (https://doa.gov.lk/). Accordingly, considering the adequacy of water for cultivation during *Maha* season, the score value scale was developed for the parameters (Table 2).

III. **Frequency of spilling the tanks within a specific period of time (per year)**

People in village tank cascade systems highly depend on the availability of tank water for agriculture and other livelihood activities. Therefore, people expect the tank to be filled during the rainy season. If there is adequate rainfall, farmers can cultivate during *Maha* season mainly with rainwater, and the excess water can be stored in the tanks for cultivating during *Yala* (relatively dry minor cultivation season) season. Assuming that tanks should spill minimum once per year most probably during North-East monsoon rains, a score of 100 was given to the tanks which spill once or more than once per year. A score of 0 was given when the tanks do not spill at least once a year. The timing and duration of spilling differ with the location of the tank in the cascade system. The downstream tanks spill for a long time compared to upstream tanks since they receive water from a large catchment area above them. However, the spilling duration was not considered as a parameter in the sustainability index.

IV. **Existence of ecological components**

Essential ecological components of VTCs such as Interceptor, Tree belt, Water hole, Upstream side ridges and Tank bund provide beneficial effects to the tank cascade system, thus important for their sustainability as well (Dharmasena, 2010). Accordingly, the existence of these ecological components in individual tanks is assessed by this parameter. The given normalization scores for the existence of ecological parameters were "0" for "Not existing/ unsatisfied," "50" for "Existing but moderately satisfied" and "100" for "Existing and satisfied." The scores are given to all

five ecological components and their average value is considered as the parameter value in the index. When the index is applied to an entire tank cascade system, the average value for the ecological components of all individual tanks in the same cascade system is taken.

V. **Agro-well density in the catchment**

Agro-wells are constructed to be used as a source of supplementary irrigation in most of the catchments in dry and intermediate regions in Sri Lanka (Pelpitiya et al., 2016). However, overabstraction of water in the upper catchment area can influence water availability in the whole catchment. When this is happening in cascade systems, it can adversely influence the sustainability of the system. To maintain the sustainability, the recommended agro-well density is 7–8 wells/km^2 (7–8 wells per 100 ha) (Dharmasena and Goodwill, 1999). The score scale was developed according to this understanding (Table 3).

VI. **Percentage of Forest cover in the catchment**

The catchment land use quality is highly important to achieve a better hydrologic potential. The forests play a major role in hydrology and can increase the infiltration rate, and they can increase the water availability within the catchment (Ekhuemelo et al., 2016; Bonnesoeur et al., 2019). Therefore, this parameter is emphasizing the fact that, with the increment of the forest cover in the catchment, the sustainability of the cascade will increase. Accordingly, the scores were identified (Table 3). When the index is applied for a total cascade, the forest cover of the whole catchment of the cascade system is taken.

VII. **Presence of risky land uses in the catchment**

Since the cascade system acts as a single ecosystem, a risky human intervention in one location of the catchment can influence the whole biotic and abiotic components in different ways. This parameter looks for the existence of risky land uses such as large-scale constructions, industrial sites, large-scale deforestations. The parameter was developed to qualitatively state whether the risk is low, moderate, high or very high (Table 3).

Table 3 Score for "Agro-well density in the catchment," "Percentage of forest cover in the catchment" and "Presence of risky land uses in the catchment"

Category	Agro-well density (wells per km^2)	Percentage forest cover in the catchment	Presence of risky land uses in the catchment	Score
i	> = 50	0%	Very high risk	0
ii	30–50	1%– < 25%	High risk	25
iii	15–30	25%– < 50%	Moderate risk	50
iv	8–15	50%– < 75%	Low risk	75
v	< = 8	> = 75%	Not existing	100

VIII. **Presence of aquatic plants in tanks (% coverage)**

Aquatic plant distribution in tanks can be taken as both positive and negative for the sustainability of the system. In ancient times, people largely benefited from aquatic plants such as lotus (*Nelumbo nucifera*), Water lily (*Nymphaea*) and Kekatiya (*Aponogeton crispus*). They could also get economic benefits (flowers can be sold for religious offerings) and food security (some plant parts can be used as food items). However, there are a limited number of people who gain these benefits in the modern society.

In addition, some other plants such as Water hyacinth (*Eichhornia crassipes*) can trap sediments and fill the tanks to reduce the capacity, block the irrigation canals and can also act as weeds in agricultural fields when transported with irrigation water. When the water surface is covered with aquatic plants, water can be lost through evapotranspiration. Spreading of aquatic weeds in water bodies can also cause economic and ecological losses to the system (Wijesundara, 2010). Since the negative impacts associated with aquatic plants distribution are severe and it can affect a greater number of people and the water circulation within the overall system, the presence of plants was considered as negative for the sustainability of VTCs. Table 4 presents the score given to this parameter.

- **Socioeconomic parameters**

I. **Existence and performances of farmer organizations**

In small irrigation systems, the basic functions of water and cultivation management are done through the farmer's organizations under the guidance of the Department of Agrarian Development. Therefore, it is important to have farmer's organizations for the sustainability of VTCs.

Additionally, the performances of the farmer's organizations are very important for better management of water and other resources in the cascade system and the maintenance of the tanks which subsequently uplift the livelihood of the farmers. The performance of the farmer's organizations is a function of farmer participation in meetings, balanced gender representation in the executive committees, major functions/activities related to cascade systems and funds/savings. Accordingly, criteria such as existence of farmer organization, farmer participation in meetings, gender representation in the executive committee, major functions and activities, water management related disputes and available funds were considered to assess this parameter and the final mark itself was considered as the index score.

Table 4 Score of "Presence of aquatic plants in tanks"

Category	Percentage coverage of aquatic plants in tanks	Score
i	> = 75%	0
ii	50%– < 75%	25
iii	25%– < 50%	50
iv	< 25%	100

Table 5 Score of "Organic fertilizer usage" and "Percentage of young farmers involve in agriculture" and "Multiple water uses/users"

Category	Percentage of farmers who use organic fertilizer	Percentage of young farmers involve in agriculture	Multiple water uses/users:- Number of benefits from the cascade system/ tank	Score
i	0%	0%	0	0
ii	1%– < 10%	1%– < 10%	2– < 4	20
iii	10%– < 20%	10%– < 20%	4– < 6	40
iv	20%– < 30%	20%– < 30%	6– < 8	60
v	30%– < 50%	30%– < 50%	8– < 10	80
vi	> = 50%	> = 50%	> 10	100

II. **Healthy Agricultural practices—Organic Fertilizer Usage**

There is reuse of water in the tank cascade systems. The excess water in the upstream paddy fields is drained to the downstream tanks and that water is utilized in its command area. Therefore, the agro-chemical usage in the upstream area has influences the water quality of the whole cascade system. If higher number of organic farmers are in the cascade, there is less chance of polluting water from heavy doses of inorganic fertilizers. Since complete organic farming is very rare in these cascade systems, farmers who attempt to incorporate organic fertilizers for their farming were considered to be promoting a healthy agricultural practice. Therefore, the following score was developed to evaluate the impact of organic fertilizer usage (Table 5).

III. **Percentage of farmers who practice water conservation strategies**

The most upstream tanks which do not connect through a drainage canal in the cascade system are highly dependent on rainwater. Farmers practice some water conservation measures such as bund maintenance, proper drainage of water, timely cultivation, mulching, incorporation of organic matter with soil. Mostly in *Yala* season, farmers have to conserve water and Sri Lankan Dry Zone farmers practice "*Bethma*" as a strategy to cultivate under water scarce situation (Somarathna and Kono, 2005). Under the "Bethma" system, a part of the command area is temporarily distributed among all the farmers in the command area based on the available water in the tank during dry seasons (Oka et al., 2015). Percentage of farmers who practice water conservation strategies itself was considered as the index score.

IV. **Percentage of young farmers involved in agriculture**

Reluctance of the young generation to take up farming as the occupation is one of the common problems in many parts of Sri Lanka (Somaratne, 2002). When there are no adequate people for agricultural activities, eventually the maintenance and management of these small tank systems will face problems. Hence, this parameter was considered as important with respect to the sustainability of the tanks/tank cascades. The farmers below 40 years of age were considered as young farmers (Zondag et al., 2015). The scale used to provide scores to this parameter is presented in Table 5.

V. **Multiple water uses/users**

Livelihood of the ancient people was highly related to the village tank cascade functions. The multiple benefits of VTCs are water for irrigation, bathing, washing and drinking, sand mining, collecting firewood, harvesting sedges, collecting bee honey, maintaining groundwater table, harvesting lotus/water lily, harvesting timber, water for livestock, etc. This parameter identified the multi-purpose nature of the tanks in the cascade which is related to multiple water uses/users. Table 5 shows the normalization score of this parameter.

VI. **Population density**

Increment of population leads to overutilization of natural resources, thereby increasing environmental pollution, land encroachment and social conflicts. To avoid these problems in ancient VTCs, the village margins have been demarcated. Therefore, people were not allowed to encroach common lands and disturb the land use plan of the tank cascade system. This parameter considers the impact of population density on the sustainability of the tank cascade system. Table 6 presents the normalization score used for this parameter.

VII. **People's awareness of cascade system functions**

Traditional communities who have evolved around the village tanks used to appreciate the functions of the cascade systems since they had a good understanding of them. With time, this close relationship between tanks and the people was broken and the traditional knowledgebase also faded away. Lack of awareness about the functions of the cascade system and its components is also a parameter which is responsible for the sustainability of these systems. Knowledge about the VTCs, water utilization by different stakeholders in that area including downstream people, wild animals and overall environment are key factors with respect to the awareness. Understanding and awareness of the functionality of the entire cascade system lead to overcome the weaknesses and challenges for sustainability (Marambe et al., 2012). Accordingly, an assessment score was developed based on the awareness of defining the cascade system, identifying the different stakeholders and understanding of the multiple benefits of the cascades system.

VIII. **Women engagement in cascade activities**

According to third Dublin principle, 1992 "Women play a central part in the provision, management and safeguarding of water" (https://www.gwp.org/). It shows that

Table 6 Score of "Population density"

Category	Population density (person per sq. km)	Score
i	> = 400	0
ii	300– < 400	25
iii	200– < 300	50
iv	100– < 200	75
v	< 100	100

women play a key role in water management related activities. However, women's involvement in the farmer organizations activities, water management related decision making and problem solving are not substantial in many water management systems including cascades (https://www.gwp.org/). However, there is a tendency for females to protect water and natural resources since they are more concerned about the well-being of their families. Hence, this parameter is qualitatively looking for the level of women's engagements for the cascade activities and is considered as positively influencing the sustainability of the system. Accordingly, the scores for "Women engagement in cascade activities were given as "0" for "Not satisfied," "50" for "Moderately satisfied," "75" for "Satisfied" and "100" for "Highly satisfied."

IX. **Severity of human-elephant conflict**

Human-Elephant Conflict (HEC) is one of the national problems in Sri Lanka at present and would become worse in the future (Santiapillai et al., 2010). Mostly the elephant's damages to the cultivations are high in Dry season (Campos-Arceiz et al., 2009). Cultivations are less in dry season and elephants tend to find the few cultivated areas to fulfill their food requirements. Farmers are reluctant to cultivate when the HEC is high. Within a cascade system if the cultivations are damaged or abandoned due to HEC, it will have an adverse impact on the economy. Subsequently, it also has an impact on water and other resource management in the cascade systems. Some tanks can be completely abandoned as a result of the elephant threat (Anuradha et al., 2019). Additionally, HEC can be a huge threat to other domestic and livelihood activities. This parameter identifies the severity of HEC with respect to the sustainability of the tanks. Table 7 shows the normalization scale of HEC in the index.

X. **Percentage of Samurdhi beneficiaries**

Samurdhi is a program launched in 1995 by the Sri Lankan government to reduce poverty by providing food stamp and other financial supports for selected households based on their income levels. Therefore, the number of *Samurdhi* beneficiaries is an indirect parameter to measure existing poverty in the area. Hence, this parameter reflects the economic status of the area. When the poverty is high, people tend to exploit natural resources to fulfill their daily needs, thereby making natural systems

Table 7 Score of "Severity of HEC," "Percentage of *Samurdhi* beneficiaries" and "Average paddy yield in *Maha* season"

Category	Severity of HEC: Percentage of people affected by HEC	Percentage of *Samurdhi* beneficiaries	Average paddy yield in *Maha* season (kg per ha)	Score
i	> 75%	> 75%	< 3000	0
ii	50%– < 75%	50%– < 75%	3000– < 3500	25
iii	25%– < 50%	25%– < 50%	3500– < 4000	50
iv	0%– < 25%	1%– < 25%	4000– < 4500	75
v	0%	0%	> = 4500	100

more vulnerable. Following scale shows the normalization of percentage of *Samurdhi* beneficiaries (Table 7).

XI. **Average paddy yield in Maha season**

People are mostly cultivating paddy in *Maha* season under minor irrigation systems due to adequate presence of water with North East monsoon (Sakthivadivel, et al., 1996). Within a tank cascade system, the water management practices, water quality, the agronomic practices, etc. will influence the crop yield. Accordingly, the *Maha* season paddy yield was taken as a parameter of the sustainability of VTCs. Average paddy yield in *Maha* season in Sri Lanka is 4364 kg per ha (http://www.statistics.gov.lk). Accordingly, following scale was used to bring the paddy yield to measure sustainability (Table 7).

XII. **Cropping intensity (paddy)**

Cropping intensity can be defined as the ratio of area cultivated within a year to total command area. If both *Yala* and *Maha* are cultivated, the cropping intensity will become 2 which is generally the maximum value of cropping intensity for paddy. Hence the value varies in between 0 and 2. The cropping intensity depends on the water availability and water management of the cascade system. The index score was developed by using Eq. 1.

$$Index score = \frac{Cropping Intensity}{2} \times 100 \quad (1)$$

XIII. **Number of cascade related projects implemented during last 10 years**

The government and non-government agencies are implementing different projects to rehabilitate the village tank cascade systems. Those projects are implemented for different purposes such as renovation and rehabilitation of tanks, developing livelihood of the people in the area, improving natural environment. Since the number of projects which has been implemented would directly influence the sustainability of the VTCs, it was considered for developing the normalization score (Implementing none of the projects = 0, implementing 1–5 projects = 50 and implementing more than 5 projects = 100).

2.2.2 Calculation of Weights for the Parameters—Analytic Hierarchy Process

All the above-mentioned parameters are not contributing to the sustainability of the tanks/cascade systems in an equal scale. Hence, it is important to identify their relative contribution to the sustainability. An Analytic Hierarchy Process was used in identifying relative importance of these parameters by calculating weightages (Ishizaka and Labib, 2011; Srdjevic and Jandric, 2010). The terms of the fundamental Saaty's scale (Srdjevic and Jandric, 2010) were used to develop the pair-wise comparison matrix.

Accordingly, expert judgments were used to develop weightages for the parameters. However, relative importance of these parameters can change under individual cascade systems.

2.2.3 Aggregating the Parameters to Develop Index of Sustainability

The physical and environmental sustainability and socioeconomic sustainability were assessed separately by considering 50% contribution from each. The final sustainability index value was obtained, which is in between the range of 0–100. The index value indicates whether the tank cascade system/the individual tank is in very low sustainability (0–25)/ low sustainability (25–50)/ moderate sustainability (50–75) or high sustainability (75–100).

3 Results and Discussion

The developed sustainability index is presented by Eq. 2. It presents all the parameters with their weightages indicating the relative importance.

$$
\begin{aligned}
&Sustainability\ Index\ of\ VTCs \\
&= \left(\left(\begin{array}{l}
(0.34 \times Ratio\ of\ catchment\ area : Water\ surface\ area\ of\ tank) \\
+(0.17 \times Ratio\ of\ Live\ storage\ of\ the\ tank : Command\ area :) \\
+\left(\begin{array}{l} 0.07 \times Frequency\ of\ spilling\ the\ tanks\ within\ a\ specific \\ period\ of\ time(per\ year) \end{array} \right) \\
+(0.11 \times Agro - well\ density\ in\ the\ catchment) \\
+(0.09 \times Existence\ of\ ecological\ components) \\
+(0.16 \times Percentage\ of\ Forest\ cover\ in\ the\ catchment) \\
+(0.03 \times Presence\ of\ risky\ land\ uses\ in\ the\ catchment) \\
+(0.02 \times Presence\ of\ aquatic\ plants\ in\ tanks)
\end{array} \right) \times 50\% \right)
\end{aligned}
$$

$$+\left(\begin{array}{l}\left(\begin{array}{l}(0.21 \times Existance\,and\,performances\,of\,farmer\,organizations)\\ +\left(\begin{array}{l}0.16 \times Healthy\,agricultural\,practices - Organic\,fertilizer\\ usage\end{array}\right)\\ +\left(\begin{array}{l}0.12 \times Percentage\,of\,farmers\,who\,practice\\ water\,conservation\,stategies\end{array}\right)\\ +(0.09 \times Percentage\,of\,young\,farmers\,in\,farmer\,organization)\\ +(0.1 \times Population\,density)\\ +(0.07 \times People's \text{ awareness of cascade system functions})\\ +(0.06 \times Women\,engagement\,in\,cascade\,activities)\\ +(0.04 \times Multiple\,water\,uses\,and\,users)\\ +(0.04 \times Severity\,of\,human - elephant\,conflict)\\ +(0.04 \times Percentage\,of\,Samurdhi\,beneficiaries)\\ +(0.02 \times Average\,paddy\,yield\,in\,Maha\,season)\\ +(0.03 \times Cropping\,intensity(paddy))\\ +\left(\begin{array}{l}0.02 \times Number\,of\,cascade\,related\,projects\,which\,has\\ implemented\,during\,last\,10\,years\end{array}\right)\end{array}\right) \times 50\%\end{array}\right) \quad (2)$$

Figure 3 presents the Microsoft Excel interface of the developed index, application of an example data set and the presentation of results. Accordingly, it visualizes the input value (given example data set), its normalized scale, criteria weightage of each parameter, separately weighted assessment rank of each parameter and sustainability scores. According to the given example cascade system, overall sustainably was at the "moderate sustainable level" (sustainability score = 64). It further interprets that the physical-environmental sustainability was at highly sustainable level (sustainability score = 81) and socioeconomic sustainability was at "low sustainability level" (sustainability score = 47). Accordingly, it leads to the consideration of factors that can be changed. However, in general, physical and environmental factors are difficult to change without any financial/government/political assistance. Hence, practical and low cost approaches are needed to improve the socio-economic sustainability of the system.

Normalized scale of the individual parameters (Fig. 3) themselves presents the rehabilitation needs of the cascade system/the individual tank. According to this particular example, the parameters showing low scores such as existence of ecological components (score = 40), distribution of aquatic plants (score = 0), existence and performance of farmer organizations (score = 30), healthy agricultural practices (score = 40), percentage of farmers who practice water conservation strategies (score 20) and percentage of young farmers involved in agriculture (score = 40) can be considered in improving the sustainability.

The sustainability index of VTCs can be applied to any VTCs and for individual village tanks for quantifying their sustainability, and accordingly comparisons between tank cascades/tanks can be done. This can be helpful in selecting

Sustainability Assessment Matrix for Village Tank Cascade Systems								
	No	Parameter	Input value	Normalized scale	Criteria weight	Weighted Assessment rank	Sustainability of the tank	
Physical and environmental sustainability	1	Ratio of Catchment area: Water surface area of tank	6	75	0.34	25.65	81	64
	2	Ratio of live storage of the tank: total command area	1.5	100	0.17	16.72		
	3	Frequency of spilling of the tanks within a specific period of time (per year)	1	100	0.07	7.34		
	4	Existance of ecological components		40	0.09	3.75		
		5.1 Interceptor (Kattakaduwa)	50					
		5.2 Tree belt (Gasgommana)	50					
		5.3 Water hole (Godawala)	0					
		5.4 Upstream side ridges (Isweti)	0					
		5.5 Tank bund (Wew kandiya)	100					
	5	Agro well density in the catchment (number per km2)	9	75	0.11	8.08		
	6	Percentage of Forest cover in the catchment	80	100	0.16	16.03		
	7	Presence of risky land uses in the catchment (Large scale constructions/ Industrials/Deforestration)	0	100	0.03	3.08		
	8	Distribution of aquatic plants in tanks (% Coverage)	95	0	0.02	0.00		
Socio-Economic Sustainability	1	Existance and Performance of farmer organizations	30	30	0.21	6.37	47	
	2	Healthy agricultural practices - organic fertilizer usage	10	40	0.16	6.44		
	3	Percentage of farmers who practice water conservation strategies	20	20	0.12	2.39		
	4	Percentage of young farmers involved in agricuture	18	40	0.09	3.73		
	5	Multiple water uses		80	0.04	3.53		
		5.1. Irrigation	1					
		5.2. Bathing and washing	1					
		5.3. Drinking	0					
		5.4. Sand mining	0					
		5.5. Fishing	1					
		5.6. Collecting firewood from forested areas	1					
		5.7. Harvesting sedges	1					
		5.8. Collecting of bee honey	1					
		5.9. Maintaining the ground water table	1					
		5.10. Harvestig lotus, water lily and other flowers	1					
		5.11.Harvesting timber	0					
		5.12. Livestock	1					
		Score	9					
	5	Population density (Population per km^2)	68.43	100	0.10	9.57		
	6	People's awareness of cascade system functions	63	63	0.07	4.41		
	7	Women parcipation in cascade activities	3	100	0.06			
	9	Severity of Human Elephant conflict	20	75	0.04	3.36		
	10	Percentage of Samurdhi beneficiaries	7	75	0.04	2.94		
	11	Average paddy yield in maha season(kg per ha)	5115	100	0.02	1.59		
	12	Cropping Intensity (Total annual irrigated crop area/Total command area)	1	50	0.03	1.56		
	13	Number of cascade related projects which has implemented during last 10 years	1	50	0.02	0.78		

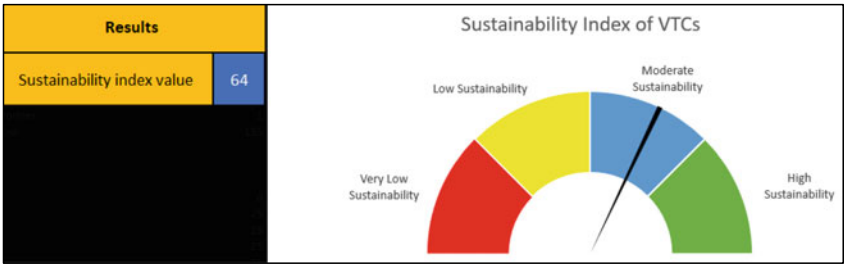

Fig. 3 Sustainability Index for Village Tank Cascade systems—the Microsoft Excel interface

tanks/cascade systems for different purposes such as tank rehabilitation, project implementations to obtain optimum benefits from these activities. The index further interprets the rehabilitation and development needs of the tank/cascade system.

According to the developed sustainability index, it is evident that the contribution of some of the parameters to the sustainability of the cascade system is significantly minimal according to the assessment. In the purpose of rapid assessment of

sustainability or in a situation where there is lack of data, it would be practically difficult to take all 21 parameters for the assessment. Hence, the parameters which have higher weights can be used in a rapid assessment. There are four physical-environmental parameters and four socioeconomic parameters which have more than 10% contribution to the developed sustainability index. These parameters are listed below:

Physical-Environmental Parameters:

- Ratio of catchment area: Water surface area of tank
- Ratio of live storage of tank: Command area
- Agro-well density in the catchment
- Percentage of forest cover in the catchment

Socio-Economic Parameters:

- Existence and performance of the farmer organization
- Healthy agricultural practices—Organic fertilizer usage
- Percentage of farmers who practice water conservation strategies
- Population density.

These parameters can again be weighted to suit different applications either for individual tanks or tank cascade systems. Accordingly, the following simplified equation presents the sustainability of VTCs.

$$
\begin{aligned}
&Sustainability\ of\ VTCs \\
&= \left(\left(\begin{array}{l} \left(\begin{array}{l} 0.44 \times Ratio\ of\ catchment\ area: \\ Water\ surface\ area\ of\ tank \end{array} \right) \\ + \left(\begin{array}{l} 0.22 \times Ratio\ of\ live\ storage\ of\ tank: \\ Command\ area \end{array} \right) \\ +(0.14 \times Agro-well\ density\ in\ the\ catchment) \\ +(0.20 \times Percentage\ forest\ cover\ in\ the\ catchment) \end{array} \right) \times 50\% \right) \\
&+ \left(\left(\begin{array}{l} \left(\begin{array}{l} 0.36 \times Existence\ and\ performance\ of \\ farmer\ organization \end{array} \right) \\ + \left(\begin{array}{l} 0.27 \times Healthy\ agricultural\ practices \\ -organic\ fertilizer\ usage \end{array} \right) \\ + \left(\begin{array}{l} 0.20 \times Percentage\ of\ farmers\ who\ practice \\ water\ conservation\ strategies \end{array} \right) \\ +(0.17 \times Population\ density) \end{array} \right) \times 50\% \right) \qquad (3)
\end{aligned}
$$

4 Conclusions

The developed sustainability index can be used in assessing the sustainability of any village tank cascade system as well as individual tanks. The sustainability index presents the overall sustainability as well as physical-environmental sustainability and socioeconomic sustainability separately. It helps in identifying the rehabilitation and development needs and comparisons of tanks and cascade systems. Out of 21 parameters considered in the sustainability index, it was identified that four physical-environmental parameters and four socio-economic parameters contribute more to the sustainability, and those eight parameters can be used in rapid assessments and in situations with poor data availability.

Acknowledgements This work was carried out with the aid of a grant from the International Development Research Center (IDRC), Ottawa, Canada. Their financial support is greatly appreciated.

References

Anuradha, J.M.P.N., Miho Fujimura, Tsukasa Inaoka, and Norio Sakai. 2019. The Role of Agricultural Land Use Pattern Dynamics on Elephant Habitat Depletion and Human-Elephant Conflict in Sri Lanka. *Sustainability* 11 (10): 2818.

Bandara, J.M.R.S., D.M.A.N. Senevirathna, D.M.R.S.B. Dasanayake, V. Herath, J.M.R.P. Bandara, T. Abeysekara, and Kolin Harinda Rajapaksha. 2008. Chronic Renal Failure Among Farm Families in Cascade Irrigation Systems in Sri Lanka Associated with Elevated Dietary Cadmium Levels in Rice and Freshwater Fish (Tilapia). *Environmental Geochemistry and Health* 30 (5): 465–478.

Bonnesoeur, Vivien, Bruno Locatelli, Manuel R. Guariguata, Boris F. Ochoa-Tocachi, Veerle Vanacker, Zhun Mao, Alexia Stokes, and Sarah-Lan. Mathez-Stiefel. 2019. Impacts of Forests and Forestation on Hydrological Services in the Andes: A Systematic Review. *Forest Ecology and Management* 433: 569–584.

Campos-Arceiz, Ahimsa, S. Takatsuki, S. Ekanayaka and T. Hasegawa. 2009. The Human-Elephant Conflict in Southeastern Sri Lanka: Type of Damage, Seasonal Patterns, and Sexual Differences in the Raiding Behavior of Elephants. *Geography* 5–14.

Dharmasena, P.B. 2009. Sustainability of Small Tank Irrigation Systems in Sri Lanka at the 21st Century. *Traversing No Man's Land: Interdisciplinary Essays in Honour of Sadurawan Madhuma Bandhura* 233–252.

Dharmasena, P.B. 2010. Essential Components of Traditional Village Tank Systems. In *Proceedings of the National Conference on Cascade Irrigation Systems for Rural Sustainability, Central Environmental Authority, Sri Lanka*, vol. 9.

Dharmasena, P.B. 2020. Cascaded Tank-Village System: Present Status and Prospects. In *Agricultural Research for Sustainable Food Systems in Sri Lanka*, 63–75. Singapore: Springer.

Dharmasena, P.B., and I.M. Goodwill. 1999. Use of Groundwater in Minor Tank Irrigation Schemes of Sri Lanka. In *ICID, 17th Congress on Irrigation and Drainage*, 175–194. Spain: Granada.

Ekhuemelo, David O., J.I. Amonum, and I.A. Usman. 2016. Importance of Forest and Trees in Sustaining Water Supply and Rainfall. *Nigeria Journal of Education, Health and Technology Research* 8: 273–280.

Geekiyanage, Nalaka, and D.K.N.G. Pushpakumara. 2013. Ecology of Ancient Tank Cascade Systems in Island Sri Lanka. *Journal of Marine and Island Cultures* 2 (2): 93–101.

http://www.statistics.gov.lk/agriculture/Paddy%20Statistics/PaddyStatsPages/AverageYield.html. Retrieved on 16.03.2020.

https://doa.gov.lk/rrdi/index.php?option=com_sppagebuilderandview=pageandid=42andlang=en. Retrieved on 12.04.2020.

https://www.centreforpublicimpact.org/case-study/samurdhi-programme-sri-lanka. Retrieved on 17.08.2021.

https://www.gwp.org/contentassets/05190d0c938f47d1b254d6606ec6bb04/dublin-rio-principles.pdf. Retrieved on 17.03.2020.

Ishizaka, Alessio, and Ashraf Labib. 2011. Review of the Main Developments in the Analytic Hierarchy Process. *Expert Systems with Applications* 38 (11): 14336–14345.

Jayarathne, K.D.B.L., N.D.K. Dayawansa, and R.P. De Silva. 2010. GIS Based Analysis of Biophysical and Socio-Economic Factors for Land Degradation in Kandaketiya DS Division. *Tropical Agricultural Research* 21 (4): 361–367.

Loucks, Daniel, P., and Eelco Van Beek. 2017. Water Resource Systems Planning And Management: An Introduction to Methods, Models, and Applications. *Springer*, 1–49.

Madduma Bandara, C. 1985. Catchment Ecosystems and Village Tank Cascades in the Dry Zone of Sri Lanka a Time-Tested System of Land and Water Resource Management. In *Strategies for River Basin Management*, 99–113. Dordrecht: Springer.

Marambe, Buddhi, Gamini Pushpakumara, and Pradeepa Silva. 2012. Biodiversity and Agrobiodiversity in Sri Lanka: Village Tank Systems. In *The Biodiversity Observation Network in the Asia-Pacific Region*, 403–430. Tokyo: Springer.

Oka, Naoko, Takeru Higashimaki, D.D.P. Witharana, and Mekonnen B. Wakeyo. 2015. Constrains and Consensus on Water Use and Land Allocation in Minor Scheme Tanks in the Dry Zone of Sri Lanka. *Scientific Papers Series Management, Economic Engineering in Agriculture and Rural Development* 15 (4): 185–190.

Panabokke, Christopher R., M. U. A. Tennakoon, and R. de S. Ariyabandu. 2001. Small Tank Systems in Sri Lanka: Issues and Considerations. In *Proceedings of the Workshop on Food Security and Small Tank Systems in Sri Lanka. National Science Foundation, Colombo, Sri Lanka*, 1–6.

Pelpitiya, I.P.S.K., N.D.K. Dayawansa, and E.R.N. Gunawardena. 2016. Impacts of Land Cover Dynamics and Shallow Groundwater Abstraction on Sustainability of Hakwatuna Oya Irrigation System. *Tropical Agricultural Research* 27 (1): 13–26.

Perera, M.P. 2016. The Hydro-Ecological Impact Assessment Scoring: A New Participatory Method to Grasp Hydro-Ecological Impact of Agro-well Development of Sri Lanka. *International Journal of Advanced Research and Review* 1 (7): 01–10.

Sakthivadivel, Ramaswamy, Christopher R. Panabokke, N. Fernando, and C. M. Wijayaratna. 1994. Guidance Package for Water Development Component of Small Tank Cascade Systems. Colombo, Sri Lanka: International Irrigation Management Institute (IIMI). Sri Lanka Field Operations (SLFO), for International Fund for Agricultural Development (IFAD).166.

Sakthivadivel, Ramaswamy, Nihal Fernando, Christopher R. Panabokke, and C. M. Wijayaratna. 1996. Nature of Small Tank Cascade Systems and a Framework for Rehabilitation of Tanks Within Them. Colombo, Sri Lanka: International Irrigation Management Institute (IIMI).54.

Samarasinghe, Y.M.P., and N.D.K. Dayawansa. 2011. Mapping Degradation Risk of Kolonnawa Marsh: A Study with Remote Sensing and GIS. Undergraduate thesis, Faculty of Agriculture, University of Peradeniya, Sri Lanka, 50.

Sangrama. 2018. Participatory Rural Appraisal Report: Participatory Climate Risk Vulnerability Capacity Assessment (pcr-vca) Palugaswewa Cascade, 43.

Santiapillai, Charles, S. Wijeyamohan, Ganga Bandara, Rukmali Athurupana, Naveen Dissanayake, and Bruce Read. 2010. An Assessment of the Human-Elephant Conflict in Sri Lanka. *Ceylon Journal of Science (biological Sciences)* 39 (1): 21–33.

Somarathna, H.M., and H. Kono. 2005. Indigenous Institutions for Irrigation Water Management and Sustainable Agriculture: A Case Study from Sri Lanka. *Journal of Agricultural Development Studies (Japan)*, 69–76.

Somaratne, W.G. 2002. Sri Lankan Agriculture for the Next Decade: Challenges and Opportunities. *Hector Kobbekaduwa Agrarian Research and Training Institute, Sri Lanka*, 123.

Srdjevic, Bojan, and Zorica Jandric. 2010. Analytic Hierarchy Process in Selecting the Best Irrigation Method. *Agricultural Systems* 103 (6): 350–358.

Wijesundara, S. 2010. Invasive Alien Plants in Sri Lanka. *Invasive Alien Species—Strengthening Capacity to Control Introduction and Spread in Sri Lanka. Biodiversity Secretariat of the Ministry of the Environment and United Nations Development Programme, Sri Lanka*, 27–38.

Zondag, Marie-José, Sacha Koppert, Carolien De Lauwere, Peter Sloot, and Andres Pauer. 2015. Needs of Young Farmers: Report I of the Pilot Project: Exchange Programmes for Young Farmers. *European Commission, Directorate-General for Agriculture and Rural Development*, 79.

An Agent Based Model of Mangrove Social-Ecological System for Livelihood Security Assessment

Shamima Airin Sweety, M. Shah Alam Khan, Anisul Haque, and Mashfiqus Salehin

Abstract Ecosystem services and livelihood security are strongly interrelated in any social-ecological system (SES), and their interdependence should be assessed using an integrated framework. Overexploitation of ecosystem resources may undermine the ecosystem services while restrictions on resource extraction may hamper the dependent livelihoods. We examine these interrelationships for the mangrove SES in Bangladesh using an Agent Based Model (ABM), a useful tool for integrated assessment of human behavior and natural processes. The model simulates the dynamics of ecosystem pressure and livelihood security by linking the supply and expenditure of ecosystem resources, exploited and/or regulated by five primary agents, viz. Bawalis, Farmers, and Fishers (livelihood agents), and Forest office and UP office (institutional agents). We find that the livelihood activities can be considerably influenced, both favorably and adversely, by the ecosystem characteristics and the institutional efficiencies. Sustainability of the livelihood activities is indicated by a change in the number of livelihood groups being able to continue their activities in the long term. This will require sound institutional policy for conservation of the ecosystem, preventing overexploitation, and supporting production of provisioning ecosystem services. Supporting optimum levels of livelihood activities and ensuring sustainability of ecosystem resources will help avert their tipping points.

Keywords Social-ecological system · Livelihood sustainability · Agent based model · Ecosystem service · Mangrove

S. A. Sweety (✉) · M. S. A. Khan · A. Haque · M. Salehin
Institute of Water and Flood Management, Bangladesh University of Engineering and Technology, Dhaka, Bangladesh

© The Author(s), under exclusive license to Springer Nature Switzerland AG 2022

G. M. Tarekul Islam et al. (eds.), *Water Management: A View from Multidisciplinary Perspectives*,
https://doi.org/10.1007/978-3-030-95722-3_16

1 Introduction

1.1 Mangrove Social-Ecological System and Ecosystem Services

Mangroves provide essential ecosystem services to the coastal population and natural environment. These services include provisioning (e.g., food and water), regulating (e.g., climate and disease control), supporting (e.g., nutrient cycling and pollination), and cultural (e.g., recreational and spiritual) dimensions that define the services. While ecosystem services ensure material and energy flows, leading to economic flow, human actions and interventions often stress the ecosystem and affect its services to varying extents. The cultural dimensions influence the way social groups act and perform. A systems view of the coupled human-natural processes is thus useful in the analysis of sustainability of the ecosystem services and resilience of the ecosystem, society, and institutions. This concept of a dynamically coupled human and natural system (CHANS) can therefore be applied more specifically to an integrated social-ecological system (SES) of the mangrove ecosystem and its dependent population.

The SES framework emerged from the concepts of common pool resources and integrated social-ecological processes (Ostrom 1990; Ostrom et al. 2007). A SES is an integrated and adaptive system representation of the social and ecological components and processes and broadly represents the human and natural domains of the system (see Fig. 1). The complex dynamics of the integrated system, particularly in different dimensions and scales, however, are yet to be fully understood and operationalized through analytical methods and tools. Virapongse et al. (2016) present a framework to translate the SES theory into practice for improved environmental management by defining the key components and processes in the system. Interaction of processes in the human and natural domains of the SES gives rise to a set of management decisions and adaptation choices, while the system and its sub-domains

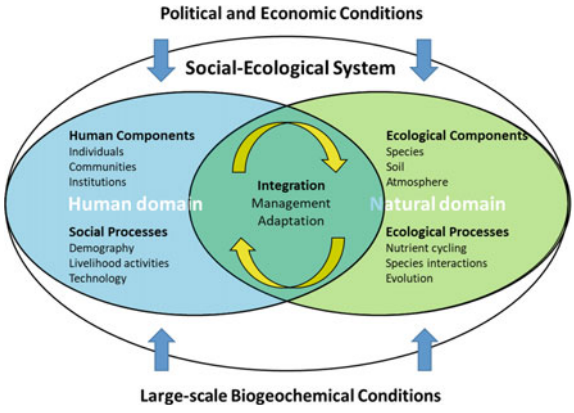

Fig. 1 Components and processes in a social-ecological system [Adapted from Virapongse et al. (2016)]

are influenced by external factors such as political, economic, and biogeochemical conditions. Other approaches to operationalization of the SES theory and representation of the nonlinear system properties and dynamics are found elsewhere in the literature (Cole et al. 2019; Forrester et al. 2014; Schlüter et al. 2012, Schlüter et al. 2014).

1.2 Livelihood Security and Dependency

The Sundarbans mangroves are rich sources of livelihood resources such as timber, mangrove palm, fish, shrimp, crab, and honey. Rice is also grown in the fringe areas of the mangroves. Household income and food security of the communities living in and around the mangroves depend mostly on these resources. Although the households are clustered and known by their main livelihood activities, household members are often engaged in multiple livelihoods to maximize the household income. Also, different livelihood groups in a community are connected and interdependent through various social and economic activities.

Local-level institutions, such as the Forest Office, regulate resource extraction to prevent overexploitation of resources and preserve ecosystem health and undertake other measures for ecosystem conservation and growth. Other institutions, such as the Union Parishad, the lowest tier local government institution, provide support to the livelihood groups through subsidies, training, and awareness campaign. Thus, sustainability of the mangrove-dependent livelihoods depends not only on the natural resources, but also on the institutional policies and broader economic, political, and environmental conditions.

1.3 SES Tipping Points

Sustainability of both the ecosystem and the dependent livelihoods is ensured when the resource extraction and ecosystem growth are balanced. This equilibrium can be achieved through regulatory policy and participatory decision making. However, environmental hazards or overexploitation often leads to negative feedback loops in the system forcing it to reach a tipping point. For example, overexploitation of fish increases household income, but rapidly depletes the fish availability, eventually leading to an overall decline of the SES sustainability. The tipping point is the 'point of no return' beyond which the SES can no longer be brought back to the previous equilibrium even by lowering the fish catch. Examples of SES feedback loop, ecosystem service trade-off, food security, and livelihood sustainability are given in Miyasaka et al. (2017), Acosta et al. (2018), Dobbie et al. (2018), and Yan et al. (2019).

1.4 Agent Based Modeling for SES Analysis

Agent based models (ABM) can help develop a simplified understanding of the complex and dynamic interaction among the ecosystem components, human actors, and institutions. This understanding is essential for sustainable environmental management and livelihood security. ABMs idealize the SES as a composition of autonomous, decision-making agents that are able to follow their goals, based on a set of rules. These agents may range from plant species to fish and animals, to households, livelihood groups, and institutions (Schulze et al. 2017; Rounsevell et al. 2012; Macal and North 2009). ABMs can also analyze the complexities such as heterogeneity, nonlinearity, and feedback in a CHANS or integrated SES, support geospatial simulation or participatory modeling of the SES, explore the system behavior across scales, and clarify the system dynamics in varying conditions (An 2012; An et al. 2014; Castle and Crooks 2006; Voinov et al. 2018; Lippe et al. 2019; Martin and Schlüter 2015; Hossain et al. 2017).

In this paper, we present an ABM application to analyze the mangrove SES-based livelihood processes, simulate the dynamics of livelihood activities and ecosystem responses, determine the efficiency of institutions in SES management, and explore how livelihood decisions and tipping points vary in different scenarios. In particular, we assess the ecosystem pressure in response to livelihood activities and try to understand how restrictions on resource extraction impact livelihoods.

2 Study Area and Methods

2.1 Study Area Description

2.1.1 SES Components and Linkages

Gabura union under Shyamnagar upazila of Satkhira district and its surrounding areas of the Sundarbans is selected as the study area (Fig. 2). Since the life and livelihoods of people in Gabura are strongly dependent on the mangrove resources, the study area is an excellent example of a SES. The mangrove forest (Sundarbans), of its total of 10,000 km^2, covers an area over 6,017 km^2 in Bangladesh. This world heritage site provides natural protection against cyclones and storm surges. The fertile soils of this area have been used intensively in agriculture for centuries, and the fringes of this ecoregion have been converted for intensive agriculture thereby decreasing the forest area alarmingly. This transition region between freshwater from the Ganges and saline water of the Bay of Bengal provides a brackish environment rich in biodiversity.

Golpata or mangrove palm (*Nypa fruticans*) is a very common palm species of the Sundarbans which grows in abundance here naturally, mainly in the less saline zone but can also grow in the moderate saline zone. Golpata is of high demand as

Fig. 2 Location and physical features of the mangrove social-ecological system under study

an economically important product for its widespread domestic and commercial use. However, the golpata stock in the Sundarbans has been severely decreasing because of both licensed and unauthorized extraction in excessive amounts, and due to the lack of proper forest management.

Fishes of the Sundarbans represent 322 species belonging to 217 genera, 96 families, and 22 orders (Habib et al. 2020), with at least 150 species of commercially important fish (Wikipedia 2021). The forest also supports the habitat for economically significant mud crabs or mangrove crabs (Banglapedia 2021). Fishing and collecting fish and crab seedlings from the mangrove and nearby offshore waters for fish farming are very common livelihoods of the people living in and around the Sundarbans. Many people are also engaged in fish farming and household fishing. Overfishing and excessive seedling collection to meet the increasing domestic and commercial demands has become a threat for the sustainability of the ecosystem services of the Sundarbans (Hoq 2007).

2.1.2 Physical and Hydro-Climatic and Settings

Gabura union is situated on the bank of the Kholpetua River, which separates this union from the Sundarbans (Fig. 2). The Kopotakkho River flows on the east side of this union, bordering with Dakshin Bedkasi union of Koyra upazila of Khulna district. Gabura is also adjacent to Padmapukur union on the north and is 27 km and 82 km away from the upazila headquarter and Satkhira district headquarter, respectively.

Gabura is one of the few areas near the Sundarbans that have been frequently affected by cyclones and storm surges. Climate change is believed to have increased the frequency of these high-energy cyclones. Fresh water availability has been severely limited in Gabura, which becomes acute after every cyclone. The brackish

water is useful for the fish farms, but adversely affects crop production and freshwater habitats. Criss-crossed with a network of rivers and canals, the area suffers from sediment deposition in the water bodies.

2.1.3 Primary and Alternative Livelihoods

The major livelihoods in this area include crab fattening, shrimp farming, agriculture, fishing, golpata and honey collection, day labor, van/auto bike pulling, and small businesses. About 42% of the people in the study area are involved in aquaculture, especially crab fattening for their livelihoods, while approximately 19% are dependent on forest resources, 16% are involved in shrimp farming, and 23% engage in agricultural activities, mainly paddy cultivation (http://www.gaburaup.satkhira.gov.bd). The primary mangrove-dependent livelihoods are fishing in mangrove water bodies and household ponds, extracting golpata and paddy cultivation. Golpata extraction is possible only in winter time in mid-March to mid-May; therefore, the Bawalis, i.e., the golpata collectors, do fishing as an alternative livelihood. Mangrove-dependent fishers of this area go into the mangroves for fishing, with a small group of them also doing fishing in household ponds. These fishers do not take other livelihood options although they are required to stop fishing in the mangroves due to fishing ban for one month of the year usually in July. Other fishers do fishing in household ponds only.

2.2 Agent Based Model for Mangrove SES

The important steps for developing an ABM for the Mangrove SES include selecting important agents, developing a conceptual model delineating how the agents interact with each other and their environment, and defining the rules; mathematically how the agents would behave, interact, and take decisions autonomously. The conceptual framework and the rules for different agents were based on review of secondary literature on Sundarban-based livelihood systems (e.g., Mallick et. al. 2021; Kabir et. al. 2019; Mozumder et. al. 2018; Getzner and Islam 2013; Sarker 2011 and https://www.ccec-bd.org › files › reports), direct mobile communication with few representatives of the primary agents (e.g., fishermen, Bawalis), and expert judgment. Some baseline data was collected from the Bangladesh Bureau of Statistics (BBS) database (http://www.bbs.gov.bd/).

The model can be considered exploratory at this stage. The conceptual model and the rules for agent behavior will require detailed verification and validation in the field with the primary agents (which was limited during this study because of the prevailing COVID situation) before the ABM for the mangrove SES can be used as a fully robust model. Nevertheless, the approximations made in the formulation are considered reasonable, if not fully accurate, and hence the model should be able to provide useful early insights.

Table 1 Agents and model environment

Class of Agents	Name of Agents	Model Environment
Livelihood Agent	Bawalis	Mangrove Socio-Ecological System
	Fishers	
	Farmers	
Institutional Agent	Union Parishad Office (UPO)	
	Forest Office (FO)	

2.2.1 Agent Selection for ABM

Agents are individual actors or actor groups of a SES who can interact with each other and their environment by autonomous decision-making based on specific rules. This study simulated the interrelations of the main mangrove-dependent livelihood groups (both individual actors and actor groups) with each other and with the environment of the SES. The livelihood activities are also linked with the regulations by the Union Parishad Office (UPO) and Forest Office (FO). For this reason, three main livelihood groups of this study area: Bawalis, Fishers, and Farmers, and these two institutions have been considered as the agents in the ABM model. The agent classification and model environment are given in Table 1.

2.2.2 Conceptual Model

Following the agent descriptions and attributes discussed earlier, Fig. 3 shows a conceptual model of interactions among the agents of the mangrove SES. Golpata is

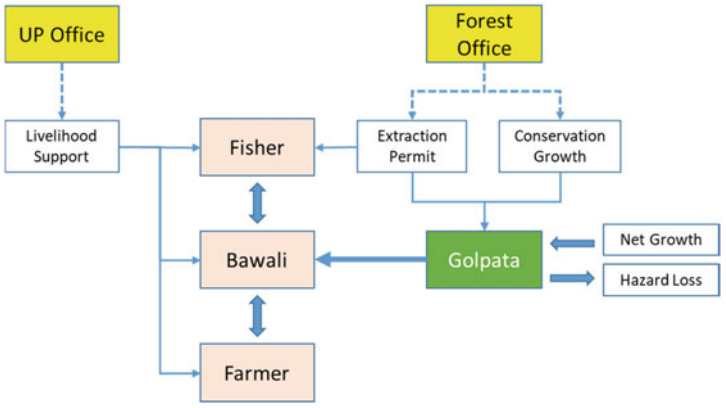

Fig. 3 Conceptual model of the mangrove social-ecological system showing the agents and their livelihood interactions

a primary source of livelihoods of the Bawalis. The Bawalis mainly extract golpata from the Sundarbans with a permit from the FO to extract a maximum fixed amount. The extraction amount of the Bawalis depends on their extraction capacity and the permitted extraction amount. The FO gives permission till the golpata stock of the patches in the forest reaches a threshold maximum amount after which the permission ceases. Also, the Bawalis need to attain a threshold capacity to go to the forest for extracting golpata even if they get a permit. Otherwise, they mainly do fishing or farming to support household activities and increase their extraction capacity gradually. Golpata grows and dies in a natural way at a net growth rate, while the golpata stock decreases due to natural hazards at an average rate. For each extraction trip, the Bawalis need to spend a portion of resources, which is subtracted from their actual extraction amount. A fraction of the remaining extracted amount contributes to increasing the extraction capacity for the next trip. Rest of the extracted amount is spent for household living and other purposes. The FO stops giving permits if the golpata stock reaches a minimum threshold amount when the FO also starts conservation activities for golpata to grow rapidly.

Two types of fishers are considered in this study. The first type of fishers mainly goes to the mangroves to catch fish using boats after getting a permit from the FO. The FO generally stops giving fishing permits for one month per year to support fish breeding, during which time these fishers remain jobless. For catching fish, they need to spend a portion of resources which is subtracted from their catching capacity in terms of the catch amount. A fraction of the catch amount contributes to increasing the catching capacity for the next year, which is proportional to the number of fish caught in the current year. Rest of this amount is spent for household living and other purposes. They can take permits from the FO many times in a year, with each permit valid for one week. Although the catch amount during a trip is uncertain, these fishers can generally catch a good amount for 7 months, a satisfactory amount for 2 months and small amounts for the rest of the year. Their expenditure, mainly on living, slightly increases if they can achieve a certain threshold of catching capacity. If their catching capacity goes down below a minimum threshold, they need to take loans for continuing fishing. They must pay back the loan with interests at a higher rate. Some of these fishers also do fishing in their household ponds.

The second type of fishers only grows fish in their own household ponds. They need to bear the production cost which is subtracted from their catching capacity. A fraction of the production increases the catching capacity for the next year and the remaining amount is used for household living and other purposes. The procedures for taking loan and repayment are similar to the first type of fishers. Fishes in the mangroves and household ponds increase due to breeding and decrease due to death and catching. Besides, if the fishes increase at a certain maximum threshold rate, a certain population of the fish dies naturally.

Farmers grow crops (mainly paddy) according to their crop production capacity and crop productivity of the agricultural land. They need to bear fertilizer cost to produce paddy which is subtracted from their crop production capacity. Crop productivity of the land decreases due to natural hazards, mainly soil salinization from storm surges. The actual production amount of paddy depends on the remaining crop

production capacity and crop productivity. A fraction of this actual amount increases the crop production capacity of the farmers for the next year. The remaining amount is used for living and other expenses at the household level. Farmers need to achieve a minimum crop production capacity to produce paddy; otherwise, they have to take loans. The loan is repaid later at a higher rate with interest.

The UPO performs regulatory functions in the study area to support financial security of the livelihood groups. It also coordinates with the FO for forest conservation. The efficiency of providing financial security depends on the capacity of livelihood activities of the livelihood groups. For example, if the number of active Bawalis decreases to a certain minimum, it indicates the lack of efficiency of the UPO in supporting their financial security. Similarly, if the number of fishers and farmers who have loans to pay increases to a certain maximum, it indicates a lower efficiency of the UPO in supporting their financial security.

The FO regulates extraction in mangroves for mangrove protection and conservation. When the natural hazard loss exceeds a certain amount, and the conservation growth rate remains low at the same time, it indicates low forest conservation efficiency. Since the livelihood groups depend on ecosystem resources directly for their livelihood activities, they produce pressure on the ecosystem. Such pressures produced by each livelihood group are calculated from the Net Primary Productivity (NPP) (from the net carbon gain) supply of the ecosystem and the NPP consumed by the livelihood group.

2.2.3 Mathematical Descriptions

Mathematical formulation of the model follows an agent-wise rule-based approach where the agents follow their own procedures according to the rules and behave autonomously while they interact with each other and with their environment. The pressures produced by the livelihood groups are calculated from the NPP supply on the ecosystem and the NPP consumed by each livelihood group where the NPP is estimated from the net carbon gain. The multipliers with variables and subtractors from variables in the equations are taken hypothetically considering logic where multipliers are numbers and subtractors have the same unit of associated variables.

Rules Related to Bawalis

The rules for the Bawalis are defined in terms of their extraction capacity, actual extraction amount, new actual extraction amount, golpata permit, golpata stock, their cost of movement, natural growth rate of golpata, conservation growth rate of golpata, and natural hazard loss of golpata. All these components are expressed in Metric tons.

1. If permit for golpata extraction remains active, then the Bawalis need to have a minimum capacity to extract golpata and they can extract the amount of golpata

according to the amount permitted by the FO and their capacity for extraction. If their capacity is higher than the permitted amount, they need to extract the amount equal to the permitted amount, otherwise they can extract equal to their capacity which is their actual extraction amount.

2. They need to spend for their movement to the mangroves and it reduces some units of their actual extraction amount as follows:

$$\begin{aligned}\text{new actual extraction amount} &= \text{actual extraction amount} \\ &\quad - \text{movement cost of bawali} \end{aligned} \tag{1}$$

3. A fraction of this increases the extraction capacity of Bawali for the next year. So, their increased capacity becomes:

$$\begin{aligned}\text{extraction capacity} &= \text{extraction capacity} \\ &\quad + (0.01 \times \text{ new actual extraction amount}) \end{aligned} \tag{2}$$

4. If the permit remains off and they have the minimum necessary capacity for extraction, then they lose some units of their extraction capacity as follows:

$$\text{extraction capacity} = \text{extraction capacity} - 10 \tag{3}$$

5. If they do not have the minimum capacity, then they increase their capacity by some units for extraction in the next year by doing fishing or farming as follows:

$$\text{extraction capacity} = \text{extraction capacity} + 2 \tag{4}$$

6. If golpata stock of patches has a certain maximum unit of golpata, then the golpata stock changes by the following equation:

$$\text{golpata stock} = \text{golpata stock} + \text{golpata natural growth rate} - \text{natural hazard loss} \tag{5}$$

7. If the golpata stock of patches reaches at a certain minimum amount, FO starts conservation. In this case,

$$\begin{aligned}\text{golpata stock} &= \text{golpata stock} + \text{natural growth rate} \\ &\quad + \text{conservation growth rate} - \text{natural hazard loss} \end{aligned} \tag{6}$$

Rules Related to Fishers

Rules for the fishers are defined in terms of their apparent and actual catching capacity, amount of loans they take, cost of ice for fish preservation, their movement cost, and fish production cost. All these components are expressed in Metric Tons.

1. Fishers who catch fishes in mangrove water area need to spend movement cost for fishing in mangroves and for carrying ice to protect fishes. It decreases some units of their capacity. So, their actual catching capacity becomes:

$$\text{actual catching capacity} = \text{catching capacity} - \text{movement cost} - \text{ice cost} \tag{7}$$

2. If they can catch a good amount of fishes for at least seven months per year, it increases their catching capacity by some units as follows:

$$\text{catching capacity} = \text{catching capacity} + (0.05 \times \text{actual catching capacity}) \tag{8}$$

Otherwise,

$$\text{catching capacity} = \text{catching capacity} - 0.075 \tag{9}$$

3. If they can catch a moderate amount of fishes for at least two months per year, it increases their catching capacity by some units as follows:

$$\text{catching capacity} = \text{catching capacity} + 0.075 \tag{10}$$

Otherwise,

$$\text{catching capacity} = \text{catching capacity} - 0.1 \tag{11}$$

4. If they can catch a small amount of fishes for a maximum of two months per year, it increases their catching capacity by some units as follows:

$$\text{catching capacity} = \text{catching capacity} + 0.05 \tag{12}$$

Otherwise,

$$\text{catching capacity} = \text{catching capacity} - 0.03 \tag{13}$$

5. Fishing in mangroves remains stopped for one month, and the fishers become jobless at this time. In this case,

$$\text{catching capacity} = \text{catching capacity} - 0.125 \tag{14}$$

6. If their catching capacity becomes greater than 2.5 Metric ton, they increase additional expenses and therefore:

$$\text{catching capacity} = \text{catching capacity} - 0.25 \tag{15}$$

7. If their catching capacity becomes less than 2 Metric ton, they need to take loan to increase some units of their catching capacity by the following equation,

$$\text{catching capacity} = \text{catching capacity} + 0.1 \tag{16}$$

8. After achieving a catching capacity greater than 2.5 Metric ton after taking loan, they pay back their loan at a slightly increased amount, which is given by the following equation:

$$\text{catching capacity} = \text{catching capacity} - 0.2 \tag{17}$$

9. Some of these fishers also do household fishing and thus increase some units of their catching capacity for fishing in mangroves by,

$$\text{catching capacity} = \text{catching capacity} + 0.005 \tag{18}$$

10. Fishers who grow fishes in household ponds need to spend a production cost and therefore their actual catching capacity becomes:

$$\text{catching capacity} = \text{catching capacity} - \text{fish production cost} \tag{19}$$

11. If the production is good for most of the year, then their catching capacity increases as:

$$\text{catching capacity} = \text{catching capacity} + (0.1 \times \text{actual catching capacity}) \tag{20}$$

12. If their fish production for the year is moderate, then:

$$\text{catching capacity} = \text{catching capacity} + (0.075 \times \text{actual catching capacity}) \tag{21}$$

13. If they produce a small amount of fishes in the year, they cannot increase their catching capacity.
14. If they produce a very low amount of fish which is not noticeable, their catching capacity decreases as follows:

$$\text{catching capacity} = \text{catching capacity} - 0.5 \tag{22}$$

15. If their catching capacity becomes greater than 2.7 Metric ton, they increase their other expenditure, and it reduces some units of their catching capacity as:

$$\text{catching capacity} = \text{catching capacity} - 0.25 \tag{23}$$

16. They need to take loan, if their catching capacity becomes less than 2 Metric ton, to increase their catching capacity as:

$$\text{catching capacity} = \text{catching capacity} + 0.1 \tag{24}$$

17. They pay back the loan after gaining a catching capacity greater than 2.5 Metric ton, which is represented by,

$$\text{catching capacity} = \text{catching capacity} - 0.2 \tag{25}$$

Rules Related to Farmers

Rules for the farmers are defined in terms of crop production capacity, actual production amount, loan, crop productivity, actual crop productivity, fertilizer cost, and natural hazard loss of crops. All these components are expressed in Metric Tons.

1. Farmers' actual crop production depends on the actual crop productivity of their agricultural land and their own capacity. They need to also pay for fertilizer. The crop productivity of agricultural land decreases due to natural hazards. If their capacity is higher than half of the actual crop productivity of the land, their actual production amount then becomes half of the actual crop productivity of the land (since it is observed that two farmers produce in each land); otherwise, they produce the amount to their capacity.
2. They need a certain minimum capacity to produce crops.
3. If the actual crop productivity is greater than 15 Metric ton, then their capacity increases as:

$$\text{crop production capacity} = \text{crop production capacity} + \left(0.1 \times \begin{pmatrix}\text{actual production amount} \\ -\text{fertilizer cost}\end{pmatrix}\right) \tag{26}$$

4. If the actual crop productivity is between 10 Metric ton and 15 Metric ton, the crop production capacity increases as:

$$\text{crop production capacity} = \text{crop production capacity} + \left(0.05 \times \begin{pmatrix}\text{actual production amount} \\ -\text{fertilizer cost}\end{pmatrix}\right) \tag{27}$$

5. If the actual crop productivity is less than 15 Metric ton, then crop production capacity becomes:

$$\text{crop production capacity} = \text{actual production amount} - \text{fertilizer cost} \tag{28}$$

6. They take loan if their crop production capacity is less than or equal to 2.5 Metric ton which is given by,

$$\text{crop production capacity} = \text{crop production capacity} + 1 \tag{29}$$

7. They pay back the loan when they regain their crop production capacity to greater than or equal to 4 Metric ton as below:

$$\text{crop production capacity} = \text{crop production capacity} - 1.25 \tag{30}$$

Rules Related to UPO

1. If the mean extraction capacity of the Bawalis, mean catching capacity of both types of Fishers, and mean crop production capacity of Farmers become less than 125, 2.3, and 4.5 Metric ton, respectively, and the number of active Bawalis becomes less than half of the total number of the Bawalis, then financial security efficiency (a dimensionless quantity or score) of the UPO will be 0.5; otherwise, it will be 1 for each of these 5 cases.
2. If the number of Fishers of both types and Farmers who have loans to pay is greater than their total number for each of these three types of livelihoods, then financial security efficiency of UPO will be 0.5; otherwise, it will be 1 for each of these 3 cases.
3. The efficiency of UPO is calculated by,

$$\begin{aligned}\text{efficiency of UP Office} = {} & \text{regulatory efficiency} \\ & + \text{support of financial security efficiency} \\ & + \text{financial safety efficiency}\end{aligned} \tag{31}$$

Rules Related to FO

1. If for natural hazard, the loss of golpata becomes greater than 1 Metric ton, and in this case conservation growth rate of golpata remains less than 4 Metric ton, the forest conservation efficiency (dimensionless quantity or score) of the FO will be 2; otherwise, it will be 4.
2. The efficiency of FO is given by,

$$\begin{aligned}\text{efficiency of Forest Office} = {} & \text{extraction control efficiency} \\ & + \text{forest conservation efficiency}\end{aligned} \tag{32}$$

Pressure on the Ecosystem

Pressure on the ecosystem is calculated by the following equation for all livelihood groups (Yan et al. 2019),

$$\text{pressure on ecosystem} = \frac{\text{NPP consumed}}{\text{NPP supply}} \tag{33}$$

Pressures on ecosystem are numbers as they are ratio of the amount of carbon.

Simulations using NetLogo

Based on the conceptual framework for the ABM, mathematical equations were set for formulating the computational framework. The NetLogo software (https://ccl.northwestern.edu/netlogo/) was used for simulations of the ABM (the interface is shown in Fig. 4). NetLogo is a multi-agent programming language and modeling environment for simulating complex systems evolving over time (Tisue and Wilenski 2004).

NetLogo visualizes the model by a 'NetLogo world' (made up of agents). It has four types of agents:

Turtles: This type of agents can move around in the world.

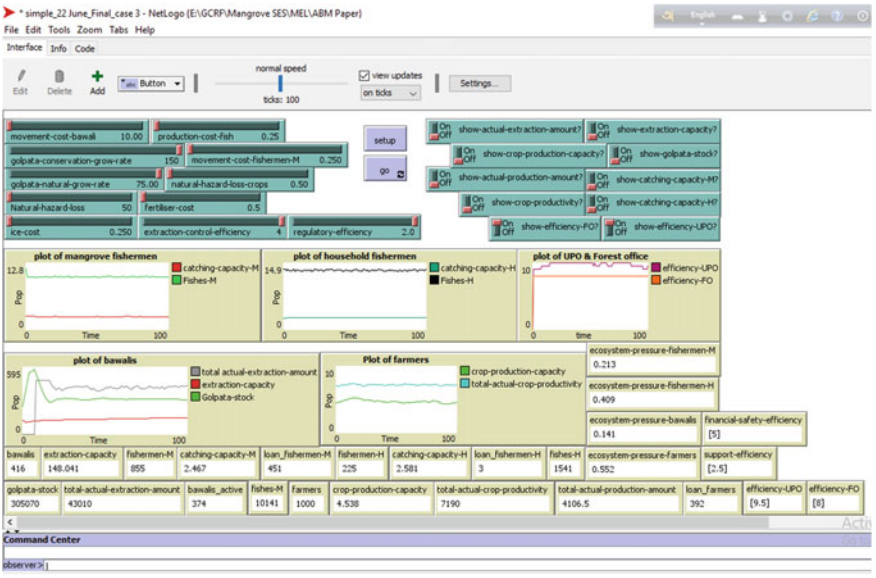

Fig. 4 NetLogo 'Interface' of the model

Patches: This type of agents has fixed coordinates, and turtles can move over patches.

Links: Links are used to connect two turtles. Links are of two types—directed and undirected.

Observers: They do not have locations and only give instruction to other agents.

Four livelihood breeds: Bawalis, Fishersmen_M (for mangrove fishermen), Fishermen_H (for household fishermen), and Farmers; and two institutional breeds: UPO and FO are used in the NetLogo model. Three types of fish breeds for the mangrove area and three types of fish breeds for household ponds are included to represent different amounts of catches during a year. These breeds are referred to as 'turtles' in NetLogo as defined earlier. The model uses four types of patch variables, which include golpata permit, golpata stock, crop productivity, and actual crop productivity. Global variables are used in the model controlled by the sliders (to define different scenarios, e.g., favorable, moderate, and critical), which include movement cost of the Bawalis, golpata growth rate (natural and conservation rates), loss of golpata, fish, and crops due to natural hazards, cost of ice for the fishermen, movement cost of fishermen, production cost of fish, fertilizer cost for the farmers, extraction control efficiency of the FO, and the regulatory efficiency of the UPO.

3 Results

3.1 Cases and Scenarios

Three cases of the SES are selected to explore the system performance and agent behavior within a feasible range of variables. These cases represent the variation in catching capacity of the two types of Fishers, crop production capacity of Farmers, and permitted amount of golpata for the Bawalis. The model variables which define the differences among the three cases are described in Table 2. Case 1 represents comparatively high golpata permit for the Bawalis, comparatively low catching capacity for both mangrove and household fishers, and comparatively high crop production capacity, while Case 2 and Case 3 represent moderate and comparatively low golpata permits for the Bawalis, moderate and comparatively high catching capacities for both mangrove and household fishers, and moderate and comparatively low crop production capacity, respectively.

Additionally, different global variables also influence agent behavior; some influence positively while others cause negative effects. These variables also influence how the ecosystem responds positively or negatively in different conditions.

Three scenarios are selected for simulation in each case: (i) a *favorable scenario* considering the highest values in the NetLogo interface slider for the global variables with positive impact and the lowest values of global variables with negative impact; (ii) a *moderate scenario* considering moderate values of all these global variables; (iii) a *critical scenario* where the highest values of global variables in the slider with

Table 2 Variable values for the three cases

Case Number	Variable	Value (Metric ton)
Case 1	golpata_permit	125
	catching_capacity_M	2.3
	catching_capacity_H	2.3
	crop_production_capacity	5
Case 2	golpata_permit	120
	catching_capacity_M	2.4
	catching_capacity_H	2.4
	crop_production_capacity	4.75
Case 3	golpata_permit	115
	catching_capacity_M	2.5
	catching_capacity_H	2.5
	crop_production_capacity	4.5

Table 3 Global variable values for the three scenarios

Global Variable	Scenario			Unit
	Favorable	Moderate	Critical	
movement_cost_bawali	10	14.75	20	Metric ton
golpata_conservation_growth_rate	150	125	100	
golpata_natural_growth_rate	75	62.5	50	
natural_hazard_loss	50	75	100	
ice_cost	0.25	0.375	0.5	
movement_cost_fishermen_M	0.25	0.375	0.5	
production_cost_fish	0.25	0.5	0.75	
natural_hazard_loss_crops	0.5	0.75	1	
fertilizer_cost	0.5	0.75	1	
extraction_control_efficiency	4	3	2	-
regulatory_efficiency	2	1.5	1	

negative impact and the lowest values of global variables with positive impact are selected. These values of the global variables are given in Table 3.

3.2 Agent Behavior in Different Conditions

NetLogo simulations of the varying behavior of the agents in different cases and scenarios are shown in Figs. 5, 6, 7, 8 and 9. In Netlogo, time is arbitrarily represented as tics, whereas one tic is equivalent to a year in this model. The figures show how

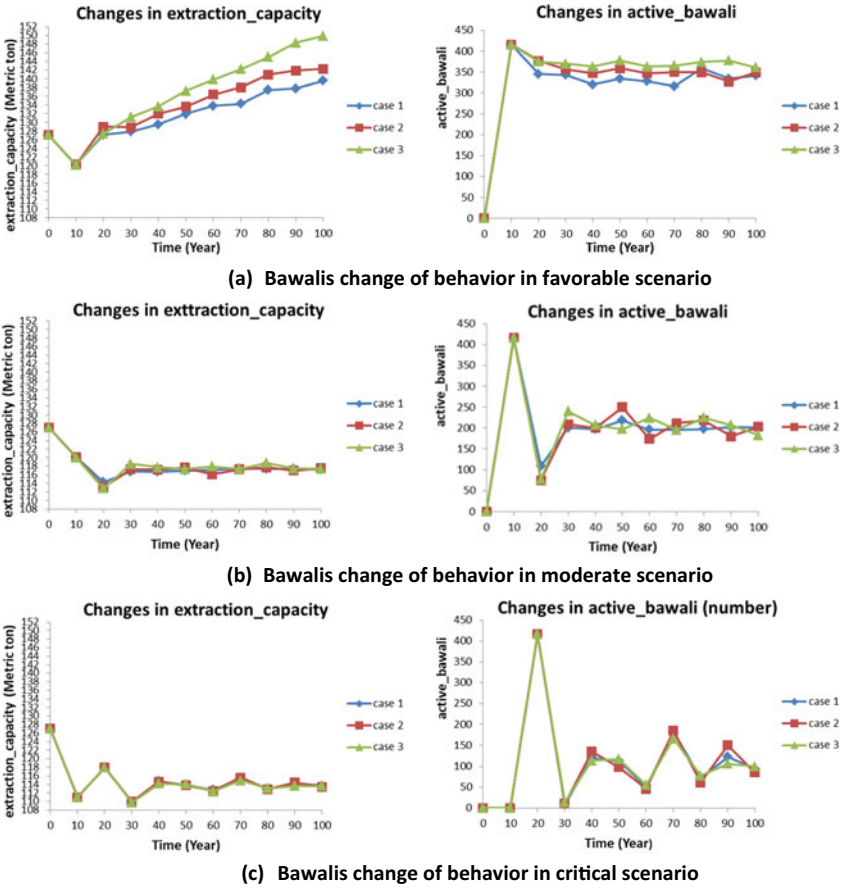

Fig. 5 Behavior change of Bawalis. Case 1: comparatively high golpata permit (Metric ton); Case 2: moderate golpata permit (Metric ton); and Case 3: comparatively low golpata permit (Metric ton)

the agents perform in different ways in different conditions, i.e., one set of variables or condition may be favorable for certain agents while the same condition may be unfavorable for the others. Individual agent behaviors are shown in these plots.

Figure 5 shows the behavior of Bawalis in different conditions. The initial extraction capacity of the Bawalis is only 127 metric ton in all scenarios for case 1, case 2, and case 3 with permit for golpata extraction 125, 120, and 115 metric ton respectively but in favorable scenario, increasing rapidly with time it reaches at almost 150, 142, and 140 Metric ton at the 100th year for case 3, case 2, and case 1 respectively. Above 365 bawalis can be active in most of the times for case 3 with extraction permit 115 Metric ton which is the best among all considered cases in this scenario. The Moderate scenario has also good extraction capacity ranges from almost 116 to 118 Metric ton and number of active Bawalis ranges from 180 to 240 in most of

the times according to different cases. The best performance of this scenario is for case 3 where extraction capacity is 117 Metric ton and the number of active Bawalis 207 are almost constant in most of the times with lowest golpata permit of the three cases, which allows better conservation of golpata stock, and as such relatively high number of Bawalis can remain active for extraction in future. In critical scenario, almost constant extraction capacity 114 Metric ton and the number of active Bawalis below 100 in all cases indicate critical situation of Bawalis.

Figure 6(A) indicates that the catching capacity of the mangrove fishers remains constant with value above 2.45 Metric tons for all cases and scenarios. The number of this type of fishers who have to pay loan increases gradually with time, for a long period and then becomes constant. This implies that the mangrove fishers struggle initially with repaying loan, but eventually overcome this with the attainment of stable catching capacity. The number is, however, the highest in the critical scenario of Case 2 (ranges from 122 to 641) and lowest in the favorable scenario of Case 2 (ranges from 123 t0 468) where catching capacity is moderate to comparatively high. In moderate scenario, the number of this type of fishers to pay loan has values ranging from 119 to 552, comparatively lower than the critical scenario and comparatively higher than the favorable scenario. This number in different times of the moderate scenario is the lowest for case 3 of all the cases and remains constant after the 80th years. Figure 6(B) indicates that catching capacity of household fishers for all cases does not change significantly with the scenarios (ranges between 2.55 and 2.6 Metric ton) but changes with time, and this value remains constant most of the times for case 3 in favorable and moderate scenarios. The number of this type of fishers having loan remains very low in all scenarios (ranges from 1 to 8).

Figure 7 represents the behavior change of farmers for case 1, case 2, and case 3 with crop production capacity 5, 4.75, and 4.5 Metric ton respectively in favorable, moderate, and critical scenario. From this it is noticed that crop production capacity of farmers remains the highest (above 4.7 Metric ton) in the favorable scenario in Case 3 with lowest number (below 400) of farmers having loan to pay of all conditions. In the critical scenario, crop production capacity indicates critical values (3.8 to 4.2 Metric ton) in most of the times for all cases. The number of farmers who have to pay loan is the lowest (below 450) in the favorable scenario and highest (above 500) in critical scenario for all cases for most of the times. The Moderate scenario of all cases indicates moderate number (about 500 to 525) of such farmers which does change significantly with time. In this scenario, Case 3 indicates the highest catching capacity whose values are above 4.3 Metric ton with lowest number of farmers having loan to pay whose maximum value is 500 in different times.

Figure 8 shows the efficiency change of FO and UPO for Case 1 with extraction permit 125, catching capacity 2.3 and crop production capacity 5 metric ton respectively, Case 2 with extraction permit 120, catching capacity 2.4 and crop production capacity 4.75 metric ton respectively, and Case 3 with extraction permit 115, catching capacity 2.5 and crop production capacity 4.5 metric ton respectively in favorable, moderate, and critical scenario. Figure 8(A) shows that the FO works with the best efficiency 8 in the favorable scenario. The efficiencies are comparatively lower in the moderate and critical scenarios which are 7 and 6, respectively. This efficiency

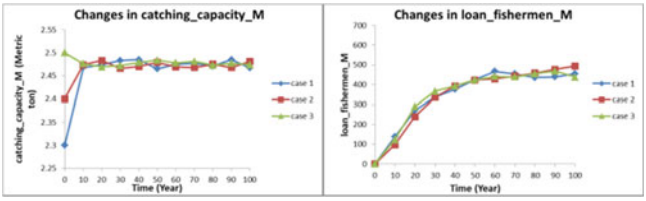

(a) fishermen_M change of behavior in favorable scenario

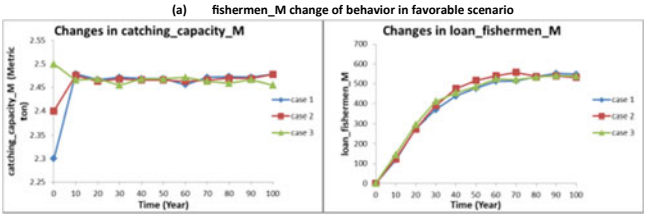

(b) fishermen_M change of behavior in moderate scenario

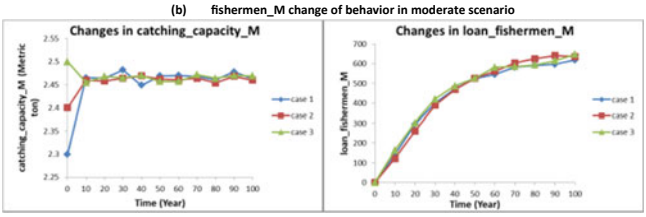

(c) fishermen_M change of behavior in critical scenario

(B) Behavior changes of fishermen_H

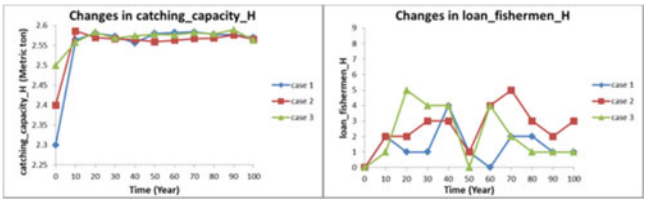

(a) fishermen_M change of behavior in favorable scenario

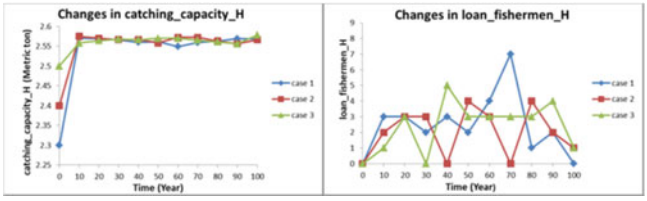

(b) fishermen_M change of behavior in moderate scenario

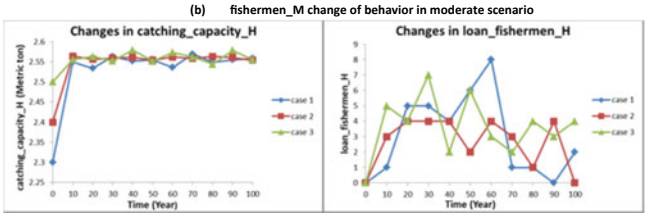

(c) fishermen_M change of behavior in critical scenario

Fig. 6 Behavior change of Fishers. Case 1: comparatively low catching capacity; Case 2: moderate catching capacity; Case 3: comparatively high catching capacity

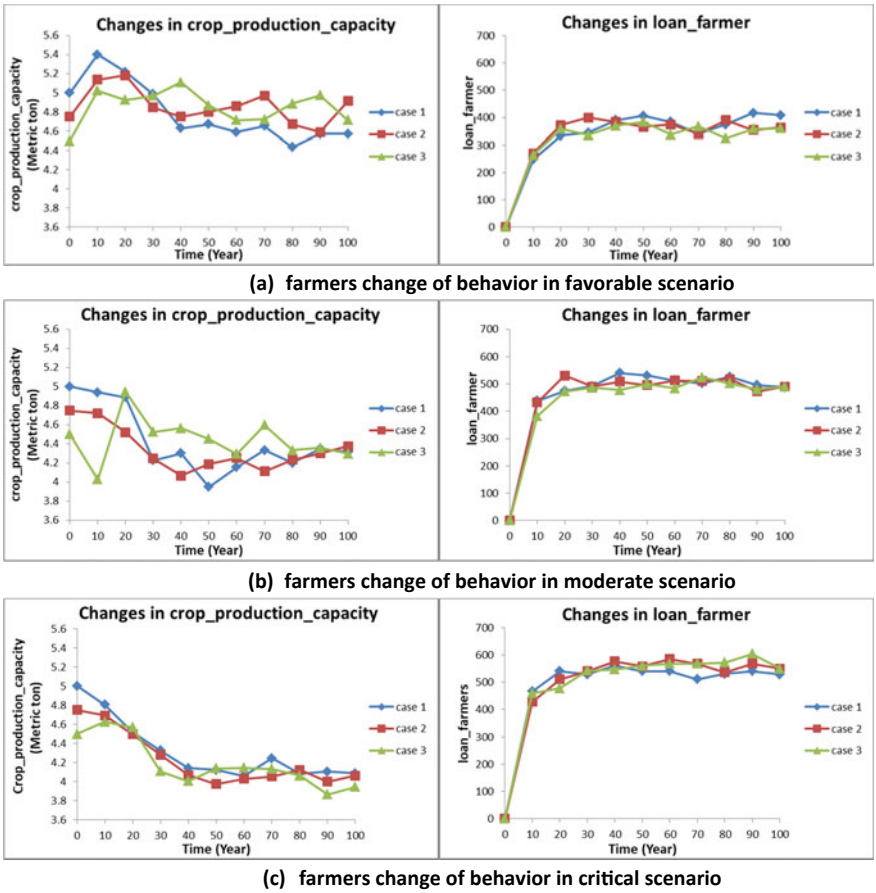

Fig. 7 Behavior change of Farmers. Case 1: comparatively high crop production capacity (Metric ton); Case 2: moderate crop production capacity (Metric ton); Case 3: comparatively low crop production capacity (Metric ton)

does not change according to cases. Figure 8(B) shows variations in efficiency of the UPO with different conditions. The efficiency is the best ranges from (9.5 to 10) in the favorable scenario. However, the efficiency remains at a reasonably satisfactory and constant level in the moderate scenario of Case 3 (ranges from 7.5 to 9). This efficiency is the lowest in the critical scenarios for all cases and has a value of 6.5 most of the times.

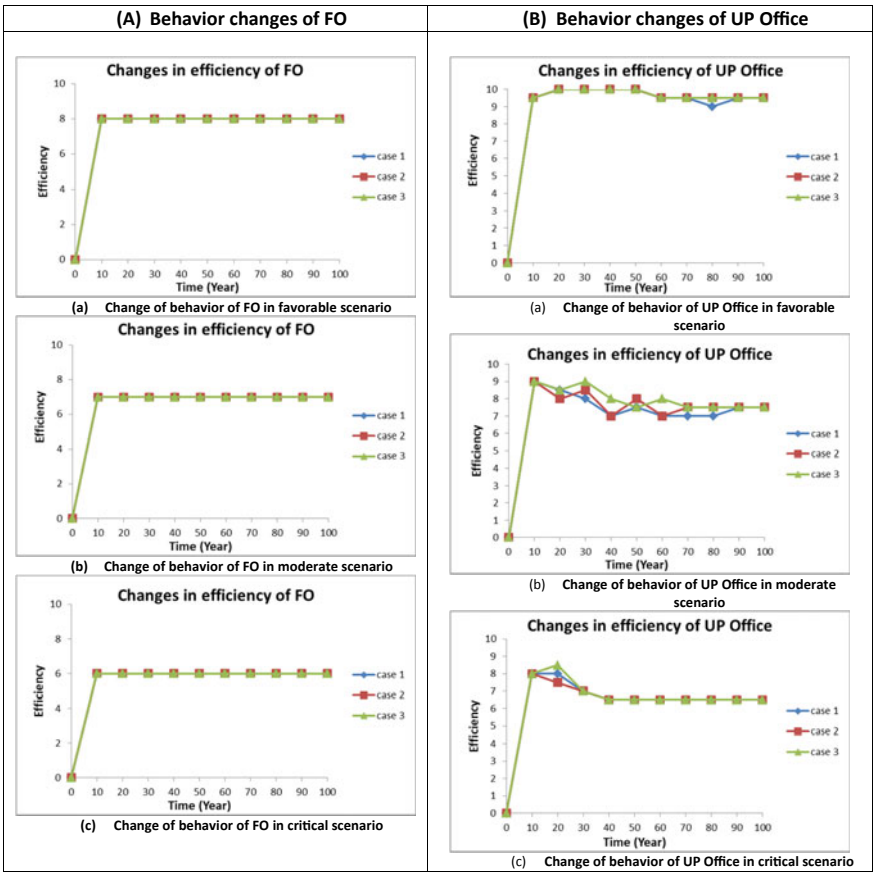

Fig. 8 Behavior change of institutional agents: (A) Forest Office; (B) UP Office

3.3 Ecological and Livelihood Tipping Points

Figure 9 shows the pressure on the ecosystem due to livelihood activities, and how the system reaches at an equilibrium condition (stable condition) or a tipping point (unstable condition) in different cases and scenarios. Figure 9(A) shows that in the favorable scenario of Case 3, the pressure on the ecosystem caused by the Bawalis increases rapidly, and after the 30th year its value remains almost constant with time. This value has the highest range (0.12 to 0.14), moderate range (0.06 to 0.08) in favorable scenario and moderate scenario, respectively. In critical scenario, this value remains very low most of the times but changes significantly with time. 9(B) shows that the mangrove fishers cause pressure constantly with time and cases. The pressure is the lowest (below 0.17) in the critical scenario and the highest (above 0.21) in the favorable scenario, the moderate scenario indicates value almost 0.18. Figure 9(C) shows that the household fishers cause the minimum pressure in the

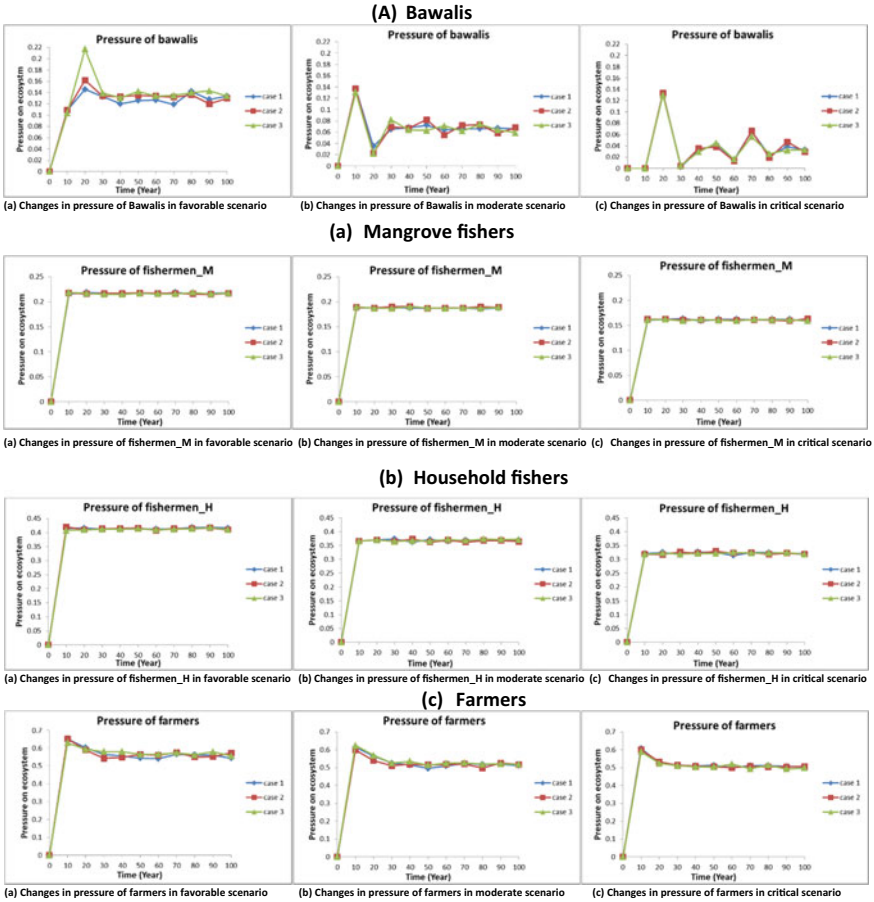

Fig. 9 Pressure on the ecosystem in different conditions caused by: (A) Bawalis; (B) Mangrove fishers; (C) Household fishers; and (D) Farmers

critical scenario (below 0.35) and the maximum pressure in the favorable scenario (above 0.4) where this pressure is about 0.35 in moderate scenario. The pressure remains constant with time and cases. Figure 9(D) shows that the pressure caused by the farmers remains the highest for Case 3 (almost 0.6) in the favorable scenario for a long period of time. The pressure remains consistently moderate in Case 3 (ranges from 0.51 to 0.53). This pressure is about 0.5 for all cases of critical scenario.

4 Discussion

4.1 Sensitivity Analysis

From the NetLogo simulation results, it is clear that moderate scenario of Case 3 is the best condition for livelihood activities by keeping balance with ecosystem pressure where the favorable scenario gives the best livelihood performance by creating excessive pressure on the ecosystem, and the critical scenario creates the minimum pressure on the ecosystem by giving poor livelihood performance. In this regard, we have tried to find out the conditions when livelihood performance will be better than moderate scenario, creating lower pressure than favorable scenario considering case 3. To do this we have taken the same values for all global variables as considered for moderate scenario except only four most sensitive global variables and considered 2 other conditions under case 3 which are case 3A and case 3B. Since golpata_conservation_growth_rate has positive effects on livelihood activities, increased values than the moderate scenario of case 3 (i.e., case 3_moderate) at the same rate have taken for case 3A and case 3B respectively. Again, movement_cost and fertilizer_cost have negative effects and therefore their decreased values than case 3_moderate have taken for case 3A and case 3B. The only global variable in this case related to fishermen_H is production_cost_fish. So, increased and decreased values at the same rate from case 3_moderate have taken for case 3A and case 3B respectively. The detailed values with variables name are given for different conditions in the Table 4.

Figure 10 shows the changes of behavior of agents for different conditions with time comparing with the moderate scenario of case 3 (case 3_moderate). From Fig. 10(A), it is shown that the extraction capacity and number of active bewail

Table 4 Global variable values for the three conditions

Global variables	case 3A	case 3_moderate	case 3B	Unit
movement_cost_bawali	14.75	14.75	14.75	Metric ton
golpata_conservation_growth_rate	137.5	125	150	
golpata_natural_growth_rate	62.5	62.5	62.5	
natural_hazard_loss	75	75	75	
ice_cost	0.375	0.375	0.375	
movement_cost_fishermen_M	0.3125	0.375	0.25	
production_cost_fish	0.625	0.5	0.375	
natural_hazard_loss_crops	0.75	0.75	0.75	
fertilizer_cost	0.625	0.75	0.5	
extraction_control_efficiency	3	3	3	-
regulatory_efficiency	1.5	1.5	1.5	-

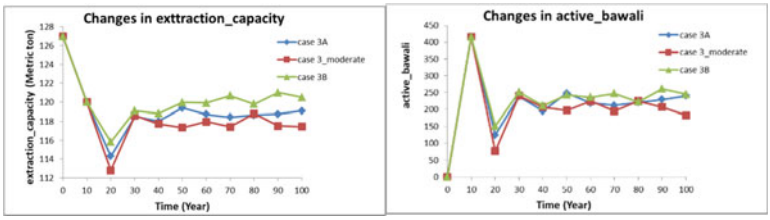

(a) bawalis change of behavior

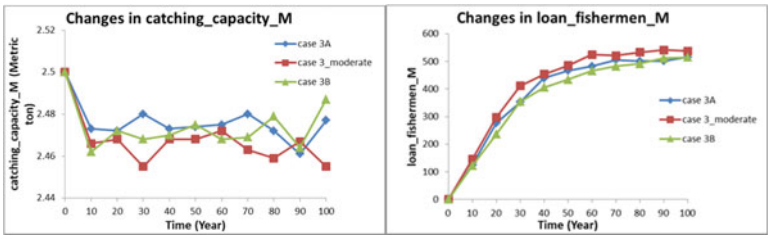

(b) fishermen_M change of behavior

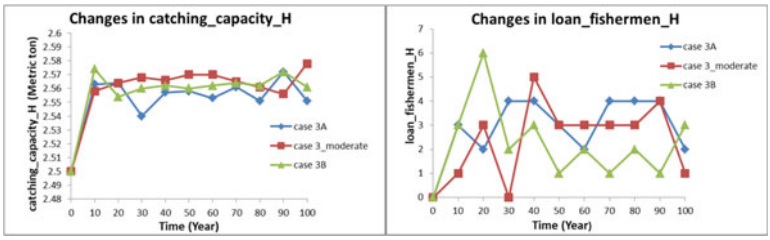

(c) fishermen_H change of behavior

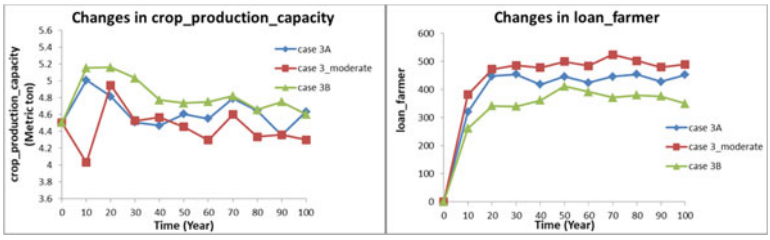

(d) farmers change of behavior

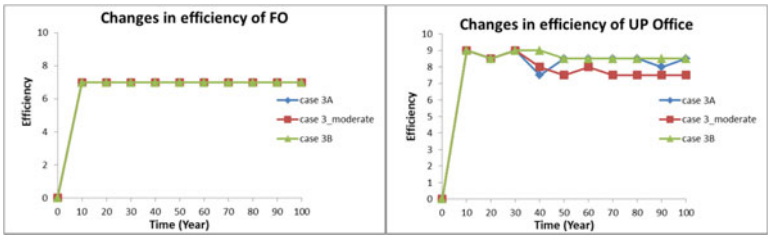

(e) Change of behavior of FO and UPO

Fig. 10 Behavior change of agents: (A) Bawalis; (B) Mangrove fishers; (C) Household fishers; and (D) Farmers

increase rapidly with time for the case 3A and case 3B than case 3_moderate condition and case 3B give the best performance with extraction_capacity 122 Metric ton and 225 number of active bawali most of the times. Figure 10(A) represents that the catching capacity of mangrove fishers also increases than case 3_moderate condition for case 3A and case 3B but does not vary much for these conditions. But the number of mangrove fishermen who have to pay loan is the lowest for case 3B (highest 515). Figure 10(C) indicates that the values of catching capacity of household fishermen and number of household fishermen to pay loan do not change significantly for case 3A and case 3B. From Fig. 10(D), it is noticed that crop production capacity and the number of farmers who have loan increase and decrease respectively from case 3_moderate for case 3A and case 3B, and case 3 gives the best performance. Again, from Fig. 10(E), it can be realized that efficiency of FO remains constant for all conditions where efficiency of UPO increases for case 3A and case 3B than case 3_moderate.

Figure 11 is for showing change of pressure on ecosystem for different livelihood groups with time comparing with the favorable scenario of case 3 (case 3_favorable). Figure 11(A) shows that in case 3A and case 3B bawalis give a very low pressure (0.07 to 0.08) on ecosystem than case 3_favorable (0.14) most of the time, and this value does not change significantly for case 3A and case 3B. From Fig. 11(B), it is noticed that in case 3_favorable condition, mangrove fishermen create pressure of almost 0.23 whereas for case 3A and case 3B, this value remains as 0.2 most of the times. Figure 11(C) represents that the pressure of household fishers on the ecosystem has almost similar values for case 3_favorable and case 3B (0.42 and 0.4 respectively) where the value is comparatively lower in case 3A about 0.35) most of the times. From Fig. 11(D), it can be realized that for case 3A farmers give the lowest pressure on ecosystem (about 0.55) and this value is significantly higher for case 3B (about 0.55) and case 3_favorable (about 0.6) most of the times.

So, by analyzing Figs. 10 and 11, it can be decided that in the moderate condition of case 3 we need to keep conservation_growth_rate between 137.5 and 150 Metric ton, movement_cost of mangrove fishermen between 0.25 and 0.3125 Metric ton, production_cost_fish for household fisher between 0.5 and 0.25 Metric ton, and fertilizer_cost of farmers between 0.625 and 0.75 Metric ton, in order to maintain better livelihood security with ecosystem sustainability.

4.2 Livelihood and Ecosystem Sustainability

NetLogo simulation results indicate that the livelihood activities of the livelihood groups can be considerably influenced, both favorably and adversely, by the ecosystem characteristics and the institutional efficiencies. These influences vary in a range of cases and scenarios represented by the agents and global variables. Sustainability of the livelihood activities is also indicated by a change in the number of livelihood groups able to continue their activities in the long term. In general, the extraction or production capacities is relatively high in the favorable scenarios

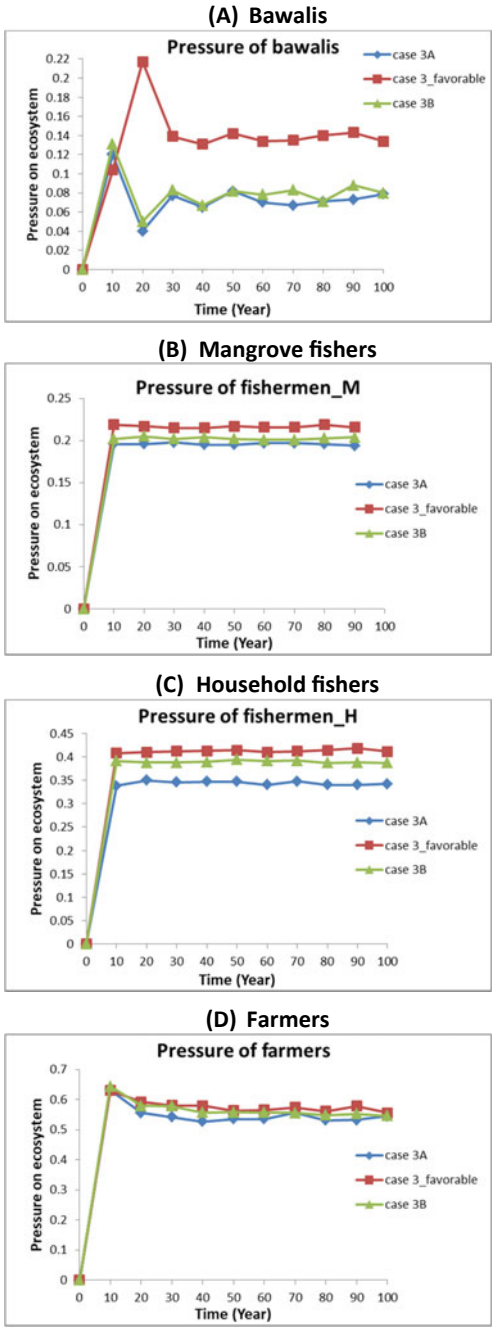

Fig. 11 Pressure on the ecosystem in different conditions caused by: (A) Bawalis; (B) Mangrove fishers; (C) Household fishers; and (D) Farmers

where the livelihood activities can sustain over a long period of time. However, this can lead to increased pressure on the ecosystem. In the critical scenario, low livelihood activity is associated with low pressure on the ecosystem, but reduced capacity, reflected in increase in number of people taking loans. Hence, this does not represent an optimal case, where livelihood is maximized and at the same time ecosystem is best preserved. The optimal balance may be found under the moderate scenario.

Ecosystem sustainability is, however, more sensitive to and dependent on the institutional policy for conservation of the ecosystem and preventing overexploitation. Providing financial security to the vulnerable livelihood groups encourages a lower level of resource exploitation thus indirectly contributing to ecosystem sustainability.

4.3 SES Equilibrium and Tipping Points

Livelihoods of the main communities considered in this study—Farmers, Bawalis, and Fishers—are closely related. They are part of the same SES and share resources, and often shift their livelihoods either to overcome a temporary financial crisis or on a more regular seasonal basis. This situation leads to a more dynamic complexity than what could be represented in this simplified model. However, it is evident that the SES reaches an equilibrium condition and averts a tipping point if institutional policies are formulated to support optimum levels of livelihood activities and to ensure that the ecosystem resources do not deplete in the long term.

4.4 Role of Institutional Agents: Sensitivity of Policy Change

As evident from the results, the institutional agents have significant influence on both the livelihood activities and ecosystem response. Efficient performance of the institutions is therefore essential to conserve the mangrove and secure the livelihoods. The ABM results indicate that protection and conservation of golpata in the Sundarbans is not only good for the livelihood groups but it also sustains the overall ecosystem. Similarly, fish conservation in the mangroves ensures continued ecosystem services as well as higher levels of fish catch.

We observed that comprehensive institutional policies to ensure mangrove SES sustainability and participatory management are missing in Bangladesh. All current policies are arbitrarily set either for a specific livelihood group, or within an administrative boundary of the local government, or only for forest management. The conservation rules and extraction licensing are based on approximate estimates rather than scientific observations such as fish catch and composition assessment or satellite data-based assessment.

5 Conclusion

ABM simulations and stakeholder interactions indicate that the vulnerable livelihood groups of the Sundarbans mangrove SES require policy support to sustain their livelihoods. Economic returns at the household level increase with an improved level of institutional decision-making based on scientific assessment. This, in turn, sustains the mangrove-dependent livelihoods, optimizes the availability of ecosystem resources, and ensures continued ecosystem services.

We conclude that a comprehensive policy is essential to ensure sustainability of the mangrove SES. Such policy should outline the roles of relevant institutions and stakeholders, the approach to science-based decision-making, the method to identify vulnerabilities of the livelihood groups and the ecosystem, and the priorities to provide support to the livelihood groups.

Acknowledgements We acknowledge the funding received from the UKRI GCRF Living Deltas Hub under Grant Reference NE/S008926/1.

References

Acosta, L.A., D.B. Magcale-Macandog, J. Manuta, A.J. Jacildo, E.R. Abucay, J.P. Talubo, E.A. Eugenio, P.B.M. Macandog, I.M.H. Escamos, and M. Gonzalo. 2018. Agent-Based Modeling of Sustainable Livelihoods for Vulnerable People to Adapt to the Impacts of Flood-Related Landslides in the Philippines. Technical Report, The Oscar M. Lopez Center for Climate Change Adaptation and Disaster Risk Management Foundation, Inc. and University of the Philippines Los Baños.

An, Li. 2012. Modeling Human Decisions in Coupled Human and Natural Systems: Review of Agent-Based Models. *Ecological Modelling* 229: 25–36. https://doi.org/10.1016/j.ecolmodel.2011.07.010.

An, Li, Alex Zvoleff, Jianguo Liu, and William Axinn. 2014. Agent-Based Modeling in Coupled Human and Natural Systems (CHANS): Lessons from a Comparative Analysis. *Annals of the Association of American Geographers* 104 (4): 723–745. https://doi.org/10.1080/00045608.2014.910085.

Banglapedia. 2021. The Sundarbans. https://en.banglapedia.org/index.php/Sundarbans,_The#:~:text=Sundarbans%2C%20The%20largest%20single%20block,with%20the%20bay%20of%20bengal.&text=The%20Sundarbans%20was%20originally%20measured,of%20about%2016%2C700%20sq%20km.

Castle, Christian J.E., and Andrew T. Crooks. 2006. Principles and Concepts of Agent-Based Modelling for Developing Geospatial Simulations. Working Papers Series, Paper 110, September2006, Centre for Advanced Spatial Analysis, University College London.

Cole, Daniel H., Graham Epstein, and Michael D. McGinnis. 2019. Combining the IAD and SES Frameworks. *International Journal of the Commons* 13 (1): 1–32. https://doi.org/10.18352/ijc.xxx.

Dobbie, Samantha, Kate Schreckenberg, James G. Dyke, Marije Schaafsma, and Stefano Balbi. 2018. Agent-Based Modelling to Assess Community Food Security and Sustainable Livelihoods. *Journal of Artificial Societies and Social Simulation* 21 (1): 1. https://doi.org/10.18564/jasss.3639.

Forrester, John, Richard Greaves, Howard Noble, and Richard Taylor. 2014. Modeling Social-Ecological Problems in Coastal Ecosystems: A Case Study. *Wiley Periodicals* 19(6) Complexity 73. https://doi.org/10.1002/cplx.21524.

Getzner, Michael and Muhammad Shariful Islam. 2013. Natural Resources, Livelihoods, and Reserve Management: A Case Study from Sundarbans Mangrove Forests, Bangladesh. International Journal of Sustainable Development and Planning. https://doi.org/10.2495/SDP-V8-N1-75-87.

Habib, Kazi Ahsan, Amit Kumer Neogi, Najmun Nahar, Jina Oh, Youn-Ho Lee and Choong-Gon Kim. 2020. An Overview of Fishes of the Sundarbans, Bangladesh and Their Present Conservation Status. *Journal of Threatened Taxa* 12 (1): 15154–15172. https://doi.org/10.11609/jott.4893.12.1.15154-15172.

Hoq, M. Enamul. 2007. An Analysis of Fisheries Exploitation and Management Practices in Sundarbans Mangrove Ecosystem Bangladesh. *Ocean & Coastal Management* 50 (5–6): 411–427. https://doi.org/10.1016/j.ocecoaman.2006.11.001.

Hossain, M. Sarwar, John Dearing, Felix Eigenbrod, and Fiifi Amoako Johnson. 2017. Operationalizing Safe Operating Space for Regional Social-Ecological Systems. *Science of the Total Environment* 584–585: 673–682. https://doi.org/10.1016/j.scitotenv.2017.01.095.

http://www.gaburaup.satkhira.gov.bd. 2021.

Kabir, K.A., S.B. Saha, and Michael Phillips. 2019. Aquaculture and Fisheries in the Sundarbans and Adjacent Areas in Bangladesh: Resources, Productivity, Challenges and Opportunities. Aquaculture and Fisheries in the Sundarbans and Adjacent Areas in Bangladesh: Resources, Productivity, Challenges and Opportunities. In Sen H. (ed), The Sundarbans: A Disaster-Prone Eco-Region. Coastal Research Library, vol 30. Springer, Cham. https://doi.org/10.1007/978-3-030-00680-8_9.

Lippe, M., M. Bithell, N. Gotts, et al. 2019. Using Agent-Based Modelling to Simulate Social-Ecological Systems Across Scales. *GeoInformatica* 23: 269–298. https://doi.org/10.1007/s10707-018-00337-8.

Mallick, Bishawjit Rupkatha, Jude N. Priodarshini, Bangkim Biswas Kimengsi, Alexander E. Hausmann, Safiqul Islam, Saleemul Huq, and Joachim Vogt. 2021. Livelihoods Dependence on Mangrove Ecosystems: Empirical Evidence from the Sundarbans. *Current Research in Environmental Sustainability* 3 (2021). https://doi.org/10.1016/j.crsust.2021.100077.

Macal, Charles M., and Michael J. North. 2009. Agent-Based Modeling and Simulation. Proceedings of the 2009 Winter Simulation Conference, M. D. Rossetti, R. R. Hill, B. Johansson, A. Dunkin and R. G. Ingalls, eds., December 13–16, 2009, Austin, Texas, USA, pp. 86–98. https://doi.org/10.1109/WSC.2009.5429324.

Martin, R., and M. Schlüter. 2015. Combining System Dynamics and Agent-Based Modeling to Analyze Social-Ecological Interactions—An Example from Modeling Restoration of a Shallow Lake. *Frontiers in Environmental Science* 3: 66. https://doi.org/10.3389/fenvs.2015.00066.

Miyasaka, T., Q.B. Le, T. Okuro, et al. 2017. Agent-Based Modeling of Complex Social–Ecological Feedback Loops to Assess Multi-Dimensional Trade-Offs in Dryland Ecosystem Services. *Landscape Ecol* 32: 707–727. https://doi.org/10.1007/s10980-017-0495-x.

Mozumder, Mohammad Mojibul Hoque, Md. Mostafa Shamsuzzaman, Md. Rashed-Un-Nabi, Ehsanul Karim. 2018. Social-Ecological Dynamics of the Small-Scale Fisheries in Sundarban Mangrove Forest, Bangladesh. *Aquaculture and Fisheries.* https://doi.org/10.1016/j.aaf.2017.12.002.

Ostrom, Elinor. 1990. *Governing the Commons.* Cambridge, UK: Cambridge University Press.

Ostrom, Elinor, M. Janssen, and J.M. Anderies. 2007. Going Beyond Panaceas. *Proceedings of the National Academy of Sciences* 104 (39): 15176–15178. https://doi.org/10.1073/pnas.0702288104.

Rounsevell, M.D.A., D.T. Robinson, and D. Murray-Rust. 2012. From Actors to Agents in Socio-Ecological Systems Models. *Philosophical Transactions of the Royal Society* B367: 259–269. https://doi.org/10.1098/rstb.2011.0187.

Sarker, Khalekuzzaman. 2011. Fisher Livelihoods in the Sundarbans. Rural Livelihoods and Protected Landscape: Co-management in the Wetlands and Forests of Bangladesh.

Schlüter, M., R.R.J. Mcallister, R. Arlinghaus, N. Bunnefeld, K. Eisenack, F. Hölker, E.J. Milner-Gulland, B. Müller, E. Nicholson, M. Quaas, and M. Stöven. 2012. New Horizons for Managing the Environment: A Review of Coupled Social-Ecological Systems Modeling. *Natural Resource Modeling* 25 (1): 219–272. https://doi.org/10.1111/j.1939-7445.2011.00108.x.

Schlüter, M., J. Hinkel, P.W.G. Bots, and R. Arlinghaus. 2014. Application of the SES Framework for Model-Based Analysis of the Dynamics of Social-Ecological Systems. *Ecology and Society* 19 (1): 36. https://doi.org/10.5751/ES-05782-190136.

Schulze, Jule, Birgit Müller, Jürgen. Groeneveld, and Volker Grimm. 2017. Agent-Based Modelling of Social-Ecological Systems: Achievements, Challenges, and a Way Forward. *Journal of Artificial Societies and Social Simulation* 20 (2): 8. https://doi.org/10.18564/jasss.3423.

Tisue, Seth and Uri Wilensky. 2004. NetLogo: A Simple Environment for Modeling Complexity. International Conference on Complex Systems, Boston, May 16–21, 2004.

Training_Report_of_Sundarbans_Nypa_Collector 2012. https://www.ccec-bd.org › files › reports.

Virapongse, Arika, Samantha Brooks, Elizabeth Covelli Metcalf, Morgan Zedalis, Jim Gosz, Andrew Kliskey, and Lilian Alessa. 2016. A Social-Ecological Systems Approach for Environmental Management. *Journal of Environmental Management* 178: 83–91. https://doi.org/10.1016/j.jenvman.2016.02.028.

Voinov, Alexey, Karen Jenni, Steven Gray, Nagesh Kolagani, Pierre D. Glynn, Pierre Bommel, Christina Prell, Moira Zellner, Michael Paolisso, Rebecca Jordan, Eleanor Sterling, Laura Schmitt Olabisi, Philippe J. Giabbanelli, Zhanli Sun, Christophe Le Page, Todd K. SondossElsawah, Klaus Hubacek BenDor, Bethany K. Laursen, Laura Basco-Carrera. AntonieJetter, Alison Singer, Laura Young, Jessica Brunacini, and Alex Smajgl. 2018. Tools and Methods in Participatory Modeling: Selecting the Right Tool for the Job. *Environmental Modelling & Software* 109: 232–255. https://doi.org/10.1016/j.envsoft.2018.08.028.

Wikipedia. 2021. Sundarbans. https://en.wikipedia.org/wiki/Sundarbans.

Yan, Huimin, Lihu Pan, Zhichao Xue, Lin Zhen, Xuehong Bai, Yunfeng Hu, and He-Qing Huang. 2019. Agent-Based Modeling of Sustainable Ecological Consumption for Grasslands: A Case Study of Inner Mongolia, China. *Sustainability* 11 (8): 2261. https://doi.org/10.3390/su11082261.

Drought Management by Integrated Approaches in T. Aman Rice Season to Escalate Rice Productivity in Drought Prone Regions of Bangladesh

Debjit Roy, Md. Belal Hossain, Mohammad Rezoan Bin Hafiz Pranto, and Md. Towfiqul Islam

Abstract Erratic rainfall often causes water shortage for wet season rice (T. Aman) cultivation, which has a negative impact on crop growth and yield. The long-term rainfall analysis of drought prone North-West region of Bangladesh indicated that moderate to severe drought occurred in this region if monsoon ceased between the last week of September and the first week of October. Integrated management approaches could help reduce the impact of drought on T. Aman rice production. The approaches include (i) applying supplemental irrigation when needed after rainfall stops; (ii) introducing drought-escaping, short duration rice variety; and (iii) adjustment of transplanting time to escape drought spells. Applying supplemental irrigation two to three times during the critical stages of rice (from flowering to grain filling), reduced 20–40% yield loss over fully rainfed conditions. Timely transplantation of drought-escaping, short duration variety allows the crop to mature before a drought is exposed. Farmer has comparative flexibility when choosing the transplanting date for the long duration variety. If T. Aman rice could be transplanted between 10 and 24 July, drought implications on critical stages could be avoided. Integrated drought management approaches have been found to increase the productivity of T. Aman rice in the drought suffered regions.

Keywords Drought management · Erratic rainfall · T. Aman rice · Supplemental irrigation · Transplanting window

1 Introduction

Rainfed Aman (T. Aman) rice is one of the major crops representing the Bangladesh agricultural sector, and it constitutes about 39% of total rice production of Bangladesh (BBS 2019). In the last few decades, Bangladesh has achieved tremendous advancements in agricultural technology such as developing high yielding rice varieties and

D. Roy (✉) · Md. B. Hossain · M. R. B. H. Pranto · Md. T. Islam
Irrigation and Water Management Division, Bangladesh Rice Research Institute, Gazipur, Bangladesh
e-mail: debjit.iwm@brri.gov.bd

© The Author(s), under exclusive license to Springer Nature Switzerland AG 2022

G. M. Tarekul Islam et al. (eds.), *Water Management: A View from Multidisciplinary Perspectives*,
https://doi.org/10.1007/978-3-030-95722-3_17

introducing modern irrigation water management practices. Despite the technological progress, the fate of T. Aman rice production still largely depends on timely occurrence of rainfall. The rainfall amount and distribution pattern throughout the season determine the irrigation demand and act as a prime climatic factor that affects rice grain yield (Sattar and Parvin 2009a). The changed climatic situation is causing erratic rainfall distribution, reduces the rainfall occurrences at critical period of crop, thus results water stress to crop due to insufficient moisture in soil profile (Rosenzweig et al. 2002). In the coming future, lengthy rainless dry spells will bring agriculture droughts and raise the water demand for rainfed rice (Fischer et al. 2007). Agricultural drought acts as the most influential abiotic stress hampering T. Aman yield (Biswas 2011). Agricultural drought usually occurs when there is a lack of adequate rainfall. Due to insufficient rainfall, soil moisture depletes and crop root zone suffers from water deficit. When water storage in vadose zone becomes limited, the soil profile cannot provide enough water for the crop to sustain. As such, the situation is termed as agricultural drought, which significantly affects rice plant growth and yield (Biswas et al. 2019, MDMR-CEGIS 2013).

Annually, on average, the north-west and central parts of Bangladesh receive 1500 mm rainfall, when the north-east and south-east parts get more than 3000 mm rainfall (Roy et al. 2014). Around 90% of total annual rainfall occurs between April and October, commonly known as the monsoon season. T. Aman rice is typically cultivated between these months in a year. However, in some years, rainfall caused by monsoon ceases early in between mid-September and early October. This creates irrigation demand for existing T. Aman rice being grown in the field and causes moderate to severe agricultural drought (Saleh 1991). Agricultural drought occurrence in September and October months often leads to drastic reduction of rice yield because the crop is usually in between its flowering and grain filling stages of growth, which are very sensitive to water stress (Sattar and Parvin 2009b). T. Aman rice is very sensitive to water stress at this reproductive stage because water shortage at flowering stage reduces crop yield significantly (Yang et al. 2019). The loss in yield is usually irreversible since rice plant's physiological features are completely dependent on the fulfilment of water needs for its reproductive phase. Drought occurrence at the vegetative phase causes 20–25% yield loss, whereas the yield loss could be more than 50% if drought occurs at the reproductive phase (Yang et al. 2019; Sattar 1993). Drought management to mitigate the hike in crop water requirements during this period can ensure sustainable T. Aman production (BRRI 1991; Haq et al. 1985; Islam 2007; Khan 1979; Roy et al. 2010; Saleh 1987).

Many researchers (Ibrahim 2001, Islam et al. 2009, Biswas et. al. 2019, Islam and Biswas 2010) have suggested several options for drought management. However, a complete management package is still lacking for farmers in drought prone areas where they can only choose one appropriate drought escape or mitigation technique depending on their resources. The present study aimed to evaluate the opportunity to apply integrated drought management approaches consisting of three practices to avoid the drought risk in T. Aman rice cultivation. These are: (i) applying supplemental irrigation when needed after rainfall stops; (ii) introducing drought-escaping, short duration rice variety; and (iii) adjustment of transplanting time to escape drought

spells. Integrated drought management approaches would be effective in moderate to severe drought affected areas and it will ensure that T. Aman yield would not decrease due to water stress during critical stages of crop production.

2 Methodology

2.1 Study Area

The North-West region of Bangladesh usually suffers from very severe to moderate agricultural drought (Fig. 1), mainly affecting the production of T. Aman rice. For the experimentation of different approaches for drought management, the trials were conducted in three locations in the North-West region, namely Kushtia (23.92° N, 89.2° E), Pabna (24.35° N, 89.73° E), and Rajshahi (24.72° N, 88.97° E). The experimental sites belong to the Agro-Ecological Zone (AEZ)-11, i.e. the High Ganges River flood plain. The region has medium–high, typical rice growing lands. The soil is moderately fertile and varies from clay loam to sandy loam texture. The average high and low temperatures are 37.8° C and 9.2° C, 31.2° C and 20.8 °C, and 32.2° C and 20.6° C in Kushtia, Pabna and Rajshahi, respectively. The mean annual rainfall is 1478 mm, 1603 mm, and 1542 mm in Kushtia, Pabna, and Rajshahi, respectively. The long-term monthly rainfall distribution in these locations, as presented in Fig. 2, reveals that the premature cessation of monsoon after September is increasing in frequency and becoming the normal rainfall pattern in the North-West region.

2.2 Supplemental Irrigation

The first study was conducted for three treatments with four replications. Among the treatments, first treatment was rainfed, i.e. no supplemental irrigation was applied throughout the growth duration. For the second treatment, two supplemental irrigations were applied at critical stages of T. Aman rice (flowering to grain filling stage), and for the third treatment, three supplemental irrigations were applied at critical stages. The second study was set up with five treatments and replicated thrice. The treatments were: T1—solely rainfed, T2—supplemental irrigation applied just after transplanting, T3—supplemental irrigation applied from transplanting to panicle initiation, T4—supplemental irrigation applied during transplanting to flowering, and T5—supplemental irrigation applied when perched water table had gone 15 cm below soil surface. The perched water table was measured by installing a polyvinyl chloride (PVC) pipe. BR11 was transplanted in both experiments and fertilizer management practices recommended by the Bangladesh Rice Research Institute (BRRI) were followed. Seedlings of 30 days were transplanted at 20 × 20 cm spacing after proper

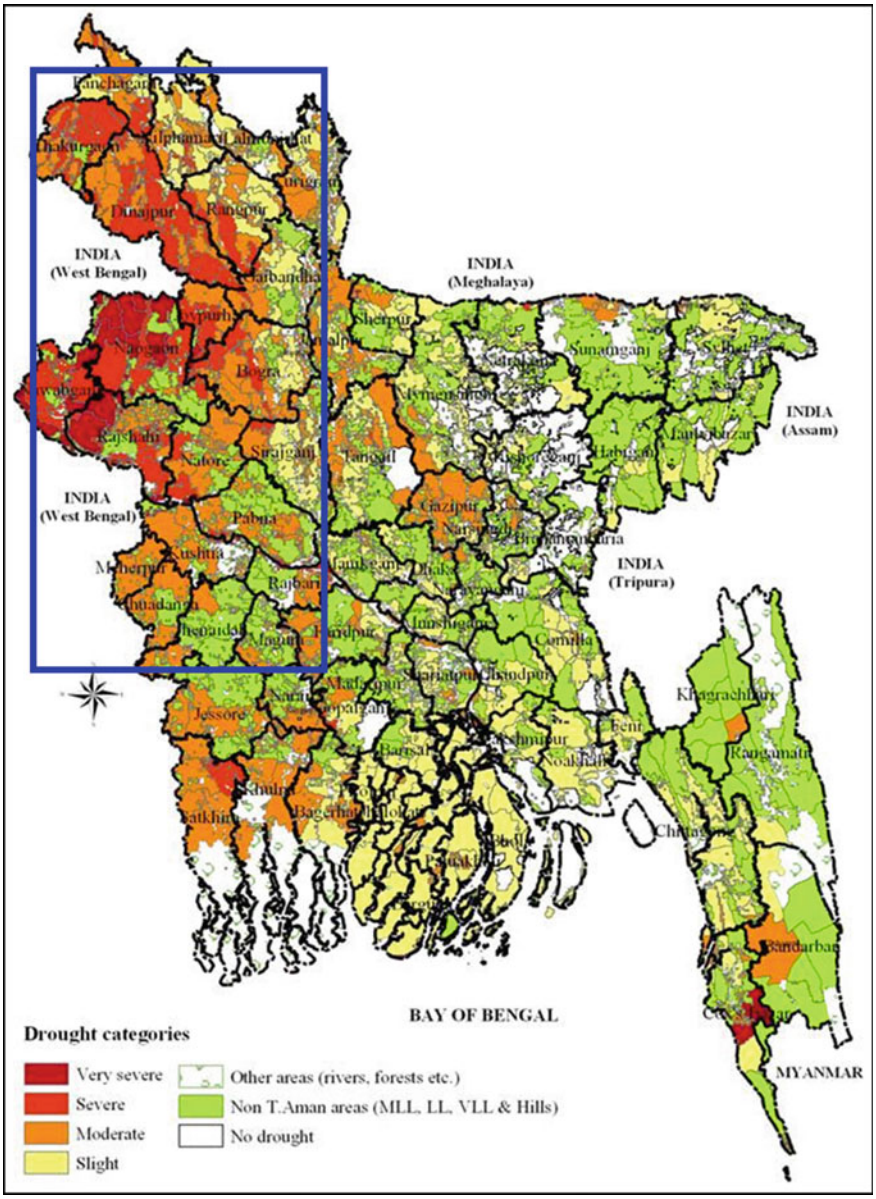

Fig. 1 T. Aman rice growing area of Bangladesh under different agricultural drought conditions. The study area (inside the box) in North-West region is under moderate to very severe drought

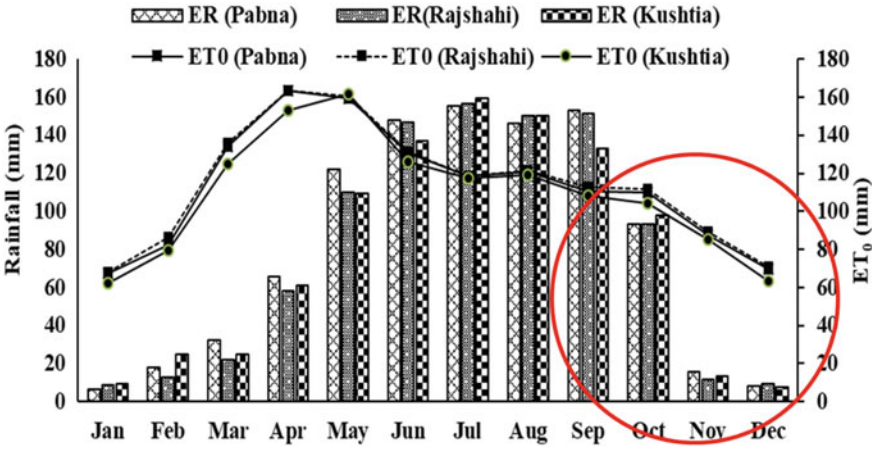

Fig. 2 Monthly distribution of normalize (1981–2017) effective rainfall (ER) and potential evapotranspiration (ET_0) in Kushtia, Pabna and Rajshahi areas

land preparation. Individual plot size was 4 × 5 m with 20 × 40 cm levees. Each plot was separated by buffer zone of 1 × 1 m.

2.3 Short Duration T. Aman Rice Variety Cultivation

The experiment was set up with four treatments and was replicated thrice. The treatments were: T1 = Date of Transplanting 10 July; T2 = Date of Transplanting 17 July; T3 = Date of Transplanting 24 July; and T4 = Date of Transplanting 31 July. A well-recommended short duration variety BRRI dhan33, especially suitable for the North-West region of Bangladesh, was used for the experiment during T. Aman season. The drought amount was calculated using a water balance-based drought model. Cultural and fertilizer management practices recommended by BRRI were followed in growing the crop. Seedlings were raised outside the experimental field and 30 days old seedlings were transplanted after proper land preparation with 20 × 20 cm spacing. Individual plot size was 4 × 5 m, separated by 20 × 40 cm levees.

2.4 Adjustment of Transplanting Time

In this study, rain gauges were installed near the experimental field to collect rainfall data throughout the growing period. The daily weather data of three North-West region districts, namely Kushtia, Pabna, and Rajshahi, were collected from the Bangladesh Meteorological Department (BMD). FAO developed CROPWAT 8.0

model was used to determine potential evapotranspiration, actual crop water requirement, effective rainfall, and irrigation demand (ID) from collected daily weather data. Six transplanting dates, namely 10 July, 17 July, 24 July, 31 July, 7 August, and 14 August, were considered for this experiment. A long duration T. Aman rice variety, BR11, was taken as test cultivar for this experiment. The seasonal and phase-wise crop water requirement, effective rainfall, and irrigation demand for Kushtia, Pabna and Rajshahi, under varying transplanting dates during T. Aman, 2013 to T. Aman, 2015, were calculated. A threshold yield of 5.5 t/ha equal to the national yield average (BRRI 2019) was considered as selection criteria for identifying suitable transplanting window.

3 Results

3.1 Supplemental Irrigation

Table 1 presents the treatment and replication-wise water requirement, water applied, yield obtained, and yield increment due to the application of supplemental irrigation at critical stages for the first study of supplemental irrigation application. The research findings showed that two supplemental irrigations, during the critical stages of T. Aman rice (i.e. flowering to grain filling), could reduce yield loss by 18–20% over completely rainfed conditions. The yield loss would be minimized more, by 40–45%, if three supplemental irrigations were applied.

Table 1 Effect of supplemental irrigation on T. Aman rice yield

Treatment	Replication	Water requirement (mm)	Water applied (mm)	Yield (t/ha)	Yield increased (%)	Average yield increased (%)
Rainfed	R1	833	833	3.7	-	
	R2	840	840	3.5	-	
	R3	892	892	3.55	-	
	R4	957	957	3.72	-	
Two irrigations at critical stages	R1	810	910	4.56	23.2	22.0
	R2	779	879	4.4	18.9	
	R3	860	960	4.38	18.4	
	R4	884	984	4.71	27.3	
Three irrigations at critical stages	R1	658	808	5.29	43.0	41.9
	R2	689	839	5.17	39.7	
	R3	747	897	5.35	44.6	
	R4	762	912	5.19	40.3	

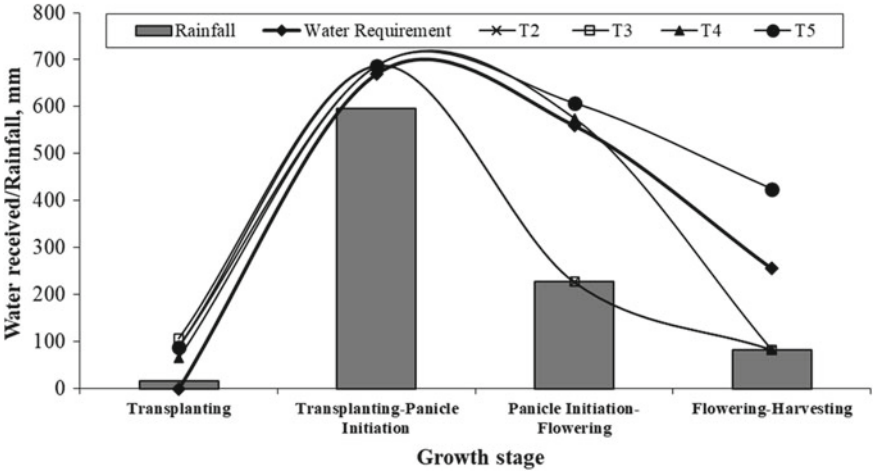

Fig. 3 Rainwater vs. Water requirement for different treatments

From the second study of supplemental irrigation, it was observed that the period from panicle initiation (PI) to flowering was critical, because difference between the water requirement (560 mm) and rainfall received (227 mm) during this period was very high compared to other periods, as depicted in Fig. 3. This difference caused maximum amount of water shortage during this period, as rainfall was not sufficient to meet the crop water requirement. Hence, at this period, when supplemental irrigations were applied in treatment T4 and T5 in addition to rainfall in order to meet the water stress, the crop did better than that of other treatments.

3.2 Short Duration T. Aman Variety

In this experiment, after transplanting the short duration T. Aman rice variety BRRI dhan33, the highest total drought amount was observed for transplanting date of 31 July and the lowest total for transplanting date of 17 July (Table 2). T. Aman rice transplanted on 10 July and 17 July faced drought during the vegetative stage, of

Table 2 Drought amount at different growth stages of BRRI dhan33

Treatment	Vegetative Stage (mm)	Reproductive Stage (mm)	Ripening Stage (mm)	Total
10 July	61.97	0	0	61.97
17 July	20.89	0	16.39	37.28
24 July	0	0	55.99	55.99
31 July	0	1.55	79.34	80.89

61.97 mm, and 20.89 mm, respectively. Drought at ripening stage was observed for all dates of transplanting except 10 July, and the highest was found for 31 July. Drought amount during the reproductive stage was not considerable in any treatment. Figure 4 represents transplanting date-wise drought pattern throughout the growth duration of BRRI dhan33 and demonstrates the safe escaping of drought at reproductive stages. BRRI dhan33, that was transplanted on 24 July, yielded higher (4.60 t/ha) than the other treatments for that variety (Table 3). In this case, the rice did not suffer from drought during its vegetative and reproductive stages. However, it faced relatively higher drought amount in the ripening stage. The next highest yield was observed for date of transplanting 31 July (4.23 t/ha). In the other two treatments, yields were comparatively lower than that of 24 July and 31 July transplanting. Considerable amount of drought was observed in the vegetative stages of rice transplanted on 10 July and 17 July. Drought at the ripening stage did not have a negative impact on rice yield at any treatment. Therefore, considering the drought amount at different growth stages, short duration T. Aman rice variety like BRRI dhan33 could easily escape drought during the critical stages.

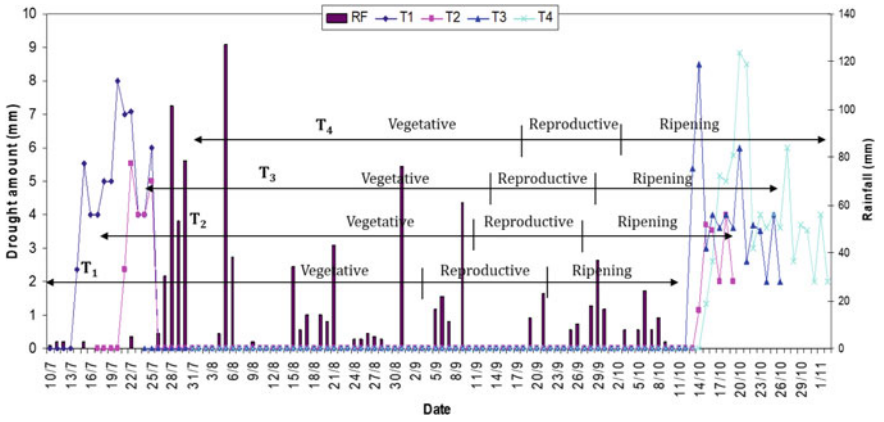

Fig. 4 Drought patterns for BRRI dhan33

Table 3 Yield performance of BRRI dhan33

Treatment	Plant height (cm)	Panicle/m^2	Yield (t/ha)
10 July	108	231	3.85
17 July	105	228	3.93
24 July	106	266	4.60
31 July	109	241	4.23

3.3 Adjustment of Transplanting Time

From Table 4, it can be observed that the vegetative phase did not have any irrigation demand in all three years (2013–2015). In all years, irrigation demand at the reproductive stage showed increasing trend due to transplanting delay. In 2014, irrigation demand was the highest in the reproductive stage due to limited rainfall failing to effectively meet the water requirement for that stage. However, irrigation demand in the reproductive and ripening stages was considerable in all three years except 2013.

Table 4 Growth stage-wise effective rainfall (ER in mm) and Irrigation demand (ID in mm) for different transplanting dates during T. Aman 2013 to 2015 at Kushtia

Growth Phase		10-Jul	17-Jul	24-Jul	31-Jul	07-Aug	31-Aug
2013							
Vegetative phase	ER	358	350	349	344	335	320
	ID	0	0	0	0	0	0
Reproductive phase	ER	118	115	111	84	80	55
	ID	0	0	0	18	21	44
Ripening phase	ER	48	29	0	0	0	0
	ID	50	71	99	97	98	92
Seasonal	ER	524	494	461	428	415	386
	ID	0	3	22	35	30	22
2014							
Vegetative phase	ER	435	435	391	356	333	317
	ID	0	0	0	0	0	0
Reproductive phase	ER	78	75	77	58	43	27
	ID	62	60	52	67	80	89
Ripening phase	ER	27	0	0	0	0	0
	ID	81	109	106	102	101	91
Seasonal	ER	539	510	467	414	376	344
	ID	8	22	55	93	105	93
2015							
Vegetative phase	ER	467	450	429	395	366	336
	ID	0	0	0	0	0	0
Reproductive phase	ER	81	81	82	69	59	49
	ID	45	43	41	52	60	59
Ripening phase	ER	31	19	1	1	1	1
	ID	71	82	94	89	87	74
Seasonal	ER	580	551	512	465	426	386
	ID	0	0	0	0	19	8

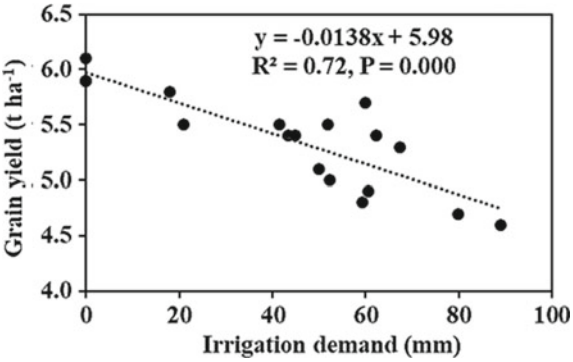

Fig. 5 Relationship between grain yield and irrigation demand of BR11 at reproductive phase in Kushtia

Figure 5 illustrates yield response to irrigation demand (ID) in the reproductive phase. From the relationship ($P < 0.01$), it could be reported that the grain yield decreased by 0.0138 t/ha if irrigation demand (ID) increased by 1 mm. This result supports the findings from Yang et al. (2019), which stated that the effect of drought stress at flowering stage was significant as it affected physiological traits and decreased grain yield. In a study conducted in Tamil Nadu, India, researchers have found a reduction of grain yield by 28% due to mild water stress in the reproductive phase of rainfed rice during 1999–2000 (Babu et al. 2003). Water stress at the reproductive stage caused significant grain yield reduction (Kamoshita et al. 2008).

BR11 yield performance was analysed for the three locations and has been illustrated in Fig. 6. The yields were estimated using the relationship developed between grain yield and irrigation demand (ID). For Kushtia, the yields of BR11 were equal to or higher than the threshold limit (5.5 t/ha) for transplanting window of 10–24 July. In Pabna, considering the threshold limit, 10–24 July was found as the suitable transplanting window (Fig. 6). In Rajshahi, the yields for different transplanting dates did not come close to the threshold limit. Hence, considering the reduced limit as 5 t/ha, the suitable transplanting window was found to be 10–24 July. In all locations, yield went down drastically if the transplanting date was outside of the suitable window.

4 Discussion

Supplemental irrigation plays a vital role in alleviating the impact of drought, especially on T. Aman rice production. T. Aman rice always suffers from either short or long-spell drought at the reproductive stage of the crop. Sattar (1993) stated that water stress at the vegetative stage can cause a yield loss of about 25% and this may be as high as 50% at the reproductive stage. Therefore, supplemental irrigation should be applied by any means from any source. It has also been observed from the effect of drought on Aman rice growth phases (BRRI 2008), that under a drought spell, percentage of yield reduction was higher at the reproductive phase than at the

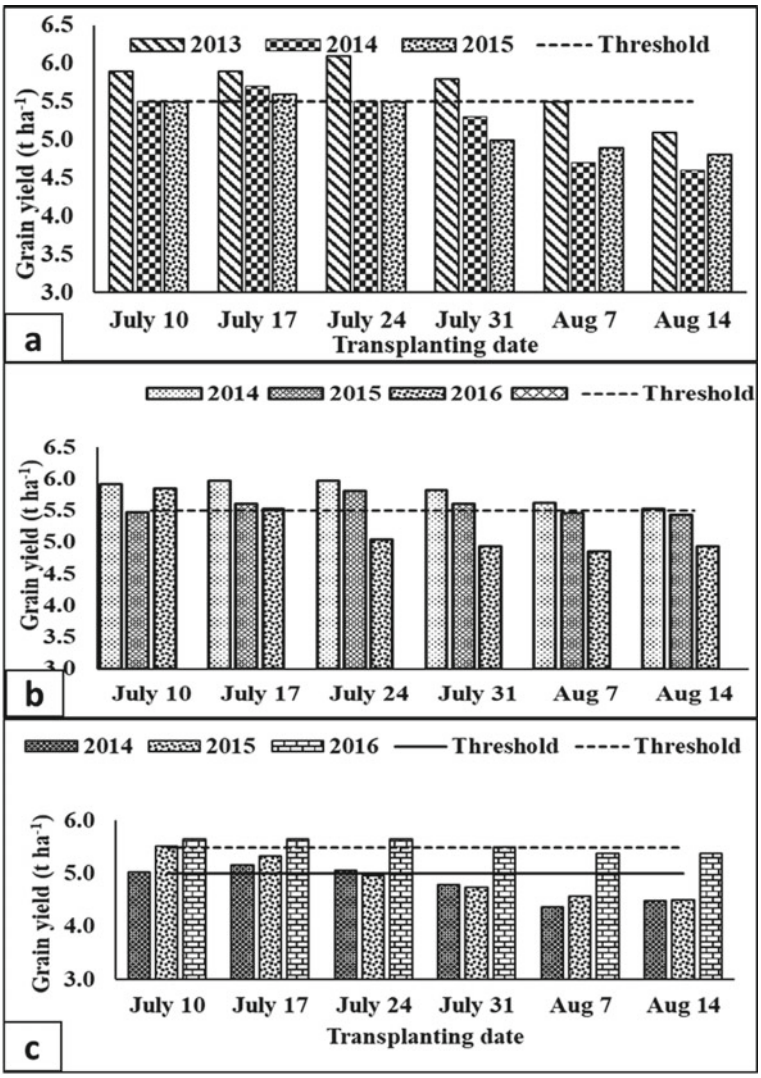

Fig. 6 Yield performance of BR 11 over threshold under different transplanting dates at (a) Kushtia, (b) Pabna and (c) Rajshahi

ripening phase. Hence, the reproductive phase is considered more vulnerable to water stress in comparison with the ripening stage. BRRI research results showed that two or three supplemental irrigations in proper time could increase T. Aman rice production by 40–45% (Table 1). However, Incremental yield was completely dependent on water shortage minimization by supplemental irrigation in excess to rainfall. The period from panicle initiation to flowering stages was critical as maximum water

stress occurred during this period due to insufficient rainfall. T. Aman rice cultivation largely depends on rain for its water supply. So, the source of supplemental irrigation water is a major concern during T. Aman season. Rainwater harvesting by mini-pond and levee management could be the best solution to this problem. The stored water in mini-ponds can be used for land preparation and for irrigation under a drought spell during the vegetative and reproductive stages of T. Aman rice (BRRI 1991). A 15 cm-levee height management can give the highest yield of T. Aman rice by conservation of maximum effective rainwater. These can be effectively used for improving land productivity in the rainfed areas.

Cultivation of short duration variety is another effective means for mitigating the effects of agricultural drought by escaping it altogether. Findings of this study show that if the cultivar could be transplanted at a recommended time, critical stages of growth duration like flowering and grain filling stages would be completed before the drought appeared. However, the yield of short duration rice variety was comparatively lower than that of the long duration variety. But at least, drought could not be able to hamper the rice production of short duration variety compared to long duration variety.

For transplanting long duration variety like BR11, the transplanting window of 10–24 July was suitable for Kushtia and Rajshahi while 10–17 July window was appropriate for Pabna. The farmers who are interested to cultivate long duration variety must adopt the recommended transplanting dates so that they do not need to cultivate short duration variety or apply supplemental irrigation.

Although all three approaches are beneficial in varying extents, farmers are not always interested or able to pick any of those, and there are a number of factors that they need to take into consideration. Supplemental irrigation application is usually the best option to mitigate agricultural drought at latter part of the season. But application of supplemental irrigation includes cost and labour. To reap maximum benefit from short duration variety, timely transplanting is critical. However, it may not be possible to prepare the land for transplanting in due time. Adjusting the transplanting dates for long duration variety would be a flexible choice for farmers. However, timely land preparation, availability of seeds and fertilizers, and cost of inputs are all key factors for transplanting T. Aman rice within the suitable window.

5 Conclusion

Drought management using integrated approaches in T. Aman season offers an effective solution for the North-West region of Bangladesh. The current rainfall pattern bears evidence that the monsoon is beginning to cease at the end of September, propagating the permanent risk of drought occurrence at the later part of T. Aman rice season. Supplemental irrigation is the first suggested approach to mitigate terminal drought at the critical reproductive stages by applying lifesaving water to the plant. As a second choice, farmers can cultivate short duration crop variety and escape the effects of drought during critical stages. Adjusting the transplanting dates for

long duration T. Aman rice cultivar can also successfully overcome the irrigation demand at the reproductive phase. Delay in transplanting demands more irrigation and reduces yield.

Acknowledgements The author would like to express heartiest gratitude to Bangladesh Rice Research Institute (BRRI) for providing research facilities and funding. The authors are also thankful to Agricultural Land and Water Resources Management (ALAWRM) Research Group, Irrigation and Water Management (IWM) Division, Bangladesh Rice Research Institute (BRRI) for their kind support and help throughout the study. The authors would like to convey their special thanks to ICWFM 2021 organizer and the scientific committee for accepting the abstract, giving the opportunity to make an oral presentation, and finally selecting the paper for publishing in conference proceedings.

References

Babu, R., B. Nguyen, V. Chamarerk, P. Shanmugasundaram, P. Chezhian, P. Jeyaprakash, et al. 2003. Genetic Analysis of Drought Resistance in Rice by Molecular Markers. *Crop Science* 43 (4): 1457–1469. https://doi.org/10.2135/cropsci2003.1457.

BBS (Bangladesh Bureau of Statistics). 2019. *"Yearbook of Agricultural Statistics of Bangladesh" Planning Division, Ministry of Planning*. Dhaka: Government of the People's Republic of Bangladesh.

Biswas, J.K. 2011. Climate Adversaries: Coping with Rice Agriculture. *J. Asiatic Soc. Bangladesh* 37: 359–374.

Biswas, J.K., Kabir S, Rahman S, Nahar K, and Hasanuzzaman M. 2019. Managing Abiotic Stresses with Rice Agriculture to Achieve Sustainable Food Security: Bangladesh Perspective. In *Advances in Rice Research for Abiotic Stress Tolerance*, ed. M. Hasanuzzaman et al., 23–46. Duxford: Woodhead Publishing, Elsevier Inc. https://doi.org/10.1016/B978-0-12-814332-2.00002-2.

BRRI (Bangladesh Rice Research Institute). 1991. Internal Review Report, 149–155. Gazipur: Irrigation and Water Management Division.

BRRI (Bangladesh Rice Research Institute). 2008. Annual Report. Irrigation and Water Management Division. Gazipur: Bangladesh Rice Research Institute.

BRRI (Bangladesh Rice Research Institute). 2019. Modern rice cultivation. Gazipur: Bangladesh Rice Research Institute.

Fischer, G., F.N. Tubiello, H. Van Velthuizen, and D.A. Wilberg. 2007. Climate Change Impacts on Irrigation Water Requirements: Effects of Mitigation, 1990–2080. *Technological Forecasting and Social Change* 74 (7): 1083–1107.

Haq, K.A., Islam, J., and Sattar, M.A. 1985. Low Irrigation Strategies for Rice Production. *Proc. of the Seminar on Low Water Demanding Crops*. Dhaka: BARC.

Ibrahim, A. 2001. Application of Agroecological Zones Database in Drought Management and Water Availability Assessment. Environment and GIS support project for water sector planning, 7–11. Dhaka.

Islam, M.T. 2007. "Modeling of Drought for Aman Rice in the Northwest Region of Bangladesh." Ph. D. Thesis. Mymensingh: Department of IWM, BAU.

Islam, M.T., and J.K. Biswas. 2010. Natural Hazard Management in Rice Production. *J Agric Engin* 38: 63–69.

Islam, M.T., L.R. Khan, and K.M. Hassanuzzaman. 2009. Integrated Approach for Mitigating Drought in Transplanted Aman Rice in Northwest Region of Bangladesh. *Bangladesh Rice Journal* 14 (1&2): 169–173.

Kamoshita, A., R.C. Babu, N.M. Bhupathi, and S. Fukai. 2008. Phenotypic and Genotypic Analysis of Drought-Resistance Traits for Development of Rice Cultivars Adapted to Rainfed Environments. *Field Crops Res.* 109: 1–23. https://doi.org/10.1016/j.fcr.2008.06.010.

Khan, H.R. 1979. Determination of Transplanting Date and Supplementary Irrigation Requirement for HYV Monsoon Rice Using Rainfall. *Bangladesh Journal of Water Resource Research* 1 (1): 76–85.

MDMR-CEGIS (Ministry of Disaster Management and Relief-Center for Environmental and Geographic Information Services). 2013. Vulnerability to Climate Induced Drought: Scenario & Impact. Center for Environmental and Geographic Information Services. Comprehensive Disaster Management Programme (CDMP II), Ministry of Disaster Management and Relief, 134.

Rosenzweig, C.E., F. Tubiello, R. Goldberg, E. Mills, and J. Bloomfield. 2002. Increased Crop Damage in the U.S. from Excess Precipitation under Climate Change. *Global Environment Change* A (12): 197–202.

Roy, D., Ahmmed, M.U., and Mahmud, N.H. 2014. Water Management Technologies for Sustainable Rice Cultivation Under Changing Climate. *J. Agric. Engin* 41/AE (1): 3–52.

Roy, D., M.T. Islam, and B.C. Nath. 2010. Impact of Supplemental Irrigation Applied at Different Growth Stages of Transplanted Aman Rice (Oryza Sativa). *The Agriculturists* 8 (1): 109–114.

Saleh, A.F.M. 1987. The Effect of Supplementary Irrigation on Rice Yield in Bangladesh. *International Rice Research Newsletter* 2 (1): 25–26.

Saleh, A.F.M. 1991. Supplementary Irrigation in Bangladesh: Requirements, Benefits, and Prospects. *Proc. of the Special Technical Session Proceedings, International Commission on Irrigation and Drainage* China 1-A: 96–105.

Sattar, M.A. 1993. Water Management and Technology Adoption for Direct Seeded Rice in an Irrigation System. Dissertation. Philippines: Central Luzon State University.

Sattar, M.A., and Parvin, M.I. 2009a. "Sustainable T. Aman Rice Production in North-West Region of Bangladesh for Food Security Under Climate Change Situation." *Proc. of International Conference on Climate Change Impacts and Adoption Strategies for Bangladesh*, 289. Dhaka: BUET.

Sattar, M.A., and Parvin, M.I. 2009b. Assessment of Vulnerability of Drought and Its Remedial Measures for Sustainable T. Aman Rice Production in the Selected Locations of Bangladesh." *Proc. of 2nd International Conference on Water and Flood Management (ICWFM 2009)*, 109. Dhaka.

Yang, X., B. Wang, L. Chen, P. Li, and C. Cao. 2019. The Different Influences of Drought Stress at the Flowering Stage on Rice Physiological Traits, Grain Yield, and Quality. *Scientific Reports* 9: 3742. https://doi.org/10.1038/s41598-019-40161-0.

Actual Evapotranspiration Estimation Using Remote Sensing: Comparison of Sebal and Metric Models

Sumit Kumar Saha, Rubel Ahmmed, and Nasreen Jahan

Abstract Evapotranspiration (ET) is the sum of evaporation from earth's surface and transpiration from plants to the atmosphere. Accurate quantification of ET is crucial for hydrologic modeling, optimizing crop production, drought monitoring, irrigation management, and overall water resource planning. For monitoring evapotranspiration, remote sensing-based Surface Energy Balance Algorithm for Land (SEBAL) and Mapping Evapotranspiration (ET) at high Resolution with Internalized Calibration (METRIC) have been applied extensively. However, the complexity of selecting hot and cold pixels has made the operational use of these models challenging. In this study, an automated implementation of these models called Land MOD ET mapper has been tested in two agricultural sites of Bangladesh using Landsat-4-5 TM images, DEM and weather data from the Modern-Era Retrospective analysis for Research and Applications, version 2 (MERRA-2). Merra-2 is a global atmospheric reanalysis produced by the NASA. The evapotranspiration calculated by the SEBAL and METRIC models were compared with the recorded pan evaporation and the Penman–Monteith method. Comparison of the results from the SEBAL and METRIC shows some differences in ET estimation. This is probably due to the differences in calculation of sensible heat and the assumptions of SEBAL and METRIC in extrapolating instantaneous ET to the daily ET. This study demonstrates the considerable potential of SEBAL and METRIC models for estimation of spatiotemporal distribution of ET from Landsat satellite images and Merra-2 weather data for the agricultural regions of Bangladesh.

Keywords Evapotranspiration · SEBAL · METRIC · Landsat · MERRA-2

S. K. Saha (✉) · R. Ahmmed · N. Jahan
Department of Water Resources Engineering, Bangladesh University of Engineering and Technology, Dhaka, Bangladesh

N. Jahan
e-mail: jahan@ualberta.ca

© The Author(s), under exclusive license to Springer Nature Switzerland AG 2022

G. M. Tarekul Islam et al. (eds.), *Water Management: A View from Multidisciplinary Perspectives*,
https://doi.org/10.1007/978-3-030-95722-3_18

1 Introduction

1.1 Background of the Study

Evapotranspiration (ET) refers to the conveyance of water vapor from earth's surface to the atmosphere. ET is the sum of evaporation and transpiration from the surface of the earth to the atmosphere. The flow of water to the air from sources such as the soil, canopy interception, and water bodies is accounted for by evaporation. On the other hand, transpiration can be defined as loss of water as vapor through stomata in the leaves. Evapotranspiration is an important phenomenon within the land–atmosphere interface that regulates the earth's energy and water cycles. Both evaporation and transpiration take place at the same time and are influenced by solar radiation, air temperature, relative humidity, vapor pressure deficit, and wind speed. Crop characteristics, environmental factors, and cultivation practices influence the rate of transpiration. Transpiration rates also vary depending on the type of plant.

Evapotranspiration is a vital nexus between terrestrial water, carbon, and surface energy exchanges and is a fundamental component of the global water cycle (Zhang et al. 2016). It is an important process in the water cycle because it is responsible for 15% of the atmosphere's water vapor (ScienceDaily 2021). Accurate estimation of ET is essential for undertaking research on climate change, and for managing agricultural water requirements, drought forecasting and monitoring, and optimal water resource development and exploitation, among other things. Bangladesh is an agriculture-based country where Boro rice cultivation during the dry season depends almost entirely on groundwater irrigation (Kirby et al. 2016). Climate change is expected to cause a decrease in soil moisture, an increase in daily ET, and these will increase the irrigation demand and cause further depletion of groundwater level (Shahid 2011). For South and East Asia, the total annual water withdrawal is roughly 1981 km^3, which is about 50% of the global aggregate, and agriculture constitutes around 82% of the total freshwater withdrawal in Asia (FAO 2016). Past studies have reported significant increasing trend of irrigation water quantity due to expanded areas in the Northwest region of Bangladesh (Mojid et al. 2021). Consequently, high water withdrawal and the rapid decline of groundwater resources in Bangladesh due to excessive irrigation during the dry season have become a severe concern that requires awareness regarding optimal on-field water requirements (GoB and FAO 2018). In addition to the rapid rise in groundwater-dependent irrigation, wastage of water by irrigating more than the crop water demand also contributes to this alarming groundwater depletion. Studies have shown that 21% of the water lifted for irrigation is left unused and lost in Bangladesh (BRAC and BUET, 2013). Therefore, proper management of groundwater resources for agricultural uses is extremely necessary to maintain a sustainable balance between groundwater supply and demand, and thereby ensure food security in the coming decades for Bangladesh. Therefore, an accurate estimation of evapotranspiration is necessary for calculating irrigation demand accurately and managing available water resources in Bangladesh.

ET can be estimated using empirical equation or remote sensing algorithm or can be measured by traditional methods (Liou and Kar 2014). Lysimeter and eddy covariance method offer in-situ measurement of ET. But they are costly, time-consuming, and works only at the local scale for a particular crop. A complementary relationship-based model developed by Anayah and Kaluarachchi (2014) has been used to compute actual evapotranspiration in a recent study in the Ganges Delta (Murshed and Kaluarachchi 2018; Murshed, Rahman, and Kaluarachchi 2019) where meteorological data have been used. The Penman–Monteith formula is used frequently to overcome this problem, but it requires several climate data and surface variables that are not easily available (Stannard 1993). Although MODIS satellite provides actual ET data based on both climate and remote sensing (RS) variables, the output showed a discrepancy with the observed ET in some studies (Ruhoff et al. 2013). So, past research on evapotranspiration estimation in Bangladesh have mainly studied reference ET instead of actual ET because it requires only a moderate amount of data in comparison with actual ET calculation (Karim et al. 2020). Under this perspective, Surface Energy Balance Algorithm for Land (SEBAL) or Mapping Evapotranspiration (ET) at high Resolution with Internalized Calibration (METRIC) can therefore be an alternative and reliable method of estimating actual ET at local to regional scales (Li et al. 2009). Remote sensing-based algorithms are cost-effective and spatiotemporal variation of ET can be monitored easily. The water stress is also considered here which is not generally considered in the empirical approach. Rojas and Sheffield (2013) evaluated daily reference evapotranspiration methods using five different methods including the ASCE-EWRI Penman–Monteith equation in Northeast Louisiana (Rojas and Sheffield 2013). Reyes-González et al. (2017) compared actual Evapotranspiration values estimated from the METRIC model with other Methods in Eastern South Dakota(Reyes-González et al. 2017). Bose et al. (2021) used SEBAL for operational irrigation advisory in Pakistan (Bose et al. 2021).

Past studies on ET estimation in Bangladesh have employed mostly the Penman–Monteith equation. Sahid, S., (2011) has shown that the climate change will increase the ET and irrigation rate. He used FAO Penman model for the computation of ET (Shahid 2011). Some of the past research studied the crop evapotranspiration (ETc) based on Penman–Monteith method and predicted future irrigation requirements of Boro rice (Acharjee et al. 2017). Kanoua and Merkel (2015) used the Two-Source Trapezoid Model for Evapotranspiration and the SEBAL model to estimate the spatiotemporal variation in actual evapotranspiration in Titas Upazila, Bangladesh (Kanoua and Merkel 2015). SEBAL was used to estimate ET in a study on the availability of groundwater for crops in the Northwest zone of Bangladesh (Dey et al. 2017). Hossen et al. (2012) reported surface energy components and evapotranspiration over a double-cropping paddy field in Bangladesh (Hossen et al. 2012).

The objective of the study is to assess the potential of Surface Energy Balance Algorithm for Land (SEBAL) and Mapping Evapotranspiration at high Resolution with Internalized Calibration (METRIC) model in estimating ET for agricultural fields of Bangladesh. An automated implementation of these models called LandMOD ET mapper has been used herein for this purpose at two agricultural

study sites. The estimated ET from SEBAL and METRIC model was also compared with the ET estimation obtained from the FAO Penman–Monteith equation and the observed pan evaporation data from Bangladesh Meteorological Department (BMD) for both stations.

1.2 Study Area

In this study, evapotranspiration has been estimated for Mymensingh Sadar Upazila and Bogra Sadar Upazila of Bangladesh. Bangladesh Meteorological Department (BMD) monitors evaporation only at a limited number of agro-meteorological stations. Two stations out of those have been randomly chosen for the study. The Mymensingh site (Fig. 1) is a paddy field located at the Bangladesh Agricultural University Farmland (24.73°N, 90.42°E, and 18 m above the mean sea level). This 1420 sq. m field has been used exclusively for paddy cultivation for about 40 years. It provides a sufficient upwind fetch of uniform land cover for measuring mass and energy fluxes using tower-based eddy covariance systems. The soil type of this field is dark-gray non-calcareous floodplain (UNDP and FAO, 1988) with a sandy loam texture. The location experiences a tropical monsoon-type climate, with a hot and

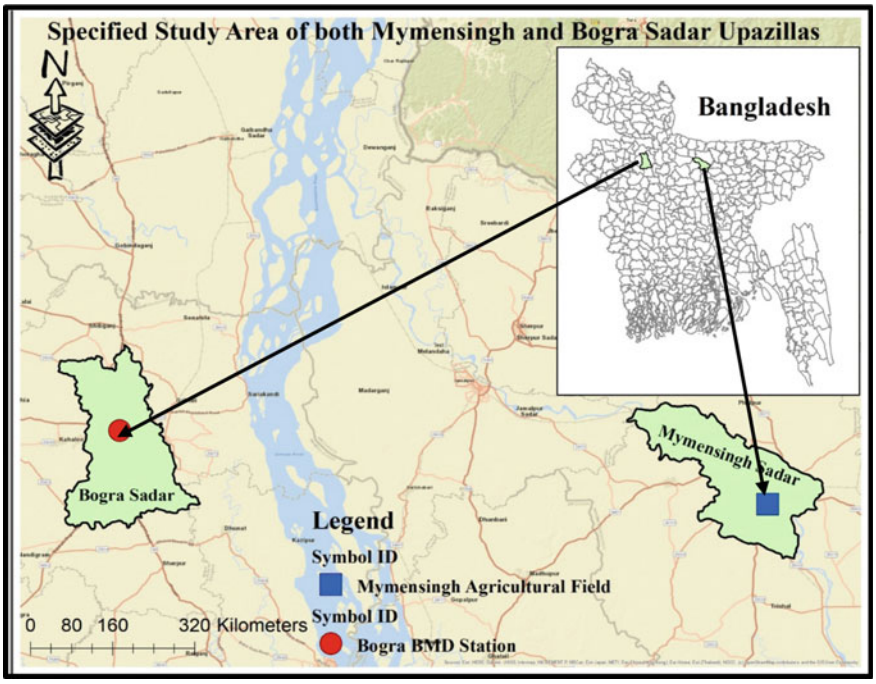

Fig. 1 Mymensingh and Bogra study sites

rainy summer, and dry winter. Annual mean air temperature was 298.66 K, and annual rainfall was 2055 mm. The usual cropping pattern is rice, with two rice crops per year. One crop is dry-season rice, locally called "Boro" rice, which is cultivated from late winter (February) to midsummer (May). The other crop is wet-season rice, locally called "Aman" rice, which is cultivated from late summer (August) to early winter (December). The field is mostly irrigated during the Boro rice period, while it is rain-fed during the Aman rice period.

The Bogra site (Fig. 1) is located around the Bangladesh Meteorological Department's climate station at Bogra (24°51'N and 89°22'E). Total Area of Bogra Sadar is 17734 ha in which 150 ha area is used for Annual crop, 1940 ha for Double crop, 8700 ha for Triple crop and 300 ha for Quadrated crop. The other 110 ha and 11,200 ha are non-cultivable areas. These two stations have been selected as we have measured pan evaporation data for these locations. The time period of the study has been chosen based on the availability of pan evaporation data of ET (Table 1).

1.2.1 Weather Data

All required weather data were collected from Modern-Era Retrospective analysis for Research and Applications, version 2 (MERRA-2) which is a global atmospheric reanalysis produced by the NASA. Following variables were collected.

I. Instantaneous Relative humidity (%) at the image time (rh_inst)
II. Instantaneous Air temperature in kelvin at the image time (t_inst)
III. Instantaneous Wind speed in m/s at the image time (u_inst)
IV. Instantaneous Incoming solar radiation in wm^{-2} at the image time (solar_inst)
V. Maximum daily air temperature in kelvin (tmax_daily)
VI. Mean daily air temperature in kelvin (tmean_daily)
VII. Minimum daily air temperature in kelvin (tmin_daily)
VIII. Daily mean solar radiation wm^{-2} (solar_daily)
IX. Daily mean Relative humidity % (rh_daily)
X. Daily mean wind speed m/s (u_daily).

1.2.2 Other Remote Sensing Data

Land surface temperature (LST) has been collected from remote sensing lab of landsat-5. Emissivity has been collected from MERRA-2. Spatial resolution has been maintained as 30 m by 30 m.

After calculating the reflectance from the digital numbers of the satellite images, NDVI is calculated by using **Eq.** 1:

$$\text{NDVI} = \frac{R_{\lambda(\text{NIR})} - R_{\lambda(\text{RED})}}{R_{\lambda(\text{NIR})} + R_{\lambda(\text{RED})}} \tag{1}$$

Table 1 Description of the data for Mymensingh and Bogra Sadar Upazilla

SL. No	Date of Collection	Day of Year	Sun Elevation Angle (Degree)	Image Collection Time		Earth Sun Shine Distance (d)
				Hour	Minute	
Mymensingh Sadar Upazilla						
01	22 Jan, 2007	22	38.257	10	19	0.98419
02	23 Feb, 2007	54	46.007	10	19	0.98944
03	11 Mar, 2007	70	51.227	10	19	0.98717
04	27 Mar, 2007	86	57.676	10	19	0.99782
05	28 pr, 2007	118	65.068	10	19	1.00679
06	30 May, 2007	150	67.715	10	18	1.01371
07	18 Aug, 2007	230	63.161	10	17	1.01225
08	19-Sep, 2007	262	56.826	10	17	1.00457
09	05 Oct, 2007	278	53.813	10	17	1.00005
Bogra Sadar Upazilla						
01	24 Jan, 2011	24	38.0341	10	20	0.98439
02	09 Feb, 2011	40	41.4123	10	20	0.98662
03	25 Feb, 2011	56	45.9611	10	20	0.98989
04	13 Mar, 2011	72	51.1584	10	20	0.99392
05	16 May, 2011	136	66.2923	10	19	1.01011
06	08 Nov, 2011	312	43.6547	10	18	1.01403

where $R_{\lambda(\mathrm{NIR})}$ is Reflectance of Near Infrared Band (band 4 of Landsat 5), $R_{\lambda(\mathrm{RED})}$ is Reflectance of Near Red Band (band 3 for Landsat 5). Albedo is a measure of how much radiation is reflected from a surface. It is a ratio of the reflected radiation to the radiation reached to the ground. Albedo has been computed following Allen et al. (2007) using the bands of the landsat images and DEM (Digital Elevation Model) of the selected sites (Allen et al. 2007).

Surface roughness (z0m) was computed using **Eq.** 2: (Su and Jacobs 2001)

$$z0m = 0.005 + 0.5 * \left(\frac{NDVI}{NDVI_{max}}\right)^{2.5} \quad (2)$$

where z0m = Surface roughness in meter, NDVI is normalized difference vegetation index, $NDVI_{max}$ is maximum value of NDVI.

2 Background of Models

2.1 Sebal

The Surface Energy Balance Algorithm for Land (SEBAL) proposed by (Bastiaanssen et al. 1998) is one of the most widely used remote sensing-based algorithm for computing energy balance (Bhattarai and Liu 2019). SEBAL estimates actual evapotranspiration (ET_a) from remotely sensed land surface temperature, surface emissivity, NDVI, and some routine ground meteorological observation data, i.e., sunshine duration and wind speed. The core assumption in SEBAL is that there is a linear relation between near-surface vertical temperature gradient and land surface temperature, and this relationship is determined by two extreme hydrological pixels, i.e., extreme wet/cold and extreme dry/hot pixels (Wang et al. 2014).

SEBAL model estimates the surface net radiation flux R_n ($W \bullet m^{-2}$), the soil heat flux G ($W \bullet m^{-2}$), and the sensible heat flux H ($W \bullet m^{-2}$) first and then estimates the latent heat flux LE ($W \bullet m^{-2}$) as an energy residual by **Eq.** 3:

$$LE = R_n - G - H \quad (3)$$

R_n is computed by **Eq.** 4:

$$R_n = (1 - \alpha)R_s + \varepsilon_a \sigma T_a^4 - \varepsilon_s \sigma T_s^4 - (1 - \varepsilon_s)\varepsilon_a \sigma T_s^4 \quad (4)$$

where R_s is the solar shortwave radiation ($W \bullet m^{-2}$), which is estimated by the empirical parameterization of (Zillman et al. 1972). ε_s and ε_a are the surface emissivity and atmospheric emissivity, respectively; α is albedo (dimensionless); σ is the Stefan-Botlzmann constant (5.67×10^{-8} $W \bullet m^{-2} \bullet K^{-4}$); T_s and T_a are the land surface temperature (in K) and air temperature (in K) at satellite observation time.

G is calculated as a fraction of R_n. The ratio G/R_n is usually defined as a function of leaf area index (LAI) or Normalized Difference Vegetation Index (NDVI). In SEBAL, G is calculated by **Eq.** 5:

$$\frac{G}{R_n} = \frac{(T_s - 273.15)}{\alpha}\left(0.0032\alpha_{avg} + 0.0062\alpha_{avg}^2\right)\left(1 - 0.978NDVI^4\right) \quad (5)$$

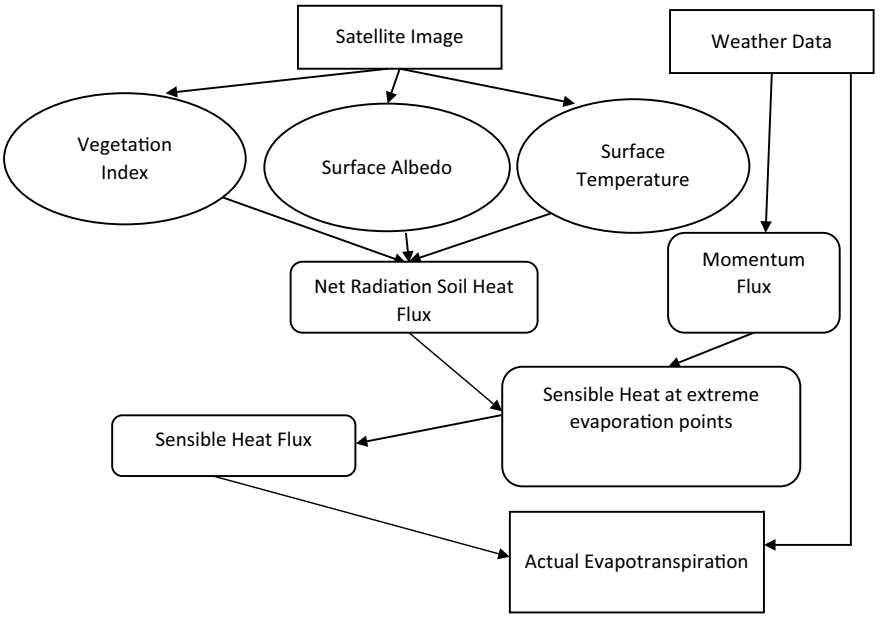

Fig. 2 SEBAL algorithm

where α_{avg} is the daily average albedo which is readily available as remotely sensed images. As the variation in albedo under all clear sky presents a U-shape, high at the sunrise and sunset and low at the noon, therefore a linear algorithm was suggested to calculate α_{avg} using instantaneous α, i.e., $\alpha_{avg} = 1.02\alpha + 0.01$ (Teixeira et al. 2008).

H is calculated by **Eq.** 6 following Anderson et al. 2011.

$$H = \rho C_p(T_0 - T_a)/r_a \tag{6}$$

where ρ is the air density ($kg \bullet m^{-3}$), C_p is the air specific heat at constant pressure ($1004\ J \bullet K^{-1} \bullet kg^{-1}$), T_0 is the aerodynamic temperature (K), r_a is the aerodynamic resistance ($m \bullet s^{-1}$). Figure 2 describes the full process.

2.2 METRIC Model

METRIC (Mapping Evapotranspiration at high Resolution with Internalized Calibration) model is another widely used actual ET estimation model (Allen et al. 2007). It is a remote sensing-based model that computes instantaneous ET values as a residual of the surface energy balance equation which is **Eq. (3)**.

The key component of METRIC model is self-calibration of H using an iterative process based on manually or automatically selected hot and cold pixels. The METRIC model works best in flat regions. However, it can be used in mountainous regions if some corrections are added based on digital elevation model, slope and aspect data (Allen et al. 2007).

METRIC is based on the commonly used principle that ET can be estimated from the residual term of the surface energy balance equation. The available energy (R_n − G) is computed first and then partitioned into H and LE. R_n is computed for clear sky conditions as following Allen et al. (2007) as given in **Eq.** 7:

$$R_n = G_{sc} \cos\theta \, d_r \tau_{sw} (1-\alpha) \, \varepsilon_o \varepsilon_a \sigma T_a^4 - \varepsilon_o \sigma T_s^4 \tag{7}$$

where G_{SC} (1367 W m − 2) is a solar constant, θ is the solar incidence angle computed from the sun elevation angle (β) where θ = (90 − β), d_r is the inverse squared relative earth-sun distance, and τ_{sw} (dimensionless) is the broad-band atmospheric transmissivity (Allen et al. 2007). ε_a is the atmospheric emissivity computed as a function of air temperature and vapor pressure (Wilfried 1975).

In METRIC model, the soil heat flux (G) is computed following Tasumi (2003). This process computes G from R_n, surface temperature, albedo, and NDVI following Bastiaanssen et al. (1998) on **Eq.** 8:

$$G = (T_s - 273.15)\, \alpha \left(0.0038\alpha \, 0.0074\alpha^2\right) \left(1 - 0.98\mathrm{NDVI}^4\right) R_n \tag{8}$$

The key part of the METRIC model is the determination of H, which uses the formulation given in **Eq.** 9:

$$H = \frac{\rho_a c_c dT}{r_{ah}} \tag{9}$$

where ρ_a is air density, c_c is the specific heat of the air, dT is temperature difference, and r_{ah} is aerodynamic resistance (Fig. 3).

2.3 Penman–Monteith Equation

To estimate evapotranspiration from various meteorological factors, a large number of empirical approaches have been developed. Some of them were derived from popular Penman equation (Penman 1948), which used a mix of an energy balance and an aerodynamic formula to calculate evaporation from open water, bare soil, and grass

$$\lambda E = \frac{\Delta(Rn - G) + \gamma \lambda Ea}{\Delta + \lambda} \tag{10}$$

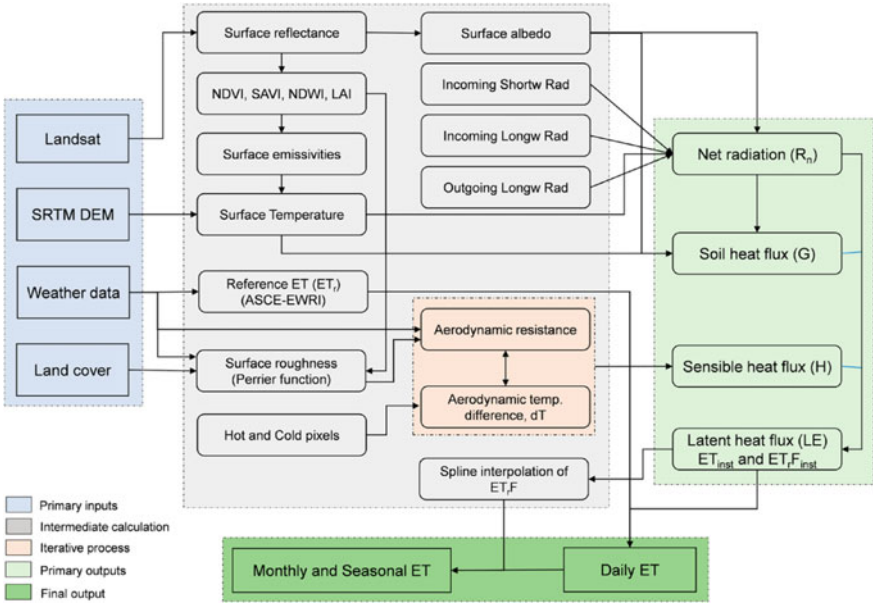

Fig. 3 METRIC algorithm (Numata et al. 2017)

where λE = evaporative latent heat flux (MJ m^{-2} d^{-1}), Δ = slope of the saturated vapor pressure curve [e^o/T, where e^o = saturated vapor pressure (kPa) and Tmean = daily mean temperature (°C)]; Rn = net radiation flux (MJ m^{-2} d^{-1}), G = sensible heat flux into the soil (MJ m^{-2} d^{-1}), ^{3} = psychometric constant (kPa $°C^{-1}$), and Ea = vapor transport of flux (mm/day).

A bulk surface resistance term was introduced in various derivations of the Penman equation (Monteith 1965), and the resulting equation is now known as the Penman–Monteith equation, which can be stated for daily values as in **Eq.** 11:

$$\lambda ET_0 = \frac{\Delta(R_n - G) + 86400\frac{\rho_a C_p (e_s^o - e_a)}{r_{av}}}{\Delta + \gamma(1 + \frac{r_s}{r_{av}})} \tag{11}$$

where ρ_a = air density (kg m^{-3}), Cp = specific heat of dry air, $e_s{}^o$ = mean saturated vapor pressure (kPa) computed as the mean e^o at the daily minimum and maximum air temperature (°C), rav = bulk surface aerodynamic resistance for water vapor (s m^{-1}), e_a = mean daily ambient vapor pressure (kPa), and r_s = the canopy surface resistance (s m^{-1}). An updated equation was recommended by FAO (Allen et al. 1998) known as the FAO-56 Penman–Monteith equation, simplifying Eq. 11 by utilizing some assumed constant parameters for reference crop. It was assumed that the definition for the reference crop was a hypothetical reference crop with crop height of 0.12 m, a fixed surface resistance of 70 s m − 1 and an albedo of 0.23 (Smith et al. 1992). The new equation is:

$$ET_0 = \frac{0.408\Delta(R_n - G) + \gamma \frac{900}{T+273} u_2(e_s - e_a)}{\Delta + \gamma(1 + 0.34u_2)} \quad (12)$$

where ET_0 = reference evapotranspiration rate (mm/day), T = mean air temperature (°C), and u_2 = wind speed (m s^{-1}) at 2 m above the ground. This equation can be applied using hourly data if the constant value "900" is divided by 24 for the hours in a day and the R_n and G terms are expressed as MJ m^{-2} h^{-1}.

2.4 LandMOD ET Mapper

Bhattarai and Tao Liu (2019) have developed a new MATLAB-based ET mapping toolbox named "LandMOD ET Mapper" for automated implementation of SEBAL and METRIC to facilitate their widespread applications among new users with any level of prior modeling experiences(Bhattarai and Liu 2019). The automation of anchor pixels uses a modified version of Bhattarai et al. (2017) that eliminates the need of having a reference weather station within the image.

The automation of hot and cold pixel starts with the selection of candidate pixels based on a simple decision tree classifier and an exhaustive search used to select a subset of pixels that could potentially be selected as hot and cold pixels. The final hot and cold pixels are based on the ranking of each pixel based on its LST and NDVI values. The pixel with the highest LST and lowest NDVI value is selected as the hot pixel, while the pixel with the lowest LST and highest NDVI is taken as the cold pixel. The automatically selected hot and cold pixels are used to internally calibrate H (Sensible Heat Flux) and follow the stabilization correction procedures explained in R. Allen et al. (2011). LE is then used to estimate evaporative fraction or reference ET fraction (ETrF), which is assumed to be constant during the day to produce daily ET maps, as in Allen et al.(2011) and (Bhattarai et al. 2017).

3 Results

3.1 Comparison of Daily Evapotranspiration for Mymensingh Sadar Upazilla

In comparing the daily ET between SEBAL and METRIC algorithms (Table 2), it has been found that METRIC ET are lower than SEBAL ET. The reason behind this can be the internal calibration of two different methods. This study is limited to seven days due to the unavailability of cloud-free Landsat images and measured data. We have selected the dates when both cloud-free remote sensing images and measured ET data were available. In comparison with SEBAL and METRIC ET against Penman–Monteith method, we have noticed that the Penman–Monteith method shows higher

Table 2 Comparison of Daily ET estimated by SEBAL, METRIC, FAO Penman–Monteith equation and Pan Evaporation methods for Mymensingh Sadar Upazilla

Serial Nos	Date of 2007	DOY	SEBAL ET (mm/day)	METRIC ET (mm/day)	Pan Evaporation (mm/day)	Penman–Monteith ET (mm/day)
1	22 Jan	022	2.52	2.67	-	5.34
2	23 Feb	054	2.14	2.33	3.13	4.66
3	11 Mar	070	3.02	2.43	3.49	4.86
4	27 Mar	086	2.80	2.41	4.41	4.82
5	28 Apr	118	3.40	2.52	-	5.60
5	30 May	150	3.68	2.65	4.19	5.30
6	19 Sep	262	1.40	1.77	5.35	3.54
7	05 Oct	278	2.36	2.25	4.40	4.49

values than the SEBAL and METRIC models. This is expected because Penman–Monteith provides potential ET but SEBAL and METRIC provide actual ET. On the other hand, pan evaporation is comparable to Penman–Monteith ET. The actual ET from the SEBAL and METRIC models have been found to be significantly correlated with the Penman–Monteith (P-M) ET with a correlation coefficient of 0.86 and 0.95, respectively, for the Mymensingh site (Fig. 4).

It has also been noticed that actual ET gradually increases in Boro season during the growth stage. In fallow period, (between Boro and Aman cultivation) ET eventually decreases. Lower ET value in September indicates the initial stage of Aman rice period. The spatial variation of daily ET from the models, across the study area, is shown in Fig. 5. The values of ET vary from 0 to 7.35 mm/day. The lowest ET have been observed from bare soil near the river bank and built up-areas (Fig. 5).

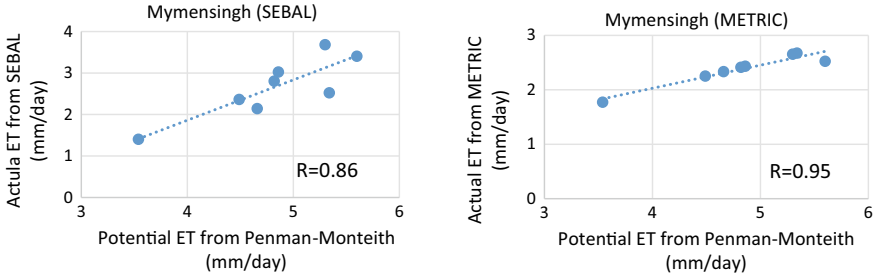

Fig. 4 Comparison of the Penman–Monteith potential ET with the remote sensing-based estimates of actual ET from the SEBAL and METRIC models for the Mymensingh site

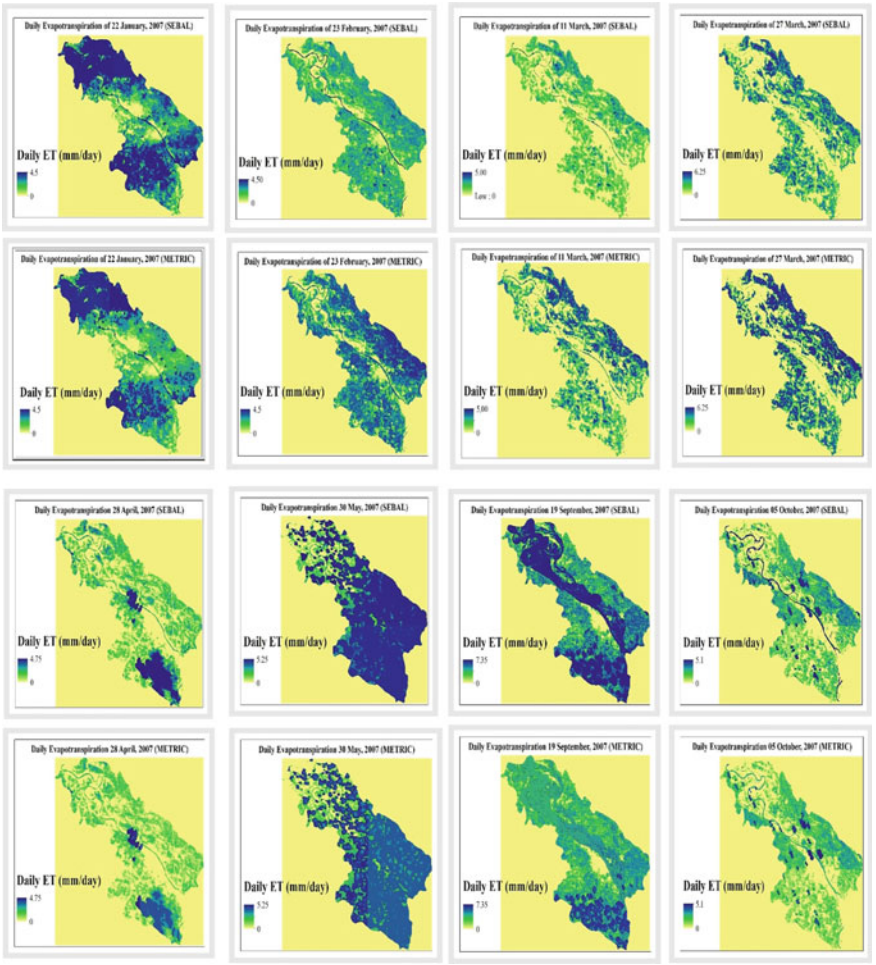

Fig. 5 Comparison of daily ET between SEBAL and METRIC method for Mymensingh Sadar Upazilla

3.2 Comparison of Daily Evapotranspiration for Bogra Sadar Upazilla

The spatial and temporal variation of ET is shown in Fig. 6 for the Bogra station. The values of ET vary from 0 to 5.65 mm/day near the BMD station. The lowest ET have been observed from bare soil near the river bank and built up-areas. The actual ET from the SEBAL and METRIC models have been found to be highly correlated with the Penman–Monteith (P-M) ET. The correlation coefficient is 0.98 between the SEBAL and P-M method while it is 0.88 between the METRIC and P-M method (Fig. 7). In comparison with daily ET between SEBAL and METRIC

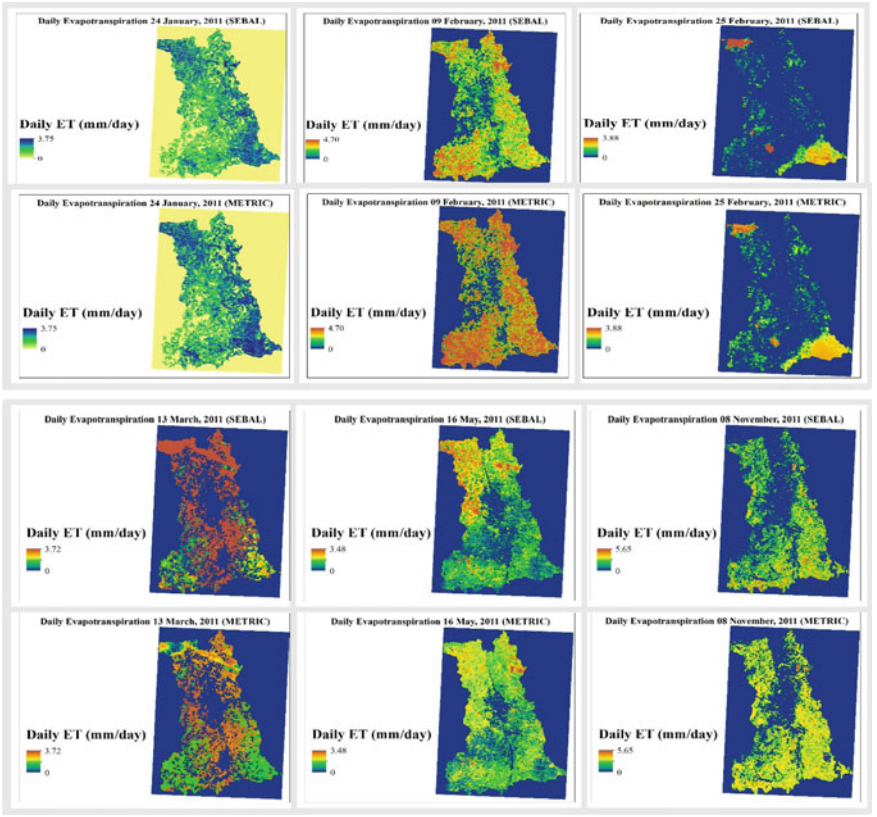

Fig. 6 Comparison of daily ET between SEBAL & METRIC method for Bogra Sadar Upazilla

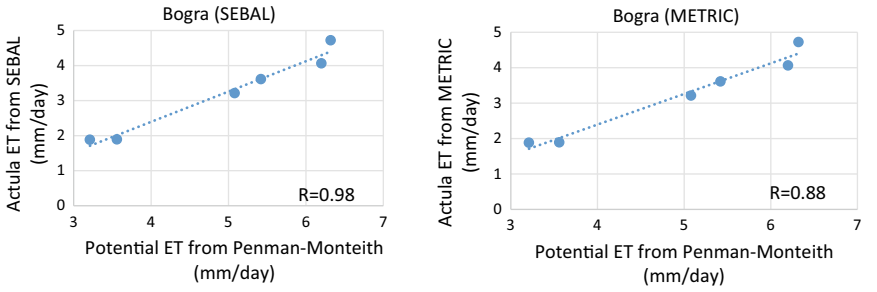

Fig. 7 Comparison of the Penman–Monteith potential ET with the remote sensing-based estimates of actual ET from the SEBAL and METRIC models for the Bogra Site

Table 3 Comparison of Daily ET estimated by SEBAL, METRIC, FAO Penman–Monteith equation, and Pan Evaporation methods for Bogra Sadar Upazilla

Serial Nos	Date of 2011	DOY	SEBAL ET (mm/day)	METRIC ET (mm/day)	Pan Evaporation (mm/day)	Penman–Monteith ET (mm/day)
1	24 Jan	24	1.88	2.85	-	3.21
2	09 Feb	40	3.21	3.41	-	5.08
3	25 Feb	56	3.61	3.62	-	5.42
4	13 Mar	72	4.72	5.64	-	6.32
5	16 May	136	4.06	4.35	5.1	6.20
6	08 Nov	312	1.89	2.26	3.3	3.56

algorithm, it has been found that METRIC ET is higher than the SEBAL ET, but the difference is moderate. One reason behind this mismatch can be the internal calibration of these two models. The differences in calculation of sensible heat in these two models and the assumptions of SEBAL and METRIC in extrapolating instantaneous ET to the daily ET may also contribute to the mismatch. Moreover accuracy of ET estimation highly depends on the accuracy of weather data. Since no actual weather data have been found available on an hourly scale, instead of actual weather data, coarse resolution weather data from Merra 2 have been used. The SEBAL and METRIC ET also differ from the pan evaporation. One reason behind this difference can be the fact that no pan coefficient has been applied to get the actual evaporation from measured evaporation. Besides these, the presence of partial cloud shadow in some dates may also cause some errors in remote sensing-based estimation (Table 3).

4 Conclusion

Evapotranspiration (ET) is a major component of the global water cycle. Measurement of evapotranspiration is essential for regional water resources management, irrigation scheduling, hydrologic modeling as well as for global climate change studies. The northwest region of Bangladesh depends highly on groundwater-based irrigation during the dry season for cultivating Boro crop. An accurate estimation of ET can be helpful in estimating irrigation demand precisely and can minimize the over extraction of groundwater in this region. In this study, the potential of SEBAL and METRIC models in estimating ET have been assessed for two agricultural fields of Bangladesh. A new MATLAB-based ET mapping toolbox named "LandMOD ET Mapper" has been used for automated implementation of these models. SEBAL and METRIC are more advantageous than conventional methods of evapotranspiration estimation using crop coefficient curves or vegetation indices because SEBAL/METRIC models

do not require any specific crop or vegetation information, and they consider the effect of water shortage, salinity or frost as well as evaporation from bare soil.

The spatial variation of ET estimated from the SEBAL and METRIC model have been found to be comparable in this study. But the magnitudes are a little different. This is probably due to the inherent differences in the algorithms of these two models. The results show that the actual ET from SEBAL and METRIC are lower than the ET from the FAO Penman–Monteith as the latter provides potential ET instead of actual ET. This study used Landsat data. Future studies can be conducted by using MODIS data instead of Landsat images. As MODIS acquire data on a daily basis, there is a better chance of obtaining more cloud-free images. This study reveals a promising potential of estimating ET from SEBAL and METRIC which can be very important to better understand and address a variety of water resources related issues. There is a need, however, to further test the model using additional datasets, and to examine the performance of the model in other sites under different soil, climate, cropping, and terrain conditions of Bangladesh. The results from this study are based on our initial efforts to assess the operational characteristics and performance of the automated SEBAL and METRIC model in the context of Bangladesh. Both models require reliable hourly weather data, including solar radiation, air temperature, relative humidity, and wind speed, in order to compute reference evapotranspiration. Reference evapotranspiration is then used to compute and interpolate the evapotranspiration for the days in between two satellite passes. The accuracy of this interpolation depends on the quality of the dataset used to compute reference ET. Especially, in developing countries like Bangladesh, hourly or even daily weather data are extremely limited. Therefore, Merra-2 weather data have been used in this study as input in the SEBAL and METRIC model. As measured weather data are not available on an hourly basis in these sites, no validation of the dataset was possible. So, data from other global gridded dataset can be used in the future as input in SEBAL and METRIC model to check whether better results can be achieved. Both models have their operational advantages and shortcomings depending on the conditions that are being applied. As the SEBAL method requires lower number of ground measured weather data, it can be said that it will be advantageous to use the SEBAL method over the METRIC model for data-scarce locations like Bangladesh. Further research is needed to evaluate the practicality and value of both models in the context of Bangladesh to predict surface ET throughout a growing season for different surfaces.

Acknowledgements The authors would like to express their gratitude to Nishan Bhattarai, Postdoctoral Research Scientist, United States Department of Agriculture (USDA), for his immense help with the LandMOD ET Mapper toolbox.

References

Acharjee, Tapos Kumar, Fulco Ludwig, Gerardo van Halsema, Petra Hellegers, and Iwan Supit. 2017. Future Changes in Water Requirements of Boro Rice in the Face of Climate Change in

North-West Bangladesh. *Agricultural Water Management* 194. Elsevier B.V.: 172–183. https://doi.org/10.1016/j.agwat.2017.09.008.

Allen, R. G., L. S. Pereira, D. Raes, and M. Smith. 1998. FAO Irrigation and Drainage Paper No. 56—Crop Evapotranspiration, no. March.

Allen, Richard G., Masahiro Tasumi, Anthony Morse, Ricardo Trezza, James L. Wright, Wim Bastiaanssen, William Kramber, Ignacio Lorite, and Clarence W. Robison. 2007. Satellite-Based Energy Balance for Mapping Evapotranspiration with Internalized Calibration (METRIC)—Applications. *Journal of Irrigation and Drainage Engineering* 133 (4): 395–406. https://doi.org/10.1061/(asce)0733-9437(2007)133:4(395).

Allen, Richard, Ayse Irmak, Ricardo Trezza, Jan M.H.. Hendrickx, Wim Bastiaanssen, and Jeppe Kjaersgaard. 2011. Satellite-Based ET Estimation in Agriculture Using SEBAL and METRIC. *Hydrological Processes* 25 (26): 4011–4027. https://doi.org/10.1002/hyp.8408.

Anayah, F.M., and J.J. Kaluarachchi. 2014. Improving the Complementary Methods to Estimate Evapotranspiration under Diverse Climatic and Physical Conditions. *Hydrology and Earth System Sciences* 18 (6): 2049–2064. https://doi.org/10.5194/hess-18-2049-2014.

Anderson, M.C., W.P. Kustas, J.M. Norman, C.R. Hain, J.R. Mecikalski, L. Schultz, M.P. González-Dugo, et al. 2011. Mapping Daily Evapotranspiration at Field to Continental Scales Using Geostationary and Polar Orbiting Satellite Imagery. *Hydrology and Earth System Sciences* 15 (1): 223–239. https://doi.org/10.5194/hess-15-223-2011.

Bastiaanssen, W.G.M., M. Meneti, R.A. Feddes, and A.A.M. Holtslag. 1998. A Remote Sensing Surface Energy Balance Algorithm for Land (SEBAL). *Journal of Hydrology* 212–213 (JANUARY): 198–212.

Bhattarai, Nishan, and Tao Liu. 2019. LandMOD ET Mapper: A New Matlab-Based Graphical User Interface (GUI)for Automated Implementation of SEBAL and METRIC Models in Thermal Imagery. *Environmental Modelling and Software* 118 (April). Elsevier: 76–82. https://doi.org/10.1016/j.envsoft.2019.04.007.

Bhattarai, Nishan, Lindi J. Quackenbush, Jungho Im, and Stephen B. Shaw. 2017. A New Optimized Algorithm for Automating Endmember Pixel Selection in the SEBAL and METRIC Models. *Remote Sensing of Environment* 196. Elsevier Inc., 178–92. https://doi.org/10.1016/j.rse.2017.05.009.

Bose, Indira, Faisal Hossain, Hisham Eldardiry, Shahryar Ahmad, Nishan K. Biswas, Ahmad Zeeshan Bhatti, Hyongki Lee, Mazharul Aziz, and Md Shah Kamal Khan. 2021. Integrating Gravimetry Data With Thermal Infra-Red Data From Satellites to Improve Efficiency of Operational Irrigation Advisory in South Asia." *Water Resources Research* 57 (4). https://doi.org/10.1029/2020WR028654.

Dey, Nepal C., Ratnajit Saha, Mahmood Parvez, Sujit K. Bala, A.K.M. Saiful Islam, Joyanta K. Paul, and Mahabub Hossain. 2017. Sustainability of Groundwater Use for Irrigation of Dry-Season Crops in Northwest Bangladesh. *Groundwater for Sustainable Development* 4: 66–77. https://doi.org/10.1016/j.gsd.2017.02.001.

"Evapotranspiration in an Arid Environment: Quantifying the Moisture Input of Landscape Trees and Turfgrass—ScienceDaily. 2021. Accessed August 19. https://www.sciencedaily.com/releases/2020/12/201215164914.htm.

Hossen, Md Shahadat, Masayoshi Mano, Akira Miyata, Md Abdul Baten, and Tetsuya Hiyama. 2012. Surface Energy Partitioning and Evapotranspiration Over a Double-Cropping Paddy Field in Bangladesh. *Hydrological Processes* 26 (9): 1311–1320. https://doi.org/10.1002/hyp.8232.

Kanoua, Wael, and Broder Merkel. 2015. Comparison Between the Two-Source Trapezoid Model for Evapotranspiration (TTME) and the Surface Energy Balance Algorithm for Land (SEBAL) in Titas Upazila in Bangladesh. *FOG-Freiberg Online Geoscience* 39: 65–86.

Karim, Fazlul, Mohammed Mainuddin, Masud Hasan, and Mac Kirby. 2020. Assessing the Potential Impacts of Climate Changes on Rainfall and Evapotranspiration in the Northwest Region of Bangladesh. *Climate* 8 (8). https://doi.org/10.3390/CLI8080094.

Kirby, J.M., M. Mainuddin, F. Mpelasoka, M.D. Ahmad, W. Palash, M.E. Quadir, S.M. Shah-Newaz, and M.M. Hossain. 2016. The Impact of Climate Change on Regional Water Balances in Bangladesh. *Climatic Change* 135 (3–4): 481–491. https://doi.org/10.1007/s10584-016-1597-1.

Li, Zhao Liang, Ronglin Tang, Zhengming Wan, Yuyun Bi, Chenghu Zhou, Bohui Tang, Guangjian Yan, and Xiaoyu Zhang. 2009. A Review of Current Methodologies for Regional Evapotranspiration Estimation from Remotely Sensed Data. *Sensors* 9 (5): 3801–3853. https://doi.org/10.3390/s90503801.

Liou, Yuei An, and Sanjib Kumar Kar. 2014. Evapotranspiration Estimation with Remote Sensing and Various Surface Energy Balance Algorithms-a Review. *Energies* 7 (5): 2821–2849. https://doi.org/10.3390/en7052821.

Mojid, Mohammad A., Mohammed Mainuddin, Khandakar Faisal Ibn Murad, and John Mac Kirby. 2021. Water Usage Trends under Intensive Groundwater-Irrigated Agricultural Development in a Changing Climate—Evidence from Bangladesh. *Agricultural Water Management* 251 (May). Elsevier: 106873. https://doi.org/10.1016/J.AGWAT.2021.106873.

Monteith, John L. 1965. Evaporation and the Environment. *19th Symposia of the Society for Experimental Biology* 19: 205–234.

Murshed, Sonia Binte, and Jagath J. Kaluarachchi. 2018. Scarcity of Fresh Water Resources in the Ganges Delta of Bangladesh. *Water Security* 4–5 (May). Elsevier: 8–18. https://doi.org/10.1016/j.wasec.2018.11.002.

Murshed, Sonia Binte, Md Rezaur Rahman, and Jagath J. Kaluarachchi. 2019. Changes in Hydrology of the Ganges Delta of Bangladesh and Corresponding Impacts on Water Resources. *Journal of the American Water Resources Association* 55 (4): 800–823. https://doi.org/10.1111/1752-1688.12775

Numata, Izaya, Kul Khand, Jeppe Kjaersgaard, Mark A. Cochrane, and Sonaira S. Silva. 2017. Evaluation of Landsat-Based Metric Modeling to Provide High-Spatial Resolution Evapotranspiration Estimates for Amazonian Forests. *Remote Sensing* 9 (1). https://doi.org/10.3390/rs9010046.

Penman, Howard Latimer. 1948. Natural Evaporation from Open Water, Bare Soil and Grass. *Proceedings of the Royal Society of London* 193: 120–145. https://doi.org/10.1098/rspa.1948.0037.

Reyes-González, Arturo, Jeppe Kjaersgaard, Todd Trooien, Christopher Hay, and Laurent Ahiablame. 2017. Comparative Analysis of METRIC Model and Atmometer Methods for Estimating Actual Evapotranspiration. *International Journal of Agronomy* 2017.https://doi.org/10.1155/2017/3632501

Rojas, Jose P., and Ronald E. Sheffield. 2013. Evaluation of Daily Reference Evapotranspiration Methods as Compared with the ASCE-EWRI Penman-Monteith Equation Using Limited Weather Data in Northeast Louisiana. *Journal of Irrigation and Drainage Engineering* 139 (4): 285–292. https://doi.org/10.1061/(asce)ir.1943-4774.0000523.

Ruhoff, A.L., A.R. Paz, L.E.O.C. Aragao, Q. Mu, Y. Malhi, W. Collischonn, H.R. Rocha, and S.W. Running. 2013. Evaluation de l'algorithme MODIS d'estimation de l'évapotranspiration Globale Utilisant Des Mesures de Covariance de La Turbulence et La Modélisation Hydrologique Dans Le Bassin Du Rio Grande. *Hydrological Sciences Journal* 58 (8): 1658–1676. https://doi.org/10.1080/02626667.2013.837578.

Shahid, Shamsuddin. 2011. Impact of Climate Change on Irrigation Water Demand of Dry Season Boro Rice in Northwest Bangladesh. *Climatic Change* 105 (3–4): 433–453. https://doi.org/10.1007/s10584-010-9895-5.

Smith, M., R.G. Allen, J.L. Monteith, L.S. Pereira, A. Perrier, and W.O. Pruitt. 1992. Report on the Expert Consultation on Procedures for Revision of FAO Guidelines for Prediction of Crop Water Requirements. Land and Water Development Division, United Nations Food and Agriculture Service, Rome.

Stannard. 1993. Modified Priestley-Taylor Evapotranspiration Models. *Water Resources* 29 (5): 1379–1392.

Su, Z., and C. Jacobs (2001). Advanced Earth Observation: Land Surface Climate Final Report. BCRS Report 2001: USP-2 Report 2001 01–02. Delft, Beleidscommissie Remote Sensing (BCRS), 183.

Tasumi, M. 2003. *Progress in Operational Estimation of Regional Evapotranspiration Using Satellite Imagery*. Ph.D. Dissertation. Moscow: University of Idaho.

Teixeira, A.H. de. C., Wim G.M. Bastiaanssen, Mobin-ud-Din Ahmad, and M.G. Bos. 2008. Reviewing SEBAL Input Parameters for Assessing Evapotranspiration and Water Productivity for the Low-Middle Sao Francisco River Basin, Brazil: Part A—Calibration and Validation. https://cgspace.cgiar.org/handle/10568/40785.

Wang, Xiao Gang, Wen Wang, Dui Huang, Bin Yong, and Xi Chen. 2014. Modifying SEBAL Model Based on the Trapezoidal Relationship Between Land Surface Temperature and Vegetation Index for Actual Evapotranspiration Estimation. *Remote Sensing* 6 (7). MDPI AG: 5909–5937. https://doi.org/10.3390/rs6075909.

Wilfried, Brutsaert. 1975. On a Derivable Formula for Long-Wave Radiation from Clear Skies FLD. *Water Resources Research* 11 (5): 742–744.

Zhang, Ke, John S. Kimball, and Steven W. Running. 2016. A Review of Remote Sensing Based Actual Evapotranspiration Estimation. *Wiley Interdisciplinary Reviews: Water* 3 (6): 834–853. https://doi.org/10.1002/wat2.1168.

Zillman, J.W. 1972. A Study of Some Aspects of the Radiation and Heat Budgets of the Southern Hemisphere Oceans/by J.W.|National Library of Australia. https://catalogue.nla.gov.au/Record/2267389.